



HAL
open science

Conception de matériaux hybrides peptidiques biomimétiques

Cécile Echalier

► **To cite this version:**

Cécile Echalier. Conception de matériaux hybrides peptidiques biomimétiques. Matériaux. Université Montpellier, 2016. Français. NNT: . tel-01476825

HAL Id: tel-01476825

<https://hal.science/tel-01476825>

Submitted on 25 Feb 2017

HAL is a multi-disciplinary open access archive for the deposit and dissemination of scientific research documents, whether they are published or not. The documents may come from teaching and research institutions in France or abroad, or from public or private research centers.

L'archive ouverte pluridisciplinaire **HAL**, est destinée au dépôt et à la diffusion de documents scientifiques de niveau recherche, publiés ou non, émanant des établissements d'enseignement et de recherche français ou étrangers, des laboratoires publics ou privés.

THÈSE

Pour obtenir le grade de
Docteur

Délivré par l'Université de Montpellier

**Préparée au sein de l'école doctorale
ED 459 Sciences Chimiques Balard
Et des unités de recherche
UMR 5247 – Institut des Biomolécules Max
Mousseron et UMR 5253 – Institut Charles Gerhardt
Montpellier**

Spécialité : Ingénierie biomoléculaire

Présentée par Cécile ECHALIER

CONCEPTION DE MATERIAUX HYBRIDES PEPTIDIQUES BIOMIMETIQUES

Soutenue le 21 novembre 2016 devant le jury composé de

M. Jean MARTINEZ, Professeur, Université de Montpellier	Président du jury
M. Thibaud CORADIN, DR CNRS, Chimie de la Matière Condensée de Paris	Rapporteur
M. Steven BALLETT, Professeur, Vrije Universiteit Brussel	Rapporteur
Mme Laetitia MESPOUILLE, Maître de conférences, Université de Mons	Examineur
M. Ahmad MEHDI, Professeur, Université de Montpellier	Directeur de thèse
M. Gilles SUBRA, Professeur, Université de Montpellier	Directeur de thèse



IBMM
Institut des
Biomolécules
Max Mousseron

Biomimetic Peptide Hybrid Materials

Remerciements

Ce travail de thèse est issu d'une collaboration entre l'équipe "Amino acides, Hétérocycles, Peptides et Protéines" (AHPP) de l'Institut des Biomolécules Max Mousseron (IBMM) et l'équipe "Chimie Moléculaire et Organisation du Solide" (CMOS) de l'Institut Charles Gerhardt (ICGM).

Je remercie tout d'abord la Région Languedoc-Roussillon d'avoir financé en grande partie ce travail au travers de la bourse "Chercheur d'Avenir" attribuée au Pr. Gilles Subra. De même, je remercie l'équipe CMOS pour avoir complété ce financement.

J'adresse mes remerciements au Dr. Thibaud Coradin et au Pr. Steven Ballet pour avoir accepté d'être les rapporteurs de ce manuscrit. Je remercie également le Dr. Laetitia Mespouille d'avoir accepté d'être examinateur lors de ma soutenance de thèse.

Je remercie chaleureusement le Pr. Jean Martinez, directeur de l'IBMM au début de ma thèse, pour m'avoir accueillie dans son institut et avoir initié la collaboration entre les équipes AHPP et CMOS sur le thème des peptides hybrides. Je remercie le Dr. François Fajula, directeur de l'ICGM au début de ma thèse, pour m'avoir permis de réaliser ma thèse au sein de son institut. Merci également aux Drs. Muriel Amblard et Hubert Mutin de m'avoir accueillie dans leur équipe respective.

Mes remerciements vont bien sûr à mes directeurs de thèse. Je remercie du fond du cœur le Pr. Gilles Subra non seulement pour son encadrement, son implication dans mon projet et ses conseils scientifiques mais aussi pour sa bonne humeur, son soutien infaillible et son optimisme à toute épreuve. Je le remercie de m'avoir transmis sa passion pour la recherche. Je n'aurais pas pu rêver meilleur directeur de thèse. Et pourtant, la chance m'a offert un deuxième directeur de thèse formidable. Je remercie le Pr. Ahmad Mehdi pour ses conseils et sa disponibilité. A tous les deux, vous formez une équipe extraordinaire.

Je remercie vivement le Pr. Xavier Garric, Audrey Bethri et le Dr. Hélène Van Den Berghe pour leur aide en culture cellulaire et en rhéologie respectivement. Merci au Pr. Estelle Bilak de m'avoir ouvert la porte de son laboratoire pour les expériences de bactériologie et à Agnès Masnou pour son aide. Je remercie le Dr. Elisabeth Engel et les membres de son équipe, les Dr. Riccardo Levato et Oscar Castaño, de m'avoir accueillie dans leur équipe et initiée à l'impression 3D. Un merci tout particulier au Dr. Miguel Angel Mateos Timoneda pour son aide précieuse et sa gentillesse. J'adresse également mes remerciements au Dr. Danièle Noël et à son équipe, en particulier au Dr. Marie Maumus, au Dr. Karine Toupet et à Gauthier Tejedor pour leur aide concernant les tests biologiques et les observations de mes échantillons au microscope confocal.

Merci aux Drs. Said Jebors, Jérémie Ciccione et Coline Pinese qui ont travaillé à mes côtés sur les peptides silylés. Je remercie le Dr. Baptiste Legrand pour les études RMN qu'il a réalisées. Merci à Pierre Sanchez et Guillaume Cazals pour les analyses de spectrométrie de masse, à

Aurélien Lebrun et Karine Parra pour les analyses RMN. Merci au Dr. Guillaume Laconde, au Dr. Pascal Verdie et à Léa Causse pour leur implication dans le projet "collagène". Un grand merci à Luc Brunel qui, outre sa participation dans ce projet, œuvre tous les jours au bon fonctionnement du laboratoire avec le sourire et avec beaucoup de dévouement.

Je remercie les Drs. Vincent Martin, Lubomir Vezekov et Matthieu Simon avec qui j'ai partagé mon bureau et de passionnantes conversations. Merci à tous mes collègues de travail et amis qui ont partagé mon quotidien pendant trois ans et l'ont égayé : Dominique, Alexandre, Barbara, Laurent S, Khoubaib, Matthieu, Clément B, Clément S, Loïc, Thibault, Aleksandra, Morgan, Marion, Camille, Juan, Salomé, Nicolas, Jean-François, JAF, Séverine, Vincent L, Laurent G, Ludovic, Youssef, Bruno, Sylvie, Jocelyne, Aymara, Sandrine, Lyne-Rose, Marion P. Un merci tout particulier à Elise et Carmen pour leur écoute attentive et leurs encouragements. Je remercie toute l'équipe CMOS pour leur accueil, bien que j'aie été une collègue très peu présente. J'adresse également mes remerciements à toute l'équipe du Dr. Marcel Garcia pour leurs conseils et leur gentillesse.

Je n'oublie pas mes amis : Justine W, Thomas, Ludo, Pierre, Rémy, Audrey, Justine G, Clémentine, Manon et Laura. Vous êtes le meilleur des réconforts après une manip ratée et tous les moments que nous passons ensemble constituent de merveilleux souvenirs. Un merci particulier à toi Michou.

Enfin, je remercie vivement ma famille. Merci à mes parents et à mes grands-parents pour leur soutien constant et leur amour inconditionnel. Je remercie ma sœur, Delphine, et son mari de toujours me réserver le 3^{ème} tabouret. Merci à mon filleul, Théo, d'avoir coloré l'année écoulée de ses sourires.

Table of contents

Remerciements	5
Table of contents.....	7
Table of figures.....	10
Abbreviations	12
List of L-amino acids	15
Introduction.....	19
Chapter I. State of the art: hydrogels for cell encapsulation	23
I.1. Cell-encapsulating hydrogels	23
I.1.1. Applications of cell-encapsulating hydrogels.....	23
I.1.1.1. 3D cell culture platforms	23
I.1.1.2. Cell-based therapies.....	23
I.1.1.3. Tissue engineering applications	24
I.1.2. Native extracellular matrix.....	26
I.1.3. Hydrogels.....	27
I.1.3.1. Hydrogels as artificial ECM.....	27
I.1.3.2. Physical hydrogels	28
I.1.3.3. Chemical hydrogels	31
I.2. Cross-linking strategies.....	31
I.2.1. Free-radical photopolymerization.....	32
I.2.1.1. Chain-growth photopolymerization.....	32
I.2.1.2. Step-growth photopolymerization.....	35
I.2.2. Click chemistry.....	37
I.2.2.1. Michael-type addition	37
I.2.2.2. Azide-alkyne cycloaddition.....	39
I.2.2.3. Diels-Alder cycloaddition	42
I.2.2.4. Native chemical ligation	44
I.2.2.5. Imine, hydrazone and oxime formation.....	45
I.2.2.6. Disulfide formation	47
I.2.3. Enzyme-mediated cross-linking	48
I.2.3.1. Enzyme-triggered free-radical polymerization	49
I.2.3.2. Enzyme-mediated ligation	50
I.2.4. Sol-gel chemistry	53
I.2.4.1. Overview	53
I.2.4.2. Hydrolysis step	54
I.2.4.3. Condensation step.....	56
I.2.4.4. Hydrogels cross-linked by the sol-gel process	57
Chapter II. Hybrid silylated peptides.....	65
II.1. Hybrid peptides	65
II.2. Hybrid peptide synthesis.....	65

II.2.1. General considerations	65
II.2.2. Triethoxysilyl peptide synthesis	66
II.2.3. Chlorodimethylsilyl peptide synthesis	67
II.3. Hybrid peptide utilization	68
II.3.1. Trialkoxysilyl peptide utilization	69
II.3.1.1. Trialkoxysilyl peptides for grafting on silica	69
II.3.1.2. Trialkoxysilyl peptides for direct synthesis of hybrid silica	70
II.3.2. Restricting the number of bonds: dimethylchlorosilyl hybrid peptides	71
II.3.2.1. Grafting of dimethylchlorosilyl hybrid peptides	71
II.3.2.2. Direct synthesis of 'silicone-based' polymers	71
II.4. Stability studies of siloxane bond and synthesis of bioactive dimers	72
II.5. Publication n°1 – Selective homodimerization of unprotected peptides using hybrid hydroxydimethylsilane derivatives	75
Chapter III. PEG-based bioactive hybrid hydrogels	87
III.1. Selection of the hydrogel precursors	87
III.2. Preparation of the hybrid precursors	88
III.3. Development of the sol-gel gelation process	89
III.3.1. Gelation conditions: pH, temperature and catalyst	89
III.3.2. NMR studies	90
III.3.2.1. Hydrolysis monitored by liquid-state ¹ H NMR	90
III.3.2.2. Condensation monitored by solid-state ²⁹ Si NMR	92
III.3.1. Rheology study	94
III.4. Selection of a hydrogel	96
III.5. Hybrid PEG 2000 hydrogels	98
III.5.1. Mechanical properties	98
III.5.2. Microscopic images	98
III.5.3. Cytotoxicity assays	99
III.6. PEG-based bioactive hybrid hydrogels	99
III.7. Publication n°2 – Easy synthesis of tunable hybrid bioactive hydrogels	101
Chapter IV. Collagen-inspired peptide hydrogel	109
IV.1. Natural collagen	109
IV.1.1. Structure and function	109
IV.1.2. Applications of collagen-based biomaterials	110
IV.1.3. Limitations of natural collagen extracts	110
IV.2. Collagen-like peptides	111
IV.2.1. Pro-Hyp-Gly based peptides as synthetic collagen mimics	111
IV.2.2. Design of the hybrid collagen-inspired peptide sequence	111
IV.3. Sol-gel derived collagen-inspired hydrogel	112
IV.3.1. Optimization of the hydrogel composition	112
IV.3.2. Monitoring of the hydrogel formation and characterization	113
IV.4. Biological assessment of the hydrogel	114

IV.4.1. Influence of the functionalization of the hybrid collagen-inspired peptide hydrogel with RGD ligand on transparency.....	114
IV.4.2. Influence of the functionalization of the hybrid collagen-inspired peptide hydrogel with RGD ligand on cell adhesion.....	115
IV.4.3. Benchmarking of hybrid collagen-inspired peptide hydrogels vs commercial collagen foams and cell encapsulation	116
IV.5. Collagen-inspired peptide membranes.....	116
IV.5.1. Synthesis of hybrid membranes by the sol-gel process.....	116
IV.5.2. Physical properties of collagen-inspired peptide membranes	117
IV.5.3. Preliminary biological assays: adhesion and proliferation of L929 fibroblasts on hybrid collagen-inspired peptide membranes	118
IV.6. Publication n°3 – Sol-gel synthesis of collagen-inspired peptide hydrogel	121
Chapter V. 3D printing of hydrogels.....	137
V.1. Applications of 3D printed hydrogels	137
V.2. Extrusion 3D printing	138
V.3. Sol-gel derived hybrid hydrogels as bioinks.....	139
V.3.1. Viscosity monitoring.....	139
V.3.2. 3D printing.....	139
V.3.3. Biological assessment of 3D scaffolds.....	140
V.4. Publication n°4 – Modular bioink for 3D printing of biocompatible hydrogels: sol-gel polymerization of hybrid peptides and polymers.....	141
Conclusion and perspectives.....	147
References.....	151
Experimental section.....	175
Supporting information for publication n°1	
Supporting information for publication n°2	
Supporting information for publication n°3	
Supporting information for publication n°4	
Annexes	281
Publication: Simple and specific grafting of antibacterial peptides on silicone catheters	281
Patent: Nouveaux hydrogels de structure silylée et procédé d'obtention.....	296

Table of figures

Figure 1. Principle of tissue engineering	25
Figure 2. Schematic representation of the extracellular matrix	26
Figure 3. Chain-growth photopolymerization mechanism.	32
Figure 4. Chemical structures of vinyl groups used for preparation of hydrogels by chain-growth photopolymerization.	33
Figure 5. Structures of some photoinitiators used for hydrogel preparation by photopolymerization.	34
Figure 6. Step-growth photopolymerization mechanism	35
Figure 7. 4-arm PEG norbornene	36
Figure 8. Michael-type addition involving a thiol as Michael donor.....	37
Figure 9. Michael acceptors and their reactivity towards thiols.....	37
Figure 10. Example of a functional hydrogel prepared by Michael addition.....	39
Figure 11. Alkyne-azide cycloadditions yielding 1,2,3-triazoles.....	40
Figure 12. Proposed mechanism for the Copper(I)-catalyzed alkyne-azide cycloaddition.	41
Figure 13. Strain-promoted azide alkyne cycloaddition (SPAAC) between an azide and a cyclooctyne.....	41
Figure 14. Structures of activated yne groups used for metal-free azide-alkyne cycloaddition	42
Figure 15. Diels-Alder reaction.....	42
Figure 16. Diels-Alder reaction between furane and maleimide moities	43
Figure 17. Inverse electron demand Diels-Alder reaction	43
Figure 18. Tetrazine-norbornene inverse electron demand hetero Diels-Alder-retro-Diels-Alder cascade.	44
Figure 19. Native chemical ligation	44
Figure 20. Reactions of a aldehyde with a primary amine, a hydrazine, a hydrazide and a O-substituted hydroxylamine to form an imine, a hydrazine, an acylhydrazone and an oxime.	45
Figure 21. Disulfide bond formation and reduction.....	47
Figure 22. Example of thiol-disulfide exchange reaction used by S.-Y. Choh and co-workers to prepare a hydrogel.....	48
Figure 23. Enzyme-mediated redox reactions triggering free-radical polymerization.....	49
Figure 24. Horseradish peroxidase (HRP)-mediated oxidative cross-linking of phenol derivatives.	50
Figure 25. Chemical structures of carboxylic acid derivatives coupled on hydrogel precursors to enable enzyme-mediated oxidative cross-linking.	50
Figure 26. Oxidative coupling of tyrosine residues by tyrosinase.....	51
Figure 27. Transglutaminase (TG)-catalyzed acyl transfer between a glutamine and a lysine side-chains.....	52
Figure 28. Phosphopantetheinyl transferase (PPTase)-catalyzed reaction between serine residue of ACP and CoA-functionalized PEG.	52
Figure 29. Principle of the sol-gel process.	54
Figure 30. Overall equation of the hydrolysis of a silicon alkoxide into silanol.....	54
Figure 31. Reaction rates of tetraethyl orthosilicate hydrolysis (blue curve) and condensation (green curve) as a function of pH.....	55
Figure 32. Acid-catalyzed hydrolysis of a silicon alkoxide group	55
Figure 33. Base-catalyzed hydrolysis of a silicon alkoxide group.....	55
Figure 34. Fluoride-catalyzed hydrolysis of a silicon alkoxide group.....	56
Figure 35. Condensation reactions via oxolation or alkoxolation.....	56
Figure 36. Influence of the catalyst on the type of hydrogels obtained.....	57
Figure 37. Synthesis of a functional hybrid hydrogel thanks to the sol-gel process.....	58
Figure 38. Encapsulation of E. coli cells in a silica hydrogel formed by the sol-gel process.....	58
Figure 39. Sol-gel cross-linking of a hybrid silylated polymer.....	60
Figure 40. Functionalization of polymers with trialkoxysilylated reagents.	61
Figure 41. General formula of hybrid silylated peptides	65
Figure 42. Hybrid silylated peptides used for the preparation of hybrid materials via the sol-gel process.....	65

Figure 43. Preparation of hybrid silylated peptides.....	66
Figure 44. Principle of the synthesis of hybrid materials using a silylated and protected peptide.	67
Figure 45. Principle of the synthesis of hybrid materials using a hybrid hydroxydimethylsilyl peptide	68
Figure 46. Principle of silicon oxide material grafting with hybrid peptides	69
Figure 47. Synthesis of multifunctional fluorescent silica nanoparticles.....	70
Figure 48. Principle of the direct synthesis of a hybrid peptide material using hybrid triethoxysilyl peptides.....	70
Figure 49. Silicone-based dimers and polymers obtained from chlorodimethylsilyl hybrid peptides or dihydroxymethylsilyl peptides.....	72
Figure 50. Preparation of the dimers used as models for the siloxane stability study and their hydrolysis into monomers.....	73
Figure 51. ¹ H NMR studies of siloxane dimer hydrolysis	73
Figure 52. Polycondensation of hybrid triethoxysilyl PEG	88
Figure 53. Preparation of hybrid silylated polyethylene glycol	89
Figure 54. Prepared hybrid silylated PEGs	89
Figure 55. Formation of PEG-based hydrogels via the sol-gel process.....	90
Figure 56. Hydrolysis of hybrid triethoxysilyl PEG	91
Figure 57. ¹ H NMR spectra of the hybrid PEG 2000 at a 10 wt% concentration in DPBS containing 0.3 wt% of NaF	91
Figure 58. Integration of ¹ H NMR signals of the CH ₃ group of ethanol	92
Figure 59. Nomenclature used to designate silicon atoms in hybrid structures and ²⁹ Si NMR chemical shifts associated.....	92
Figure 60. ²⁹ Si NMR spectra of 10 wt% hybrid PEG 2000 hydrogels lyophilized after 0, 2 or 4 days.....	93
Figure 61. Possible structures for T ³ silicon species.....	93
Figure 62. Comparison of networks formed from hybrid triethoxysilyl PEG (A) and hybrid dimethylhydroxysilyl PEG (B)	94
Figure 63. AR 2000 rheometer fitted with a 20 mm parallel geometry	95
Figure 64. G' (in blue) and G'' (in green) moduli measured on a 10 wt% hybrid PEG 2000 solution in DPBS with sodium fluoride (3 mg/mL) at 37°C (1% strain, 1 Hz)	95
Figure 65. 10 wt% hybrid PEG solutions in DPBS after 24 h at 37°C.....	97
Figure 66. SEM images of 10 wt% hybrid PEG 2000 hydrogel.	99
Figure 67. Preparation of covalent hybrid bioactive hydrogels thanks to the sol-gel process	100
Figure 68. Structure of natural collagen	109
Figure 69. Commercially available collagen foam (ACE Surgical Supply Co, inc.) engineered from highly purified cross-linked bovine type I collagen and used as a resorbable material in periodontal defects to aid in wound healing	110
Figure 70. Hybrid collagen-inspired peptide used as a building block for hydrogel preparation	112
Figure 71. Appearance of different hydrogels prepared in DPBS.....	112
Figure 72. CryoSEM images of a 10 wt% hybrid collagen-inspired peptide hydrogel prepared in cell culture medium with sodium fluoride (3 mg/mL)	113
Figure 73. Appearance of hybrid collagen-inspired peptide hydrogels prepared in cell culture plates.	114
Figure 74. mMSC adhesion on hybrid collagen-inspired peptide hydrogels containing 0 or 10 mol% of hybrid RGD peptide.....	115
Figure 75. Synthesis of a hybrid peptide membrane by the sol-gel process	117
Figure 76. Hybrid collagen-inspired peptide membranes.....	117
Figure 77. SEM image of a hybrid collagen-inspired peptide membrane.....	118
Figure 78. Commercially available natural collagen membrane.....	119
Figure 79. L929 adhesion and proliferation on hybrid collagen-inspired peptide membranes.	119
Figure 80. Computer-aided design (CAD) process for automated printing of 3D shape imitating target tissue or organ developed by H.-W. et al.....	137
Figure 81. nScript 3Dn-300 rapid prototyping machine used in IBEC to print 3D scaffolds .	138

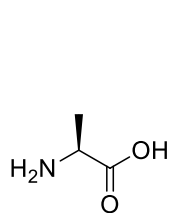
Abbreviations

2D, 3D	two-dimensional, three-dimensional
ACN	acetonitrile
Alloc	allyloxycarbonyl
APTES	aminopropyltriethoxysilane
BBFO	broad band fluorine observation
Boc	<i>tert</i> -butyloxycarbonyl
CAD	computer-aided design
cat	catalyst
CD	circular dichroism
CFU	colony-forming unit
CM	ChemMatrix
CuAAC	copper(I)-catalyzed alkyne-azide cycloaddition
DA	Diels-Alder
DCM	dichloromethane
DEPT	distortionless enhancement by polarization transfer
DIEA	N,N-diisopropylethylamine
DMEM	Dulbecco's modified eagle medium
DMF	N-N'-dimethylformamide
DMSO	dimethylsulfoxide
DOPA	3,4-dihydroxyphenylalanine
DPBS	Dulbecco's phosphate-buffered saline
ECM	extracellular matrix
EDC	1-ethyl-3-(3-dimethylaminopropyl)-carbodiimide
EDG	electron-donating group
eq	equivalent
ESI	electrospray ionization
EthD-III	ethidium homodimer III
EWG	electron-withdrawing group
FBS	fetal bovine serum
Fmoc	fluorenylmethoxycarbonyl
FPPS	fast parallel peptide synthesis
GHRP-6	growth hormone releasing hexapeptide
GOx	glucose oxidase enzyme
GPMDS	3-(glycidoxypropyl)methyldiethoxysilane
GPTMS	3-(glycidoxypropyl)trimethoxysilane
HA	hyaluronic acid
HATU	1-[Bis(dimethylamino)methylene]-1H-1,2,3-triazolo[4,5-b]pyridinium 3-oxid hexafluorophosphate

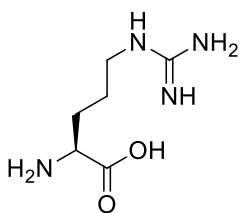
HBTU	N,N,N',N'-tetramethyl-O-(1H-benzotriazol-1-yl)uronium phosphate	hexafluoro-
HFIP	hexafluoroisopropanol	
HOSu	N-hydroxysuccinimide	
HPA	3-(4-hydroxyphenyl)propionic acid	
HPMC	hydroxypropylmethylcellulose	
HRP	horseradish peroxidase	
HTRF	homogenous time resolved fluorescence	
HPLC	high performance liquid chromatography	
HRMS	high resolution mass spectrometry	
ICPDMCS	3-isocyanatopropyltrimethylchlorosilane	
ICPTES	3-isocyanatopropyltriethoxysilane	
IP1	inositol monophosphate	
LC/MS	tandem liquid chromatography/ mass spectrometry	
MMP	matrix metalloproteinase	
MSC, mMSC, hMSC	mesenchymal stem cell, mouse MSC, human MSC	
MW	molecular weight	
n. a.	non applicable	
NCL	native chemical ligation	
n. d.	non determined	
NIPAM	poly(N-isopropylacrylamide)	
NMP	N-methyl-2-pyrrolidone	
NMR	nuclear magnetic resonance	
OMNCL	oxo-ester mediated chemical ligation	
OMS	ordered mesoporous silica	
PA	polyacrylamide	
Pbf	2,2,4,6,7-pentamethyldihydrobenzofuran-5-sulfonyl	
PDMS	polydimethylsiloxane	
PEG	polyethylene glycol	
PEGDA	polyethylene glycol diacrylate	
PEGDM	polyethylene glycol dimethacrylate	
PHEMA	polyhydroxyethylmethacrylate	
PI	photoinitiator	
pip	piperidine	
PLA	poly(L,D-lactic acid)	
PLGA	poly(lactic-co-glycolic acid)	
PP	polypropylene	
PPII	polyproline II helix	
PPTase	phosphopantetheinyl transferase	
PVA	poly(vinyl alcohol)	
PS	polystyrene	

ROS	reactive oxygen species
RP	reversed phase
RT	room temperature
SEM	scanning electron microscopy
SPAAC	strain-promoted alkyne-azide cycloaddition
SPPS	solid phase peptide synthesis
TC-PS	tissue culture polystyrene
TEOS	tetraethyl orthosilicate
TFA	trifluoroacetic acid
TG	transglutaminase
THF	tetrahydrofuran
TIS	triisopropylsilane
TMSP	trimethylsilyl-3-propionic acid 2,2,3,3-sodium salt
Trt	trityl
TSA	tryptic soy agar
UV	ultra-violet
VEGF	vascular endothelial growth factor

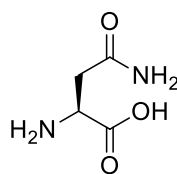
List of L-amino acids



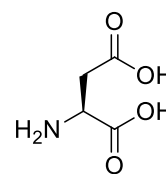
Alanine
Ala - A



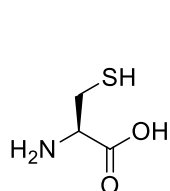
Arginine
Arg - R



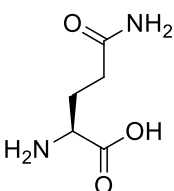
Asparagine
Asn - N



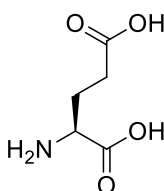
Aspartic acid
Asp - D



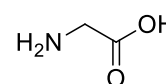
Cysteine
Cys - C



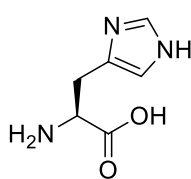
Glutamine
Gln - Q



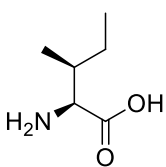
Glutamic acid
Glu - E



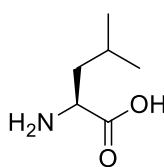
Glycine
Gly - G



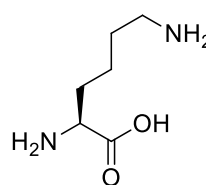
Histidine
His - H



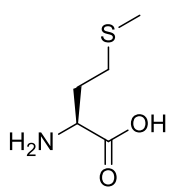
Isoleucine
Ile - I



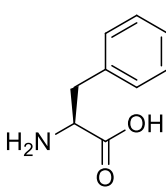
Leucine
Leu - L



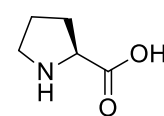
Lysine
Lys - K



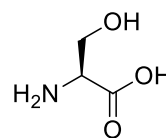
Methionine
Met - M



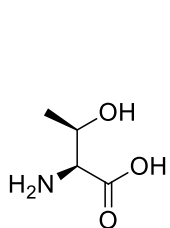
Phenylalanine
Phe - F



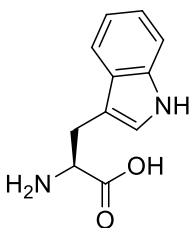
Proline
Pro - P



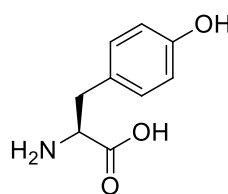
Serine
Ser - S



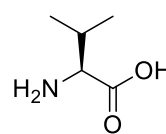
Threonine
Thr - T



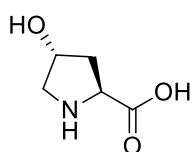
Tryptophan
Trp - W



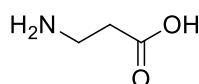
Tyrosine
Tyr - Y



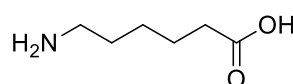
Valine
Val - V



Hydroxyproline
Hyp - O



β -Alanine
 β Ala - β A



6-aminohexanoic acid
Ahx

Introduction

Introduction

In living tissues, cells are surrounded by a complex and bioactive matrix which provides them mechanical support while directing their behavior. Interactions between this extracellular matrix (ECM) and cells are crucial for cell survival, proliferation, migration and differentiation. Consequently, ECMs are the object of many research projects that aim at studying their properties and understanding their regulation pathways both under healthy and disease conditions. The knowledge gained through these studies helps producing artificial ECMs.

The design of biomaterials in which cells could behave like in their native environment is of tremendous interest in regenerative medicine. Tissue engineering is the field of regenerative medicine dedicated to the production of living tissues intended to be used as tissue grafts or organ replacements. Developments in this area could address the organ donor shortage which is a major public health issue. To achieve this objective, tissue engineering relies on biomaterials able to act as artificial ECM to guide cells towards the development of a new tissue. ECM substitutes have also found applications in *in vivo* cell delivery for the treatment of hormone and enzyme deficiencies or for cancer therapy. Therefore, considerable efforts have been made to develop biomimetic materials and it remains a real challenge. My PhD project fits in with this context.

The approach selected herein for the design of new bioactive materials is supported by the complementary skills of the two research groups involved in this PhD. On the one hand, the team "*Aminoacides, Hétérocycles, Peptides et Protéines*" (AHPP) of the Institute of Biomolecules Max Mousseron has expertise in (bio)organic and peptide chemistry at the interface with biology. On the other hand, the team "*Chimie Moléculaire et Organisation du Solide*" (CMOS) of the Institute Charles Gerhardt is specialized in inorganic chemistry and materials science. This collaboration gave birth to a modular bottom-up approach in which hybrid molecules are combined to build a multifunctional material. These hybrid building blocks are made of a (bio)organic unit, which affords its bioactivity to the resulting material, and an inorganic moiety, which allows the polymerization by the sol-gel process. The sol-gel chemistry involves the hydrolysis and the condensation of metal alkoxide precursors to form an oxide network. In our case, polymers are modified with trialkoxysilane groups ($-\text{Si}(\text{OR})_3$) to yield hydrogels cross-linked by siloxane (Si-O-Si) bonds. This chemistry was chosen for its softness and good compatibility with living cells. The process is carried out in aqueous solution at physiological pH and body temperature. It is chemoselective and bioorthogonal, *i. e.* it could occur in living systems without interfering with biological processes. In addition, it allows the combination of hybrid precursors for the preparation of multifunctional tailor-made materials.

The **first chapter** of this thesis draws attention on the applications of the biomaterials we intend to develop because these applications impose some designing constraints. The notions of extracellular matrix and hydrogel are defined. The different cross-linking methods available

for the preparation of chemical hydrogels under conditions compatible with living cells are reviewed, highlighting the advantages and limitations of each strategy.

The **second chapter** is dedicated to a preliminary study of hybrid hydroxydimethylsilyl peptides. Before introducing hybrid molecules in hydrogels, we evaluated the stability of the siloxane bond in aqueous media. NMR was used to monitor the hydrolysis of siloxane dimers in different experimental conditions. Then, we showed that the functionalization of peptides with a hydroxydimethylsilyl group was a straightforward dimerization method and we applied this strategy to bioactive sequences. **[Publication n°1 – Selective homodimerization of unprotected peptides using hybrid hydroxydimethylsilane derivatives]** Hybrid hydroxydimethylsilyl peptides were also used for the grafting of silicone catheters. This work, in which I was involved, is beyond the scope of this PhD project and the corresponding **publication (Simple and specific grafting of antibacterial peptides on silicone catheters)** will be found in the annex section at the end of the manuscript.

The development of polyethylene glycol-based hydrogels is presented in the **third chapter**. After their modification with triethoxysilyl groups, PEG units were cross-linked *via* a sol-gel process carried out in physiological medium at 37°C. The one-pot covalent functionalization of these hydrogels during the sol-gel process was demonstrated with fluorescein derivatives and then applied to the preparation of cell adhesive and antibacterial hydrogels using hybrid peptides. **[Publication n°2 – Easy synthesis of tunable hybrid bioactive hydrogels]**

Then, the bio-inert PEG was replaced by a synthetic peptide to prepare hydrogel networks with inherent cell-friendly properties. The sequence of the peptide was inspired by natural collagen sequence. The resulting hydrogels were suitable for cell adhesion and proliferation. We demonstrated that the sol-gel process enabled the encapsulation of stem cells. These results are described in the **fourth chapter**. **[Publication n°3 – Sol-gel synthesis of collagen-inspired peptide hydrogel]**

Finally, in the **fifth chapter**, we focused our efforts on hydrogel shaping. We demonstrated that sol-gel chemistry and extrusion 3D printing could be combined. A colloidal solution of hydrogel precursors was used as a bioink for the 3D printing of grid-patterned scaffolds. **[Publication n°4 – Modular bioink for 3D printing of biocompatible hydrogels: sol-gel polymerization of hybrid peptides and polymers]**

Concluding remarks and perspectives will be found at the end of the manuscript before the experimental section. Applications of the method developed herein for the preparation of biocompatible hydrogels were protected by a patent that is also enclosed in the annex section.

Chapter I.

Hydrogels for

cell encapsulation

State of the art

Chapter I. State of the art: hydrogels for cell encapsulation

I.1. Cell-encapsulating hydrogels

I.1.1. Applications of cell-encapsulating hydrogels

I.1.1.1. 3D cell culture platforms

In vitro culture of adherent cells is classically carried out on flat, rigid 2D tissue culture polystyrene. However, in spite of its extensive use, this environment is far from native three-dimensional cell environment and often induces unnatural cell behavior.¹ Therefore, the development of matrices for 3D cell culture is of interest. Hydrogels suitable for cell encapsulation have become popular as 3D cell culture platforms.² In particular, they can be used as models to study cell behavior. They provide more biologically relevant conclusions than 2D models, allowing reliable predictions for *in vivo* cell behavior.

For example, K. S. Anseth and co-workers engineered a hydrogel containing embryonic stem cell-derived motor neurons to measure the forces and energies involved in neurite extension.³ Recently, S. Pedron *et al.* designed a hydrogel that replicates the native tumor environment enabling the study of glioma cells at molecular and genomic levels.⁴ Cell-encapsulating hydrogels are also useful in drug discovery.⁵ L. A. Gurski *et al.* encapsulated metastatic prostate cancer cells in hyaluronic acid-based hydrogels and demonstrated the efficacy of this 3D system for anti-cancer drug screening.⁶

As a consequence, 3D cell culture platforms based on cell-encapsulating hydrogels can be considered as precious tools for biological research.

I.1.1.2. Cell-based therapies

Applications of injectable cell-laden hydrogels can also cover therapies based on a cell-mediated drug release. Indeed, cells can be delivered *in situ* to secrete a molecule of interest.

This approach is investigated as a treatment for enzyme and hormone deficiencies. For instance, type 1 diabetes is an autoimmune disease in which insulin-producing pancreatic β -cells are destroyed by the immune system. Because insulin is responsible for the regulation of blood glucose levels, the β -cell destruction leads to hyperglycemia that can cause serious damages to the body. The main treatment consists of multiple daily insulin injections to maintain glucose homeostasis. Successful delivery of insulin-producing cells could replace the burden of injections and considerably improve the daily life of patients affected by type 1 diabetes. Therefore, the encapsulation of insulin-producing cells or pancreatic islets in

matrices that allow the diffusion of the secreted insulin while protecting the cells from the immune system is of interest.⁷⁻⁹

Cell-encapsulating hydrogels are also promising for cancer treatment. The 20 kDa C-terminal fragment of collagen XVIII, the endostatin protein, has been identified as an endothelial proliferation inhibitor.¹⁰ It has been proven to be an effective inhibitor of tumor angiogenesis and growth. However, the use of endostatin for cancer therapy faces several problems. In fact, it is difficult to produce the purified biologically active protein and huge quantities of the protein are required for cancer therapy. Once administered, endostatin is rapidly cleared from the blood. Consequently, the encapsulation of cells that have the capacity to continuously release endostatin has been investigated. *In vivo* studies on mice demonstrated that the injection of encapsulated baby hamster kidney-endo (BHK) cells in the close proximity of a tumor significantly inhibited its growth.^{11,12}

Both examples illustrate the importance of cell-laden hydrogels for the development of therapies that involve the continuous release of a therapeutically relevant biomolecule.

I.1.1.3. Tissue engineering applications

Above all, cell-laden hydrogels are of paramount importance in tissue engineering. This area of research aims at producing living tissues for medical purposes.^{13,14} These artificial tissues are intended to be used as tissue grafts to repair or replace damaged biological tissues/organs. They are engineered to be functional *in vivo*. Here a particular focus is placed on hydrogels encapsulating cells. The preparation and applications of cell-free scaffolds intended to be colonized *in vivo* will not be discussed in this manuscript.

Developments in tissue engineering seek to address the overwhelming need for organs and tissues. In France, 21 464 people were waiting for a lifesaving organ transplant in 2015.¹⁵ Only 5 746 of these patients received a transplant. In addition, a successful transplantation implies a heavy follow-up with a lifelong therapeutic treatment. The production of artificial organs from patients' cells would address both the organ donor shortage and the graft rejection issues.

The principle of tissue engineering is to construct biological substitutes from cells taken from the patients (Figure 1). Differentiated cells can be used but stem cells are preferred since they are the "wild cards" of the body. They have the ability to renew themselves ad infinitum and differentiate into any specific cell in the body. Their plasticity makes them a perfect fit for tissue engineering.^{16,17} Stem cells were originally isolated from bone marrow but can now be isolated from a large number of adult tissues. First, they are cultured *in vitro* under conditions maintaining their undifferentiated state to preserve their capacity for self-renewal and pluripotency. Then, they are seeded in a scaffold that will support them and provide signals to guide them towards the development of new functional tissue. Hence, they will differentiate, proliferate and produce the matrix of the artificial tissue. Ultimately, the

engineered tissue will be transplanted to the patient where it is expected to restore biological tissue function.

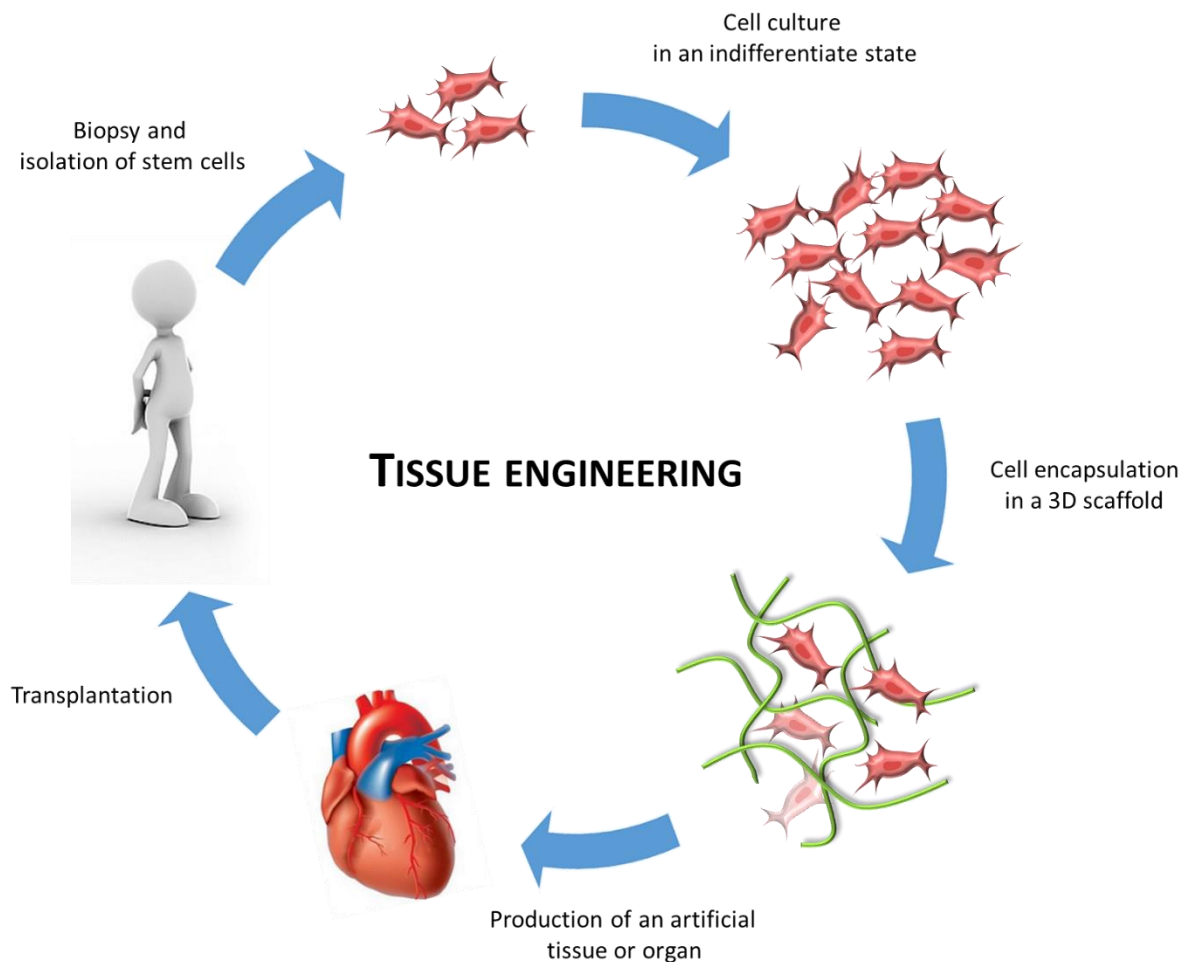


Figure 1. Principle of tissue engineering

Alternatively, cells can be encapsulated in injectable *in situ* gelling hydrogels.^{18–20} In this case, cells are suspended in a precursor solution that forms a cell-laden hydrogel after injection *in vivo*. These hydrogels enable cell delivery at the site of interest for *in situ* regeneration of a tissue. The procedure is minimally invasive compared to surgery. The hydrogel serves as temporary scaffold which provides mechanical support and appropriate signals until a newly tissue is formed by the injected cells. Eventually, the regenerated tissue should be identical to the native healthy tissue in terms of structure and function. This regenerative strategy is investigated for instance for articular cartilage repair.^{21,22}

In both cases, the choice of the biomaterial in which cells are embedded is crucial for tissue development. This material must provide to the cells an environment as similar as possible to their native environment.

As a consequence, whatever the intended application, the development of cell-laden hydrogels requires a comprehensive knowledge of the extracellular matrix (ECM), the native environment of the encapsulated cells.

I.1.2. Native extracellular matrix

In biological tissues, cells are surrounded by a complex and bioactive matrix, the extracellular matrix (ECM). It is both the physical scaffold responsible for tissue 3D structure and an orchestra conductor for cells.^{23–26}

Within the same living organism, the ECM composition varies from tissue to tissue. The main components are proteins, polysaccharides and water. An interstitial fluid is entrapped in a network constituted of hydrated proteoglycans and fibrous proteins (Figure 2). Proteoglycans are made of polysaccharides, such as hyaluronic acid, attached to a core protein. These polysaccharides are called glycosaminoglycans (GAG), they are negatively charged which allows them to sequester water and cations. Proteoglycans are coiled around fibrous proteins such as collagen, fibronectin, elastin and laminin. Collagen is the most abundant fibrous protein in the ECM, its fibers provide tensile strength to the surrounding tissue. All together, these components confer a hydrogel-like consistency to the ECM.

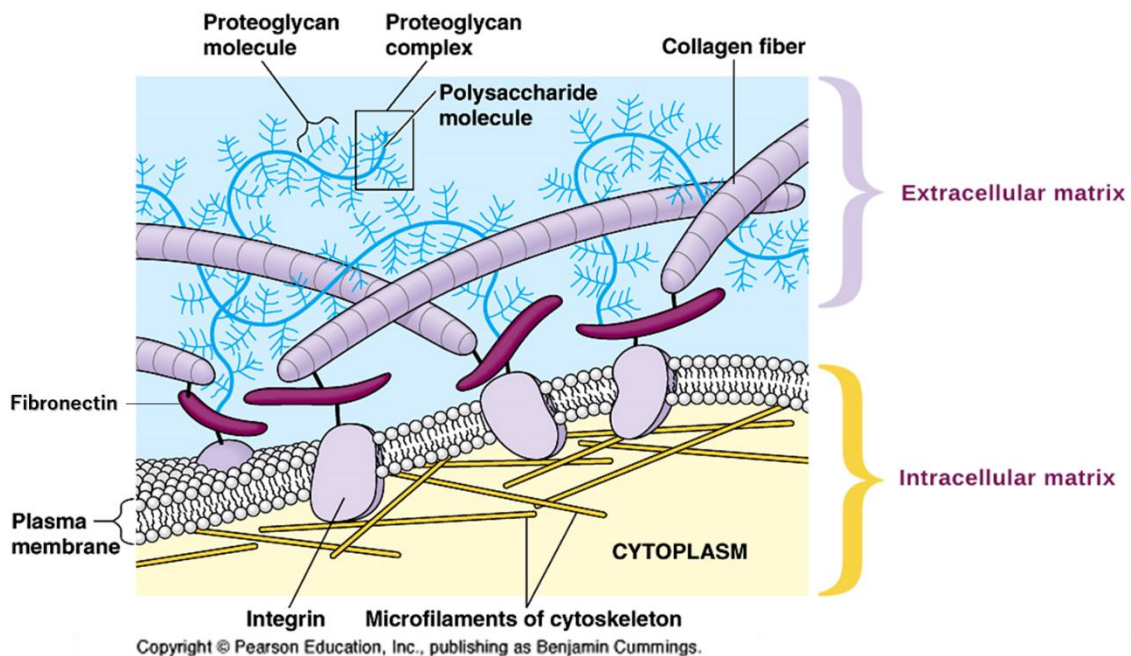


Figure 2. Schematic representation of the extracellular matrix

The role of the ECM is not only to provide mechanical support to the cells but also to regulate their behavior. Indeed, ECM is involved in cell survival, proliferation, migration and differentiation, in other words, it directs cell fate. This matrix holds cells into tissues and maintains cells in a buffered aqueous environment. It enables the diffusion of oxygen, nutrients and metabolic products. It sequesters and delivers growth factors and other biological signaling molecules while controlling the diffusion of cell secreted substances. Bioavailability of signaling factors is controlled spatially and temporally by the establishment of chemical gradients. Consequently, ECM is highly involved in intercellular communication.

In addition, it provides cell-matrix interactions. For instance, fibronectin presents cell adhesion sites to attachment dependent cells. ECM serves as movement track for cell migration. Mechanical signals from ECM also affect cell fate. Matrix rigidity greatly influences cell differentiation. At last, ECM is highly dynamic, it is constantly undergoing remodeling. It is produced by cells and degraded by proteases and matrix metalloproteinases (MMPs) to allow cell migration and proliferation. ECM structure and composition result from a reciprocal relationship with cells.

Considering the importance of ECM to so many cellular processes, it is a challenge to design artificial matrices that recapitulate faithfully the structure and functions of native ECM.

I.1.3. Hydrogels

I.1.3.1. Hydrogels as artificial ECM

Hydrogels are water-swollen three-dimensional polymeric matrices.²⁷ They are made of hydrophilic polymers cross-linked into water-insoluble polymeric networks. This property allows them to retain large amounts of water while maintaining their three-dimensional structure.

Given their high water content (typically $w_{\text{water}} \gg w_{\text{polymer}}$, with w the mass fraction), hydrogels have been investigated as artificial ECM.^{2,28–30} Their elastic properties provide a mechanical environment close to native soft tissues. Their mechanical properties can be tuned by modifying the degree of cross-linking. However, although a high cross-linking density leads to high mechanical strength, it also results in lower swelling capabilities and decreased mesh sizes, which has an impact on biomolecule diffusion and cell migration. Therefore, a subtle balance should be struck between the physical properties of the hydrogel.

Natural ECM components such as collagen and hyaluronic acid have been used to prepare ECM substitutes.³¹ These biopolymers are inherently biocompatible and bioactive. However, because they are extracted from natural sources, they present several drawbacks such as a high cost of production, a weak batch-to-batch reproducibility, potential microbial contamination during the isolation process and risks of immunogenicity.

In contrast, synthetic polymers such as polyethylene glycol (PEG) and poly(vinyl alcohol) (PVA) are easy to produce on a large scale and are well-defined. Their chemical modification is simple. Hydrogels formed entirely from these polymers are highly reproducible and able to maintain cell viability. They are bio-inert, in the sense that they are biocompatible but cannot promote cell behavior. The term permissive hydrogels is used for them, as opposed to promoting hydrogels made of natural polymers.²

Nevertheless, it is possible to confer some bioactivity to permissive hydrogels by functionalizing them.³² The modification of artificial matrices with cell adhesive peptides is very common. Peptide sequences are often derived from ECM proteins.³³ Among them, the

fibronectin-derived Arg-Gly-Asp (RGD) sequence which is a recognition motif for cell integrins is the most frequently used.^{34,35} Other peptide sequences of interest have proven to be useful in designing artificial ECM. K. S. Anseth and co-workers demonstrated that KLER sequence could promote cartilage-specific matrix deposition and organization by binding and stabilizing collagen.³⁶ Growth factors have also been introduced in artificial matrices. For instance, E. D. Phelps *et al.* engineered a system in which vascular endothelial growth factor (VEGF) was sequestered within a hydrogel and delivered to the cells upon proteolytic degradation of the gel.⁸ M. V. Tsurkan *et al.* described a PEG-heparin hydrogel in which heparin serves as reservoir for growth factors.³⁷ The degradability of the network is also a key feature as it allows cell growth and migration leading to the replacement of artificial matrix by natural tissue.^{32,38} Hydrolysable bonds can be introduced in the network providing a time-dependent degradation.³⁹⁻⁴¹ More interestingly, cell-responsive hydrogels can be obtained with enzyme-sensitive peptide cross-linkers, ensuring that the gel degradation will match cell growth. J. Patterson and J. A. Hubell reported hydrogels sensitive to matrix metalloproteinases (MMPs).^{42,43}

Depending on the type of interactions involved in the formation of the matrix, two types of hydrogels can be defined: physical and chemical hydrogels.

I.1.3.2. Physical hydrogels

Physical hydrogels result from the formation of a physical network involving weak interactions such as ionic interactions, hydrogen bonds, π - π stacking, Van der Waals forces or hydrophobic interactions.²⁷ The weakness of the interactions can be counterbalanced by their large number to give rather strong hydrogels.

Natural polymers, like collagen, hyaluronic acid, alginate, chitosan, dextran and fibrin, readily form physical hydrogels. Alginate in particular has been extensively investigated as ECM substitute.⁴⁴ Nonetheless, as already pointed out, biopolymers suffer several drawbacks. They are expensive to produce and often ill-defined. Their properties may vary from batch to batch and are difficult to tune. In addition, they present a risk of contamination with pathogenic substances and they might be immunogenic. Therefore, we will focus on synthetic physical hydrogels.

Physical hydrogels can be obtained from small synthetic molecules, called hydrogelators, that self-assemble in water to form three-dimensional supramolecular networks.⁴⁵ Self-assembling peptides hold a prime position among hydrogelators.⁴⁶⁻⁵⁰ They have been extensively used for drug delivery as many of them exhibit a shear-thinning behavior.⁵¹ Indeed, due to the dynamic nature of the physical interactions, the self-assembled peptide network can be dissociated when shear is applied, leading to a decrease in viscosity that allows injection. When shear is removed, peptides reassemble into hydrogels. This property can be advantageously used for cell delivery. In this case, special attention has to be paid not to damage the cells during pressure application.

Table 1. Some examples of self-assembling peptides used to prepare cell-encapsulating hydrogels

Peptide	Sequence	Design and structure	Hydrogel conc. (wt%)	Encapsulated cells
RADA₁₆ (RAD₁₆-I)	Ac-RADARADARADARADA-NH ₂	Hydrophobic/charged residue alternation, β -sheet structure	0.1-1	neural stem cells, ⁵² umbilical vein endothelial cells, ⁵³ Schwann cells. ⁵⁴
RADA₁₆-IKVAV	Ac-RADARADARADARADAIKVAV-NH ₂	Hydrophobic/charged residue alternation, β -sheet structure	1	neural stem cells. ⁵²
RAD₁₆-II	Ac-RARADADARARADADA-NH ₂	Hydrophobic/charged residue alternation, β -sheet structure	0.1-1	embryonic stem cells, ⁵⁵ microvascular endothelial cells, ⁵⁶ umbilical vein endothelial cells. ⁵³
KLD-12	Ac-KLDLKLKLDL-NH ₂	Hydrophobic/charged residue alternation, β -sheet structure	0.5-1	chondrocytes, ⁵⁷ umbilical vein endothelial cells. ⁵³
FEFEFKFK	H-FEFEFKFK-OH	Aromatic/charged residue alternation, β -sheet structure	0.5-4	chondrocytes. ⁵⁸
MAX8	H-VKVKVKVKvPPTKVEVKVKV-NH ₂	Hydrophobic/charged residue alternation flanking a β -turn sequence, β -hairpin structure	0.5-0.75	mesenchymal stem cells, ⁵⁹ progenitor osteoblast cells. ⁶⁰
Multidomain peptides	Ac-KKSLSLSLSLSLK-NH ₂ Ac-KSLSLSLRGSLSLKGRGDS-NH ₂	Amphiphilic core flanked by charged regions, sandwich-like β -sheet assembly	1	mesenchymal stem cells, ⁶¹ dental pulp stem cells. ⁶²
Fmoc-F₂	Fmoc-FF-OH	Assembly driven by hydrogen bonding and π - π interactions, β -sheets interlocked by Fmoc π - π stacks	0.22-2.14	chondrocytes, ⁶³⁻⁶⁵ dermal fibroblasts. ^{66,67}

The table 1 summarizes the examples of self-assembled peptide hydrogels discussed below. T.-Y. Cheng *et al.* reported an injectable hydrogel encapsulating neural stem cells for the repair of injured brain tissue. The hydrogel was based on the self-assembly of RADA₁₆, a 16-mer ionic self-complementary peptide. They added a laminin-derived peptide sequence to RADA₁₆ peptide to promote stem cell adhesion and differentiation.⁵² RADA₁₆ peptide and RAD₁₆-II peptide, whose sequence is closely related, were also used by R. T. Lee and co-workers for the regeneration of vascularized tissues,^{55,56} and by F. Moradi *et al.* for spinal cord regeneration.⁵⁴ Another ionic self-complementary peptide, KLD-12, was used to prepare chondrocyte-encapsulating hydrogels for cartilage tissue repair.⁵⁷ As another example of hydrogel precursor for chondrocyte encapsulation, we can mention FEFKFK.⁵⁸ β -hairpin self-assembling peptides were also designed. MAX8 peptide is made of an alternation of hydrophilic and hydrophobic residues flanking a β -turn sequence. In presence of DMEM, a common cell culture media, it adopts a β -hairpin conformation and undergoes self-assembly into a β -sheet-rich injectable hydrogel. It was shown to be suitable for cell-encapsulation.^{59,60} K. M. Galler *et al.* worked with amphiphilic peptides in which cationic lysine residues flanked a hydrophobic sequence. They showed that RGD cell adhesive and MMP-cleavable sequences could be added to the initial gelator sequence to improve its biocompatibility.⁶¹ Their system was applied to dental pulp engineering.⁶² In an original way, Ulijn group focused on Fmoc-protected dipeptides, with a particular interest for the PhePhe dipeptide.⁶³⁻⁶⁵ Fmoc-FF-OH self-assembles through hydrogen-bonding and π - π stacking. They demonstrated that Fmoc-FF-OH and Fmoc-RGD-OH could be used in combination to yield bioactive hydrogels.^{66,67} At last, some groups investigated self-assembled peptide hydrogels as 3D cell culture platforms,⁶⁸ in particular as 3D cancer models.^{69,70}

These examples demonstrate the potential of self-assembled peptide hydrogels for tissue engineering and other applications of cell-encapsulating hydrogels. Besides their injectability that has already been highlighted, one of the main advantages of physical hydrogels is that no reactive functional group is required for cross-linking and establishment of the tridimensional network. Thus, the synthesis of precursors is straightforward (no further modification with reactive groups is required) and cross-reactions *in vivo* are avoided. In addition, peptide synthesis is well-mastered and generates well-defined products that can be isolated and purified. However, physical hydrogels often suffer from poor mechanical properties owing to the weak interactions involved in their formation. While shear-thinning behavior is an asset for hydrogel injection, it prevents applications, such as articular cartilage repair, in which the hydrogel will be subjected to shear forces. Overall, the mechanical properties of physical hydrogels are difficult to tune. It is impossible to play with the cross-linking density. The concentration in precursors can be increased to get stiffer gels but it may create large osmotic gradients *in vivo*. It is also difficult to control the degradability of physical hydrogels. When associations between the molecules are weak, the local concentration can be reduced over time by dilution with physiological fluids which leads to loss of integrity. When interactions are strong, the backbone of the gelator itself has to be degradable. At last, although a few examples described above demonstrated that functionalization with active sequences such as

RGD motives is feasible, it is challenging to add functionalities to a system without disrupting its capacity to gelate. Consequently, although self-assembled peptide hydrogels have been extensively used for drug delivery with excellent results, they are not as widespread as chemical hydrogels regarding tissue engineering applications.

I.1.3.3. Chemical hydrogels

Chemical hydrogels are cross-linked through covalent bonds. Covalent cross-linking provides improved mechanical properties and stability compared to physical cross-linking. A wide range of precursors, displaying reactive functions, are available to prepare chemical hydrogels *via* different methods. The strengths and weaknesses of each method will be highlighted in the next section.

I.2. Cross-linking strategies

Herein, we will discuss the cross-linking methods leading to a covalent hydrogel. We chose to limit the scope of the discussion to the methods compatible with live cell encapsulation. The main parameters for cell-friendly embedment are summarized below.

- Organic solvents have to be avoided.
- The gelation has to proceed in an aqueous solution isotonic to cytosol.
- The pH must be kept between 7.2 and 7.5.
- Phosphate-buffered saline or, even better, cell culture media are well-suited.
- The temperature has to be maintained between room temperature and 37°C. Ideally, the *in vitro* gelation process is conducted at 37°C in a humidified 5% CO₂ atmosphere.⁷¹

These requirements have a strong impact on the hydrogel precursors and the cross-linking chemistries. First of all, cross-linking proceeds in aqueous conditions. As a consequence, hydrogel precursors have to be water-soluble. For a homogeneous cell distribution within the hydrogel, the precursor solution has to turn rather quickly into a solid hydrogel to avoid sedimentation of the cells after their introduction. Precursors, catalysts, initiators, cofactors, additional reagents, etc. must be cytocompatible and the cross-linking reaction must not release cytotoxic by-products. This is the reason why macromolecular precursors are often preferred since most of the time they are less cytotoxic than small molecules. The cytotoxicity is often related to a lack of selectivity of the reactive functions displayed by the precursors. For example, aldehydes and epoxides may react with biomolecules from live cells, thus interfering with native biological processes. Indeed small bifunctional molecules such as epichlorohydrin,⁷² glyoxal⁷³ and 1,4-butanediol diglycidyl ether⁷⁴ have been used to cross-link polymers, but presented some cytotoxicity because of their lack of selectivity. The 'bio-

orthogonality', which regarding materials is the selectivity of precursors for network formation *versus* reaction with biological molecules, is an important issue for the design of convenient hydrogels.⁷⁵ Therefore, we will report herein only bioorthogonal cross-linking strategies. Noteworthy, recent reviews summarizing advances in the cross-linking chemistries are available.^{76,77} They are focused on commonly used PEG-based hydrogels.

1.2.1. Free-radical photopolymerization

Light-activated cross-linking is of particular interest as it offers spatial and temporal control of the hydrogel formation. Indeed, in this case, the gelation is triggered by a light beam that can be applied with high precision at precise moments on the precursor solution. Free-radical photopolymerization is the most common method to prepare hydrogels under physiological conditions.^{78,79} Multifunctional macromolecular precursors can undergo chain-growth or step-growth polymerization depending on the chosen functionalizing moieties.

1.2.1.1. Chain-growth photopolymerization

Vinyl-functionalized macromolecules are subjected to chain-growth polymerization. This process requires a photoinitiator. Upon irradiation with the appropriate wavelength, the photoinitiator absorbs the light energy and dissociates into free-radical reactive species (Figure 3). These reactive species add to vinyl groups on macromolecular precursors by opening homolytically the π -bond and forming new free radical species. Hence, the reactive center is propagated as covalent bonds are formed between precursors resulting in the formation of a polymer network within seconds to minutes.

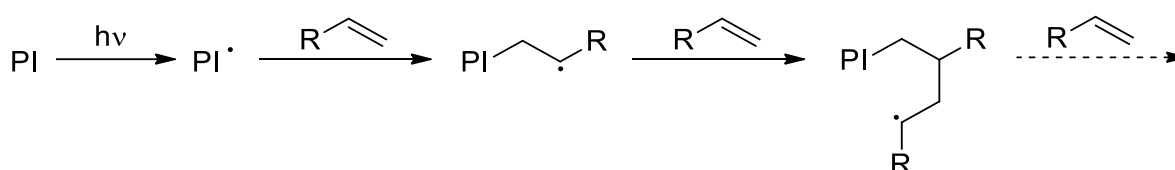


Figure 3. Chain-growth photopolymerization mechanism. PI: photoinitiator, hv: light source.

Most of the time, ultra-violet light is chosen to trigger the polymerization, 365 nm being the most common wavelength.⁸⁰ Among the different vinyl groups introduced on precursors (Figure 4), acrylates are the most popular. They can be introduced on hydroxyl groups using acryloyl chloride in presence of a base, trimethylamine for instance.^{81,82} PEG-diacrylates (PEGDA) are commercially available. F. Yang *et al.* investigated osteogenesis of bone marrow stromal cells in a 3D environment formed by photopolymerization of PEGDA and a PEG acrylate functionalized with peptide ligands promoting cell adhesion.³⁵ S. R. Peyton *et al.* used the same strategy to study smooth muscle cell behavior in a 3D model system.³³ Methacrylate groups are also suitable for hydrogel photopolymerization. Weber *et al.* encapsulated murine pancreatic islets in dimethacrylated PEG (PEGDM) hydrogels for insulin-producing cell delivery

applications.⁸³ PEGDM can be mixed with other synthetic or natural methacrylated polymers. S. J. Bryant *et al.* designed degradable hydrogels by copolymerizing PEG with PLA.⁸⁴ The same group also prepared hydrogels from PVA and a natural polymer, chondroitin sulfate. Both polymers were functionalized with methacrylate by reacting their hydroxy groups with 2-isocyanatoethylmethacrylate and methacrylic anhydride respectively.⁸⁵ Methacrylated alginate⁸⁶ and hyaluronic acid⁸⁷ were also described. Diacrylamide groups are less common than (meth)acrylates. However, PEG diacrylamide conjugated to collagen enabled the preparation of a hydrogel in which the co-culture of endothelial cells and fibroblasts led to the formation of capillary vessel-like networks.⁸⁸

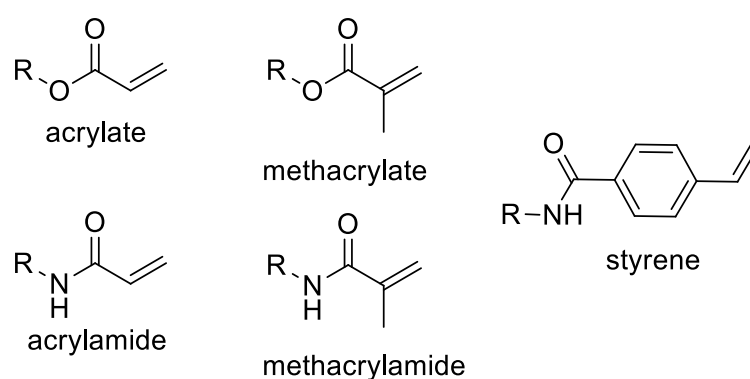
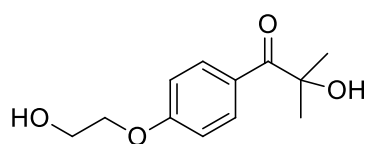


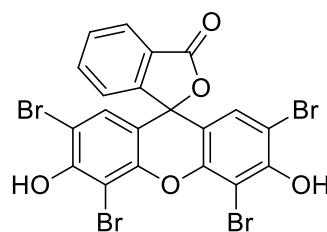
Figure 4. Chemical structures of vinyl groups used for preparation of hydrogels by chain-growth photopolymerization.

Although this chain-growth photopolymerization cross-linking strategy was successfully applied to the preparation of numerous cell-laden hydrogels, careful consideration must be taken in choosing the photoinitiating conditions. On the one hand, cytotoxicity of several photoinitiators was investigated.^{80,89,90} Cell viability in their presence was found to be dependent of cell types and cell division rate. Irgacure 2959 (2-hydroxy-1-(4-(2-hydroxyethoxy)phenyl)-2-methylpropan-1-one, Figure 5) proved to be well-tolerated by a broad range of mammalian cells and is the most frequently-used photoinitiator for cell encapsulation.^{41,81,84} Nevertheless, Fedorovitch *et al.* observed adverse effects of Irgacure 2959-initiated photopolymerization on MSC monolayers.⁹¹ Likewise, A. D. Rouillard *et al.* demonstrated that Irgacure 2959-photogenerated radical species were cytotoxic and led to cell viabilities below 70%.⁸⁶



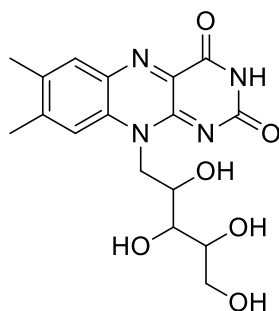
Irgacure 2959

$\lambda_{\max} = 280 \text{ nm}$



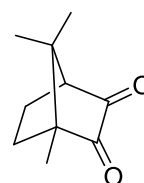
Eosin Y

$\lambda_{\max} = 524 \text{ nm}$



Riboflavin

$\lambda_{\max} = 450 \text{ nm}$



Camphorquinone

$\lambda_{\max} = 468 \text{ nm}$

Figure 5. Structures of some photoinitiators used for hydrogel preparation by photopolymerization.

On the other hand, UV photons carry more energy than visible-light photons, this is why UV wavelengths were selected in the first place for efficient photoactivation. Yet, it is well-known that UV exposure can damage cells.^{91,92} As a consequence, significant efforts have been made in developing visible light-initiated systems.⁹³ Most of the time, visible blue light was chosen. Eosin Y (Figure 5) and triethanolamine were used several times as photoinitiator and co-initiator respectively, sometimes with N-vinylpyrrolidone (NVP) to accelerate the gelation.^{94,95} For instance, this initiator solution allowed the visible-light cross-linking of collagen methacrylamide.⁹⁶ Methacrylated glycol chitosan, obtained by reacting commercially available glycol chitosan with glycidyl methacrylate, was photocrosslinked at 400-500 nm with riboflavin photoinitiator.^{97,98} A. Hoshikawa *et al.* described the photopolymerization of styrene-modified gelatin with camphorquinone photoinitiator.⁹⁹

Nevertheless, cells can be damaged even when visible light is used to initiate the polymerization process. Indeed, during the chain-growth polymerization, molecular oxygen acts as a radical scavenger leading to the formation of reactive oxygen species (ROS). ROS are known to generate oxidative stress in cells.¹⁰⁰ J. J. Roberts and S. J. Bryant showed that chondrocytes exhibited high levels of intracellular ROS immediately after their encapsulation in a PEGDA hydrogel.¹⁰¹ According to these authors, step-growth polymerization should be preferred since this mechanism consumes ROS.

I.2.1.2. Step-growth photopolymerization

Step-growth photopolymerization requires two functional groups, a vinyl and a thiol. Thus, it is often referred to as thiol-ene photopolymerization.¹⁰² The process can be initiated under conditions similar to chain-growth photopolymerization conditions (UV or visible light, same photoinitiators). Upon irradiation, the photoinitiator decomposes into free-radical species. A radical abstracts a hydrogen atom from a thiol group to produce a thiyl radical that reacts with a double bond (Figure 6). The resulting alkane radical abstracts a hydrogen atom from another thiol group, thus forming a thioether bond and regenerating a thiyl radical. The thiol-ene coupling and the thiyl radical generation occur alternatively in a stoichiometric ratio until one of the precursors is entirely consumed. When precursors are multi-functionalized, a 3D network with thioether linkages is formed.

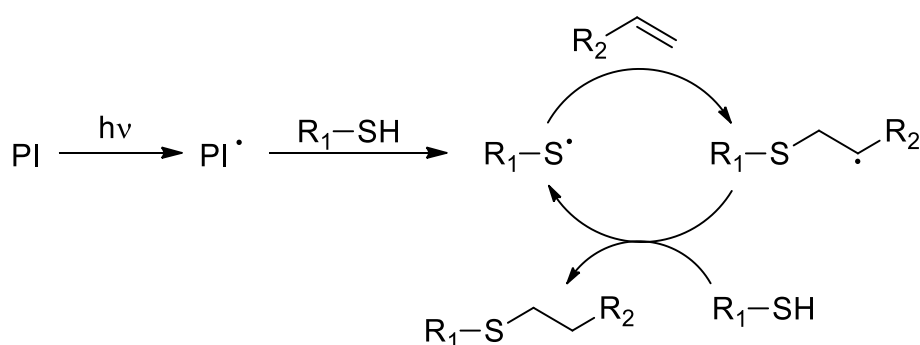


Figure 6. Step-growth photopolymerization mechanism. PI: photoinitiator, hv: light source.

The radical-mediated process can be propagated by ROS which results in low ROS level in the hydrogel. As a consequence, step-growth polymerization was found to be cell-friendlier than chain-growth mechanism.^{101,103} In addition, PEG hydrogels formed by step-growth mechanisms featured superior physical properties compared to PEG hydrogels obtained by chain-growth mechanism. The resulting network was more homogeneous and had a higher functional group conversion.¹⁰³

When (meth)acrylates are chosen as vinyl moieties for thiol-ene photopolymerization, the step-growth mechanism is not guaranteed anymore and a mixed-mode photopolymerization can occur. In this case, the free-radical species formed by irradiation of the photoinitiator can react both with the thiol and (meth)acrylate groups leading to a combination of step and chain-growth polymerization. After studying the formation of thiol-acrylate networks through mixed-mode photopolymerization and investigating the mechanical properties and degradation behavior of resulting hydrogels,¹⁰⁴ K. S. Anseth and co-workers applied this strategy to the encapsulation of human mesenchymal stem cells (hMSCs).¹⁰⁵ The hydrogel was obtained by mixed-mode photopolymerization of PEGDA with cell-adhesion peptides containing a cysteine. Y. Hao *et al.* used the same strategy with visible-light irradiation.¹⁰⁶ In another study, these later authors compared the gelation kinetics when using different tetra-functionalized PEG (acrylate, methacrylate, acrylamide and allylether) in a mixed-mode thiol-ene polymerization.¹⁰⁷

To ensure a step-growth mechanism a thiol-norbornene combination can be chosen for thiol-ene photopolymerization.¹⁰⁸ This system was developed by B. D. Fairbanks *et al.*¹⁰⁹ They first described the preparation of a proteolitically degradable hydrogel by step-growth photopolymerization of a norbornene-functionalized 4-arm PEG (Figure 7) and a chymotrypsine-degradable peptide containing two cysteines. The norbornene moieties were introduced on PEG by coupling norbornene acid activated as a symmetrical anhydride. The thiol groups were brought by the side-chains of the cysteines. hMSCs were successfully encapsulated in this hydrogel using Irgacure 2959 (Figure 5) as photoinitiator with irradiation at 352 nm. C.C. Lin reported a similar system with irradiation at 365 nm.¹⁰³ The thiol-norbornene photopolymerization was then adapted for initiation with visible light.^{110,7,111} In this system, homopolymerization between norbornenes does not happen which guarantees a step-growth mechanism.

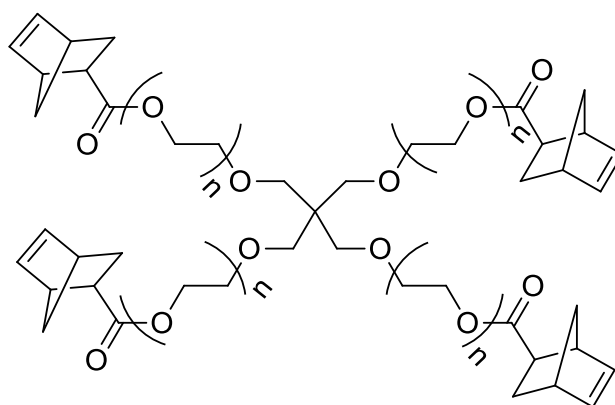


Figure 7. 4-arm PEG norbornene

All together, these examples demonstrate the utmost importance of free-radical photopolymerization for the preparation of cell-laden biomimetic hydrogels. The main advantage of this cross-linking strategy is the spatial and temporal control over gelation kinetics. On the other hand, the main limitation of this method is the adverse effects on encapsulated cells. Whatever the polymerization mechanism (chain or step-growth) and the wavelength used for irradiation, the radical species involved may interact with encapsulated cells and be detrimental to their survival and differentiation.

Besides, the covalent functionalization of hydrogels with bioactive molecules is of interest. It is theoretically possible to mix hydrogels precursors with vinyl-modified or thiol-containing molecules to covalently attach these molecules to the network during its formation by photopolymerization. However, the immobilization efficiencies of pendent monofunctionalized bioactive molecules on the cross-linked network are often rather low and the unreacted free bioactive molecules can lead to undesired biological responses. To overcome this issue, two separate chemistries have to be used: the first one to conjugate the bioactive molecule to multifunctional macromolecular precursor and the second one to cross-link these precursors.

hydride. Acrylated polymers were also used as Michael acceptors to prepare hydrogels.¹²² In particular, chondrocytes and embryonic stem cells were encapsulated in hydrogel formed by cross-linking thiol-functionalized dextran with a tetra-acrylated 4-arm PEG.¹²³ As another example, X. Zheng Shu *et al.* investigated the reaction of thiol-functionalized hyaluronan with PEG diacrylate, dimethacrylate, diacrylamide and dimethacrylamide in order to encapsulate fibroblasts.¹²⁴

Triethanolamine and HEPES (2-[4-(2-hydroxyethyl)piperazin-1-yl]ethanesulfonic acid) are often used as catalysts to facilitate the Michael addition reaction.¹²⁵ At high concentrations, these compounds may be toxic to cells. To overcome this issue, A. J. Garcia *et al.* investigated the reactivity of PEG maleimide, PEG vinyl-sulfone and PEG-acrylate as Michael acceptors. They demonstrated that PEG maleimide afforded the fastest reaction kinetics and required much less triethanolamine to form a gel, resulting in a higher encapsulated cell viability.¹²⁶ They illustrated these results through the encapsulation of pancreatic islets in a hydrogel obtained by Michael addition of a cross-linking degradable peptide containing 2 cysteines on a 4-arm PEG tetra-maleimide (Figure 10). In this example, the Michael addition chemistry was also used to functionalize the hydrogel with a cell adhesion peptide and VEGF.⁸

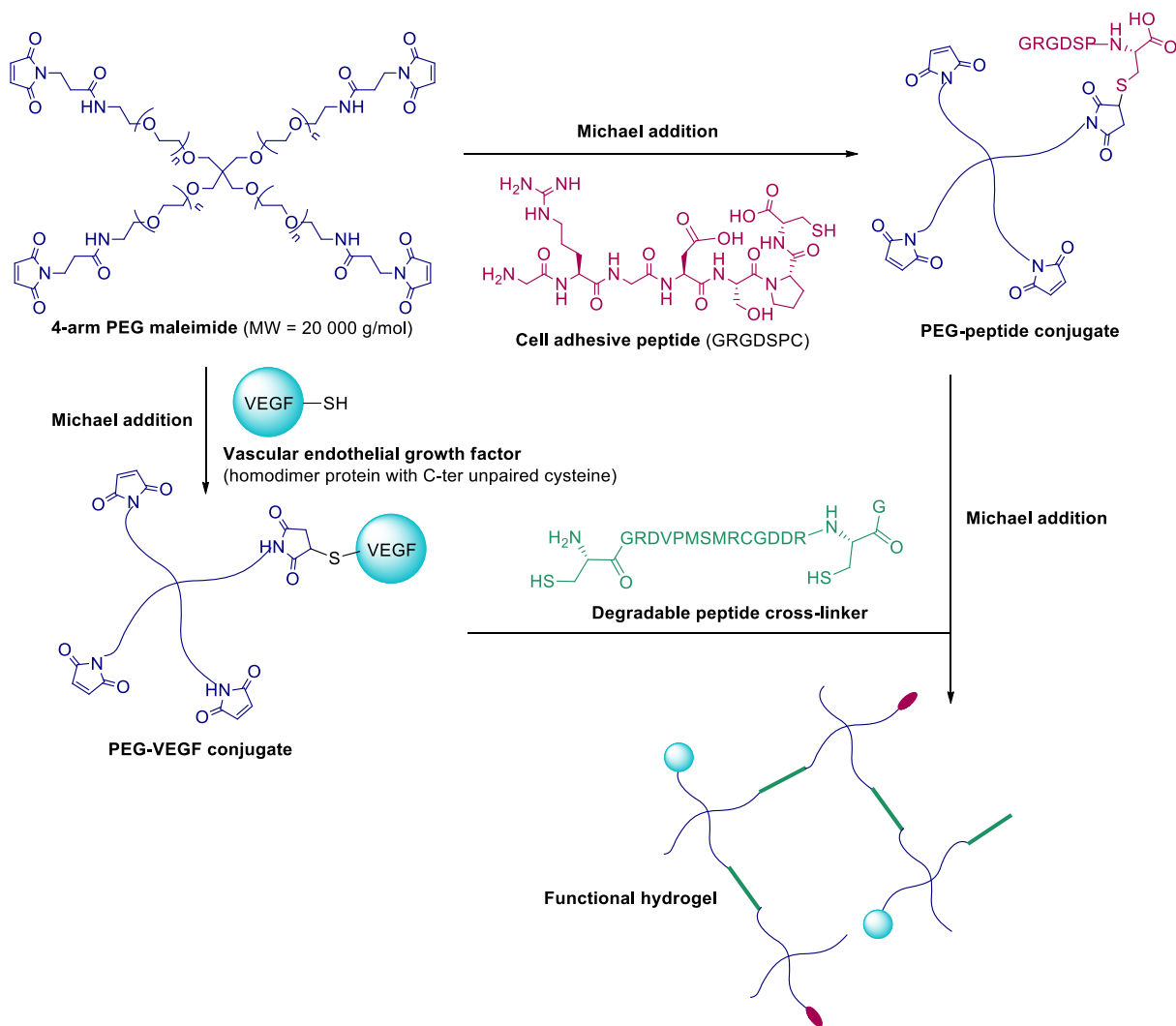


Figure 10. Example of a functional hydrogel prepared by Michael addition⁸

A. D. Baldwin and K. L. Kiick showed that the succinimide thioether linkage resulting from the Michael addition of thiols to maleimides could undergo retro and exchange reactions at physiological pH and temperature.¹²⁷ It is possible to stabilize the thioether linkage by ring-opening the succinimide. Alternatively, the authors proposed to take advantage of these properties to control the release of a drug or to tune the degradability of the hydrogel.¹²⁸

Although the thiol-Michael addition is attractive for the design of biomimetic hydrogels, a limitation of this strategy could arise from the use of thiol-functionalized molecules for *in vivo* gelation. Indeed, thiols are naturally occurring chemical groups. Thus, their administration *in vivo* could lead to undesired cross-reactivity, oxidation or metabolism.

1.2.2.2. Azide-alkyne cycloaddition

Cycloaddition of monosubstituted alkynes and azides gives 1,2,3-triazoles. While the thermal Huisgen 1,3-dipolar cycloaddition often produces a mixture of two regioisomers, the

copper(I)-catalyzed alkyne-azide cycloaddition (CuAAC) gives selectively 1,4-disubstituted regioisomers (Figure 11).¹²⁹

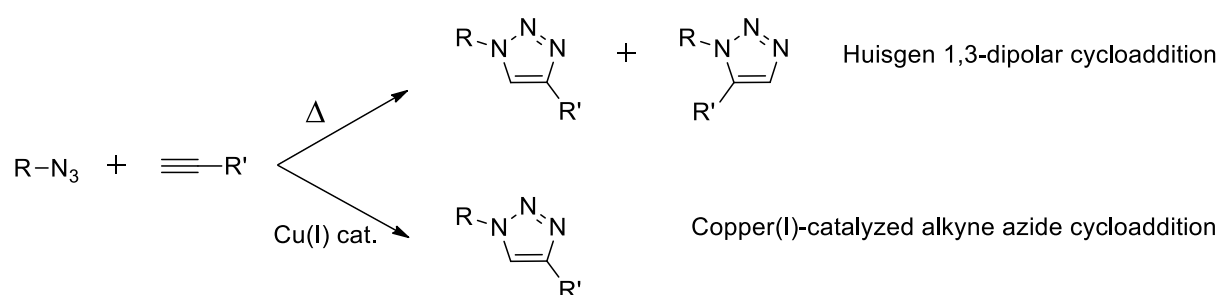


Figure 11. Alkyne-azide cycloadditions yielding 1,2,3-triazoles

This reaction can proceed under physiological conditions and is bioorthogonal since it involves two mutual reactive groups, azides and alkynes, which are not found naturally in living cells. Cu(I) species can be used directly to catalyze the reaction. However, most of the time, Cu(I) active catalyst is generated *in situ* from Cu(II) salts using a reducing agent such as sodium ascorbate. Alternatively, B. J. Adzima *et al.* demonstrated that Cu(II) could be photochemically reduced to Cu(I), affording spatial and temporal control over CuAAC-based gels.¹³⁰ In contrast to the concerted Huisgen cycloaddition mechanism, CuAAC proceeds through a stepwise mechanism (Figure 12).¹³¹ It begins with the formation of a copper acetylide. Then, the azide binds to the copper acetylide and a six-membered copper(III) metallacycle forms. Ring contraction to a triazolyl-copper derivative and protonolysis yield the 1,4-disubstituted 1,2,3-triazole product.

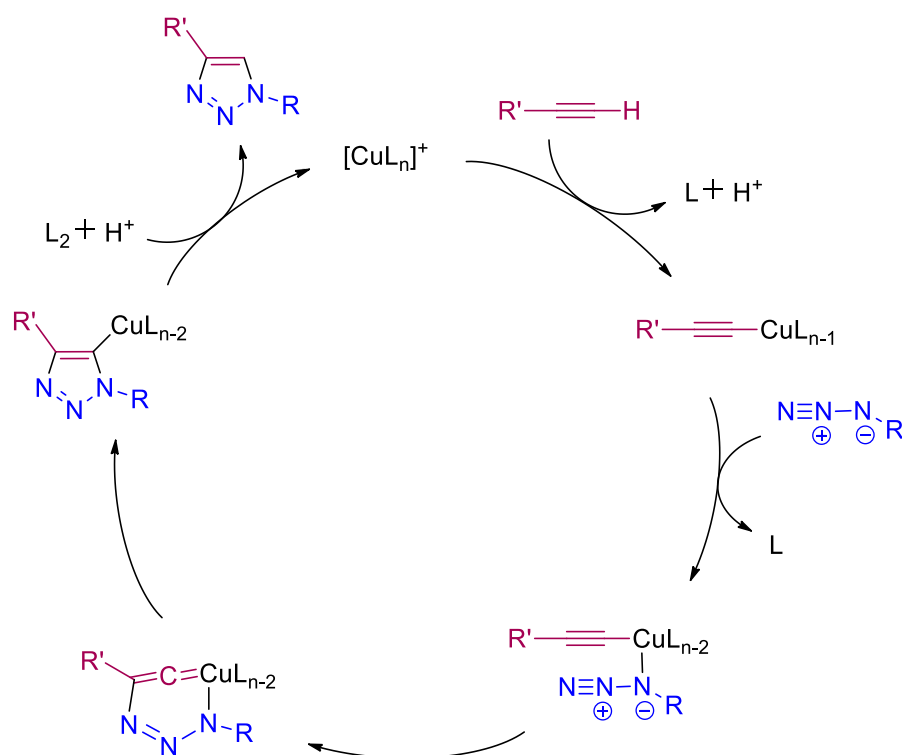


Figure 12. Proposed mechanism for the Copper(I)-catalyzed alkyne-azide cycloaddition.¹³¹
L: ligand, H₂O for example.

D. A. Ossipov and J. Hilborn were the first to apply the CuAAC to the preparation of hydrogels using alkyne and azide-functionalized PVA and PEG.¹³² Alkyne and azide groups were introduced on polymers by reaction with propargylamine derivatives and 2-azidoethylamine or sodium azide respectively. Several hydrogels were prepared with the CuAAC strategy,^{133–137} but only V. Crescenzi *et al.* reported the encapsulation of cells in a CuAAC cross-linked hyaluronan hydrogel.¹³⁸ Indeed, the major limitation of CuAAC strategy is the cytotoxicity of copper ions and their ability to generate ROS *in vivo*.¹³⁹

To avoid the use of toxic copper ions, an alternative metal-free approach was developed in which ring strain was used to promote the azide-alkyne cycloaddition.¹⁴⁰ The reaction between a strained cyclooctyne and an azide, called strain-promoted alkyne-azide cycloaddition (SPAAC), proceeds under physiological conditions without additional reagent (Figure 13).

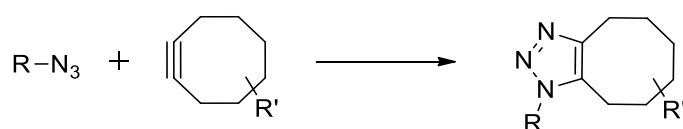


Figure 13. Strain-promoted azide alkyne cycloaddition (SPAAC) between an azide and a cyclooctyne.

SPAAC has been successfully applied to the preparation of injectable hydrogels¹⁴¹ and cell-encapsulating hydrogels. C. L DeForest and K. S. Anseth have worked extensively on SPAAC cross-linking.^{142–147} In their system, gelation was achieved by a SPAAC reaction between a cyclooctyne-functionalized 4-arm PEG and a bis(azide)-functionalized peptide,^{144,145,147} or

alternatively between a 4-arm PEG azide and a cyclooctyne-functionalized peptide.^{142,143} For most of their studies,^{142–145} C. L. Deforest and co-workers chose a gem-difluoro cyclooctyne (DIFO, Figure 14) since the presence of strong electron withdrawing fluorines enhances the SPAAC kinetics and affords a faster gelation.¹⁴⁸ Dibenzylcyclooctyne-functionalized PEG were also reported for hydrogel preparation allowing for cell encapsulation.^{149,150,146}

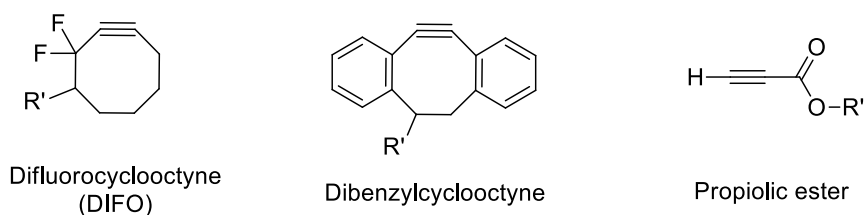


Figure 14. Structures of activated yne groups used for metal-free azide-alkyne cycloaddition

The main limitation of the SPAAC cross-linking strategy comes from the syntheses of cyclooctyne derivatives that involve over 10 steps with a low overall yield. Recently, V. X. Truong *et al.* overcame this issue by taking advantage of the reaction of azides with propiolic esters (Figure 14).¹⁵¹ In propiolic esters, the triple bond is activated by the neighboring electron-withdrawing ester group. The electron-deficiency of the alkyne allows the cycloaddition to proceed without catalyst. V. X. Truong *et al.* demonstrated that a cell-laden hydrogel could be obtained from 3-arm PEG propiolate and azide-functionalized chitosan.¹⁵² Proceeding under physiological conditions between two functions that are not found in the biomolecules of living organisms without any additional reagent, the cycloaddition between azides and propiolic esters appears as a promising tool for biomimetic hydrogel preparation.

1.2.2.3. Diels-Alder cycloaddition

The Diels-Alder reaction (DA) refers to a [4+2] cycloaddition of a conjugated diene to a dienophile (Figure 15). Ideally, it occurs between an electron-rich diene and an electron-deficient double bond. It was first reported in 1928 by Otto Diels and Kirk Alder.¹⁵³ The reaction is spontaneous under physiological conditions. Neither catalyst nor additional reagent is needed and no by-product is formed. It proceeds through a concerted mechanism and the reaction rate is advantageously enhanced in water compared to organic solvents.^{154,155}

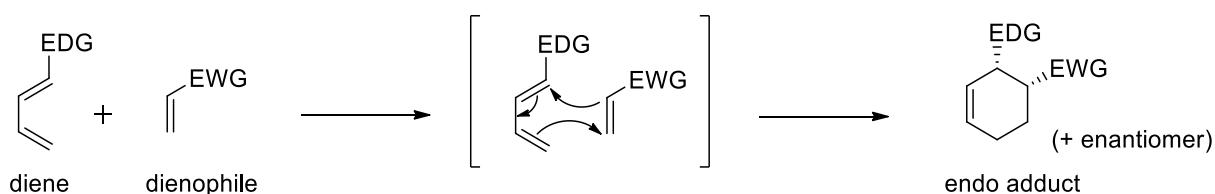


Figure 15. Diels-Alder reaction. EDG: Electron-donating group, EWG: Electron-withdrawing group.

Furan and maleimide are the most commonly used diene and dienophile for the preparation of Diels-Alder cross-linked hydrogels (Figure 16).¹⁵⁶⁻¹⁶² For instance, Yu et al. functionalized hyaluronic acid (HA) with furylamine after activation of HA carboxyl groups with (4,6-dimethoxy-1,3,5-triazin-2-yl)-4-methylmorpholiniumchloride (DMTMM). The resulting HA-furan and commercially available bis(maleimide)-PEG underwent Diels-Alder reaction in DPBS. Murine chondrocytic cells were successfully encapsulated during the process.¹⁶³

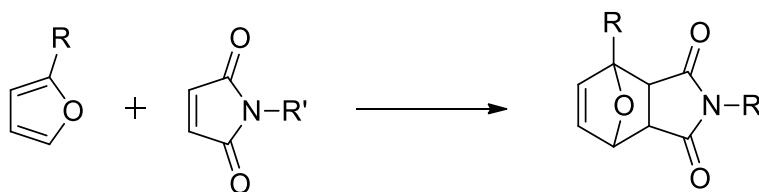


Figure 16. Diels-Alder reaction between furane and maleimide moieties

Furthermore, it has been shown that the Diels-Alder adducts were reversible and that the equilibrium could be shifted towards the reverse Diels-Alder reaction under physiological conditions.¹⁶⁴ This reversibility was advantageously used to modulate the degradation of the hydrogels,¹⁶⁵ to promote the controlled release of a drug^{166,167} or to prepare self-healing hydrogels.¹⁶⁸

The click Diels-Alder reaction with its reversibility seems attractive for the preparation of engineered biocompatible hydrogels. Yet, very few authors reported direct encapsulation of cells in the gels using the Diels-Alder strategy. This may be attributed to rather long gelation time (> 50 min)¹⁶³. Besides, another limitation could arise from the reactivity of maleimide towards thiol-containing biomolecules *in vivo*, undergoing Michael-type 1,4-addition yielding thioether ligation product.

Noteworthy, a second type of Diels-Alder cycloaddition was investigated as a coupling tool: the inverse electron demand Diels-Alder reaction.^{169,170} This reaction involves an electron deficient diene and an electron rich dienophile to yield a formal [4+2] Diels-Alder adduct (Figure 17). 1,2,4,5 tetrazines are the most popular diene for this reaction. In presence of strained dienophiles such as norbornene or trans-cyclooctene, they undergo an inverse electron demand hetero-Diels-Alder reaction, instantly followed by a retro Diels-Alder reaction releasing nitrogen (Figure 18).

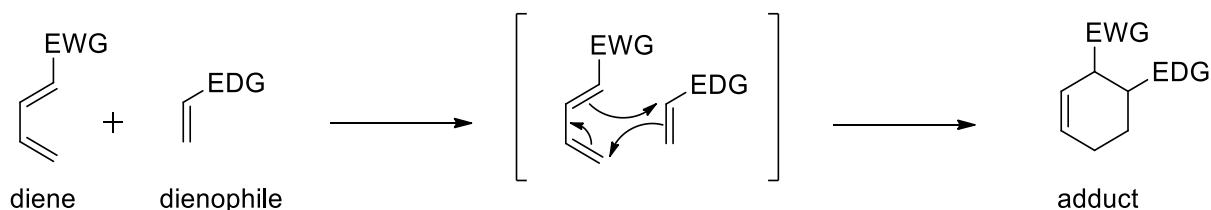


Figure 17. Inverse electron demand Diels-Alder reaction. EDG: Electron-donating group, EWG: Electron-withdrawing group.

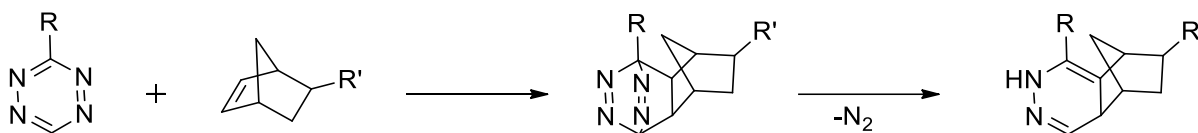


Figure 18. Tetrazine-norbornene inverse electron demand hetero Diels-Alder-retro-Diels-Alder cascade.

K. S. Anseth and co-workers applied the inverse electron demand Diels-Alder reaction to the preparation of cell-encapsulating hydrogels. The hydrogel formed within minutes from a multi-arm PEG tetrazine and a cell degradable dinorbornene cross-linker peptide. When functionalized with a norbornene-bearing cell adhesion peptide, these hydrogels allowed the encapsulation of hMSC with high viability.¹⁷¹ As another example, H. Zhang *et al.* encapsulated prostate cancer LNCaP cells in hydrogel microspheres by reacting tetrazine-modified hyaluronic acid with a bis-*trans*-cyclooctene cross-linker.¹⁷²

1.2.2.4. Native chemical ligation

Native chemical ligation was initially developed for polypeptide and protein syntheses.¹⁷³ This method allows the coupling of two unprotected peptide sequences through the formation of a peptide bond. The reaction occurs between a C-terminal thioester peptide and an N-terminal cysteine residue from another peptide. The first step is a reversible, chemoselective and regioselective transthioesterification (Figure 19). The thiol side-chain of the cysteine residue attacks the thioester to form a thioester intermediate. Then, an intramolecular S→N acyl shift results in the formation of a 'native' amide bond.

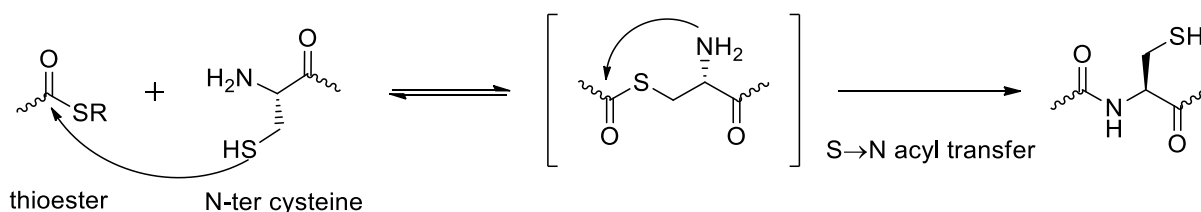


Figure 19. Native chemical ligation

P. B. Messersmith and co-workers were the first to describe hydrogels cross-linked by NCL.¹⁷⁴ They prepared thioester-terminated PEG by coupling ethyl 3-mercaptopropionate succinic acid onto PEG amine. Cysteine-terminated PEGs were obtained by coupling Boc-Cys(Trt)-OH or the dipeptide Boc-Cys(Trt)-AA-OH onto PEG amine followed by Boc removal in acidic conditions. Later on, they reported encapsulation of pancreatic islets and stem cells in these PEG-based hydrogels.^{175,176} Noteworthy, NCL ligation has also been used to chemically cross-link physical hydrogels.¹⁷⁷

The oxo-ester mediated chemical ligation (OMNCL) was proposed as a variant of the NCL reaction, in which thioesters are replaced by activated oxo-esters such as *para*-nitrophenyl ester.¹⁷⁸ P. B. Messersmith and colleagues applied this reaction to the cross-linking of hydrogels.¹⁷⁹ They successfully encapsulated cells in an OMNCL cross-linked hydrogel. The

hydrogel network resulted from the amide bond formation between 8-arm PEG functionalized with N-hydroxysuccinimide oxo-esters and cysteines via an OMNCL reaction. However, due to the reactivity of the *para*-nitrophenyl ester, side products generated by direct nucleophilic addition of primary amino groups (Lysine side chains, protein N terminus) are highly probable.

NCL is still under investigation as cross-linking method. The hydrolytic instability of thioesters may be a limitation for its applications. In addition, the use of free sulfhydryl cysteine residues may require the presence of reducing agents to prevent the formation of disulfide bonds. It may also lead to cross-reactions *in vivo* with cysteine-containing proteins which are commonly present in the cell membrane. And last but not least, special attention has to be paid to the thiol leaving group that could generate adverse biological effects.

1.2.2.5. Imine, hydrazone and oxime formation

Imines, hydrazones, acylhydrazones and oximes are formed through the reversible reaction of a carbonyl group (an aldehyde or a ketone) with an amino group (a primary amine, a hydrazine, a hydrazide or a hydroxylamine respectively) (Figure 20). These reactions expand the toolbox of cross-linking strategies. Most of the time, aldehydes are chosen as carbonyl groups because of their higher reactivity towards nucleophiles compared to ketone.

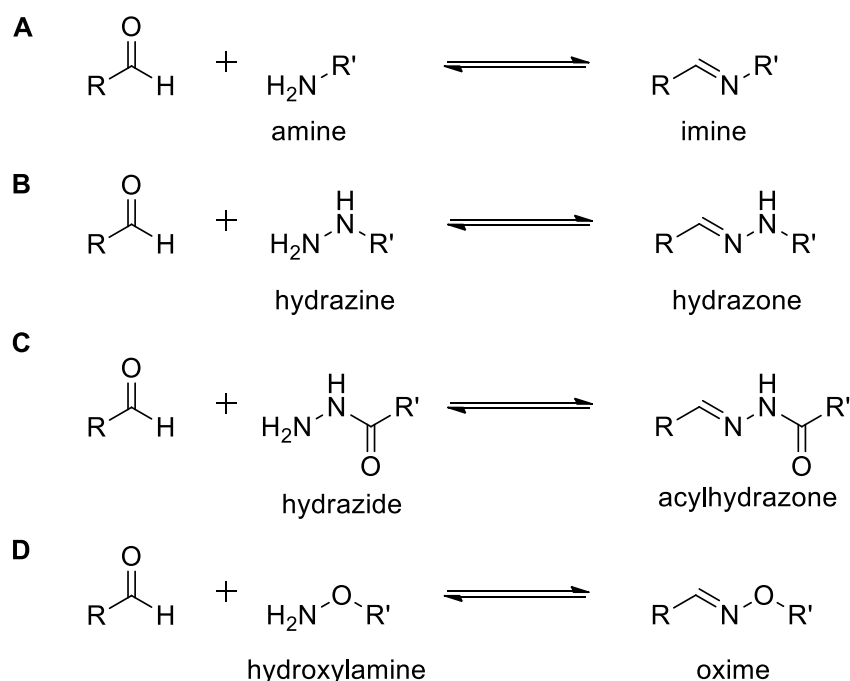


Figure 20. Reactions of a aldehyde with a primary amine, a hydrazine, a hydrazide and a O-substituted hydroxylamine to form an imine, a hydrazone, an acylhydrazone and an oxime

Hydrogel preparation through imine formation, also known as Schiff's base formation, is limited by the low hydrolytic stability of imine linkages. Nevertheless, it was investigated by several groups.^{180–188} In particular, H. Tan *et al.* developed an imine cross-linked hydrogel for cartilage tissue engineering. The hydrogel was obtained from modified chitosan and aldehyde

hyaluronic acid.¹⁸⁹ L. Weng *et al.* described *in situ* gelable hydrogels by imine formation between aldehyde groups from oxidized dextran and amino groups from N-carboxyethyl chitosan.¹⁹⁰ Most of the time, imine cross-linked hydrogels involve aldehyde groups from an oxidized polysaccharide since such polysaccharides are easy to access. But synthetic aldehyde derivatives can also be used. For instance, B. Yang *et al.* reported an injectable cell therapy carrier hydrogel by cross-linking glycol chitosan with a bis(formyl)PEG.¹⁹¹

Unfortunately, this strategy is not properly biorthogonal. Indeed, the nucleophile used is a primary amine which is, as already stated in this manuscript, commonly found in proteins (Lysine side chains and N terminus). Thus, the use of more potent nucleophiles at physiological pH (hydrazines, hydrazides, *O*-substituted hydroxylamines) seems more attractive to increase the selectivity of the reaction and minimize biological material-reagent unwanted side reactions.

(Acyl)hydrazone bonds exhibit a higher hydrolytic stability than imines and thus afford a hydrogel degradation rate more compatible with drug delivery and tissue engineering applications.¹⁹² Hydrazone and acylhydrazone cross-linking has been widely used for injectable hydrogel preparation.^{193–200} As far as 3D culture systems are concerned, D. D. McKinnon *et al.* presented a hydrogel to 3D culture mouse myoblasts made from hydrazine and aldehyde-modified multi-arm PEGs in combination with a aldehyde-functionalized cell adhesion peptide.²⁰¹ Then, they showed how this hydrogel could be used to study the biophysical forces involved in neurite extension.³ Following the work of D. A. Ossipov *et al.*,²⁰² P. J. Martens and colleagues reported cell encapsulation in acylhydrazone cross-linked PVA or PVA-heparin hydrogels.^{39,203} L. A. Gurski *et al.* developed a 3D matrix for *in vitro* anti-cancer drug screening and cancer cell motility study. The system consisted of a acylhydrazone cross-linked hyaluronic acid hydrogel encapsulating cancer cells.^{6,204} Many more examples of (acyl)hydrazone cross-linked hydrogels exist.^{205–209} As a last illustration, we can mention the hydrogels developed by J. Dahlmann *et al.* for myocardial tissue engineering. They produced spontaneously contracting bioartificial cardiac tissue by encapsulating neonatal rat heart cells in acylhydrazone cross-linked alginate-HA hydrogels with additional human type I collagen.²¹⁰

Oxime bonds are close relatives to imines and hydrazones but they exhibit a higher hydrolytic stability.²¹¹ They have received little attention as cross-linkages. G. N. Grover *et al.* worked on oxime cross-linked hydrogels.^{212,213} They cross-linked an aminoxy-8arm-PEG with glutaraldehyde in presence of a ketone-containing cell adhesion peptide. Although glutaraldehyde is known to be cytotoxic,^{214,215} they showed that MSC could be encapsulated in this hydrogel with high viability.²¹²

Due to their reversibility, imine, hydrazine, acylhydrazone and, to a lesser extent, oxime bonds are dynamic cross-links. They can provide self-healing properties to materials and enable a controlled degradation.²¹⁶ Aldehyde groups are preferred over ketones for their higher reactivity. However, because of this high reactivity, aldehydes can react *in vivo* with amines from biomolecules and lead to toxicity.

I.2.2.6. Disulfide formation

Disulfide bonds play a key role in protein folding and stability.^{217,218} They result from the oxidation of two thiol groups (Figure 21). Mild oxidizers, such as O₂, are sufficient to drive the oxidative coupling. Thus, cross-linking of thiol-containing polymers can be achieved under physiological conditions with atmospheric oxygen. For instance, G. D. Prestwich and co-workers functionalized hyaluronic acid with dithiobis(propanoic dihydrazide) and dithiobis(butyric dihydrazide).^{219,220} The initial disulfide bonds were reduced with dithiothreitol to give thiolated HA that could turn into a hydrogel upon oxidation of the thiols with air. They demonstrated that encapsulated L929 fibroblasts could proliferate in this disulfide cross-linked HA hydrogel.²²⁰ Chitosan,²²¹ PEG²²² and gellan²²³ have also been modified by thiol moieties and cross-linked into hydrogels. Thiol groups are often introduced via the coupling of a cysteine residue. However, K. E. Swindle-Reilly *et al.* prepared hydrogels from thiolated poly(acrylamide) obtained by copolymerization of acrylamide and bisacryloylcystamine.²²⁴

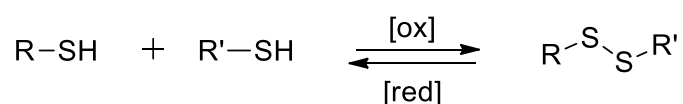


Figure 21. Disulfide bond formation and reduction

Cross-linking of hydrogels through oxidation of free thiols often requires long gelation times. Alternatively, polymers can be cross-linked via thiol-disulfide exchange reaction (Figure 22).²²⁵ This reaction is a nucleophilic substitution between a thiol and an activated disulfide that leads to the formation of a new disulfide and a thiol. Unlike the disulfide bond formation from sulfhydryl derivatives, this strategy ensures the formation of intermolecular linkages, avoiding the risk of intermolecular cyclized side products. S.-Y. Choh *et al.* used pyridyl-disulfide-modified HA and PEG dithiol to encapsulate several cell types in a disulfide cross-linked hydrogel.²²⁶ In this case, cellular effects of thiols released during thiol-disulfide exchange reactions have to be carefully studied.

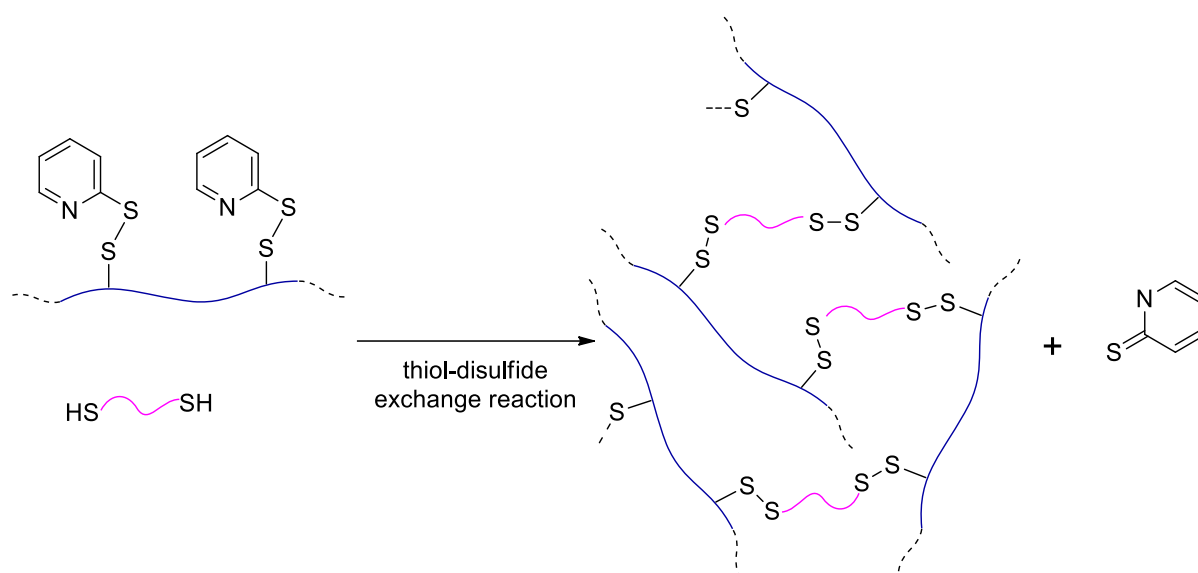


Figure 22. Example of thiol-disulfide exchange reaction used by S.-Y. Choh and co-workers to prepare a hydrogel.²²⁶

J. Lee *et al.* showed that compression or tension applied to PEG hydrogels with disulfide linkages induced disulfide bond rupture. They took advantage of the compression-induced generation of free sulfhydryl groups to functionalize these hydrogels with a maleimide-containing fluorophore through a Michael-type addition.²²⁷ Nonetheless, disulfide bond rupture in response to applied force could be limiting for applications of disulfide cross-linked hydrogels as ECM substitutes for tissues subjected to high physical forces. In addition, disulfide cross-linked hydrogels are rapidly reduced by glutathione [H-Glu(CysGlyOH)-OH], a naturally occurring anti-oxidant tripeptide synthesized in human cells. Therefore, they are more appropriate for short-term applications. As already mentioned for Michael-type additions and native chemical ligation, thiols can lead to cross-reactivity with proteins and peptides *in vivo*.

Overall, the application of click reactions to the cross-linking of hydrogels allowed a ground breaking development in the field of biomaterials. However, the design of cell-encapsulating hydrogels remains a challenge. Some other biorthogonal ligation reactions are only starting to be explored by a few groups. For instance, C. L. Stabler *et al.* worked on Staudinger ligation and showed that this reaction could be advantageously used to encapsulate pancreatic islets in alginate-PEG hydrogels.^{228,229} R. Tamate and co-workers cross-linked a hydrogel by photoinduced dimerization of coumarin moieties.²³⁰ Z. Zong *et al.* focused their efforts on tetrazole-alkene photo-click chemistry but have not proved yet that this method allowed cell encapsulation.^{231,232}

1.2.3. Enzyme-mediated cross-linking

It is well known that enzymes catalyze specific reactions with high selectivity and efficiency. Their potential has been used in chemical synthesis as a convenient alternative to traditional

organic chemistry.^{233,234} As enzymes work under physiological conditions, they are suitable for biocompatible cross-linking strategies.²³⁵

Enzyme can be used in two ways for hydrogel formation: either as a mean to *in situ* generate initiators for free-radical polymerization of hydrogel precursors, or to catalyze specific covalent bond formation between two mutually reactive moieties displayed by hydrogel precursors.

I.2.3.1. Enzyme-triggered free-radical polymerization

The oxidation of glucose by the glucose oxidase enzyme (GOx) produces hydrogen peroxide. In the presence of Fe^{2+} , hydrogen peroxide generates hydroxyl radicals that can initiate a polymerization according to a mechanism described above in section I.2.1. (Figure 23, pathway A). C. N. Bowman and K. S. Anseth used GOx to cross-link PEGDA.^{236–238} This system was applied to the coating of cell-encapsulating hydrogels but was never described as a cross-linking method to prepare cell-laden hydrogels.²³⁷ Recently, Q. Wei *et al.* combined two enzyme-mediated redox reactions in a single system (Figure 23, pathway B). The hydrogen peroxide released by GOx oxidation of glucose was used by horseradish peroxidase (HRP) to oxidize acetyl acetone, a diketone mediator, as a ternary initiating system to trigger the radical-mediated polymerization of PEG methacrylate (Figure 23).²³⁹ In these cases, enzymes are not directly involved in the cross-linking process, they are used as initiators for chain-growth polymerization. In that sense, enzyme-triggered free-radical polymerization cannot be properly considered as an enzyme-mediated cross-linking method.

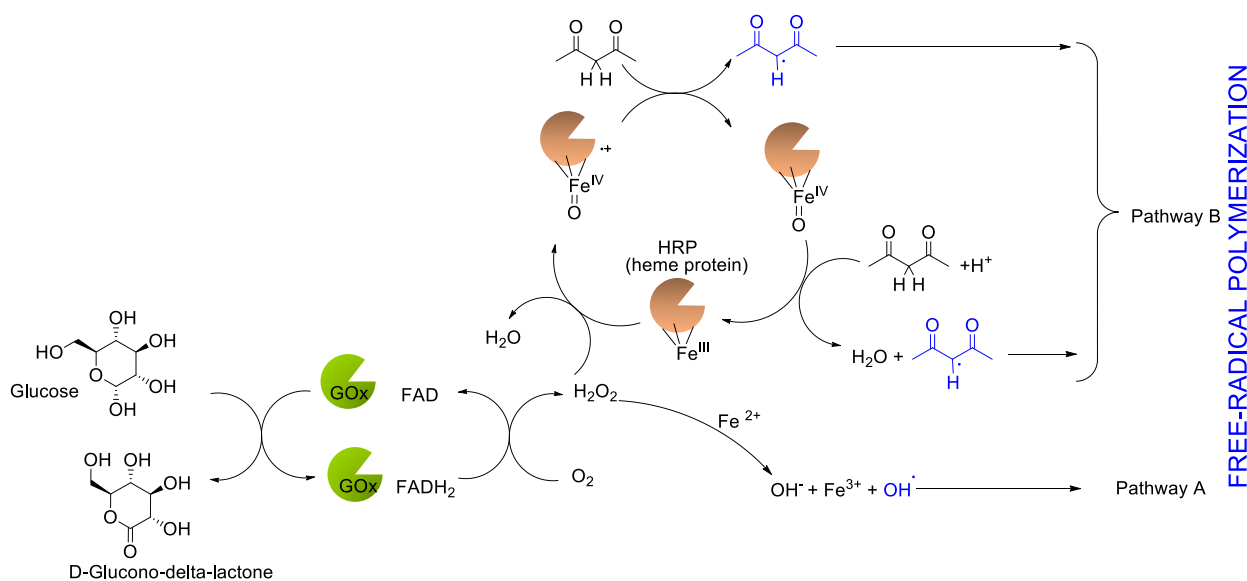


Figure 23. Enzyme-mediated redox reactions triggering free-radical polymerization

1.2.3.2. Enzyme-mediated ligation

The potential of enzymes can be used more interestingly to catalyze the reaction between two reactive groups leading to the formation of a cross-link.

Horseshoe peroxidase (HRP), which was reported above for triggering free-radical polymerization, can also catalyze the oxidative coupling of phenol moieties in the presence of hydrogen peroxide. A cross-link is formed between two carbon-centered radicals at the *ortho*-position to the phenolic hydroxyl groups, or between an *ortho*-carbon radical and a phenolic hydroxyl group (Figure 24). L.-S. Wang *et al.* functionalized gelatin with 3-(4-hydroxyphenyl)propionic acid (HPA) (Figure 25) and reported the encapsulation of hMSCs in a hydrogel formed by the HRP-catalyzed cross-linking of HPA groups.²⁴⁰ Likewise, D. J. Menzies *et al.* prepared cell-laden hydrogels from branched-PEG-HPA.²⁴¹ Tyramine and tyrosine derivatives can also undergo HRP-mediated cross-linking.^{242–244} For instance, F. Chen and co-workers encapsulated chondrocytes in a HRP cross-linked hydrogel obtained from carboxymethyl pullulan-tyramine and chondroitin sulfate-tyramine.²⁴⁵

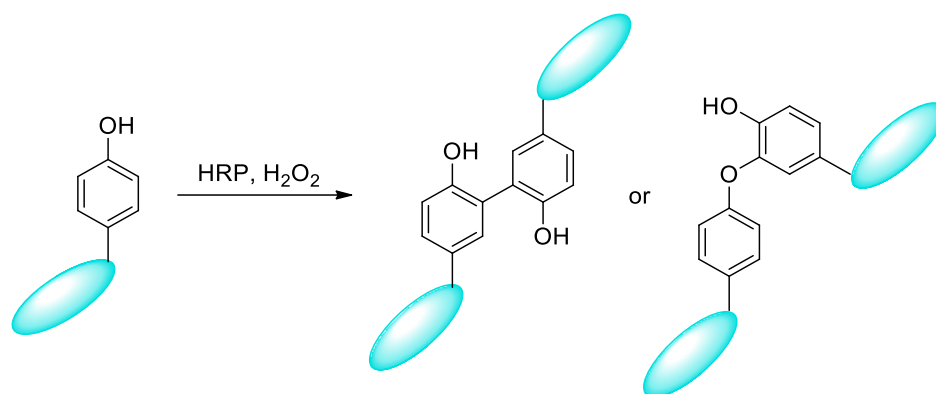


Figure 24. Horseradish peroxidase (HRP)-mediated oxidative cross-linking of phenol derivatives.

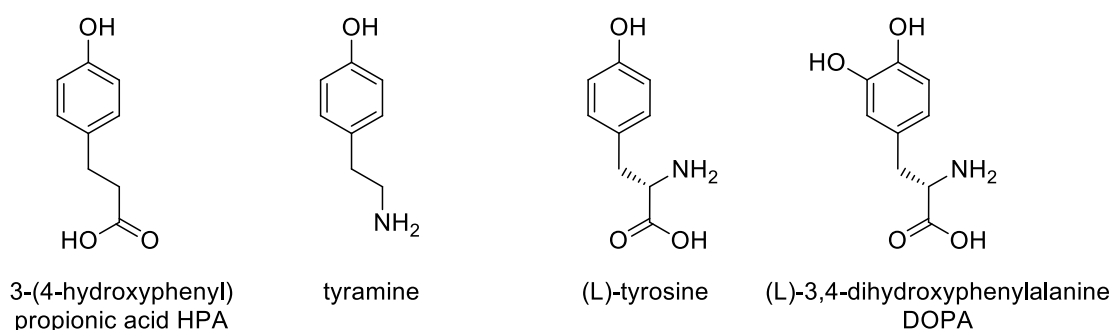


Figure 25. Chemical structures of carboxylic acid derivatives coupled on hydrogel precursors to enable enzyme-mediated oxidative cross-linking.

Tyrosinase is another oxidative enzyme able to cross-link phenol and catechol-functionalized molecules in the absence of hydrogen peroxide (Figure 26). This is of interest given the adverse cellular effects of H_2O_2 . However, few studies have investigated tyrosinase-mediated cross-linking for biomedical applications.^{246–248} S. Das *et al.* reported the encapsulation of mesenchymal progenitor cells in a silk fibroin-gelatin hydrogel. In this work, mushroom

tyrosinase was used to create cross-links between tyrosine residues of silk and gelatin.²⁴⁹ Tyramine and DOPA derivatives were also used to enable tyrosinase-mediated cross-linking.^{248,246} Noteworthy, the oxidative coupling of DOPA-bearing polymers can also be achieved with a chemical oxidant such as sodium periodate.^{246,250–252}

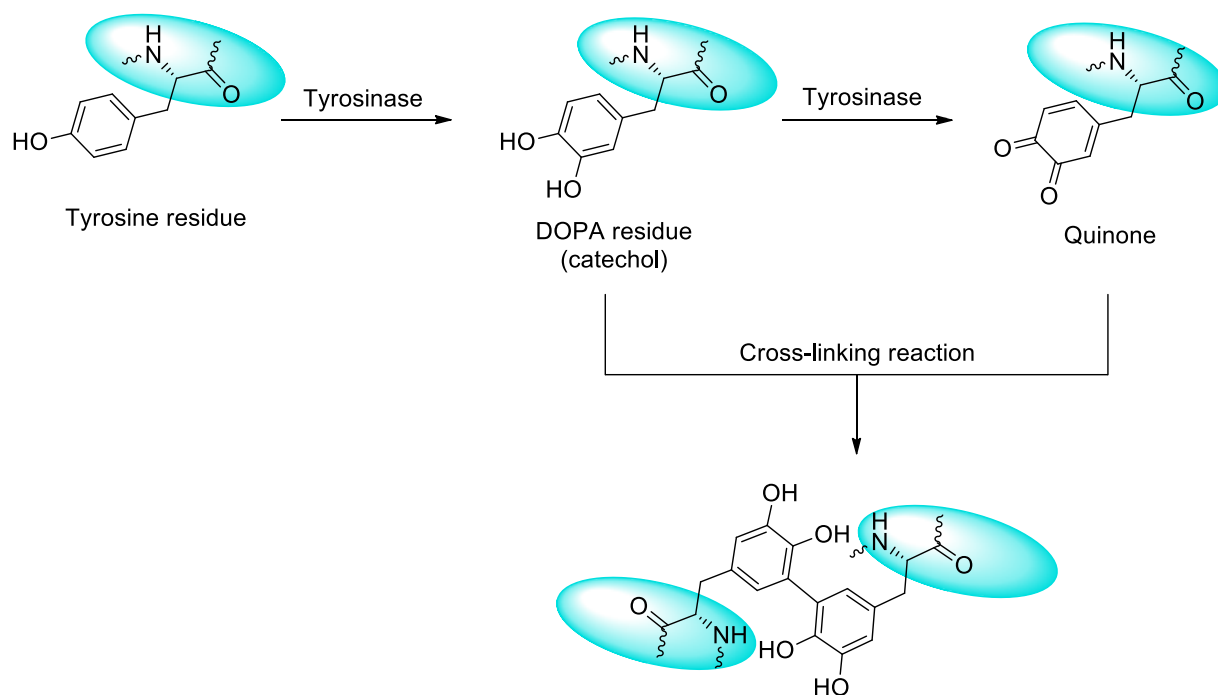


Figure 26. Oxidative coupling of tyrosine residues by tyrosinase

Transglutaminase (TG) cross-links peptides and proteins by catalyzing an acyl-transfer between the side-chain of a glutamine residue and the side-chain of lysine residue in the presence of its cofactor, Ca^{2+} ion (Figure 27). This reaction is highly selective for the two substrates (*i. e.* the Lysine containing sequence acting as acyl acceptor and the Glutamine-containing peptide acting as acyl donor). Thus, macromolecules that are functionalized with two rationally designed TG substrates can be cross-linked by TG. This strategy was used by B.-H. Hu and P. B. Messersmith, they conjugated TG peptide substrates to PEG chains and demonstrated hydrogel formation under physiological conditions.²⁵³ Prior to their study, J. J. Sperinde and L. G. Griffith had already obtained TG cross-linked hydrogels from a glutaminamide-functionalized PEG and a poly(LysPhe) peptide.²⁵⁴ M. K. McHale *et al.* reported chondrocyte encapsulation in an elastin-like polypeptide hydrogel with TG-mediated gelation.²⁵⁵ A thermally responsive gelation system was developed by T. J. Sanborn and co-workers based on the controlled release of the enzyme cofactor. Indeed, calcium-loaded liposomes allowed TG activation only when the system temperature was raised to 37°C , releasing the calcium ions during the phase transition of the liposome.²⁵⁶ Finally, M. Ehrbar *et al.* engineered cell-laden hydrogels whose network was formed by combining different molecules functionalized with TG peptide substrates, in particular multi-arm PEGs, cell

adhesion peptide and MMP-sensitive peptide.^{257–259} Interestingly, the later gave to the resulting network interesting enzymatic degradation properties.

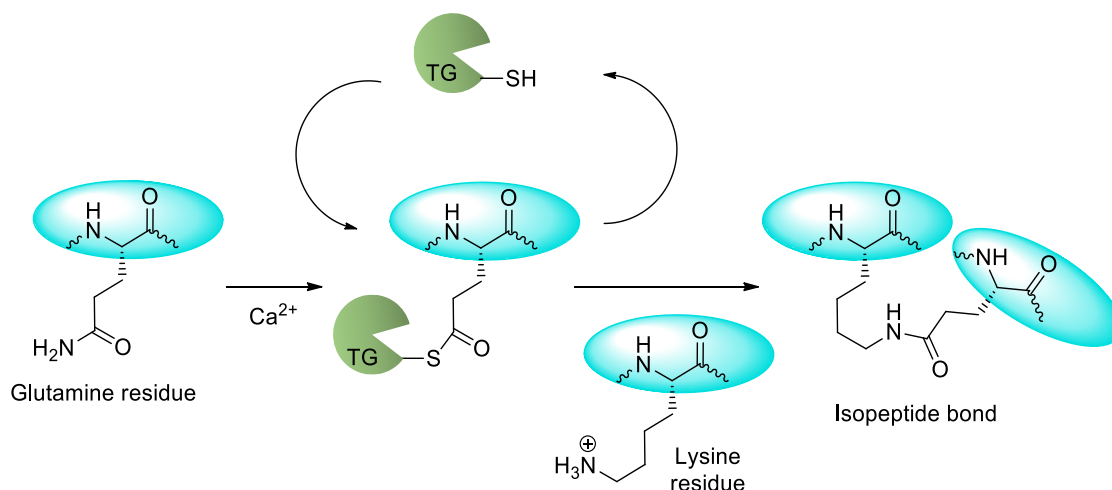


Figure 27. Transglutaminase (TG)-catalyzed acyl transfer between a glutamine and a lysine side-chains.

At last, the phosphopantetheinyl transferase (PPTase) was also successfully used for tissue engineering applications. This enzyme catalyzes the covalent attachment of the 4-phosphopantetheine moiety of coenzyme A (CoA) to a specific serine residue on the apo-acyl carrier protein (ACP) (Figure 28). Hydrogels were formed from 3-arm PEG multi-functionalized with CoA and an engineered ACP dimer. The PPTase-mediated cross-linking was conducted in the presence of cells demonstrating its biocompatibility.²⁶⁰

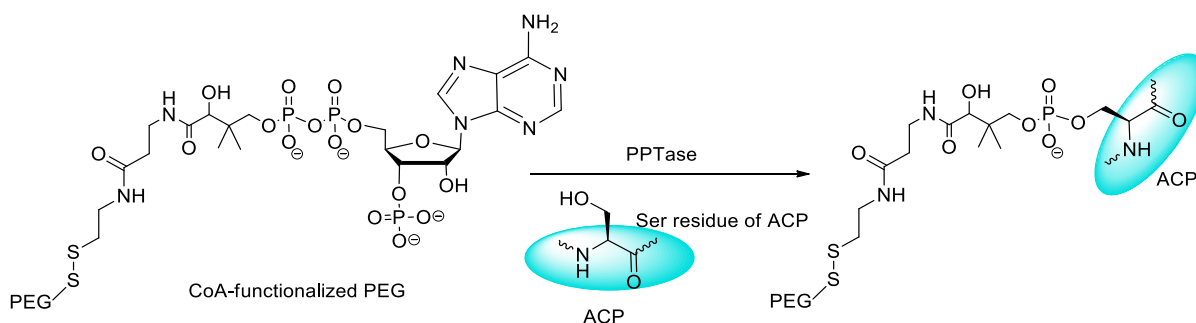


Figure 28. Phosphopantetheinyl transferase (PPTase)-catalyzed reaction between serine residue of ACP and CoA-functionalized PEG.

The examples discussed in this section show that enzymes are well-suited for the cross-linking of hydrogels. Nevertheless, special attention has to be paid to enzymes that work in an oxidative medium either because they require H₂O₂ or because they generate it.²⁶¹ In addition, the enzymes used for cross-linking are not physiologically present in cell culture media or they are present in too low quantities to avoid their additional introduction during hydrogel formation. It implies that they could lead to immune responses and cross-reactions *in vivo*. Lastly, diffusion of enzymes in the medium during the gelation process is limited which often results in heterogeneous hydrogels with poor mechanical properties.

I.2.4. Sol-gel chemistry

Numerous methods have already been investigated to cross-link cell-containing hydrogels but the potential of inorganic sol-gel polymerization as a cross-linking method for cell encapsulation in hydrogels has not been fully exploited. This PhD work was performed in this context and aims at preparing hybrid hydrogels thanks to the sol-gel process. Therefore, the following section is dedicated to the basics of inorganic sol-gel polymerization and highlights the main features that make it attractive for the preparation of cell-encapsulating hydrogels.

I.2.4.1. Overview

The sol-gel chemistry was pioneered by M. Ebelman^{262,263} and T. Graham²⁶⁴ in the 19th century. They observed that the hydrolysis of $\text{Si}(\text{OEt})_4$ (tetraethyl orthosilicate, TEOS), under acidic conditions yielded silica in the form of a "glass-like material". Since then, the sol-gel processes have had a tremendous development as demonstrated in the numerous books and reviews dedicated to this chemistry.^{265–271}

The sol-gel process refers to an inorganic polymerization of molecular precursors to form an oxide network at low temperature and under mild conditions. Precursors are generally metal alkoxides whose general formula is $\text{M}(\text{OR})_n$ with M a metal (Si, Al, Ti, etc.) and R an alkyl group (Me, Et, iPr, etc.). Alternatively, metal halides can be used (MX_n). The process is characterized by a sol to gel transition. A sol is a stable suspension of colloidal particles within a liquid and a gel is a 3-dimensionnally interconnected solid network holding large amounts of solvent (Figure 29).

The sol-gel process is based on two steps, hydrolysis and condensation, which are described in detail in the following sections. Water is involved as a reagent but can also be used as a solvent. Interestingly, homogeneous multi-component systems can be easily accessed by simply mixing different molecular precursors.

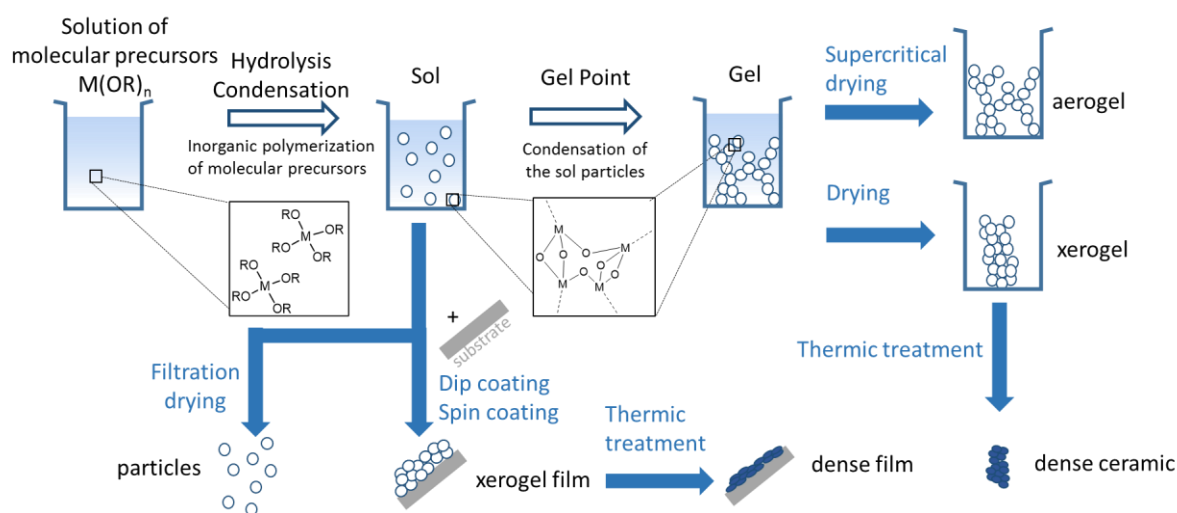


Figure 29. Principle of the sol-gel process.²⁷²

The sol-gel chemistry was first applied to the preparation of glasses and ceramics.^{266,273,274} The advantages of this approach were lower processing temperatures compared to conventional glass melting and ceramic powder methods and a higher homogeneity. Sol-gel derived nanoparticles, in particular nanoparticles obtained via the Stöber process,²⁷⁵ have received considerable attention and find applications in medicine for site-specific drug delivery and bio-imaging.^{276–279} The strength of the sol-gel chemistry is its compatibility with lots of processing methods, e. g. spinning and dip coating, that lead to a wide range of products: fibers, coatings, films, xerogels, aerogels, etc. It enables the preparation of advanced tailor-made materials.

Silicon is the second most abundant element in the Earth's crust after oxygen.²⁸⁰ Silicon alkoxides, $\text{Si}(\text{OR})_4$, are stable and easy to handle. Therefore, they are the most commonly used precursors for the sol-gel process. Herein, we will discuss the hydrolysis and condensation steps undergone by silicon alkoxides in aqueous media.

I.2.4.2. Hydrolysis step

The sol-gel process starts with the hydrolysis of alkoxysilyl groups (Si-OR) into silanols (Si-OH) and the resulting release of an alcohol (ROH) (Figure 30). At neutral pH, this reaction is very slow (Figure 31). However, acids, bases and nucleophiles can be used as catalysts to increase the reaction rate.

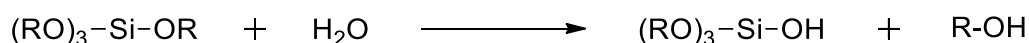


Figure 30. Overall equation of the hydrolysis of a silicon alkoxide into silanol

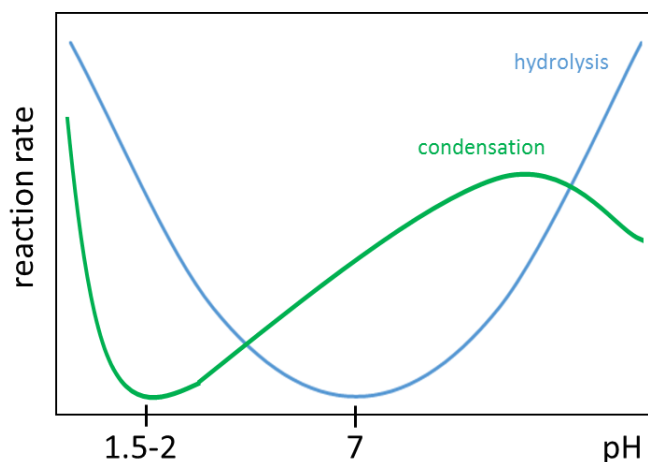


Figure 31. Reaction rates of tetraethyl orthosilicate hydrolysis (blue curve) and condensation (green curve) as a function of pH.²⁶⁵

In the acid-catalyzed process, an oxygen from an alkoxysilyl group is protonated (Figure 32). On the one hand, this protonation increases the electrophilicity of the silicon atom and favors the nucleophilic attack of water. On the other hand, it makes ROH a better leaving group. Both effects contribute to a high hydrolysis rate.

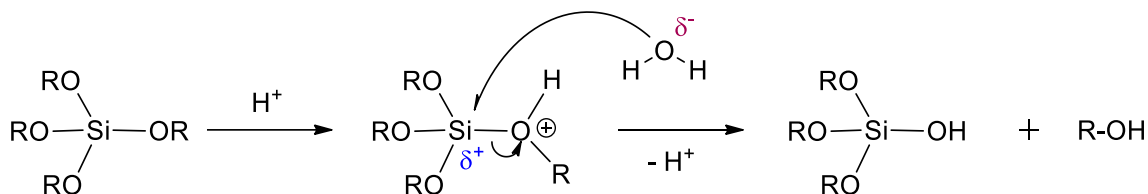


Figure 32. Acid-catalyzed hydrolysis of a silicon alkoxide group

Under basic conditions, hydroxyl ions form and add to the silicon center to yield a penta-coordinate silicon intermediate with a negative charge (Figure 33). The product of hydrolysis results from the departure of an alcoholate. Finally, OH⁻ catalyst can be regenerated by reaction between the alcoholate and water. The overall reaction rate is lower than the acid-catalyzed reaction.

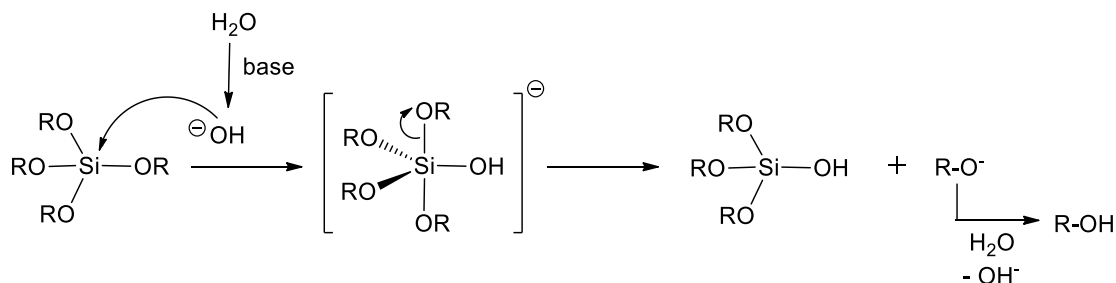


Figure 33. Base-catalyzed hydrolysis of a silicon alkoxide group

Alternatively, nucleophile catalysts can be used to speed the process at neutral or physiological pH. Owing to their high affinity for silicon, fluorides hold a prime position as nucleophile catalysts for this reaction. The addition of a fluoride onto a silicon atom give a penta-coordinate silicon intermediate similar to the intermediate observed in the base-

catalyzed reaction (Figure 34). The penta-coordinate silicon is transformed into a hexa-coordinate silicon upon attack of a water molecule. The product of hydrolysis is formed upon the departure of an alcohol and the regeneration of the fluoride catalyst.

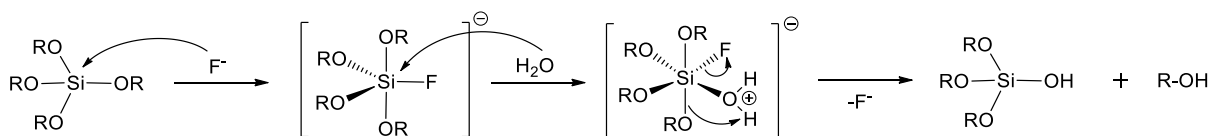


Figure 34. Fluoride-catalyzed hydrolysis of a silicon alkoxide group

The precursor may undergo four successive hydrolyses until $\text{Si}(\text{OH})_4$ forms but as soon as one alkoxide group has been hydrolyzed, condensation can also begin.

1.2.4.3. Condensation step

The condensation step leads to the formation of siloxane bonds (Si-O-Si). When the condensation reaction occurs between two hydroxysilyl groups with release of water, it is called oxolation (Figure 35). When it involves a hydroxide and an alkoxide with release of an alcohol, it is called alkoxolation.

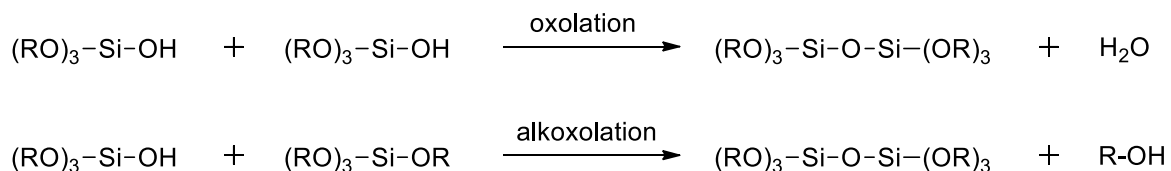


Figure 35. Condensation reactions via oxolation or alkoxolation

The condensation step can also be catalyzed by acids, bases and nucleophiles. The mechanisms of the reaction are exactly the same as the mechanisms of hydrolysis except that silanols and silanolates are the nucleophilic species instead of H_2O and HO^- under acid and basic conditions respectively. Likewise, in the presence of fluorides, a penta-coordinate silicon fluoride is formed and evolves towards a hexa-coordinate silicon specie upon nucleophilic attack of a silanol. The condensation reaction ends with the departure of H_2O (oxolation) or ROH (alkoxolation) and the regeneration of the fluoride ion.

In the sol-gel process, the choice of the catalyst is crucial and will influence the texture (porosity, surface area...) of the resulting material. Two types of gels can be distinguished: colloidal gels whose network is made of colloidal sol particles and polymeric gels whose network is made of sub-colloidal chemical units such as macromolecules. An acid pH favors hydrolysis over condensation and leads preferably to a polymeric gel whereas a basic pH induces nucleation and generates a colloidal gel (Figure 36). Fluorides catalyze equally both hydrolysis and condensation at neutral pH which leads preferably to a colloidal gel. Of course, the nature of the metal alkoxide, the concentration and the temperature are parameters that also influence the process.

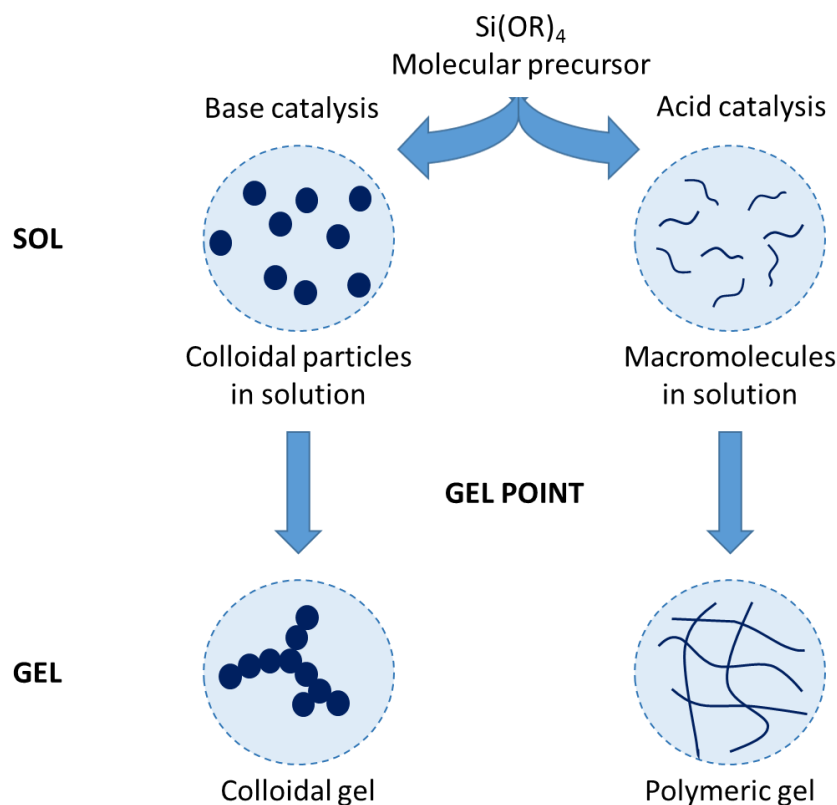


Figure 36. Influence of the catalyst on the type of hydrogels obtained

The sol-gel process was given the label “Chimie douce” by Jacques Livage.²⁸¹ The mild conditions under which the sol-gel process occurs make it compatible with organic molecules and biological molecules. Combination of organic and inorganic components leads to the formation of hybrid materials.

1.2.4.4. Hydrogels cross-linked by the sol-gel process

In the sol-gel chemistry, gels are usually considered as intermediates and dried to produce xerogels and aerogels for example. However, several sol-gel characteristics suggest that sol-gel chemistry would be well-suited for the preparation of cell-encapsulating hydrogels. Indeed, gelation can occur in aqueous media, at physiological pH and at room or body temperature. Importantly, the condensation reaction is chemoselective. As no biomolecule contains silicon atoms, the process is completely biorthogonal. In addition, the Si-O-Si bond formation is a symmetrical reaction, involving twice the same reactive moiety. As a consequence, it is theoretically possible to combine molecular precursors tailored to establish the tridimensional network and precursors affording additional biological or physical properties into a single and homogeneous multi-component system. One single chemistry (Si-O-Si bond formation) can be used both for cross-linking and functionalizing the hydrogel (Figure 37).

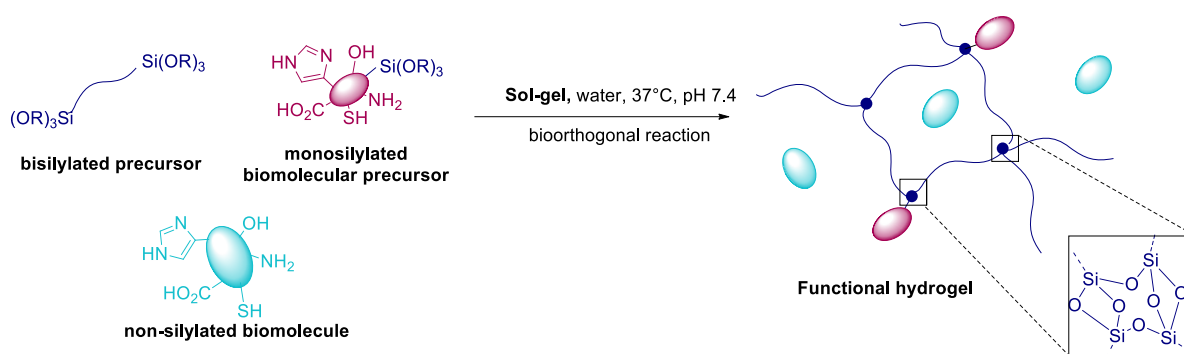


Figure 37. Synthesis of a functional hybrid hydrogel thanks to the sol-gel process

Cell encapsulation in silica hydrogels

The encapsulation of cells in sol-gel materials was pioneered by G. Carturan *et al.* who encapsulated yeast cells into thin layers of SiO_2 gel.^{282,283} Then it was demonstrated that bacteria could also remain viable in silica hydrogels (Figure 38), some of them even seemed to be stabilized by sol-gel encapsulation.^{284–287} Unfortunately, animal cells could not tolerate to be readily suspended in silica solutions because of the acidic pH required and the large quantities of alcohol released by the hydrolysis of alkoxide precursors. Therefore, J. Livage and co-workers suggested to protect the biological load by immobilizing it in a suitable microphase prior to coating with sol-gel silica.²⁸⁸ Hence, Sakai *et al.* encapsulated pancreatic cells and islets in sol-gel coated alginate microcapsules.^{289,290} However, this approach requires the use of an initial system with its own capacity to gelate, in this example alginate. In order to improve encapsulated cell viability, some researchers focused on experimental conditions and reduced the contact time between cells and precursor solution,^{291–293} while others proposed sodium silicate aqueous solutions as an alternative to alkoxide precursors to avoid alcohol release.²⁹⁴ The ‘Biosil’ method was also developed to avoid alcohol release in the medium and thus improve encapsulated cell viability. In this process, living cells are coated by a silica film via sol-gel reactions occurring at the surface of the cells in a water layer. Molecular silicon precursors are continuously provided in the gas phase, *i. e.* an inert gas carrier saturated by silicon alkoxides is directed to the cell surface, and by-products, herein alcohol, are removed in the out flow.²⁸³

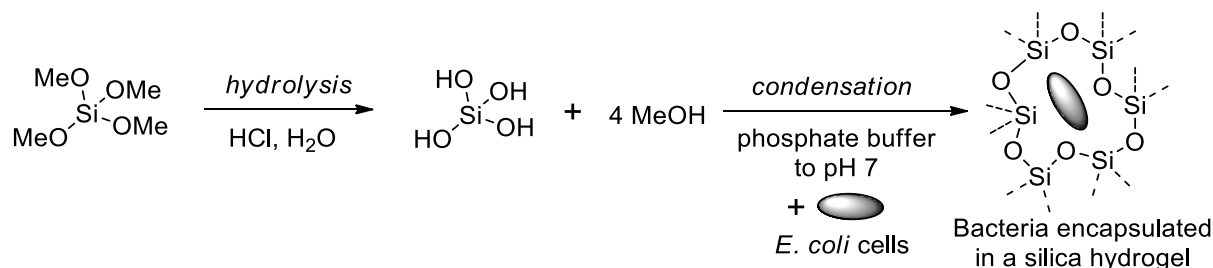


Figure 38. Encapsulation of *E. coli* cells in a silica hydrogel formed by the sol-gel process.²⁸⁴

Interestingly, amorphous silica is considered non-toxic, being used commonly as additive in food and drugs and recognized as safe (GRAS) by the American Food and Drug Administration.²⁹⁵ Toxicity issues raised about silica were mainly due to the size and shape of silica materials and were particularly discussed in the case of silica nanoparticles.²⁹⁶ The degradation of silica hydrogels leads to the formation of polysilicic acids and ultimately to the ortho-silicic acid (Si(OH)_4). This latter is naturally present in food and water. It is non-toxic and plays a crucial role in delivering silicon to cells in the body. As silicon has been shown to be involved in many biological functions such as bone mineralization, collagen synthesis and hair condition, therapeutic effects of silicic acid were investigated.²⁹⁷ A wound dressing made of silica fibers releasing ortho-silicic acid was even reported.²⁹⁸ Nevertheless, the intermediate degradation products of silica, the polysilicic acids, were shown to present some adverse effects by interacting with proteins.²⁹⁹

If numerous examples demonstrate that cells encapsulated in sol-gel silica are viable, it is obvious that a promoting bioorganic network is necessary for soft tissue growth. As a consequence, we will focus our attention on hydrogels in which silicon atoms are used only as cross-linkers. Precursors of such hydrogels are 'hybrid' molecules in the sense that they display both an (bio)organic moiety and inorganic silane groups. Systems in which silica precursors are mixed with polymers to improve their mechanical properties will not be discussed.

Cell-encapsulation in hybrid hydrogels cross-linked by the sol-gel process

To obtain a cell-friendly environment, it is relevant to keep the silicon amount as low as possible to maximize the resemblance of the hydrogel with native ECM and limit the release of alcohol when alkoxide precursors are used. This can be achieved by modifying covalently a (bio)polymer to introduce a trialkoxysilane moiety. In this case, the silicon atom is linked to the polymer via a C-Si bond. The network results from the formation of siloxane bonds (Figure 39). The C-Si bond being stable to hydrolysis, the network can be degraded either by hydrolysis of the siloxane bonds or by biodegradation of the backbone by pathways specific to each polymer. Depending on the silylation reagent chosen, the link between the polymer and the silylation reagent can also be cleaved. Toxicity may arise from silylation reagents left unreacted in the hydrogel. To overcome this problem, it is possible to perform the modification of the polymer separately from the formation of the hydrogel. Washings between the two steps enable to get rid of free reagents and potential side-products. Then hydrogel biocompatibility is often evaluated via cytotoxicity assays. Hybrid hydrogels showed good overall cytocompatibility but an in-deep study of the toxicity of potential biodegradation products has never been performed.

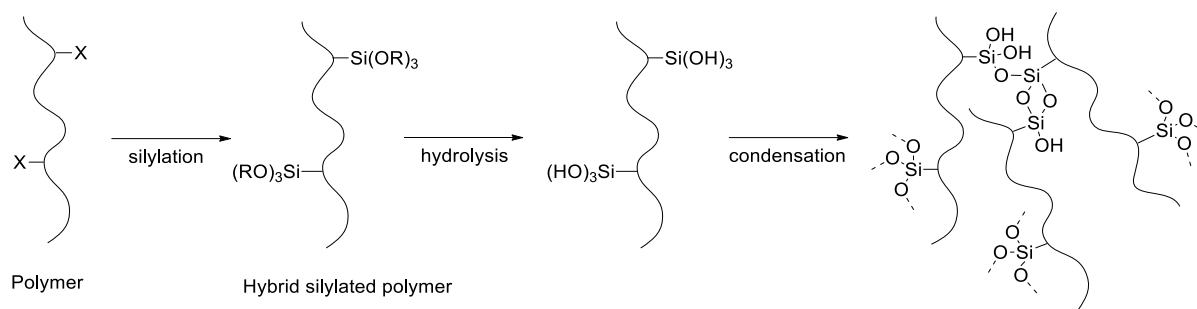


Figure 39. Sol-gel cross-linking of a hybrid silylated polymer. X: reactive function of the polymer.

Hybrid precursors are obtained by covalent modification of polymers with alkoxy silane moieties (Figure 40). The choice of the silylating reagent depends on the available reactive functions (e.g. alcohol, amine, carboxylic acid) displayed by the polymer. S. Jo and K. Park described the functionalization of the hydroxyle extremities of PEG and Pluronic F-127 (block copolymer $\text{HO}-[\text{CH}_2\text{CH}_2\text{O}]_n-[\text{CH}(\text{CH}_3)\text{CH}_2\text{O}]_m-[\text{CH}_2\text{CH}_2\text{O}]_n-\text{H}$ with $n \approx 98$ and $m \approx 67$) with 3-isocyanatopropyl triethoxysilane (ICPTES) but they used a sol-gel procedure involving ethanol, acidic pH and solvent evaporation.³⁰⁰ L. Ren *et al.* used 3-(glycidoxypropyl)trimethoxysilane (GPTMS) to functionalize gelatin, a biopolymer derived from collagen that displays both hydroxyle and primary amine functions. The reactivity of GPTMS towards nucleophiles was studied.^{301,302} The preparation of the hybrid polymer and its gelation were carried out one pot in a 0.1 M HCl solution at 40°C. The hydrogels were then dried.³⁰³ Based on this work, J. R. Jones *et al.* used hybrid gelatin in combination with TEOS to prepare materials with an increased inorganic content for a better control over mechanical and degradation properties. Sol-gel precursors were hydrolyzed in a HCl solution and condensation was catalyzed by hydrofluoric acid. A surfactant, Triton X-100, was used to generate porosity.³⁰⁴ Then the same group prepared silica-chitosan hybrid scaffolds. Hybrid chitosan was obtained by reaction with GPTMS and the sol-gel process was carried out in acidic conditions. The structure of the scaffolds could be directed by freeze-drying.^{305,306} In both cases, J. R. Jones and co-workers selected hydrogel formation conditions that are not compatible with cell encapsulation. Therefore, they had to develop processing methods to generate highly porous structures and thus facilitate cell penetration in the freeze-dried scaffolds. N. Hanagata *et al.* used the same silylation reagent, GPTMS, to cross-link collagen fibril hydrogels. Preformed collagen hydrogels were soaked in a HCl/ethanol solution containing GPTMS. After dehydration, drying and rehydration, hybrid cross-linked hydrogels could support osteoblast proliferation.³⁰⁷ K. Hosoya *et al.* coupled 3-aminopropyltriethoxysilane (APTES) on alginate. For that purpose, they activated carboxylic acid functions of alginate with a carbodiimide (EDC, 1-ethyl-3-(3-dimethylaminopropyl)-carbodiimide) in the presence of an auxiliary nucleophile (N-hydroxysuccinimide, HOSu). The hybrid alginate was not isolated, it underwent gelation right after its formation. Urea by-product resulting from carbodiimide activation and HOSu were then washed away and the resulting hydrogels were freeze-dried.³⁰⁸ None of these procedures was compatible with cell encapsulation. Most of the hydrogels mentioned above were prepared under acidic conditions and they were all dried before cell seeding.

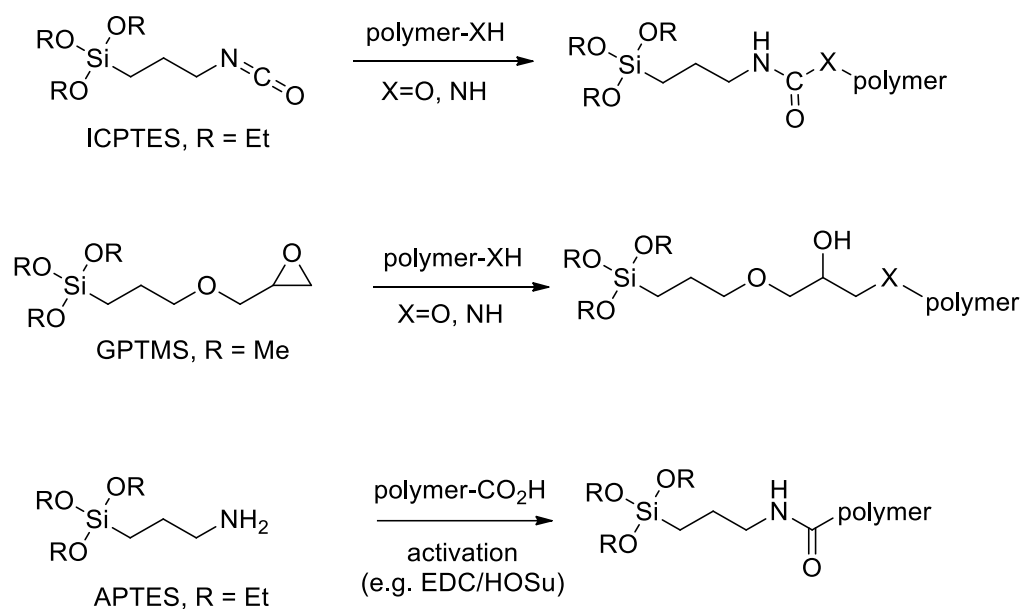


Figure 40. Functionalization of polymers with trialkoxysilylated reagents.

Y. Shirotsaki *et al.* added GPTMS to chitosan in 0.25 M acetic acid aqueous solution. These conditions allowed both the covalent modification of chitosan with a trimethoxysilane group and the acid-catalyzed hydrolysis of methoxy groups into hydroxyl groups. Under such acidic conditions, condensation was very slow. Therefore, the solution was then neutralized with sodium hydroxide to promote condensation. At this stage, the hybrid chitosan solution was injectable. A 2 wt% chitosan solution could turn into a gel at 37°C within 60 or 200 minutes with 5 or 1 molar ratio of GPTMS respectively. This hydrogel was intended to be used as a resorbable vehicle for bone graft.³⁰⁹

Finally, P. Weiss and co-workers developed hybrid cellulose-based hydrogels. They functionalized different cellulose derivatives, in particular hydroxypropylmethylcellulose (HPMC), with GPTMS or 3-glycidopropylmethyldiethoxysilane (GPMDS) via a Williamson reaction between the hydroxyl groups of the biopolymer and the epoxide.^{310,311} In organic solvents, the cellulose derivatives were not soluble and the reaction occurred in heterogeneous medium. In order to increase the modification homogeneity, they developed and patented a silylation method in homogeneous medium by using ionic liquids.³¹² Their sol-gel procedure consisted of a hydrolysis step at pH > 12.3 and condensation upon neutralization. At high pHs, the hybrid polymer, named Si-HPMC, is the form of sodium silanolate. The charge repulsion prevents condensation and allows the storage of the solution as a viscous liquid for a prolonged period. Condensation occurs upon neutralization at room or body temperature. They demonstrated that the Si-HPMC hydrogels could encapsulate chondrocytes and could also be injected for cartilage tissue repair.³¹³ Eventually, they used Si-HPMC as a base for the development of several materials for tissue regeneration.³¹⁴⁻³¹⁹

The Si-HMPC hydrogels developed by P. Weiss and co-workers are very promising for tissue engineering. However, their system relies on a natural biopolymer. As discussed earlier, the use of natural biopolymers has some shortcomings. Therefore, the development of a similar

approach based on synthetic molecules would be of interest. In addition, their two-steps sol-gel procedure requires a careful pH monitoring. A protocol involving hydrolysis and condensation at physiological pH in a cell culture medium would be simpler. Nucleophile-catalyzed sol-gel process at physiological pH was never exploited for cell encapsulation in hydrogels made of hybrid alkoxy silane polymers. The functionalization of this kind of hydrogels with hybrid silylated peptides was never reported neither. Accordingly, we decided to investigate both.

Chapter II.

Hybrid silylated peptides

*Publication 1 – Selective
homodimerization of unprotected
peptides using hybrid
hydroxydimethylsilane derivatives*

Echalier C. *et al.*, *RSC Adv.*, 2016, **6**, 32905-32914

My contribution to this paper: I prepared all the NMR samples, designed the NMR analyses, processed and interpreted the data. I participated in the synthesis, silylation, purification and characterization of the peptides. I participated in the writing of the paper.

Chapter II. Hybrid silylated peptides

II.1. Hybrid peptides

Ahead of this PhD project, the “Amino acides, Hétérocycles, Peptides et Protéines” team of IBMM and the “Chimie Moléculaire et Organisation du solide” team of ICGM had developed hybrid silylated peptides and patented their applications for the synthesis of materials.³²⁰ For these groups and throughout this manuscript, hybrid silylated peptides refer to peptides functionalized by one or several silyl groups (Figure 41). The silicon atom of these silyl moieties is linked to the peptide part through a covalent and highly stable C-Si bond. The three other groups born by the silicon atoms can be hydroxy, alkyl, alkoxy groups or halogen atoms. Hydroxydimethylsilyl, dihydroxymethylsilyl and triethoxysilyl groups have been particularly investigated as they can form one, two or three siloxane bonds respectively during the sol-gel process (Figure 42).

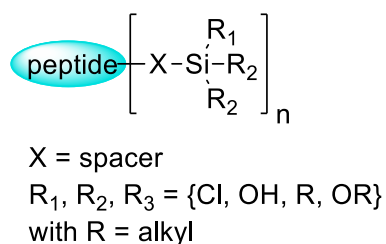


Figure 41. General formula of hybrid silylated peptides

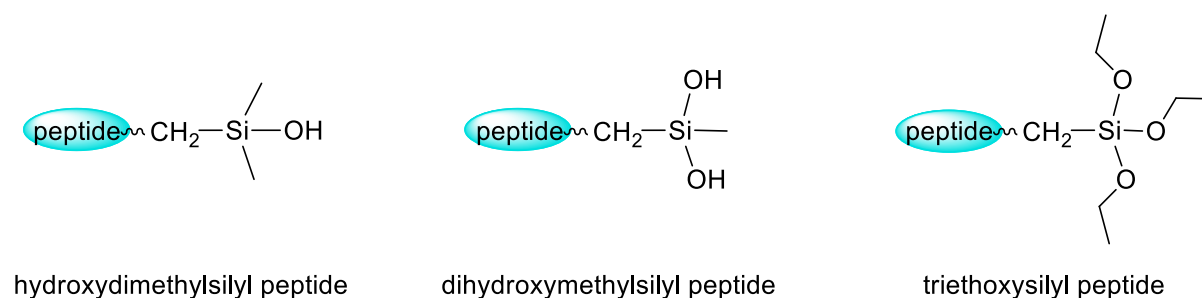


Figure 42. Hybrid silylated peptides used for the preparation of hybrid materials via the sol-gel process.

II.2. Hybrid peptide synthesis

II.2.1. General considerations

Several methods for the introduction of silyl groups on peptides were investigated in the laboratory before the beginning of my PhD, including the coupling of an amino derivative to an activated acid function of the peptide or the reaction of an isocyanate derivative with an amine function of the peptide. The reaction of an isocyanate with a primary or secondary amine results in a urea bond between the linker displaying the silicon atom and the peptide

(Figure 43). The use of isocyanatopropylsilyl derivatives was preferred over other methods of silylation for several reasons. First, these reagents are commercially available (ICPTES was obtained from Alfa Aeser, other silylated isocyanates were obtained from SIKEMIA, France). Second, isocyanates are very reactive towards nucleophiles. The quick reaction between an isocyanate and a free amino group limits the risks of premature hydrolysis of silyl groups which could lead to unwanted condensation. No coupling agent is needed, only a base (N,N-diisopropylethylamine, DIEA) is added to deprotonate ammoniums and form nucleophile amines ready to attack the isocyanate function. At last, this reaction proceeds without generating any side-product which simplifies the subsequent work-up and isolation of the hybrid building blocks. This is of interest considering the risk of premature hydrolysis and condensation. Most of hybrid peptides are not soluble in diethyl ether while silylated isocyanate derivatives are. As a consequence, the excess of isocyanate can be easily removed at the end of the reaction by precipitation of the hybrid peptide in diethyl ether. Usually, the hybrid silylated peptide is recovered quantitatively after centrifugation, removal of the supernatant and evaporation of diethyl ether traces.

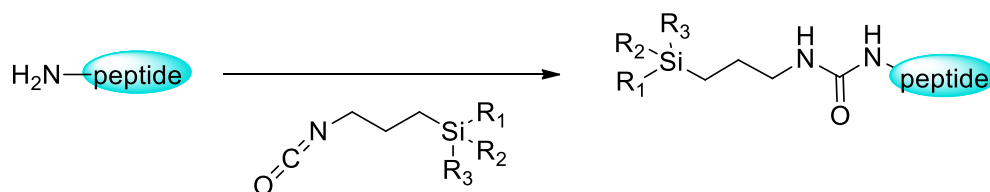


Figure 43. Preparation of hybrid silylated peptides. R_1, R_2, R_3 = halogen atoms, alkyl or alkoxy groups.

However, peptides can display nucleophilic side-chains that are not intended to be modified by silyl groups. When a stoichiometric amount of isocyanate is used, amino groups selectively react with the isocyanate in the presence of Serine or Threonine alcohol side chains. However, when several amino groups are present on the target peptide, side-chains must be protected. The most commonly used peptide synthesis strategy, the Fmoc/tBu solid phase peptide synthesis (SPPS) strategy, involves acid-labile side-chain protecting groups and acid-labile linkers.³²¹ The resin cleavage and/or the removal of these protecting groups from a hybrid silylated peptide under acidic conditions (trifluoroacetic acid, TFA) results in the concomitant hydrolysis of chlorosilane and alkoxy silane and the formation of silanols, due to the presence of traces of water during TFA-mediated cleavage and subsequent workup.

II.2.2. Triethoxysilyl peptide synthesis

Triethoxysilyl hybrid peptides are prepared by reacting the N-terminal amine and/or a lysine side-chain of a peptide with 3-isocyanatopropyltriethoxysilane (ICPTES). During acidic mediated removal of protecting groups and resin cleavage, triethoxysilyl group is hydrolysed into trihydroxysilyl group which leads to a significant extend of premature undesired polycondensation of the hybrid peptide.

Several strategies were used to overcome this limitation. Peptides which don't display any other amino group than the one intended to be reacted with isocyanate, can be functionalized with ICTES after cleavage and purification in their fully unprotected form.³²² As an alternative, a partially protected peptide, displaying a single free amino function, can be prepared in solution or on solid support, using suitable orthogonal linkers. It can be isolated and purified in its partially protected form before introduction of the triethoxysilyl group by reaction with ICTPES. The protected hybrid peptide can then be engaged in the sol-gel process to yield a bioorganic-inorganic material including the protected peptide. Eventually, this material is submitted to an acidic treatment for the removal of the peptide protecting groups (Figure 44).^{323,324} For example, the use of gaseous HCl was performed on hybrid silica materials for removal of Boc protection. Unfortunately, this strategy is limited to the hybrid materials that are not damaged by an acidic treatment and that can be further washed and/or dry to remove the acid. It is not friendly with the encapsulation of fragile biological cargo and living cells.

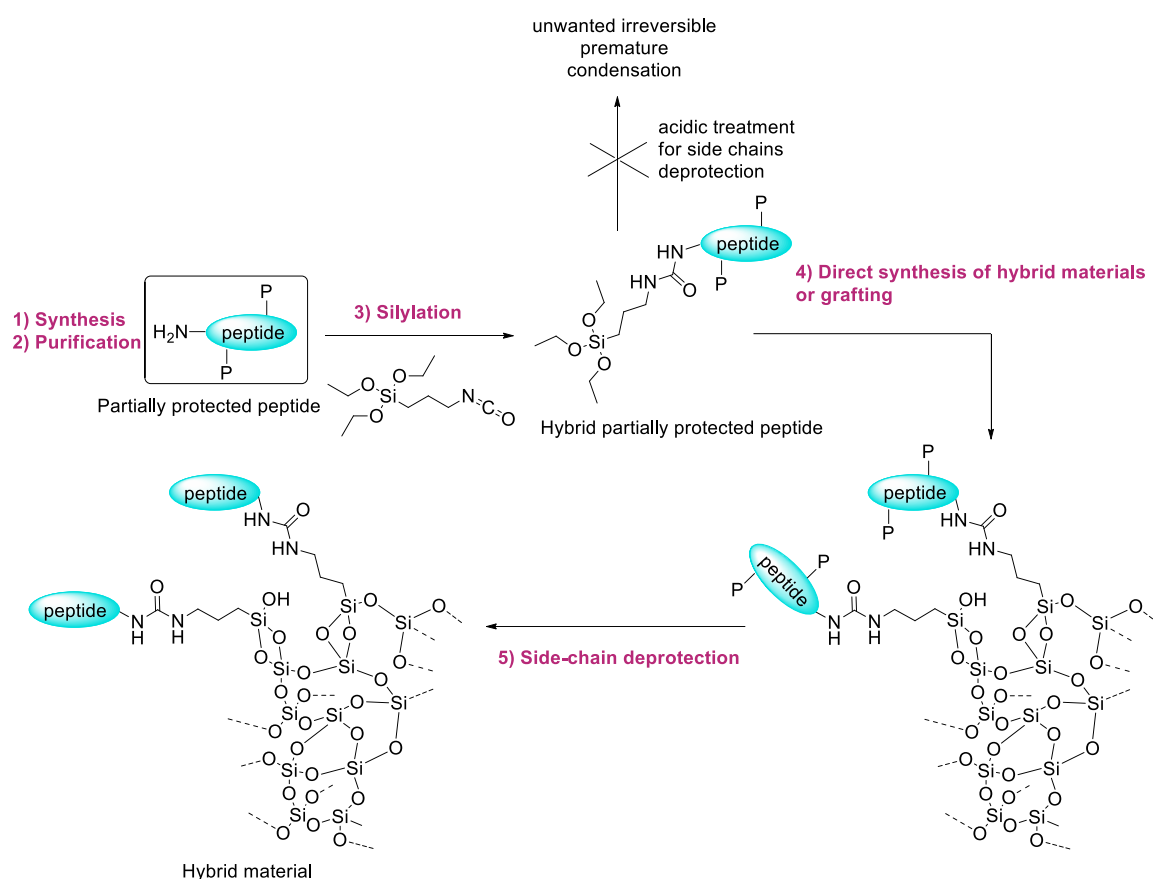


Figure 44. Principle of the synthesis of hybrid materials using a silylated and protected peptide.

II.2.3. Chlorodimethylsilyl peptide synthesis

The synthesis and the handling of chlorodimethylsilyl hybrid peptides are easier than their triethoxysilyl counterparts. They are obtained by reacting peptides with 3-isocyanatopropylchlorodimethylsilane (ICPCDMS).³²⁵ When chlorodimethylsilyl peptides are subjected to a TFA treatment for removal of peptide side-chain protections,

chlorodimethylsilanes are immediately hydrolyzed into hydroxydimethylsilanes. In the same way than trihydroxysilyl derivatives, condensation between two hybrid hydroxydimethylsilyl peptides can occur. However, and in contrast to the multiple bonds formed by trihydroxysilyl analogues, $\text{Me}_2\text{Si-O-SiMe}_2$ siloxane bond can easily be hydrolyzed in H_2O 1% TFA mixture to recover the hybrid hydroxydimethylsilyl monomers. This feature opens the way to a wider range of synthetic strategies, including silylation directly on the solid support used for the peptide synthesis (Figure 45). When the reaction is performed on solid support, the excess of ICPCDMS is removed by simple washings of the resin beads. Then the hybrid peptide is cleaved from the support using TFA. Side-chain protections are removed simultaneously and the chlorosilyl group is hydrolyzed into a hydroxysilyl group. The crude hydroxydimethylsilyl peptide can be easily purified as monomer by preparative RP-HPLC using acidic buffers (*i. e.* acetonitrile and water with 1% TFA).

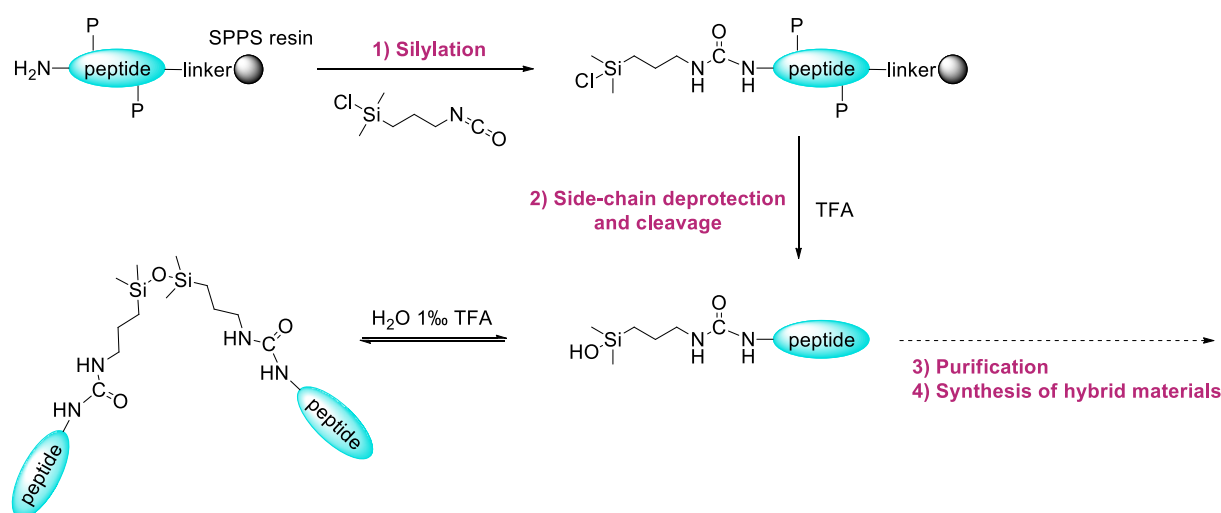


Figure 45. Principle of the synthesis of hybrid materials using a hybrid hydroxydimethylsilyl peptide

II.3. Hybrid peptide utilization

The more obvious utilization of hybrid silylated peptides is the surface modification of materials by grafting. In this case, the main advantage of hybrid peptides is the chemoselectivity of the SiOSi bond formation in the presence of other reactive side chains of amino acids. Theoretically, any metal oxide surface can be modified by grafting of hybrid peptides through the formation of a **M-O-Si**(R_1R_2)-peptide bond. However, most of the work performed so far with hybrid peptides concerns silicon oxide materials (Figure 46).

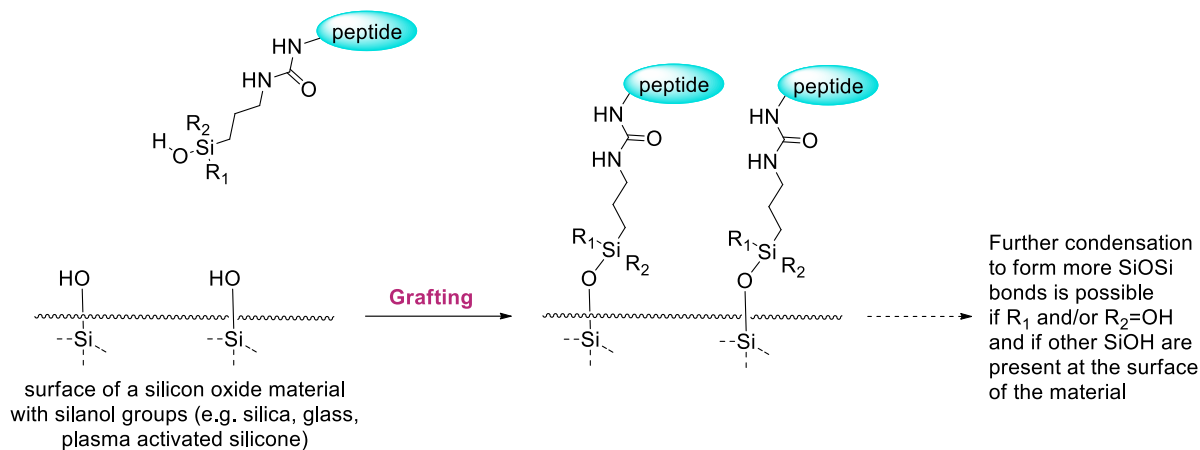


Figure 46. Principle of silicon oxide material grafting with hybrid peptides

Hybrid silylated peptides can also be engaged in a sol-gel process for the one-pot synthesis of hybrid materials. They can be used alone or in combination with silicon oxide precursors such as tetraethyl orthosilicate (TEOS). Upon hydrolysis and condensation of silyl groups, a hybrid bioorganic-inorganic material is formed.

II.3.1. Trialkoxysilyl peptide utilization

II.3.1.1. Trialkoxysilyl peptides for grafting on silica

In the first place, trialkoxysilyl groups were chosen over other silylated groups for silica surface modification because it was hypothesized that attachment through three siloxane bonds would be stronger than attachment through 1 or 2 bonds (Figure 46 with $R_1 = R_2 = OH$). First, S. Jebors *et al.* described the surface modification of silica materials with trialkoxysilyl peptides.³²³ They grafted a triethoxysilyl peptide into the pores of ordered mesoporous silica (OMS). The peptide sequence H-ProProAspLys-NH₂ was chosen for its ability to catalyze aldolisation reactions. The peptide was modified at its N terminus with a triethoxysilyl moiety and it was demonstrated that the resulting hybrid peptide retained its catalytic properties once anchored on the silica.³²³ More recently, J. Ciccione *et al.* reported the preparation of multi-ligand fluorescent silica nanoparticles with an accurate control of the grafting ratio of each ligand by using two triethoxysilyl peptide ligands in appropriate concentration (Figure 47).³²²

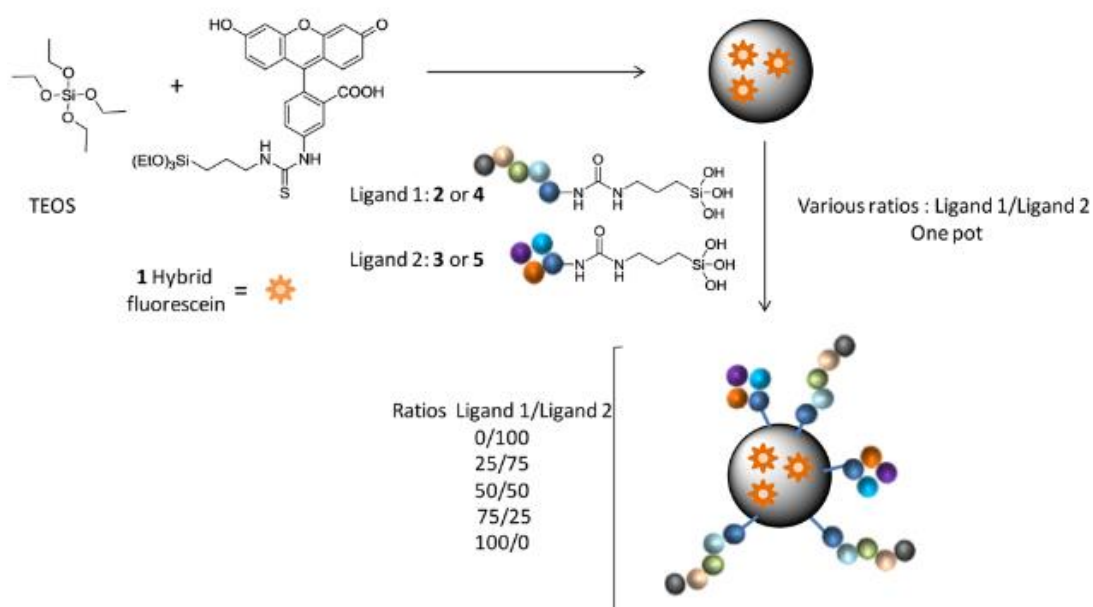


Figure 47. Synthesis of multifunctional fluorescent silica nanoparticles. Reprinted from.³²²

II.3.1.2. Trialkoxysilyl peptides for direct synthesis of hybrid silica

Hybrid triethoxysilyl peptides were used for the one-step synthesis of bioorganic-silica hybrid materials (Figure 48). S. Jebors *et al.* used the hybrid triethoxysilyl catalytic peptide that they already used for grafting, in combination with tetraethyl orthosilicate (TEOS). They showed that, in presence of a structure-directing agent, a peptide-hybrid ordered mesoporous silica could be successfully obtained in a single step.³²⁴ In the same paper, they selected an antibacterial peptide sequence (H-AhxArgArg-NH₂) and prepared an antifouling film by dip-coating with the corresponding triethoxysilyl hybrid antibacterial peptide analogue.³²⁴

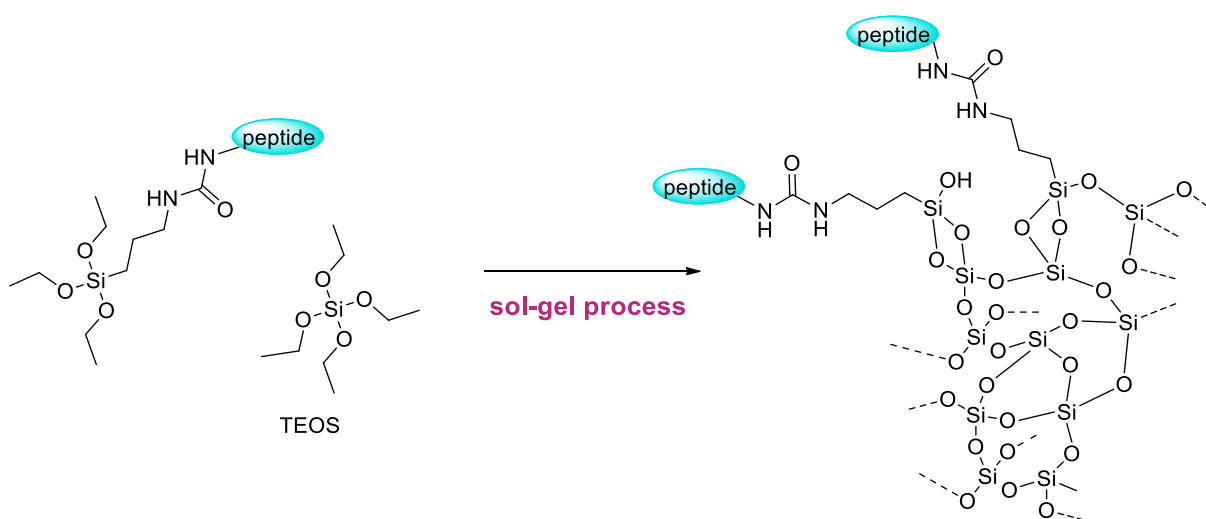


Figure 48. Principle of the direct synthesis of a hybrid peptide material using hybrid triethoxysilyl peptides

II.3.2. Restricting the number of bonds: dimethylchlorosilyl hybrid peptides

II.3.2.1. Grafting of dimethylchlorosilyl hybrid peptides

In our laboratory, C. Pinese *et al.* used hybrid hydroxydimethylsilyl peptides for the grafting of silicone surface.³²⁶ Silicone devices are made of cross-linked polydimethylsiloxane (PDMS) and do not display reactive silanol functions on the surface. Thus, in order to graft hybrid peptides on them, an oxygen plasma activation was performed, generating SiOH moieties (Figure 46). Commercially available silicone catheters were grafted with N-terminal hydroxydimethylsilyl derivative of the antibacterial H-AhxArgArg-NH₂ peptide. The functionalized catheters exhibited a prolonged antibacterial activity. Consequently, this grafting strategy could be useful to fight against bacterial colonization of implantable medical devices. This work, in which I was involved, does not fall into the topic of this PhD manuscript and will not be discussed in details. However, the corresponding paper can be found in the annex section at the end of the manuscript.

II.3.2.2. Direct synthesis of 'silicone-based' polymers

S. Jebors and co-workers focused their attention on the synthesis of peptide-functionalized polysiloxane polymers obtained by polymerization of hybrid peptides functionalized with two chlorodimethylsilyl groups. These polymers were designed as 'silicone-based' polymers because they share the same repetitive motif $-(\text{Me})_2\text{Si}-\text{O}-\text{Si}(\text{Me})_2-$ with the most common silicone material, the polydimethylsiloxane (PDMS). Chlorodimethylsilanes undergo hydrolysis into hydroxydimethylsilanes and condensation to form siloxane bonds. The bis-functionalized peptides yielded silicone-peptide polymers (Figure 49) whose geometry (linear or comb-like) resulted from the position of the chlorodimethylsilyl moiety within the peptide sequence.³²⁵ Alternatively, comb-like silicone-peptide polymers could be obtained from dihydroxymethylsilyl hybrid peptides. This strategy was applied to the synthesis of antibacterial silicone-peptide polymers.³²⁷

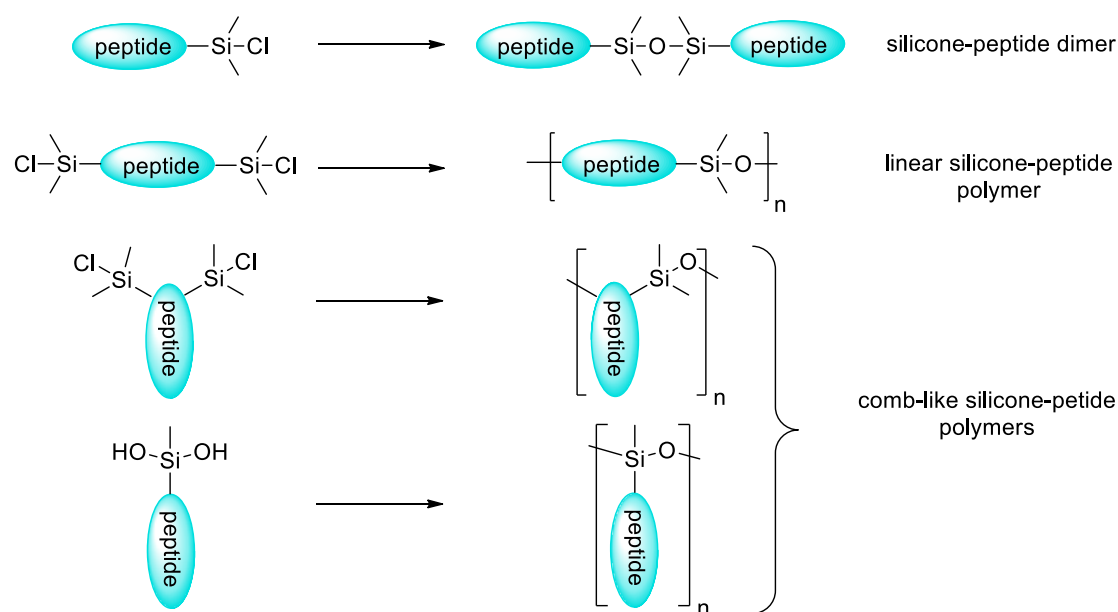


Figure 49. Silicone-based dimers and polymers obtained from chlorodimethylsilyl hybrid peptides or dihydroxymethylsilyl peptides^{325,327}

Interestingly, a monofunctionalized peptide could lead to silicone-peptide dimers. At the beginning of my PhD, although hybrid hydroxydimethylsilyl peptides were routinely used in the laboratory, the stability of the siloxane bond they form had never been investigated. On the contrary of ‘silicone-based polymers’ which were all insoluble in water and whose stability was difficult to evaluate in biological conditions, dimers were soluble and appeared to be an interesting model to study siloxane bond hydrolysis in different experimental conditions. This fundamental work was of interest to get an insight in the stability of the hydrogels that we wanted to develop. It could help to modulate hydrogel degradability or design systems for time-dependent release of active compounds.

II.4. Stability studies of siloxane bond and synthesis of bioactive dimers

Accordingly, we chose a simple model that possessed the same dimerization arm as the hybrid hydroxydimethylsilyl peptides developed in the team: the commercially available 1,3-bis(3-aminopropyl)tetramethyl disiloxane and its monomer (Figure 50). As this dimer was not soluble in water, we prepared its chloride and trifluoroacetate salts.

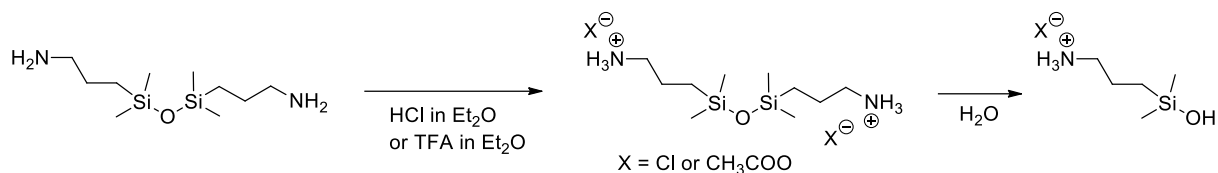


Figure 50. Preparation of the dimers used as models for the siloxane stability study and their hydrolysis into monomers

First, we needed to identify an analysis method suitable for the monitoring of dimer hydrolysis. The method should give two different quantitative signals for the monomer and the dimer. It should be non-destructive and allow analysis in different solvents (organic or aqueous), at different pHs. At last, it should be quick enough to allow correct sampling for kinetic studies. ²⁹Si NMR met the two first criteria. However, owing to the low natural abundance of ²⁹Si isotope and its weak detection sensitivity, ²⁹Si NMR analyses are long and do not address the last criterion. In this study, we demonstrated that ¹H NMR signals of the methylene and methyl groups connected to the silicon atom (CH₂-Si and Si-CH₃) can be used as sensitive probes to monitor the hydrolysis of dimers by ¹H NMR.

Hence, ¹H NMR kinetic studies allowed us to estimate the half-lives of the model dimer in dimethylsulfoxide (DMSO) and in water at different pHs. As expected, the dimer was stable in the absence of water (Figure 51). In aqueous solutions, the further the pH was to the neutrality, the faster was the hydrolysis. Importantly, at physiological pH, the dimer was rather stable with a half-life of about 439 h. In view of this stability, we envisioned biological applications for the dimers of hydroxydimethylsilyl peptides.

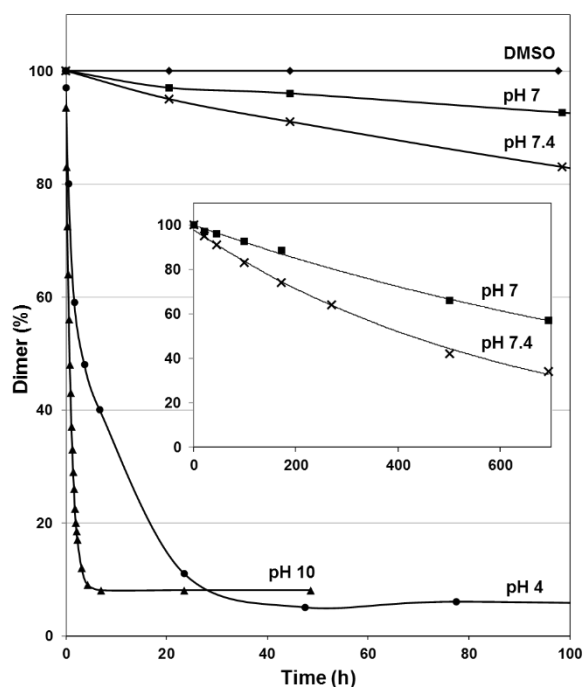


Figure 51. ¹H NMR studies of siloxane dimer hydrolysis

We showed that homodimers of peptides could be easily obtained from hydroxymethylsilyl peptides upon freeze-dried right after purification. It is well-known that homodimerization of a bioactive molecule can improve its pharmacological profile.³²⁸ Therefore, we functionalized the growth hormone releasing hexapeptide (GHRP-6) with a hydroxydimethylsilyl group at three different positions of the peptide sequence: C-terminal, N-terminal and intra-sequence through a modified lysine residue. Thus, we obtained three GHRP-6 dimers and found that they exhibited different *in vitro* behaviors, demonstrating thereby that the bioactivity of a drug can be modulated by its dimerization and more importantly by the position of the dimerization.

All these results are presented in detail in the enclosed publication entitled “Selective homodimerization of unprotected peptides using hybrid hydroxydimethylsilane derivatives” (RSC Advances).

Cite this: *RSC Adv.*, 2016, 6, 32905

Selective homodimerization of unprotected peptides using hybrid hydroxydimethylsilane derivatives†

Cécile Echalié,^{ab} Aleksandra Kalistratova,^{ac} Jérémie Ciccione,^{ab} Aurélien Lebrun,^a Baptiste Legrand,^a Emilia Naydenova,^c Didier Gagne,^a Jean-Alain Fehrentz,^a Jacky Marie,^a Muriel Amblard,^a Ahmad Mehdi,^b Jean Martinez^a and Gilles Subra^{*a}

We developed a simple and straightforward way to dimerize unprotected peptide sequences that relies on a chemoselective condensation of hybrid peptides bearing a hydroxydimethylsilyl group at a chosen position (either C-ter, N-ter or side-chain linked) to generate siloxane bonds upon freeze-drying. Interestingly, the siloxane bond sensitivity to hydrolysis is strongly pH-dependent. Thus, we investigated the stability of siloxane dimers in different experimental conditions. For that purpose, ²⁹Si, ¹³C and ¹H NMR spectra were recorded to accurately quantify the ratio of dimer/monomer. More interestingly, we showed that ¹H resonances of the methylene and methyl groups connected to the Si can be used as sensitive probes to monitor siloxane hydrolysis and to determine the half-lives of the dimers. Importantly, we showed that the dimers were rather stable at pH 7.4 ($t_{1/2} \approx 400$ h) and we applied the dimerization strategy to bioactive sequences. Once optimized, three dimers of the growth hormone releasing hexapeptide (GHRP-6) were prepared. Interestingly, their pharmacological evaluation revealed that the activity of the dimeric ligands could be switched from agonist to inverse agonist depending on the position of dimerization.

Received 7th March 2016
Accepted 23rd March 2016

DOI: 10.1039/c6ra06075g

www.rsc.org/advances

Introduction

Homodimerization of bioactive molecules is a well-known strategy to improve the pharmacological profile of the corresponding monomer. Dimerization was first applied to increase the local concentration of a ligand in the neighborhood of a receptor. In some reported cases, such a strategy leads to a large increase of the dimer affinity for its receptor. There are three hypotheses to explain such a phenomenon.¹ First, a dimer may connect two binding sites in close proximity (*i.e.* two receptors or an additional binding subsite). Alternatively, a dimer may first bind to a single receptor and help in the recruitment of another receptor. This is particularly relevant when signaling is initiated by receptor oligomerization.² At last, a “statistical binding effect” has to be taken into account: binding of a dimeric ligand is favored by the higher local concentration of binding elements at

the neighborhood of the receptor. The dimerization may also improve the stability towards proteases particularly in the case of peptide ligands and may affect the selectivity³ and the biological activity of the resulting compounds. Dimerization strategy was applied to numerous peptide hormones including serotonin,^{4,5} enkephalins,⁶ bradykinin,⁷ TGF- β .⁸ More recently, dimerization was also applied to the design of protein–protein interaction inhibitors.⁹ Several chemical strategies, in solution or on solid support, were used for peptide dimerization using specific functional groups and spacer arms. As examples of peptide dimer syntheses, we can cite the anchorage of a bifunctionalized spacer on a solid support and the simultaneous synthesis of the two ligand peptides from C to N-terminus,¹⁰ the coupling of two identical protected peptides which bear a single free reactive function on a bifunctionalized spacer.⁷

In this study, we focused our efforts on an alternate dimerization process based on hydroxydimethylsilane peptides. To our knowledge, most of the existing strategies require orthogonal protecting groups and multistep procedures to obtain homodimeric peptides at the exception of dimerization of unprotected peptide sequence containing cysteine residue through the formation of a disulfide bond.¹¹ Advantageously, the use of dimethylhydroxysilane peptides allows the dimerization of any peptides, even those containing a Cys residue and greatly simplifies and speeds up the process. Indeed, dimerization occurs chemoselectively in the presence of unprotected side chains.

^aInstitut des Biomolécules Max Mousseron (IBMM), UMR5247 Université de Montpellier, CNRS, ENSCM, Faculté de Pharmacie, 15 avenue Charles Flahault, 34093 Montpellier, France. E-mail: gilles.subra@univ-montp1.fr; Tel: +33 4 11 75 96 06

^bInstitut Charles Gerhardt (ICGM), UMR5253 Université de Montpellier, CNRS, ENSCM, Place Eugène Bataillon, 34095 Montpellier, France. Tel: +33 4 67 14 38 32

^cUniversity of Sofia, boulevard “Sveti Kliment Ohridski” 8, Sofia, Bulgaria

† Electronic supplementary information (ESI) available: NMR spectra, kinetic studies, compound characterization, monomeric ligand binding assays and bioactivity. See DOI: 10.1039/c6ra06075g

Moreover, it is of particular interest that hybrid dimethylhydroxysilane monomers are prepared by classical peptide synthesis and can be purified before dimerization. We recently applied this strategy to the synthesis of linear and branched peptide-polymers and tripeptide dimers.¹² In this work, we aimed at demonstrating that the strategy is not only applicable to the synthesis of N-ter dimers but also to C-ter and internal bioactive peptide sequence dimerization. Interestingly we proved here that siloxane formation simply occurred during lyophilization after preparative RP-HPLC of the hybrid monomer. The ²⁹Si NMR signals were different in siloxane bonds and silanols but we demonstrated that, ¹H NMR could be used advantageously to measure the SiOH/SiOSi ratio. Thanks to quick and sensitive ¹H NMR analyses, we monitored the stability of siloxane bonds in different solvents but more importantly in water at various pHs. At last, we synthesized three types of dimers based on the sequence of the growth hormone releasing hexapeptide (GHRP-6). The dimerization strategy was applied at three different positions of the peptide sequence: C-terminal, N-terminal and intra-sequence through a modified lysine residue (Scheme 1). Then, the binding and signaling properties of these dimers were evaluated on intact HEK293T cells expressing the growth hormone secretagogue receptor 1a (GHS-R1a) involved in important physiological pathways.¹³

Materials and methods

All solvents and reagents were used as supplied. Solvents used for LC/MS were of HPLC grade. Dichloromethane (DCM); *N,N*-dimethylformamide (DMF) were obtained from Carlo Erba. Fmoc amino acid derivatives, [benzotriazol-1-yloxy(dimethylamino)methylidene]dimethylazanium hexafluorophosphate (HBTU), Fmoc-Rink amide CM resin, 2-chloro chlorotrityl PS resin, were purchased from Iris Biotech (Marktredwitz, Germany). Diisopropylcarbodiimide (DIC), diisopropylethylamine (DIEA), trifluoroacetic acid (TFA) were obtained from Sigma-Aldrich (St. Louis, MO, USA). Hexafluoroisopropanol (HFIP) and triisopropylsilane (TIS) were obtained from Alfa Aesar and Acros respectively. 3-Isocyanatopropyl dimethylchlorosilane was purchased from Sikemia (France).

The following abbreviations were used: ICPDMCS – isocyanatopropyl dimethylchlorosilane. Other abbreviations used are recommended by the IUPAC-IUB Commission.

Peptide synthesis

Microwave assisted peptide syntheses were performed using Fmoc/*t*Bu SPPS strategy on a Liberty™ Microwave Peptide Synthesizer (CEM Corporation, Matthews, NC) providing MW irradiation at 2450 MHz. Temperature consign was set up at 70 °C as previously described.^{14,15}

Ethane-1,2-diamine anchoring on chloro-2-chlorotrityl PS resin

The chloro-2-chlorotrityl chloride PS resin (4.00 g, 8.8 mmol, initial theoretical loading = 2.2 mmol g⁻¹) was conditioned for

15 min in DCM. The resin was filtered and a solution of ethane-1,2-diamine (1.175 mL, 17.6 mmol, 2 eq.) in DMF (40 mL) containing DIEA (3.060 mL, 17.6 mmol, 2 eq.) was added. The resin was stirred overnight and washed with DMF (2×), DCM/MeOH 1/1 v/v (2×), DMF (2×), DCM (2×) and dried overnight *in vacuo*. The experimental loading of the resin was determined after the first amino acid coupling. Optical density of dibenzofulvene-piperidine adduct formed during Fmoc deprotection with a piperidine/DMF 2/8 v/v solution was measured at 299 nm and the loading was calculated according to a previously reported method.¹⁵

Coupling step

On a 0.1 mmol resin scale (either H-Rink amide ChemMatrix resin 1.2 mmol g⁻¹ or H₂N(CH₂)₂NH-chlorotrityl-PS resin 0.8 mmol g⁻¹), coupling reactions were performed with 5 eq. of amino acid (0.5 mmol, 2.5 mL of 0.2 M solution in DMF), 5 eq. of HBTU (0.5 mmol, 2.5 mL of 0.2 M solution in DMF), and 10 eq. of DIEA (1 mmol, 0.5 mL of 2 M NMP solution). Resin was stirred for 90 minutes at room temperature or heated at 70 °C under microwave irradiation (50 W) for 10 minutes. The resin was filtered and then washed with DMF (2×) and DCM (2×).

Fmoc deprotection step

Fmoc removal was carried out in DMF/pip 8/2 v/v solution for 3 minutes under stirring, at room temperature. The resin was filtered and a DMF/pip solution was added again and stirred for 20 minutes. When MW irradiation was used (50 W, 70 °C), two cycles of 30 s and 3 minutes were used. In both cases, the resin was filtered and then washed with DMF (2×) and DCM (2×).

Alloc deprotection

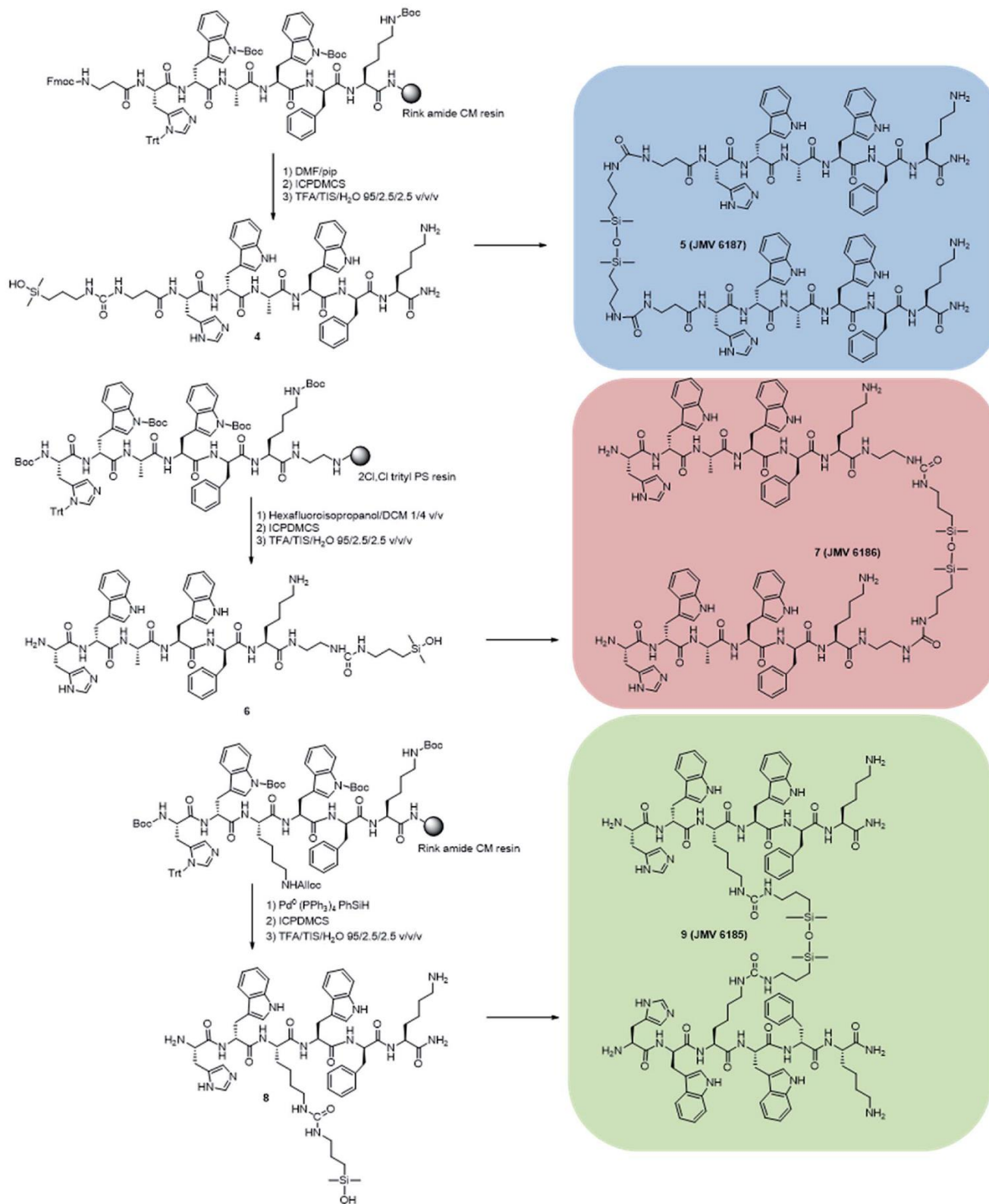
The Alloc lysine side-chain protecting group of the peptide anchored on a Rink amide resin was removed selectively. Phenylsilane (20 eq.) was added to a solution of Pd(PPh₃)₄ (0.1 eq.) in DCM (4 mL g⁻¹ of resin). The resulting solution was poured on the peptidyl-resin (1 eq.) in an open vessel. The resin was stirred for 2 h and then washed with DCM (2×) and DMF (2×). A solution of potassium *O*-ethyl dithiocarbonate in DMF (50 mg in 10 mL) was added and the resin was stirred for 20 minutes before final washings with DMF (2×) and DCM (2×).

HFIP-mediated cleavage of protected peptide from 2-chlorotrityl resin

The peptidyl-resin was stirred in a solution of hexafluoroisopropanol/DCM 1/4 v/v (40 mL g⁻¹ of resin) for 30 min. The resin was filtered. The solution was concentrated under vacuum to yield the protected peptide.

Silylation in solution

The peptide to be silylated was solubilized in anhydrous DMF under argon. DIEA (4 eq.) and 3-isocyanatopropylchlorodimethylsilane (1 eq.) were added. The released hydrogen chloride released was removed under an argon flow. The



Scheme 1 Synthesis of GHRP-6 peptide homodimers based on dimethylhydroxysilyl peptides. 5: N-terminal dimerization; 7: C-terminal dimerization; 9: internal residue dimerization.

mixture was stirred for 2 h and then concentrated under vacuum. The hybrid peptide was precipitated by addition of diethyl ether and dried under vacuum.

Side-chain deprotection in solution

Side-chain amino acid protecting groups were removed in TFA/triisopropylsilane/H₂O 95/2.5/2.5 v/v/v. After 30 minutes under

stirring, the solution was concentrated under vacuum. The unprotected dimethylhydroxysilyl peptide was precipitated in diethyl ether and dried under vacuum.

Silylation on solid support

3-Isocyanatopropylchlorodimethylsilane (3 eq.) was added in a solution of DIEA (3 eq.) in anhydrous DMF (10 mL g⁻¹ of resin). The resulting solution was poured on the peptidyl resin and the resin was stirred overnight before being filtered and washed with DMF (2×) and DCM (2×).

Cleavage from Rink amide ChemMatrix resin along with side-chain deprotection

The peptide was cleaved from Rink amide ChemMatrix resin in TFA/triisopropylsilane/H₂O 95/2.5/2.5 v/v/v. The resin was stirred in the cleavage mixture for 2 × 2 h. The resin was filtered and the solution was concentrated under vacuum. The unprotected peptide was precipitated by addition of diethyl ether.

Purification

Hybrid hydroxydimethylsilyl-peptides were purified by preparative chromatography. Purifications were performed using a Waters HPLC 4000 instrument, equipped with a UV detector 486 and a Waters Delta-Pack 40 × 100 mm, 100 Å, 15 µm, C18 reversed-phase column using a flow rate of 50 mL min⁻¹. Solvents employed were water/0.1% TFA and ACN/0.1% TFA. UV detection was performed at 214 nm. Only the hybrid monomers were recovered. Condensation into dimers occurred after purification, during lyophilization.

NMR analysis

NMR samples contained 0.06 mmol (3-aminopropyl)dime-thylsilyl compounds dissolved in DMSO-*d*₆ or D₂O (600 µl). The ²⁹Si, ¹³C and ¹H spectra were collected on a Bruker AVANCE III 600 MHz spectrometer at 298 K. Peptide dimers (4 µmol) were dissolved in DMSO-*d*₆ and spectra were collected on a Bruker AVANCE III HD 400 MHz spectrometer at 298 K. Both spectrometers were equipped with a 5 mm BroadBand Observation BBFO probe. The deuterated solvent was used as an internal deuterium lock. Chemical shifts are given in δ ppm calibrated with residual protic solvent (e.g., DMSO: 2.50 ppm). A quantitative inverse-gated experiment was used for ²⁹Si NMR using a recovery delay of 60 s (128 scans with a spectral width of 5950 Hz). The same sequence was used for quantitative ¹³C NMR with the same recovery delay (64 scans with a spectral width of 15 120 Hz). For determination of silicon chemical shifts, a DEPT sequence was used to benefit from the polarization transfer of hydrogens near the silicon atom (256 scans, spectral width of 11 900 Hz and recovery delay of 2 s). ¹H NMR spectra were typically recorded using 16 scans with a spectral width of 6000 Hz and a recovery delay of 2 s. Spectra were processed and visualized either with Topspin 3.2 (Bruker Biospin) on a Linux station or with MestReNova 6.0.2 (Mestrelab research).

Ligand binding assay

K_i values were determined from binding competition experiments performed on intact HEK293T cells expressing the GHS-R1a using a Homogenous Time Resolved Fluorescence (HTRF) assay as previously described.¹⁶ The HTRF signal was collected in a PHERAstar microplate reader (BMG LABTECH). K_i values were obtained from binding curves using GraphPad Prism software (GraphPad Software, Inc., San Diego, CA).

Inositol phosphate assay

Inositol phosphate accumulation assay was carried out 48 h after transfection on adherent cells in 96-well plates at a density of 50 000 cells per well. IP1 production was measured using the IP-One HTRF kit (Cisbio Bioassays) as previously described.¹⁶ Briefly, cells were stimulated for 30 min at 37 °C with the ligand to be tested in 70 µl of IP1 stimulation buffer. An anti-IP1 antibody labelled with Lumi4-Tb (15 µl) and an IP1-d2 derivative (15 µl), were added on cells. The medium was incubated for 1 h at room temperature. Signals at 665 nm and 620 nm were detected using a PHERAstar (BMG LABTECH) fluorescence reader. Values are expressed as Δ*F*. Δ*F* corresponded to: (ratio 665 nm/620 nm of the assay – ratio 665 nm/620 nm of the negative control)/ratio 665 nm/620 nm of the negative control. The negative control corresponded to the Lumi4-Tb blank and was used as an internal assay control. Inositol phosphate accumulation was expressed as the percentage of the maximal ghrelin response using the formula: (Δ*F* mock cells – Δ*F* receptor transfected cells)/(Δ*F* mock cells – Δ*F* maximal ghrelin stimulation for receptor transfected cells). EC₅₀ values were determined from dose–response curves using GraphPad Prism software (GraphPad Software, Inc., San Diego, CA).

Results and discussion

In the frame of this study, characterization of the dimeric siloxane species was of first importance. *In vitro* biological assays mostly require small quantities of bioactive compounds and thus, peptide analogues to be tested are mostly synthesized at a small scale (<0.1 mmol). In this context, sensitive and non-destructive methods have to be privileged. In a general manner, NMR is the method of choice considering nuclei having detectable isotopes of high abundance. The distinction between dimethylsiloxane (dimer) or hydroxydimethylsilane (monomer) could be achieved by ²⁹Si NMR; chemical shifts being different between a monomer and a dimer. However, due to the low natural abundance and the rather weak detection sensitivity of ²⁹Si isotope, ²⁹Si NMR analyses was not sufficient for a convenient characterization of hybrid peptides, their corresponding dimers and the study of the dimers stability. Thus, despite a narrow spectral width and the numerous peptides resonances in the ¹H dimension, we first showed that quick ¹H NMR analyses allowed us to readily quantify the relative proportions of monomers and dimers both in D₂O and DMSO-*d*₆ and to measure the half-lives of the dimers in different conditions. Indeed, the ¹H resonances of methylene and methyl groups connected to the Si allow to discriminate the dimeric from the monomeric peptide state.

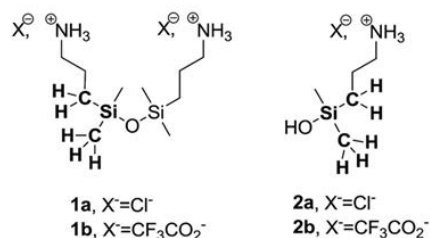


Fig. 1 Model compounds for NMR determination of ¹H, ¹³C and ²⁹Si shifts. Representative atoms of interest for the identification of both dimer and monomer are marked in bold.

²⁹Si, ¹³C and ¹H NMR chemical shifts assignment of (3-aminopropyl)dimethylsilyl compounds as model for the hybrid peptide characterization

First, we assigned the NMR chemical shifts of the simple model 1,3-bis(3-aminopropyl)tetramethyl disiloxane (Fig. 1) and its monomer, which possessed the same dimerization arm as the hybrid peptides of the study.

Compound **1a** was obtained from commercially available 1,3-bis(3-aminopropyl)tetramethyl disiloxane poured into hydrogen chloride ether solution. On the contrary of its neutral counterpart, **1a** was soluble in water enabling the NMR analysis in aqueous solutions. Compound **1a** was solubilized either in DMSO-*d*₆ or D₂O and analyzed by ¹H, ¹³C and ²⁹Si NMR. Results are reported in Table 1 (first column, dimer **1a**). As expected, when compound **1a** was left in D₂O for a prolonged time, monomer **2a** appeared upon hydrolysis. This latter was analyzed by NMR (Table 1). Hydrochloric acid was added to dimer **1a** in DMSO-*d*₆ to force hydrolysis and subsequently identify the chemical shifts of monomer **2a** (Table 1). Since all the peptides were purified in trifluoroacetic acid-containing solvents and therefore recovered as trifluoroacetate salts, dimer **1b** was also prepared. It was prepared from 1,3-bis(3-aminopropyl)tetramethyl disiloxane poured into trifluoroacetic acid ether solution and solubilized in DMSO-*d*₆ or D₂O. Partial hydrolysis occurred with time and the mixture of monomer **2b** and dimer **1b** was analyzed by ¹H, ¹³C and ²⁹Si NMR. Chemical shifts of monomer **2b** and dimer **1b** are reported in Table 1.

Analyses of monomer/dimer mixtures by ²⁹Si NMR showed two signals at 8.0 and 10.8 (±0.1) ppm in DMSO-*d*₆ and 11.4 and 18.1 (±0.1) ppm in D₂O that corresponded to the silicon signal involved in siloxane Si–O–Si and hydroxysilane Si–OH bonds respectively

(Fig. 2). Whatever the conditions of analysis, ²⁹Si NMR unambiguously allowed the identification of hybrid monomeric and dimeric species. The ¹³C NMR spectra also allowed us to readily discriminate the monomer from the dimer signals looking at the methyl and the methylene resonances connected to the Si. ²⁹Si and ¹³C NMR have the advantage to display a large spectral width and only few ²⁹Si and ¹³C signals are present in our systems. Nevertheless, due to the low natural abundance (4.7% and 1.1%, respectively) and low NMR sensitivity of ²⁹Si and ¹³C, long acquisition times are required even at 0.1 M concentration. In this context, we investigated the characterization of all derivatives using ¹H NMR spectra which are far more sensitive than ²⁹Si and ¹³C NMR despite a narrowest spectral width and the larger number of ¹H resonances. In this context, we switched our attention to the NMR signals of the hydrogen on carbon atoms in alpha position to the silicon atoms (Fig. 1). Interestingly, ¹H chemical shifts of –CH₂Si and CH₃Si of the monomer and dimer were localized in a rather clear region of the ¹H NMR spectra of the hybrid peptides (≤0.7 ppm) (Table 1). These resonances should not overlapped with those of the methyl groups of the Leu, Ile and Val expected around 0.7–0.8 ppm. In addition, we showed with the model compounds **1a–b** and **2a–b** that in DMSO-*d*₆ ¹H NMR chemical shifts of the monomer and dimer were clearly different whatever the amine counter-ion, thereby hybrid dimers and monomers could be unambiguously identified by a simple ¹H NMR. In D₂O, ¹H NMR methyl signals of monomer and dimer as hydrochloride salts were partially overlapped. However, the counter-ion switch from hydrochloride to trifluoroacetate induced a splitting of monomer and dimer signals (ESI Fig. S22†). As a consequence, TFA salts should be preferred for a better signal separation in D₂O. In contrast to the ²⁹Si and the ¹³C resonances, the ¹H chemical shifts values of the –CH₂Si (~0.7 ppm) and CH₃Si (~0.2 ppm) were rather close in both species and sensitive to the pH which could lead to confusion between monomer and dimer during assignment. When both monomer and dimer were present, signal assignment was easy as NMR peaks always came out in the same order: in D₂O, dimer protons were typically more shielded than monomer hydrogens. In case of any doubt about a sample containing only one species, ²⁹Si NMR analyses had to be undertaken. In order to significantly decrease the experiment time, we used a DEPT24 sequence instead of the typical ²⁹Si quantitative sequence (ESI Fig. S23†).

When both monomer and dimer are present in a sample, determination of their proportion is valuable. For that, we

Table 1 ¹H, ¹³C and ²⁹Si NMR shifts (in ppm) of siloxane dimer **1** and monomer **2**

Solvent	Nucleus	Dimer 1a		Monomer 2a		Dimer 1b		Monomer 2b	
		–CH ₂ Si	CH ₃ Si	–CH ₂ Si	CH ₃ Si	–CH ₂ Si	CH ₃ Si	–CH ₂ Si	CH ₃ Si
DMSO- <i>d</i> ₆	¹ H	0.53	0.06	0.48	0.00	0.52	0.06	0.48	0.01
	¹³ C	14.6	0.2	14.5	0.0	14.5	0.1	14.4	–0.1
	²⁹ Si		8.0		10.9		8.0		10.8
D ₂ O	¹ H	0.71	0.22	0.74	0.23	0.70	0.21	0.72	0.22
	¹³ C	13.6	–1.2	12.9	–2.3	13.6	–1.2	12.9	–2.3
	²⁹ Si		11.4		18.2		11.4		18.1

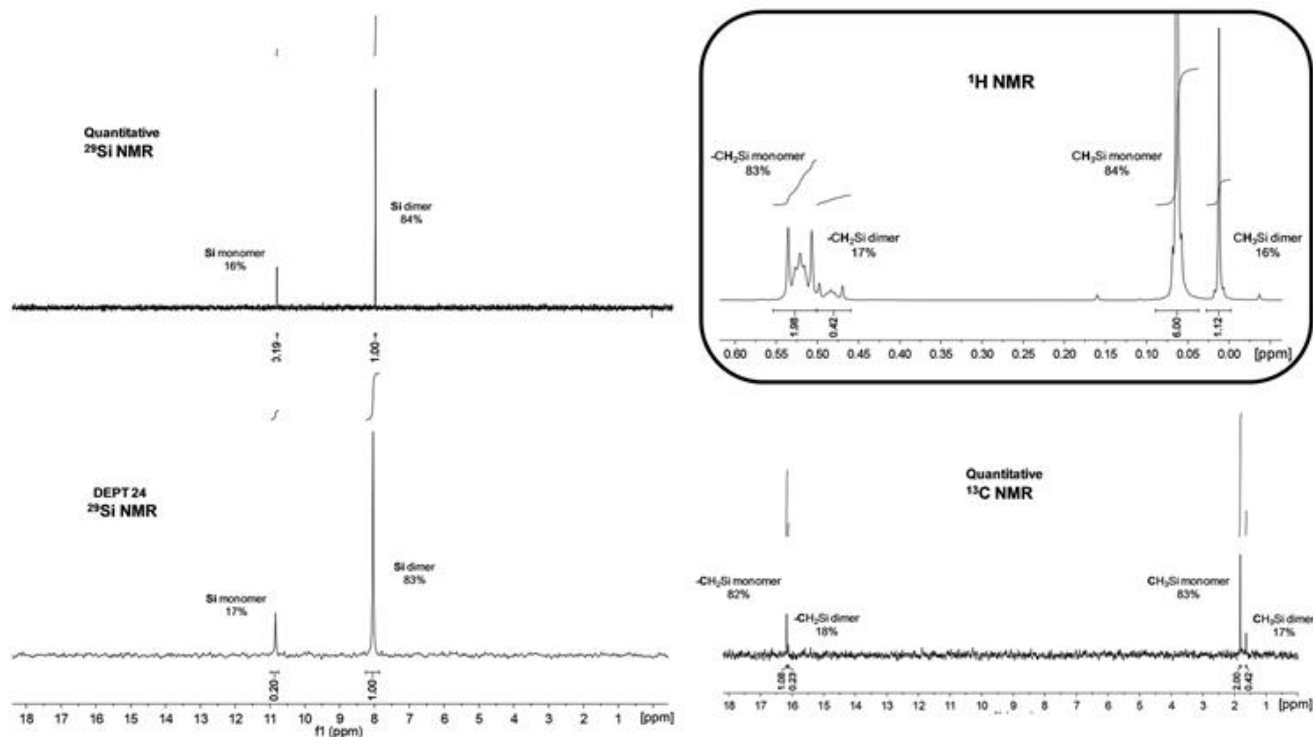


Fig. 2 ^{29}Si , ^{13}C and ^1H NMR spectra of the dimer **1b**/monomer **2b** mixture recorded in $\text{DMSO}-d_6$. Chemical shifts of relevant signals (protons, carbons, and silicon atoms of $-\text{CH}_2\text{Si}$ and CH_2Si) are reported in Table 1. Integrations suggested that the sample contained 83% of dimer **1b** and 17% of monomer **2b**.

used ^{13}C and ^{29}Si quantitative sequences which require long acquisition times. Interestingly, the ^{29}Si DEPT sequence was not expected to be quantitative; however we noticed that when applied to our hybrid systems, signal integrations reflected the proportion of monomer and dimer in the sample (Fig. 2, ^{29}Si spectra). To go further, signal integrations of ^1H spectra were compared with ^{29}Si NMR spectra. Interestingly, integration of NMR signals related to dimer or monomer showed that the monomer/dimer ratio was unchanged (Fig. 2). Thus, ^1H could be used to determine the proportion of monomer and dimer in a sample. This was particularly advantageous for kinetic studies where high rate sampling was required to monitor the hydrolysis of siloxane bond. Indeed, long acquisition times provided an average ratio that did not make sense when sample evolution was fast. Furthermore, due to the high sensitivity of ^1H NMR, the spectra always presented a higher ratio signal to noise by comparison to those of ^{29}Si , which led to a lower detection limit and more accurate integrations.

We showed that simple ^1H NMR can be routinely used to analyze hybrid peptides and quantify hydroxydimethylsilane/dimethylsiloxane ratio. The presence of TFA salts seemed to be preferable in D_2O for a better signal separation. However, when possible, $\text{DMSO}-d_6$ should be preferred as solvent since chemical shifts in $\text{DMSO}-d_6$ were less sensitive to salts and pH, resulting in an easier signal assignment. The analysis of hybrid peptide ligands (**4**–**9**) used for biological assays was performed by ^1H NMR in $\text{DMSO}-d_6$.

Stability studies of the siloxane bond in different solutions by ^1H NMR

The applicability of the dimerization method based on the dimethylhydroxysilane peptides is subjected to the stability of the siloxane bond towards hydrolysis. It is well known that acid- or base-catalyzed polycondensation reactions are reversible and the hydrolysis rate of siloxanes is pH-dependent. This phenomenon was well studied in silica matrixes which quickly dissolve in alkali aqueous solution ($\text{pH} > 10$).¹⁷ However, to the best of our knowledge, no general study was reported for the type of siloxane bonds we used in the dimerization arm. Thus, we investigated the kinetic of hydrolysis of the 1,3-bis(3-aminopropyl)tetramethyl disiloxane in water at different pH by ^1H NMR (Fig. 3). First of all, dimer **1a** was dissolved in $\text{DMSO}-d_6$ and ^1H NMR analyses were carried out regularly for one week. No monomer was detected, which confirmed the dimer was stable in the absence of water. This result was in agreement with what we already observed on siloxane polymers.¹² In the presence of water, dimer **1** was hydrolyzed. To study the influence of pH on the dimer hydrolysis rate, dimer **1a** was dissolved at 0.1 M in D_2O at pH 4, 7, 7.4 and 10. ^1H signals from the $-\text{CH}_2\text{Si}$ group of monomer and dimer were integrated and the dimer percent was plotted as a function of time (Fig. 3).

As expected, the closer the pH was to the neutrality, the slower was the dimer hydrolysis. When the media is moved to acidic and basic pH (4 and 10, respectively), the hydrolysis rate increased, particularly in basic medium. The half-life of dimer **1a** was 203 min at pH 4 and 54 min at pH 10. Most of the time, bioactive

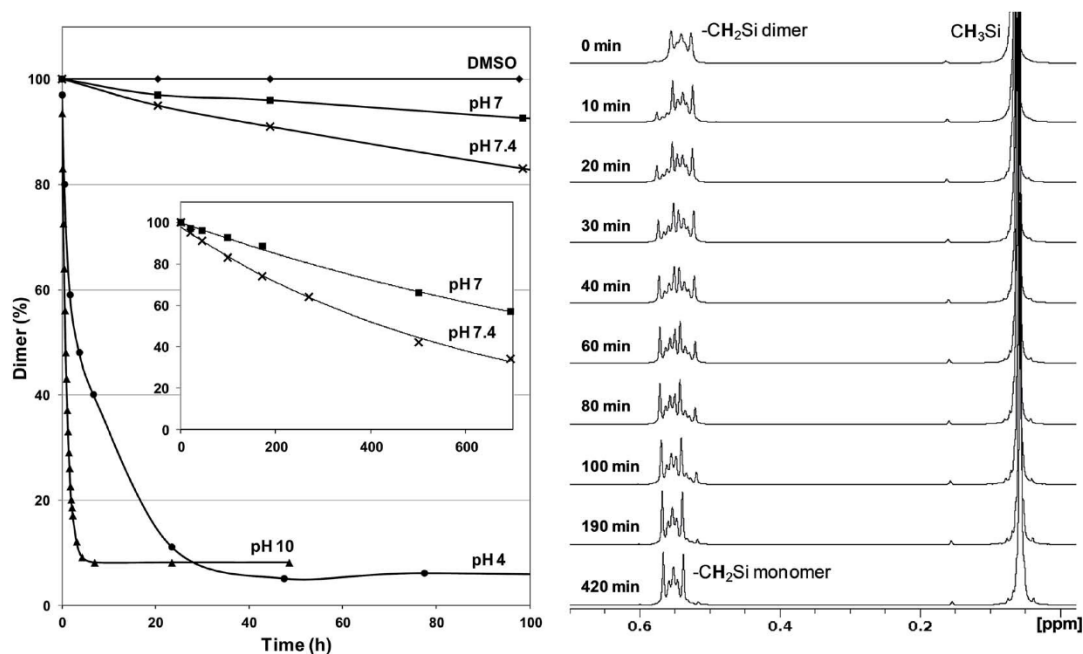


Fig. 3 ¹H NMR kinetic studies. Left panel: dimer percent reported as a function of time. ◆ DMSO; ■ pH 7; × pH 7.4; ● pH 4; ▲ pH 10. Full sets of data for pH 7 and 7.4 are presented in the box. Right panel: ¹H NMR spectra at pH 10.

peptides are administered intravenously. As a consequence, a good stability of hybrid peptide dimers at blood pH was mandatory. Importantly, at pH 7.4, the half-life of dimer **1a** was 439 h, with less than 10% of hydrolysis within 2 days. This stability allows envisioning biological applications for hybrid dimers.

In order to mimic the RP-preparative HPLC experimental conditions, the behavior of dimer **1a** in more acidic conditions (pH 2) was studied. As expected a few minutes after solubilization of dimer **1a** in D₂O/0.1% TFA, only monomer was detected (Fig. S33[†]). Thus, when RP-preparative HPLC is required, hybrid compounds need to be purified as monomer species prior to dimerization.

Synthesis of GHRP-6 analogues

Having studied the stability of the dimer **2** at physiological pH, we decided to apply this strategy of dimerization to a relevant bioactive sequence. We selected the growth hormone releasing hexapeptide (GHRP-6) of sequence H-His-DTrp-Ala-Trp-DPhe-Lys-NH₂. Both binding properties and bioactivity of dimers was assayed on intact HEK293T cells expressing the GHS-R1a. Apart

from controlling growth hormone secretion, this receptor is involved in many physiological processes such as energy homeostasis,¹⁸ glucose metabolism,¹⁹ gastric acid secretion²⁰ and cardiovascular activity.²¹ Besides, the study of this ligand/receptor system is particularly relevant to witness an eventual switch in the behavior of dimer analogues depending on their structure. Indeed GHSR-1a possesses a remarkable high constitutive activity. Indeed, ~50% of its maximal activity is observed in the absence of its natural agonist, ghrelin (Ghr).²²

We evaluated the impact of GHRP-6 dimerization in terms of binding affinity and more importantly, in terms of bioactivity. Indeed, we hypothesized that, depending on the position of the bridge between monomers, the agonism behavior of GHRP-6 sequence could be impacted. To answer these questions, three hybrid derivatives of GHRP-6 were prepared (Fig. 4).

Peptide sequences of the three hybrid derivatives of GHRP-6 were prepared on solid support by conventional Fmoc/*t*Bu strategy. For N-terminus dimerization, a β-alanine spacer was added after the last amino acid and the peptidyl resin was reacted with the 3-isocyanatopropyl dimethylchlorosilane

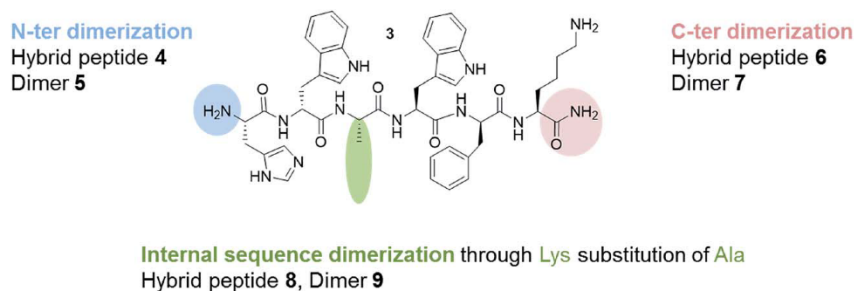


Fig. 4 Peptide **3**, H-His-DTrp-Ala-Trp-DPhe-Lys-NH₂ (GHRP-6) and potential points of dimerization.

(ICPDMCS) to yield the hybrid monomer **4** after cleavage and side-chain deprotection. In contrast, the C-terminus modification was performed through introduction of an ethylene diamine. For that purpose, ethane-1,2-diamine was anchored on 2-chloro chlorotriyl PS resin and the sequence was elongated to the N-terminus *via* conventional Fmoc/*t*Bu SPPS. The N-Boc, fully protected peptide was cleaved from the solid support by mild acidic treatment (HFIP/DCM 1/4 v/v, 30 min) to maintain the side chain protecting groups. The protected peptide was then reacted with ICPDMCS in solution, precipitated in diethyl ether and treated by TFA to remove the side-chain protecting groups to yield the hybrid peptide **6**. To conserve the N and C-termini unchanged, dimerization within the peptide sequence was performed, which might induce a non-negligible steric hindrance in the center of the sequence. Alanine residue in position 3 of GHRP-6 was swapped with a lysine, which served as anchoring point for ICPDMCS. Selective removal of Alloc protecting group on the Lys³ side-chain was performed with phenylsilane and Pd⁰(PPh₃)₄ on the sequence still anchored on solid support. The ε-amino group was reacted with ICPDMCS before cleavage of the hybrid peptide from Rink amide resin, yielding hybrid peptide **8**.

In all cases, the last step of the synthesis of dimethylhydroxysilyl hybrid peptides was a TFA treatment, which removed the acid sensitive protecting groups of the side chains and cleaved the linker when the synthesis was entirely performed on solid support (compounds **4** and **8**). TFA was removed under reduced pressure and the hybrid peptide was recovered as its monomeric form by precipitation in diethyl ether. Hybrid monomers **4**, **6** and **8** were purified by preparative RP HPLC. We then applied the dimerization procedure by solubilization of the hybrid peptide monomers in aqueous solution at pH 7.4 at high concentration (>0.2 M) as previously described for polymers obtained from bis-silylated precursors.¹² In most cases, a precipitate appeared at this stage and condensation products were recovered by centrifugation. This procedure proved to be efficient for dimer **5**, which precipitated and was recovered by centrifugation with good yield (90%). Only dimer **5** was observed by ¹³C NMR. However, a more sensitive ¹H NMR analysis indicated the presence of 3% of monomer **4**. Unfortunately, no precipitation occurred for dimers **7** and **9**, probably because of the presence of the free N-terminal amine, which enhanced water solubility.

Optimization of the dimerization

We hypothesized that the condensation could also happen during lyophilization. To verify it, a solution of the model

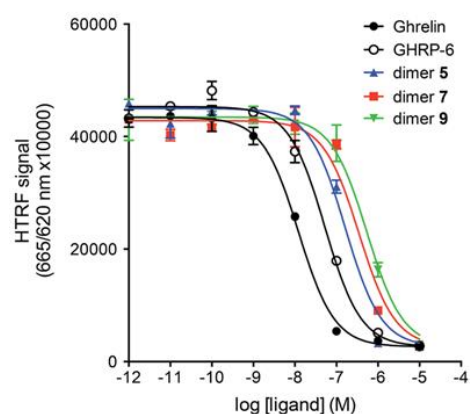


Fig. 5 Binding of dimer ligands to GHS-R1a. Ligands affinities were determined by HTRF-based competition binding assay performed on intact HEK293T cells as described in Materials and methods. Results are from one representative experiment of three, each performed in triplicate.

monomer **2a** was analyzed by ¹H NMR before and after freeze-drying (ESI Fig. S34†). The percent of dimer increased from 6% to 100% upon lyophilization. As a consequence, the lyophilization constitutes an easy procedure to obtain dimers directly from hybrid monomers species. This procedure was applied to the synthesis of three analogues of the growth hormone releasing hexapeptide (GHRP-6). In agreement with these results, monomers **6** and **8** were purified by preparative HPLC to get rid of buffer salts used during the precipitation attempts. They were freeze-dried at a concentration of 0.1 mM approximately. After lyophilisation, dimer **7** and dimer **9** were obtained. ¹H NMR analysis revealed that 10% of monomer was still present in both cases. However, they were used without further processing for biological studies.

Binding property of ligands

The affinity of ligands was determined by competition binding assay on HEK293T cells expressing the Growth Hormone Secretagogue type 1 receptor (GHS-R1a). Competition binding curves are reported in Fig. 5 and binding affinities are reported in Table 2.

First of all, all dimers were able to bind to ghrelin receptor in the 100 nM range. However, compared to GHRP-6, a 5 to 10-fold decrease of binding was observed for compounds **5** and **7**. Internal dimerization (compound **9**) induced a 15-fold loss of affinity. N-Terminus dimerization (compound **5**) had the less impact on the binding affinity. These results could be related to the steric hindrance of the dimeric molecule to approach GHS-

Table 2 Binding properties of dimers compared to GHRP-6 and ghrelin

Compound	N-ter dimer 5 JMV 6187	C-ter dimer 7 JMV 6186	Internal dimer 9 JMV 6185	Compound 3 GHRP-6	Ghrelin
K_i^a (nM)	59.7 ± 21.4	173 ± 2	319.5 ± 49.5	18.8 ± 8	7.8 ± 1.8

^a K_i values (mean ± S.E.M)s were obtained from competition binding curves analysis with GraphPad Prism v5 software.

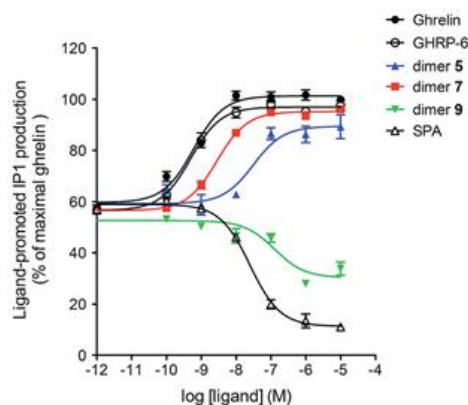


Fig. 6 Signaling property of ligands. Efficacy of ligands to stimulate IP1 production was measured on HEK293T cells expressing the GHS-R1a as described in Materials and methods. Results are one representative experiment of three, each performed in triplicate.

R1a binding sites, the transmembrane region 3 of the GHS-R1a in which peptide ligands and small molecules can bind.²³ However, binding behavior cannot be associated to bioactivity by a direct relationship. We thus investigated the biological activity of the ligands by measuring their ability to promote inositol phosphate (IP) production in HEK293T cells expressing the GHS-R1a. The production of IP, reported as % of ghrelin-induced maximal responses, are reported in Fig. 6 and summarized in Table 3. The peptide [*D*-Arg¹, *D*-Phe⁵, *D*-Trp^{7,9}, Leu¹¹]-substance P (noted SPA for substance P analogue)²⁴ is a non selective ligand of GHS-R1a, which behaves as an inverse agonist. It was also included in the same experiments.

Interestingly very different behaviors were obtained for the three dimers. N-Terminal dimer 5 which was the best binder within the dimer series, proved to be a partial agonist with an EC₅₀ of 20 nM. It induced 86.5 ± 2.7% of the maximal effect of the ghrelin. In contrast, the C-terminal dimer 7, which had a three-fold lower affinity for GHS-R1a, was a full agonist with an EC₅₀ of 2.57 nM, close to that of GHRP-6 (1.2 nM). The most striking result was obtained with dimer 9, which behaved as an inverse agonist with an efficacy of 38 ± 3% (Table 3). Interestingly, it was reported that the peptide *D*-Lys³-GHRP-6 displayed some inverse agonist activity in the sea bream²⁵ but behaved as an antagonist in mammals.^{26,27} In the case of dimer 9, a *L*-lysine was introduced as an anchoring point of the dimethylhydroxysilane moiety. Therefore, it could not be excluded that the inverse agonist effect was not induced by dimerization but simply by the Lys/Ala substitution, even though the stereochemistry was not the same (*D*-Lys in the reported monomeric inverse agonist and *L*-Lys in the dimer 9). Thus, to know the significance of either the dimerization or the modification of the linear sequence itself in inducing the inverse agonist activity, two other compounds were prepared (Fig. 7). Compound 10 was obtained in the same way as monomer 8 except isocyanopropyltrimethylsilane was used instead of ICPDMCS for the formation of the urea bond. Lys³-GHRP-6 (compound 11) was also prepared. Bioactivity of 10, 11 and of Lys³ *N*-ε acetylated analogue 12 was also evaluated on HEK293T cells expressing the GHS-R1.

Interestingly none of them displayed any inverse agonist activity and all behaved as neutral ligands (ESI Fig. S54†). This last result showed that the dimerization in itself induced a complete switch of activity and the position of the

Table 3 Efficacy of ligands to stimulate inositol phosphate production

Compound	N-ter dimer 5 JMV 6187	C-ter dimer 7 JMV 6186	Internal dimer 9 JMV 618	SPA	Compound 3 GHRP-6	Ghrelin
EC ₅₀ ^a (nM)	20.4 ± 6.8	2.57 ± 0.35	160 ± 44	27 ± 2	1.18 ± 0.82	0.85 ± 0.29
E _{max} (%)	86.5 ± 2.7	97.8 ± 1.7	38 ± 3	77.5 ± 7.5	99.5 ± 2.2	100
Behaviour	Partial agonist	Full agonist	Inverse agonist	Inverse agonist	Full agonist	Full agonist

^a EC₅₀ and E_{max} were obtained from dose–response curve analysis with GraphPad Prism v5 software. For agonist compounds, E_{max} is expressed as the % of maximal ghrelin. For inverse agonists, E_{max} is expressed as the maximal basal inhibition (100% inhibition corresponding to the basal of mock-transfected HEK293T cells). Values are mean ± S.E.M of three independent experiments.

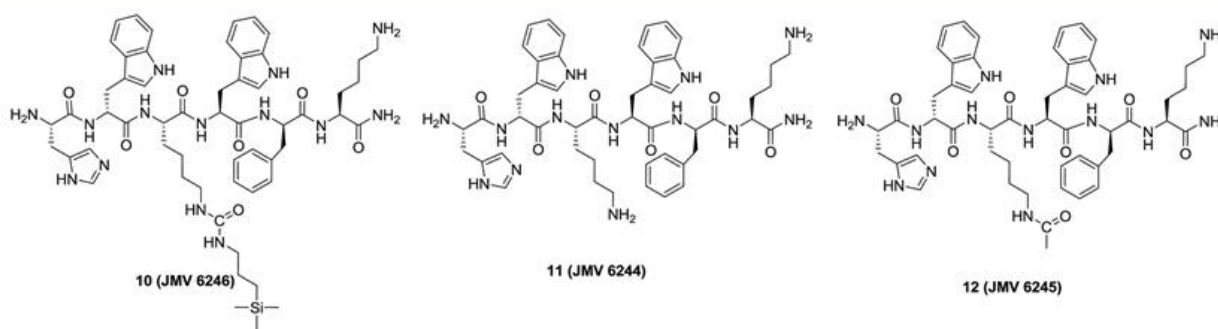


Fig. 7 Peptides 10, 11 and 12 monomeric analogues of dimer 9.

dimerization within the active sequence is accordingly of great impact. Further pharmacological studies will be performed to investigate the structure–activity relationships of GHRP-6 analogues.

Conclusions

In this paper, we demonstrated that formation of siloxane bound could be a simple and useful tool to yield homodimers of peptide ligands. Formation of siloxane bonds starting from hydroxydimethylsilane could be easily monitored by NMR spectroscopy, especially by measuring the proton signals of the methyl groups linked to silicon atoms. This study clearly demonstrated that the bond was relatively stable at neutral pH but was hydrolyzed in basic or acidic conditions. Noteworthy, the position of dimerization and thus, the orientation of the bioactive sequence could be controlled by introduction of a hydroxydimethylsilane moiety either at the N-terminus, C-terminus or within the sequence *via* the side chain of a lysine. Using GHRP-6 as an example, we demonstrated that the position of the dimerization could be crucial for modulating bioactivity, dimers being agonists, inverse agonists or partial agonists.

Acknowledgements

C. Echalié's Ph.D. is partly founded by Region Languedoc Roussillon through 'Chercheur d'avenir' grant attributed to G. Subra. Peptide syntheses were performed using the facilities of SynBio3 IBISA platform supported by ITMO cancer. NMR analyses were performed using the facilities of the 'Laboratoire de Mesures Physiques' (LMP) from the University of Montpellier.

Notes and references

- J. E. Gestwicki, C. W. Cairo, L. E. Strong, K. A. Oetjen and L. L. Kiessling, *J. Am. Chem. Soc.*, 2002, **124**, 14922–14933.
- C. Valant, J. Robert Lane, P. M. Sexton and A. Christopoulos, *Annu. Rev. Pharmacol. Toxicol.*, 2012, **52**, 153–178.
- C. Hiller, J. Kühhorn and P. Gmeiner, *J. Med. Chem.*, 2013, **56**, 6542–6559.
- S. Halazy, M. Perez, C. Fourrier, I. Pallard, P. J. Pauwels, C. Palmier, G. W. John, J. P. Valentin, R. Bonnafous and J. Martinez, *J. Med. Chem.*, 1996, **39**, 4920–4927.
- M. Perez, P. J. Pauwels, C. Fourrier, P. Chopin, J. P. Valentin, G. W. John, M. Marien and S. Halazy, *Bioorg. Med. Chem. Lett.*, 1998, **8**, 675–680.
- Y. Shimohigashi, T. Costa, H.-C. Chen and D. Rodbard, *Nature*, 1982, **297**, 333–335.
- I. Daffix, M. Amblard, G. Bergé, P. Dodey, D. Pruneau, J.-L. Paquet, C. Fouchet, R.-M. Franck, E. Defrère, J.-M. Luccarini, P. Bélichard and J. Martinez, *J. Pept. Res.*, 1998, **52**, 1–14.
- G. Subra, M. Amblard, P. Verdie, S. Komesli, P. Dutartre, P. Durand, P. Renaut and J. Martinez, *QSAR Comb. Sci.*, 2007, **26**, 496–510.
- D. Lecis, E. Mastrangelo, L. Belvisi, M. Bolognesi, M. Civera, F. Cossu, M. De Cesare, D. Delia, C. Drago, G. Manenti, L. Manzoni, M. Milani, E. Moroni, P. Perego, D. Potenza, V. Rizzo, C. Scavullo, C. Scolastico, F. Servida, F. Vasile and P. Seneci, *Bioorg. Med. Chem.*, 2012, **20**, 6709–6723.
- G. Subra, M. Amblard and J. Martinez, *Tetrahedron Lett.*, 2002, **43**, 9221–9223.
- S. Mitra, S. Duggineni, M. Koolpe, X. Zhu, Z. Huang and E. B. Pasquale, *Biochemistry*, 2010, **49**, 6687–6695.
- S. Jebors, J. Ciccione, S. Al-Halifa, B. Nottelet, C. Enjalbal, C. M'Kadmi, M. Amblard, A. Mehdi, J. Martinez and G. Subra, *Angew. Chem., Int. Ed.*, 2015, **54**, 3778–3782.
- C. M'Kadmi, J.-P. Leyris, L. Onfroy, C. Galés, A. Saulière, D. Gagne, M. Damian, S. Mary, M. Maingot, S. Denoyelle, P. Verdié, J.-A. Fehrentz, J. Martinez, J.-L. Banères and J. Marie, *J. Biol. Chem.*, 2015, **290**, 27021–27039.
- S. Coantic, G. Subra and J. Martinez, *Int. J. Pept. Res. Ther.*, 2008, **14**, 143–147.
- C. Echalié, S. Al-Halifa, A. Kreiter, C. Enjalbal, P. Sanchez, L. Ronga, K. Puget, P. Verdié, M. Amblard, J. Martinez and G. Subra, *Amino Acids*, 2013, **45**, 1395–1403.
- J.-P. Leyris, T. Roux, E. Trinquet, P. Verdié, J.-A. Fehrentz, N. Oueslati, S. Douzon, E. Bourrier, L. Lamarque, D. Gagne, J.-C. Galleyrand, C. M'kadmi, J. Martinez, S. Mary, J.-L. Banères and J. Marie, *Anal. Biochem.*, 2011, **408**, 253–262.
- R. Corriu and N. Trong Anh, *Molecular Chemistry of Sol–Gel Derived Nanomaterials*, Wiley, 2009.
- M. Kojima, H. Hosoda, Y. Date, M. Nakazato, H. Matsuo and K. Kangawa, *Nature*, 1999, **402**, 656–660.
- W. Zhang, M. Chen, X. Chen, B. J. Segura and M. W. Mulholland, *J. Physiol.*, 2001, **537**, 231–236.
- V. Sibilía, F. Pagani, F. Guidobono, V. Locatelli, A. Torsello, R. Deghenghi and C. Netti, *Neuroendocrinology*, 2002, **75**, 92–97.
- E. Bollano, C.-H. Bergh, C. Kjellström, E. Omerovic, V. Kujacic, K. Caidahl, B.-Å. Bengtsson, F. Waagstein and J. Isgaard, *Eur. J. Heart Failure*, 2001, **3**, 651–660.
- Y. Mear, A. Enjalbert and S. Thirion, *Front. Neurosci.*, 2013, **7**, 87.
- S. D. Feighner, A. D. Howard, K. Prendergast, O. C. Palyha, D. L. Hreniuk, R. Nargund, D. Underwood, J. R. Tata, D. C. Dean, C. P. Tan, K. K. McKee, J. W. Woods, A. A. Patchett, R. G. Smith and L. H. Van der Ploeg, *Mol. Endocrinol.*, 1998, **12**, 137–145.
- B. Holst, M. Lang, E. Brandt, A. Bach, A. Howard, T. M. Frimurer, A. Beck-Sickinger and T. W. Schwartz, *Mol. Pharmacol.*, 2006, **70**, 936–946.
- C.-B. Chan, P.-K. Leung, H. Wise and C. H. K. Cheng, *FEBS Lett.*, 2004, **577**, 147–153.
- R. G. Smith, *Endocr. Rev.*, 2005, **26**, 346–360.
- M. Kojima and K. Kangawa, *Physiol. Rev.*, 2005, **85**, 495–522.

Chapter III.

PEG-based bioactive hybrid hydrogels

*Publication 2 – Easy synthesis of
tunable hybrid bioactive hydrogels*

Echalier C. *et al.*, *Chem. Mater.*, 2016, **28**, 1261-1265

My contribution to this paper: I carried out all the experiments: synthesis of the hybrid PEG, peptides and fluorescein derivatives, preparation of the hydrogels, determination of gelation times, rheology, fluorescein release experiments, cell adhesion assays, antibacterial assays. I wrote the paper.

Chapter III. PEG-based bioactive hybrid hydrogels

After the preliminary study of hybrid silylated peptides and siloxane bonds described in the last chapter, we sought to prepare bio-functionalized hydrogels thanks to the sol-gel process. Thus, we synthesized hybrid silylated PEG and hybrid silylated bioactive peptides and, based on these hybrid blocks, we developed a modular method for the one-pot synthesis of covalent bioactive hybrid hydrogels.

III.1. Selection of the hydrogel precursors

Polyethylene glycol (PEG) has been widely used for various biomedical applications ranging from tissue engineering and drug delivery to diagnostics and drug development.^{77,329,330} For instance, the addition of one or several PEG chains to a bioactive compound (*i. e.* 'pegylation') is used to improve its solubility and its pharmacokinetic profile.^{331,332} PEG is a synthetic polymer with $\text{HO}(\text{CH}_2\text{CH}_2\text{O})_n\text{H}$ as general formula. It is prepared by the polymerization of ethylene oxide.³³³ A wide range of PEG units are commercially available: linear or branched PEG with low to very high molecular weights (from a few ethylene glycol monomers to several millions Da) and with different functional terminal groups. PEG is soluble both in water and in a wide range of organic solvents. The end-primary alcohol functions of PEG are easy to modify since the backbone of the polymer does not display any other reactive moiety. In addition, PEG is non-toxic and non-immunogenic, it has been approved by the US Food and Drug Administration (FDA) for many applications. Almost all the cross-linking strategies reported in the first chapter have been applied to the preparation of PEG-based hydrogels.⁷⁶ These hydrogels are valuable thanks to their good biocompatibility, their high capability to retain water and their tissue-like elastic properties. They are considered as 'bio-inert' that is to say that they behave as passive environment for the cells.³²

For all these reasons and as many other researchers, we selected polyethylene glycol as building blocks for the design of hybrid hydrogels. We decided to functionalize PEG with triethoxysilane groups which can be hydrolyzed and polycondensed to establish three siloxane bonds. These three bonds can link a single pair of silicon atoms, thus lengthening the polymeric chain in one dimension (Figure 52, pathway A) or, more likely, they can link a silicon atom to two or three other molecules, thus creating a cross-link node (Figure 52, pathway B). In that case, triethoxysilane groups allow the growing of a three-dimensional network, starting from linear bifunctional triethoxysilyl PEG.

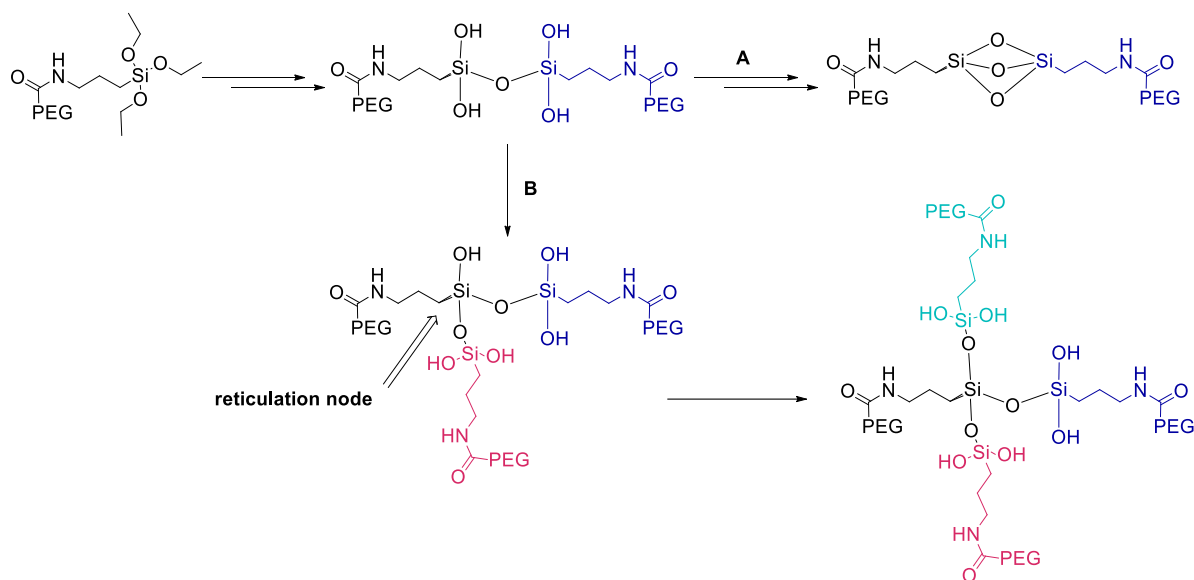


Figure 52. Polycondensation of hybrid triethoxysilyl PEG

III.2. Preparation of the hybrid precursors

PEGs are considered as monodisperse polymers, they are a mixture of molecules with a very narrow distribution of molecular weights. The number indicated in PEG names refers to their average molecular weights. For instance, PEG 2000 designates a PEG unit with an average molecular weight of 2000 daltons. The silica/organic ratio in hybrid triethoxysilyl PEG is directly related to the number of cross-links that can be formed in a hybrid hydrogel. Low molecular weight PEGs are expected to yield highly cross-linked networks and stiff hydrogels, while high molecular weight PEGs should lead to soft hydrogels after a prolonged gelation time. As a compromise between gel time and mechanical properties, we selected PEG with an average molecular weight of a few kilodaltons.

Hybrid PEG building blocks were prepared by reacting the hydroxyle extremities of PEG with 3-isocyanatopropyltriethoxysilane resulting in a carbamate linkage (Figure 53). Carbamates exhibit a higher hydrolytic stability than esters but are still susceptible to cleavage by esterases.³³⁴ It is worth noting that hydroxyle groups are less nucleophilic than amine groups. Thus, the reaction between PEG and ICPTES requires tougher conditions than the introduction of silyl groups on peptide amines which was described in the previous chapter. The reaction proceeds to completion by heating THF at reflux for 48 h, in the presence of triethylamine.³³⁵ Then the reaction mixture is concentrated under reduced pressure. The hybrid PEG is washed three times in hexane to eliminate the excess of ICPTES and the traces of triethylamine. After removal of residual hexane, the hybrid PEG can be stored under argon at 4°C for several months. A dry storage is important to avoid the hydrolysis of triethoxysilyl groups and their premature polycondensation. Indeed, moisture can significantly reduce the hybrid PEG

utilization to several weeks, after which the precursor cannot be fully solubilized in aqueous solutions anymore, witnessing a premature polymerization.

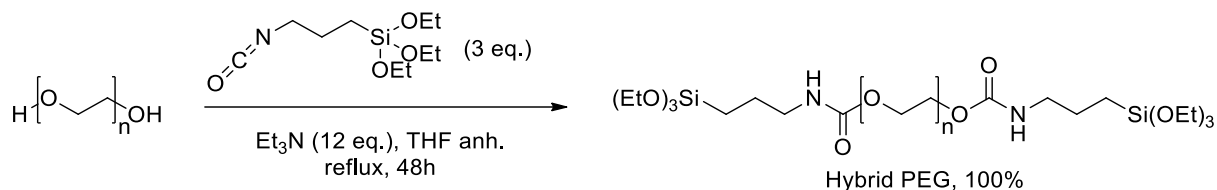


Figure 53. Preparation of hybrid silylated polyethylene glycol

We applied this protocol to the preparation of linear and branched PEG units (Figure 54). Equivalents of reagents were adjusted proportionally to the number of reactive hydroxyle extremities. Hybrid PEGs were characterized by ^1H , ^{13}C and ^{29}Si NMR in CDCl_3 .

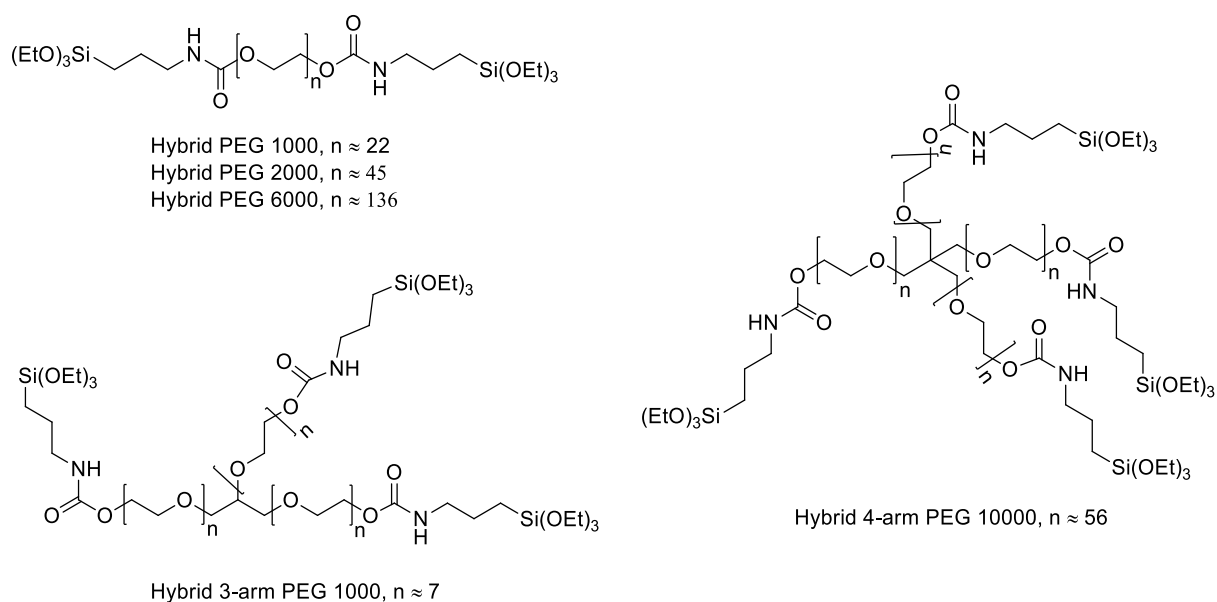


Figure 54. Prepared hybrid silylated PEGs

III.3. Development of the sol-gel gelation process

III.3.1. Gelation conditions: pH, temperature and catalyst

With these hybrid PEG-based building blocks in hand, we focused on a gelation process at physiological pH. Therefore, we chose a phosphate buffer at pH 7.2 as solvent: Dulbecco's Phosphate-Buffered Saline (DPBS, Gibco 14190) containing NaCl (138 mM), Na_2HPO_4 (8.06 mM), KCl (2.67 mM) and KH_2PO_4 (1.47 mM). Hybrid PEG 2000 was first selected as a model to study and optimize the gelation process. A 10 wt% (mass/volume, 40 mM) solution of hybrid PEG 2000 in DPBS could turn into a solid-like hydrogel at room temperature but it required

nearly a week. In order to decrease the gelation time, the temperature was increased to 37°C, the highest temperature compatible with living cells.

Nucleophile catalysts, in particular proline, glycine and fluorides were investigated. The catalyst was added to DPBS and the hybrid PEG 2000 was simply dissolved in this solution. The dissolution of the hybrid PEG occurred spontaneously but could be accelerated by trituration, stirring or sonication. Gelation times were determined using the 'tilting method', *i. e.* gelation was observed when the sample could not flow anymore upon inversion of the vial. Sodium fluoride (NaF) afforded the fastest gelation times and was retained to catalyze the sol-gel process (Figure 55). However, exposition to high fluoride doses has been shown to results in adverse cell effects,^{336–338} and we envisioned that careful optimization of the fluoride concentration would have to be performed before using hybrid PEG hydrogels in biological assays.

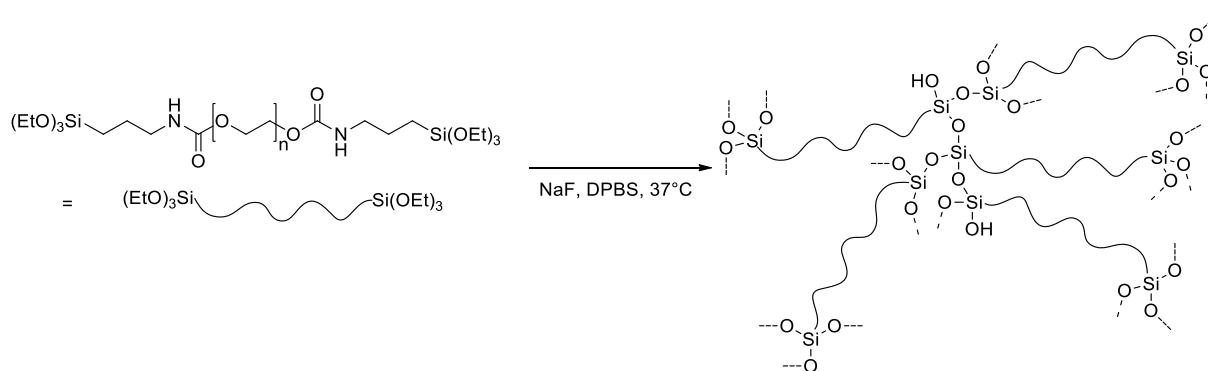


Figure 55. Formation of PEG-based hydrogels via the sol-gel process

III.3.2. NMR studies

III.3.2.1. Hydrolysis monitored by liquid-state ¹H NMR

The evolution of the sol-gel process was monitored by liquid ¹H NMR. The hybrid PEG 2000 was dissolved in a DPBS/D₂O 90/10 mixture at a 10 wt% concentration in the presence of sodium fluoride (3 mg/ mL, 71 mM, 0.9 eq. F⁻/Si). The hybrid solution was immediately introduced in an NMR tube and spectra were recorded at 37°C (Figure 57). The hydrolysis of ethoxysilyl groups (Figure 56) was monitored by quantification of the released amount of ethanol (Figure 58). Based on the integration of the CH₃ signal of EtOH, it appeared that two thirds of the ethoxysilane groups were hydrolyzed after 1 h. The hydrolysis reached a plateau after 2 h. The disappearance of the signal attributed to -Si(OCH₂CH₃)₃ also confirmed these results. A regular decrease of the overall signal of the hybrid PEG was observed and resulted from the decrease in the concentration of free hybrid PEG molecules in solution upon condensation. The solution turned into a gel after 2 h. It is worth noting that gelation limits the movement of polymer chains thus preventing the completion of the condensation reaction. Therefore, at the end of the process, some hybrid PEG molecules are expected to

display free Si-OH functions but all of them are supposed to be covalently linked within the network.

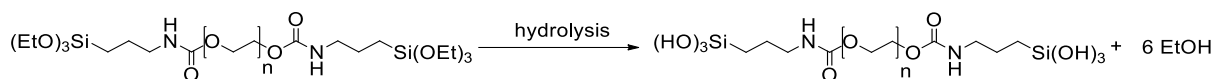


Figure 56. Hydrolysis of hybrid triethoxysilyl PEG

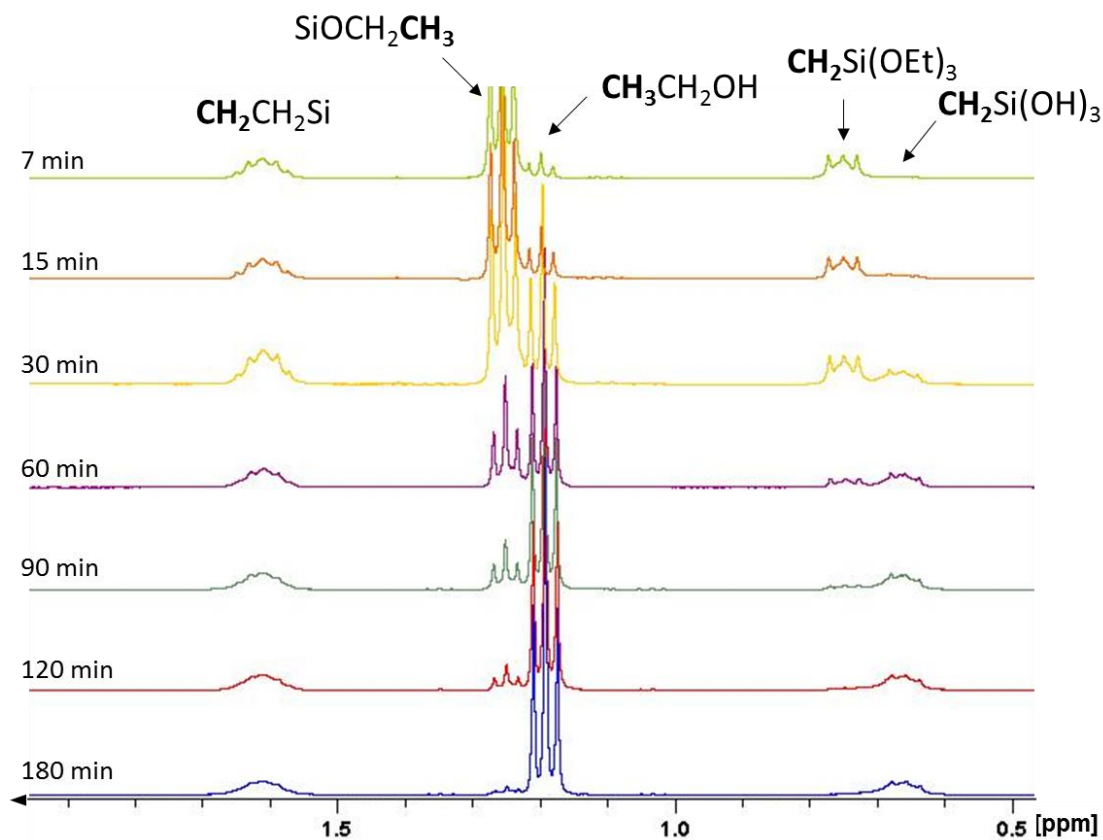


Figure 57. ¹H NMR spectra of the hybrid PEG 2000 at a 10 wt% concentration in DPBS containing 0.3 wt% of NaF

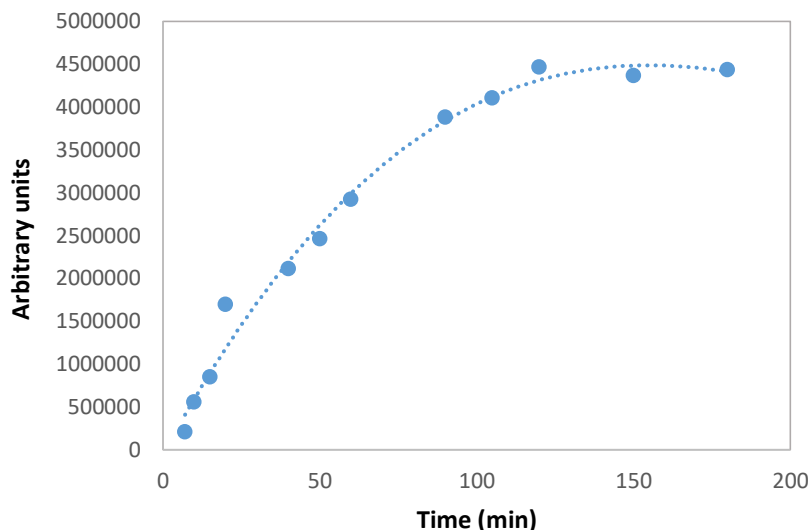


Figure 58. Integration of ^1H NMR signals of the CH_3 group of ethanol

III.3.2.2. Condensation monitored by solid-state ^{29}Si NMR

^{29}Si NMR can provide information relative to the degree of condensation in the hydrogels. Indeed, silicon atoms exhibit ^{29}Si NMR signals with different chemical shifts depending on the number of siloxane bonds they are involved in (Figure 59).³³⁹ Liquid-state ^{29}Si NMR was not appropriate for our study due to the disappearance of free hybrid PEG in solution upon condensation. As a consequence, we turned to solid-state ^{29}Si NMR. A 10 wt% solution of hybrid PEG 2000 in DBPS with sodium fluoride (25 mg/mL, for a fast gelation) was prepared. The gelation time of this hybrid solution at 37°C was found to be 35 min. Samples of this hydrogel were lyophilized immediately after gelation, two days and four days after gelation. Solid-state ^{29}Si NMR spectra of the residues were recorded (Figure 60). T^2 and T^3 silicon species were observed, resulting from condensation. ^{29}Si quantitative sequences required very long acquisition times and therefore could not be used. Moreover, we showed previously that condensation can occur during lyophilization.³⁴⁰ Nevertheless, as all the samples underwent the same treatment, we can say that the proportion of T^3 species increases with time, suggesting that the hydrogel is evolving towards a highly condensed network.

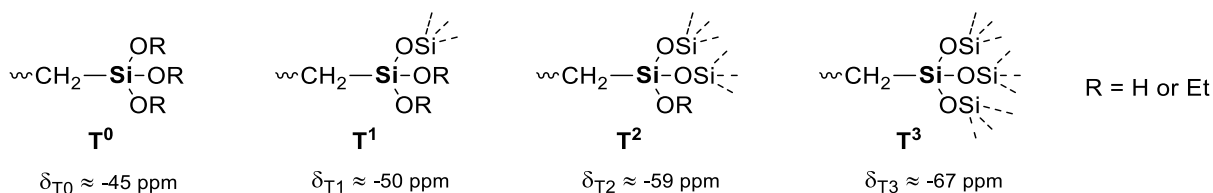


Figure 59. Nomenclature used to designate silicon atoms in hybrid structures and ^{29}Si NMR chemical shifts associated

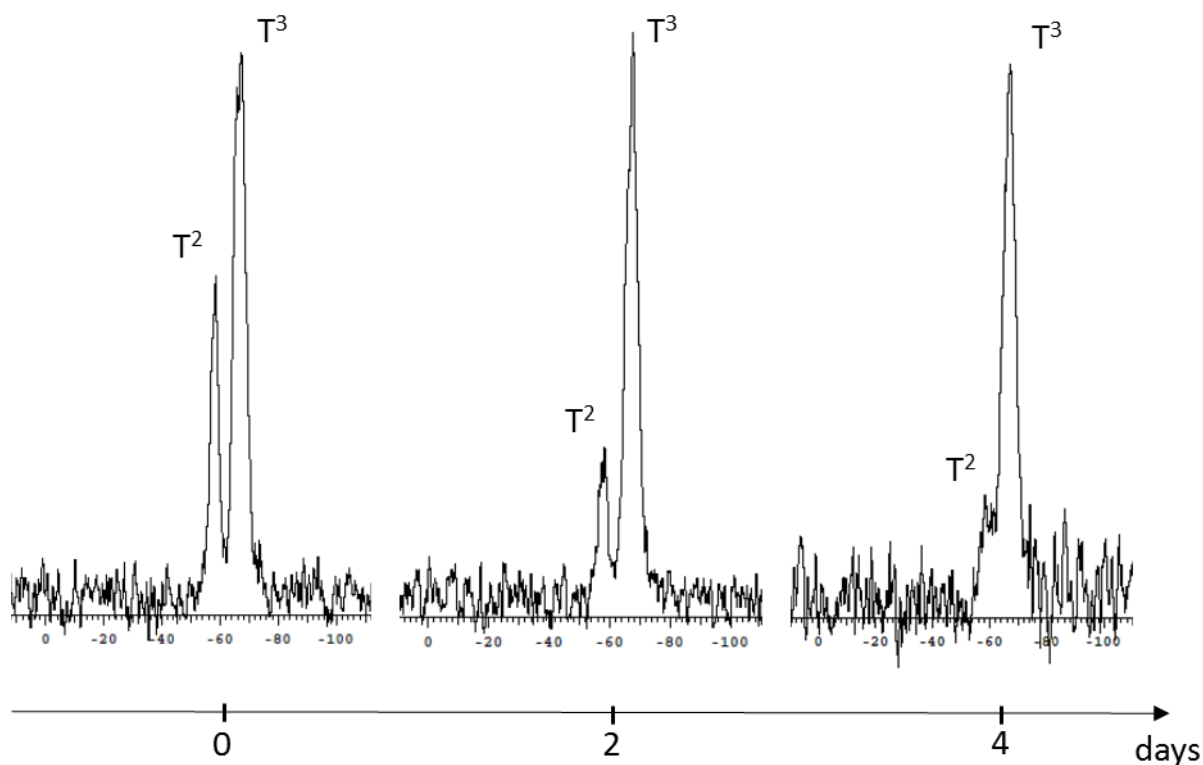


Figure 60. ^{29}Si NMR spectra of 10 wt% hybrid PEG 2000 hydrogels lyophilized after 0, 2 or 4 days.

^{29}Si NMR does not show whether the three siloxane bonds of T^3 species are established between only two hybrid PEG molecules or link four different hybrid PEG molecules (Figure 61). To elucidate this point, a bis(hydroxydimethylsilyl) hybrid PEG 2000 was prepared. Hydrogels could not be obtained from this hybrid block (Figure 62, B). This result suggests that a three-dimensional cross-linkage is required to yield a hydrogel (Figure 62, A) and that some T^3 silicon atoms link more than two PEG molecules in the network.

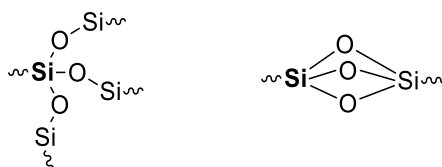


Figure 61. Possible structures for T^3 silicon species

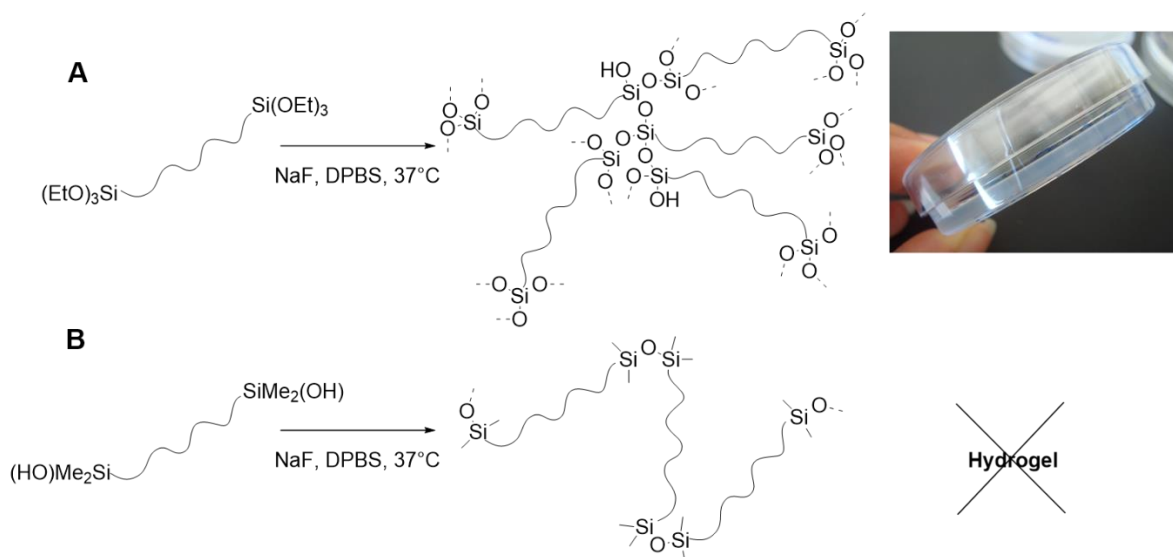


Figure 62. Comparison of networks formed from hybrid triethoxysilyl PEG (A) and hybrid dimethylhydroxysilyl PEG (B)

III.3.1. Rheology study

The gelation process was also monitored by rheology. The viscoelastic behavior of a system can be characterized by the storage (G') and loss (G'') moduli. These moduli respectively quantify the solid-like and fluid-like contributions to the measured response when a sinusoidal shear deformation is applied to the system. Rheology can provide gel time values that are more accurate than the one determined by the tilting method. Oscillatory shear measurements were performed on a 10 wt% hybrid PEG 2000 solution in DPBS (Gibco 14040 with calcium and magnesium) in the presence of sodium fluoride (3 mg/mL). Experiments were carried out at 37°C using an AR 2000 rheometer (TA Instruments, Inc) with a 20 mm diameter parallel geometry (Figure 63). The hybrid solution was deposited on the Peltier plate and the gap was set at 500 μm . The dependence of G' and G'' moduli was measured as a function of time with a 1% strain and at 1 Hz frequency (Figure 64).

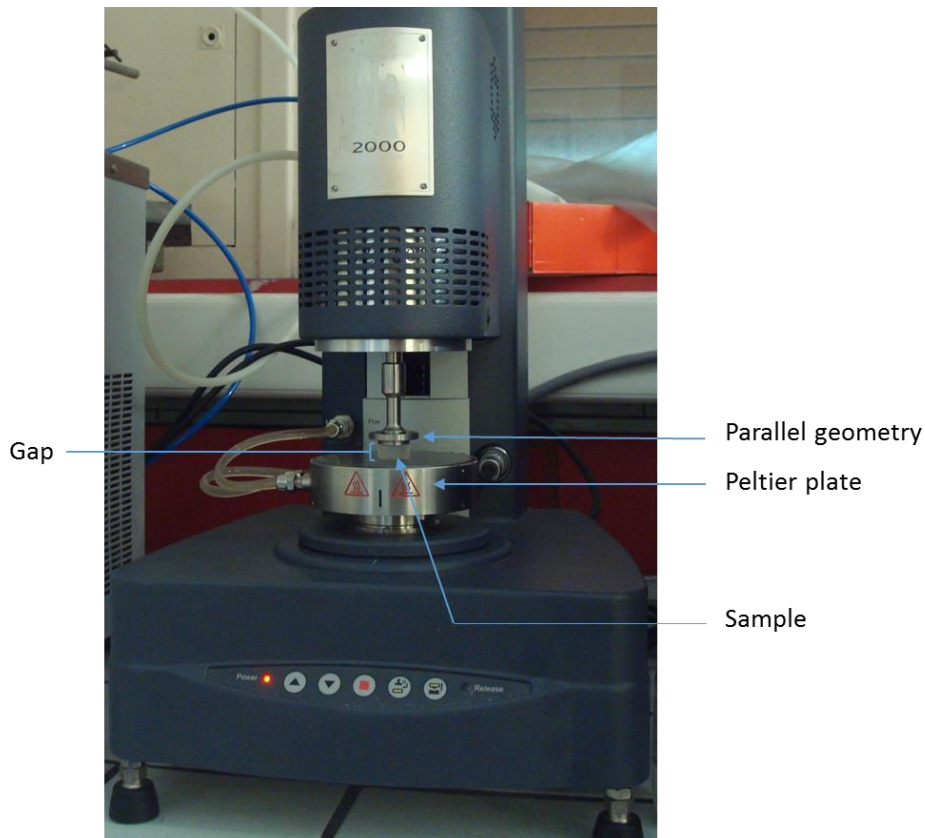


Figure 63. AR 2000 rheometer fitted with a 20 mm parallel geometry

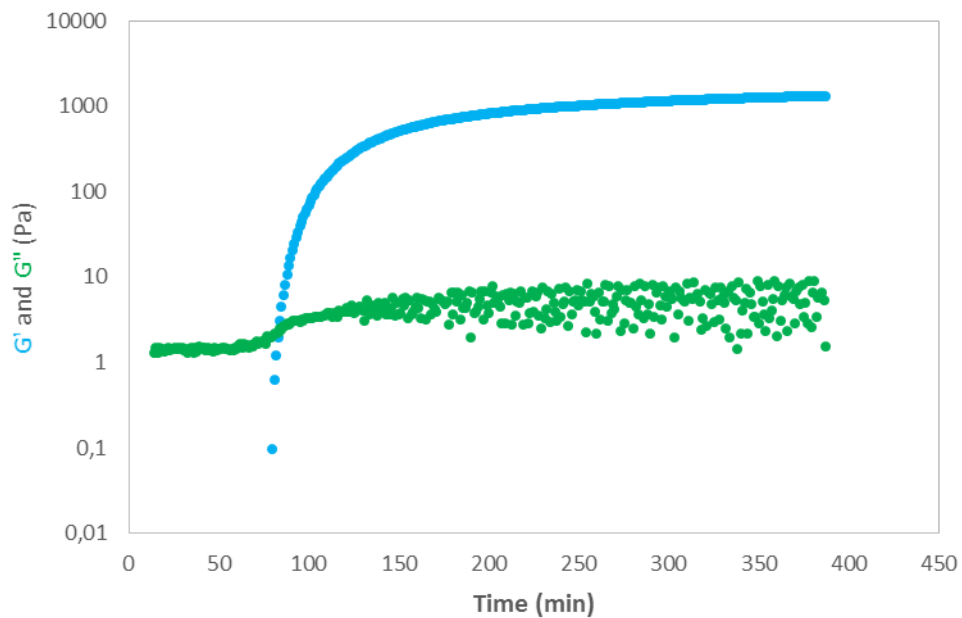

















Figure 64. G' (in blue) and G'' (in green) moduli measured on a 10 wt% hybrid PEG 2000 solution in DPBS with sodium fluoride (3 mg/mL) at 37°C (1% strain, 1 Hz)

Initially, G'' was greater than G' which indicated a fluid-like behavior of the sample. During the experiment, G' increased quickly due to the formation of siloxane cross-links while G'' increased negligibly. Thus a crossover of G' and G'' was observed at 84 min corresponding to the gel point. Then, the sample presented solid-like properties.

III.4. Selection of a hydrogel

After the general studies of the gelation process, we compared the five different hybrid PEG blocks prepared (Figure 54) in order to choose one of them for further experiments (Table 2). First of all, the hydrogel formation was assayed. All hybrid PEG units were soluble in DPBS except the 3-arm PEG 1000. This latter formed a second oily phase in DPBS and could not lead to the formation of a homogeneous hydrogel. The other hybrid PEG units (hybrid PEG 1000, 2000, 6000 and 4-arm PEG 10000) were dissolved in DPBS at a 10 wt% concentration in the presence of sodium fluoride (25 mg/ mL). All these hybrid solutions could turn into hydrogels within 1 h at 37°C except the hybrid PEG 6000 solution that yielded a viscous liquid after 24 h (Figure 65). This can be explained by a decrease in cross-links due to a lower silica/organic ratio.

Table 2. Selection of the best hybrid PEG candidate for the preparation of hydrogels with good stability and mechanical properties

Hybrid silylated unit	Dissolution in DPBS ^a	Hydrogel formation ^b	Stability ^c	Mechanical properties ^d
Hybrid PEG 1000				
Hybrid PEG 2000				
Hybrid PEG 6000			n. a.	n. a
Hybrid 3-arm PEG 1000			n.a.	n. a.
Hybrid 4-arm PEG 10000				n. d.

^a Assay of solubilisation of the hybrid unit in DPBS at a 10 wt% concentration.

^b Capacity of a 10 wt% hybrid PEG solution in DPBS with NaF (25 mg/mL) to form a hydrogel within 1 h.

^c Stability of the hydrogel in DPBS at 37°C.

^d Mechanical properties assessed by rheological measurements. High elasticity was sought.

n.a.: non applicable; n. d.: non determined



Figure 65. 10 wt% hybrid PEG solutions in DPBS after 24 h at 37°C. Top: hybrid PEG 2000; bottom: hybrid PEG 6000.

We carried out some comparative degradation studies on hybrid PEG 1000, 2000 and hybrid 4-arm PEG 10000 hydrogels. These degradation experiments are not described in detail but we used an indirect evaluation based on the release of a hybrid fluorophore witnessing the degradation of the network. These experiments are related to fluorescein release experiments described in publication n°2 (“Easy synthesis of tunable hybrid bioactive hydrogels”). After gelation, hydrogels were unmolded and placed in DPBS at 37°C. We observed that the hybrid 4-arm PEG 10000 hydrogels were the first one to dissolve in the buffer. Thus, we selected linear hybrid PEGs 1000 and 2000 for a better hydrolytic stability.

It is noteworthy that hybrid PEG 1000 was obtained as a paste with a melting point close to room temperature whereas hybrid PEG 2000 is a solid. Therefore, hybrid PEG 1000 was less easy to handle than hybrid PEG 2000. We decided to compare the mechanical properties of hybrid PEG 1000 and 2000 hydrogels. Cylindrical hydrogels were prepared at 37°C from a 10 wt% hybrid PEG 1000 or 2000 solution in DPBS with sodium fluoride (25 mg/mL). These hydrogels were unmolded after 24 h at 37°C. Oscillatory shear measurements were performed at 37°C using an AR 2000 rheometer with a 20 mm diameter parallel geometry (1 N normal force). Storage (G') and loss (G'') moduli were recorded as a function of frequency within the linear viscoelastic regime at 0,1% strain. Both samples presented solid-like properties with G' higher than G'' . The storage modulus values were compared to evaluate the hydrogel elasticity. Surprisingly, G' value of hybrid PEG 1000 gel (7973 Pa) was lower than that of hybrid PEG 2000 (10630 Pa). An increase in the PEG chain length should induce a higher mesh size and reduce the number of cross-links. Therefore, we could suspect a reduction of G' for hybrid PEG 2000 gel. In our case, observed evolution can be explained by the higher crystallinity of PEG 2000 which could result in a self-assembly of PEG units in the gel.³⁴¹ The presence of crystalline regions in the gels could be evidenced by differential scanning calorimetry experiments.

Since hybrid PEG 2000 was easier to handle than hybrid PEG 1000 and yielded more elastic hydrogels, hybrid PEG 2000 hydrogels were retained for further experiments.

III.5. Hybrid PEG 2000 hydrogels

Based on these results, we focused our attention on hybrid PEG 2000 hydrogels. We studied their mechanical properties, examined their structure by scanning electron microscopy and assessed their cytotoxicity in order to validate a hydrogel composition that would be suitable for further investigations.

III.5.1. Mechanical properties

The effect of hybrid PEG concentration on mechanical properties of the gels was studied by rheology and is described in the following publication. The increase in PEG/water ratio conferred higher values to the viscoelastic parameters. On the other hand, high water content is preferable for cell culture. Therefore, 10 wt% hybrid PEG 2000 hydrogels were selected as a good compromise between mechanical properties and assumed cell culture properties. We also observed that G' values of the hydrogels increased in a minor contribution with higher NaF concentration.

III.5.2. Microscopic images

The morphology of 10 wt% hybrid PEG 2000 hydrogels was examined by scanning electron microscopy (SEM). Environmental SEM was chosen in the first place to observe the hydrogel in its wet state. Unfortunately, the resolution was not high enough to distinguish between the hybrid network and the aqueous environment. Consequently, the samples were freeze-dried and coated with a gold layer. SEM images show a featureless homogeneous and dense matrix whether for broad and magnified top views. However, it is worth noting that the freeze-drying process may have denatured the hydrogel. No porosity could be observed.

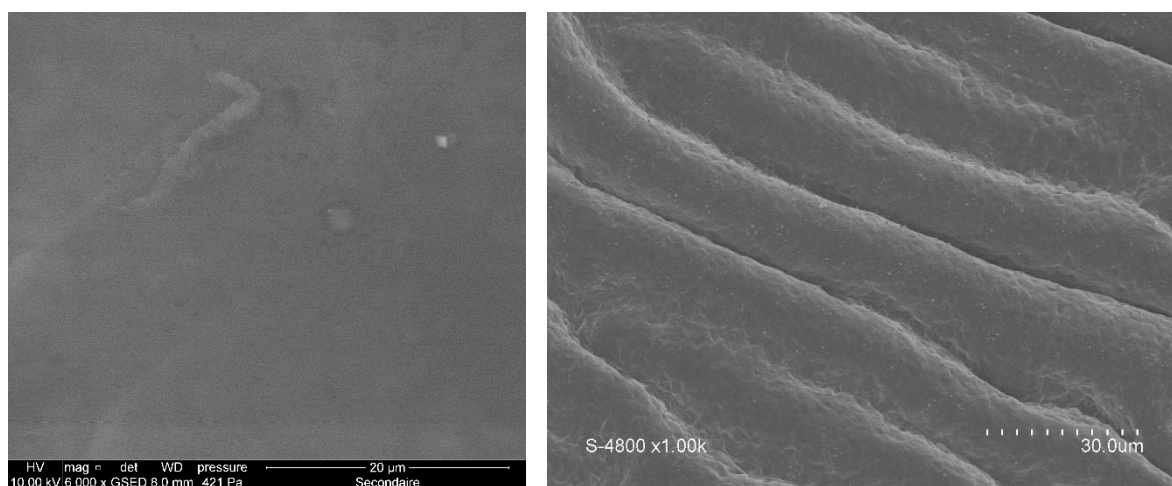


Figure 66. SEM images of 10 wt% hybrid PEG 2000 hydrogel. Left: environmental SEM; right: SEM after freeze-drying and coating

III.5.3. Cytotoxicity assays

Cytotoxicity of 10 wt% hybrid PEG 2000 hydrogels in DPBS containing 0.3 wt% or 2.5 wt% of sodium fluoride was assessed on L929 mouse fibroblasts. This experiment is described in the following publication. Gels containing 2.5 wt% of sodium fluoride were toxic to the cells while a good cell viability was observed with 0.3 wt% of sodium fluoride. As a consequence, 10 wt% hybrid PEG 2000 hydrogels in DPBS containing 0.3 wt% of sodium fluoride were used for further studies. Noteworthy, they exhibited a gel time of 2 h at 37°C.

III.6. PEG-based bioactive hybrid hydrogels

Hybrid PEG 2000 was able to form a bio-inert network intended to be used as the skeleton of the hydrogel. The second step was to covalently functionalize the hydrogel to give it interesting properties.

While capture and release of active substances within the gel matrix can be achieved quite easily, covalent attachment of molecules of interest to the scaffold is much more challenging and offers attractive features. Several groups have already modified PEG hydrogels to afford them bioactivity.³² Among the molecules of biological interest used to functionalize hydrogels, peptides are the most common as they are easy to synthesize and can exhibit a high biological activity. The Arg-Gly-Asp sequence (RGD) found in fibronectin has been identified more than 30 years ago as a minimal cell adhesion peptide sequence.³⁴² Since then, it has been by far the most often used peptide sequence to promote cell adhesion on/in materials.³⁴ Different strategies have been investigated to attach RGD peptides to the hydrogel scaffold. Two main methods arise. In the first method, RGD-PEG conjugates are obtained through a Michael type addition: a thiol containing RGD peptide is reacted with a Michael acceptor-modified PEG

unit.^{42,126} In the second method, the N-terminal amine of RGD peptide reacts with a N-hydroxysuccinimide-containing PEG.^{33,35,81} In both cases, RGD-PEG conjugates are prepared before the hydrogel synthesis to ensure a homogeneous repartition of the peptide in the hydrogel and avoid the presence of unreacted free peptides that could lead to undesired biological responses. When a combination of active peptides is desired, each peptide-PEG conjugate has to be prepared prior to gelation. In contrast with these examples, we proposed to use a single chemistry, the sol-gel process, to build up the hydrogel network and covalently functionalize it one pot with bioactive peptides.

In the following article, we demonstrated the one-pot covalent incorporation of molecules within the gel using hybrid silylated fluorescein derivatives. Then, two hybrid silylated peptides were synthesized, a RGD peptide and an antibacterial peptide. Cell adhesion or antibacterial properties were given to hybrid PEG-based hydrogels by incorporation of these active hybrid peptides (Figure 67).

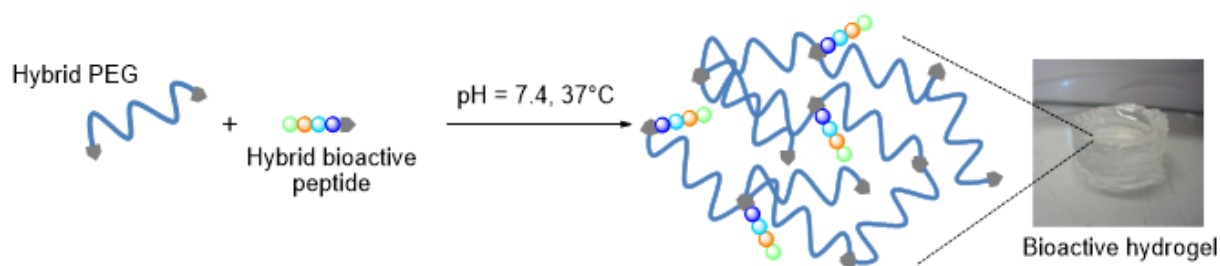


Figure 67. Preparation of covalent hybrid bioactive hydrogels thanks to the sol-gel process

Easy Synthesis of Tunable Hybrid Bioactive Hydrogels

Cécile Echalié,^{†,‡} Coline Pinese,[†] Xavier Garric,[†] Hélène Van Den Berghe,[†] Estelle Jumas Bilak,[§] Jean Martinez,[†] Ahmad Mehdi,^{*,‡} and Gilles Subra^{*,†}

[†]Institut des Biomolécules Max Mousseron (IBMM), UMR5247 CNRS, ENSCM, Université de Montpellier, 15 avenue Charles Flahault, 34093 Montpellier Cedex 05, France

[‡]Institut Charles Gerhardt (ICG), UMR5253 CNRS, ENSCM, Université de Montpellier, Equipe Chimie Moléculaire et Organisation du Solide, Place Eugène Bataillon, 34095 Montpellier Cedex 05, France

[§]HydroSciences Montpellier, UMR5569 CNRS, Université de Montpellier, 15 avenue Charles Flahault, 34093 Montpellier Cedex 05, France

Supporting Information

Hydrogels play a central role in the field of biomedical materials. Indeed, their high water content makes them the ideal candidates as extracellular matrix substitutes. They are of high interest for biomedical applications such as reconstructive surgery and tissue engineering^{1–4} but also drug delivery.⁵ One of the main challenges is to synthesize scaffolds where cells will be able to proliferate, differentiate and behave like in their natural environment. This can be achieved by introduction of bioactive molecules like growth factors but also shorter peptide ligands that can promote, for example, the cell adhesion and mobility into the artificial matrix.^{6–8} In the later case, immobilization of the suitable ligand on the material offers attractive features. While noncovalent entrapment of such active substances within a gel matrix can be achieved quite easily, covalent attachment of peptides of biological interest to the scaffold often requires UV activation⁹ or functionalization of precursors with different chemical groups to ensure selectivity.^{10,11} In this context, we propose a modular strategy based on alkoxy silane hybrid biomolecules that can be engaged in a sol–gel process to yield covalently bound functional hybrid hydrogels. Few hybrid alkoxy silane polymers were already used to obtain biomaterials¹² or modified silica hydrogels¹³ but their further functionalization with bioactive peptides has never been reported. In our case, synthesis of the hydrogel covalently functionalized with active peptides proceeds in a single step, in biocompatible conditions and do not require any bioconjugation chemistry, chemical reagent or solvents (Figure 1).

We chose polyethylene glycol (PEG) as the basic building block for this study because of its nontoxicity and its high hydrophilicity. Indeed, PEG-based hydrogels already demonstrated promising results as biocompatible materials.^{14–17} Finally, we proved that the resulting hybrid silylated functional

hydrogels exhibited biological properties depending on the nature of the covalently bound bioactive peptide, promoting cell adhesion or displaying antibacterial properties (Scheme 1, hybrid peptides 2 and 3 respectively).

Before preparing functional gels containing peptides, we optimized the preparation of the gel matrix itself. First, the bifunctional PEG hybrid unit 1 was synthesized by reacting polyethylene glycol (MW = 2000 Da) with 3-isocyanatopropyltriethoxysilane (Scheme 1).¹⁸ Then, the hybrid silylated PEG block was engaged in sol–gel process, consisting in hydrolysis of ethoxysilyl groups into silanols and their condensation to form siloxane bonds.¹⁹ This process was carried out at 37 °C, in pH 7.4 phosphate buffer (DPBS). These conditions were chosen to eventually allow injection and in vivo gelation.²⁰ Sodium fluoride was used as a nucleophile catalyst to accelerate the condensation reactions.²¹ Different concentrations of hybrid PEG and sodium fluoride were assayed, greatly influencing the gelation time (Table 1).

The effect of water/PEG ratio and NaF concentration on mechanical properties of hydrogels was also studied. Oscillatory shear measurements of the hydrogel viscoelastic response were performed using an AR 2000 rheometer (TA Instruments, Inc.) with a 20 mm diameter parallel geometry (1 N normal force). The dependence of the storage (G') and loss (G'') moduli was measured as a function of the oscillation frequency (f) at different PEG and NaF concentrations at 37 °C within the linear viscoelastic regime (0.1% strain, from 0.01 to 10 Hz). Moduli values at 1 Hz frequency for 24 h old hydrogels are presented in Table 1. It was observed that all the samples present solid-like properties with G' higher than G'' . The storage modulus value was used as a measurement of the hydrogel elasticity. The loss modulus increased negligibly for all hydrogels. Storage moduli remained constant over 1 week and were ranging from 2500 to 55 000 Pa, covering an important range of physiologically tunable stiffness. The increase in PEG concentration involved the formation of a strong network that confers higher values to the viscoelastic parameters. One can also notice that G' values increased in a minor contribution with higher NaF concentration. Thus, depending on the aimed

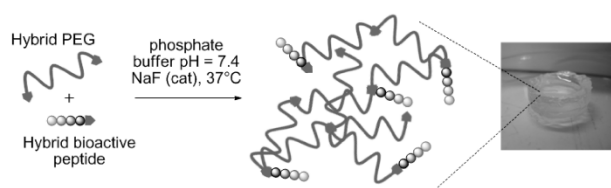


Figure 1. One pot preparation of hybrid functional silylated PEG-based hydrogels containing covalently bound bioactive peptides.

Received: December 23, 2015

Revised: February 8, 2016

Published: February 9, 2016

Scheme 1. Synthesis of Hybrid Bis-silylated PEG 1 and Hybrid Silylated Peptides 2 and 3

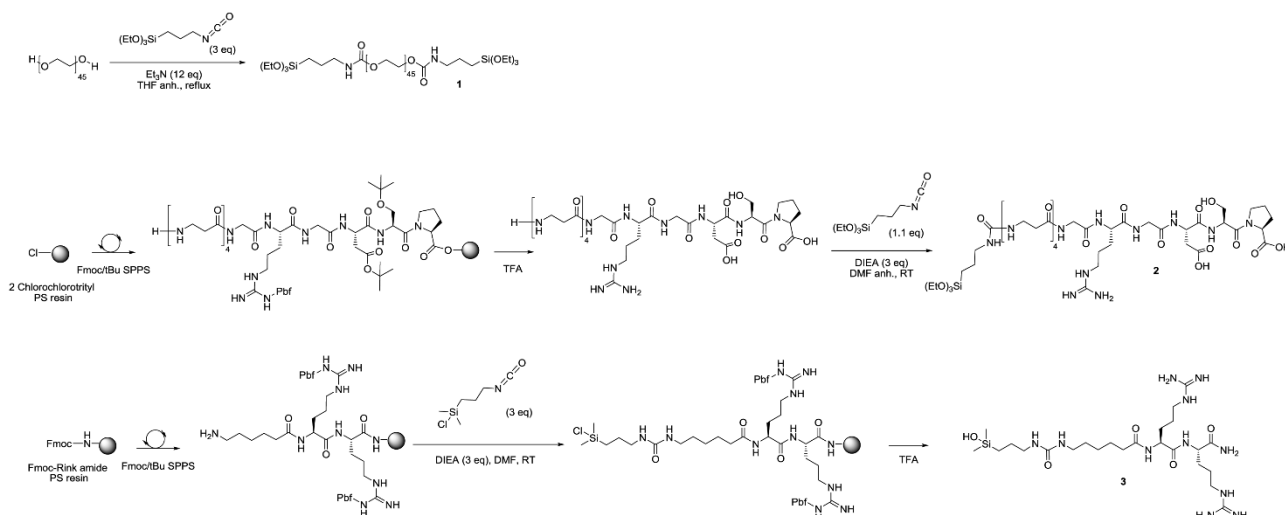


Table 1. Gelation Time of Hybrid PEG Solutions in DPBS at 37 °C and Viscoelastic Moduli of Resulting Hydrogels

gel composition		gelation time (min)	G' (Pa)	G'' (Pa)
hybrid PEG (wt %)	NaF (wt %)			
20	5.0	10	n.d.	n.d.
20	2.5	15	55 160	131
10	5.0	20	12 370	140
10	2.5	35	10 630	37
10	0.3	120	6088	-33
5	5.0	50	n.d.	n.d.
5	2.5	220	2518	14

application, the stiffness of these hybrid hydrogels can be easily modulated by varying hybrid bis-silylated PEG 1 and/or NaF concentrations.

The influence of PEG molecular weights on hydrogel mechanical properties was also studied, and the results are presented in the [Supporting Information](#).

Ten wt % hybrid hydrogels were examined by scanning electron microscopy (SEM) ([Supporting Information](#)). Images show a featureless homogeneous and dense matrix whether for broad and magnified top views.

Cytotoxicity assays were conducted on 10 wt % hybrid hydrogels containing respectively 0.3 or 2.5 wt % of NaF. L929 mouse fibroblasts were chosen for the tests as recommended by ISO specifications and especially for the evaluation of medical device cytotoxicity.²² Cells were seeded on tissue culture treated polystyrene. After 24 h of proliferation, they were incubated with the hydrogels for 24 h. Cell viability was measured with a LDH based cytotoxicity assay monitoring the apparition of a red formazan product.²³ Poly(D,L-lactic acid) was used as a positive control as it is a well-known biocompatible polymer currently used for pharmaceutical and medical device applications. As expected, gels containing the higher concentration of NaF were toxic. However, over 80% of cell viability was observed with 3 mg/mL NaF concentration; this latter result is similar to cell viability observed with PLA control, meaning we obtained a noncytotoxic gel ([Figure 2](#), left).²² These results were confirmed by microscopic observations and showed spindle-shaped and healthy cells

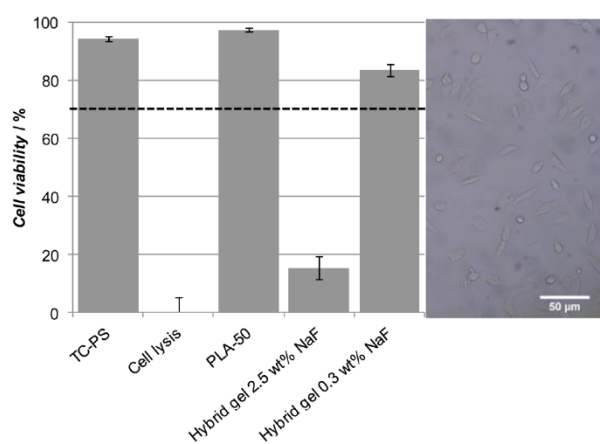


Figure 2. Left: cytotoxicity assays on L929 Fibroblasts. TC-PS, cell viability on TC-PS without gel; cell lysis, complete lysis; PLA-50 control, cells in the presence of poly(D,L-lactic acid); hybrid gels, 10 wt % hybrid PEG gels containing respectively 2.5 or 0.3 wt % of NaF; ---cytotoxicity limit. Right: L929 fibroblasts under hybrid gel containing 0.3 wt % NaF after 24 h of incubation at 37 °C.

([Figure 2](#), right). Hence, 10 wt % hybrid PEG gels with 0.3 wt % NaF were selected as biocompatible scaffolds featuring good mechanical properties for further studies. Noteworthy, NaF could be used at a higher concentration and removed by gel washings.

At this stage, we wanted to demonstrate the covalent incorporation of a biomolecule within the gel and the absence of leaking as a function of time. To that purpose, fluorescein derivatives were chosen as models for the ease of release monitoring and they were prepared from fluorescein isothiocyanate (FITC) ([Supporting Information](#)). Two types of fluorescein derivatives yielding covalent bonds were tested (triethoxysilane derivative 4 and dimethylhydroxysilane derivative 5) as well as the nonsilylated derivative 6 ([Figure 3](#)). Each fluorescein derivative was dissolved in 10 wt % hybrid PEG solution at a concentration of 4.3 mol % regarding hybrid PEG concentration (1.7 mM). Sodium fluoride was added and solutions were homogenized.

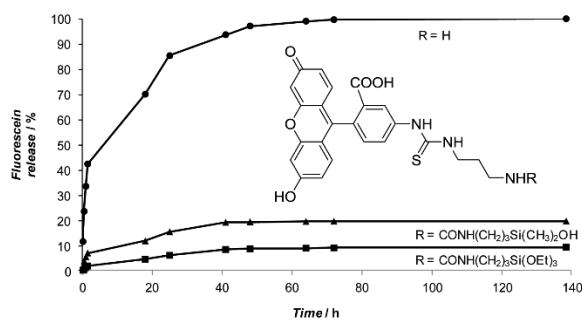


Figure 3. Fluorescein release from hybrid gels. ● Nonsilylated fluorescein 6; ▲ dimethylhydroxysilyl fluorescein 5; ■ triethoxysilyl fluorescein 4.

Fluorescent hybrid gels were obtained at 37 °C in 30 min (See the video in the [Supporting Information](#)). The different gels were placed in phosphate buffer (10 mL) and fluorescein release was monitored by HPLC. In the case of noncovalent entrapment of 6, a complete release was observed within 72 h. As expected, the release of fluorescein in covalent gels reached a plateau after 72 h, indicating the stability of the hybrid covalent linkages. A maximum of 9% and 20% release was observed for the triethoxysilyl derivative 4 and for the dimethylchlorosilyl derivative 5, respectively (Figure 3). This release could be attributed to hybrid molecules noncovalently entrapped that did not react to form the network during gelation process. This is consistent with the fact that triethoxysilyl derivative 4 should be more reactive in the condensation reaction than dimethylhydroxysilane 5.²⁴

Having demonstrated that covalent introduction of an organic moiety within the hybrid gel was possible, two hybrid bioactive peptides (Scheme 1) were prepared to yield functional hybrid PEG gels. The hybrid peptide 2 containing RGD sequence was selected to promote cell adhesion.^{25,6,26} On the other hand, the cationic hybrid peptide 3 was chosen for its antibacterial effects. Indeed, a triethoxysilyl analogue of 3 was already used to prepare antibacterial glass surfaces.²⁷ The utilization of 3-isocyanatopropylchlorodimethylsilane (ICPCDMS) instead of 3-isocyanatopropyltriethoxysilane to obtain hybrid silylated peptides facilitates the removal of acid sensitive protecting groups such as the 2,2,4,6,7-pentamethyl-dihydrobenzofuran-5-sulfonyl (Pbf), which protects the arginine side-chains of 3. ICPCDMS was already used to prepare silicone-based peptide polymers.²⁸

The unprotected peptide H-GRGDSP-OH was first prepared by Fmoc/tBu solid phase peptide synthesis and functionalized with a triethoxysilyl group using ICPTES to yield 2 (Scheme 1). A 10 wt % solution of the hybrid PEG 1 containing 0.3 wt % of NaF was prepared and the hybrid block 2 was added to this solution at a concentration of 10 mol % or 20 mol % regarding hybrid block 1 (i.e., at 4.0 mM or 8.0 mM). Hybrid solutions were placed at 37 °C overnight, to yield PEG/RGD silylated hybrid gels.

L929 fibroblasts were seeded onto the surface of PEG/RGD hybrid hydrogels and on a nonfunctionalized hybrid PEG hydrogel. Adherent cells were quantified with PrestoBlue cell viability reagent after 30 min, 1 and 2 h (Figure 4). As expected, hybrid PEG gel prevented cell adhesion. In contrast, cell adhesion was very efficient on 20 mol % hybrid PEG/RGD hydrogels and provided even better results after 30 min than polystyrene treated for tissue culture (TC-PS) for a similar

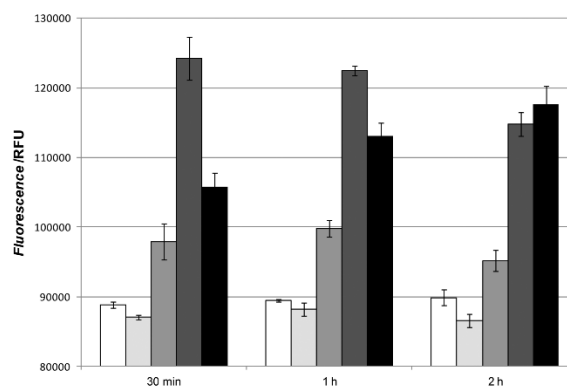


Figure 4. Cell adhesion on hybrid PEG gels. White, fluorescence of the medium without cells; light gray, cells on 10 wt % hybrid PEG gel; medium gray, cells on 10 wt % hybrid PEG gel containing 10 mol % of hybrid RGD peptide; dark gray, cells on 10 wt % hybrid PEG gel containing 20 mol % of hybrid RGD peptide; black, cells on TC-PS.

surface area. Noteworthy, cell adhesion values increased proportionally with the amount of hybrid RGD peptide in hydrogels.

Similarly, hydrogels with antibacterial properties were prepared using the hybrid peptide 3. H-Ahx-Arg(Pbf)-Arg-(Pbf)-Rink amide resin was functionalized on the N-terminal by a dimethylhydroxysilyl group before cleavage from the resin and deprotection of side chains (Scheme 1). The resulting hybrid peptide was added to gel solutions in the conditions previously described for hybrid RGD 2. Another cationic hybrid peptide 7, (EtO)₃Si-(CH₂)₃-NHCO-LeuLeuLeuArgArgNH₂ was prepared as a control. This cationic peptide is similar to 3 in terms of charge, size and lipophilicity but exhibited poor antibacterial activity in solution. It was chosen to demonstrate that the bioresponse is specific and peptide-dependent. Antibacterial activity of hydrogels was evaluated against *Escherichia coli* and *Staphylococcus aureus*. These infectious agents display different bacterial cell structures and different mechanisms of antimicrobial resistance. They are major pathogens particularly involved in healthcare associated infections. Hydrogel surfaces were inoculated with a bacteria suspension (10³ CFU/mL) and covered with tryptic soy agar (TSA) culture medium. After 24 h at 37 °C, bacterial colonies growing on hydrogels containing 0, 7.5, or 15 mol % of hybrid peptide 3 or 7 were counted and compared to a bacterial growth control performed on agar culture medium instead of hydrogel (Figure 5). In the absence of peptides, hybrid PEG hydrogels did not inhibit *E. coli* and *S. aureus* growth. As expected, the hybrid peptide 7 showed a poor antibacterial activity. However, 15 mol % of the antibacterial peptide 3 induced a complete inhibition of *S. aureus* growth and reduced *E. coli* growth by 80%. Thus, a specific antibacterial effect was provided by the hybrid peptide 3.

Herein, we presented an easy and original method to prepare PEG-based hydrogels by the sol-gel process at physiological temperature and pH. We demonstrated through two examples that bioactive peptides can be covalently incorporated into these gels and can confer their biological properties to the gels. Materials described above could find applications in tissue engineering or in controlling postsurgical adhesions. Finally, this one-pot method to prepare biocompatible and bioactive hydrogels is highly adaptable. Indeed, gel properties can be

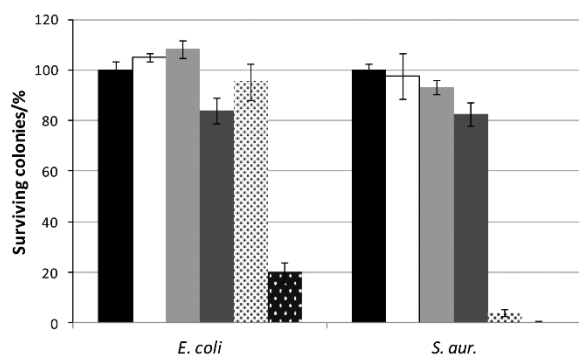


Figure 5. Bacteria survival rate on hybrid gels. Black, agar; white, 10 wt % hybrid PEG gel; light gray, 10 wt % hybrid PEG gel containing 7.5 mol % of hybrid peptide 7; dark gray, 10 wt % hybrid PEG gel containing 15 mol % of hybrid peptide 7, white with black dots, 10 wt % hybrid PEG gel containing 7.5 mol % of hybrid antibacterial peptide 3, black with white dots, 10 wt % hybrid PEG gel containing 15 mol % of hybrid antibacterial peptide 3.

finely tuned by mixing different building blocks to address a specific need for healthcare.

■ ASSOCIATED CONTENT

📄 Supporting Information

The Supporting Information is available free of charge on the ACS Publications website at DOI: 10.1021/acs.chemmater.5b04881.

Fluorescent hybrid gel synthesis (AVI).

Hybrid molecule syntheses, hydrogel preparation, viscometry, rheology, SEM images, cell culture assays and antibacterial assays (PDF).

■ AUTHOR INFORMATION

Corresponding Authors

*G. Subra. E-mail: gilles.subra@umontpellier.fr.

*A. Mehdi. E-mail: ahmad.mehdi@umontpellier.fr.

Notes

The authors declare no competing financial interest.

■ ACKNOWLEDGMENTS

C. Echaliér's Ph.D. is partly founded by Region Languedoc Roussillon through "Chercheur d'avenir" grant attributed to G. Subra. Peptide syntheses were performed using the facilities of SynBio3 IBISA platform supported by ITMO cancer.

■ REFERENCES

- (1) Slaughter, B. V.; Khurshid, S. S.; Fisher, O. Z.; Khademhosseini, A.; Peppas, N. A. Hydrogels in Regenerative Medicine. *Adv. Mater.* **2009**, *21*, 3307–3329.
- (2) Tibbitt, M. W.; Anseth, K. S. Hydrogels as Extracellular Matrix Mimics for 3D Cell Culture. *Biotechnol. Bioeng.* **2009**, *103*, 655–663.
- (3) Drury, J. L.; Mooney, D. J. Hydrogels for Tissue Engineering: Scaffold Design Variables and Applications. *Biomaterials* **2003**, *24*, 4337–4351.
- (4) Kim, B.-S.; Park, I.-K.; Hoshiba, T.; Jiang, H.-L.; Choi, Y.-J.; Akaike, T.; Cho, C.-S. Design of Artificial Extracellular Matrices for Tissue Engineering. *Prog. Polym. Sci.* **2011**, *36*, 238–268.
- (5) Vashist, A.; Vashist, A.; Gupta, Y. K.; Ahmad, S. Recent Advances in Hydrogel Based Drug Delivery Systems for the Human Body. *J. Mater. Chem. B* **2014**, *2*, 147–166.

(6) Hersel, U.; Dahmen, C.; Kessler, H. RGD Modified Polymers: Biomaterials for Stimulated Cell Adhesion and beyond. *Biomaterials* **2003**, *24*, 4385–4415.

(7) Auernheimer, J.; Zukowski, D.; Dahmen, C.; Kantlehner, M.; Enderle, A.; Goodman, S. L.; Kessler, H. Titanium Implant Materials with Improved Biocompatibility through Coating with Phosphonate-Anchored Cyclic RGD Peptides. *ChemBioChem* **2005**, *6*, 2034–2040.

(8) Kantlehner, M.; Schaffner, P.; Finsinger, D.; Meyer, J.; Jonczyk, A.; Diefenbach, B.; Nies, B.; Hölzemann, G.; Goodman, S. L.; Kessler, H. Surface Coating with Cyclic RGD Peptides Stimulates Osteoblast Adhesion and Proliferation as Well as Bone Formation. *ChemBioChem* **2000**, *1*, 107–114.

(9) Yang, F.; Williams, C. G.; Wang, D.; Lee, H.; Manson, P. N.; Elisseeff, J. The Effect of Incorporating RGD Adhesive Peptide in Polyethylene Glycol Diacrylate Hydrogel on Osteogenesis of Bone Marrow Stromal Cells. *Biomaterials* **2005**, *26*, 5991–5998.

(10) Du, H.; Zha, G.; Gao, L.; Wang, H.; Li, X.; Shen, Z.; Zhu, W. Fully Biodegradable Antibacterial Hydrogels via Thiol–ene "click" Chemistry. *Polym. Chem.* **2014**, *5*, 4002–4008.

(11) Jiang, H.; Qin, S.; Dong, H.; Lei, Q.; Su, X.; Zhuo, R.; Zhong, Z. An Injectable and Fast-Degradable Poly(ethylene Glycol) Hydrogel Fabricated via Bioorthogonal Strain-Promoted Azide–alkyne Cycloaddition Click Chemistry. *Soft Matter* **2015**, *11*, 6029–6036.

(12) Vinatier, C.; Magne, D.; Weiss, P.; Trojani, C.; Rochet, N.; Carle, G. F.; Vignes-Colombeix, C.; Chadjichristos, C.; Galera, P.; Daculsi, G.; Guicheux, J. A Silanized Hydroxypropyl Methylcellulose Hydrogel for the Three-Dimensional Culture of Chondrocytes. *Biomaterials* **2005**, *26*, 6643–6651.

(13) Beltrán-Osuna, Á. A.; Cao, B.; Cheng, G.; Jana, S. C.; Espe, M. P.; Lama, B. New Antifouling Silica Hydrogel. *Langmuir* **2012**, *28*, 9700–9706.

(14) Zhu, J. Bioactive Modification of Poly(ethylene Glycol) Hydrogels for Tissue Engineering. *Biomaterials* **2010**, *31*, 4639–4656.

(15) Lin, C.-C.; Anseth, K. S. PEG Hydrogels for the Controlled Release of Biomolecules in Regenerative Medicine. *Pharm. Res.* **2009**, *26*, 631–643.

(16) Bakaic, E.; Smeets, N. M. B.; Hoare, T. Injectable Hydrogels Based on Poly(ethylene Glycol) and Derivatives as Functional Biomaterials. *RSC Adv.* **2015**, *5*, 35469–35486.

(17) Lin, C.-C. Recent Advances in Crosslinking Chemistry of Biomimetic Poly(ethylene Glycol) Hydrogels. *RSC Adv.* **2015**, *5*, 39844–39853.

(18) Grandsire, A. F.; Laborde, C.; Lamaty, F.; Mehdi, A. Palladium Supported on Polyether-Functionalized Mesoporous Silica. Synthesis and Application as Catalyst for Heck Coupling Reaction. *Appl. Organomet. Chem.* **2010**, *24*, 179–183.

(19) Zha, J.; Roggendorf, H. In *Sol–Gel Science, the Physics and Chemistry of Sol–Gel Processing*; Brinker, C. J.; Scherer, G. W., Eds.; Academic Press: Boston, 1990; ISBN 0-12-134970-5.

(20) Nguyen, M. K.; Lee, D. S. Injectable Biodegradable Hydrogels. *Macromol. Biosci.* **2010**, *10*, 563–579.

(21) Mehdi, A.; Reyé, C.; Brandès, S.; Guillard, R.; Corriu, R. J. P. Synthesis of Large-Pore Ordered Mesoporous Silicas Containing Aminopropyl Groups. *New J. Chem.* **2005**, *29*, 965–968.

(22) AAFNOR. EN ISO 10993-5: Biological evaluation of medical devices - Part 5: tests for in vitro cytotoxicity. 1999. Cell viability of more than 70% is considered noncytotoxic.

(23) Decker, T.; Lohmann-Matthes, M.-L. A Quick and Simple Method for the Quantitation of Lactate Dehydrogenase Release in Measurements of Cellular Cytotoxicity and Tumor Necrosis Factor (TNF) Activity. *J. Immunol. Methods* **1988**, *115*, 61–69.

(24) Livage, J.; Henry, M. In *Ultrastructure Processing of Advanced Ceramics*; Mackenzie, J. D.; Ulrich, D. R., Eds.; Wiley: Hoboken, NJ, 1988; pp 183–195.

(25) Pierschbacher, M. D.; Ruoslahti, E. Cell Attachment Activity of Fibronectin Can Be Duplicated by Small Synthetic Fragments of the Molecule. *Nature* **1984**, *309*, 30–33.

(26) Li, B.; Chen, J.; Wang, J. H.-C. RGD Peptide-Conjugated Poly(dimethylsiloxane) Promotes Adhesion, Proliferation, and Colla-

gen Secretion of Human Fibroblasts. *J. Biomed. Mater. Res., Part A* **2006**, *79A*, 989–998.

(27) Jebors, S.; Cecillon, S.; Faye, C.; Enjalbal, C.; Amblard, M.; Mehdi, A.; Subra, G.; Martinez, J. From Protected Trialkoxysilyl-Peptide Building Blocks to Bioorganic-Silica Hybrid Materials. *J. Mater. Chem. B* **2013**, *1*, 6510–6515.

(28) Jebors, S.; Ciccione, J.; Al-Halifa, S.; Nottelet, B.; Enjalbal, C.; M'Kadmi, C.; Amblard, M.; Mehdi, A.; Martinez, J.; Subra, G. A New Way to Silicone-Based Peptide Polymers. *Angew. Chem., Int. Ed.* **2015**, *54*, 3778–3782.

Chapter IV.

Collagen-inspired peptide hydrogel

*Publication 3 – Sol-gel synthesis of
collagen-inspired peptide hydrogel*

Echalier C. et al., submitted, under consideration.

My contribution to this paper: I performed the synthesis of the hybrid collagen-inspired peptide on a small scale, I prepared the hydrogels, I carried out the rheological measurements with the help of H el ene Van Den Berghe, I prepared the samples for microscopy, I performed cell adhesion, proliferation and encapsulation assays. I participated in the writing of the paper.

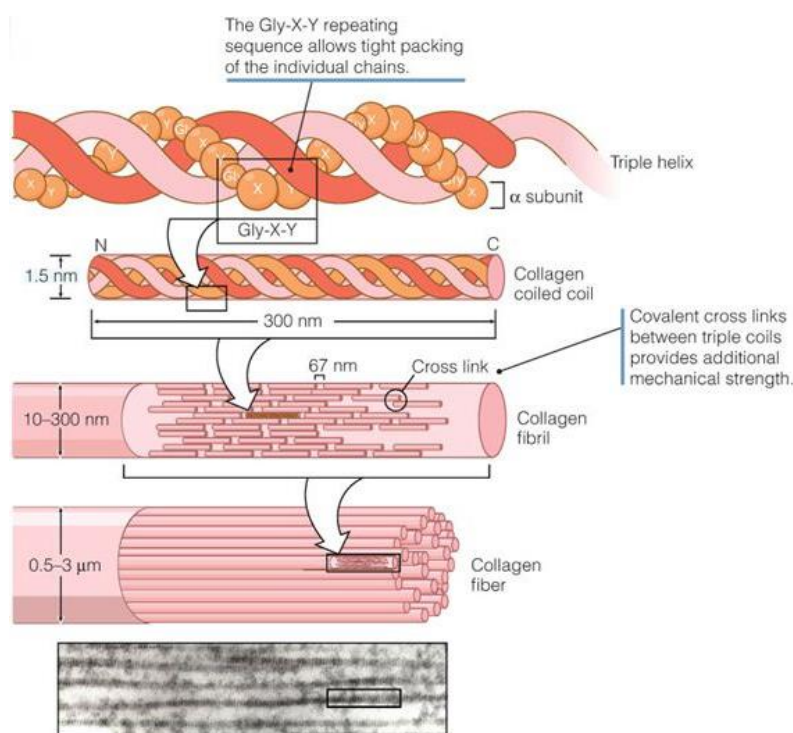
Chapter IV. Collagen-inspired peptide hydrogel

In the previous chapter, we presented a method for the one-pot preparation of functional PEG-based hydrogels. As already mentioned, PEG is a bio-inert polymer and PEG-based hydrogels have to be functionalized to afford an environment conducive to cell adhesion and proliferation. With tissue engineering applications in mind, we wanted to substitute PEG by a synthetic hydrogel precursor having inherent cell-friendly properties. We took inspiration from natural collagen.

IV.1. Natural collagen

IV.1.1. Structure and function

Collagen is the most abundant protein in the human body.³⁴³ It is a major component of the extracellular matrix. Collagen fibers form a three-dimensional network that provides tensile strength to the surrounding tissue. Different types of collagen have been identified and all of them share a common structure. Collagen is made of polypeptide chains whose sequence is composed of X-Y-Gly repetitive triplets. Exceptions to these repeat are very rare.³⁴⁴ X and Y can be any amino acid. However, the Pro-Hyp-Gly sequence has been identified as the most common triplet in collagen.³⁴⁵ These polypeptide chains are twisted in a left-handed polyproline II-type (PPII) helix. Three PPII helices wrap around each other to form a right-handed triple helix. Eventually, triple helices can self-assemble into fibrils which can agglomerate to form fibers (Figure 68).



Copyright © 2013 by Jones & Bartlett Learning, LLC an Ascend Learning Company
www.jblearning.com

Figure 68. Structure of natural collagen

IV.1.2. Applications of collagen-based biomaterials

Natural collagen can be used to design biomaterials (e.g. foams, films, hydrogels) which intrinsically provide a cell-friendly environment.³⁴⁶ It is of tremendous interest for wound healing and tissue engineering applications (Figure 69).^{347,348} For instance, Y. Zhao *et al* encapsulated hepatocytes in collagen hydrogels to reconstitute three-dimensional, vascularized hepatic tissue *in vivo*.³⁴⁹

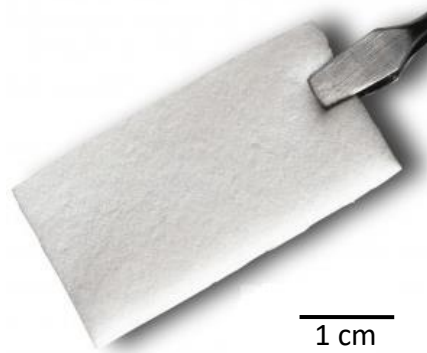


Figure 69. Commercially available collagen foam (ACE Surgical Supply Co, inc.) engineered from highly purified cross-linked bovine type I collagen and used as a resorbable material in periodontal defects to aid in wound healing

IV.1.3. Limitations of natural collagen extracts

Natural collagen is usually extracted from animal tissues (e. g. bovine tendon, porcine skin, rat tail).³⁴⁶ Animal-derived collagens are costly because their production requires large amount of animal tissues and their isolation and purification is challenging.³⁴⁷ They are sterilized to avoid infection but this do not alleviate the risk of contamination by pathogenic substances such as prions.³⁵⁰ In addition, remnant xenogeneic and allogeneic cellular antigens but also antigenic determinants located on the collagen molecule itself due to interspecies variation can trigger an immune response.^{351,352} At last, as for other natural extracts, they suffer from a poor batch-to-batch reproducibility.

Alternatively, recombinant systems have been investigated to produce human type collagen, in a large scale.³⁵³ Collagen was produced in transfected mammalian cells, insect cells, yeasts, transgenic tobacco, mice and silkworms. Some transgenic systems hold great promises for the production of recombinant human collagen. However, none of these recombinant collagens have received approval for clinical use yet.

IV.2. Collagen-like peptides

IV.2.1. Pro-Hyp-Gly based peptides as synthetic collagen mimics

Owing to the limitations of natural collagen mentioned above, several groups have investigated the synthesis of collagen-like polypeptides.^{354–358} For example, S. E. Paramonov *et al.* prepared peptides containing the Pro-Hyp-Gly triplet and used native chemical ligation to polymerize these peptides. They showed that the polymers obtained exhibited some basic features of natural collagen, in particular the triple-helical character and the nanofibrous structure.³⁵⁹ J. D. Hartgerink and co-workers designed the collagen mimetic peptide (Pro-Lys-Gly)₄(Pro-Hyp-Gly)₄(Asp-Hyp-Gly)₄ that formed a triple helix stabilized by electrostatic interactions between lysine and aspartic acid. Nanofibers were observed that could self-assemble into hydrogels.³⁵⁵

It is noteworthy that three repeated sequences of the Pro-Hyp-Gly triplet were found to be sufficient for a peptide to adopt a PPII conformation. However, a minimum of nine triplets is required to form a triple helix stable at 37°C.³⁶⁰

IV.2.2. Design of the hybrid collagen-inspired peptide sequence

We chose the nonapeptide (Pro-Hyp-Gly)₃ as a building block for hydrogel preparation. This sequence was expected to adopt a PPII helix conformation but was not intended to assemble into a triple helix. Indeed, our goal was not to reproduce the supramolecular structure of natural collagen but rather to build a three-dimensional matrix displaying multiple Pro-Hyp-Gly motifs. We took advantage of the sol-gel process to prepare a fully synthetic but collagen-inspired hydrogel from a very short peptide sequence. We were hoping that this artificial matrix would be more conducive to cell adhesion and proliferation than synthetic polymer-based hydrogels such as PEG or PVA-based hydrogels.

The (Pro-Hyp-Gly)₃ peptide sequence was flanked by two lysine residues whose side-chains were intended to be used for the introduction of silyl groups (Figure 70). The N-terminus was acetylated while the C-terminus was amidated. Two triethoxysilyl groups were introduced on the amino side-chains of lysines by reaction with 3-isocyanatopropyltriethoxysilane as previously described in the second chapter yielding however urea linkages instead of the carbamate linkages of the silylated PEGs.

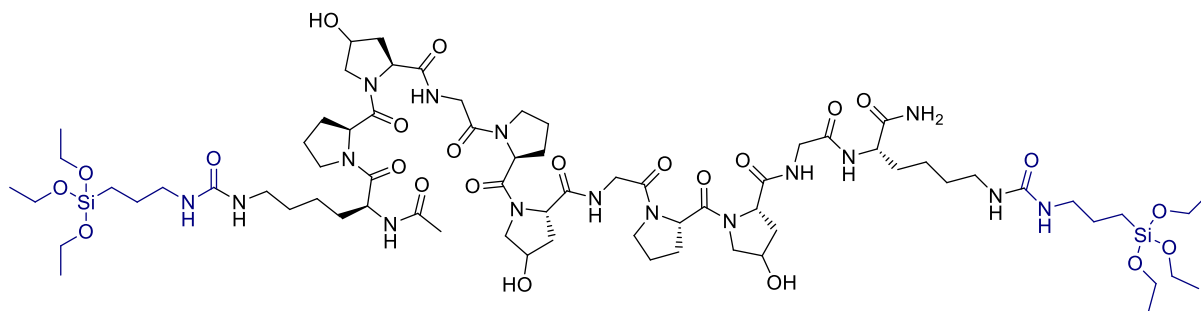


Figure 70. Hybrid collagen-inspired peptide used as a building block for hydrogel preparation

The synthesis of the hybrid collagen-inspired peptide is described in the following publication. The structure of this hybrid peptide in physiological buffer was studied by NMR and circular dichroism (CD). These experiments confirmed that the peptide adopted a PPII conformation but was too short to form a triple helix.

IV.3. Sol-gel derived collagen-inspired hydrogel

IV.3.1. Optimization of the hydrogel composition

The experimental procedure developed in the third chapter for the preparation of hybrid PEG-based hydrogels was applied to the hybrid collagen-inspired peptide. Hydrogels could be obtained by dissolution of this hybrid peptide in DPBS or cell culture media in the presence of sodium fluoride (3 mg/mL) and incubation at 37°C. A 10 wt% (62 mM) hybrid peptide solution yielded a hydrogel after 1h30. We tried to decrease the concentration in hybrid peptide but a 5 wt% solution was not able to form a hydrogel. It is noteworthy that 10 wt% hybrid peptide hydrogels were not as transparent as 10 wt% hybrid PEG 2000 hydrogels (Figure 71). They had a milky appearance already observed for 5 wt% hybrid PEG 2000 hydrogels. This milky appearance seems to indicate a concentration limit below which it is not possible to form hydrogels. Higher concentrations in hybrid collagen-inspired peptide were not investigated, we assumed that denser hydrogels would be less valuable for cell culture.

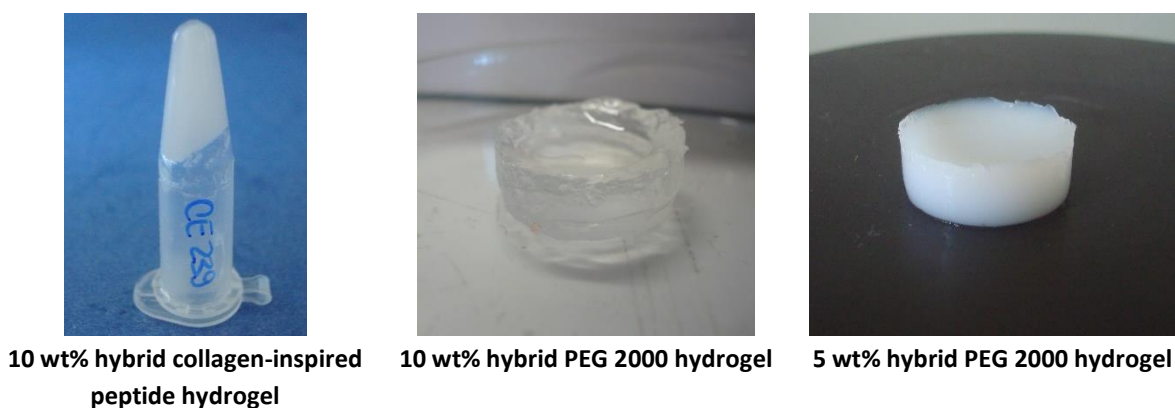


Figure 71. Appearance of different hydrogels prepared in DPBS

As a consequence, in all the following experiments, including the ones described in the enclosed paper Echalier *et al.* "Sol-gel synthesis of collagen-inspired peptide hydrogel", a 10 wt% concentration in hybrid collagen-inspired peptide was chosen.

IV.3.2. Monitoring of the hydrogel formation and characterization

The gelation of a 10 wt% hybrid peptide solution at 37°C was monitored by liquid ^1H NMR and rheology. These studies are described in the following publication. It is worth noting that the rheological measurements showed the same pattern as for the gelation of hybrid PEG, suggesting that the nature of the organic part of the hybrid block is not determinant for the sol-gel gelation process. The resulting hydrogel was also examined by scanning electron microscopy. Like for the hybrid PEG hydrogels previously, environmental SEM images and conventional SEM images of the freeze-dried samples were not satisfactory and showed a featureless dense matrix. The porosity of the hydrogel was brought to light by cryoSEM technique. In this case, the hydrogel sample is frozen in slush nitrogen which enables to preserve the inner structure of the matrix. Then it is fractured and only a thin layer of water is removed to observe the surface of the sample at low temperature. CryoSEM images showed a porous matrix with a quite homogeneous distribution of micrometric alveoli (Figure 72) that allowed us to envision cell encapsulation.

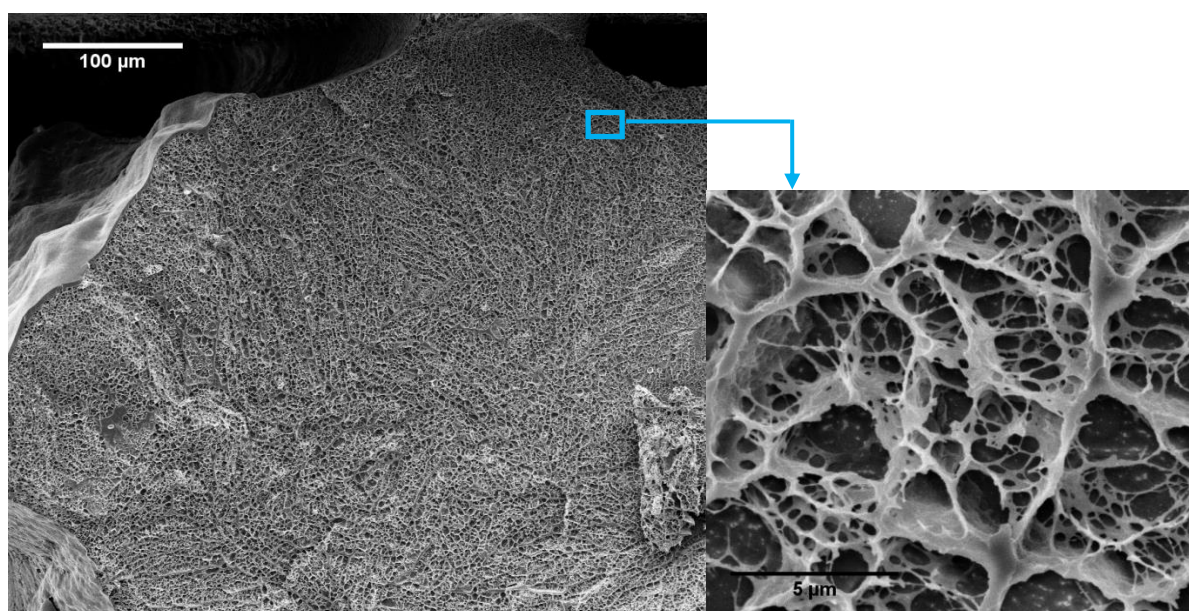


Figure 72. CryoSEM images of a 10 wt% hybrid collagen-inspired peptide hydrogel prepared in cell culture medium with sodium fluoride (3 mg/mL)

IV.4. Biological assessment of the hydrogel

Cell adhesion properties of the hybrid collagen-inspired peptide hydrogel were evaluated on mouse mesenchymal stem cells (mMSC). Stem cells were selected considering their significance in tissue engineering (cf. Chapter I).

IV.4.1. Influence of the functionalization of the hybrid collagen-inspired peptide hydrogel with RGD ligand on transparency

Two hybrid solutions were prepared for cell adhesion assays. The first one consisted of the hybrid collagen-inspired peptide dissolved in cell culture medium (high glucose DMEM containing phenol red and GlutaMAX – Gibco ref. 31966 – with 10% FBS and 1% penicillin-streptomycin) at a 10 wt% concentration in presence of sodium fluoride (3 mg/mL). The second solution was obtained from the first one by addition of hybrid RGD peptide (this hybrid peptide was already described and used to prepare bioactive PEG-based hydrogels in the second chapter) at a 10 mol% concentration regarding the hybrid collagen-inspired peptide. These hybrid solutions were deposited in 96 well cell culture plate (30 μ L per well) and incubated at 37°C overnight to allow the formation of hydrogels.

We noticed that the second hybrid solution yielded hydrogels more transparent than the first one (Figure 73 left), suggesting that the addition of another hybrid block strengthens the network. This observation was in accordance with the evolution of PEG hydrogel transparency as a function of hybrid PEG concentration (Figure 71). To confirm this tendency, 300 μ L hybrid collagen-inspired peptide hydrogels with 0, 10 or 20 mol% of hybrid RGD peptide were prepared (Figure 73 right).

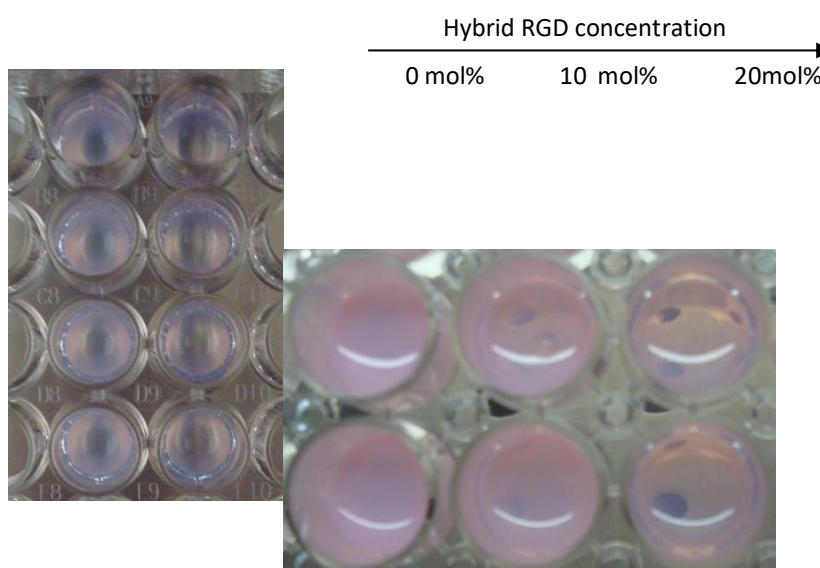


Figure 73. Appearance of hybrid collagen-inspired peptide hydrogels prepared in cell culture plates. Left picture: 30 μ L hybrid collagen-inspired hydrogels without hybrid RGD (left column) and with 10 mol% hybrid RGD peptide (right column) in a 96 well cell culture plate. Right picture: 300 μ L hybrid collagen-inspired hydrogels in a 24 well cell culture plate.

Obviously, the higher the concentration in silicon atom is in the hydrogel, the more transparent is the hydrogel. These results were not discussed in the publication n°3 (“Sol-gel synthesis of collagen-inspired peptide hydrogel”).

IV.4.2. Influence of the functionalization of the hybrid collagen-inspired peptide hydrogel with RGD ligand on cell adhesion

The hydrogels prepared in the 96 well cell culture plate were washed with cell culture media before mMSC were seeded on their surface. Cells were allowed to adhere for 1 h, 2 h and 4 h at 37°C. Then cell culture media were removed and wells were washed with DPBS. Adherent cells were quantified with the CellTiter-Glo luminescent cell viability assay (Figure 74). This cell viability assay is based on the quantification of the adenosine-triphosphate (ATP) released upon cell lysis. The ATP amount is directly proportional to the number of cells present in each well. The number of adherent cells on hybrid hydrogels was compared to the number of adherent cells on tissue-culture polystyrene (TC-PS). Results were normalized to a set of samples that was left intact after cell seeding (no washing) and thus provided the value corresponding to 100% adhesion. Interestingly, cell adhesion on hybrid peptide hydrogels was found to be far more efficient than on TC-PS. In addition, no significant difference was observed between the samples containing the hybrid RGD peptide and the others. It means that the hybrid collagen-inspired peptide is sufficient in it-self to afford an environment favourable for cell adhesion without the need of modification with cell adhesion peptides. This result has to be underlined because it is rather rare that synthetic hydrogels exhibit good cell adhesion properties prior to modification with cell adhesion ligands.

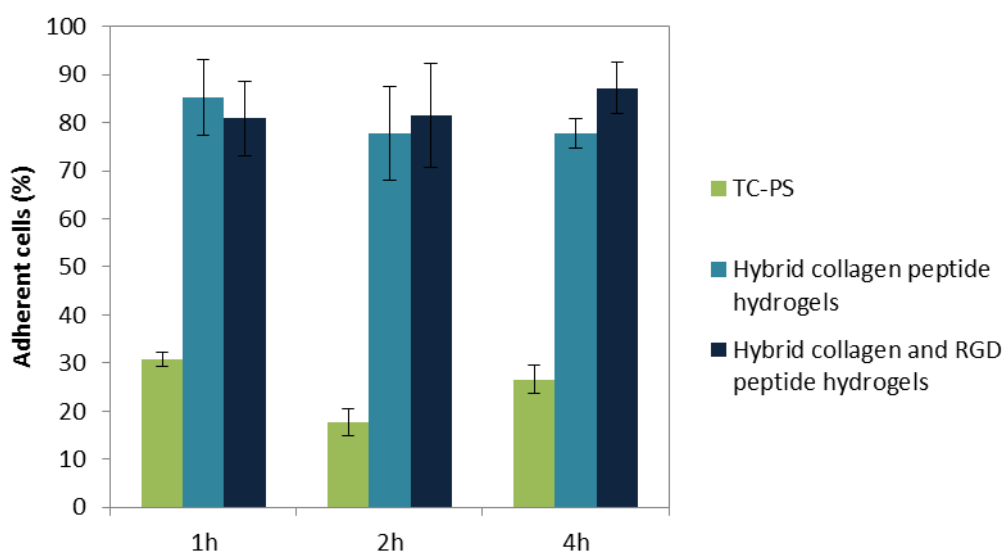


Figure 74. mMSC adhesion on hybrid collagen-inspired peptide hydrogels containing 0 or 10 mol% of hybrid RGD peptide

IV.4.3. Benchmarking of hybrid collagen-inspired peptide hydrogels vs commercial collagen foams and cell encapsulation

Other cell adhesion experiments were set up to compare cell adhesion on hybrid collagen-inspired peptide hydrogels and on natural collagen substrates (Figure 69), they are described in the following paper. After 4 h of contact between cells and substrates, cell adhesion on hybrid peptide gels was equivalent to the cell attachment on natural collagen foams. Cell proliferation assays on the hybrid hydrogels were also performed and are discussed in the enclosed publication. Interestingly, cell proliferation on hybrid peptide hydrogels was as efficient as on natural collagen foams. At last, we demonstrated that stem cells could be encapsulated within the hybrid collagen-inspired peptide hydrogels with a good viability provided that the sodium fluoride concentration was decreased. These results suggested that hybrid collagen-inspired peptide hydrogels could be useful matrices for cell encapsulation and applications in tissue engineering. In view of these applications, an efficient and cell-friendly catalyst of the sol-gel process that could replace sodium fluoride is of interest to enable a tighter control over the gelation time while preserving cell viability.

IV.5. Collagen-inspired peptide membranes

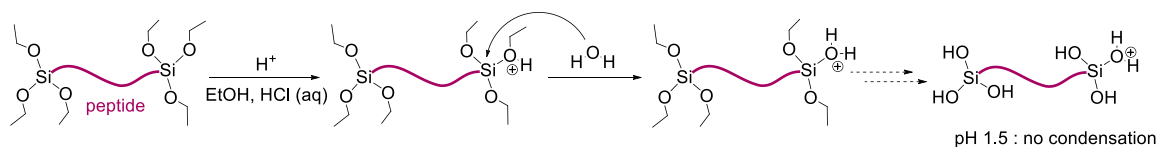
Collagen membranes are of tremendous interest for wound healing.³⁴⁶ They serve primarily as a barrier to protect the wound from the external environment, role that is usually held by the skin. Thus, collagen membranes decrease the risk of infection while reinforcing compromised tissues and guiding their regeneration. They can be loaded with growth factors for a sustained release that will improve wound healing.³⁶¹ In view of the significance of collagen membranes as wound dressings and the shortcomings of natural collagen, the preparation of synthetic hybrid collagen-inspired peptide membranes was of interest.

IV.5.1. Synthesis of hybrid membranes by the sol-gel process

Accordingly, alongside the results obtained with the hybrid collagen-inspired peptide hydrogel and described in the following publication, we investigated the use of this hybrid peptide for the preparation of collagen-inspired peptide membranes by the sol-gel process. While hydrogels are prepared in aqueous solutions and used in their wet state, membranes are synthesized in a volatile solvent and obtained in their dried form. The hybrid collagen-inspired peptide was dissolved in absolute ethanol at a 12 wt% concentration. A 0.1 M solution of chlorhydric acid (50 μ L/mL of ethanol) was added (Figure 75). The resulting hybrid solution was poured in a Petri dish or a cap and incubated at 37°C overnight to yield a membrane (Figure 76). Herein, HCl catalyzes the hydrolysis of ethoxysilyl groups. The condensation of silanols is triggered by the increase in concentration resulting from ethanol evaporation. The

high concentration in silyl precursors at the end of the process, the low amount of water and the temperature contribute to the formation of a highly cross-linked network.

A - Acid-catalyzed hydrolysis



B - Condensation

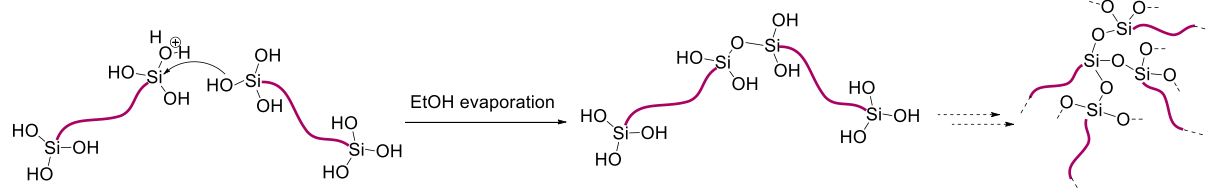


Figure 75. Synthesis of a hybrid peptide membrane by the sol-gel process



Figure 76. Hybrid collagen-inspired peptide membranes. Left: raw membrane after unmolding. Right: cut membrane.

IV.5.2. Physical properties of collagen-inspired peptide membranes

As shown in Figure 76, hybrid membranes are highly transparent. Their homogeneity was confirmed by scanning electron microscopy. SEM images showed a dense matrix and absence of aggregated domains (Figure 77).

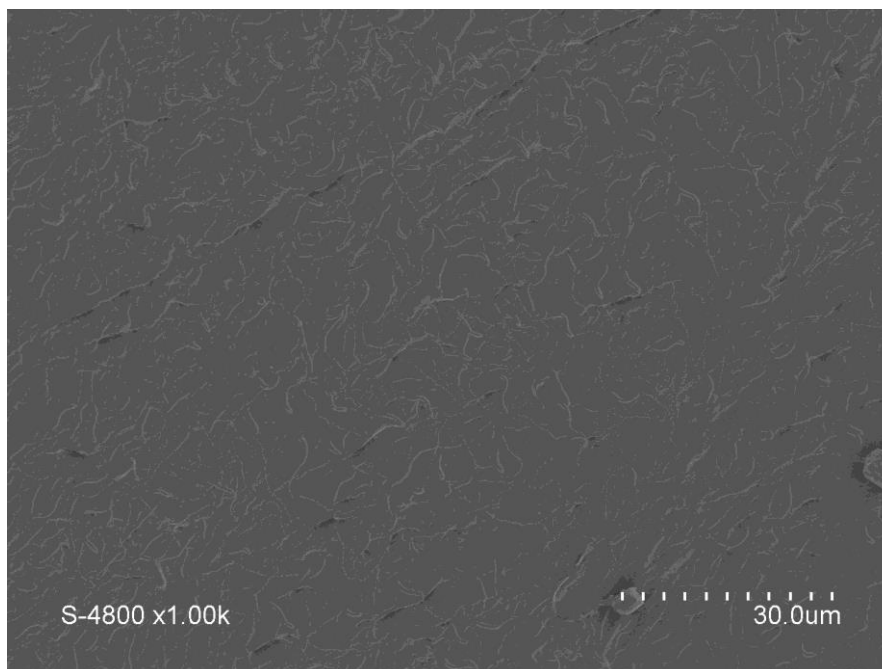


Figure 77. SEM image of a hybrid collagen-inspired peptide membrane.

Hybrid membranes can be cut, sterilized in 70% ethanol baths and washed with cell culture media. They are easy to handle and exhibit low swelling capacity due to their high degree of condensation.

Further characterizations of the hybrid membranes would be required to envision wound healing applications. In particular, mechanical properties of the membranes have to be studied: elastic modulus, tensile strength and elongation at break are important parameters for wound dressings.

IV.5.3. Preliminary biological assays: adhesion and proliferation of L929 fibroblasts on hybrid collagen-inspired peptide membranes

The adhesion and proliferation of L929 mouse fibroblasts was measured on these hybrid membranes. Fibroblasts were chosen because they are of interest for wound healing applications. Membranes were cut to fit in a 24 well cell culture plate. They were maintained in the bottom of the wells using O-rings. Cells were seeded on top of the hybrid membranes and allowed to adhere for 30 min. After washing, adherent cells were quantified with a PrestoBlue cell viability assay. PrestoBlue reagent is reduced by metabolically active cells into a fluorescent dye. Thus, fluorescence reading values provide a quantitative measure of cell viability. This cell viability assay was chosen because it doesn't require cell lysis. After removal of the reagent and addition of fresh cell culture medium, cell culture can be continued to monitor proliferation.

Hence, the proliferation of cells on hybrid membranes was followed for 7 days using the PrestoBlue assay (Figure 79). Adhesion and proliferation results on hybrid membranes were

compared to results on polystyrene (PS), on TC-PS and on a commercially available natural collagen membrane (RCM6 resorbable collagen membrane ACE, Figure 78) cut into samples of the same size as hybrid membranes. As expected, the number of cells on PS was very low since non-treated PS is a very poor substrate for cell culture. Herein, it was used as a negative control. In contrast, cell adhesion and proliferation on TC-PS was very efficient. Cell adhesion on hybrid membranes was lower than on TC-PS but similar to cell adhesion on natural collagen membranes. In the first five days, cells grew efficiently on natural collagen membranes and were even able to catch up with cells on TC-PS. Inexplicably, a slight decrease in the number of cells on natural collagen membranes was observed on the 7th day. In comparison, cell proliferation on hybrid membranes was lower and seemed to reach a plateau after 72 hours.



Figure 78. Commercially available natural collagen membrane.

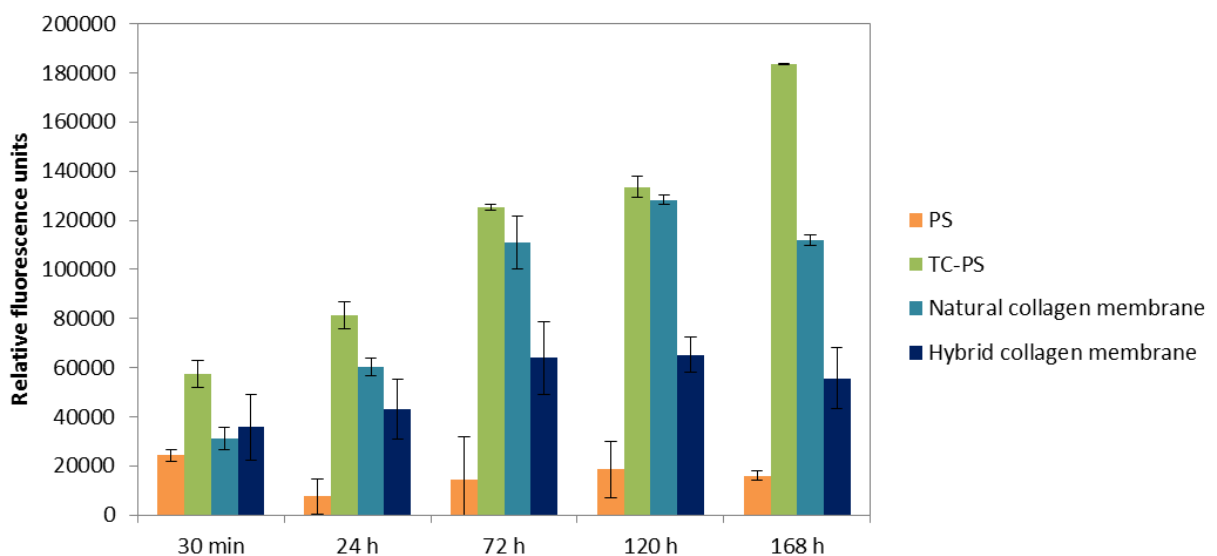


Figure 79. L929 adhesion and proliferation on hybrid collagen-inspired peptide membranes.

These results might be due to the morphology of the hybrid membranes and their high

density. More efficient membranes could be obtained by introducing some macroporosity (50-500 μm) in the artificial network. This could be achieved by using porogens during the sol-gel process. When casted with material precursors, porogens, such as sodium chloride, form particles that can be removed after establishment of the network, yielding pores in the resulting materials ("porogen leaching" method).³⁶² A looser network could also be accessed by increasing the length of the hybrid peptide (*i. e.* 4 or more ProHypGly repeats) and/or adding monosilylated species. Such membranes could be of interest for wound healing. As a conclusion concerning this last section, the hybrid collagen-inspired peptide developed for the preparation of hydrogels in the beginning of this chapter was also used to prepare membranes through the sol-gel process. These membranes seemed to be biocompatible and exhibited correct cell adhesion properties but were not fully optimized to promote efficient cell proliferation.

IV.6. Publication n°3 – Sol-gel synthesis of collagen-inspired peptide hydrogel

The publication n°3 was under consideration at the time of printing of this manuscript (25th September 2016). It is not an accepted work but, for the ease of reading, it has been included in this manuscript in the form of its current submission.

Sol-gel synthesis of collagen-inspired peptide hydrogel

Cécile Echalié^{1,2}, Said Jebors¹, Guillaume Laconde¹, Luc Brunel¹, Pascal Verdié¹, Léa Causse¹, Audrey Bethry¹, Baptiste Legrand¹, Hélène Van Den Berghe¹, Xavier Garric¹, Danièle Noël³, Jean Martinez¹, Ahmad Mehdi², Gilles Subra¹

¹ Institut des Biomolécules Max Mousseron (IBMM), UMR5247 Université de Montpellier, CNRS, ENSCM, France.

² Institut Charles Gerhardt de Montpellier (ICGM), UMR5253 Université de Montpellier, CNRS, ENSCM, France.

³ Institute for Regenerative Medicine and Biotherapy (IRMB), Inserm U1183, CHU, Université de Montpellier, France.

Correspondence should be addressed to G.S. (gilles.subra@umontpellier.fr)

Conceiving biomaterials able to mimic the specific environments of extracellular matrices are a prerequisite for tissue engineering applications. Numerous types of polymers (PEG, PLA, etc.) have been used for the design of biocompatible scaffolds, but they are still less efficient than natural biopolymers such as collagen extracts. Chemically modified and loaded with different bioactive factors, biopolymers afford an environment favourable to cell proliferation and differentiation. Unfortunately, they present several drawbacks, such as weak batch-to-batch reproducibility, potential immunogenicity and high cost of production. Herein we propose a fully synthetic covalent hydrogel obtained by sol-gel polymerisation of a silylated peptide. We selected a short and low molecular building-block derived from the consensus collagen sequence [Pro-Hyp-Gly]. Interestingly, the sol-gel process occurs in physiological buffer, enabling the embedment of stem cells. This collagen-inspired hydrogel provides a cell-friendly environment comparable to natural collagen substrates, demonstrating its potency as a biomimetic scaffold.

Introduction

Hydrogels are exceptional biomaterials, especially for their use as scaffolds for tissue engineering and as matrices for drug and gene delivery. Depending on the type of bonds that are formed during their fabrication process, physical or chemical hydrogels can be obtained. Physical hydrogels are reversible, due to the weak interactions involved in the biomaterial (e.g. hydrogen and ionic bonds), and are attractive as injectable materials due to their shear thinning (or thixotropic behavior). On the other hand, chemical hydrogels cross-linked by covalent bonds, are more stable and thus suitable for a wider range of applications including cell culture. A large family of them is based on synthetic polymers such as poly(lactic-co-glycolic acid) PLGA,¹ polyacrylamides,^{2,3} polyhydroxyethylmethacrylate (PHEMA)⁴ or polyethyleneglycol (PEG)⁵. However all these materials fail to mimic the complexity of natural tissues and have to be further functionalized with peptide ligands derived from extracellular matrix (ECM) proteins (e.g. fibronectin, laminin) for efficient cell adhesion.^{6,7}

To improve the resemblance with natural tissues, it is also possible to form a hydrogel by covalently linking chemically-modified synthetic polymers [*i. e.* poly(N-isopropylacrylamide)

(NIPAM), PEG, etc.] with chemically-modified natural biopolymers [*i. e.* polysaccharides, heparin, etc.]. For example, hydrazide-modified NIPAM was reacted with aldehyde-modified carboxymethyl cellulose, to yield injectable hydrogels.⁸ A starPEG-heparin hydrogel was obtained after chemical modification of both starPEG and heparin with a maleimide (via carbodiimide/active ester)⁹, which can be cross-linked with the thiol side-chains of a cysteine-containing peptide by Michael addition.^{10,11} A analogue method was used to cross-link thiol-modified gelatin and hyaluronic acid with PEG bis-acrylate.¹² Among the described conjugation methods that have been employed for polymer cross-linking, the embedment of cells drastically restrains the choice to non-toxic reagents, and to the absence of side-products coming from the reticulation reaction (*i. e.* active esters, metals, etc.).

Hydrogels obtained directly from cross-linked natural biopolymers are more adapted to cell survival and proliferation. Photopolymerization of methacrylated gelatin¹³, chitosan¹⁴ and hyaluronic acid¹⁵ were used to prepare hydrogels. Nevertheless, these natural polymers are usually costly, they encounter low batch-to-batch reproducibility, microbial contaminants during the isolation process and potential immunogenicity in the case of animal extracts.

In this context, we propose a novel type of biomaterial, combining the biocompatibility of natural polymers, with the ease of synthesis and modification afforded by synthetic molecules. We defined four requirements to address the problems raised by existing materials.

(i) The starting materials should be synthetic to avoid purification problems encountered with extraction of natural biopolymers, and to facilitate the scale-up of the synthesis; (ii) The formation of the hydrogel network should be compatible with the inclusion of cells, avoiding the use of any chemical reagent; (iii) The process should be modular and should allow the covalent incorporation of any bioactive moiety in one single step; (iv) The resulting hydrogels should favour cell adhesion and proliferation, without the need of further addition of adhesion ligands.

These challenges were tackled by the design and synthesis of a bis-silylated low molecular building block (1612 g/mol) able to undergo sol-gel process, through hydrolysis and condensation in a biological buffer, yielding a three-dimensional network (Figure 1 A). We have already reported the synthesis of bioactive PEG-based chemical hydrogels by this type of soft chemistry route¹⁶. In this study, we substituted the biologically inert PEG by a peptide to give inherent cell-friendly properties to the network.

Considering the significance of collagen in tissue engineering¹⁷, extensive work has been performed to mimic its multi-hierarchical structure with synthetic peptides. Among the general repetitive triplet motifs X-Y-Gly, the Pro-Hyp-Gly tripeptide is one of the most common stabilizing sequence found in collagens.¹⁸ Very short oligopeptides based on this sequence were shown to adopt a polyproline II (PPII) helix conformation.¹⁹ In natural collagen, three peptide sequences adopting a PPII structure wrap around each other to form a right-handed supercoil triple helix. It has been established that a minimal oligopeptide length is required to get stable triple helix structure. This latter structure was generally observed using nine or more X-Y-Gly triplets.²⁰⁻²³ Moreover, to stabilize the self-assembly of synthetic collagen peptides, several strategies have been developed such as disulphide bridges formation,^{24,25} ionic interactions between anionic and cationic side chains,^{26,27} and hydrogen bond networks.²⁸

In contrast with the ongoing research related to the design of peptide-based collagen mimics, we did not aim at reproducing the supramolecular structure of natural collagen. We focussed on the multiple presentation of Pro-Hyp-Gly motif, structured in PPII conformation, within a tri-dimensional matrix. We hypothesise that such artificial but collagen-inspired matrix could advantageously replace polymers to form hydrogels favouring cell culture with an efficiency comparable to that of collagen-based materials. We selected the peptide sequence (Pro-Hyp-Gly)₃ whose size was too small to expect the formation of triple helix, but long enough to adopt a well-defined PPII structure.¹⁹ At last, the collagen-inspired sequence was flanked by two lysine residues and triethoxysilane groups were introduced on the lysine side-chains using a

flexible linker. Silyl moieties are the anchoring points promoting the covalent assembly of the network.

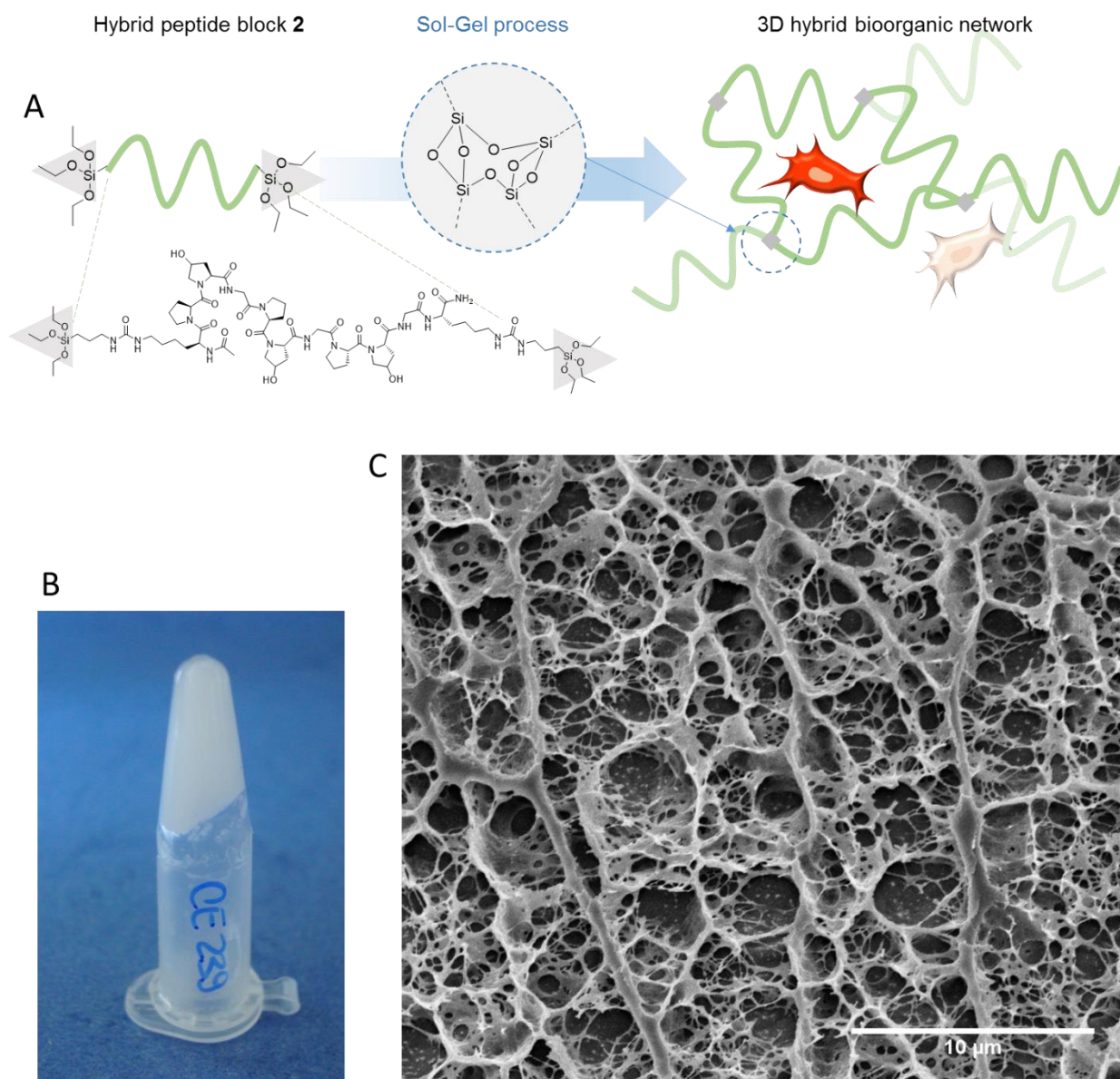


Figure 1. Schematic representation (A), photo (B) and cryo-SEM image (C) of the hybrid collagen-inspired hydrogel.

Results and discussion

Synthesis of a bis-silylated undecapeptide as hydrogel building block

A convergent synthesis was first set up to prepare the undecapeptide **1**. It involved the synthesis of the Fmoc-Pro-Hyp-Gly-OH tripeptide in solution, and its use as a building block for the stepwise synthesis on solid support (S.I. figure S1). In the meantime, we developed a novel methodology for rapid peptide synthesis called Fast Parallel Peptide Synthesis (FPPS).²⁹ This

methodology was successfully applied to the synthesis of peptide **1** that was obtained in only 3 hours (Figure 2, S.I. p S3).

After N-terminus acetylation, the peptide **1** was cleaved from the resin concomitantly with the removal of the N-terbutyloxycarbonyl (Boc) and t-butyl ester (tBu) groups, which protected respectively the side chains of lysine and hydroxyproline residues. At this stage, compound **1** has been purified by RP-preparative HPLC (yield 50%, > 99% purity). The synthesis was repeated several times and the large-scale RP-HPLC purification was optimized (S.I. p S3). The overall process proved to be robust enough to provide multi-gram batches of pure peptide **1**. The key step of the synthesis was the introduction of the two alkoxyisilane moieties. N- ϵ amino groups of lysine residues reacted quantitatively with 3-isocyanatopropyltriethoxysilane (ICPTES) in the presence of DIEA, to yield the bis-functionalized undecapeptide **2** (Figure 2). The hybrid peptide building block **2** was recovered quantitatively by precipitation in diethyl ether and characterized by ^1H , ^{13}C , ^{29}Si NMR, and LC/MS (S.I. figures S3-S7).

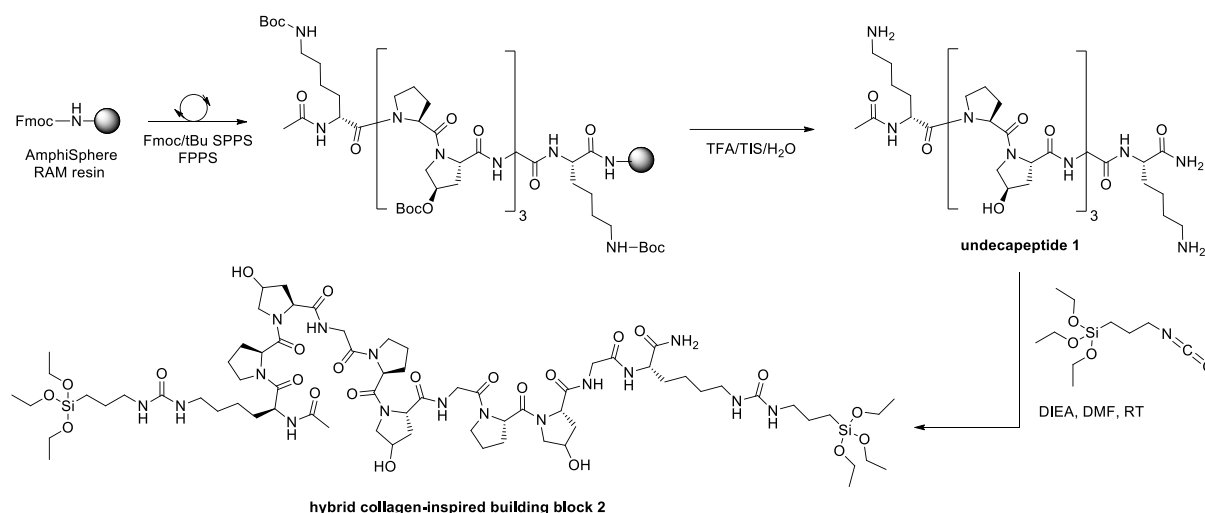


Figure 2. Synthesis of the hybrid bis-silylated undecapeptide **2**, Ac-Lys[CONH-(CH₂)₃-Si(OEt)₃]-[Pro-Hyp-Gly]₃-Lys[CONH-(CH₂)₃-Si(OEt)₃]-NH₂

We investigated the propensity of the short peptide sequence of **2** to adopt a PPII helix structure and self-assemble in triple helix by circular dichroism (CD) and NMR spectroscopies in DPBS buffer, pH 7.2. The CD spectrum of **2** showed a typical PPII signature with negative and positive maxima at 200 and 224 nm, respectively (S.I. Figure S13). Moreover, characteristic NOE correlations of the PPII helical fold were found on the ROESY spectrum of **2** (i.e, strong and medium H α (i),H δ (i+1) and H β (i),H δ (i+1) NOE peaks). In this context, the three Pro-Hyp-Gly repeats adopt a PPII while the lysine residues and the silylated arms were disordered since few NOEs could be detected in these moieties, as expected. The building block has a maximal dimension of 66 Å, with a length of 26 Å for the PPII secondary structure. Finally, the ^1H resonances of **2** were similar at 62 mM and 0.62 mM (10 and 0.1 wt%, respectively) showing that this undecapeptide was too short to assemble in triple helix (S.I. Figure S9).

Hydrogel formation

The sol-gel process consists in the hydrolysis of alkoxyisilyl groups followed by condensation to yield siloxane bonds.³⁰ Depending on the conditions (e.g. pH, catalyst) these two processes happen either sequentially or concomitantly. Cross-linked hydrogels of biopolymers such as

gelatin,³¹ alginate³², chitosan,³³ and hydroxypropylmethyl cellulose (HMPC)³⁴ have already been obtained by the sol-gel process. However, such protocols involve either a pH solution that is not compatible with live cells or toxic chemical reagents that have to be removed prior to biological assays. Alternatively, they are based on hydrolysis of the alkoxysilanes in acidic or basic conditions, followed by condensation upon neutralization of the medium. The method we have developed proceeds at 37°C, at physiological pH (7.4), in suitable biological buffer (DPBS or DMEM). It could be compatible with the inclusion of stem cells and, more importantly, could allow injection, and *in vivo* gelation.³⁵

Accordingly to our previous study,¹⁶ sodium fluoride was used to catalyse both the condensation, and the hydrolysis process (S.I. figure S8 A and B respectively), at physiological pH. Each of the silane group of the hybrid collagen peptide might undergo three successive condensations to yield three Si-O-Si bonds, which might link the same pair of atoms. Such 'intra' condensation can be considered as a linear enlargement of the polymeric chain. Alternatively, each silicon atom can be linked to two or three different partners. In this case, a reticulation node was created which can be considered as a chemical cross-link between the polymer chains. Hence, a covalent three-dimensional network was established, made of short (Pro-Hyp-Gly)₃ sequences linked by siloxane bonds (Figure 1).

In practice, building block **2** was dissolved in cell culture medium (62 mM in DMEM with 10% FBS), at a concentration of 10 wt%. 0.3 wt% of sodium fluoride was added and the hybrid solution was placed at 37°C to form a gel. The evolution of the sol-gel process was monitored by liquid ¹H NMR. For this study, cell culture medium was replaced by DPBS (DPBS × 10/D₂O/H₂O 1/1/8 v/v/v). The hybrid solution was introduced in a NMR tube and spectra were performed at 37°C (Figure 3 and S.I. pp S9-S13). The hydrolysis of ethoxysilanes was monitored by quantification of the released ethanol. Based on the integration of the CH₃ signal of EtOH, it appeared clearly that 70% of SiOEt groups were hydrolysed after 5 minutes. The hydrolysis was found to be complete after 60 min. These results were also confirmed by the disappearance of the signal attributed to -Si(OCH₂CH₃)₃. Since the hydrolysis and the polycondensation reactions operated at the same time under nucleophile (F⁻ herein) catalyst, a regular decrease of the overall signal of peptide was also observed, resulting from the disappearance of free peptides in solution upon condensation. No precipitation was observed but the solution turned into a gel after 90 minutes. It is worth noting that the condensation was incomplete even after several hours, due to the gelation which limited the movement of polymer chains.

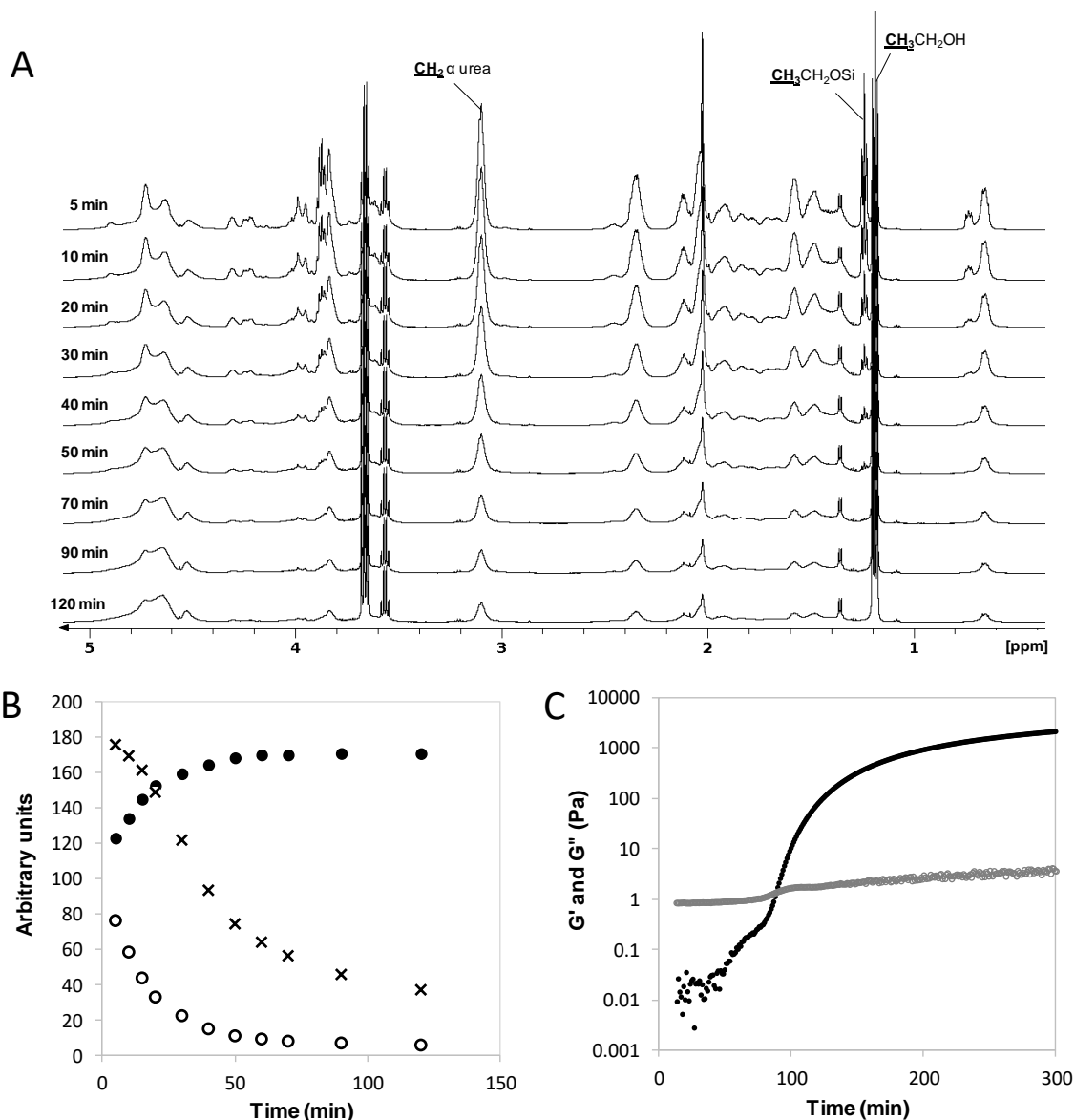


Figure 3. Monitoring of hydrogel formation by ^1H NMR and rheology. A: ^1H NMR spectra of the hybrid peptide **2** at a 10 wt% concentration in DPBS containing 0.3 wt% of NaF. B: Integration of ^1H NMR signals of the CH_3 group of ethanol ($\delta = 1.18$ ppm, ●), $\text{Si}(\text{OCH}_2\text{CH}_3)_3$ of the hybrid peptide ($\delta = 1.24$ ppm, o) and CH_2 groups of the hybrid peptide located in α position of ureas ($\delta = 3.10$ ppm, x). C: G' (●) and G'' (o) moduli measured on a hybrid peptide **2** solution (10 wt% in cell culture media containing 0.3 wt% of NaF) at 37°C (25% strain, 1 Hz).

The gelation process was also monitored by rheology in order to determine the gel point (Figure 3, C). The viscoelastic behavior of a system is characterized by the storage (G') and loss (G'') moduli which respectively quantify the solid-like and fluid-like contributions to the measured response when a sinusoidal shear deformation is applied to the system. Oscillatory shear measurements were performed on the hybrid peptide **2** solution (10 wt% in cell culture media with 0.3 wt% of NaF) at 37°C using an AR 2000 rheometer (TA Instruments, Inc) with a 20 mm diameter parallel geometry. The hybrid solution was deposited on the Peltier plate and the gap was set at 500 μm . The dependence of G' and G'' moduli was measured as a function of time within the linear viscoelastic regime of the hydrogel (25% strain, 1 Hz). Initially, G'' was greater than G' which indicated a viscous behavior of the sample. During the experiment, G' increased quickly due to the formation of elastic intermolecular cross-links upon

polycondensation while G'' increased negligibly. Thus a crossover of G' and G'' was observed at 90 min corresponding to the gel point. Afterwards, the sample presented solid-like properties. Frequency sweep experiment was also carried out and showed no dependence of the G' modulus as a function of the frequency at 25% strain. (S.I. figure S14).

These hybrid hydrogels were examined by Scanning Electron Microscopy (SEM). Images obtained in wet state by environmental SEM or after freeze-drying and gold coating by conventional SEM were not satisfactory due to either a low resolution or the denaturation of the hydrogel during the freeze-drying process (S.I. figure S15). We then turn our attention to cryoSEM technique which enables to freeze the inner structure of the hydrogel. Only a thin layer of water is removed from the sample to observe its surface. Interestingly, cryoSEM images showed a homogeneous porous matrix all over the different samples. Interestingly, micrometric alveoli were observed (Figure 1C and S.I. figure S16), whose size was comparable to alveoli obtained in elastin porous hydrogels.³⁶ The size of the pores suggested that collagen-inspired hydrogels could be suitable for the inclusion of cells.

Biological assessment

Cell adhesion and proliferation properties of hybrid (Pro-Hyp-Gly)₃-based hydrogels were assayed using mouse mesenchymal stem cells (mMSC). This cell line was chosen in the perspective of tissue engineering applications. Indeed, MSC are a promising alternative to chondrocytes to treat osteoarthritis or other osteochondral defects, a major cause of disability and pain among the ageing population.³⁷ MSC are the most attractive stem cells for cartilage repair,³⁸ as they can be readily isolated from various tissues such as bone marrow, adipose tissue, umbilical cord, synovia and synovial fluid. These cells are characterized by their capacity to differentiate into three main lineages, bone, fat, and cartilage. On the contrary to chondrocytes, they can be isolated and expanded quite easily. To optimize their differentiation, to improve their viability and to limit their dissemination after implantation, it is highly important to associate the MSC with a support.³⁹

Cell adhesion

The hybrid collagen-inspired peptide **2** was dissolved in cell culture media at a concentration of 10 wt%, in the presence of sodium fluoride (0.3 wt%). The hybrid solutions were poured into 96-well cell culture plates, and incubated overnight at 37°C. The resulting hydrogels were washed with cell culture media, and mMSC were seeded onto their surface. Adherent cells were quantified with the CellTiter-Glo luminescent cell viability assay after 30 min, 1 h, 2 h, and 4 h (Figure 4, A). These results were compared to cell adhesion on tissue culture polystyrene (TC-PS), and commercially available foams made of cross-linked type I bovine collagen (ACE surgical). As expected, the number of cells measured out on bovine collagen foams after washing was very high, since cells could be retained in their porous structure. Interestingly, cell adhesion on hybrid peptide gels was more efficient than on TC-PS, and increased as a function of time. After 4 hours of contact between cells and substrates, cell attachment on hybrid peptide gels was more than twice higher than on TC-PS, and interestingly was equivalent to the cell attachment on commercially available collagen foams.

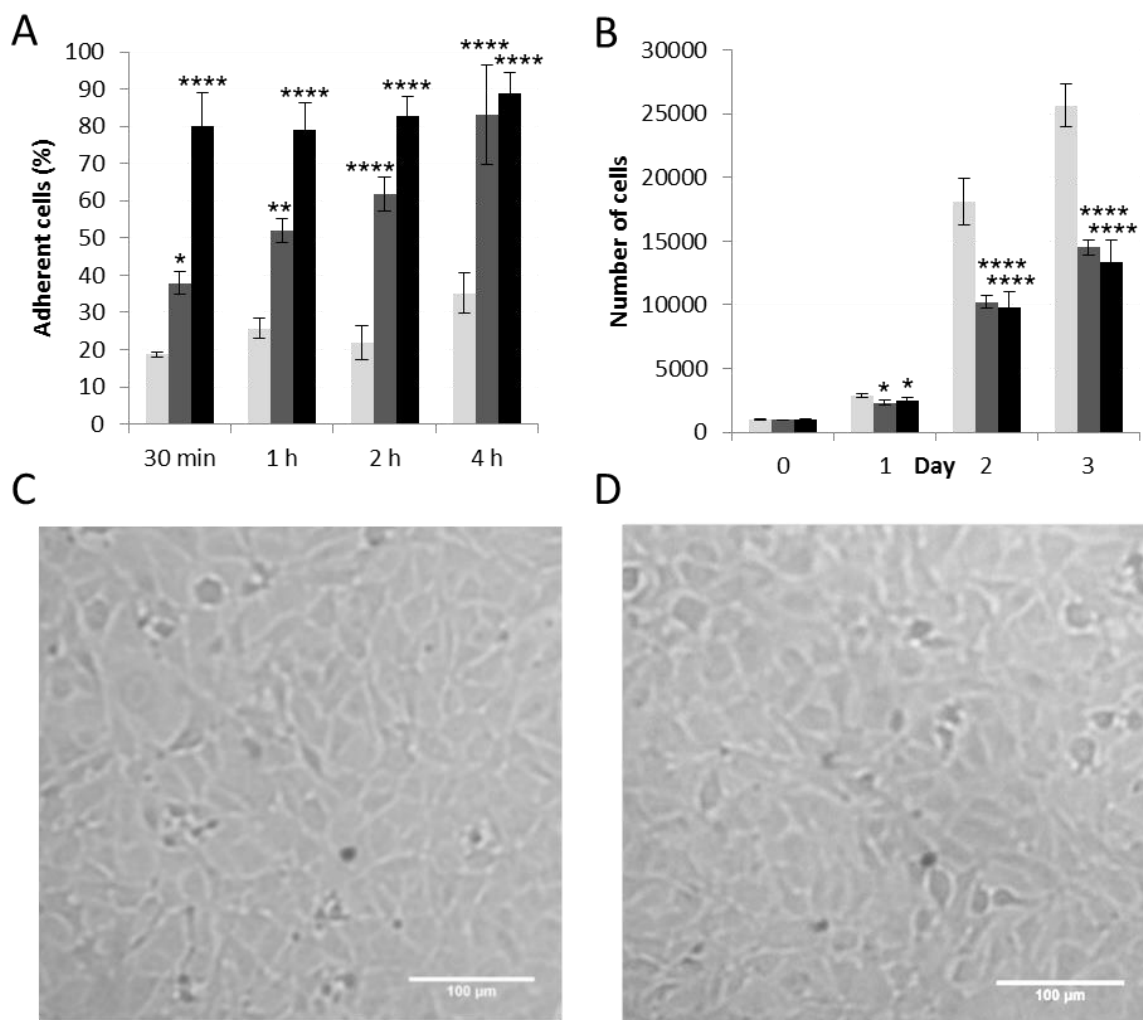


Figure 4. mMSC adhesion (A) and proliferation (B) on TC-PS (light grey), on hybrid collagen-inspired peptide **2** hydrogels (dark grey) and on commercially available bovine collagen foams (black). Microscopic images of cells after 3 days of culture on TC-PS (C) and on hybrid collagen-inspired peptide **2** hydrogel (D).

Cell proliferation

Encouraged by the cell attachment results, we investigated the cell proliferation on the surface of hybrid gels. Gels were prepared according to the procedure described above for adhesion assays. TC-PS and commercially available bovine collagen foam were used as controls. mMSC were seeded on the surface of the samples, and allowed to proliferate until confluence was reached on the TC-PS control. Every day, cells were quantified with the CellTiter-Glo assay (Figure 4, B). The cell proliferation on hybrid peptide hydrogels was as efficient as on bovine collagen foams. To complement the proliferation assay, direct optical microscopy observation was performed on TC-PS and hybrid gels which were transparent. Such direct observation was not possible on the collagen foams because of their opacity. Although the number of cells on hybrid gels was lower than on TC-PS by the end of the experiment, microscopic observations showed that cells had reached confluence in both cases (Figure 4, C and D). A possible explanation for this phenomenon was that the meniscus shape of the gel surface prevented cells from migrating to the edges of the gels, thus reducing the available surface for proliferation.

Cell encapsulation

After demonstrating that cells could proliferate at the surface of hybrid gels, we wanted to take advantage of the sol-gel process to encapsulate live cells in the hybrid gels before the gel point. mMSC were seeded in a hybrid peptide **2** solution with the same composition as previously (10 wt% of **2** in cell culture media with 0.3 wt% NaF). After 25 hours of incubation, cells were stained with a Live/Dead assay kit and their viability was checked by observation with a fluorescent microscope. Live cells appeared in green (calcein) while dead cells were stained in red (EthD-III). On the first attempt, most cells died. However, after decreasing the amount of sodium fluoride from 0.3 wt% to 0.01 wt%, the viability of the stem cells in the hybrid gels was fully conserved (Figure 5). Confocal microscopy images showed that cell distribution was rather homogeneous, except in the area impacted by the meniscus of the gel surface.

Noteworthy, special attention has to be paid to sodium fluoride concentration. Cell-free hydrogels are attractive as cell culture supports or as implantable materials aiming at filling a gap or a defect inside native tissues, which are further colonized by endogenous cells. Hydrogel dressings⁴⁰ or scaffold designed for spinal cord injuries⁴¹ fall in this category. For such applications, hydrogels can be washed before putting them in contact with living cells and thus a high concentration in sodium fluoride, even cytotoxic, can be used to increase the gelation speed. However, when cells are embedded in the hydrogel matrix, a low NaF concentration should be preferred. These conditions decrease the gelation rate. As a consequence, in our study, the hybrid peptide solution was prepared 17 hours before cell seeding. At this point, the mMSC were suspended in the viscous solution and did not sediment during the 25 h-incubation, as witnessed by the lateral microscopic view (Figure 5, C). The good cell viability observed using this procedure enlarge the range of potential applications of hybrid peptide hydrogels to cell-laden matrixes.

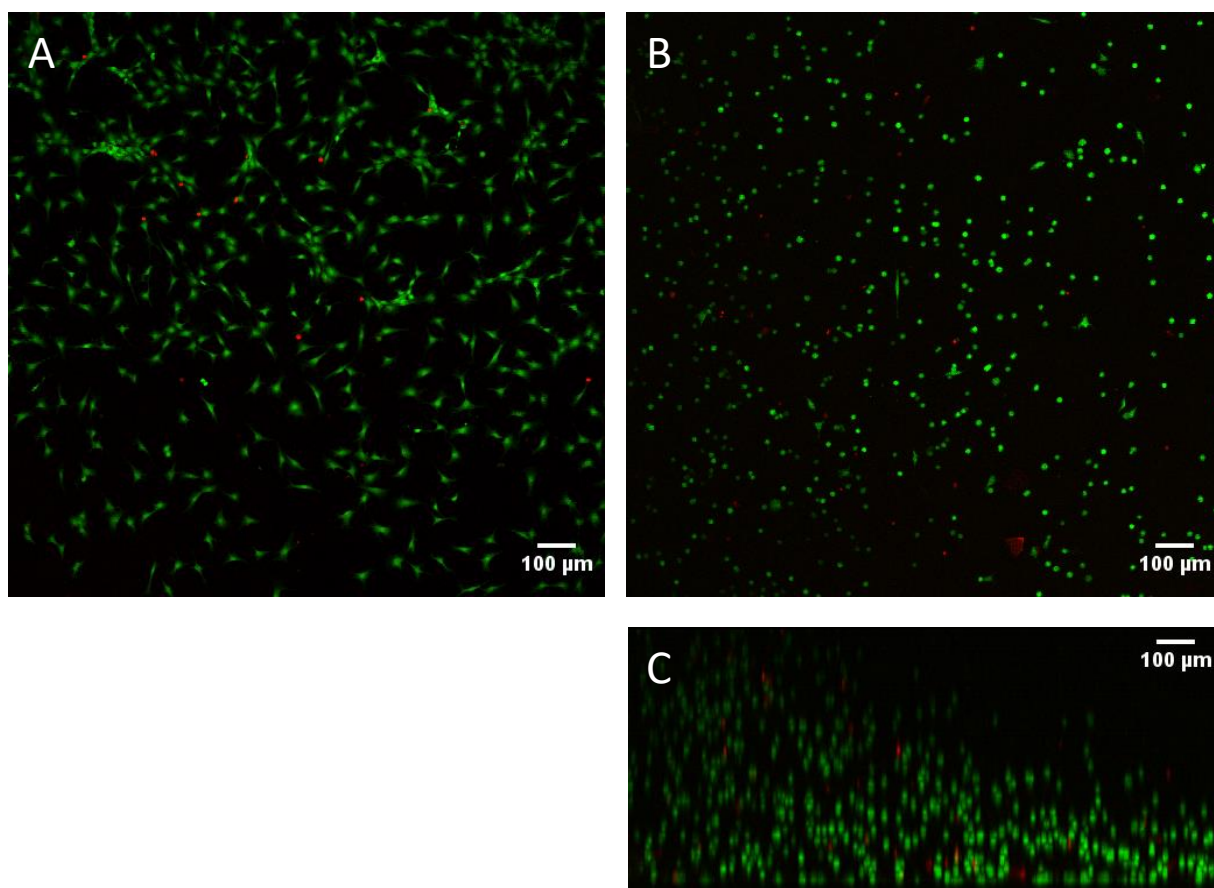


Figure 5. Confocal microscopy images of mMSC 25h after seeding. (A) top view of a 2D-culture on TC-PS. (B) top view (z-projection) and (C) side view (y-projection) of a 3D-culture inside a hybrid collagen-inspired peptide hydrogel.

Conclusion

In contrast to natural collagen scaffolds, the use of a short bis-silylated peptide to prepare biocompatible hydrogels presents several interesting features. Firstly, the technology offers the possibility to create biocompatible gels from a synthetic starting material, which is of a paramount interest in terms of safety, cost of production and putative translation to the clinics. Secondly, the NaF catalyzed sol-gel process we described is straightforward and proceeds entirely in biological media. The sol-gel process has already been exploited to form hydrogels from biopolymers such as chitosan,³³ gelatin³¹ and modified-cellulose,³⁴ that were cross-linked by silylation with 3-(glycidoxypropyl)trimethoxysilane. However, in these studies, the hydrolysis was performed in strong acidic or basic media, and condensation occurred either at a pH non-compatible with cell survival, or separately from hydrolysis upon careful neutralisation. In addition, the fact that the mixture containing hydrogel precursors, nutrients, factors and cells can be handled as a solution, is of great advantage when injection is required, or even when scaffold 3D printing is envisioned. Biofabrication using different silylated bioinks that could polymerize simply by the sol-gel process is of great significance for future developments. It is important to notice that the nature of the silanol chemistry itself unlocks the possibility to design and synthesize multifunctional and tailored hydrogels. In fact, Si-O-Si bond formation is chemoselective, but it is also a 'symmetrical' reaction, involving the same reactive moiety, several times. This represents a ground breaking improvement over systems of chemical cross-linking such as maleimide/thiol¹¹ or photoactivation,⁴² which involve two different chemical groups. Although the Si-O-Si bond formation does not allow the control of directed assemblies (e.g. regular formation of -A-B-A-B- from A and B blocks), a single type of functionalization is sufficient to get a covalent network bringing together any type of silylated building blocks (*i. e.* polymers, peptides, fluorophores, drugs, etc.). The control of the cross-linking degree could be easily tuned by varying the length of precursors but also by introducing tri or tetra-silylated molecules. Taking into account the diversity of natural tissues in terms of biochemical composition and structural features, a versatile and generic method to build dedicated hydrogels is of high interest. In this perspective, the hybrid collagen-inspired peptide forming hydrogel is a promising brick for the straightforward synthesis of biomimetic structures.

Methods

Silylation of peptide 1: Ac-Lys-[Pro-Hyp-Gly]₃-Lys-NH₂ was reacted with 3-isocyanatopropyltriethoxysilane (2.2 eq) in DMF at a concentration of 100 mM, in the presence of DIEA (4 eq) for 50 min. The bis-silylated hybrid block **2** was obtained after precipitation and washings with diethyl ether.

Collagen-inspired hybrid hydrogel preparation: The hybrid peptide **2** (200 mg) was dissolved in 10% FBS supplemented DMEM (Gibco, ref. 31966, 2 mL) at a 10 wt% concentration. The solution was filtered on a 0.22 μm pore size filter. Sodium fluoride (0.3 wt%, 6 mg) was added. The hybrid solution was incubated at 37 °C overnight to yield the hybrid hydrogel.

For peptide synthesis, NMR studies, rheology, SEM images, CD spectra and cell culture assays, see supplementary information.

Acknowledgements

C. Echali er’s PhD was partly founded by the “Region Languedoc Roussillon”, grant attributed to G. Subra, through the program ‘Chercheur d’Avenir’. Peptide syntheses were performed using the facilities of SynBio3 IBISA platform supported by IBMM and ITMO cancer. Cryo-SEM analyses were realized by the CT  (Centre technique des microstructures) from EZUS-Lyon 1 University. Karine Toupet and Gautier Tejedor performed confocal microscopy observations, using the facilities of the Institute for Regenerative Medicine and Biotherapy (IRBM, Montpellier).

Author contributions

C.E. performed all the syntheses of hybrid peptides, hybrid gels, performed the assays and participated in the writing of the paper. S.J. synthesized the first collagen-inspired sequence. G.L. optimized the synthesis of peptide **1** on the FPPS platform. P.V. and L.C. performed the large-scale synthesis of peptide **1**. L.B. performed the large-scale purification of peptide **1**. A.B. provided advices for biological assessment of the gels. B.L. performed the NMR and CD studies. H.V. helped for the set up of the rheological study. X.G. helped in the design of bioassays and in the interpretation of data. D.N. provided the cell line and helped in the design of bioassays and analysis of proliferation data. J.M. provided scientific advices in chemistry and biology, and initiated the project of hybrid peptides. G.S. and A.M. supervised the project and wrote the paper.

Additional information

The authors declare no competing financial interests.

References

1. Taba, M., Jin, Q., Sugai, J. V. & Giannobile, W. V. Current concepts in periodontal bioengineering. *Orthod. Craniofac. Res.* **8**, 292–302 (2005).
2. Barry, R. A. *et al.* Direct-Write Assembly of 3D Hydrogel Scaffolds for Guided Cell Growth. *Adv. Mater.* **21**, 2407–2410 (2009).
3. Cretu, A., Castagnino, P. & Assoian, R. Studying the Effects of Matrix Stiffness on Cellular Function using Acrylamide-based Hydrogels. *J. Vis. Exp. JoVE* (2010). doi:10.3791/2089
4. Guvendiren, M. & Burdick, J. A. The control of stem cell morphology and differentiation by hydrogel surface wrinkles. *Biomaterials* **31**, 6511–6518 (2010).
5. Lin, C.-C. Recent advances in crosslinking chemistry of biomimetic poly(ethylene glycol) hydrogels. *RSC Adv.* **5**, 39844–39853 (2015).
6. Hersel, U., Dahmen, C. & Kessler, H. RGD modified polymers: biomaterials for stimulated cell adhesion and beyond. *Biomaterials* **24**, 4385–4415 (2003).
7. Lin, C.-Y. *et al.* Peptide-Modified Zwitterionic Porous Hydrogels for Endothelial Cell and Vascular Engineering. *BioResearch Open Access* **3**, 297–310 (2014).
8. Patenaude, M. & Hoare, T. Injectable, Mixed Natural-Synthetic Polymer Hydrogels with Modular Properties. *Biomacromolecules* **13**, 369–378 (2012).
9. Freudenberg, U. *et al.* Using Mean Field Theory to Guide Biofunctional Materials Design. *Adv. Funct. Mater.* **22**, 1391–1398 (2012).
10. Tsurkan, M. V. *et al.* Defined Polymer–Peptide Conjugates to Form Cell-Instructive starPEG–Heparin Matrices In Situ. *Adv. Mater.* **25**, 2606–2610 (2013).
11. Watarai, A. *et al.* TGF  functionalized starPEG-heparin hydrogels modulate human dermal fibroblast growth and differentiation. *Acta Biomater.* **25**, 65–75 (2015).
12. Vanderhooft, J. L., Alcoutlabi, M., Magda, J. J. & Prestwich, G. D. Rheological Properties of Cross-Linked Hyaluronan–Gelatin Hydrogels for Tissue Engineering. *Macromol. Biosci.* **9**, 20–28 (2009).
13. Nichol, J. W. *et al.* Cell-laden microengineered gelatin methacrylate hydrogels. *Biomaterials* **31**, 5536–5544 (2010).

14. Hu, X. & Gao, C. Photoinitiating polymerization to prepare biocompatible chitosan hydrogels. *J. Appl. Polym. Sci.* **110**, 1059–1067 (2008).
15. Park, Y. D., Tirelli, N. & Hubbell, J. A. Photopolymerized hyaluronic acid-based hydrogels and interpenetrating networks. *Biomaterials* **24**, 893–900 (2003).
16. Echaliier, C. *et al.* Easy Synthesis of Tunable Hybrid Bioactive Hydrogels. *Chem. Mater.* **28**, 1261–1265 (2016).
17. Chattopadhyay, S. & Raines, R. T. Review collagen-based biomaterials for wound healing. *Biopolymers* **101**, 821–833 (2014).
18. Ensanya A Abou Neel, L. B. Collagen - Emerging collagen based therapies hit the patient. *Adv. Drug Deliv. Rev.* (2012). doi:10.1016/j.addr.2012.08.010
19. Feng, Y., Melacini, G., Taulane, J. P. & Goodman, M. Acetyl-terminated and template-assembled collagen-based polypeptides composed of Gly-Pro-Hyp sequences. 2. Synthesis and conformational analysis by circular dichroism, ultraviolet absorbance, and optical rotation. *J. Am. Chem. Soc.* **118**, 10351–10358 (1996).
20. Kotch, F. W. & Raines, R. T. Self-assembly of synthetic collagen triple helices. *Proc. Natl. Acad. Sci. U. S. A.* **103**, 3028–3033 (2006).
21. Cejas, M. A. *et al.* Collagen-Related Peptides: Self-Assembly of Short, Single Strands into a Functional Biomaterial of Micrometer Scale. *J. Am. Chem. Soc.* **129**, 2202–2203 (2007).
22. Cejas, M. A. *et al.* Thrombogenic collagen-mimetic peptides: Self-assembly of triple helix-based fibrils driven by hydrophobic interactions. *Proc. Natl. Acad. Sci.* **105**, 8513–8518 (2008).
23. Jenkins, C. L. & Raines, R. T. Insights on the conformational stability of collagen. *Nat. Prod. Rep.* **19**, 49–59 (2002).
24. Saccá, B. & Moroder, L. Synthesis of heterotrimeric collagen peptides containing the $\alpha 1\beta 1$ integrin recognition site of collagen type IV. *J. Pept. Sci.* **8**, 192–204 (2002).
25. Ottil, J. & Moroder, L. Disulfide-Bridged Heterotrimeric Collagen Peptides Containing the Collagenase Cleavage Site of Collagen Type I. Synthesis and Conformational Properties. *J. Am. Chem. Soc.* **121**, 653–661 (1999).
26. Kumar, V. A. *et al.* A Nanostructured Synthetic Collagen Mimic for Hemostasis. *Biomacromolecules* **15**, 1484–1490 (2014).
27. O’Leary, L. E. R., Fallas, J. A., Bakota, E. L., Kang, M. K. & Hartgerink, J. D. Multi-hierarchical self-assembly of a collagen mimetic peptide from triple helix to nanofibre and hydrogel. *Nat. Chem.* **3**, 821–828 (2011).
28. Luo, J. & Tong, Y. W. Self-Assembly of Collagen-Mimetic Peptide Amphiphiles into Biofunctional Nanofiber. *ACS Nano* **5**, 7739–7747 (2011).
29. Laconde, G. *et al.* Fast parallel peptide synthesis - FPPS: A methodology for the rapid and efficient preparation of peptide libraries. *Submitted*
30. Zha, J. & Roggendorf, H. Sol–gel science, the physics and chemistry of sol–gel processing, Ed. by C. J. Brinker and G. W. Scherer, Academic Press, Boston 1990, xiv, 908 pp., bound—ISBN 0-12-134970-5. *Adv. Mater.* **3**, 522–522 (1991).
31. Ren, L., Tsuru, K., Hayakawa, S. & Osaka, A. Synthesis and characterization of gelatin-siloxane hybrids derived through sol-gel procedure. *J. Sol-Gel Sci. Technol.* **21**, 115–121 (2001).
32. Hosoya, K. *et al.* A novel covalently crosslinked gel of alginate and silane with the ability to form bone-like apatite. *J. Biomed. Mater. Res. A* **71A**, 596–601 (2004).
33. Shirotsaki, Y., Botelho, C. M., Lopes, M. A. & Santos, J. D. Synthesis and Characterization of Chitosan-Silicate Hydrogel as Resorbable Vehicle for Bonelike® Bone Graft. *J. Nanosci. Nanotechnol.* **9**, 3714–3719 (2009).

34. Vinatier, C. *et al.* A silanized hydroxypropyl methylcellulose hydrogel for the three-dimensional culture of chondrocytes. *Biomaterials* **26**, 6643–6651 (2005).
35. Nguyen, M. K. & Lee, D. S. Injectable Biodegradable Hydrogels. *Macromol. Biosci.* **10**, 563–579 (2010).
36. Annabi, N., Mithieux, S. M., Weiss, A. S. & Dehghani, F. The fabrication of elastin-based hydrogels using high pressure CO₂. *Biomaterials* **30**, 1–7 (2009).
37. Makris, E. A., Gomoll, A. H., Malizos, K. N., Hu, J. C. & Athanasiou, K. A. Repair and tissue engineering techniques for articular cartilage. *Nat. Rev. Rheumatol.* **11**, 21–34 (2015).
38. Vinatier, C., Mrugala, D., Jorgensen, C., Guicheux, J. & Noël, D. Cartilage engineering: a crucial combination of cells, biomaterials and biofactors. *Trends Biotechnol.* **27**, 307–314 (2009).
39. Morille, M., Toupet, K., Montero-Menei, C. N., Jorgensen, C. & Noël, D. PLGA-based microcarriers induce mesenchymal stem cell chondrogenesis and stimulate cartilage repair in osteoarthritis. *Biomaterials* **88**, 60–69 (2016).
40. Murakami, K. *et al.* Hydrogel blends of chitin/chitosan, fucoidan and alginate as healing-impaired wound dressings. *Biomaterials* **31**, 83–90 (2010).
41. Tukmachev, D. *et al.* Injectable Extracellular Matrix Hydrogels as Scaffolds for Spinal Cord Injury Repair. *Tissue Eng. Part A* **22**, 306–317 (2016).
42. Nichol, J. W. *et al.* Cell-laden microengineered gelatin methacrylate hydrogels. *Biomaterials* **31**, 5536–5544 (2010).

Chapter V.

3D printing of hydrogels

Publication 4 – Modular bioink for 3D printing of biocompatible hydrogels: sol-gel polymerization of hybrid peptides and polymers

Echalier C. et al., submitted, under consideration.

My contribution to this paper: I performed the synthesis of the hybrid compounds and prepared the hydrogels. I performed the viscometry experiments. I printed the 3D scaffolds after optimization of the printing settings by Riccardo Levato. I designed and carried out the biological experiments. I participated in the writing of the paper.

Chapter V. 3D printing of hydrogels

V.1. Applications of 3D printed hydrogels

Hydrogel shapes that can be accessed by molding are very limited. In contrast, 3D printing allows the design of scaffolds of almost any geometrical complexity.³⁶³ One of its main applications in medicine is the fabrication of customized implants for reconstructive surgery.^{364,365} Materials with a patient-specific geometry can be designed, printed and implanted at the site of the defect with a perfect fit. In addition, cell-friendly 3D-printing methods hold great promises in tissue engineering.^{366,367} For instance, L. K. Narayanan *et al.* bioprinted layer-by-layer a cell-laden human medial knee meniscus based on magnetic resonance scans of the patient's knee.³⁶⁸ Cell-laden hydrogels with a well-defined structure can be printed and used as vessels for the transplantation of cells into the body of the patient. This method affords a better control over graft size and shape than the injection of a cell-laden *in situ* gelling hydrogel. Living cells and scaffolding materials can thus be delivered *in vivo* in a well-organized manner. In this case, the printed scaffold provides a 3D architectural template for tissue regeneration. Porous scaffolds (100-1000 μm pores) with well-defined strand-pore structure can be printed which is of interest to enhance cell viability.³⁶⁹ Indeed, higher cell viability was observed in porous scaffolds compared non-porous scaffolds.³⁷⁰ This may be related to a lack of nutrient perfusion and waste removal for the cells embedded in thick hydrogels. The ultimate application of 3D printing is the construction of live tissues and organs, this is the aim of "organism manufacturing engineering" (OME).³⁷¹ OME uses modern manufacturing techniques to create live tissues and organs through 3D assembly of cells. It is based on the principle that every tissue, organ or organism can be regarded as assembled from parts. All these parts can be created by co-printing several materials with different chemical compositions, microstructures, mechanical and biological properties.³⁷² Recently, H.-W. Kang *et al.* reported an "integrated tissue-organ printer" that can fabricate human-scale tissue constructs (*Figure 80*).³⁷³

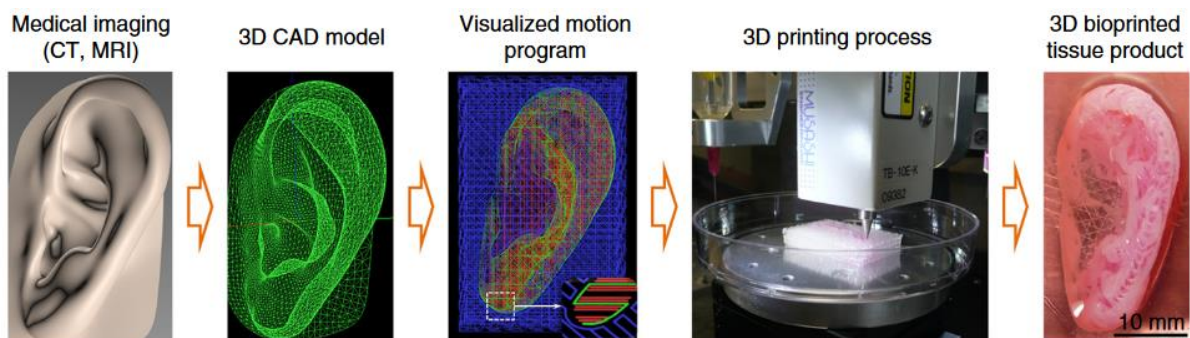


Figure 80. Computer-aided design (CAD) process for automated printing of 3D shape imitating target tissue or organ developed by H.-W. *et al.*. A 3D CAD model is generated from medical image data. Based on this model, a visualized motion program is created, which includes instructions for XYZ stage movements and actuating pneumatic pressure to achieve 3D printing. Reprinted from.³⁷³

V.2. Extrusion 3D printing

In order to meet this challenge, we focus our efforts on 3D printing which enables the on-demand design of structurally complex scaffolds and is a method of choice for the handling of soft hydrogels.³⁷⁴ A collaboration was established with the “Biomaterials for regenerative therapies” group led by Dr. Elisabeth Engel in the Institute for BioEngineering of Catalonia (IBEC, Barcelona). This group has a rapid prototyping machine (nScrypt 3Dn-300-TE, Orlando, FL) which is well-suited for the 3D printing of hydrogels (Figure 81). This machine pneumatically dispenses an ink to build up scaffolds layer by layer on a stationary platform. The ink, which is a printable material such as a viscous solution or hydrogel, is loaded in a syringe equipped with an air pressure-driven piston. Upon application of pressure over the piston, a filament of the ink is extruded. The x/y/z movement of the printhead enables to produce the desired shape.

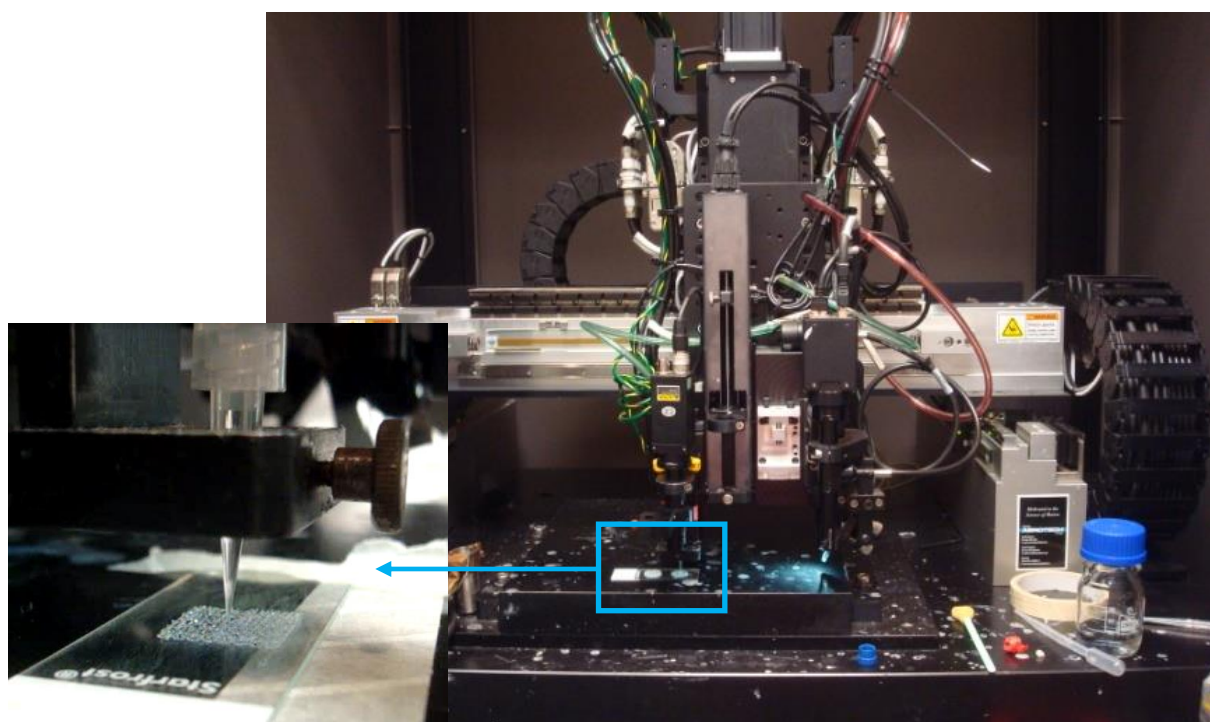


Figure 81. nScrypt 3Dn-300 rapid prototyping machine used in IBEC to print 3D scaffolds

Extrusion-based 3D printing is one of the most widespread method for tissue engineering applications because it is cell-friendly.³⁷⁵ Cells can be embedded in the bioink and printed concomitantly with the biomaterial. Processing conditions are gentle: printing can be performed at room temperature and cells are exposed to low shear forces due the rather large nozzle orifices. The other size of the coin is that print resolution is limited by the nozzle diameter. Only a milli/micron-scale resolution is achieved.

V.3. Sol-gel derived hybrid hydrogels as bioinks

A critical aspect for 3D printing is the choice of the bioink. This latter should be able to flow through the printing nozzle and gelate quickly enough upon deposition on the printing platform to allow the building up of a self-supporting 3D scaffold. Different chemical and physical hydrogels were investigated to address this challenge.³⁶⁷ We wanted to demonstrate that sol-gel chemistry was also well-suited for the preparation of bioinks and their printing by extrusion technique. Indeed, published examples combining sol-gel and 3D printing relates to inorganic pattern direct writing³⁷⁶ or ink-jet printing under non-biocompatible conditions.³⁷⁷ Recently, A. Chiappone *et al.* printed 3D structured hybrid materials using polyethylene glycol diacrylate (PEGDA), tetraethyl orthosilicate and methacryloyloxypropyl trimethoxysilane (MEMO). Photopolymerization of PEGDA led to the formation of an organic network while TEOS yielded inorganic nanoparticles by the sol-gel process. MEMO was used as a bridging monomer between the organic and inorganic network. In this case, the sol-gel process was performed after printing, under conditions non-compatible with live cells.³⁷⁸ In contrast, we would like to print 3D hybrid scaffolds under cell-friendly conditions thanks to a soft sol-gel process occurring simultaneously with the printing process.

V.3.1. Viscosity monitoring

We took as a starting point the 10 wt% hybrid PEG-based hydrogels developed previously (“Easy synthesis of tunable hybrid bioactive hydrogels”). As the control of the bioink viscosity is of high importance to prevent the collapse of the printed scaffold, we monitored the evolution of hybrid PEG solution viscosity as a function of time. This study is presented in the following publication and allowed us to determine when the hybrid solution could be printed. The hydrogel was printed after gel point, it looked like the solid hydrogel was temporarily broken during extrusion and then repaired after printing thanks to the still on-going sol-gel process. We demonstrated that the hybrid solution could be maintained in the printable viscosity range (between 2500 and 4500 mPa.s) for 2 h.

V.3.2. 3D printing

Consequently, grid-patterned 3D scaffolds were printed from a 10 wt% hybrid PEG 2000 solution in DPBS containing sodium fluoride (3 mg/mL) and hybrid RGD peptide (1 wt%), thus demonstrating for the first time that sol-gel process and extrusion 3D printing could be combined.

The modularity of the sol-gel process makes this approach highly promising. Indeed, the sol-gel chemistry enables the one-pot synthesis of covalently functionalized hydrogels. Different hybrid building blocks can be combined in desired ratio to design a tailor-made hydrogel. This broadens the panel of available bioinks. In addition, as a single chemistry is used for cross-

linking and functionalization, bioinks with different compositions in bioactive components could be prepared and printed sequentially to yield heterogeneous hydrogels in which ligand distribution would be spatially-controlled. For example, in the case of cartilage defects where both cartilage and the sub-chondral bone are degraded, a bilayer scaffold that could repair both tissues by presenting to stem cells two different environments, would be of utmost interest.

V.3.3. Biological assessment of 3D scaffolds

Cell adhesion and proliferation assays were carried out on printed hybrid scaffolds. Unfortunately, these experiments did not provide reliable results. Several technical problems were encountered.

Firstly, when cells were seeded on top on the scaffolds, they could pass under the scaffold because of the grid-pattern and proliferate on the bottom of cell culture plate wells. To overcome this issue and ensure uniform cell seeding, a dynamic cell seeding procedure was selected. The printed hydrogels were immersed in a cell suspension and continuously rotated on a MACSmix tube rotator at 37°C for 4 h. Then, cell-laden scaffolds were washed and placed in non-treated polystyrene cell-culture plates. However, we observed that cells were able to migrate from the scaffolds to the cell culture plate surface and proliferated under the scaffolds. Eventually, we placed the cell-laden scaffolds in conical polypropylene (PP) tubes after dynamic cell seeding and washing. Hence, the contact between scaffolds and tubes was minimized and cell migration onto PP tubes was disfavored. An overall good cell viability was observed on the printed scaffolds but precise and reproducible quantitative results could not be obtained. Standard deviations were high within one set of samples. Differences in cell adhesion and proliferation were observed from batch-to-batch. A stricter protocol for scaffold processing and cell culture assays has to be established for a better reproducibility.

The progress on this project was also limited by the fact that the printing step was performed in IBEC in Barcelona and the biological assessment of the printed scaffolds was carried out in IBMM in Montpellier. Frequent trips back and forth would have been required to go beyond the proof of concept and develop functional scaffolds. Given the limited amount of time for this PhD, we could not improve the printing process and investigate changes in the bioink composition and the scaffold pattern. The acquisition of an extrusion 3D printer in IBMM will boost this project.

The publication n°4 (“Modular bioink for 3D printing of biocompatible hydrogels: sol-gel polymerization of hybrid peptides and polymers”) was under consideration at the time of printing of this manuscript (25th September 2016). It is not an accepted work but, for the ease of reading, it has been included in this manuscript in the template of its current submission.

Modular bioink for 3D printing of biocompatible hydrogels: sol-gel polymerization of hybrid peptides and polymers

Received 00th January 20xx,
Accepted 00th January 20xx

C. Echalié,^{a,b} R. Levato,^c M.A. Mateos-Timoneda,^{c,f} O. Castaño,^c S. Déjean,^a X. Garric,^a C. Pinese,^a
D. Noël,^d E. Engel,^c J. Martinez,^a A. Mehdi,^{b*} and G. Subra^{a*}

DOI: 10.1039/x0xx00000x

www.rsc.org/

An unprecedented generic system allowing the 3D printing of peptide-functionalized hydrogels by soft sol-gel inorganic polymerization is presented. Hybrid inorganic/bioorganic blocks are mixed in biological buffer in an appropriate ratio, to yield a multicomponent bioink that can be printed as a hydrogel without using any photochemical or organic reagent. The resulting scaffolds were suitable for cell culture.

3D printing raised high hopes in regenerative medicine, enabling the on-demand design of structurally complex scaffolds for tissue regeneration. Due to their high content in water, hydrogels are highly attractive biomaterials for 3D printing as efficient extracellular matrix surrogates.^{1–3} Extrusion, due to the affordability of commercially available 3D printers, and the compatibility with a large number of polymers, has emerged as a method of choice for rapid fabrication of hydrogel constructs.⁴ It is one of the most straightforward methods for biofabrication: a continuous filament of hydrogel is extruded while the x/y/z movement of the printhead enables to craft the desired shape. Blueprints from a CAD file are constructed into 3D architectures in a layer-by-layer fashion. The bioink contains the hydrogel precursors and has to be carefully chosen to avoid premature collapse of the printed structure.

Various types of physical and chemical hydrogels have been tailored to address this challenge.³ Among physical hydrogels,

self-assembling peptide hydrogels are very promising for *in vivo* applications.^{5,6} They can be injected thanks to their shear-thinning behavior and are degraded by proteolytic enzymes, yielding non-toxic amino acids and short peptides as metabolites. However, although widely used as drug delivery systems,⁷ such hydrogels are less favoured for biofabrication as their network only relies on weak non-covalent interactions which impacts their stability and structural integrity when placed in contact with biological fluids and extracellular matrices. The main class of materials used for biofabrication remains chemical hydrogels based on natural or synthetic polymers.³ The control of gelation is of high importance and constitutes the main limitation in the panel of polymers that are used. To prevent the spreading of hydrogel after printing, the viscosity has to be precisely controlled. This entails the careful handling of a pre-polymer solution, which has to gelate quickly enough upon deposition on the printing platform. Biopolymers have their own gelation methods such as complexation of calcium ions for alginate,⁸ pH adjustment of an acidic solution for collagen,⁹ and cooling a hot viscous solution for agarose,¹⁰ to name a few. One of the concerns about biopolymer is the batch-to-batch reproducibility impacting the gelation kinetics. Cross-linking of soluble polymer was generally employed to increase the stability of the hydrogel. For example, methacrylate groups introduced on biopolymers are commonly used for that purpose, reacting with sulfhydryl containing cross-linkers¹¹ through a Michael-type addition. They may also be used for photo cross-linking.¹² Diels alders reaction between furan-modified gelatin and maleimide cross-linkers,¹³ hydrazone formation between aldehyde-modified alginate and hydrazide cross-linkers¹⁴ as well as copper-free azide-alkyne cycloaddition^{15,16} were also investigated. The range of cross-linking strategies is even wider for hydrogels prepared from synthetic polymers. Photo cross-linking remains the most commonly used method,^{17,18,19} the transparency of the material enabling an efficient curing process.

^a Institut des Biomolécules Max Mousseron (IBMM), UMR5247 Université de Montpellier, CNRS, ENSCM, Faculté de Pharmacie, 15 avenue Charles Flahault, 34093 Montpellier, France. gilles.subra@umontpellier.fr

^b Institut Charles Gerhardt de Montpellier (ICGM), UMR 5253 Université de Montpellier, CNRS, ENSCM, Place E. Bataillon, 34095 Montpellier Cedex 5, France. Ahmad.mehdi@umontpellier.fr

^c Institute for Bioengineering of Catalonia (IBEC), Barcelona, Spain Dr. M.A. Mateos

^d CIBER en Bioingeniería, Biomateriales y Nanomedicina (CIBER-BBN), Barcelona, Spain

^e Institute for Regenerative Medicine and Biotherapy (IRMB), Inserm U1183, Montpellier, France

^f CIBER en Bioingeniería, Biomateriales y Nanomedicina (CIBER-BBN), Barcelona, Spain

† Electronic Supplementary Information (ESI) available: See DOI: 10.1039/x0xx00000x

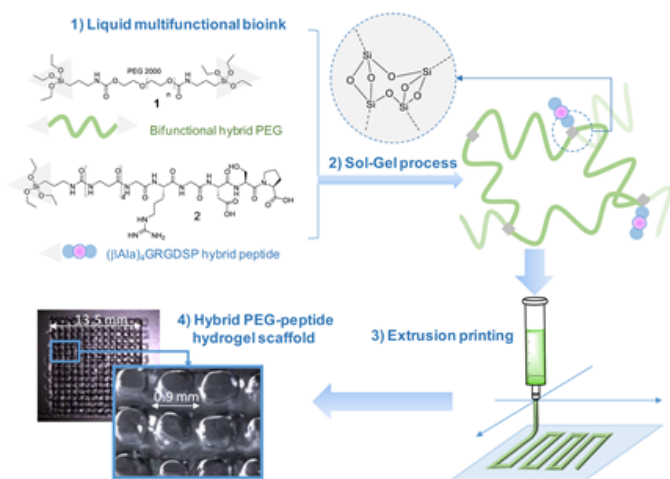


Fig. 1 Principle of sol-gel extrusion printing of hybrid functional hydrogels

The bioink, which contains soluble functionalized polymers or monomers and photoinitiators, is UV-irradiated. This can be done while the bioink is flowing out of the nozzle or after printing. Polyhydroxyethylmethacrylate (PHEMA)²⁰ and polyacrylamide (PA)²¹ scaffolds have been printed by this way.

In this study, we propose a novel methodology to 3D print chemically cross-linked hydrogels by using the sol-gel process. To the best of our knowledge, sol-gel was never exploited for biofabrication with hydrogel inks. All examples combining sol-gel and 3D printing deal either with inorganic pattern direct writing²² or with ink-jet printing under non-biocompatible conditions.²³ In this latter case, silane-modified polymers were pre-hydrolysed and used as printable inks. Gel formation was promoted by Si-O-Si formation upon solvent evaporation. The bioink we have developed enables printing at room temperature, in physiological buffer (pH 7.2), without photoactivation or additional chemical reagents. An alkoxy-silane-derivatized synthetic polymer (Figure 1, bifunctional hybrid PEG **1**) solubilized in DPBS undergoes hydrolysis and condensation in the course of the printing process, yielding a covalent hydrogel (Figure 1).

To succeed in an efficient cell colonization of artificial materials and its progressive replacement with natural matrices, cells seeded in the artificial substrate have to differentiate, to migrate and to behave like in their natural environment. This can be induced by diverse biochemical (e.g. growth factors, cell-adhesion peptide ligands) and physical (e.g. pore size, stiffness, rigidity) stimuli distributed within the tissues.²⁴ The sol-gel approach presented in this study is highly attractive since its modularity simplifies the covalent modification of the hydrogel with peptide ligands exhibiting biological activities (i.e. enhancing cell adhesion, stimulating proliferation; etc.). This is a significant breakthrough in this technology, since available 3D printable synthetic polymers such as PEG, PHEMA or PA are not ideal supports as such for cell attachment and have to be further functionalized to improve their cell compatibility.^{20,25,26} Interestingly, sol-gel could simplify the biofabrication of hydrogel scaffolds of heterogeneous

composition. Indeed, as a single chemistry system is involved, different bioinks can be prepared to sequentially print layers with different compositions in bioactive components, eliciting specific cell responses in a spatially controlled environment.

We recently demonstrated the feasibility of the sol-gel approach to obtain functional PEG-based hydrogels with either antibacterial or cell-adhesive properties, depending on the hybrid peptide that was used.²⁷ We thus determined a hydrogel composition suitable for cell adhesion which included hybrid RGDSP ligand **2** which displays a trialkoxysilane function at its N-terminus. Once homogeneously mixed in the bioink at the chosen concentration, hybrid blocks (**1** and **2**) reacted together chemoselectively to form Si-O-Si bonds, guaranteeing both the desired orientation and the correct density of bioactive ligand within the hydrogel matrix.

After solubilization of the hybrid silylated precursors **1** and **2** in DPBS, the sol-gel process started with a constant increase of the bioink viscosity. First of all, the progress of sol-gel reaction (i.e. hydrolysis and condensation) was monitored by viscometry. The bioink viscosity was measured as a function of time in order to precisely determine when the bioink could be printed. To do so, a 10 wt% hybrid PEG **1** solution in DPBS containing 0.3 wt% of NaF was prepared and poured into the sample cup of sine-wave vibro viscometer SV-10 (A&D). This apparatus measures the viscosity by detecting the driving electric current necessary to resonate two sensor plates at a constant frequency. Its wide measurement range was well suited to follow the gelation process without damaging the hydrogel. The viscosity of the solution was recorded at 37 °C (Figure 2) until it reached 10 000 mPa.s, which was the highest value measurable with the apparatus. At the beginning of the experiment, the viscosity of the solution was quite low, around 1.5 mPa.s. It increased negligibly for the first two hours when hydrolysis occurred and condensation started. The gel point was observed at 120 min. Afterwards the viscosity increased sharply. We found that printing should be performed when hydrogel viscosity was comprised between 2 000 and 5 000 mPa.s: below 2 000 mPa.s, the hydrogel tended to spread, whereas above 5 000 mPa.s, a continuous filament could not be extruded. More precisely, a viscosity between 2 500 and 4 500 mPa.s was ideal for a neat deposition of the hydrogel and was consequently selected for further studies. In order to maintain the hydrogel in the appropriate viscosity range for a prolonged period, we investigated printing at room temperature. After gelation occurred at 37 °C, the temperature was lowered to 25 °C to slow down the sol-gel process. The viscosity was recorded in these conditions (Figure 2). This change in temperature allowed widening the printing time window from 1 to 2 hours. As already pointed out, one objective of this work was to print RGD-functionalized scaffolds. So the hybrid GRGDSP ligand **2** (20 mol% in regards to **1**, 1 wt% in regards to the solvent) was added to the hybrid PEG **1** solution, and the influence on viscosity evolution was studied (Figure 2). One can notice that gelation was faster with the hybrid GRGDSP **2**, gel point was observed at 84 min that is to say 36 min earlier.

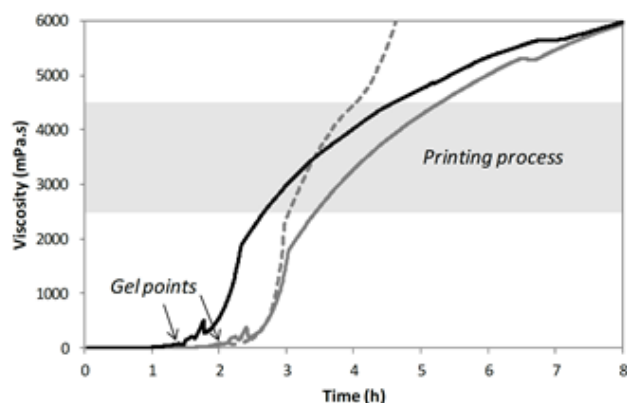


Fig. 2 Viscosity of the hybrid solutions recorded as a function of time. Dashed grey line: hybrid PEG solution at 37°C; solid grey line: hybrid PEG solution at 37°C until gel point and then at 25°C; black line: hybrid PEG-GRGDSP solution at 37°C until gel point and then at 25°C.

Nonetheless, the presence of the hybrid RGD 2 did not seem to induce any change in the final viscosity and still allowed printing in the same range of viscosity (2 500 – 4 500 mPa.s) within a 2 hour time frame. All the printing assays were performed on an nScript 3Dn-300-TE rapid prototyping machine (nScript, Orlando, FL). This 3D dispensing machine pneumatically deposits a bioink to build up scaffolds layer by layer on a stationary platform. The bioink was prepared by solubilization of the hybrid PEG 1 (10 wt%) and the hybrid GRGDSP peptide 2 (1 wt%) in DPBS containing NaF (0.3 wt%). It was loaded in a 3 mL syringe (fluid dispensing system Nordson EFD) equipped with an air pressure-driven piston. The syringe was incubated at 37 °C until gelation occurred (84 min). Then, it was kept at room temperature (25 °C) for 76 min. The bioink reached the appropriate viscosity for printing (2500 mPa.s) 160 min after the beginning of the sol-gel process. At this point, the syringe was fitted with a 27 G conical nozzle (Nordson EFD). A pressure comprised between 0.15 and 0.28 MPa was applied over the piston to dispense the hydrogel. It was tuned to be consistent with the increasing viscosity. A grid pattern was chosen. The scaffold design was a 5 layer stack of porous 13.5 mm squares with 0.9 mm strand spacing (Figure 3).

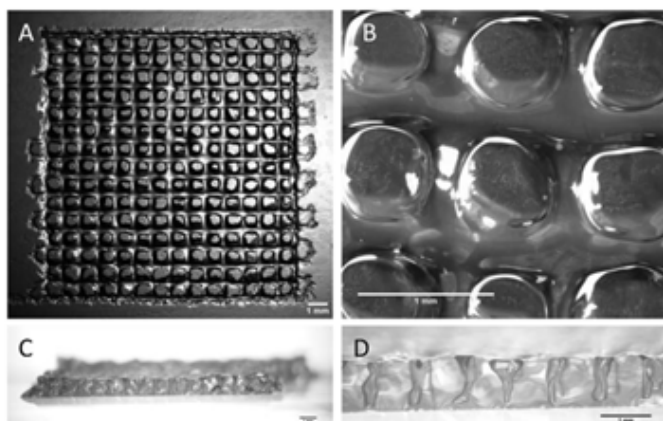


Fig. 3 Stereomicroscopy images of the 3D-printed scaffolds. (A,B) top views; (C,D) side views. All the scale bars represent 1 mm.

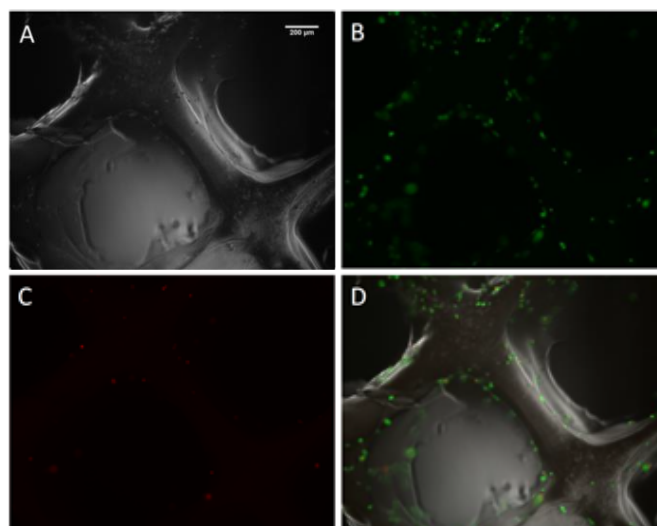


Fig. 4 Fluorescent microscopy images of mMSC after 4 days of culture on a hybrid 3D-printed scaffold. (A) transmitted light image; (B) calcein-AM stain showing live cells in green; (C) EthD-III stain showing dead cells in red; (D) merged images.

The deposition of the first layer was crucial for the scaffolding. In order to make the first strands stick and stay in place, glass slides were coated with a thin layer of bioink before printing.

Porous 3D scaffolds were successfully printed as the printhead moved at a constant speed of 3 mm/s in the xy plane. The biocompatibility of the 3D printed scaffolds was assessed on mouse mesenchymal stem cells (mMSC). This cell line was chosen in the perspective of tissue engineering applications. After printing, the scaffolds were stored in their wet state (in a humidified environment). Since the printing environment was not sterile, the scaffolds were sterilized in an autoclave. Then, they were allowed to swell in cell culture medium before being cut into discs of 7 mm in diameter. The printed hydrogels were immersed in a cell suspension to undergo a dynamic cell seeding procedure at 37 °C, in a rotating device. Then, the cell-laden constructs were washed with cell culture media and placed in polypropylene tubes filled with media. After 4 days of proliferation, a Live/Dead assay was performed on the scaffolds. Upon observation with a fluorescent microscope, live cells appeared in green whereas dead cells were marked in red (Figure 4). These results were compared to cells cultured on a PLA scaffold under the same conditions (ESI† Fig. S6). Excellent cell viability was observed in both cases, indicating that the hybrid PEG-peptide 3D scaffolds were suitable for cell culture.

Beyond the printing of hydrogel scaffolds made out of hybrid PEG and hybrid integrin ligand, the combination of sol-gel chemistry and 3D extrusion printing paves the way to unlimited customization of biomimetic matrices. The functionalization of (bio)polymers and small molecules, in particular bioactive peptides, with silyl groups enables formation of the desired network in water, using a single soft chemoselective chemistry. Proceeding at room temperature in biological buffer with mild pressure constraint, this process could be a promising way to prepare cell-laden scaffolds. Moreover, the combination of several syringes filled with

different hybrid bioinks is envisioned to open the way to the biofabrication of multilayer and non-homogeneous biomaterials, mimicking even more closely the complexity of natural tissues in terms of shape and biochemical composition.

C. Echalié's PhD was partly funded by the "Région Languedoc Roussillon through the program "Chercheur d'Avenir", grant attributed to G. Subra. Peptide synthesis and purification were performed using SynBio3 platform facilities supported by GIS IBISA and ITMO Cancer. The 3D scaffold fabrication was performed using the facilities of the platform of Production of Biomaterials and Biomolecules of the ICTS "NANBIOSIS", more specifically by the U5 Unit of the CIBER in Bioengineering, Biomaterials & Nanomedicine (CIBER-BBN) at the Institute for Bioengineering of Catalonia (IBEC).

Notes and references

§ Hybrid PEG and hybrid peptide syntheses: the synthesis of hybrid blocks was achieved using 3-isocyanatopropyltriethoxysilane following a previously described procedure.²⁷

§ Preparation of the bioink: hybrid PEG **1** (10 wt%, 300 mg) and hybrid GRGDSP peptide **2** (1 wt%, 30 mg) were dissolved in DPBS (3 mL) containing sodium fluoride (0.3 wt%, 9 mg).

§ 3D printing: 3D printing was performed on an nScript rapid prototyping machine (3Dn-300-TE) at RT using a 3 mL syringe filled with the bioink and fitted with a 200 µm tip. The hydrogel was dispensed on a glass slide at a constant speed of 3 mm.s⁻¹ under a pressure ranging from 0.15 to 0.28 MPa.

- 1 M. Guvendiren, J. Molde, R. M. D. Soares and J. Kohn, *ACS Biomater. Sci. Eng.*, 2016.
- 2 P. Bajaj, R. M. Schweller, A. Khademhosseini, J. L. West and R. Bashir, *Annu. Rev. Biomed. Eng.*, 2014, **16**, 247–276.
- 3 J. Malda, J. Visser, F. P. Melchels, T. Jüngst, W. E. Hennink, W. J. A. Dhert, J. Groll and D. W. Huttmacher, *Adv. Mater.*, 2013, **25**, 5011–5028.
- 4 M. E. Hoque, Y. L. Chuan and I. Pashby, *Biopolymers*, 2012, **97**, 83–93.
- 5 A. Dasgupta, J. H. Mondal and D. Das, *RSC Adv.*, 2013, **3**, 9117–9149.
- 6 A. Altunbas and D. J. Pochan, *Top. Curr. Chem.*, 2012, **310**, 135–167.
- 7 A. Altunbas, S. J. Lee, S. A. Rajasekaran, J. P. Schneider and D. J. Pochan, *Biomaterials*, 2011, **32**, 5906–5914.
- 8 F. You, X. Wu, N. Zhu, M. Lei, B. F. Eames and X. Chen, *ACS Biomater. Sci. Eng.*, 2016.
- 9 N. Rajan, J. Habermehl, M.-F. Coté, C. J. Doillon and D. Mantovani, *Nat. Protoc.*, 2006, **1**, 2753–2758.
- 10 M. S. Shoichet, R. H. Li, M. L. White and S. R. Winn, *Biotechnol. Bioeng.*, 1996, **50**, 374–381.
- 11 S. Khetan and J. A. Burdick, *Biomaterials*, 2010, **31**, 8228–8234.
- 12 H. Aubin, J. W. Nichol, C. B. Hutson, H. Bae, A. L. Sieminski, D. M. Cropek, P. Akhyari and A. Khademhosseini, *Biomaterials*, 2010, **31**, 6941–6951.
- 13 C. García-Astrain, A. Gandini, C. Peña, I. Algar, A. Eceiza, M. Corcuera and N. Gabilondo, *RSC Adv.*, 2014, **4**, 35578.
- 14 N. Huebsch, P. R. Arany, A. S. Mao, D. Shvartsman, O. A. Ali, S. A. Bencherif, J. Rivera-Feliciano and D. J. Mooney, *Nat. Mater.*, 2010, **9**, 518–526.
- 15 C. A. DeForest and K. S. Anseth, *Nat. Chem.*, 2011, **3**, 925–931.
- 16 H. Jiang, S. Qin, H. Dong, Q. Lei, X. Su, R. Zhuo and Z. Zhong, *Soft Matter*, 2015, **11**, 6029–6036.
- 17 H. Shih and C.-C. Lin, *Biomacromolecules*, 2012, **13**, 2003–2012.
- 18 E. A. Phelps, N. O. Enemchukwu, V. F. Fiore, J. C. Sy, N. Murthy, T. A. Sulchek, T. H. Barker and A. J. García, *Adv. Mater.*, 2012, **24**, 64–70.
- 19 J. J. Moon, S.-H. Lee and J. L. West, *Biomacromolecules*, 2007, **8**, 42–49.
- 20 J. N. Hanson Shepherd, S. T. Parker, R. F. Shepherd, M. U. Gillette, J. A. Lewis and R. G. Nuzzo, *Adv. Funct. Mater.*, 2011, **21**, 47–54.
- 21 R. A. Barry, R. F. Shepherd, J. N. Hanson, R. G. Nuzzo, P. Wiltzius and J. A. Lewis, *Adv. Mater.*, 2009, **21**, 2407–2410.
- 22 E. B. Duoss, M. Twardowski and J. A. Lewis, *Adv. Mater.*, 2007, **19**, 3485–3489.
- 23 G. Orsi, C. De Maria, F. Montemurro, V. M. Chauhan, J. W. Aylott and G. Vozzi, *Curr. Top. Med. Chem.*, 2015, **15**, 271–278.
- 24 B.-S. Kim, I.-K. Park, T. Hoshiba, H.-L. Jiang, Y.-J. Choi, T. Akaike and C.-S. Cho, *Prog. Polym. Sci.*, 2011, **36**, 238–268.
- 25 F. Yang, C. G. Williams, D. Wang, H. Lee, P. N. Manson and J. Elisseeff, *Biomaterials*, 2005, **26**, 5991–5998.
- 26 U. Hersel, C. Dahmen and H. Kessler, *Biomaterials*, 2003, **24**, 4385–4415.
- 27 C. Echalié, C. Pinese, X. Garric, H. Van Den Berghe, E. Jumas Bilak, J. Martinez, A. Mehdi and G. Subra, *Chem. Mater.*, 2016, **28**, 1261–1265.

Conclusion and Perspectives

Conclusion and perspectives

During my PhD work, an easy and tunable method for the preparation of hybrid hydrogels was developed. We combined the advantages of the sol-gel chemistry with peptide chemistry to design new hybrid bioactive matrices.

First, polyethylene glycol blocks were functionalized with triethoxysilyl groups. The resulting hybrid building blocks were simply dissolved in a physiological buffer to form hydrogels thanks to the sol-gel process which consists in a soft inorganic polymerization. This process was monitored by NMR, rheology and viscometry. It involves two steps: the hydrolysis of ethoxysilyl groups into silanols and their condensation into siloxanes (Si-O-Si) bonds. Thus a three-dimensional covalent network in which PEG units were linked through siloxane bonds was obtained. Interestingly, the whole gelation process occurred at pH 7.4 and 37°C in a biologically relevant buffer. Gel times within minutes or hours could be achieved by the addition of sodium fluoride which catalyzes the sol-gel process. The mechanical properties of the resulting hybrid PEG hydrogels were studied by rheology and their cytocompatibility was investigated.

Secondly, we demonstrated that different hybrid silylated blocks could be combined and engaged in the sol-gel process to yield covalently functionalized hydrogels. Hybrid triethoxysilyl or hydroxydimethylsilyl peptides were synthesized and covalently incorporated into hybrid PEG hydrogels. We showed that these hybrid peptides could confer their biological properties to the gels. Indeed, depending on the type of bioactive peptides introduced, hydrogels exhibited either antibacterial or cell adhesion properties.

Thirdly, we substituted the biologically inert PEG units by a peptide to give inherent cell-friendly properties to the network. A short peptide (11-mer), whose sequence was inspired from natural collagen, was synthesized and modified with triethoxysilane moieties. Hybrid collagen-inspired peptide hydrogels were prepared according to the sol-gel method developed previously. Stem cell proliferation assays suggested that these hydrogels provided a cell-friendly environment comparable to natural collagen substrates. Interestingly, cells could be encapsulated in the hybrid peptide hydrogel during its formation with a good viability.

Finally, the fabrication of hybrid hydrogels with a designed shape was explored. We showed that hybrid solutions resulting from the dissolution of hybrid building blocks in physiological buffer could be used as bio-inks to print 3D scaffolds.

The general aim of this PhD work was to demonstrate the potential of the sol-gel chemistry for the preparation of biocompatible hydrogels with finely tuned properties. The proof of concept was clearly established during these three years of PhD. The versatility of this sol-gel method allowed us to envision a huge number of applications which were protected by a patent (Martinez J. *et al.* "Nouveaux hydrogels de structure silylée et procédé d'obtention" FR 1556628, PCT/EP2016/066215).

Of course, a lot of work has to be done to move from the proof of concept to medical applications. In that context, during my last year of PhD, several research programs started on that topic in collaboration between IBMM, ICGM and other laboratories.

As a first follow-up of this work, hybrid hydrogels will be investigated for stem cell-based therapies. These studies will be performed in the frame of the “LEGOGEL” project starting in October 2016 and funded by the French National Agency for Research (ANR). Along with IBMM and ICGM, this project involves the Institute for Regenerative Medicine and Biotherapy (IRMB, Montpellier). It aims at developing functional hydrogels for the reparation of osteo-articular damages. Mesenchymal stem cells (MSC) will be embedded in hybrid hydrogels mimicking cartilage and bone extracellular matrix. The MSC proliferation and targeted differentiation into chondrocytes will be evaluated *in vitro* and *in vivo* after injection of a MSC-laden hybrid precursor solution. Multilayer implantable scaffolds that could repair both cartilage and sub-chondral bone by presenting to MSCs two different environments will be 3D printed.

One of the challenges to tackle will be to find an alternative to sodium fluoride as sol-gel catalyst since this latter leads to adverse cell effects at concentrations high enough to catalyze fast gelation. On-going experiments aims at finding an efficient and non-toxic organic catalyst. This would enable a tighter control over the gelation time.

Another important point to be optimized is the control of the nanometric structure of the network. Indeed, the extracellular matrix provides information to the cells not only in the form of biochemical signals but also through mechanical and topographic stimuli. It has been demonstrated that network density, pore size and topographic features affect cell behavior, in particular cell adhesion and migration. As an example, improvements can be achieved by preparing longer collagen-inspired hybrid peptides leading to hydrogels with larger mesh size that would be more suitable for cell encapsulation.

So far, we have used only PEG and synthetic collagen sequences as blocks for the hydrogel network. Nevertheless, it would be interesting to design and synthesize other hybrid blocks inspired from important native extracellular matrix (ECM) components such as polysaccharides. In particular, efforts are being made to silylate hyaluronic acid, a major glycosaminoglycan of ECM. In the same way, selective introduction of silyl groups on proteins, like growth factors, would allow their covalent immobilization in hydrogel network. This challenging task would enable a tight spatial and temporal control over the presentation of such factors in biomaterials.

Another promising and yet unexplored perspective of this PhD work is the use of hydrogels as functional substrates for the controlled release of active substances. The later could be viewed as ‘smart’ hydrogel dressings or drug reservoirs. As pointed out in chapter 3, we have demonstrated that it could be possible to release a fluorescent dye. One can play on numerous triggers to finely tune the release of a drug from hybrid hydrogels. First, the susceptibility to hydrolysis of the silicon-oxygen-silicon bond depends on the substituents on the silicon atom

and on the number of siloxane bonds linking the drug to the network. Secondly, peptide sequences sensitive to enzymes of the extracellular matrix such as matrix metalloproteinases, could be used as spacers between the bioactive compound to be released and the hydrogel network. Enzymatic-responsive hydrogels could thus be obtained, resulting in the release of a compound upon enzymatic cleavage. Enzyme-sensitive sequences could also be included as bridges within the tridimensional network. Large molecules such as proteins could be non-covalently trapped in tight meshes and released upon loosening of the network by enzymatic cleavage.

At last, matrices responsive to external stimuli would be of utmost interest. These hydrogels could be 'activated' on demand to trigger the release of a drug like analgesics or to stimulate the encapsulated cells. Two types of hydrogels whose shape and physical properties could be modified by an external stimulus have been considered. On the one hand, hydrogels incorporating a hybrid photoisomerizable block, such as azobenzene derivative, would respond to light. On the other hand, hydrogels containing magnetic nanoparticles would be sensitive to magnetic fields.

Summing up, beyond the first series of results and achievements obtained during this PhD, the simplicity and versatility of the soft and modular sol-gel strategy developed paves the way to a wide range of biomaterials that could be tailored to address multiple challenges in healthcare.

References

- (1) Antoni, D.; Burckel, H.; Josset, E.; Noel, G. Three-Dimensional Cell Culture: A Breakthrough in Vivo. *Int. J. Mol. Sci.* **2015**, *16* (3), 5517–5527.
- (2) Tibbitt, M. W.; Anseth, K. S. Hydrogels as Extracellular Matrix Mimics for 3D Cell Culture. *Biotechnol. Bioeng.* **2009**, *103* (4), 655–663.
- (3) McKinnon, D. D.; Domaille, D. W.; Brown, T. E.; Kyburz, K. A.; Kiyotake, E.; Cha, J. N.; Anseth, K. S. Measuring Cellular Forces Using Bis-Aliphatic Hydrazone Crosslinked Stress-Relaxing Hydrogels. *Soft Matter* **2014**, *10* (46), 9230–9236.
- (4) Pedron, S.; Becka, E.; Harley, B. A. Spatially Graded Hydrogel Platform as a 3D Engineered Tumor Microenvironment. *Adv. Mater.* **2015**, *27* (9), 1567–1572.
- (5) Edmondson, R.; Broglie, J. J.; Adcock, A. F.; Yang, L. Three-Dimensional Cell Culture Systems and Their Applications in Drug Discovery and Cell-Based Biosensors. *Assay Drug Dev. Technol.* **2014**, *12* (4), 207–218.
- (6) Gurski, L. A.; Jha, A. K.; Zhang, C.; Jia, X.; Farach-Carson, M. C. Hyaluronic Acid-Based Hydrogels as 3D Matrices for in Vitro Evaluation of Chemotherapeutic Drugs Using Poorly Adherent Prostate Cancer Cells. *Biomaterials* **2009**, *30* (30), 6076–6085.
- (7) Shih, H.; Mirmira, R. G.; Lin, C.-C. Visible Light-Initiated Interfacial Thiol-Norbornene Photopolymerization for Forming Islet Surface Conformal Coating. *J. Mater. Chem. B Mater. Biol. Med.* **2015**, *3* (2), 170–175.
- (8) Phelps, E. A.; Templeman, K. L.; Thulé, P. M.; García, A. J. Engineered VEGF-Releasing PEG-MAL Hydrogel for Pancreatic Islet Vascularization. *Drug Deliv. Transl. Res.* **2015**, *5* (2), 125–136.
- (9) McEwan, K.; Padavan, D. T.; Ellis, C.; McBane, J. E.; Vulesevic, B.; Korbitt, G. S.; Suuronen, E. J. Collagen-Chitosan-Laminin Hydrogels for the Delivery of Insulin-Producing Tissue. *J. Tissue Eng. Regen. Med.* **2013**.
- (10) O'Reilly, M. S.; Boehm, T.; Shing, Y.; Fukai, N.; Vasios, G.; Lane, W. S.; Flynn, E.; Birkhead, J. R.; Olsen, B. R.; Folkman, J. Endostatin: An Endogenous Inhibitor of Angiogenesis and Tumor Growth. *Cell* **1997**, *88* (2), 277–285.
- (11) Nedovic, V.; Willaert, R. *Applications of Cell Immobilisation Biotechnology*; Springer Science & Business Media, 2006.
- (12) Sorensen, D. R.; Read, T.-A. Delivery of Endostatin in Experimental Cancer Therapy. *Int. J. Exp. Pathol.* **2002**, *83* (6), 265–274.
- (13) *Principles of Tissue Engineering*, Fourth edition.; Lanza, R. P., Langer, R. S., Vacanti, J., Eds.; Academic Press, an imprint of Elsevier: Amsterdam, 2014.
- (14) *Tissue Engineering*; Blitterswijk, C. A. van, Thomsen, P., Eds.; Academic Press series in biomedical engineering; Elsevier, Acad. Press: Amsterdam, 2008.
- (15) Agence de la biomédecine. Dons et Greffes D'organes : Les Chiffres Clés 2015. *Press Release* **2016**.
- (16) Pavlovic, M.; Balint, B. *Stem Cells and Tissue Engineering*; SpringerBriefs in Electrical and Computer Engineering; Springer: New York, 2013.
- (17) Warburton, D. *Stem Cells, Tissue Engineering, and Regenerative Medicine*; World Scientific Publishing Company: Singapore, 2015.
- (18) Sivashanmugam, A.; Arun Kumar, R.; Vishnu Priya, M.; Nair, S. V.; Jayakumar, R. An Overview of Injectable Polymeric Hydrogels for Tissue Engineering. *Eur. Polym. J.* **2015**, *72*, 543–565.

- (19) Patenaude, M.; Smeets, N. M. B.; Hoare, T. Designing Injectable, Covalently Cross-Linked Hydrogels for Biomedical Applications. *Macromol. Rapid Commun.* **2014**, *35* (6), 598–617.
- (20) Tan, H.; Marra, K. G. Injectable, Biodegradable Hydrogels for Tissue Engineering Applications. *Materials* **2010**, *3* (3), 1746–1767.
- (21) Huang, B. J.; Hu, J. C.; Athanasiou, K. A. Cell-Based Tissue Engineering Strategies Used in the Clinical Repair of Articular Cartilage. *Biomaterials* **2016**, *98*, 1–22.
- (22) Spiller, K. L.; Maher, S. A.; Lowman, A. M. Hydrogels for the Repair of Articular Cartilage Defects. *Tissue Eng. Part B Rev.* **2011**, *17* (4), 281–299.
- (23) Theocharis, A. D.; Skandalis, S. S.; Gialeli, C.; Karamanos, N. K. Extracellular Matrix Structure. *Adv. Drug Deliv. Rev.* **2016**, *97*, 4–27.
- (24) Yue, B. Biology of the Extracellular Matrix: An Overview. *J. Glaucoma* **2014**, S20–S23.
- (25) *The Extracellular Matrix: An Overview*; Mecham, R. P., Ed.; Biology of extracellular matrix; Springer Verlag: Berlin ; New York, 2011.
- (26) Frantz, C.; Stewart, K. M.; Weaver, V. M. The Extracellular Matrix at a Glance. *J. Cell Sci.* **2010**, *123* (24), 4195–4200.
- (27) Ahmed, E. M. Hydrogel: Preparation, Characterization, and Applications: A Review. *J. Adv. Res.* **2015**, *6* (2), 105–121.
- (28) Geckil, H.; Xu, F.; Zhang, X.; Moon, S.; Demirci, U. Engineering Hydrogels as Extracellular Matrix Mimics. *Nanomed.* **2010**, *5* (3), 469–484.
- (29) Slaughter, B. V.; Khurshid, S. S.; Fisher, O. Z.; Khademhosseini, A.; Peppas, N. A. Hydrogels in Regenerative Medicine. *Adv. Mater.* **2009**, *21* (32–33), 3307–3329.
- (30) Kim, B.-S.; Park, I.-K.; Hoshiba, T.; Jiang, H.-L.; Choi, Y.-J.; Akaike, T.; Cho, C.-S. Design of Artificial Extracellular Matrices for Tissue Engineering. *Prog. Polym. Sci.* **2011**, *36* (2), 238–268.
- (31) Badylak, S. F.; Freytes, D. O.; Gilbert, T. W. Extracellular Matrix as a Biological Scaffold Material: Structure and Function. *Acta Biomater.* **2009**, *5* (1), 1–13.
- (32) Zhu, J. Bioactive Modification of Poly(ethylene Glycol) Hydrogels for Tissue Engineering. *Biomaterials* **2010**, *31* (17), 4639–4656.
- (33) Peyton, S. R.; Raub, C. B.; Keschrums, V. P.; Putnam, A. J. The Use of Poly(ethylene Glycol) Hydrogels to Investigate the Impact of ECM Chemistry and Mechanics on Smooth Muscle Cells. *Biomaterials* **2006**, *27* (28), 4881–4893.
- (34) Hersel, U.; Dahmen, C.; Kessler, H. RGD Modified Polymers: Biomaterials for Stimulated Cell Adhesion and beyond. *Biomaterials* **2003**, *24* (24), 4385–4415.
- (35) Yang, F.; Williams, C. G.; Wang, D.; Lee, H.; Manson, P. N.; Elisseeff, J. The Effect of Incorporating RGD Adhesive Peptide in Polyethylene Glycol Diacrylate Hydrogel on Osteogenesis of Bone Marrow Stromal Cells. *Biomaterials* **2005**, *26* (30), 5991–5998.
- (36) Salinas, C. N.; Anseth, K. S. Decorin Moieties Tethered into PEG Networks Induce Chondrogenesis of Human Mesenchymal Stem Cells. *J. Biomed. Mater. Res. A* **2009**, *90* (2), 456–464.
- (37) Tsurkan, M. V.; Chwalek, K.; Prokoph, S.; Zieris, A.; Levental, K. R.; Freudenberg, U.; Werner, C. Defined Polymer-Peptide Conjugates to Form Cell-Instructive starPEG-Heparin Matrices In Situ. *Adv. Mater.* **2013**, *25* (18), 2606–2610.
- (38) Nicodemus, G. D.; Bryant, S. J. Cell Encapsulation in Biodegradable Hydrogels for Tissue Engineering Applications. *Tissue Eng. Part B Rev.* **2008**, *14* (2), 149–165.

- (39) Alves, M. H.; Young, C. J.; Bozzetto, K.; Poole-Warren, L. A.; Martens, P. J. Degradable, Click Poly(vinyl Alcohol) Hydrogels: Characterization of Degradation and Cellular Compatibility. *Biomed. Mater.* **2012**, *7* (2), 024106.
- (40) Benoit, D. S. W.; Durney, A. R.; Anseth, K. S. Manipulations in Hydrogel Degradation Behavior Enhance Osteoblast Function and Mineralized Tissue Formation. *Tissue Eng.* **2006**, *12* (6), 1663–1673.
- (41) Wang, D.; Williams, C. G.; Li, Q.; Sharma, B.; Elisseeff, J. H. Synthesis and Characterization of a Novel Degradable Phosphate-Containing Hydrogel. *Biomaterials* **2003**, *24* (22), 3969–3980.
- (42) Patterson, J.; Hubbell, J. A. Enhanced Proteolytic Degradation of Molecularly Engineered PEG Hydrogels in Response to MMP-1 and MMP-2. *Biomaterials* **2010**, *31* (30), 7836–7845.
- (43) Patterson, J.; Hubbell, J. A. SPARC-Derived Protease Substrates to Enhance the Plasmin Sensitivity of Molecularly Engineered PEG Hydrogels. *Biomaterials* **2011**, *32* (5), 1301–1310.
- (44) Andersen, T.; Auk-Emblem, P.; Dornish, M. 3D Cell Culture in Alginate Hydrogels. *Microarrays* **2015**, *4* (2), 133–161.
- (45) Du, X.; Zhou, J.; Shi, J.; Xu, B. Supramolecular Hydrogelators and Hydrogels: From Soft Matter to Molecular Biomaterials. *Chem. Rev.* **2015**, *115* (24), 13165–13307.
- (46) Worthington, P.; Pochan, D. J.; Langhans, S. A. Peptide Hydrogels – Versatile Matrices for 3D Cell Culture in Cancer Medicine. *Front. Oncol.* **2015**, *5*.
- (47) Dasgupta, A.; Mondal, J. H.; Das, D. Peptide Hydrogels. *RSC Adv.* **2013**, *3* (24), 9117.
- (48) *Peptide-Based Materials*; Deming, T., Ed.; Topics in Current Chemistry; Springer Berlin Heidelberg: Berlin, Heidelberg, 2012; Vol. 310.
- (49) Jonker, A. M.; Löwik, D. W. P. M.; van Hest, J. C. M. Peptide- and Protein-Based Hydrogels. *Chem. Mater.* **2012**, *24* (5), 759–773.
- (50) Altunbas, A.; Pochan, D. J. Peptide-Based and Polypeptide-Based Hydrogels for Drug Delivery and Tissue Engineering. In *Peptide-Based Materials*; Deming, T., Ed.; Springer Berlin Heidelberg: Berlin, Heidelberg, 2011; Vol. 310, pp 135–167.
- (51) Guvendiren, M.; Lu, H. D.; Burdick, J. A. Shear-Thinning Hydrogels for Biomedical Applications. *Soft Matter* **2011**, *8* (2), 260–272.
- (52) Cheng, T.-Y.; Chen, M.-H.; Chang, W.-H.; Huang, M.-Y.; Wang, T.-W. Neural Stem Cells Encapsulated in a Functionalized Self-Assembling Peptide Hydrogel for Brain Tissue Engineering. *Biomaterials* **2013**, *34* (8), 2005–2016.
- (53) Sieminski, A. L.; Semino, C. E.; Gong, H.; Kamm, R. D. Primary Sequence of Ionic Self-Assembling Peptide Gels Affects Endothelial Cell Adhesion and Capillary Morphogenesis. *J. Biomed. Mater. Res. A* **2008**, *87A* (2), 494–504.
- (54) Moradi, F.; Bahktiari, M.; Joghataei, M. T.; Nobakht, M.; Soleimani, M.; Hasanzadeh, G.; Fallah, A.; Zarbakhsh, S.; Hejazian, L. B.; Shirmohammadi, M.; Maleki, F. BD PuraMatrix Peptide Hydrogel as a Culture System for Human Fetal Schwann Cells in Spinal Cord Regeneration. *J. Neurosci. Res.* **2012**, *90* (12), 2335–2348.
- (55) Davis, M. E.; Motion, J. P. M.; Narmoneva, D. A.; Takahashi, T.; Hakuno, D.; Kamm, R. D.; Zhang, S.; Lee, R. T. Injectable Self-Assembling Peptide Nanofibers Create Intramyocardial Microenvironments for Endothelial Cells. *Circulation* **2005**, *111* (4), 442–450.

- (56) Narmoneva, D. A.; Oni, O.; Sieminski, A. L.; Zhang, S.; Gertler, J. P.; Kamm, R. D.; Lee, R. T. Self-Assembling Short Oligopeptides and the Promotion of Angiogenesis. *Biomaterials* **2005**, *26* (23), 4837–4846.
- (57) Kisiday, J.; Jin, M.; Kurz, B.; Hung, H.; Semino, C.; Zhang, S.; Grodzinsky, A. J. Self-Assembling Peptide Hydrogel Fosters Chondrocyte Extracellular Matrix Production and Cell Division: Implications for Cartilage Tissue Repair. *Proc. Natl. Acad. Sci.* **2002**, *99* (15), 9996–10001.
- (58) Mujeeb, A.; Miller, A. F.; Saiani, A.; Gough, J. E. Self-Assembled Octapeptide Scaffolds for in Vitro Chondrocyte Culture. *Acta Biomater.* **2013**, *9* (1), 4609–4617.
- (59) Haines-Butterick, L.; Rajagopal, K.; Branco, M.; Salick, D.; Rughani, R.; Pilarz, M.; Lamm, M. S.; Pochan, D. J.; Schneider, J. P. Controlling Hydrogelation Kinetics by Peptide Design for Three-Dimensional Encapsulation and Injectable Delivery of Cells. *Proc. Natl. Acad. Sci. U. S. A.* **2007**, *104* (19), 7791–7796.
- (60) Yan, C.; Mackay, M. E.; Czymmek, K.; Nagarkar, R. P.; Schneider, J. P.; Pochan, D. J. Injectable Solid Peptide Hydrogel as a Cell Carrier: Effects of Shear Flow on Hydrogels and Cell Payload. *Langmuir ACS J. Surf. Colloids* **2012**, *28* (14), 6076–6087.
- (61) Galler, K. M.; Aulisa, L.; Regan, K. R.; D’Souza, R. N.; Hartgerink, J. D. Self-Assembling Multidomain Peptide Hydrogels: Designed Susceptibility to Enzymatic Cleavage Allows Enhanced Cell Migration and Spreading. *J. Am. Chem. Soc.* **2010**, *132* (9), 3217–3223.
- (62) Galler, K. M.; Hartgerink, J. D.; Cavender, A. C.; Schmalz, G.; D’Souza, R. N. A Customized Self-Assembling Peptide Hydrogel for Dental Pulp Tissue Engineering. *Tissue Eng. Part A* **2012**, *18* (1–2), 176–184.
- (63) Jayawarna, V.; Ali, M.; Jowitt, T. A.; Miller, A. F.; Saiani, A.; Gough, J. E.; Ulijn, R. V. Nanostructured Hydrogels for Three-Dimensional Cell Culture Through Self-Assembly of Fluorenylmethoxycarbonyl–Dipeptides. *Adv. Mater.* **2006**, *18* (5), 611–614.
- (64) Jayawarna, V.; Smith, A.; Gough, J. E.; Ulijn, R. V. Three-Dimensional Cell Culture of Chondrocytes on Modified Di-Phenylalanine Scaffolds. *Biochem. Soc. Trans.* **2007**, *35* (Pt 3), 535–537.
- (65) Jayawarna, V.; Richardson, S. M.; Hirst, A. R.; Hodson, N. W.; Saiani, A.; Gough, J. E.; Ulijn, R. V. Introducing Chemical Functionality in Fmoc-Peptide Gels for Cell Culture. *Acta Biomater.* **2009**, *5* (3), 934–943.
- (66) Zhou, M.; Smith, A. M.; Das, A. K.; Hodson, N. W.; Collins, R. F.; Ulijn, R. V.; Gough, J. E. Self-Assembled Peptide-Based Hydrogels as Scaffolds for Anchorage-Dependent Cells. *Biomaterials* **2009**, *30* (13), 2523–2530.
- (67) Zhou, M.; Ulijn, R. V.; Gough, J. E. Extracellular Matrix Formation in Self-Assembled Minimalistic Bioactive Hydrogels Based on Aromatic Peptide Amphiphiles. *J. Tissue Eng.* **2014**, *5*, 2041731414531593.
- (68) Luo, Z.; Yue, Y.; Zhang, Y.; Yuan, X.; Gong, J.; Wang, L.; He, B.; Liu, Z.; Sun, Y.; Liu, J.; Hu, M.; Zheng, J. Designer D-Form Self-Assembling Peptide Nanofiber Scaffolds for 3-Dimensional Cell Cultures. *Biomaterials* **2013**, *34* (21), 4902–4913.
- (69) Yang, Z.; Zhao, X. A 3D Model of Ovarian Cancer Cell Lines on Peptide Nanofiber Scaffold to Explore the Cell-Scaffold Interaction and Chemotherapeutic Resistance of Anticancer Drugs. *Int. J. Nanomedicine* **2011**, *6*, 303–310.
- (70) Huang, H.; Ding, Y.; Sun, X. S.; Nguyen, T. A. Peptide Hydrogelation and Cell Encapsulation for 3D Culture of MCF-7 Breast Cancer Cells. *PLoS One* **2013**, *8* (3), e59482.

- (71) Freshney, R. I. *Culture of Animal Cells: A Manual of Basic Technique and Specialized Applications*; John Wiley & Sons, 2011.
- (72) Garnica-Palafox, I. M.; Sánchez-Arévalo, F. M.; Velasquillo, C.; García-Carvajal, Z. Y.; García-López, J.; Ortega-Sánchez, C.; Ibarra, C.; Luna-Bárceñas, G.; Solís-Arrieta, L. Mechanical and Structural Response of a Hybrid Hydrogel Based on Chitosan and Poly(vinyl Alcohol) Cross-Linked with Epichlorohydrin for Potential Use in Tissue Engineering. *J. Biomater. Sci. Polym. Ed.* **2014**, *25* (1), 32–50.
- (73) Wang, L.; Stegemann, J. P. Glyoxal Crosslinking of Cell-Seeded Chitosan/Collagen Hydrogels for Bone Regeneration. *Acta Biomater.* **2011**, *7* (6), 2410–2417.
- (74) Yang, R.; Tan, L.; Cen, L.; Zhang, Z. An Injectable Scaffold Based on Crosslinked Hyaluronic Acid Gel for Tissue Regeneration. *RSC Adv.* **2016**, *6* (20), 16838–16850.
- (75) Sletten, E. M.; Bertozzi, C. R. Bioorthogonal Chemistry: Fishing for Selectivity in a Sea of Functionality. *Angew. Chem. Int. Ed Engl.* **2009**, *48* (38), 6974–6998.
- (76) Lin, C.-C. Recent Advances in Crosslinking Chemistry of Biomimetic Poly(ethylene Glycol) Hydrogels. *RSC Adv.* **2015**, *5* (50), 39844–39853.
- (77) Bakaic, E.; Smeets, N. M. B.; Hoare, T. Injectable Hydrogels Based on Poly(ethylene Glycol) and Derivatives as Functional Biomaterials. *RSC Adv.* **2015**, *5* (45), 35469–35486.
- (78) Nguyen, K. T.; West, J. L. Photopolymerizable Hydrogels for Tissue Engineering Applications. *Biomaterials* **2002**, *23* (22), 4307–4314.
- (79) Ifkovits, J. L.; Burdick, J. A. Review: Photopolymerizable and Degradable Biomaterials for Tissue Engineering Applications. *Tissue Eng.* **2007**, *13* (10), 2369–2385.
- (80) Mironi-Harpaz, I.; Wang, D. Y.; Venkatraman, S.; Seliktar, D. Photopolymerization of Cell-Encapsulating Hydrogels: Crosslinking Efficiency versus Cytotoxicity. *Acta Biomater.* **2012**, *8* (5), 1838–1848.
- (81) Burdick, J. A.; Anseth, K. S. Photoencapsulation of Osteoblasts in Injectable RGD-Modified PEG Hydrogels for Bone Tissue Engineering. *Biomaterials* **2002**, *23* (22), 4315–4323.
- (82) Sawhney, A. S.; Pathak, C. P.; Hubbell, J. A. Bioerodible Hydrogels Based on Photopolymerized Poly(ethylene Glycol)-Co-Poly(.alpha.-Hydroxy Acid) Diacrylate Macromers. *Macromolecules* **1993**, *26* (4), 581–587.
- (83) Weber, L. M.; Lopez, C. G.; Anseth, K. S. The Effects of PEG Hydrogel Crosslinking Density on Protein Diffusion and Encapsulated Islet Survival and Function. *J. Biomed. Mater. Res. A* **2009**, *90* (3), 720–729.
- (84) Bryant, S. J.; Bender, R. J.; Durand, K. L.; Anseth, K. S. Encapsulating Chondrocytes in Degrading PEG Hydrogels with High Modulus: Engineering Gel Structural Changes to Facilitate Cartilaginous Tissue Production. *Biotechnol. Bioeng.* **2004**, *86* (7), 747–755.
- (85) Bryant, S. J.; Davis-Arehart, K. A.; Luo, N.; Shoemaker, R. K.; Arthur, J. A.; Anseth, K. S. Synthesis and Characterization of Photopolymerized Multifunctional Hydrogels: Water-Soluble Poly(Vinyl Alcohol) and Chondroitin Sulfate Macromers for Chondrocyte Encapsulation. *Macromolecules* **2004**, *37* (18), 6726–6733.
- (86) Rouillard, A. D.; Berglund, C. M.; Lee, J. Y.; Polacheck, W. J.; Tsui, Y.; Bonassar, L. J.; Kirby, B. J. Methods for Photocrosslinking Alginate Hydrogel Scaffolds with High Cell Viability. *Tissue Eng. Part C Methods* **2011**, *17* (2), 173–179.
- (87) Masters, K. S.; Shah, D. N.; Leinwand, L. A.; Anseth, K. S. Crosslinked Hyaluronan Scaffolds as a Biologically Active Carrier for Valvular Interstitial Cells. *Biomaterials* **2005**, *26* (15), 2517–2525.

- (88) Singh, R. K.; Seliktar, D.; Putnam, A. J. Capillary Morphogenesis in PEG-Collagen Hydrogels. *Biomaterials* **2013**, *34* (37).
- (89) Bryant, S. J.; Nuttelman, C. R.; Anseth, K. S. Cytocompatibility of UV and Visible Light Photoinitiating Systems on Cultured NIH/3T3 Fibroblasts in Vitro. *J. Biomater. Sci. Polym. Ed.* **2000**, *11* (5), 439–457.
- (90) Williams, C. G.; Malik, A. N.; Kim, T. K.; Manson, P. N.; Elisseeff, J. H. Variable Cytocompatibility of Six Cell Lines with Photoinitiators Used for Polymerizing Hydrogels and Cell Encapsulation. *Biomaterials* **2005**, *26* (11), 1211–1218.
- (91) Fedorovich, N. E.; Oudshoorn, M. H.; van Geemen, D.; Hennink, W. E.; Alblas, J.; Dhert, W. J. A. The Effect of Photopolymerization on Stem Cells Embedded in Hydrogels. *Biomaterials* **2009**, *30* (3), 344–353.
- (92) Pattison, D. I.; Davies, M. J. Actions of Ultraviolet Light on Cellular Structures. *EXS* **2006**, No. 96, 131–157.
- (93) Zhou, D.; Ito, Y. Visible Light-Curable Polymers for Biomedical Applications. *Sci. China Chem.* **2014**, *57* (4), 510–521.
- (94) Mishra, S.; Scarano, F. J.; Calvert, P. Entrapment of *Saccharomyces Cerevisiae* and 3T3 Fibroblast Cells into Blue Light Cured Hydrogels. *J. Biomed. Mater. Res. A* **2012**, *100A* (10), 2829–2838.
- (95) Bahney, C. S.; Lujan, T. J.; Hsu, C. W.; Bottlang, M.; West, J. L.; Johnstone, B. Visible Light Photoinitiation of Mesenchymal Stem Cell-Laden Bioresponsive Hydrogels. *Eur Cell Mater* **2011**, *22*, 43–55.
- (96) Brinkman, W. T.; Nagapudi, K.; Thomas, B. S.; Chaikof, E. L. Photo-Cross-Linking of Type I Collagen Gels in the Presence of Smooth Muscle Cells: Mechanical Properties, Cell Viability, and Function. *Biomacromolecules* **2003**, *4* (4), 890–895.
- (97) Hu, J.; Hou, Y.; Park, H.; Choi, B.; Hou, S.; Chung, A.; Lee, M. Visible Light Crosslinkable Chitosan Hydrogels for Tissue Engineering. *Acta Biomater.* **2012**, *8* (5), 1730–1738.
- (98) Park, H.; Choi, B.; Hu, J.; Lee, M. Injectable Chitosan Hyaluronic Acid Hydrogels for Cartilage Tissue Engineering. *Acta Biomater.* **2013**, *9* (1), 4779–4786.
- (99) Hoshikawa, A.; Nakayama, Y.; Matsuda, T.; Oda, H.; Nakamura, K.; Mabuchi, K. Encapsulation of Chondrocytes in Photopolymerizable Styrenated Gelatin for Cartilage Tissue Engineering. *Tissue Eng.* **2006**, *12* (8), 2333–2341.
- (100) Schieber, M.; Chandel, N. S. ROS Function in Redox Signaling and Oxidative Stress. *Curr. Biol.* **2014**, *24* (10), R453–R462.
- (101) Roberts, J. J.; Bryant, S. J. Comparison of Photopolymerizable Thiol-Ene PEG and Acrylate-Based PEG Hydrogels for Cartilage Development. *Biomaterials* **2013**, *34* (38), 9969–9979.
- (102) Hoyle, C. E.; Bowman, C. N. Thiol-Ene Click Chemistry. *Angew. Chem. Int. Ed.* **2010**, *49* (9), 1540–1573.
- (103) Lin, C.-C.; Raza, A.; Shih, H. PEG Hydrogels Formed by Thiol-Ene Photo-Click Chemistry and Their Effect on the Formation and Recovery of Insulin-Secreting Cell Spheroids. *Biomaterials* **2011**, *32* (36), 9685–9695.
- (104) Rydholm, A. E.; Bowman, C. N.; Anseth, K. S. Degradable Thiol-Acrylate Photopolymers: Polymerization and Degradation Behavior of an in Situ Forming Biomaterial. *Biomaterials* **2005**, *26* (22), 4495–4506.
- (105) Salinas, C. N.; Anseth, K. S. The Enhancement of Chondrogenic Differentiation of Human Mesenchymal Stem Cells by Enzymatically Regulated RGD Functionalities. *Biomaterials* **2008**, *29* (15), 2370–2377.

- (106) Hao, Y.; Lin, C.-C. Degradable Thiol-Acrylate Hydrogels as Tunable Matrices for Three-Dimensional Hepatic Culture: Degradable Thiol-Acrylate Hydrogels. *J. Biomed. Mater. Res. A* **2014**, *102* (11), 3813–3827.
- (107) Hao, Y.; Shih, H.; Muñoz, Z.; Kemp, A.; Lin, C.-C. Visible Light Cured Thiol-Vinyl Hydrogels with Tunable Degradation for 3D Cell Culture. *Acta Biomater.* **2014**, *10* (1).
- (108) Lin, C.-C.; Ki, C. S.; Shih, H. Thiol-Norbornene Photoclick Hydrogels for Tissue Engineering Applications. *J. Appl. Polym. Sci.* **2015**, *132* (8), n/a-n/a.
- (109) Fairbanks, B. D.; Schwartz, M. P.; Halevi, A. E.; Nuttelman, C. R.; Bowman, C. N.; Anseth, K. S. A Versatile Synthetic Extracellular Matrix Mimic via Thiol-Norbornene Photopolymerization. *Adv. Mater. Deerfield Beach Fla* **2009**, *21* (48), 5005–5010.
- (110) Shih, H.; Lin, C.-C. Visible-Light-Mediated Thiol-Ene Hydrogelation Using Eosin-Y as the Only Photoinitiator. *Macromol. Rapid Commun.* **2013**, *34* (3), 269–273.
- (111) McKinnon, D. D.; Kloxin, A. M.; Anseth, K. S. Synthetic Hydrogel Platform for Three-Dimensional Culture of Embryonic Stem Cell-Derived Motor Neurons. *Biomater. Sci.* **2013**, *1* (5), 460–469.
- (112) Kolb, H. C.; Finn, M. G.; Sharpless, K. B. Click Chemistry: Diverse Chemical Function from a Few Good Reactions. *Angew. Chem. Int. Ed.* **2001**, *40* (11), 2004–2021.
- (113) Liu, S.; Dicker, K. T.; Jia, X. Modular and Orthogonal Synthesis of Hybrid Polymers and Networks. *Chem Commun* **2015**, *51* (25), 5218–5237.
- (114) Jiang, Y.; Chen, J.; Deng, C.; Suuronen, E. J.; Zhong, Z. Click Hydrogels, Microgels and Nanogels: Emerging Platforms for Drug Delivery and Tissue Engineering. *Biomaterials* **2014**, *35* (18), 4969–4985.
- (115) Azagarsamy, M. A.; Anseth, K. S. Bioorthogonal Click Chemistry: An Indispensable Tool to Create Multifaceted Cell Culture Scaffolds. *ACS Macro Lett.* **2013**, *2* (1), 5–9.
- (116) Nimmo, C. M.; Shoichet, M. S. Regenerative Biomaterials That “Click”: Simple, Aqueous-Based Protocols for Hydrogel Synthesis, Surface Immobilization, and 3D Patterning. *Bioconjug. Chem.* **2011**, *22* (11), 2199–2209.
- (117) Michael, A. Ueber Die Addition von Natriumacetessig- Und Natriummalonsäureäthern Zu Den Aethern Ungesättigter Säuren. *J. Für Prakt. Chem.* **1887**, *35* (1), 349–356.
- (118) Friedman, M.; Cavins, J. F.; Wall, J. S. Relative Nucleophilic Reactivities of Amino Groups and Mercaptide Ions in Addition Reactions with α , β -Unsaturated compounds¹, 2. *J. Am. Chem. Soc.* **1965**, *87* (16), 3672–3682.
- (119) Nair, D. P.; Podgórski, M.; Chatani, S.; Gong, T.; Xi, W.; Fenoli, C. R.; Bowman, C. N. The Thiol-Michael Addition Click Reaction: A Powerful and Widely Used Tool in Materials Chemistry. *Chem. Mater.* **2014**, *26* (1), 724–744.
- (120) Lutolf, M. P.; Lauer-Fields, J. L.; Schmoekel, H. G.; Metters, A. T.; Weber, F. E.; Fields, G. B.; Hubbell, J. A. Synthetic Matrix Metalloproteinase-Sensitive Hydrogels for the Conduction of Tissue Regeneration: Engineering Cell-Invasion Characteristics. *Proc. Natl. Acad. Sci.* **2003**, *100* (9), 5413–5418.
- (121) Park, Y.; Lutolf, M. P.; Hubbell, J. A.; Hunziker, E. B.; Wong, M. Bovine Primary Chondrocyte Culture in Synthetic Matrix Metalloproteinase-Sensitive Poly(ethylene Glycol)-Based Hydrogels as a Scaffold for Cartilage Repair. *Tissue Eng.* **2004**, *10* (3–4), 515–522.
- (122) Cellesi, F.; Tirelli, N.; Hubbell, J. A. Towards a Fully-Synthetic Substitute of Alginate: Development of a New Process Using Thermal Gelation and Chemical Cross-Linking. *Biomaterials* **2004**, *25* (21), 5115–5124.

- (123) Jukes, J. M.; van der Aa, L. J.; Hiemstra, C.; van Veen, T.; Dijkstra, P. J.; Zhong, Z.; Feijen, J.; van Blitterswijk, C. A.; de Boer, J. A Newly Developed Chemically Crosslinked Dextran-Poly(ethylene Glycol) Hydrogel for Cartilage Tissue Engineering. *Tissue Eng. Part A* **2010**, *16* (2), 565–573.
- (124) Zheng Shu, X.; Liu, Y.; Palumbo, F. S.; Luo, Y.; Prestwich, G. D. In Situ Crosslinkable Hyaluronan Hydrogels for Tissue Engineering. *Biomaterials* **2004**, *25* (7–8), 1339–1348.
- (125) Li, G.-Z.; Randev, R. K.; Soeriyadi, A. H.; Rees, G.; Boyer, C.; Tong, Z.; Davis, T. P.; Becer, C. R.; Haddleton, D. M. Investigation into Thiol-(Meth)acrylate Michael Addition Reactions Using Amine and Phosphine Catalysts. *Polym. Chem.* **2010**, *1* (8), 1196–1204.
- (126) Phelps, E. A.; Enemchukwu, N. O.; Fiore, V. F.; Sy, J. C.; Murthy, N.; Sulchek, T. A.; Barker, T. H.; García, A. J. Maleimide Cross-Linked Bioactive PEG Hydrogel Exhibits Improved Reaction Kinetics and Cross-Linking for Cell Encapsulation and In Situ Delivery. *Adv. Mater.* **2012**, *24* (1), 64–70.
- (127) Baldwin, A. D.; Kiick, K. L. Tunable Degradation of Maleimide–Thiol Adducts in Reducing Environments. *Bioconjug. Chem.* **2011**, *22* (10), 1946–1953.
- (128) Baldwin, A. D.; Kiick, K. L. Reversible Maleimide–thiol Adducts Yield Glutathione-Sensitive Poly(ethylene Glycol)–heparin Hydrogels. *Polym. Chem.* **2012**, *4* (1), 133–143.
- (129) Rostovtsev, V. V.; Green, L. G.; Fokin, V. V.; Sharpless, K. B. A Stepwise Huisgen Cycloaddition Process: Copper(I)-Catalyzed Regioselective “Ligation” of Azides and Terminal Alkynes. *Angew. Chem. Int. Ed.* **2002**, *41* (14), 2596–2599.
- (130) Adzima, B. J.; Tao, Y.; Kloxin, C. J.; DeForest, C. A.; Anseth, K. S.; Bowman, C. N. Spatial and Temporal Control of the Alkyne–azide Cycloaddition by Photoinitiated Cu(II) Reduction. *Nat. Chem.* **2011**, *3* (3), 256–259.
- (131) Himo, F.; Lovell, T.; Hilgraf, R.; Rostovtsev, V. V.; Noodleman, L.; Sharpless, K. B.; Fokin, V. V. Copper(I)-Catalyzed Synthesis of Azoles. DFT Study Predicts Unprecedented Reactivity and Intermediates. *J. Am. Chem. Soc.* **2005**, *127* (1), 210–216.
- (132) Ossipov, D. A.; Hilborn, J. Poly(vinyl Alcohol)-Based Hydrogels Formed by “Click Chemistry.” *Macromolecules* **2006**, *39* (5), 1709–1718.
- (133) Polizzotti, B. D.; Fairbanks, B. D.; Anseth, K. S. Three-Dimensional Biochemical Patterning of Click-Based Composite Hydrogels via Thiolene Photopolymerization. *Biomacromolecules* **2008**, *9* (4), 1084–1087.
- (134) Liu, S. Q.; Ee, P. L. R.; Ke, C. Y.; Hedrick, J. L.; Yang, Y. Y. Biodegradable Poly(ethylene Glycol)-Peptide Hydrogels with Well-Defined Structure and Properties for Cell Delivery. *Biomaterials* **2009**, *30* (8), 1453–1461.
- (135) van Dijk, M.; van Nostrum, C. F.; Hennink, W. E.; Rijkers, D. T. S.; Liskamp, R. M. J. Synthesis and Characterization of Enzymatically Biodegradable PEG and Peptide-Based Hydrogels Prepared by Click Chemistry. *Biomacromolecules* **2010**, *11* (6), 1608–1614.
- (136) Hu, X.; Li, D.; Zhou, F.; Gao, C. Biological Hydrogel Synthesized from Hyaluronic Acid, Gelatin and Chondroitin Sulfate by Click Chemistry. *Acta Biomater.* **2011**, *7* (4), 1618–1626.
- (137) Tan, S.; Blencowe, A.; Ladewig, K.; Qiao, G. G. A Novel One-Pot Approach towards Dynamically Cross-Linked Hydrogels. *Soft Matter* **2013**, *9* (21), 5239.
- (138) Crescenzi, V.; Cornelio, L.; Di Meo, C.; Nardecchia, S.; Lamanna, R. Novel Hydrogels via Click Chemistry: Synthesis and Potential Biomedical Applications. *Biomacromolecules* **2007**, *8* (6), 1844–1850.

- (139) Lallana, E.; Riguera, R.; Fernandez-Megia, E. Reliable and Efficient Procedures for the Conjugation of Biomolecules through Huisgen Azide-Alkyne Cycloadditions. *Angew. Chem. Int. Ed.* **2011**, *50* (38), 8794–8804.
- (140) Agard, N. J.; Prescher, J. A.; Bertozzi, C. R. A Strain-Promoted [3 + 2] Azide–Alkyne Cycloaddition for Covalent Modification of Biomolecules in Living Systems. *J. Am. Chem. Soc.* **2004**, *126* (46), 15046–15047.
- (141) Jiang, H.; Qin, S.; Dong, H.; Lei, Q.; Su, X.; Zhuo, R.; Zhong, Z. An Injectable and Fast-Degradable Poly(ethylene Glycol) Hydrogel Fabricated via Bioorthogonal Strain-Promoted Azide–alkyne Cycloaddition Click Chemistry. *Soft Matter* **2015**, *11* (30), 6029–6036.
- (142) DeForest, C. A.; Polizzotti, B. D.; Anseth, K. S. Sequential Click Reactions for Synthesizing and Patterning 3D Cell Microenvironments. *Nat. Mater.* **2009**, *8* (8), 659–664.
- (143) DeForest, C. A.; Sims, E. A.; Anseth, K. S. Peptide-Functionalized Click Hydrogels with Independently Tunable Mechanics and Chemical Functionality for 3D Cell Culture. *Chem. Mater.* **2010**, *22* (16), 4783–4790.
- (144) DeForest, C. A.; Anseth, K. S. Cytocompatible Click-Based Hydrogels with Dynamically-Tunable Properties Through Orthogonal Photoconjugation and Photocleavage Reactions. *Nat. Chem.* **2011**, *3* (12), 925–931.
- (145) DeForest, C. A.; Anseth, K. S. Photoreversible Patterning of Biomolecules within Click-Based Hydrogels. *Angew. Chem. Int. Ed Engl.* **2012**, *51* (8), 1816–1819.
- (146) McKinnon, D. D.; Brown, T. E.; Kyburz, K. A.; Kiyotake, E.; Anseth, K. S. Design and Characterization of a Synthetically Accessible, Photodegradable Hydrogel for User-Directed Formation of Neural Networks. *Biomacromolecules* **2014**, *15* (7), 2808–2816.
- (147) DeForest, C. A.; Tirrell, D. A. A Photoreversible Protein-Patterning Approach for Guiding Stem Cell Fate in Three-Dimensional Gels. *Nat. Mater.* **2015**, *14* (5), 523–531.
- (148) Baskin, J. M.; Prescher, J. A.; Laughlin, S. T.; Agard, N. J.; Chang, P. V.; Miller, I. A.; Lo, A.; Codelli, J. A.; Bertozzi, C. R. Copper-Free Click Chemistry for Dynamic in Vivo Imaging. *Proc. Natl. Acad. Sci. U. S. A.* **2007**, *104* (43), 16793–16797.
- (149) Xu, J.; Fillion, T. M.; Prifti, F.; Song, J. Cytocompatible Poly(ethylene Glycol)-Copolycarbonate Hydrogels Cross-Linked by Copper-Free, Strain-Promoted Click Chemistry. *Chem. – Asian J.* **2011**, *6* (10), 2730–2737.
- (150) Zheng, J.; Smith Callahan, L. A.; Hao, J.; Guo, K.; Wesdemiotis, C.; Weiss, R. A.; Becker, M. L. Strain-Promoted Cross-Linking of PEG-Based Hydrogels via Copper-Free Cycloaddition. *ACS Macro Lett.* **2012**, *1* (8), 1071–1073.
- (151) Li, Z.; Seo, T. S.; Ju, J. 1,3-Dipolar Cycloaddition of Azides with Electron-Deficient Alkynes under Mild Condition in Water. *Tetrahedron Lett.* **2004**, *45* (15), 3143–3146.
- (152) Truong, V. X.; Ablett, M. P.; Gilbert, H. T. J.; Bowen, J.; Richardson, S. M.; Hoyland, J. A.; Dove, A. P. In Situ-Forming Robust Chitosan-Poly(ethylene Glycol) Hydrogels Prepared by Copper-Free Azide–alkyne Click Reaction for Tissue Engineering. *Biomater Sci* **2014**, *2* (2), 167–175.
- (153) Diels, O.; Alder, K. Synthesen in Der Hydroaromatischen Reihe. *Justus Liebigs Ann. Chem.* **1928**, *460* (1), 98–122.
- (154) Rideout, D. C.; Breslow, R. Hydrophobic Acceleration of Diels-Alder Reactions. *J. Am. Chem. Soc.* **1980**, *102* (26), 7816–7817.
- (155) Blokzijl, W.; Engberts, J. B. F. N. Enforced Hydrophobic Interactions and Hydrogen Bonding in the Acceleration of Diels–Alder Reactions in Water. In *Structure and*

- Reactivity in Aqueous Solution*; Cramer, C. J., Truhlar, D. G., Eds.; American Chemical Society: Washington, DC, 1994; Vol. 568, pp 303–317.
- (156) Wei, H.-L.; Yang, Z.; Zheng, L.-M.; Shen, Y.-M. Thermosensitive Hydrogels Synthesized by Fast Diels–Alder Reaction in Water. *Polymer* **2009**, *50* (13), 2836–2840.
- (157) Nimmo, C. M.; Owen, S. C.; Shoichet, M. S. Diels–Alder Click Cross-Linked Hyaluronic Acid Hydrogels for Tissue Engineering. *Biomacromolecules* **2011**, *12* (3), 824–830.
- (158) Tan, H.; Rubin, J. P.; Marra, K. G. Direct Synthesis of Biodegradable Polysaccharide Derivative Hydrogels Through Aqueous Diels–Alder Chemistry. *Macromol. Rapid Commun.* **2011**, *32* (12), 905–911.
- (159) Wei, H.-L.; Yao, K.; Yang, Z.; Chu, H.-J.; Zhu, J.; Ma, C.-C.; Zhao, Z.-X. Preparation of Thermosensitive Hydrogels by Means of Tandem Physical and Chemical Crosslinking. *Macromol. Res.* **2011**, *19* (3), 294–299.
- (160) Owen, S. C.; Fisher, S. A.; Tam, R. Y.; Nimmo, C. M.; Shoichet, M. S. Hyaluronic Acid Click Hydrogels Emulate the Extracellular Matrix. *Langmuir* **2013**, *29* (24), 7393–7400.
- (161) Kirchhof, S.; Gregoritzka, M.; Messmann, V.; Hammer, N.; Goepferich, A. M.; Brandl, F. P. Diels–Alder Hydrogels with Enhanced Stability: First Step toward Controlled Release of Bevacizumab. *Eur. J. Pharm. Biopharm. Off. J. Arbeitsgemeinschaft Für Pharm. Verfahrenstechnik EV* **2015**, *96*, 217–225.
- (162) Stewart, S. A.; Backholm, M.; Burke, N. A. D.; Stöver, H. D. H. Cross-Linked Hydrogels Formed through Diels–Alder Coupling of Furan- and Maleimide-Modified Poly(methyl Vinyl Ether-*Alt* -Maleic Acid). *Langmuir* **2016**, *32* (7), 1863–1870.
- (163) Yu, F.; Cao, X.; Li, Y.; Zeng, L.; Zhu, J.; Wang, G.; Chen, X. Diels–Alder Crosslinked HA/PEG Hydrogels with High Elasticity and Fatigue Resistance for Cell Encapsulation and Articular Cartilage Tissue Repair. *Polym. Chem.* **2014**, *5* (17), 5116.
- (164) Sanyal, A. Diels–Alder Cycloaddition–Cycloreversion: A Powerful Combo in Materials Design. *Macromol. Chem. Phys.* **2010**, *211* (13), 1417–1425.
- (165) Kirchhof, S.; Brandl, F. P.; Hammer, N.; Goepferich, A. M. Investigation of the Diels–Alder Reaction as a Cross-Linking Mechanism for Degradable Poly(ethylene Glycol) Based Hydrogels. *J. Mater. Chem. B* **2013**, *1* (37), 4855.
- (166) Koehler, K. C.; Alge, D. L.; Anseth, K. S.; Bowman, C. N. A Diels–Alder Modulated Approach to Control and Sustain the Release of Dexamethasone and Induce Osteogenic Differentiation of Human Mesenchymal Stem Cells. *Biomaterials* **2013**, *34* (16), 4150–4158.
- (167) Koehler, K. C.; Anseth, K. S.; Bowman, C. N. Diels–Alder Mediated Controlled Release from a Poly(ethylene Glycol) Based Hydrogel. *Biomacromolecules* **2013**, *14* (2), 538–547.
- (168) Wei, Z.; Yang, J. H.; Du, X. J.; Xu, F.; Zrinyi, M.; Osada, Y.; Li, F.; Chen, Y. M. Dextran-Based Self-Healing Hydrogels Formed by Reversible Diels–Alder Reaction under Physiological Conditions. *Macromol. Rapid Commun.* **2013**, *34* (18), 1464–1470.
- (169) Devaraj, N. K.; Weissleder, R. Biomedical Applications of Tetrazine Cycloadditions. *Acc. Chem. Res.* **2011**, *44* (9), 816–827.
- (170) Knall, A.-C.; Slugovc, C. Inverse Electron Demand Diels–Alder (iEDDA)-Initiated Conjugation: A (High) Potential Click Chemistry Scheme. *Chem. Soc. Rev.* **2013**, *42* (12), 5131–5142.
- (171) Alge, D. L.; Azagarsamy, M. A.; Donohue, D. F.; Anseth, K. S. Synthetically Tractable Click Hydrogels for Three-Dimensional Cell Culture Formed Using Tetrazine–Norbornene Chemistry. *Biomacromolecules* **2013**, *14* (4), 949–953.

- (172) Zhang, H.; Dicker, K. T.; Xu, X.; Jia, X.; Fox, J. M. Interfacial Bioorthogonal Cross-Linking. *ACS Macro Lett.* **2014**, *3* (8), 727–731.
- (173) Dawson, P. E.; Muir, T. W.; Clark-Lewis, I.; Kent, S. B. Synthesis of Proteins by Native Chemical Ligation. *Science* **1994**, *266* (5186), 776–779.
- (174) Hu, B.-H.; Su, J.; Messersmith, P. B. Hydrogels Cross-Linked by Native Chemical Ligation. *Biomacromolecules* **2009**, *10* (8), 2194–2200.
- (175) Su, J.; Hu, B.-H.; Lowe, W. L.; Kaufman, D. B.; Messersmith, P. B. Anti-Inflammatory Peptide-Functionalized Hydrogels for Insulin-Secreting Cell Encapsulation. *Biomaterials* **2010**, *31* (2), 308–314.
- (176) Jung, J. P.; Sprangers, A. J.; Byce, J. R.; Su, J.; Squirrell, J. M.; Messersmith, P. B.; Eliceiri, K. W.; Ogle, B. M. ECM-Incorporated Hydrogels Crosslinked 1 via Native Chemical Ligation to Engineer Stem Cell Microenvironments. *Biomacromolecules* **2013**, *14* (9).
- (177) Boere, K. W. M.; Soliman, B. G.; Rijkers, D. T. S.; Hennink, W. E.; Vermonden, T. Thermoresponsive Injectable Hydrogels Cross-Linked by Native Chemical Ligation. *Macromolecules* **2014**, *47* (7), 2430–2438.
- (178) Wan, Q.; Chen, J.; Yuan, Y.; Danishefsky, S. J. Oxo-Ester Mediated Native Chemical Ligation: Concept and Applications. *J. Am. Chem. Soc.* **2008**, *130* (47), 15814–15816.
- (179) Strehin, I.; Gourevitch, D.; Zhang, Y.; Heber-Katz, E.; Messersmith, P. B. Hydrogels Formed by Oxo-Ester Mediated Native Chemical Ligation. *Biomater. Sci.* **2013**, *1* (6), 603.
- (180) Balakrishnan, B.; Jayakrishnan, A. Self-Cross-Linking Biopolymers as Injectable in Situ Forming Biodegradable Scaffolds. *Biomaterials* **2005**, *26* (18), 3941–3951.
- (181) Bhatia, S. K.; Arthur, S. D.; Chenault, H. K.; Kodokian, G. K. Interactions of Polysaccharide-Based Tissue Adhesives with Clinically Relevant Fibroblast and Macrophage Cell Lines. *Biotechnol. Lett.* **2007**, *29* (11), 1645–1649.
- (182) Tan, H.; Rubin, J. P.; Marra, K. G. Injectable in Situ Forming Biodegradable Chitosan-Hyaluronic Acid Based Hydrogels for Adipose Tissue Regeneration. *Organogenesis* **2010**, *6* (3), 173–180.
- (183) Tan, H.; Li, H.; Rubin, J. P.; Marra, K. G. Controlled Gelation and Degradation Rates of Injectable Hyaluronic Acid-Based Hydrogels through a Double Crosslinking Strategy. *J. Tissue Eng. Regen. Med.* **2011**, *5* (10), 790–797.
- (184) Zhang, Y.; Tao, L.; Li, S.; Wei, Y. Synthesis of Multiresponsive and Dynamic Chitosan-Based Hydrogels for Controlled Release of Bioactive Molecules. *Biomacromolecules* **2011**, *12* (8), 2894–2901.
- (185) Zhang, Y.; Yang, B.; Zhang, X.; Xu, L.; Tao, L.; Li, S.; Wei, Y. A Magnetic Self-Healing Hydrogel. *Chem. Commun.* **2012**, *48* (74), 9305.
- (186) Li, Y.; Liu, C.; Tan, Y.; Xu, K.; Lu, C.; Wang, P. In Situ Hydrogel Constructed by Starch-Based Nanoparticles via a Schiff Base Reaction. *Carbohydr. Polym.* **2014**, *110*, 87–94.
- (187) Shi, J.; Guobao, W.; Chen, H.; Zhong, W.; Qiu, X.; Xing, M. M. Q. Schiff Based Injectable Hydrogel for in Situ pH-Triggered Delivery of Doxorubicin for Breast Tumor Treatment. *Polym Chem* **2014**, *5* (21), 6180–6189.
- (188) Morozowich, N. L.; Nichol, J. L.; Allcock, H. R. Hydrogels Based on Schiff Base Formation between an Amino-Containing Polyphosphazene and Aldehyde Functionalized-Dextran. *J. Polym. Sci. Part Polym. Chem.* **2016**, *54* (18), 2984–2991.
- (189) Tan, H.; Chu, C. R.; Payne, K.; Marra, K. G. Injectable In Situ Forming Biodegradable Chitosan-Hyaluronic Acid Based Hydrogels for Cartilage Tissue Engineering. *Biomaterials* **2009**, *30* (13), 2499–2506.

- (190) Weng, L.; Romanov, A.; Rooney, J.; Chen, W. Non-Cytotoxic, in Situ Gelable Hydrogels Composed of N-Carboxyethyl Chitosan and Oxidized Dextran. *Biomaterials* **2008**, *29* (29), 3905–3913.
- (191) Yang, B.; Zhang, Y.; Zhang, X.; Tao, L.; Li, S.; Wei, Y. Facilely Prepared Inexpensive and Biocompatible Self-Healing Hydrogel: A New Injectable Cell Therapy Carrier. *Polym. Chem.* **2012**, *3* (12), 3235.
- (192) McKinnon, D. D.; Domaille, D. W.; Cha, J. N.; Anseth, K. S. Bis-Aliphatic Hydrazone-Linked Hydrogels Form Most Rapidly at Physiological pH: Identifying the Origin of Hydrogel Properties with Small Molecule Kinetic Studies. *Chem. Mater.* **2014**, *26* (7), 2382–2387.
- (193) Jia, X.; Colombo, G.; Padera, R.; Langer, R.; Kohane, D. S. Prolongation of Sciatic Nerve Blockade by in Situ Cross-Linked Hyaluronic Acid. *Biomaterials* **2004**, *25* (19), 4797–4804.
- (194) Luo, Y.; Kobler, J. B.; Heaton, J. T.; Jia, X.; Zeitels, S. M.; Langer, R. Injectable Hyaluronic Acid-Dextran Hydrogels and Effects of Implantation in Ferret Vocal Fold. *J. Biomed. Mater. Res. B Appl. Biomater.* **2010**, *93B* (2), 386–393.
- (195) Hudson, S.; Langer, R.; Fink, G. R.; Kohane, D. S. INJECTABLE IN SITU CROSS-LINKING HYDROGELS FOR LOCAL ANTIFUNGAL THERAPY. *Biomaterials* **2010**, *31* (6), 1444.
- (196) Zhang, R.; Huang, Z.; Xue, M.; Yang, J.; Tan, T. Detailed Characterization of an Injectable Hyaluronic Acid-Polyaspartylhydrazide Hydrogel for Protein Delivery. *Carbohydr. Polym.* **2011**, *85* (4), 717–725.
- (197) Patenaude, M.; Hoare, T. Injectable, Degradable Thermoresponsive Poly(*N* - Isopropylacrylamide) Hydrogels. *ACS Macro Lett.* **2012**, *1* (3), 409–413.
- (198) Patenaude, M.; Hoare, T. Injectable, Mixed Natural-Synthetic Polymer Hydrogels with Modular Properties. *Biomacromolecules* **2012**, *13* (2), 369–378.
- (199) Lu, C.; Wang, X.; Wu, G.; Wang, J.; Wang, Y.; Gao, H.; Ma, J. An Injectable and Biodegradable Hydrogel Based on Poly(α,β -Aspartic Acid) Derivatives for Localized Drug Delivery. *J. Biomed. Mater. Res. A* **2014**, *102* (3), 628–638.
- (200) Smeets, N. M. B.; Bakaic, E.; Patenaude, M.; Hoare, T. Injectable and Tunable Poly(ethylene Glycol) Analogue Hydrogels Based on Poly(oligoethylene Glycol Methacrylate). *Chem. Commun.* **2014**, *50* (25), 3306.
- (201) McKinnon, D. D.; Domaille, D. W.; Cha, J. N.; Anseth, K. S. Biophysically Defined and Cytocompatible Covalently Adaptable Networks as Viscoelastic 3D Cell Culture Systems. *Adv. Mater. Deerfield Beach Fla* **2014**, *26* (6), 865–872.
- (202) Ossipov, D. A.; Brännvall, K.; Forsberg-Nilsson, K.; Hilborn, J. Formation of the First Injectable Poly(vinyl Alcohol) Hydrogel by Mixing of Functional PVA Precursors. *J. Appl. Polym. Sci.* **2007**, *106* (1), 60–70.
- (203) Roberts, J. J.; Naudiyal, P.; Jugé, L.; Bilston, L. E.; Granville, A. M.; Martens, P. J. Tailoring Stimuli Responsiveness Using Dynamic Covalent Cross-Linking of Poly(vinyl Alcohol)-Heparin Hydrogels for Controlled Cell and Growth Factor Delivery. *ACS Biomater. Sci. Eng.* **2015**, *1* (12), 1267–1277.
- (204) Gurski, L. A.; Xu, X.; Labrada, L. N.; Nguyen, N. T.; Xiao, L.; van Golen, K. L.; Jia, X.; Farach-Carson, M. C. Hyaluronan (HA) Interacting Proteins RHAMM and Hyaluronidase Impact Prostate Cancer Cell Behavior and Invadopodia Formation in 3D HA-Based Hydrogels. *PLoS ONE* **2012**, *7* (11).

- (205) Jia, X.; Yeo, Y.; Clifton, R. J.; Jiao, T.; Kohane, D. S.; Kobler, J. B.; Zeitels, S. M.; Langer, R. Hyaluronic Acid-Based Microgels and Microgel Networks for Vocal Fold Regeneration. *Biomacromolecules* **2006**, *7* (12), 3336–3344.
- (206) Farran, A. J. E.; Teller, S. S.; Jha, A. K.; Jiao, T.; Hule, R. A.; Clifton, R. J.; Pochan, D. P.; Duncan, R. L.; Jia, X. Effects of Matrix Composition, Microstructure, and Viscoelasticity on the Behaviors of Vocal Fold Fibroblasts Cultured in Three-Dimensional Hydrogel Networks. *Tissue Eng. Part A* **2010**, *16* (4), 1247–1261.
- (207) Oommen, O. P.; Wang, S.; Kisiel, M.; Sloff, M.; Hilborn, J.; Varghese, O. P. Smart Design of Stable Extracellular Matrix Mimetic Hydrogel: Synthesis, Characterization, and In Vitro and In Vivo Evaluation for Tissue Engineering. *Adv. Funct. Mater.* **2013**, *23* (10), 1273–1280.
- (208) Yan, S.; Wang, T.; Feng, L.; Zhu, J.; Zhang, K.; Chen, X.; Cui, L.; Yin, J. Injectable in Situ Self-Cross-Linking Hydrogels Based on poly(L-Glutamic Acid) and Alginate for Cartilage Tissue Engineering. *Biomacromolecules* **2014**, *15* (12), 4495–4508.
- (209) Boehnke, N.; Cam, C.; Bat, E.; Segura, T.; Maynard, H. D. Imine Hydrogels with Tunable Degradability. *Biomacromolecules* **2015**, *16* (7), 2101–2108.
- (210) Dahlmann, J.; Krause, A.; Möller, L.; Kensah, G.; Möwes, M.; Diekmann, A.; Martin, U.; Kirschning, A.; Gruh, I.; Dräger, G. Fully Defined in Situ Cross-Linkable Alginate and Hyaluronic Acid Hydrogels for Myocardial Tissue Engineering. *Biomaterials* **2013**, *34* (4), 940–951.
- (211) Kalia, J.; Raines, R. T. Hydrolytic Stability of Hydrazones and Oximes. *Angew. Chem. Int. Ed Engl.* **2008**, *47* (39), 7523–7526.
- (212) Grover, G. N.; Lam, J.; Nguyen, T. H.; Segura, T.; Maynard, H. D. Biocompatible Hydrogels by Oxime Click Chemistry. *Biomacromolecules* **2012**, *13* (10), 3013–3017.
- (213) Grover, G. N.; Braden, R. L.; Christman, K. L. Oxime Cross-Linked Injectable Hydrogels for Catheter Delivery. *Adv. Mater. Deerfield Beach Fla* **2013**, *25* (21), 2937–2942.
- (214) Sun, H. W.; Feigal, R. J.; Messer, H. H. Cytotoxicity of Glutaraldehyde and Formaldehyde in Relation to Time of Exposure and Concentration. *Pediatr Dent* **1990**, *12* (5), 303–7.
- (215) Gough, J. E.; Scotchford, C. A.; Downes, S. Cytotoxicity of Glutaraldehyde Crosslinked Collagen/Poly(vinyl Alcohol) Films Is by the Mechanism of Apoptosis. *J. Biomed. Mater. Res.* **2002**, *61* (1), 121–130.
- (216) Wang, H.; Heilshorn, S. C. Adaptable Hydrogel Networks with Reversible Linkages for Tissue Engineering. *Adv. Mater.* **2015**, *27* (25), 3717–3736.
- (217) Sevier, C. S.; Kaiser, C. A. Formation and Transfer of Disulphide Bonds in Living Cells. *Nat. Rev. Mol. Cell Biol.* **2002**, *3* (11), 836–847.
- (218) Tu, B. P.; Weissman, J. S. Oxidative Protein Folding in Eukaryotes Mechanisms and Consequences. *J. Cell Biol.* **2004**, *164* (3), 341–346.
- (219) Vercruyse, K. P.; Marecak, D. M.; Marecek, J. F.; Prestwich, G. D. Synthesis and *in Vitro* Degradation of New Polyvalent Hydrazide Cross-Linked Hydrogels of Hyaluronic Acid. *Bioconjug. Chem.* **1997**, *8* (5), 686–694.
- (220) Shu, X. Z.; Liu, Y.; Luo, Y.; Roberts, M. C.; Prestwich, G. D. Disulfide Cross-Linked Hyaluronan Hydrogels. *Biomacromolecules* **2002**, *3* (6), 1304–1311.
- (221) Wu, Z. M.; Zhang, X. G.; Zheng, C.; Li, C. X.; Zhang, S. M.; Dong, R. N.; Yu, D. M. Disulfide-Crosslinked Chitosan Hydrogel for Cell Viability and Controlled Protein Release. *Eur. J. Pharm. Sci.* **2009**, *37* (3–4), 198–206.

- (222) Fairbanks, B. D.; Singh, S. P.; Bowman, C. N.; Anseth, K. S. Photodegradable, Photoadaptable Hydrogels via Radical-Mediated Disulfide Fragmentation Reaction. *Macromolecules* **2011**, *44* (8), 2444–2450.
- (223) Du, H.; Hamilton, P.; Reilly, M.; Ravi, N. Injectable in Situ Physically and Chemically Crosslinkable Gellan Hydrogel. *Macromol. Biosci.* **2012**, *12* (7), 952–961.
- (224) Swindle-Reilly, K. E.; Shah, M.; Hamilton, P. D.; Eskin, T. A.; Kaushal, S.; Ravi, N. Rabbit Study of an In Situ Forming Hydrogel Vitreous Substitute. *Investig. Ophthalmology Vis. Sci.* **2009**, *50* (10), 4840.
- (225) Singh, R.; Whitesides, G. M. Thiol–disulfide Interchange. In *Sulphur-Containing Functional Groups (1993)*; Patai, S., Rappoport, Z., Eds.; John Wiley & Sons, Inc., 1993; pp 633–658.
- (226) Choh, S.-Y.; Cross, D.; Wang, C. Facile Synthesis and Characterization of Disulfide-Cross-Linked Hyaluronic Acid Hydrogels for Protein Delivery and Cell Encapsulation. *Biomacromolecules* **2011**, *12* (4), 1126–1136.
- (227) Lee, J.; Silberstein, M. N.; Abdeen, A. A.; Kim, S. Y.; Kilian, K. A. Mechanochemical Functionalization of Disulfide Linked Hydrogels. *Mater Horiz* **2016**, *3* (5), 447–451.
- (228) Gattás-Asfura, K. M.; Stabler, C. L. Chemoselective Cross-Linking and Functionalization of Alginate via Staudinger Ligation. *Biomacromolecules* **2009**, *10* (11), 3122–3129.
- (229) Hall, K. K.; Gattás-Asfura, K. M.; Stabler, C. L. Microencapsulation of Islets within Alginate/Poly(ethylene Glycol) Gels Cross-Linked via Staudinger Ligation. *Acta Biomater.* **2011**, *7* (2), 614–624.
- (230) Tamate, R.; Ueki, T.; Kitazawa, Y.; Kuzunuki, M.; Watanabe, M.; Akimoto, A. M.; Yoshida, R. Photo-Dimerization Induced Dynamic Viscoelastic Changes in ABA Triblock Copolymer-Based Hydrogels for 3D Cell Culture. *Chem. Mater.* **2016**.
- (231) Fan, Y.; Deng, C.; Cheng, R.; Meng, F.; Zhong, Z. In Situ Forming Hydrogels via Catalyst-Free and Bioorthogonal “Tetrazole–Alkene” Photo-Click Chemistry. *Biomacromolecules* **2013**, *14* (8), 2814–2821.
- (232) Jiang, Y.; Deng, C.; Meng, F.; Cheng, R.; Zhong, Z. Injectable Hydrogels Formed via Catalyst-Free “tetrazole–alkene” Photo-Click Chemistry. *J. Controlled Release* **2013**, *172* (1), e146–e147.
- (233) Koeller, K. M.; Wong, C. H. Enzymes for Chemical Synthesis. *Nature* **2001**, *409* (6817), 232–240.
- (234) Drauz, K. *Enzyme Catalysis in Organic Synthesis: A Comprehensive Handbook*; John Wiley & Sons, 2012.
- (235) Moreira Teixeira, L. S.; Feijen, J.; van Blitterswijk, C. A.; Dijkstra, P. J.; Karperien, M. Enzyme-Catalyzed Crosslinkable Hydrogels: Emerging Strategies for Tissue Engineering. *Biomaterials* **2012**, *33* (5), 1281–1290.
- (236) Johnson, L. M.; DeForest, C. A.; Pendurti, A.; Anseth, K. S.; Bowman, C. N. Formation of Three-Dimensional Hydrogel Multilayers Using Enzyme-Mediated Redox Chain Initiation. *ACS Appl. Mater. Interfaces* **2010**, *2* (7), 1963–1972.
- (237) Hume, P. S.; Bowman, C. N.; Anseth, K. S. Functionalized PEG Hydrogels through Reactive Dip-Coating for the Formation of Immunoactive Barriers. *Biomaterials* **2011**, *32* (26), 6204–6212.
- (238) Shenoy, R.; Tibbitt, M. W.; Anseth, K. S.; Bowman, C. N. Formation of Core–Shell Particles by Interfacial Radical Polymerization Initiated by a Glucose Oxidase-Mediated Redox System. *Chem. Mater.* **2013**, *25* (5), 761–767.

- (239) Wei, Q.; Xu, W.; Liu, M.; Wu, Q.; Cheng, L.; Wang, Q. Viscosity-Controlled Printing of Supramolecular-Polymeric Hydrogels via Dual-Enzyme Catalysis. *J Mater Chem B* **2016**.
- (240) Wang, L.-S.; Chung, J. E.; Pui-Yik Chan, P.; Kurisawa, M. Injectable Biodegradable Hydrogels with Tunable Mechanical Properties for the Stimulation of Neurogenic Differentiation of Human Mesenchymal Stem Cells in 3D Culture. *Biomaterials* **2010**, *31* (6), 1148–1157.
- (241) Menzies, D. J.; Cameron, A.; Munro, T.; Wolvetang, E.; Grøndahl, L.; Cooper-White, J. J. Tailorable Cell Culture Platforms from Enzymatically Cross-Linked Multifunctional Poly(ethylene Glycol)-Based Hydrogels. *Biomacromolecules* **2013**, *14* (2), 413–423.
- (242) Jin, R.; Hiemstra, C.; Zhong, Z.; Feijen, J. Enzyme-Mediated Fast in Situ Formation of Hydrogels from Dextran–tyramine Conjugates. *Biomaterials* **2007**, *28* (18), 2791–2800.
- (243) Lee, F.; Chung, J. E.; Kurisawa, M. An Injectable Enzymatically Crosslinked Hyaluronic Acid–tyramine Hydrogel System with Independent Tuning of Mechanical Strength and Gelation Rate. *Soft Matter* **2008**, *4* (4), 880–887.
- (244) Liao, S. W.; Yu, T.-B.; Guan, Z. De Novo Design of Saccharide–Peptide Hydrogels as Synthetic Scaffolds for Tailored Cell Responses. *J. Am. Chem. Soc.* **2009**, *131* (48), 17638–17646.
- (245) Chen, F.; Yu, S.; Liu, B.; Ni, Y.; Yu, C.; Su, Y.; Zhu, X.; Yu, X.; Zhou, Y.; Yan, D. An Injectable Enzymatically Crosslinked Carboxymethylated Pullulan/Chondroitin Sulfate Hydrogel for Cartilage Tissue Engineering. *Sci. Rep.* **2016**, *6*.
- (246) Lee, B. P.; Dalsin, J. L.; Messersmith, P. B. Synthesis and Gelation of DOPA-Modified Poly(ethylene Glycol) Hydrogels. *Biomacromolecules* **2002**, *3* (5), 1038–1047.
- (247) Chen, T.; Embree, H. D.; Brown, E. M.; Taylor, M. M.; Payne, G. F. Enzyme-Catalyzed Gel Formation of Gelatin and Chitosan: Potential for in Situ Applications. *Biomaterials* **2003**, *24* (17), 2831–2841.
- (248) Lee, S. H.; Lee, Y.; Lee, S.-W.; Ji, H.-Y.; Lee, J.-H.; Lee, D. S.; Park, T. G. Enzyme-Mediated Cross-Linking of Pluronic Copolymer Micelles for Injectable and in Situ Forming Hydrogels. *Acta Biomater.* **2011**, *7* (4), 1468–1476.
- (249) Das, S.; Pati, F.; Choi, Y.-J.; Rijal, G.; Shim, J.-H.; Kim, S. W.; Ray, A. R.; Cho, D.-W.; Ghosh, S. Bioprintable, Cell-Laden Silk Fibroin–gelatin Hydrogel Supporting Multilineage Differentiation of Stem Cells for Fabrication of Three-Dimensional Tissue Constructs. *Acta Biomater.* **2015**, *11*, 233–246.
- (250) Brubaker, C. E.; Kissler, H.; Wang, L.; Kaufman, D. B.; Messersmith, P. B. Biological Performance of Mussel-Inspired Adhesive in Extrahepatic Islet Transplantation. *Biomaterials* **2010**, *31* (3), 420–427.
- (251) Hong, S.; Yang, K.; Kang, B.; Lee, C.; Song, I. T.; Byun, E.; Park, K. I.; Cho, S.-W.; Lee, H. Hyaluronic Acid Catechol: A Biopolymer Exhibiting a pH-Dependent Adhesive or Cohesive Property for Human Neural Stem Cell Engineering. *Adv. Funct. Mater.* **2013**, *23* (14), 1774–1780.
- (252) Cencer, M.; Liu, Y.; Winter, A.; Murley, M.; Meng, H.; Lee, B. P. Effect of pH on the Rate of Curing and Bioadhesive Properties of Dopamine Functionalized Poly(ethylene Glycol) Hydrogels. *Biomacromolecules* **2014**, *15* (8), 2861–2869.
- (253) Hu, B.-H.; Messersmith, P. B. Rational Design of Transglutaminase Substrate Peptides for Rapid Enzymatic Formation of Hydrogels. *J. Am. Chem. Soc.* **2003**, *125* (47), 14298–14299.
- (254) Sperinde, J. J.; Griffith, L. G. Synthesis and Characterization of Enzymatically-Cross-Linked Poly (Ethylene Glycol) Hydrogels. *Macromolecules* **1997**, *30* (18), 5255–5264.

- (255) McHale, M. K.; Setton, L. A.; Chilkoti, A. Synthesis and in Vitro Evaluation of Enzymatically Cross-Linked Elastin-like Polypeptide Gels for Cartilaginous Tissue Repair. *Tissue Eng.* **2005**, *11* (11–12), 1768–1779.
- (256) Sanborn, T. J.; Messersmith, P. B.; Barron, A. E. In Situ Crosslinking of a Biomimetic Peptide-PEG Hydrogel via Thermally Triggered Activation of Factor XIII. *Biomaterials* **2002**, *23* (13), 2703–2710.
- (257) Ehrbar, M.; Rizzi, S. C.; Schoenmakers, R. G.; San Miguel, B.; Hubbell, J. A.; Weber, F. E.; Lutolf, M. P. Biomolecular Hydrogels Formed and Degraded via Site-Specific Enzymatic Reactions. *Biomacromolecules* **2007**, *8* (10), 3000–3007.
- (258) Ehrbar, M.; Rizzi, S. C.; Hlushchuk, R.; Djonov, V.; Zisch, A. H.; Hubbell, J. A.; Weber, F. E.; Lutolf, M. P. Enzymatic Formation of Modular Cell-Instructive Fibrin Analogs for Tissue Engineering. *Biomaterials* **2007**, *28* (26), 3856–3866.
- (259) Lienemann, P. S.; Karlsson, M.; Sala, A.; Wischhusen, H. M.; Weber, F. E.; Zimmermann, R.; Weber, W.; Lutolf, M. P.; Ehrbar, M. A Versatile Approach to Engineering Biomolecule-Presenting Cellular Microenvironments. *Adv. Healthc. Mater.* **2013**, *2* (2), 292–296.
- (260) Mosiewicz, K. A.; Johnsson, K.; Lutolf, M. P. Phosphopantetheinyl Transferase-Catalyzed Formation of Bioactive Hydrogels for Tissue Engineering. *J. Am. Chem. Soc.* **2010**, *132* (17), 5972–5974.
- (261) Gough, D. R.; Cotter, T. G. Hydrogen Peroxide: A Jekyll and Hyde Signalling Molecule. *Cell Death Dis.* **2011**, *2* (10), e213.
- (262) Ebelmen, M. Recherches Sur Les Combinaisons Des Acides Boriques et Siliciques Avec Les Éthers. *Ann Chim. Phys* **1846**, *16*, 129.
- (263) Ebelmen, M. Sur L’hyalite Artificielle et L’hydrophane. *C R Acad Sci* **1847**, *25*, 854.
- (264) Graham, T. On the Properties of Silicic Acid and Other Analogous Colloidal Substances. *J. Chem. Soc.* **1864**, *17*, 318–327.
- (265) Brinker, C. J.; Scherer, G. W. *Sol-Gel Science: The Physics and Chemistry of Sol-Gel Processing*; Gulf Professional Publishing, 1990.
- (266) Wright, J. D.; Sommerdijk, N. A. J. M. *Sol-Gel Materials: Chemistry and Applications*; CRC Press, 2000.
- (267) Pierre, A. C. *Introduction to Sol-Gel Processing*; Springer Science & Business Media, 2013.
- (268) Corriu, R.; Nguyễn, T. A. *Molecular Chemistry of Sol-Gel Derived Nanomaterials*; Wiley: Chichester, West Sussex, U.K, 2009.
- (269) Livage, J.; Henry, M.; Sanchez, C. Sol-Gel Chemistry of Transition Metal Oxides. *Prog. Solid State Chem.* **1988**, *18* (4), 259–341.
- (270) Livage, J.; Sanchez, C.; Henry, M.; Doeuff, S. The Chemistry of the Sol-Gel Process. *Solid State Ion.* **1989**, *32*, 633–638.
- (271) Hench, L. L.; West, J. K. The Sol-Gel Process. *Chem. Rev.* **1990**, *90* (1), 33–72.
- (272) Kołodziejczak-Radzimska, A.; Jesionowski, T. Zinc Oxide—From Synthesis to Application: A Review. *Materials* **2014**, *7* (4), 2833–2881.
- (273) Popovich, N. V. Low-Temperature Synthesis of Amorphous and Glass Ceramic Silicate Materials (Review). *Glass Ceram.* **1993**, *50* (9–10), 380–383.
- (274) Sakka, S. Sol-Gel Glasses and Their Future Applications. *Trans. Indian Ceram. Soc.* **1987**, *46* (1), 1–11.
- (275) Stöber, W.; Fink, A.; Bohn, E. Controlled Growth of Monodisperse Silica Spheres in the Micron Size Range. *J. Colloid Interface Sci.* **1968**, *26* (1), 62–69.

- (276) Owens, G. J.; Singh, R. K.; Foroutan, F.; Alqaysi, M.; Han, C.-M.; Mahapatra, C.; Kim, H.-W.; Knowles, J. C. Sol-gel Based Materials for Biomedical Applications. *Prog. Mater. Sci.* **2016**, *77*, 1–79.
- (277) De Jong, W. H.; Borm, P. J. Drug Delivery and Nanoparticles: Applications and Hazards. *Int. J. Nanomedicine* **2008**, *3* (2), 133–149.
- (278) Gupta, R.; Kumar, A. Bioactive Materials for Biomedical Applications Using Sol-gel Technology. *Biomed. Mater.* **2008**, *3* (3), 034005.
- (279) Kessler, V. G. The Chemistry behind the Sol-gel Synthesis of Complex Oxide Nanoparticles for Bio-Imaging Applications. *J. Sol-Gel Sci. Technol.* **2009**, *51* (3), 264.
- (280) Lutgens, F. K.; Tarbuck, E. J. *Essentials of Geology*; Prentice Hall, 2000.
- (281) Livage, J. Vers Une Chimie Écologique. Quand L'air et L'eau Remplacent Le Pétrole. *Le Monde* **1977**.
- (282) Carturan, G.; Camprostrini, R.; Diré, S.; Scardi, V.; De Alteriis, E. Inorganic Gels for Immobilization of Biocatalysts: Inclusion of Invertase-Active Whole Cells of Yeast (*Saccharomyces Cerevisiae*) into Thin Layers of SiO₂ Gel Deposited on Glass Sheets. *J. Mol. Catal.* **1989**, *57* (1), L13–L16.
- (283) Carturan, G.; Dal Toso, R.; Boninsegna, S.; Dal Monte, R. Encapsulation of Functional Cells by Sol-gel Silica: Actual Progress and Perspectives for Cell Therapy. *J Mater Chem* **2004**, *14* (14), 2087–2098.
- (284) Fennouh, S.; Guyon, S.; Catherine, J.; Livage, J.; Roux, C. Encapsulation of Bacteria in Silica Gels. *Comptes Rendus Académie Sci. - Ser. IIC - Chem.* **1999**, *2* (11), 625–630.
- (285) Fennouh, S.; Guyon, S.; Livage, J.; Roux, C. Sol-Gel Entrapment of *Escherichia Coli*. *J. Sol-Gel Sci. Technol.* **2000**, *19* (1–3), 647–649.
- (286) Nassif, N.; Bouvet, O.; Noelle Rager, M.; Roux, C.; Coradin, T.; Livage, J. Living Bacteria in Silica Gels. *Nat. Mater.* **2002**, *1* (1), 42–44.
- (287) Nassif, N.; Roux, C.; Coradin, T.; Rager, M.-N.; Bouvet, O. M. M.; Livage, J. A Sol-gel Matrix to Preserve the Viability of Encapsulated Bacteria. *J. Mater. Chem.* **2003**, *13* (2), 203–208.
- (288) Coradin, T.; Mercey, E.; Lisnard, L.; Livage, J. Design of Silica-Coated Microcapsules for Bioencapsulation. *Chem. Commun.* **2001**, No. 23, 2496–2497.
- (289) Sakai, S.; Ono, T.; Ijima, H.; Kawakami, K. Synthesis and Transport Characterization of Alginate/Aminopropyl-Silicate/Alginate Microcapsule: Application to Bioartificial Pancreas. *Biomaterials* **2001**, *22* (21), 2827–2834.
- (290) Sakai, S.; Ono, T.; Ijima, H.; Kawakami, K. Proliferation and Insulin Secretion Function of Mouse Insulinoma Cells Encapsulated in Alginate/Sol-Gel Synthesized Aminopropyl-Silicate/Alginate Microcapsule. *J. Sol-Gel Sci. Technol.* **2003**, *28* (2), 267–272.
- (291) Pope, E. J. A.; Braun, K.; Peterson, C. M. Bioartificial Organs I: Silica Gel Encapsulated Pancreatic Islets for the Treatment of Diabetes Mellitus. *J. Sol-Gel Sci. Technol.* **1997**, *8* (1–3), 635–639.
- (292) Pope, E. J. A. Encapsulation of Animal and Microbial Cells in an Inorganic Gel Prepared from an Organosilicon. US5739020 A, April 14, 1998.
- (293) Pope, E. J. A. Encapsulation of Living Tissue Cells in Inorganic Microspheres Prepared from an Organosilicon. US5895757 A, April 20, 1999.
- (294) Coiffier, A.; Coradin, T.; Roux, C.; Bouvet, O. M. M.; Livage, J. Sol-gel Encapsulation of Bacteria: A Comparison between Alkoxide and Aqueous Routes. *J. Mater. Chem.* **2001**, *11* (8), 2039–2044.

- (295) Fruijtjer-Pölloth, C. The Toxicological Mode of Action and the Safety of Synthetic Amorphous silica—A Nanostructured Material. *Toxicology* **2012**, *294* (2–3), 61–79.
- (296) Asefa, T.; Tao, Z. Biocompatibility of Mesoporous Silica Nanoparticles. *Chem. Res. Toxicol.* **2012**, *25* (11), 2265–2284.
- (297) Jurkić, L. M.; Capanec, I.; Pavelić, S. K.; Pavelić, K. Biological and Therapeutic Effects of Ortho-Silicic Acid and Some Ortho-Silicic Acid-Releasing Compounds: New Perspectives for Therapy. *Nutr. Metab.* **2013**, *10*, 2.
- (298) Grotheer, V.; Goergens, M.; Fuchs, P. C.; Dunda, S.; Pallua, N.; Windolf, J.; Suschek, C. V. The Performance of an Orthosilicic Acid-Releasing Silica Gel Fiber Fleece in Wound Healing. *Biomaterials* **2013**, *34* (30), 7314–7327.
- (299) He, Q.; Zhang, Z.; Gao, Y.; Shi, J.; Li, Y. Intracellular Localization and Cytotoxicity of Spherical Mesoporous Silica Nano- and Microparticles. *Small* **2009**, *5* (23), 2722–2729.
- (300) Jo, S.; Park, K. Novel Poly(Ethylene Glycol) Hydrogels from Silylated PEGs. *J. Bioact. Compat. Polym.* **1999**, *14* (6), 457–473.
- (301) Gabrielli, L.; Connell, L.; Russo, L.; Jiménez-Barbero, J.; Nicotra, F.; Cipolla, L.; Jones, J. R. Exploring GPTMS Reactivity against Simple Nucleophiles: Chemistry beyond Hybrid Materials Fabrication. *RSC Adv.* **2013**, *4* (4), 1841–1848.
- (302) Guillory, X.; Tessier, A.; Gratien, G.-O.; Weiss, P.; Collic-Jouault, S.; Dubreuil, D.; Lebreton, J.; Bideau, J. L. Glycidyl Alkoxysilane Reactivities towards Simple Nucleophiles in Organic Media for Improved Molecular Structure Definition in Hybrid Materials. *RSC Adv.* **2016**, *6* (78), 74087–74099.
- (303) Ren, L.; Tsuru, K.; Hayakawa, S.; Osaka, A. Synthesis and Characterization of Gelatin-Siloxane Hybrids Derived through Sol-Gel Procedure. *J. Sol-Gel Sci. Technol.* **2001**, *21* (1–2), 115–121.
- (304) Mahony, O.; Yue, S.; Turdean-Ionescu, C.; Hanna, J. V.; Smith, M. E.; Lee, P. D.; Jones, J. R. Silica-gelatin Hybrids for Tissue Regeneration: Inter-Relationships between the Process Variables. *J. Sol-Gel Sci. Technol.* **2013**, *69* (2), 288–298.
- (305) Connell, L. S.; Romer, F.; Suárez, M.; Valliant, E. M.; Zhang, Z.; Lee, P. D.; Smith, M. E.; Hanna, J. V.; Jones, J. R. Chemical Characterisation and Fabrication of Chitosan-silica Hybrid Scaffolds with 3-Glycidoxypropyl Trimethoxysilane. *J Mater Chem B* **2014**, *2* (6), 668–680.
- (306) Wang, D.; Romer, F.; Connell, L.; Walter, C.; Saiz, E.; Yue, S.; Lee, P. D.; McPhail, D. S.; Hanna, J. V.; Jones, J. R. Highly Flexible Silica/Chitosan Hybrid Scaffolds with Oriented Pores for Tissue Regeneration. *J Mater Chem B* **2015**, *3* (38), 7560–7576.
- (307) Chen, S.; Osaka, A.; Ikoma, T.; Morita, H.; Li, J.; Takeguchi, M.; Hanagata, N. Fabrication, Microstructure, and BMP-2 Delivery of Novel Biodegradable and Biocompatible Silicate-collagen Hybrid Fibril Sheets. *J. Mater. Chem.* **2011**, *21* (29), 10942.
- (308) Hosoya, K.; Ohtsuki, C.; Kawai, T.; Kamitakahara, M.; Ogata, S.; Miyazaki, T.; Tanihara, M. A Novel Covalently Crosslinked Gel of Alginate and Silane with the Ability to Form Bone-like Apatite. *J. Biomed. Mater. Res. A* **2004**, *71A* (4), 596–601.
- (309) Shirosaki, Y.; Tsuru, K.; Hayakawa, S.; Osaka, A.; Lopes, M. A.; Santos, J. D.; Fernandes, M. H. In Vitro Cytocompatibility of MG63 Cells on Chitosan-Organosiloxane Hybrid Membranes. *Biomaterials* **2005**, *26* (5), 485–493.
- (310) Bourges, X.; Weiss, P.; Coudreuse, A.; Daculsi, G.; Legeay, G. General Properties of Silylated Hydroxyethylcellulose for Potential Biomedical Applications. *Biopolymers* **2002**, *63* (4), 232–238.

- (311) Bourges, X.; Weiss, P.; Daculsi, G.; Legeay, G. Synthesis and General Properties of Silated-Hydroxypropyl Methylcellulose in Prospect of Biomedical Use. *Adv. Colloid Interface Sci.* **2002**, *99* (3), 215–228.
- (312) Weiss, P.; Le, B. J.; Recho, J.; Fatimi, A.; GUICHEUX, J. Method for the Silanisation of Polysaccharides. WO2010037986 A1, April 8, 2010.
- (313) Vinatier, C.; Magne, D.; Weiss, P.; Trojani, C.; Rochet, N.; Carle, G. F.; Vignes-Colombeix, C.; Chadjichristos, C.; Galera, P.; Daculsi, G.; Guicheux, J. A Silanized Hydroxypropyl Methylcellulose Hydrogel for the Three-Dimensional Culture of Chondrocytes. *Biomaterials* **2005**, *26* (33), 6643–6651.
- (314) Viguier, A.; Boyer, C.; Chassenieux, C.; Benyahia, L.; Guicheux, J.; Weiss, P.; Rethore, G.; Nicolai, T. Interpenetrated Si-HPMC/Alginate Hydrogels as a Potential Scaffold for Human Tissue Regeneration. *J. Mater. Sci. Mater. Med.* **2016**, *27* (5), 99.
- (315) Zhang, J.; Liu, W.; Gauthier, O.; Sourice, S.; Pilet, P.; Rethore, G.; Khairoun, K.; Bouler, J.-M.; Tancret, F.; Weiss, P. A Simple and Effective Approach to Prepare Injectable Macroporous Calcium Phosphate Cement for Bone Repair: Syringe-Foaming Using a Viscous Hydrophilic Polymeric Solution. *Acta Biomater.* **2016**, *31*, 326–338.
- (316) Rederstorff, E.; Rethore, G.; Weiss, P.; Sourice, S.; Beck-Cormier, S.; Mathieu, E.; Maillason, M.; Jacques, Y.; Collic-Jouault, S.; Fellah, B. H.; Guicheux, J.; Vinatier, C. Enriching a Cellulose Hydrogel with a Biologically Active Marine Exopolysaccharide for Cell-Based Cartilage Engineering. *J. Tissue Eng. Regen. Med.* **2015**.
- (317) Liu, W.; Zhang, J.; Rethore, G.; Khairoun, K.; Pilet, P.; Tancret, F.; Bouler, J.-M.; Weiss, P. A Novel Injectable, Cohesive and Toughened Si-HPMC (Silanized-Hydroxypropyl Methylcellulose) Composite Calcium Phosphate Cement for Bone Substitution. *Acta Biomater.* **2014**, *10* (7), 3335–3345.
- (318) Weiss, P.; Mathieu, E.; Guicheux, J.; Lemarchand, P. Silylated Biomolecule-Based Hydrogel for Culturing Cardiomyocytes and Stem Cells, and Use of the Hydrogel Thereof for Treating Heart Failure. US20140161775 A1, June 12, 2014.
- (319) Mathieu, E.; Lamirault, G.; Toquet, C.; Lhommet, P.; Rederstorff, E.; Sourice, S.; Biteau, K.; Hulin, P.; Forest, V.; Weiss, P.; Guicheux, J.; Lemarchand, P. Intramyocardial Delivery of Mesenchymal Stem Cell-Seeded Hydrogel Preserves Cardiac Function and Attenuates Ventricular Remodeling after Myocardial Infarction. *PLoS One* **2012**, *7* (12), e51991.
- (320) Martinez, J.; Subra, G.; Mehdi, A.; JEBORS, S.; ENJALBAL, C.; Brunel, L.; Fajula, F. Matériaux Hybrides Peptide-Silice. WO2013190148 A1, December 27, 2013.
- (321) Amblard, M.; Fehrentz, J.-A.; Martinez, J.; Subra, G. Methods and Protocols of Modern Solid Phase Peptide Synthesis. *Mol. Biotechnol.* **33** (3), 239–254.
- (322) Ciccione, J.; Jia, T.; Coll, J.-L.; Parra, K.; Amblard, M.; Jebors, S.; Martinez, J.; Mehdi, A.; Subra, G. Unambiguous and Controlled One-Pot Synthesis of Multifunctional Silica Nanoparticles. *Chem. Mater.* **2016**, *28* (3), 885–889.
- (323) Jebors, S.; Enjalbal, C.; Amblard, M.; Mehdi, A.; Subra, G.; Martinez, J. Bioorganic Hybrid OMS by Straightforward Grafting of Trialkoxysilyl Peptides. *J. Mater. Chem. B* **2013**, *1* (23), 2921–2925.
- (324) Jebors, S.; Cecillon, S.; Faye, C.; Enjalbal, C.; Amblard, M.; Mehdi, A.; Subra, G.; Martinez, J. From Protected Trialkoxysilyl-Peptide Building Blocks to Bioorganic–silica Hybrid Materials. *J. Mater. Chem. B* **2013**, *1* (47), 6510.

- (325) Jebors, S.; Ciccione, J.; Al-Halifa, S.; Nottelet, B.; Enjalbal, C.; M'Kadmi, C.; Amblard, M.; Mehdi, A.; Martinez, J.; Subra, G. A New Way to Silicone-Based Peptide Polymers. *Angew. Chem. Int. Ed.* **2015**, *54* (12), 3778–3782.
- (326) Pinese, C.; Jebors, S.; Echalié, C.; Licznar-Fajardo, P.; Garric, X.; Humblot, V.; Calers, C.; Martinez, J.; Mehdi, A.; Subra, G. Simple and Specific Grafting of Antibacterial Peptides on Silicone Catheters. *Adv. Healthc. Mater.* **2016**, In press.
- (327) Jebors, S.; Pinese, C.; Nottelet, B.; Parra, K.; Amblard, M.; Mehdi, A.; Martinez, J.; Subra, G. Turning Peptides in Comb Silicone Polymers. *J. Pept. Sci.* **2015**, *21* (3), 243–247.
- (328) Gestwicki, J. E.; Cairo, C. W.; Strong, L. E.; Oetjen, K. A.; Kiessling, L. L. Influencing Receptor-Ligand Binding Mechanisms with Multivalent Ligand Architecture. *J. Am. Chem. Soc.* **2002**, *124* (50), 14922–14933.
- (329) Hutanu, D. Recent Applications of Polyethylene Glycols (PEGs) and PEG Derivatives. *Mod. Chem. Appl.* **2014**, *02* (02).
- (330) D'souza, A. A.; Shegokar, R. Polyethylene Glycol (PEG): A Versatile Polymer for Pharmaceutical Applications. *Expert Opin. Drug Deliv.* **2016**, *13* (9), 1257–1275.
- (331) Harris, J. M.; Chess, R. B. Effect of Pegylation on Pharmaceuticals. *Nat. Rev. Drug Discov.* **2003**, *2* (3), 214–221.
- (332) Greenwald, R. B.; Choe, Y. H.; McGuire, J.; Conover, C. D. Effective Drug Delivery by PEGylated Drug Conjugates. *Adv. Drug Deliv. Rev.* **2003**, *55* (2), 217–250.
- (333) Harris, J. M. *Poly(ethylene Glycol) Chemistry: Biotechnical and Biomedical Applications*; Topics in Applied Chemistry; Springer US, 1992.
- (334) Ghosh, A. K.; Brindisi, M. Organic Carbamates in Drug Design and Medicinal Chemistry. *J. Med. Chem.* **2015**, *58* (7), 2895–2940.
- (335) Grandsire, A. F.; Laborde, C.; Lamaty, F.; Mehdi, A. Palladium Supported on Polyether-Functionalized Mesoporous Silica. Synthesis and Application as Catalyst for Heck Coupling Reaction. *Appl. Organomet. Chem.* **2010**, *24* (3), 179–183.
- (336) Jeng, J. H.; Hsieh, C. C.; Lan, W. H.; Chang, M. C.; Lin, S. K.; Hahn, L. J.; Kuo, M. Y. Cytotoxicity of Sodium Fluoride on Human Oral Mucosal Fibroblasts and Its Mechanisms. *Cell Biol. Toxicol.* **1998**, *14* (6), 383–389.
- (337) Song, J.-S.; Lee, H.-Y.; Lee, E.; Hwang, H. J.; Kim, J. H. Cytotoxicity and Apoptosis Induction of Sodium Fluoride in Human Promyelocytic Leukemia (HL-60) Cells. *Environ. Toxicol. Pharmacol.* **2002**, *11* (2), 85–91.
- (338) Agalakova, N. I.; Gusev, G. P. Molecular Mechanisms of Cytotoxicity and Apoptosis Induced by Inorganic Fluoride. *Int. Sch. Res. Not.* **2012**, *2012*, e403835.
- (339) Marsmann, P. D. H. ²⁹Si-NMR Spectroscopic Results. In *Oxygen-17 and Silicon-29; NMR Basic Principles and Progress / NMR Grundlagen und Fortschritte*; Springer Berlin Heidelberg, 1981; pp 65–235.
- (340) Echalié, C.; Kalistratova, A.; Ciccione, J.; Lebrun, A.; Legrand, B.; Naydenova, E.; Gagne, D.; Fehrentz, J.-A.; Marie, J.; Amblard, M.; Mehdi, A.; Martinez, J.; Subra, G. Selective Homodimerization of Unprotected Peptides Using Hybrid Hydroxydimethylsilane Derivatives. *RSC Adv.* **2016**, *6* (39), 32905–32914.
- (341) Li, Y.; Ma, Q.; Huang, C.; Liu, G. Crystallization of Poly (Ethylene Glycol) in Poly (Methyl Methacrylate) Networks. *Mater. Sci.* **2013**, *19* (2).
- (342) Pierschbacher, M. D.; Ruoslahti, E. Cell Attachment Activity of Fibronectin Can Be Duplicated by Small Synthetic Fragments of the Molecule. *Nature* **1984**, *309* (5963), 30–33.

- (343) Shoulders, M. D.; Raines, R. T. Collagen Structure and Stability. *Annu. Rev. Biochem.* **2009**, *78*, 929–958.
- (344) Brazel, D.; Oberbäumer, I.; Dieringer, H.; Babel, W.; Glanville, R. W.; Deutzmann, R.; Kühn, K. Completion of the Amino Acid Sequence of the $\alpha 1$ Chain of Human Basement Membrane Collagen (Type IV) Reveals 21 Non-Triplet Interruptions Located within the Collagenous Domain. *Eur. J. Biochem.* **1987**, *168* (3), 529–536.
- (345) Ramshaw, J. A.; Shah, N. K.; Brodsky, B. Gly-X-Y Tripeptide Frequencies in Collagen: A Context for Host-Guest Triple-Helical Peptides. *J. Struct. Biol.* **1998**, *122* (1–2), 86–91.
- (346) Chattopadhyay, S.; Raines, R. T. Collagen-Based Biomaterials for Wound Healing: Collagen-Based Biomaterials. *Biopolymers* **2014**, *101* (8), 821–833.
- (347) Abou Neel, E. A.; Bozec, L.; Knowles, J. C.; Syed, O.; Mudera, V.; Day, R.; Hyun, J. K. Collagen — Emerging Collagen Based Therapies Hit the Patient. *Adv. Drug Deliv. Rev.* **2013**, *65* (4), 429–456.
- (348) Dong, C.; Lv, Y. Application of Collagen Scaffold in Tissue Engineering: Recent Advances and New Perspectives. *Polymers* **2016**, *8* (2), 42.
- (349) Zhao, Y.; Xu, Y.; Zhang, B.; Wu, X.; Xu, F.; Liang, W.; Du, X.; Li, R. In Vivo Generation of Thick, Vascularized Hepatic Tissue from Collagen Hydrogel-Based Hepatic Units. *Tissue Eng. Part C Methods* **2010**, *16* (4), 653–659.
- (350) Nemoto, T.; Horiuchi, M.; Ishiguro, N.; Shinagawa, M. Detection Methods of Possible Prion Contaminants in Collagen and Gelatin. *Arch. Virol.* **1999**, *144* (1), 177–184.
- (351) Lynn, A. k.; Yannas, I. v.; Bonfield, W. Antigenicity and Immunogenicity of Collagen. *J. Biomed. Mater. Res. B Appl. Biomater.* **2004**, *71B* (2), 343–354.
- (352) Badylak, S. F.; Gilbert, T. W. Immune Response to Biologic Scaffold Materials. *Semin. Immunol.* **2008**, *20* (2), 109–116.
- (353) Olsen, D. Recombinant Collagen and Gelatin for Drug Delivery. *Adv. Drug Deliv. Rev.* **2003**, *55* (12), 1547–1567.
- (354) Fallas, J. A.; O’Leary, L. E. R.; Hartgerink, J. D. Synthetic Collagen Mimics: Self-Assembly of Homotrimers, Heterotrimers and Higher Order Structures. *Chem. Soc. Rev.* **2010**, *39* (9), 3510–3527.
- (355) O’Leary, L. E. R.; Fallas, J. A.; Bakota, E. L.; Kang, M. K.; Hartgerink, J. D. Multi-Hierarchical Self-Assembly of a Collagen Mimetic Peptide from Triple Helix to Nanofibre and Hydrogel. *Nat. Chem.* **2011**, *3* (10), 821–828.
- (356) Luo, J.; Tong, Y. W. Self-Assembly of Collagen-Mimetic Peptide Amphiphiles into Biofunctional Nanofiber. *ACS Nano* **2011**, *5* (10), 7739–7747.
- (357) Kotch, F. W.; Raines, R. T. Self-Assembly of Synthetic Collagen Triple Helices. *Proc. Natl. Acad. Sci. U. S. A.* **2006**, *103* (9), 3028–3033.
- (358) Kishimoto, T.; Morihara, Y.; Osanai, M.; Ogata, S.-I.; Kamitakahara, M.; Ohtsuki, C.; Tanihara, M. Synthesis of poly(Pro-Hyp-Gly)(n) by Direct Poly-Condensation of (Pro-Hyp-Gly)(n), Where n=1, 5, and 10, and Stability of the Triple-Helical Structure. *Biopolymers* **2005**, *79* (3), 163–172.
- (359) Paramonov, S. E.; Gauba, V.; Hartgerink, J. D. Synthesis of Collagen-like Peptide Polymers by Native Chemical Ligation. *Macromolecules* **2005**, *38* (18), 7555–7561.
- (360) Feng, Y.; Melacini, G.; Taulane, J. P.; Goodman, M. Acetyl-Terminated and Template-Assembled Collagen-Based Polypeptides Composed of Gly-Pro-Hyp Sequences. 2. Synthesis and Conformational Analysis by Circular Dichroism, Ultraviolet Absorbance, and Optical Rotation. *J. Am. Chem. Soc.* **1996**, *118* (43), 10351–10358.

- (361) Maeda, M.; Kadota, K.; Kajihara, M.; Sano, A.; Fujioka, K. Sustained Release of Human Growth Hormone (hGH) from Collagen Film and Evaluation of Effect on Wound Healing in Db/Db Mice. *J. Control. Release Off. J. Control. Release Soc.* **2001**, *77* (3), 261–272.
- (362) Tran, R. T.; Naseri, E.; Kolasnikov, A.; Bai, X.; Yang, J. A New Generation of Sodium Chloride Porogen for Tissue Engineering. *Biotechnol. Appl. Biochem.* **2011**, *58* (5), 335–344.
- (363) Giannatsis, J.; Dedoussis, V. Additive Fabrication Technologies Applied to Medicine and Health Care: A Review. *Int. J. Adv. Manuf. Technol.* **2009**, *40* (1–2), 116–127.
- (364) Parthasarathy, J. 3D Modeling, Custom Implants and Its Future Perspectives in Craniofacial Surgery. *Ann. Maxillofac. Surg.* **2014**, *4* (1), 9–18.
- (365) Liu, A.; Xue, G.; Sun, M.; Shao, H.; Ma, C.; Gao, Q.; Gou, Z.; Yan, S.; Liu, Y.; He, Y. 3D Printing Surgical Implants at the Clinic: A Experimental Study on Anterior Cruciate Ligament Reconstruction. *Sci. Rep.* **2016**, *6*, 21704.
- (366) Bajaj, P.; Schweller, R. M.; Khademhosseini, A.; West, J. L.; Bashir, R. 3D Biofabrication Strategies for Tissue Engineering and Regenerative Medicine. *Annu. Rev. Biomed. Eng.* **2014**, *16*, 247–276.
- (367) Malda, J.; Visser, J.; Melchels, F. P.; Jüngst, T.; Hennink, W. E.; Dhert, W. J. A.; Groll, J.; Hutmacher, D. W. 25th Anniversary Article: Engineering Hydrogels for Biofabrication. *Adv. Mater.* **2013**, *25* (36), 5011–5028.
- (368) Narayanan, L. K.; Huebner, P.; Fisher, M. B.; Spang, J. T.; Starly, B.; Shirwaiker, R. A. 3D-Bioprinting of Polylactic Acid (PLA) Nanofiber–Alginate Hydrogel Bioink Containing Human Adipose-Derived Stem Cells. *ACS Biomater. Sci. Eng.* **2016**.
- (369) You, F.; Wu, X.; Zhu, N.; Lei, M.; Eames, B. F.; Chen, X. 3D Printing of Porous Cell-Laden Hydrogel Constructs for Potential Applications in Cartilage Tissue Engineering. *ACS Biomater. Sci. Eng.* **2016**, *2* (7), 1200–1210.
- (370) Gaetani, R.; Doevendans, P. A.; Metz, C. H. G.; Alblas, J.; Messina, E.; Giacomello, A.; Sluijter, J. P. G. Cardiac Tissue Engineering Using Tissue Printing Technology and Human Cardiac Progenitor Cells. *Biomaterials* **2012**, *33* (6), 1782–1790.
- (371) Xiong, Z.; Yan, Y.; Zhang, R.; Wang, X. Organism Manufacturing Engineering Based on Rapid Prototyping Principles. *Rapid Prototyp. J.* **2005**, *11* (3), 160–166.
- (372) Kolesky, D. B.; Truby, R. L.; Gladman, A. S.; Busbee, T. A.; Homan, K. A.; Lewis, J. A. 3D Bioprinting of Vascularized, Heterogeneous Cell-Laden Tissue Constructs. *Adv. Mater.* **2014**, *26* (19), 3124–3130.
- (373) Kang, H.-W.; Lee, S. J.; Ko, I. K.; Kengla, C.; Yoo, J. J.; Atala, A. A 3D Bioprinting System to Produce Human-Scale Tissue Constructs with Structural Integrity. *Nat. Biotechnol.* **2016**, *advance online publication*.
- (374) Guvendiren, M.; Molde, J.; Soares, R. M. D.; Kohn, J. Designing Biomaterials for 3D Printing. *ACS Biomater. Sci. Eng.* **2016**.
- (375) Hoque, M. E.; Chuan, Y. L.; Pashby, I. Extrusion Based Rapid Prototyping Technique: An Advanced Platform for Tissue Engineering Scaffold Fabrication. *Biopolymers* **2012**, *97* (2), 83–93.
- (376) Duoss, E. B.; Twardowski, M.; Lewis, J. A. Sol-Gel Inks for Direct-Write Assembly of Functional Oxides. *Adv. Mater.* **2007**, *19* (21), 3485–3489.
- (377) Orsi, G.; De Maria, C.; Montemurro, F.; M Chauhan, V.; W Aylott, J.; Vozzi, G. Combining Inkjet Printing and Sol-Gel Chemistry for Making pH-Sensitive Surfaces. *Curr. Top. Med. Chem.* **2015**, *15* (3), 271–278.

- (378) Chiappone, A.; Fantino, E.; Roppolo, I.; Lorusso, M.; Manfredi, D.; Fino, P.; Pirri, C. F.; Calignano, F. 3D Printed PEG-Based Hybrid Nanocomposites Obtained by Sol–Gel Technique. *ACS Appl. Mater. Interfaces* **2016**, *8* (8), 5627–5633.

Experimental section

Experimental section

Supporting information for publication n°1

Homodimerization of Unprotected Peptides Using Hybrid Hydroxydimethylsilane Derivatives

Cécile Echalié, Aleksandra Kalistratova, Jérémie Ciccione, Aurélien Lebrun, Baptiste Legrand, Emilia Naydenova, Didier Gagne, Jean-Alain Fehrentz, Jacky Marie, Muriel Amblard, Ahmad Mehdi, Jean Martinez, Gilles Subra

Abbreviations.....	4
Material and Methods.....	4
1,3-bis(3-aminopropyl)tetramethyl disiloxane hydrochloride 1a	5
1,3-bis(3-aminopropyl)tetramethyl disiloxane trifluoroacetate 1b	8
(3-aminopropyl)dimethylsilanol hydrochloride 2a	10
(3-aminopropyl)dimethylsilanol trifluoroacetate 2b	14
Counter-ion effect on NMR signals.....	17
DEPT ²⁹ Si sequence optimization.....	18
Stability studies of the siloxane bond in different solutions by ¹ H-NMR.....	19
Silanol condensation upon lyophilization.....	25
N-ter hybrid monomer 4	26
N-ter hybrid dimer 5 (JMV 6187).....	27
C-ter hybrid monomer 6	29
C-ter hybrid dimer 7 (JMV 6186).....	31
Lys ³ hybrid monomer 8	33
Lys ³ hybrid dimer 9 (JMV 6185).....	35
Lys ³ (NH(CH ₂) ₃ Si(CH ₃) ₃) monomer 10 (JMV 6246).....	37
Lys ³ monomer 11 (JMV 6244).....	40
Lys ³ (Ac) monomer 12 (JMV 6245).....	43
Monomeric ligand binding assay.....	46
Bioactivity of monomeric ligands.....	47

Homodimerization of unprotected peptides using hybrid hydroxydimethylsilane derivatives

Figure S1. ¹ H NMR spectrum of 1a in DMSO-d ₆ (600 MHz)	5
Figure S2. ¹³ C NMR spectrum of 1a in DMSO-d ₆ (151 MHz).....	6
Figure S3. ²⁹ Si NMR spectrum of 1a in DMSO-d ₆ (119 MHz)	6
Figure S4. ¹ H NMR spectrum of 1a in D ₂ O (600 MHz)	7
Figure S5. ¹³ C NMR spectrum of 1a in D ₂ O (151 MHz).....	7
Figure S6. ²⁹ Si NMR spectrum of 1a in D ₂ O (119 MHz)	8
Figure S7. ¹ H NMR spectrum of 1b in DMSO-d ₆ (600 MHz)	9
Figure S8. ¹³ C NMR spectrum of 1b in DMSO-d ₆ (151 MHz).....	9
Figure S9. ²⁹ Si NMR spectrum of 1b in DMSO-d ₆ (119 MHz)	10
Figure S10. ¹ H NMR spectrum of 1a/2a in DMSO-d ₆ (600 MHz)	11
Figure S11. ¹³ C NMR spectrum of 1a/2a in DMSO-d ₆ (151 MHz)	11
Figure S12. ²⁹ Si NMR spectrum of 1a/2a in DMSO-d ₆ (119 MHz)	12
Figure S13. ¹ H NMR spectrum of 2a in D ₂ O (600 MHz)	13
Figure S14. ¹³ C NMR spectrum of 2a in D ₂ O (151 MHz).....	13
Figure S15. ²⁹ Si NMR spectrum of 2a in D ₂ O (119 MHz)	14
Figure S16. ¹ H NMR spectrum of 1b/2b in DMSO-d ₆ (600 MHz).....	14
Figure S17. ¹³ C NMR spectrum of 1b/2b in DMSO-d ₆ (151 MHz).....	15
Figure S18. ²⁹ Si NMR spectrum of 1b/2b in DMSO-d ₆ (119 MHz).....	15
Figure S19. ¹ H NMR spectrum of 1b/2b in D ₂ O (600 MHz)	16
Figure S20. ¹³ C NMR spectrum of 1b/2b in D ₂ O (151 MHz)	16
Figure S21. ²⁹ Si NMR spectrum of 1b/2b in D ₂ O (119 MHz).....	16
Figure S22. From hydrochloride to trifluoroacetate salts. Top: ¹ H NMR spectrum of 1a/2a mixture in D ₂ O. Bottom: ¹ H NMR spectrum of 1b/2b mixture in D ₂ O.....	17
Figure S23. ¹ H flip angle optimization.	18
Figure S24. ¹ H NMR spectra of 1a in DMSO-d ₆	19
Figure S25. ¹ H NMR spectra of 1a at pH 4.....	20
Figure S26. 1a hydrolysis at pH 4 based on ¹ H NMR kinetic studies	20
Figure S27. ¹ H NMR spectra of 1a at pH 7.....	21
Figure S28. 1a hydrolysis at pH 7 based on ¹ H NMR kinetic studies	21
Figure S29. ¹ H NMR spectra of 1a at pH 7.4.....	22
Figure S30. 1a hydrolysis at pH 7.4 based on ¹ H NMR kinetic studies	22
Figure S31. ¹ H NMR spectra of 1a at pH 10. Signals from the CH ₂ group in gamma position to silicon.....	23
Figure S32. 1a hydrolysis at pH 10 based on ¹ H NMR kinetic studies	24
Figure S33. ¹ H NMR spectrum of 1a in D ₂ O 0.1% TFA at t = 0.	24
Figure S34. From monomer to dimer upon lyophilization.....	25
Figure S35. LC/MS spectrum of 4	26
Figure S36. ¹ H NMR spectrum of 5 in DMSO-d ₆ (400 MHz)	27
Figure S37. ¹³ C NMR spectrum of 5 in DMSO-d ₆ (101 MHz)	28
Figure S38. HR-MS analysis of 5	29
Figure S39. LC/MS spectrum of 6	30
Figure S40. ¹ H NMR spectrum of 7 in DMSO-d ₆ (400 MHz)	31
Figure S41. ¹³ C NMR spectrum of 7 in DMSO-d ₆ (101 MHz)	32
Figure S42. HR-MS analysis of 7	33
Figure S43. LC/MS spectrum of 8	34
Figure S44. ¹ H NMR spectrum of 9 in DMSO-d ₆ (400 MHz)	35
Figure S45. ¹³ C NMR spectrum of 9 in DMSO-d ₆ (101 MHz)	36
Figure S46. HR-MS analysis of 9	37

Supporting information for publication n°1

Homodimerization of unprotected peptides using hybrid hydroxydimethylsilane derivatives

Figure S47. LC/MS spectrum of 10	38
Figure S48. HR-MS analysis of 10	39
Figure S49. LC-MS spectrum of 11	41
Figure S50. HR-MS analysis of 11	42
Figure S51. LC-MS spectrum of 12	44
Figure S52. HR-MS spectrum of 12	45
Figure S53. Binding of compounds 10 , 11 and 12	46
Figure S54. Signaling property of compounds 10 , 11 and 12	47

Abbreviations

ACN, acetonitrile; Alloc, allyloxycarbonyl; Boc, t-butyloxycarbonyl; CM, ChemMatrix; DCM, dichloromethane; DEPT, distortionless enhancement by polarization transfer; DIEA, diisopropylethylamine; DMF, N,N'-dimethylformamide; DMSO, dimethylsulfoxide; DPBS, Dulbecco's phosphate buffered saline; ESI-MS, electrospray ionization mass spectrometry; Fmoc, fluorenylmethoxycarbonyl; GHRP-6, growth hormone releasing hexapeptide; HBTU, *N,N,N',N'*-tetramethyl-*O*-(1*H*-benzotriazol-1-yl)uronium hexafluorophosphate; HFIP, hexafluoroisopropanol; HTRF, homogenous time resolved fluorescence; ICPDMCS, 3-isocyanatopropyltrimethylchlorosilane; IP1, inositol monophosphate; LC/MS, tandem liquid chromatography/ mass spectrometry; MW, microwave; NMP, N-methyl-2-pyrrolidone; NMR, nuclear magnetic resonance; pip, piperidine; PS, polystyrene; RP-HPLC, reversed phase high performance liquid chromatography; RT, room temperature; SPPS, solid phase peptide synthesis; TFA, trifluoroacetic acid; THF, tetrahydrofuran; TIS, triisopropylsilane; Trt, trityl; UV, ultra-violet. Other abbreviations used were those recommended by the IUPAC-IUB Commission (Eur. J. Biochem. 1984, 138, 9-37).

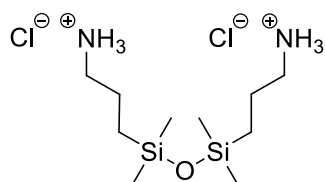
Material and Methods

All solvents and reagents were used as supplied. Solvents used for LC/MS were of HPLC grade. Dichloromethane (DCM); N,N-dimethylformamide (DMF) were obtained from Carlo Erba. Fmoc amino acid derivatives, [benzotriazol-1-yloxy(dimethylamino)methylidene]-dimethylazanium hexafluorophosphate (HBTU), Fmoc-Rink amide CM resin, 2-chloro chlorotriyl PS resin, were purchased from Iris Biotech (Marktredwitz, Germany). Diisopropylcarbodiimide (DIC), diisopropylethylamine (DIEA), trifluoroacetic acid (TFA) were obtained from Sigma-Aldrich (St. Louis, MO, USA). Hexafluoroisopropanol (HFIP) and triisopropylsilane (TIS) were obtained from Alfa Aesar and Acros respectively. NMR solvents were obtained from Euriso-top.

Samples for LC/MS analyses were prepared in acetonitrile/water (50:50, v/v) mixture, containing 0.1% TFA. The LC/MS system consisted of a Waters Alliance 2695 HPLC, coupled to a Water Micromass ZQ spectrometer (electrospray ionization mode, ESI+). All the analyses were carried out using a Phenomenex Onyx, 25 x 4.6 mm reversed-phase column. A flow rate of 3 mL/min and a gradient of (0-100)% B over 2.5 min were used. Eluent A: water/0.1% HCO₂H; eluent B: acetonitrile/0.1% HCO₂H. UV detection was performed at 214 nm. Electrospray mass spectra were acquired at a solvent flow rate of 200 µL/min. Nitrogen was used for both the nebulizing and drying gas. The data were obtained in a scan mode ranging from 100 to 1000 m/z or 250 to 1500 m/z to in 0.7 sec intervals.

High Resolution Mass Spectrometric analyses were performed with a Synapt G2-S (Waters) mass spectrometer fitted with an Electrospray Ionisation source. All measurements were performed in the positive ion mode. Capillary voltage: 1000 V; cone voltage: 30 V; source temperature: 120°C; desolvation temperature: 250°C. The data were obtained in a scan mode ranging from 100 to 1500 m/z.

1,3-bis(3-aminopropyl)tetramethyl disiloxane hydrochloride 1a



Commercially available 1,3-bis(3-aminopropyl)tetramethyl disiloxane (500 μ L, 1.8 mmol) was poured into 1 M hydrogen chloride ether solution (7.2 mL, 7.2 mmol, 4 eq) cooled in an ice bath. 1,3-bis(3-aminopropyl)tetramethyl disiloxane hydrochloride precipitated immediately. Diethyl ether was removed under reduced pressure to yield compound **1a** as a white powder (100%).

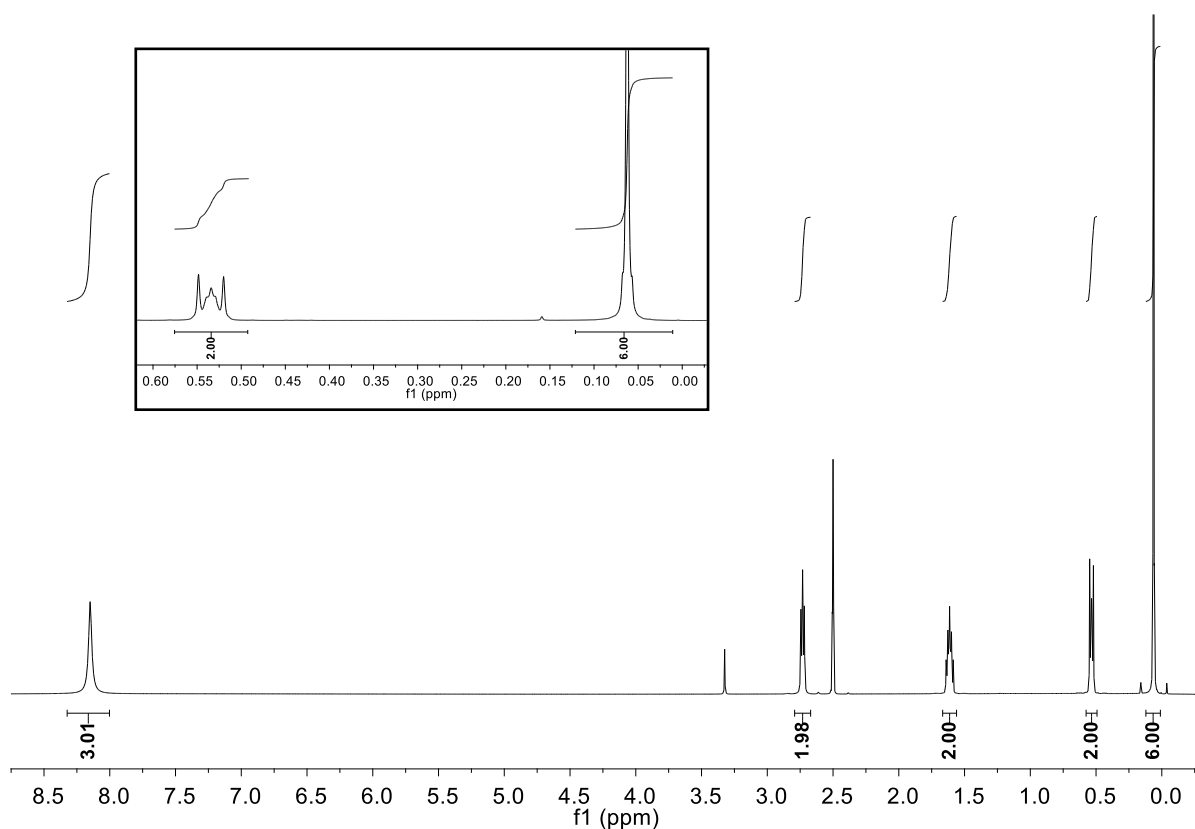


Figure S1. ^1H NMR spectrum of **1a** in $\text{DMSO-}d_6$ (600 MHz)

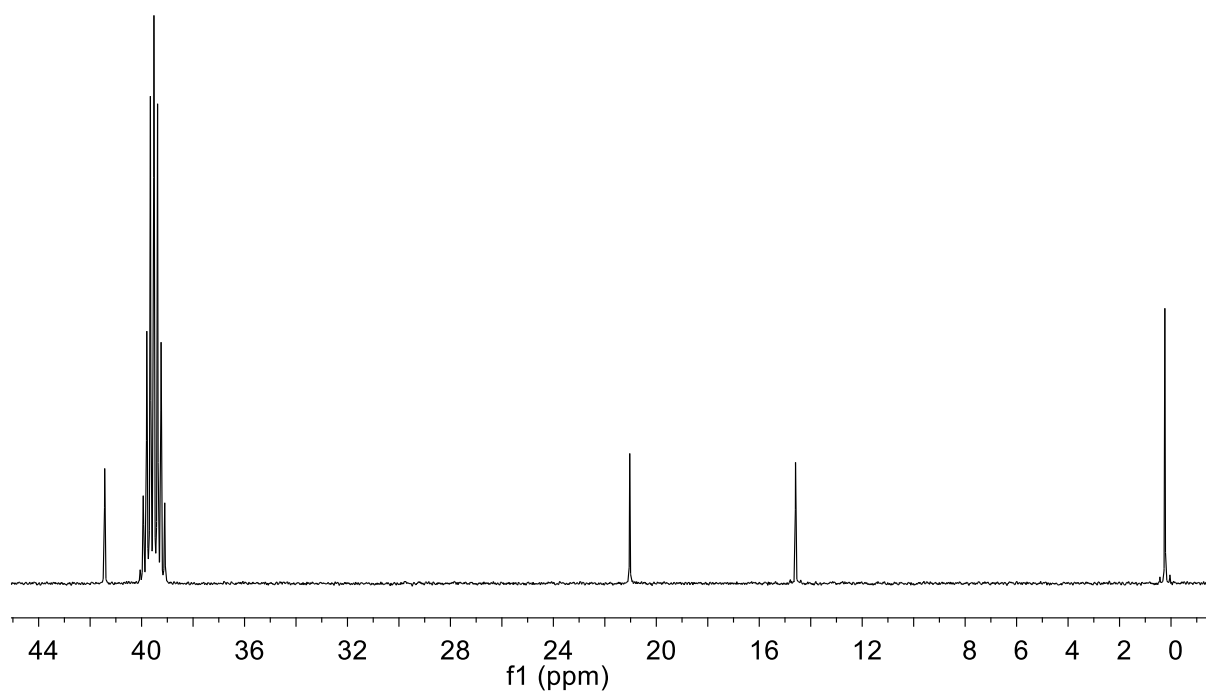


Figure S2. ^{13}C NMR spectrum of **1a** in $\text{DMSO-}d_6$ (151 MHz)

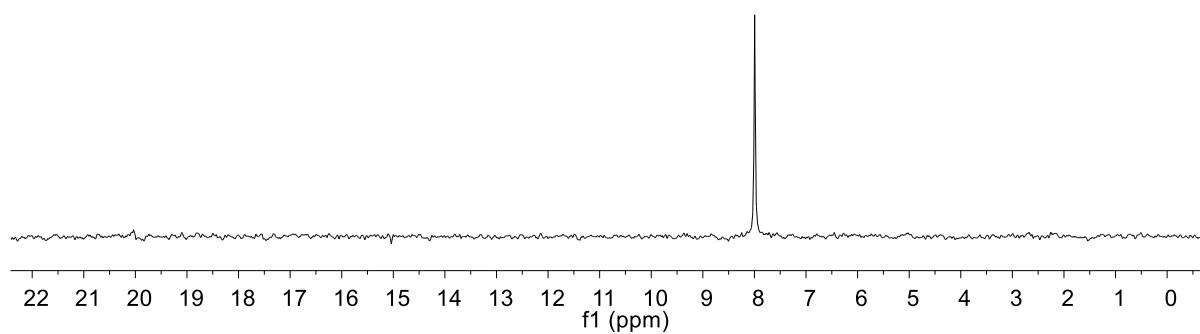


Figure S3. ^{29}Si NMR spectrum of **1a** in $\text{DMSO-}d_6$ (119 MHz)

Supporting information for publication n°1
Homodimerization of unprotected peptides using hybrid hydroxydimethylsilane derivatives

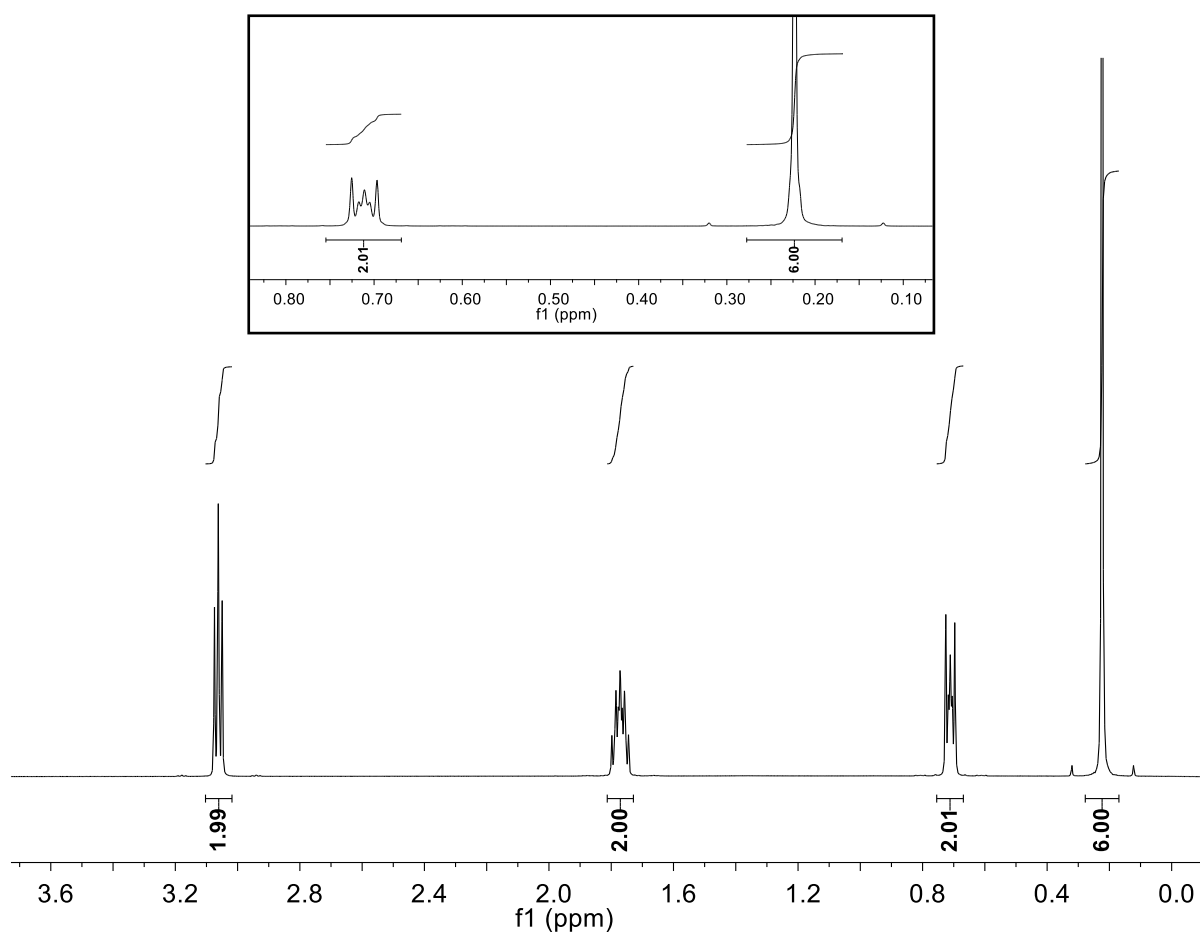


Figure S4. ¹H NMR spectrum of **1a** in D₂O (600 MHz)

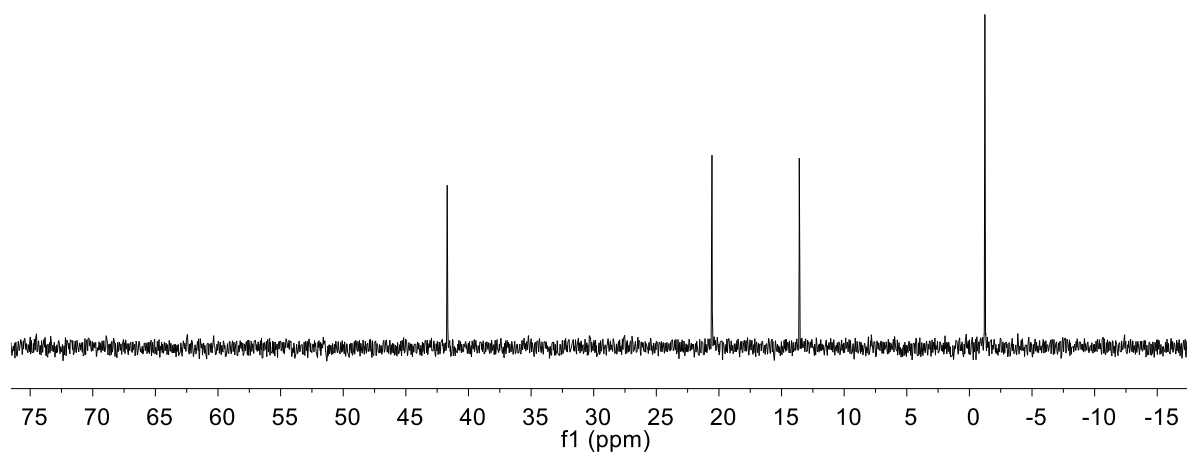


Figure S5. ¹³C NMR spectrum of **1a** in D₂O (151 MHz)

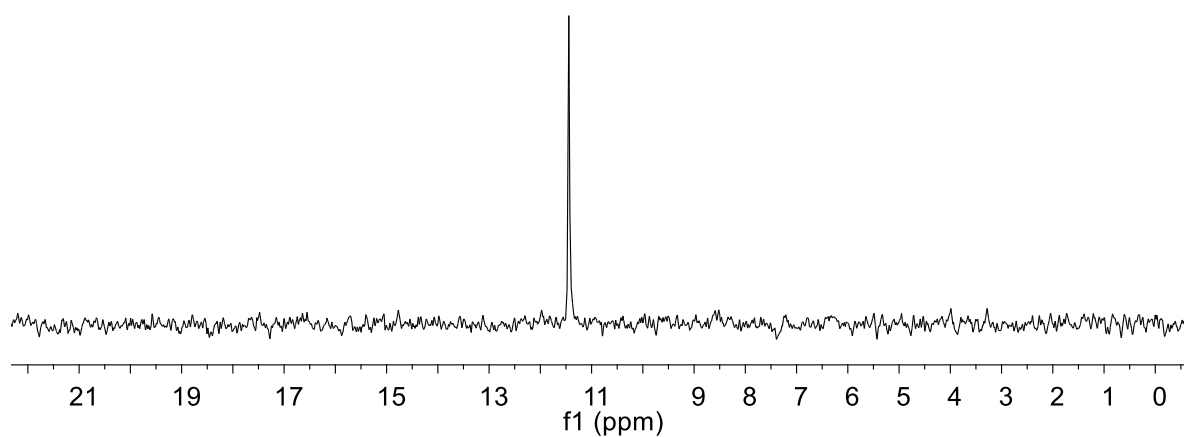
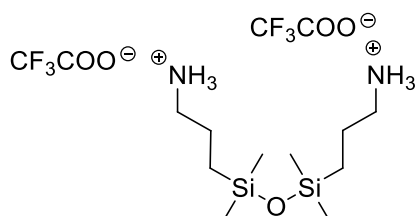


Figure S6. ^{29}Si NMR spectrum of **1a** in D_2O (119 MHz)

1,3-bis(3-aminopropyl)tetramethyl disiloxane trifluoroacetate 1b



Trifluoroacetic acid (220 μL , 2.89 mmol, 4 eq) was added on 1,3-bis(3-aminopropyl)tetramethyl disiloxane (200 μL , 0.722 mmol) in diethyl ether (2 mL) on an ice bath. Diethyl ether and TFA excess were removed under reduced pressure to yield compound **1b** as a colorless oil (100%).

Supporting information for publication n°1
Homodimerization of unprotected peptides using hybrid hydroxydimethylsilane derivatives

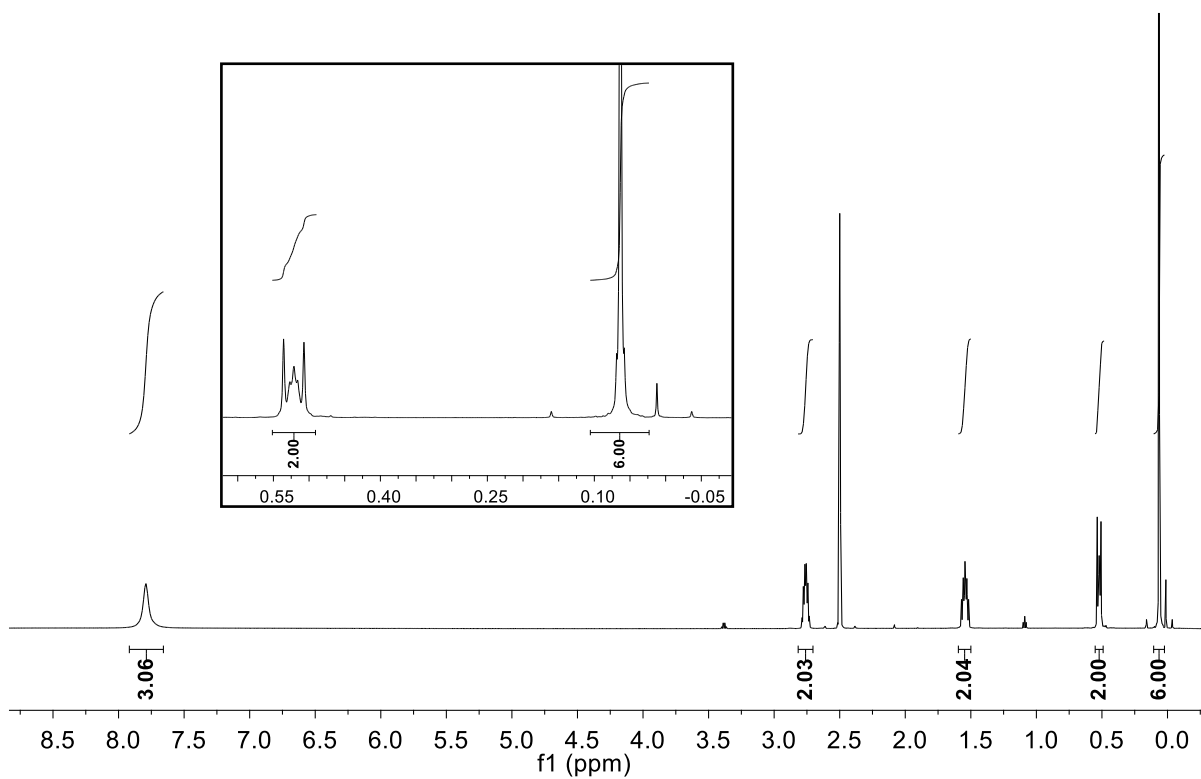


Figure S7. ^1H NMR spectrum of **1b** in DMSO-d_6 (600 MHz)

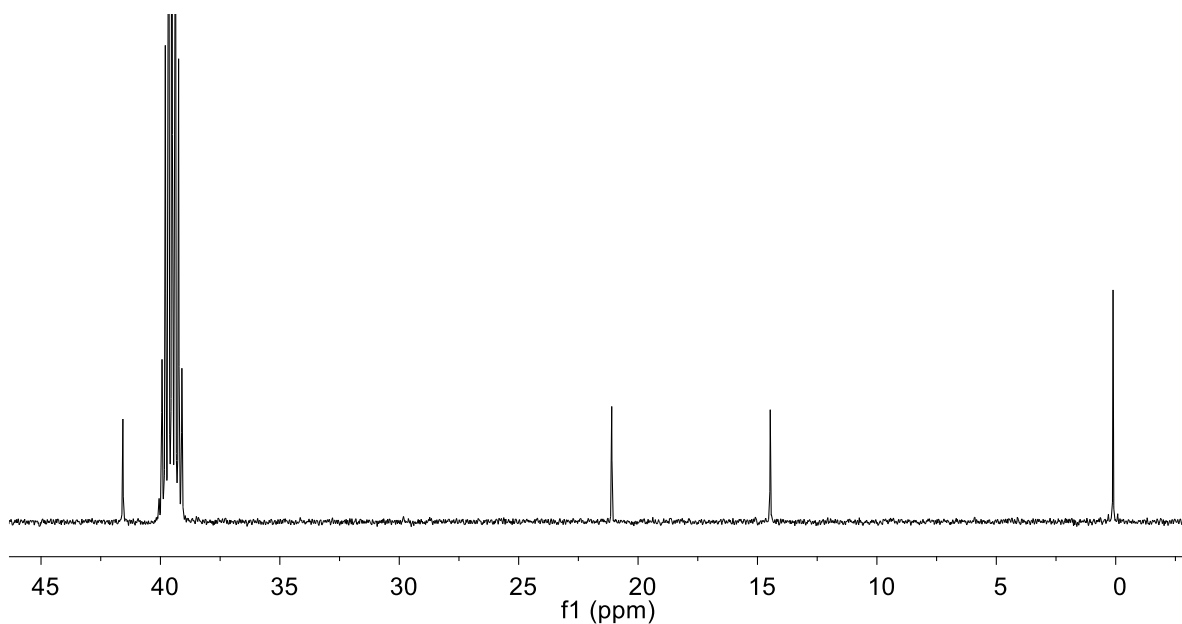


Figure S8. ^{13}C NMR spectrum of **1b** in DMSO-d_6 (151 MHz)

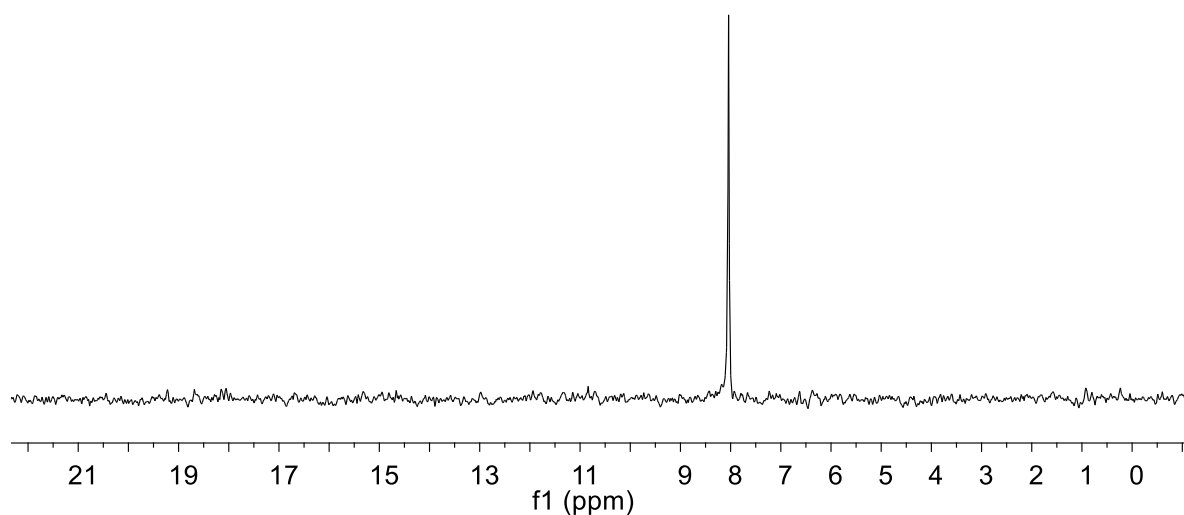
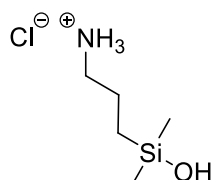


Figure S9. ^{29}Si NMR spectrum of **1b** in DMSO-d_6 (119 MHz)

(3-aminopropyl)dimethylsilanol hydrochloride 2a



On the one hand, DCI 35% in D_2O (6.00 μL) were added to **1a** (20 mg) in DMSO-d_6 (600 μL) to trigger **1a** hydrolysis into **2a**. The **1a/2a** mixture in DMSO-d_6 was analyzed by NMR.

Supporting information for publication n°1
Homodimerization of unprotected peptides using hybrid hydroxydimethylsilane derivatives

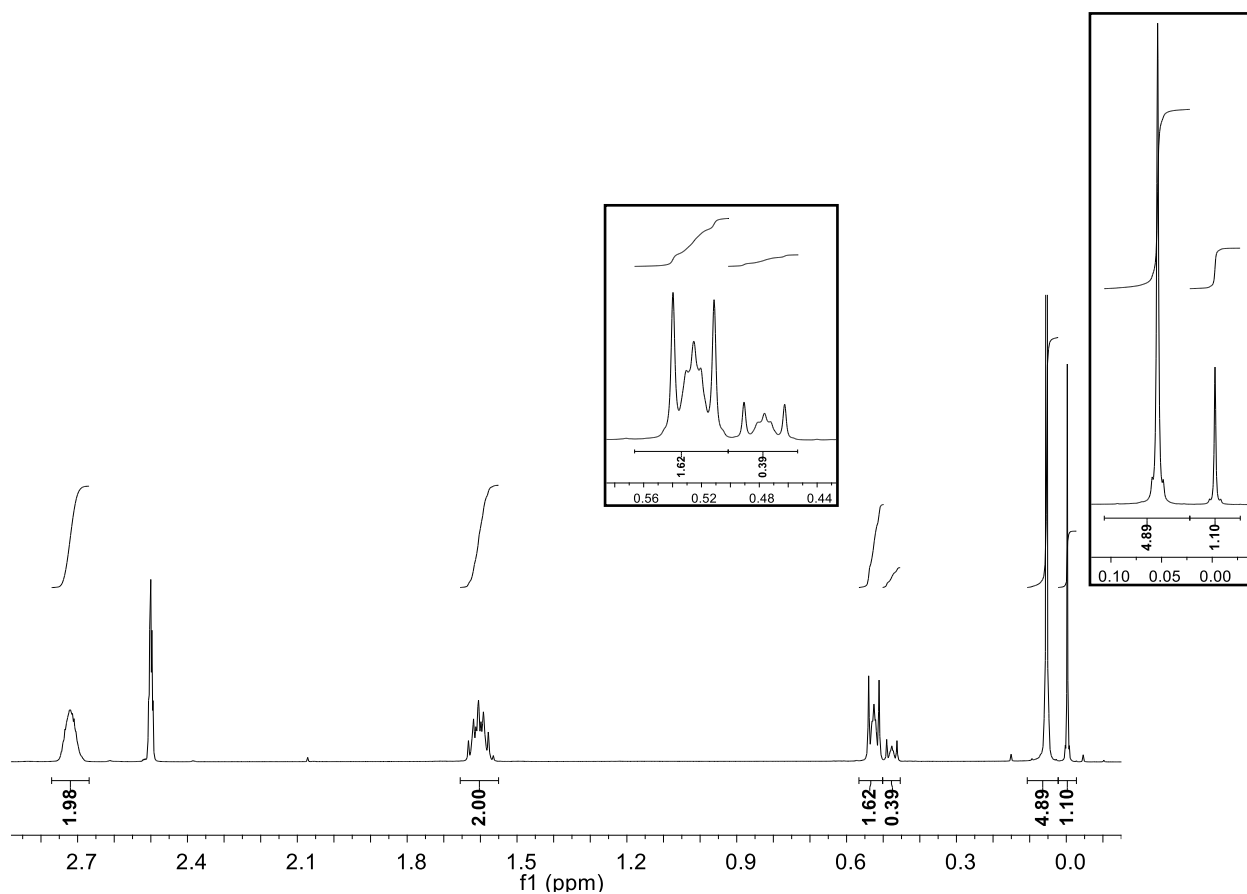


Figure S10. ^1H NMR spectrum of **1a/2a** in DMSO-d_6 (600 MHz)

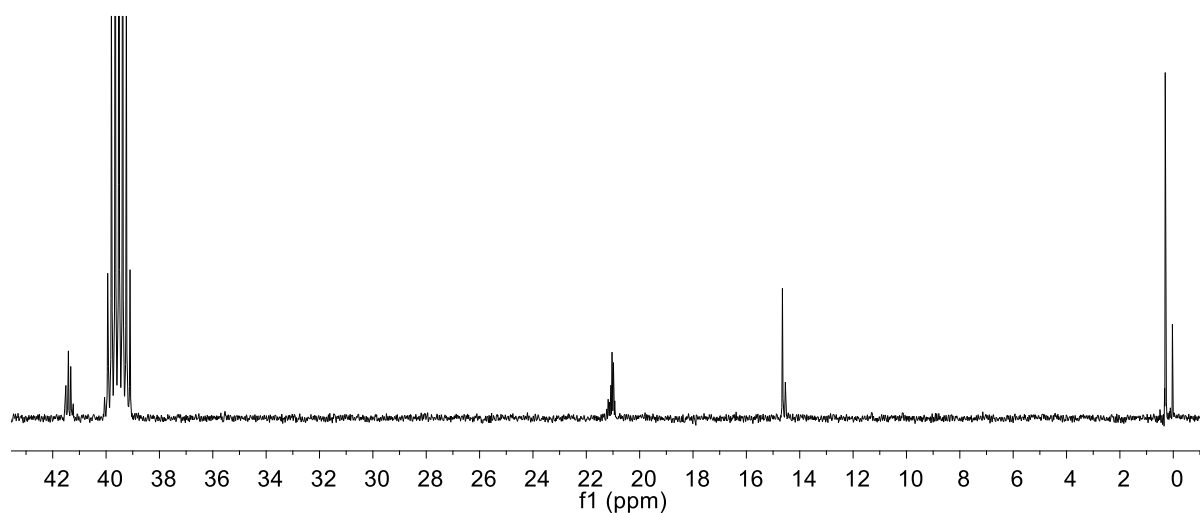


Figure S11. ^{13}C NMR spectrum of **1a/2a** in DMSO-d_6 (151 MHz)

Supporting information for publication n°1
Homodimerization of unprotected peptides using hybrid hydroxydimethylsilane derivatives

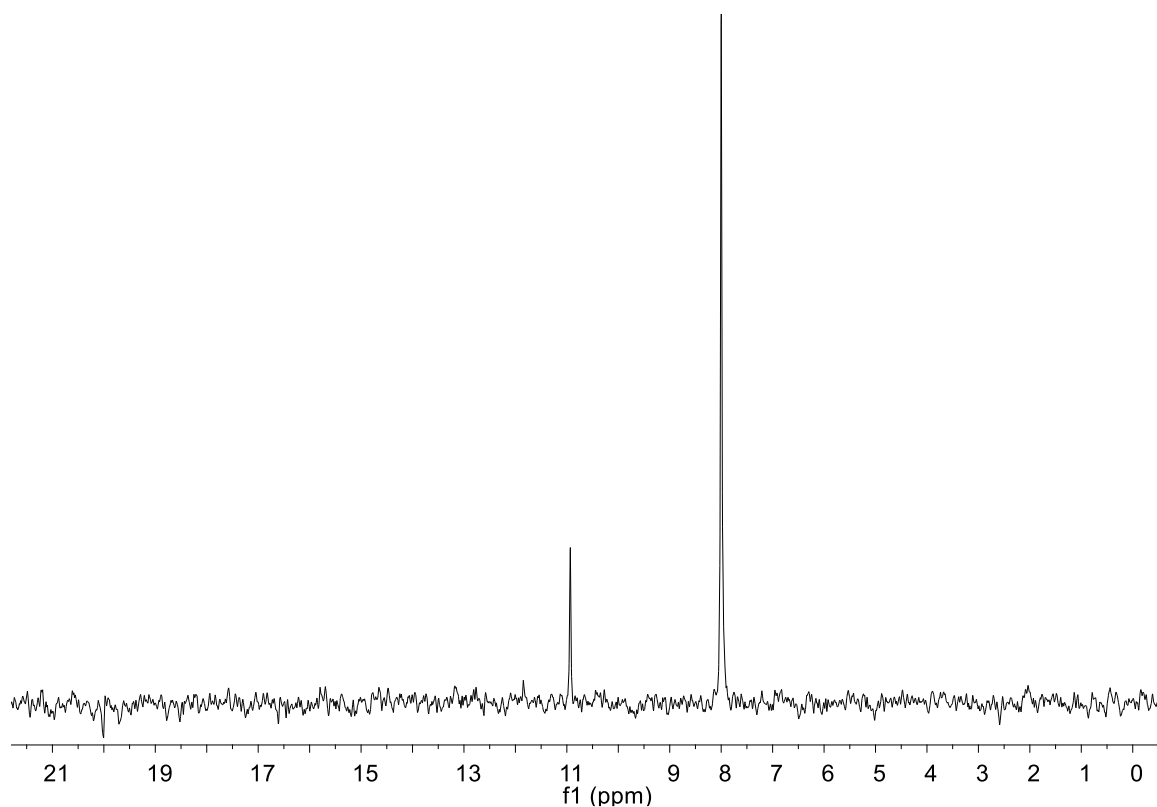


Figure S12. ^{29}Si NMR spectrum of **1a/2a** in DMSO-d_6 (119 MHz)

On the other hand, 1,3-bis(3-aminopropyl)tetramethyl disiloxane hydrochloride **1a** (20 mg) was solubilized in D_2O (600 μL) and the solution was left aside for 8 weeks to allow **1a** hydrolysis into **2a**. **2a** solution in D_2O was analyzed by NMR. Traces of **1a** are still visible on NMR spectra.

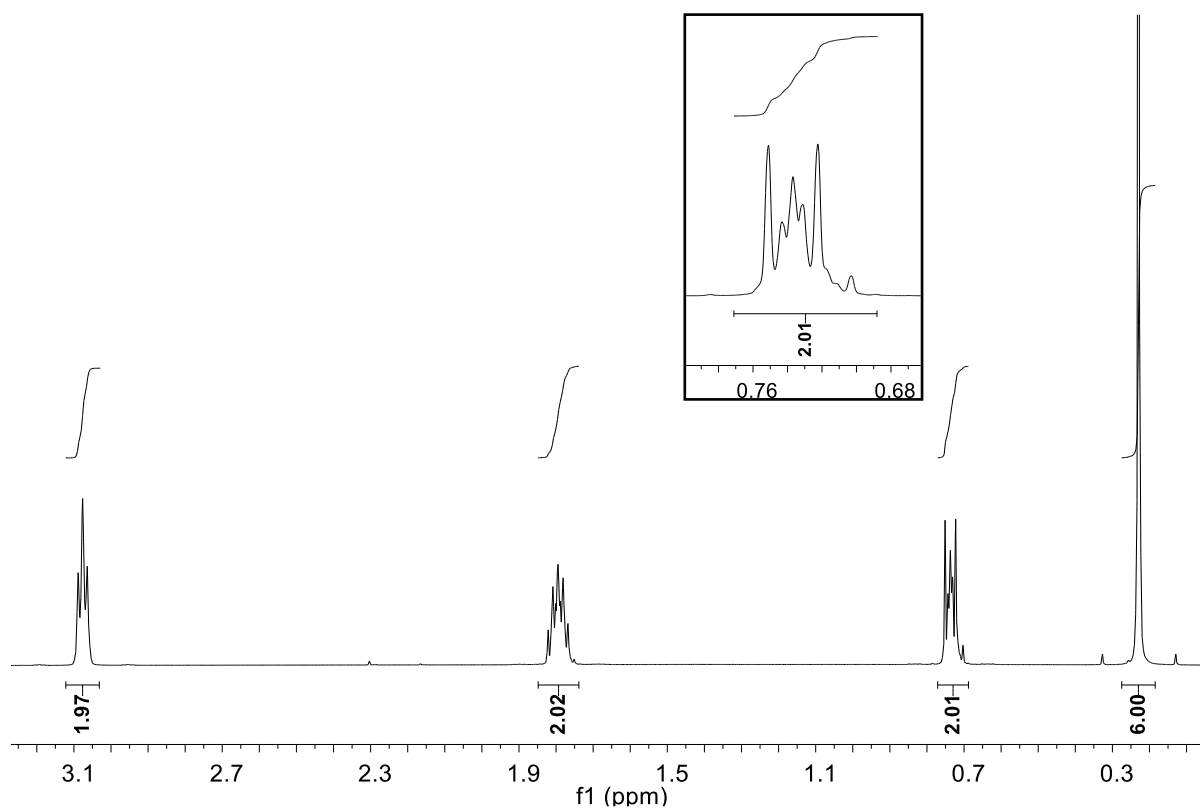


Figure S13. ¹H NMR spectrum of **2a** in D₂O (600 MHz)

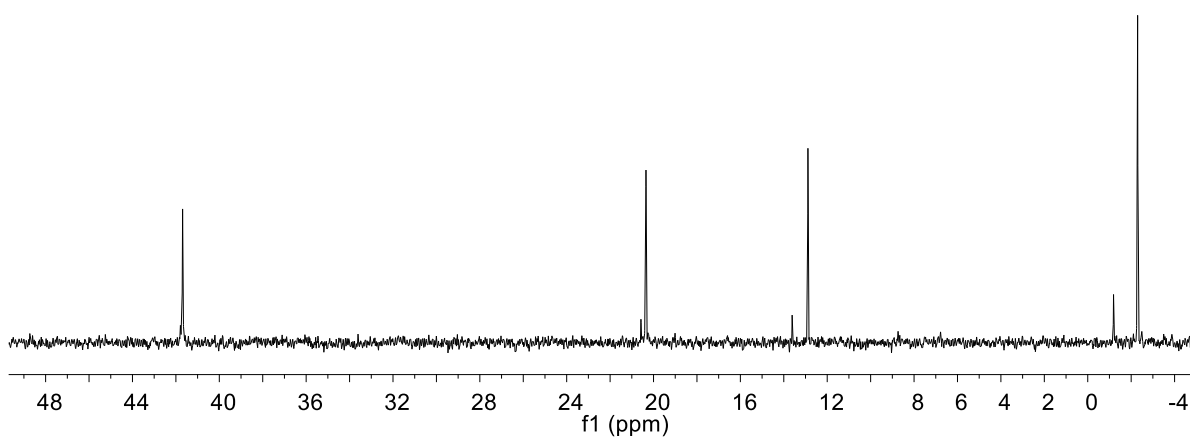


Figure S14. ¹³C NMR spectrum of **2a** in D₂O (151 MHz)

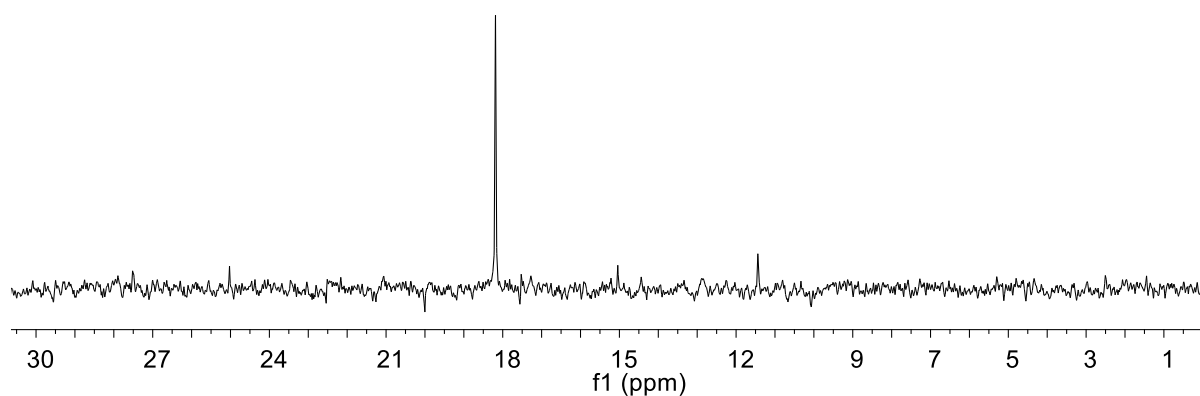
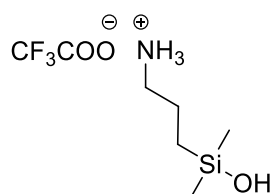


Figure S15. ^{29}Si NMR spectrum of **2a** in D_2O (119 MHz)

(3-aminopropyl)dimethylsilanol trifluoroacetate 2b



On the one hand, 3-bis(3-aminopropyl)tetramethyl disiloxane trifluoroacetate **1b** (20 mg) was dissolved in DMSO-d_6 (600 μL) and the solution was left aside for 5 weeks to allow **1b** hydrolysis into **2b**. Then the mixture **1b/2b** in DMSO-d_6 was analyzed by NMR.

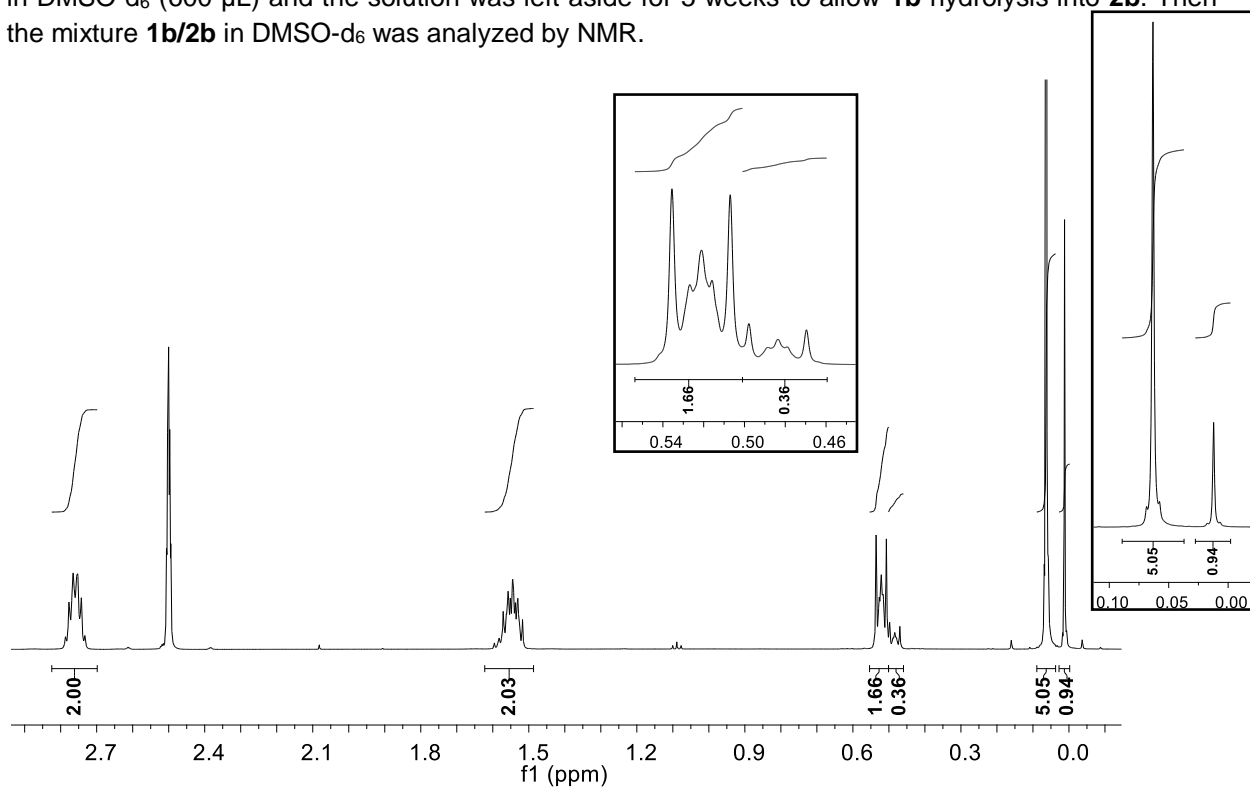


Figure S16. ^1H NMR spectrum of **1b/2b** in DMSO-d_6 (600 MHz)

Supporting information for publication n°1
Homodimerization of unprotected peptides using hybrid hydroxydimethylsilane derivatives

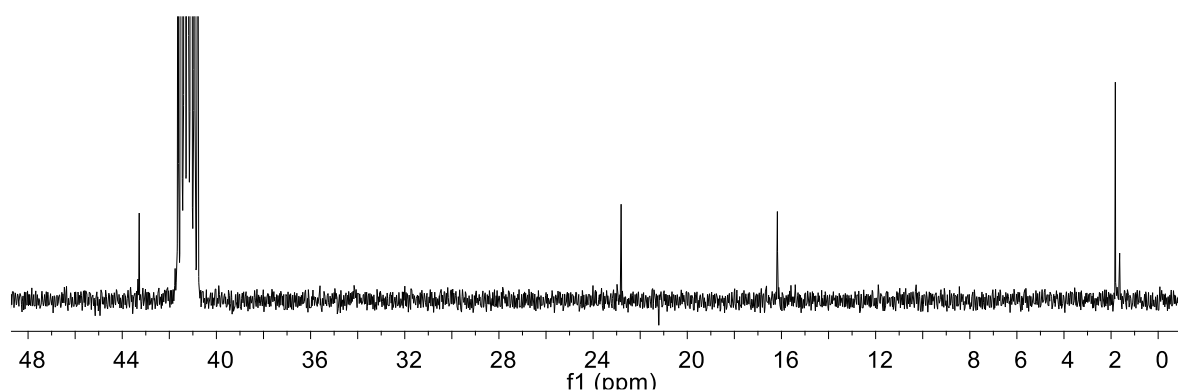


Figure S17. ^{13}C NMR spectrum of **1b/2b** in DMSO-d_6 (151 MHz)

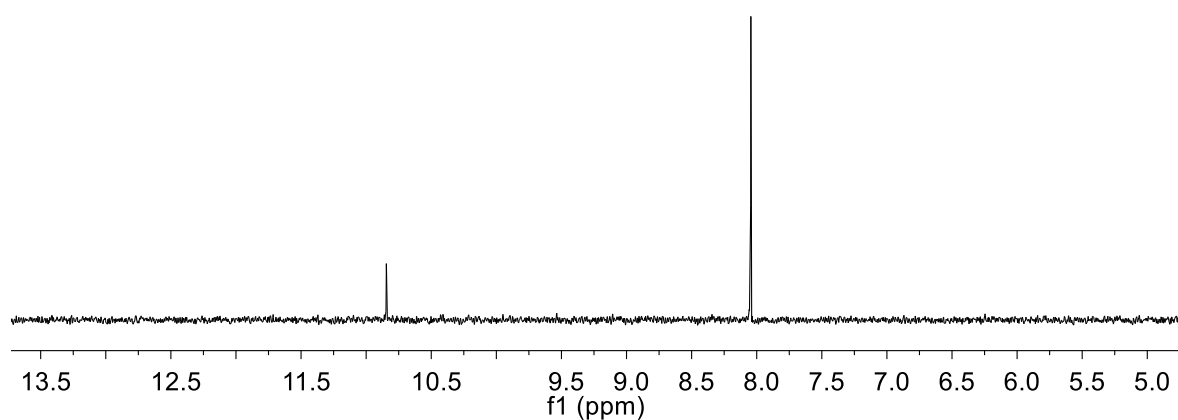


Figure S18. ^{29}Si NMR spectrum of **1b/2b** in DMSO-d_6 (119 MHz)

On the other hand, 3-bis(3-aminopropyl)tetramethyl disiloxane trifluoroacetate **1b** (20 mg) was dissolved in D_2O (600 μL). **1b** hydrolysis into **2b** occurred. The mixture **1b/2b** in D_2O was analyzed by NMR.

Supporting information for publication n°1
Homodimerization of unprotected peptides using hybrid hydroxydimethylsilane derivatives

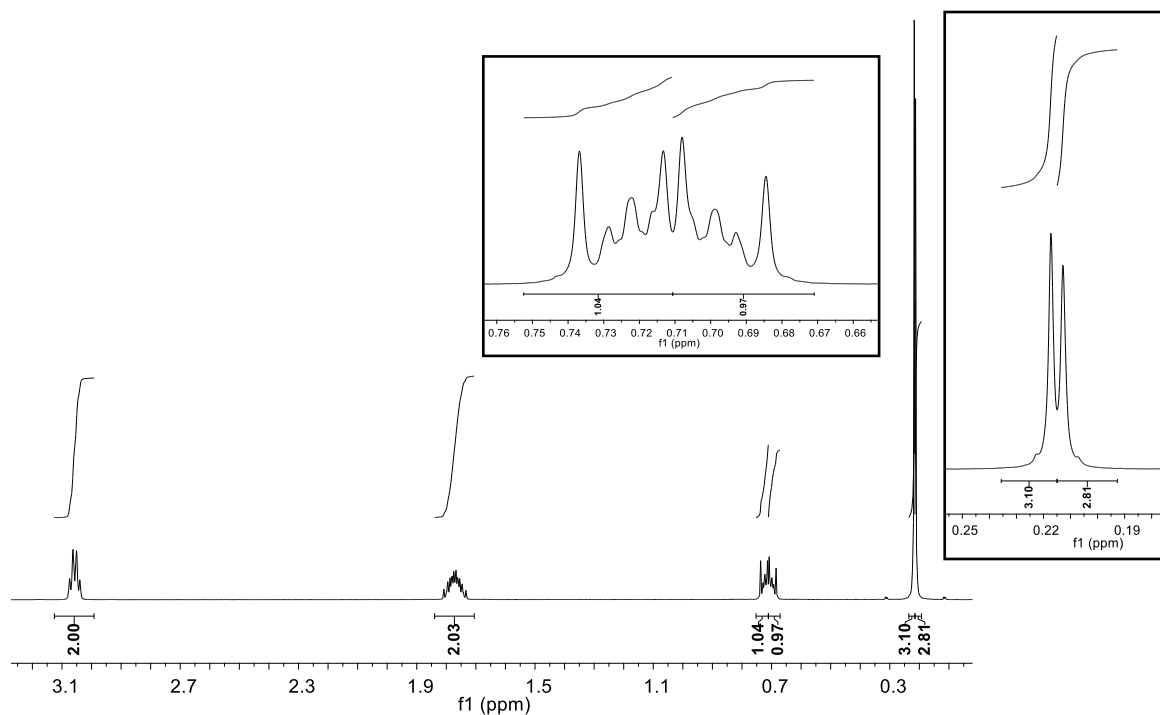


Figure S19. ¹H NMR spectrum of **1b/2b** in D₂O (600 MHz)

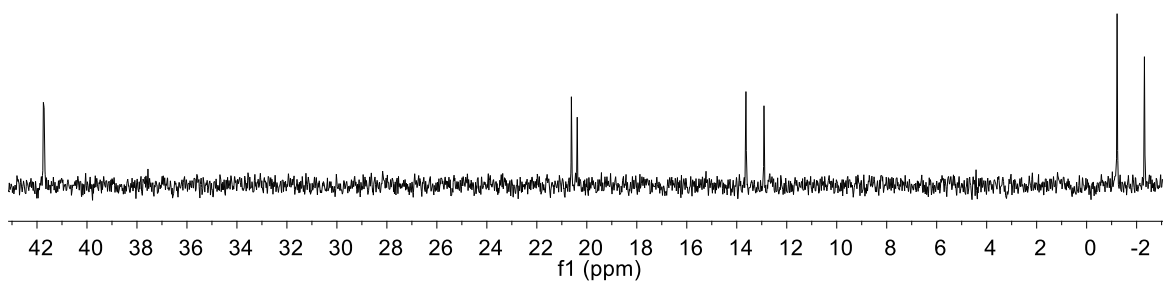


Figure S20. ¹³C NMR spectrum of **1b/2b** in D₂O (151 MHz)

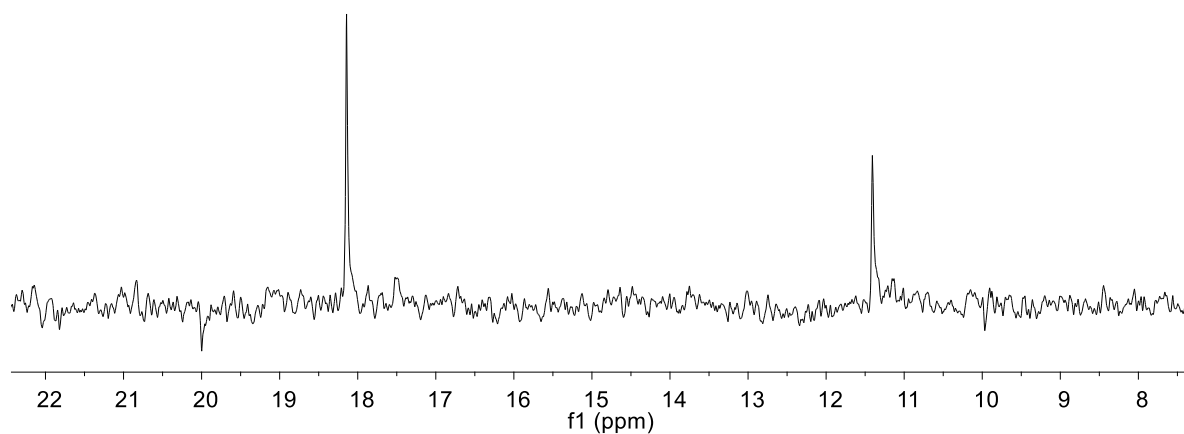


Figure S21. ²⁹Si NMR spectrum of **1b/2b** in D₂O (119 MHz)

Counter-ion effect on NMR signals

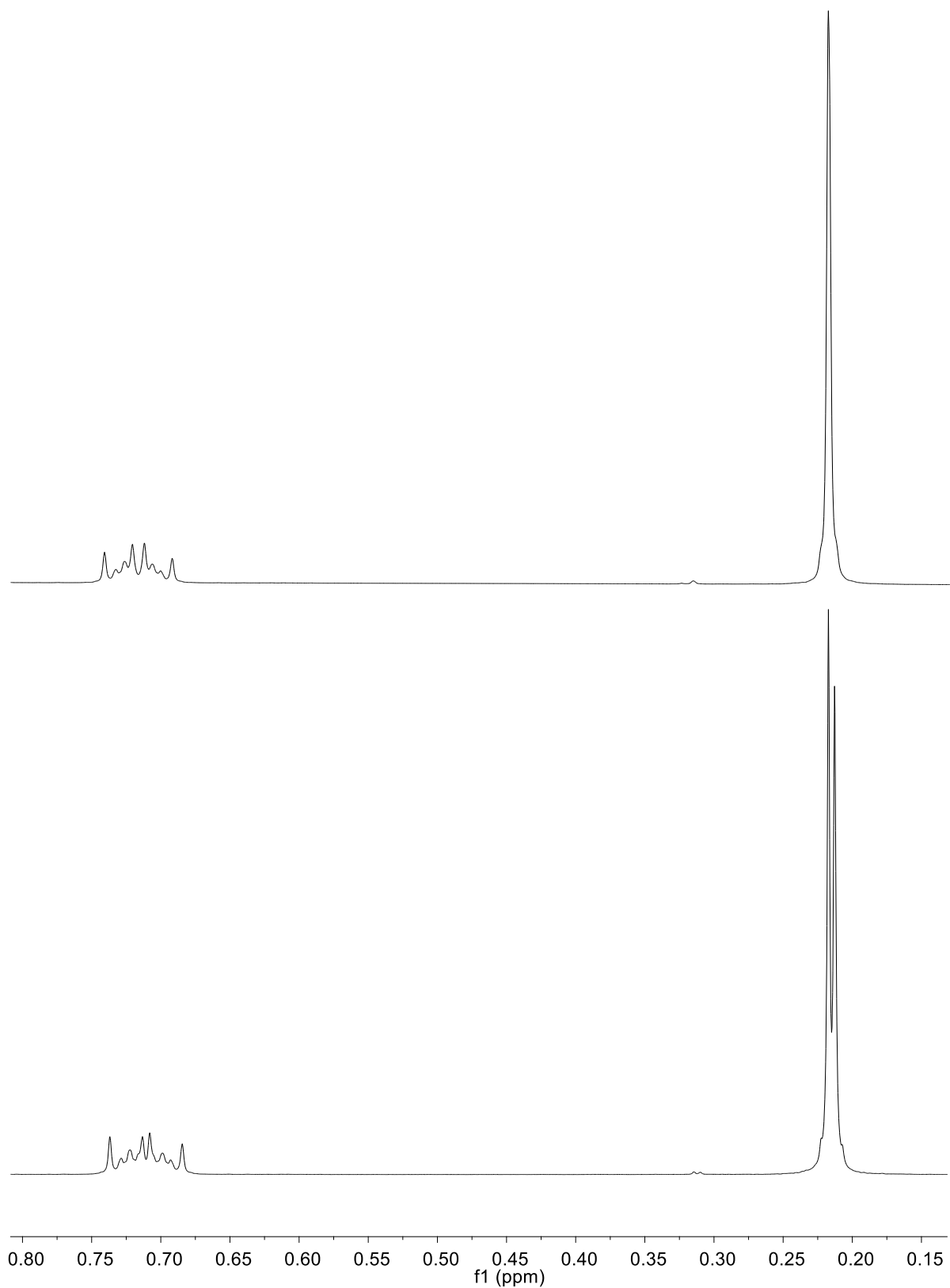


Figure S22. From hydrochloride to trifluoroacetate salts. Top: ^1H NMR spectrum of **1a/2a** mixture in D_2O . Bottom: ^1H NMR spectrum of **1b/2b** mixture in D_2O .

DEPT ^{29}Si sequence optimization

In order to decrease the experiment time, we used a DEPT ^{29}Si sequence, with a relaxation delay of 2 seconds, to take advantage of the polarization transfer from hydrogens of methylene in the alpha position to the silicon atom. An optimization was made on this sequence, where the last ^1H flip angle was moved from 17° to 45° (Figure S23). The results showed a factor of 2 gain in favor of the angle of 24° compared to the standard DEPT of 45° .

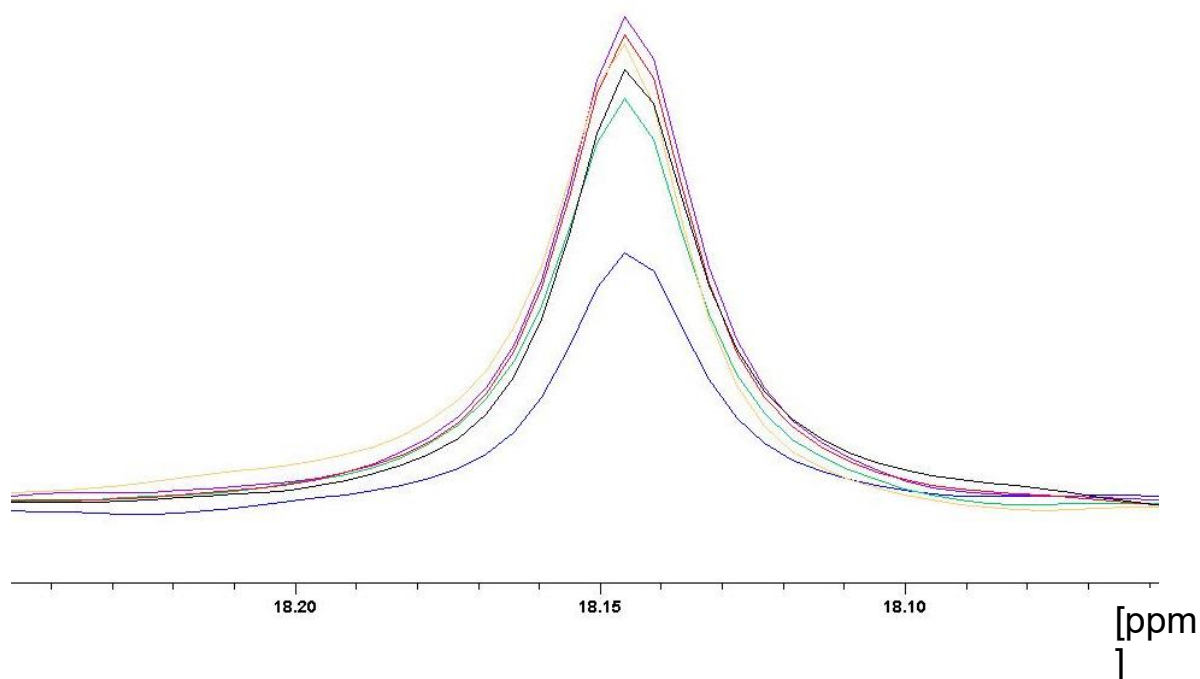


Figure S23. ^1H flip angle optimization. ^1H flip angle was moved from 17° to 45° : blue 45° , green 35° , purple 24° , red 21° , orange 19.5° , black 17°

Stability studies of the siloxane bond in different solutions by $^1\text{H-NMR}$

$t = 0$ min corresponds to the dissolution of 1,3-bis(3-aminopropyl)tetramethyl disiloxane hydrochloride **1a** (20 mg) in DMSO-d_6 or in D_2O -containing buffer that yields a solution at the desired pH. pH were adjusted in advance with Dulbecco's phosphate buffered saline, HCl or NaOH aqueous solutions on blank samples. Dimer percent was reported as a function of time based on the integration of ^1H signals from the $-\text{CH}_2\text{Si}$ group of monomer and dimer.

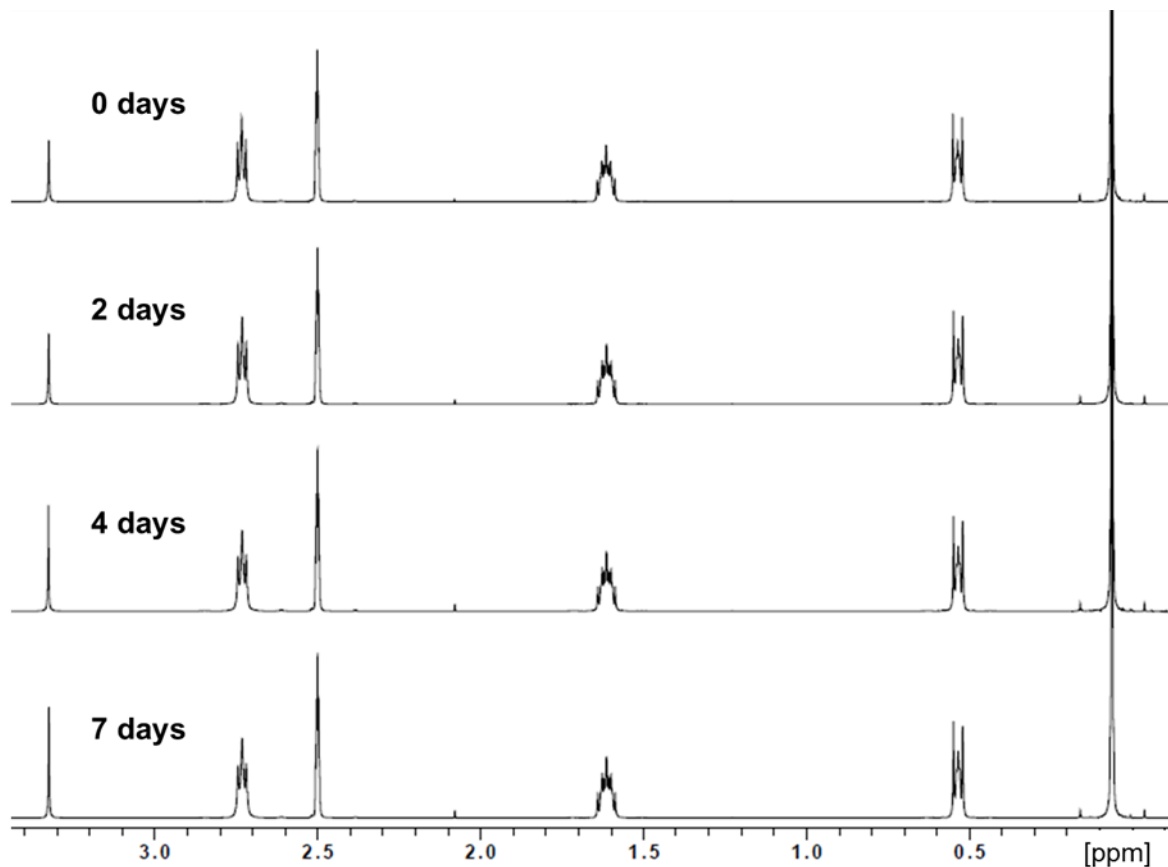


Figure S24. ^1H NMR spectra of **1a** in DMSO-d_6

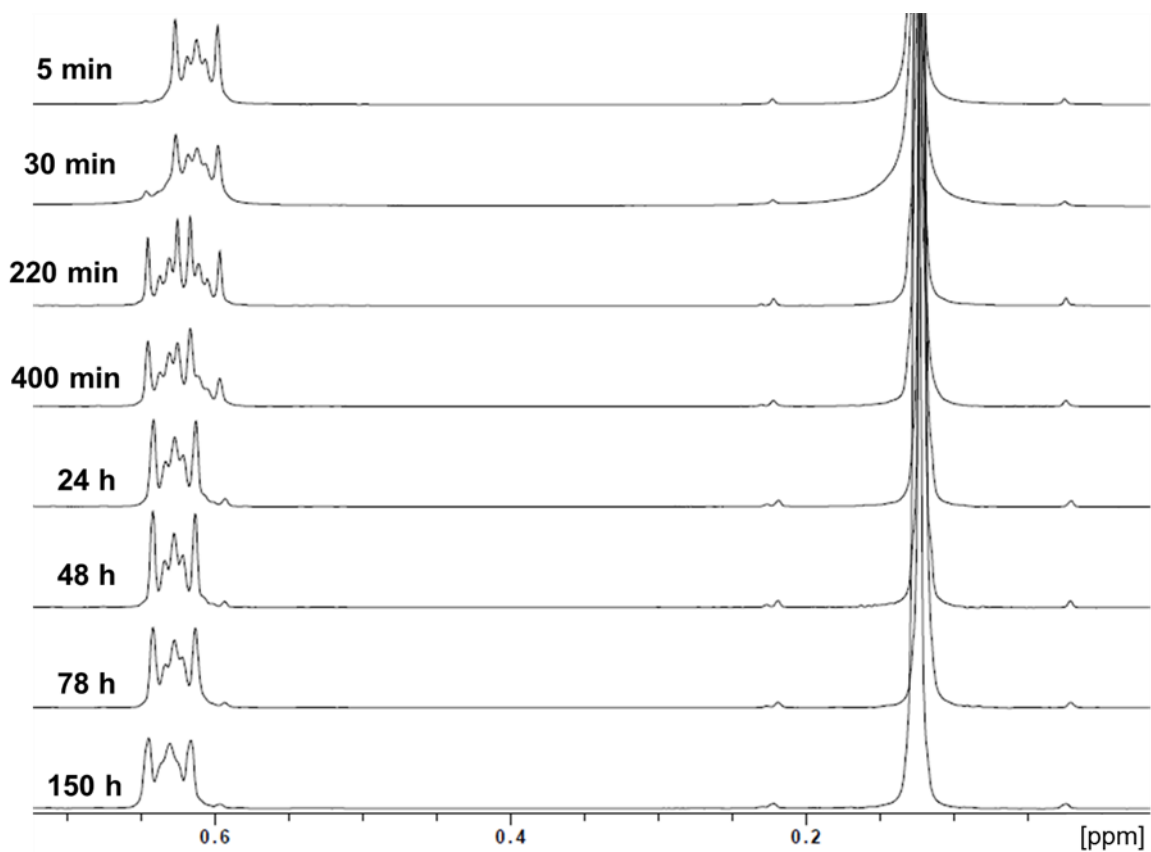


Figure S25. ^1H NMR spectra of **1a** at pH 4

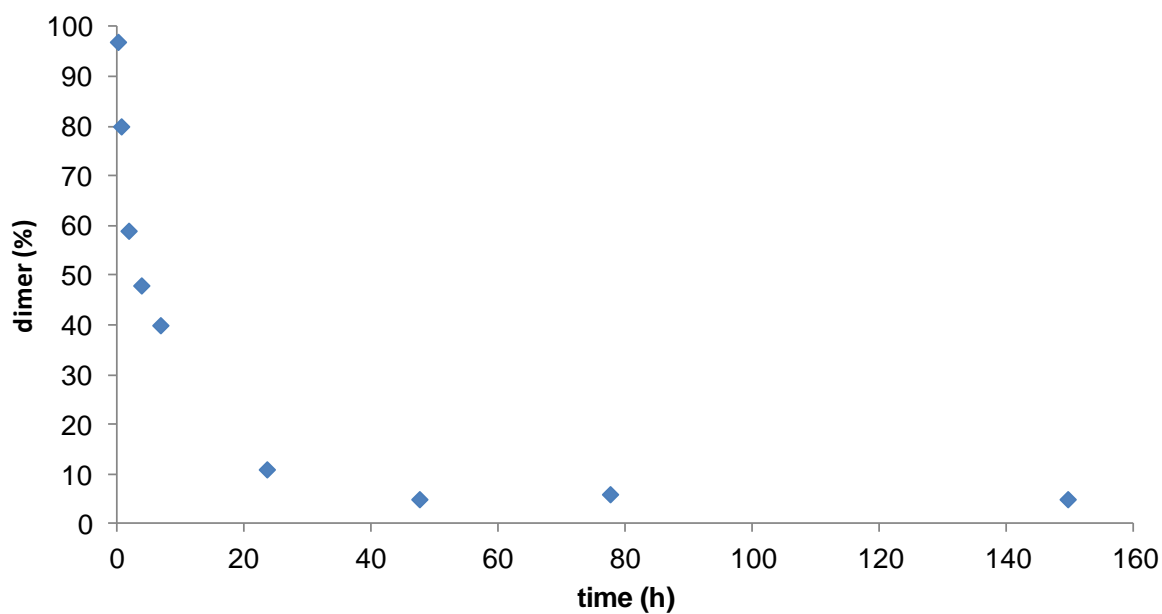


Figure S26. **1a** hydrolysis at pH 4 based on ^1H NMR kinetic studies

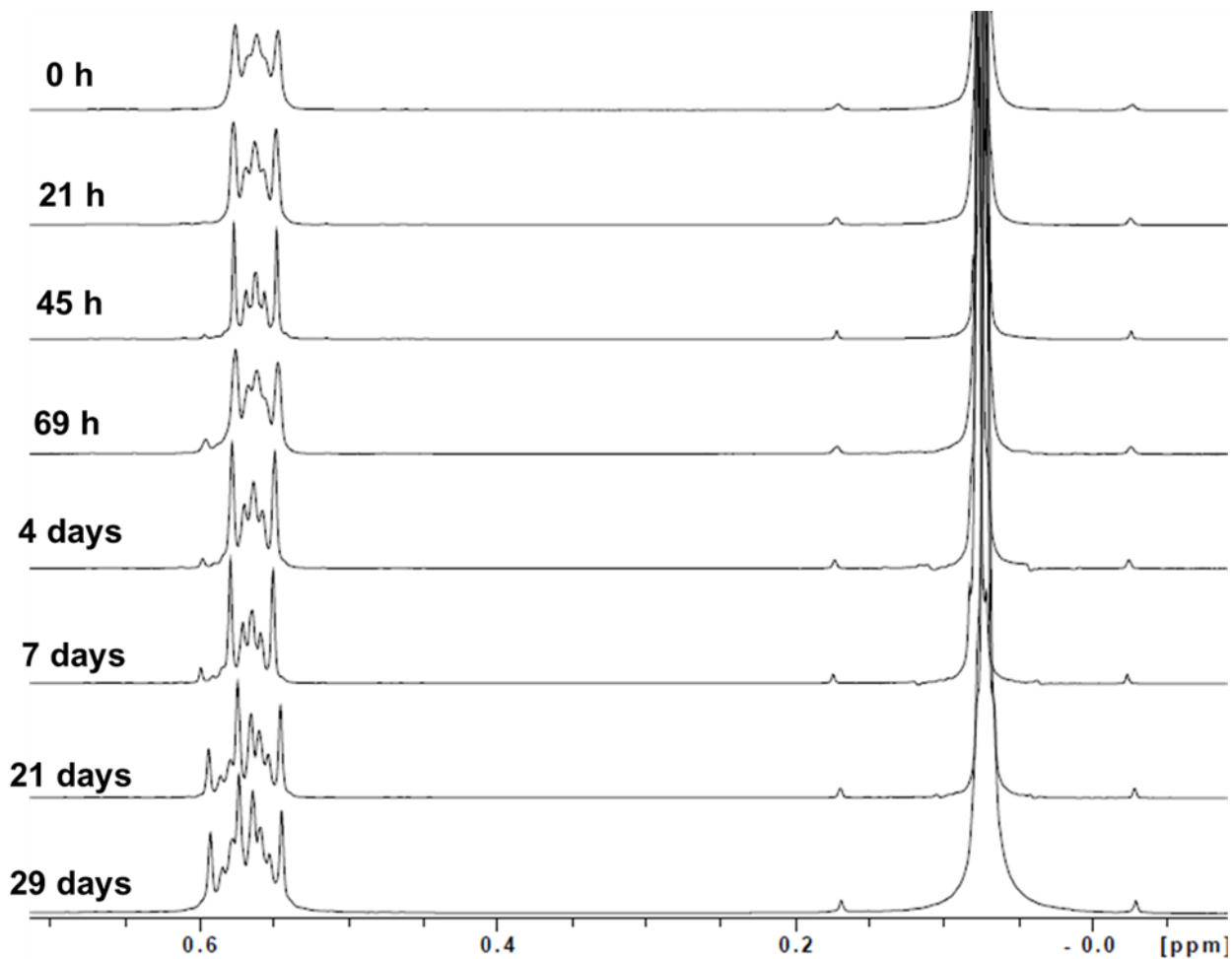


Figure S27. ^1H NMR spectra of **1a** at pH 7

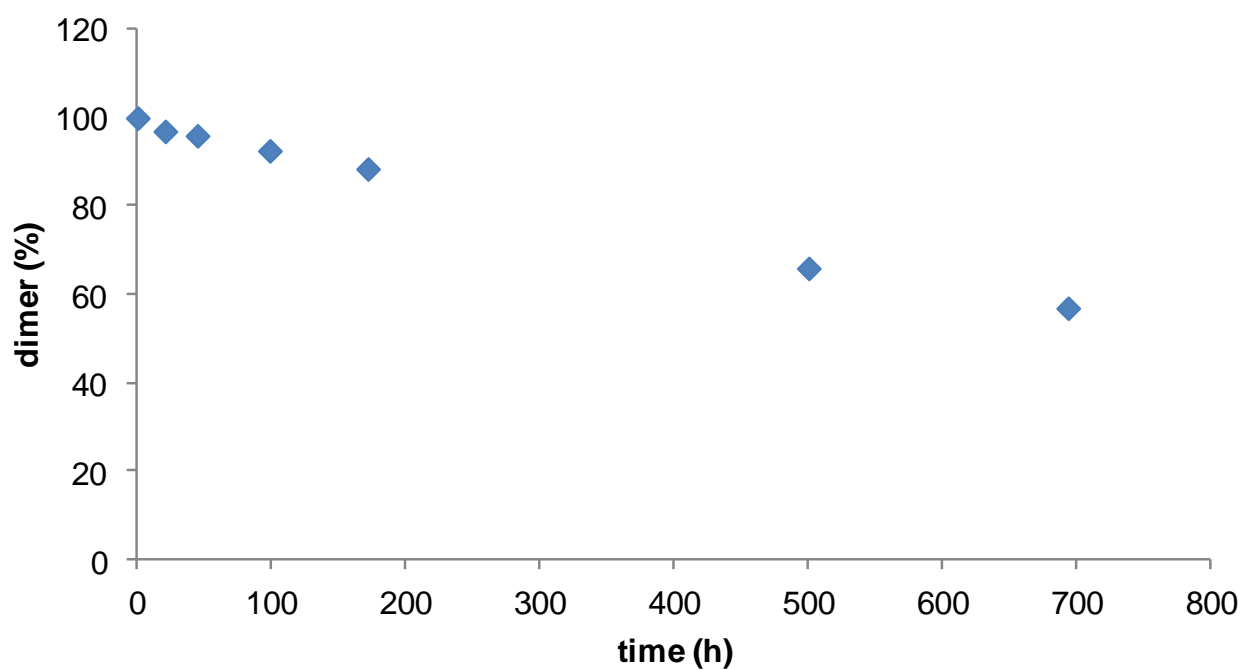


Figure S28. **1a** hydrolysis at pH 7 based on ^1H NMR kinetic studies

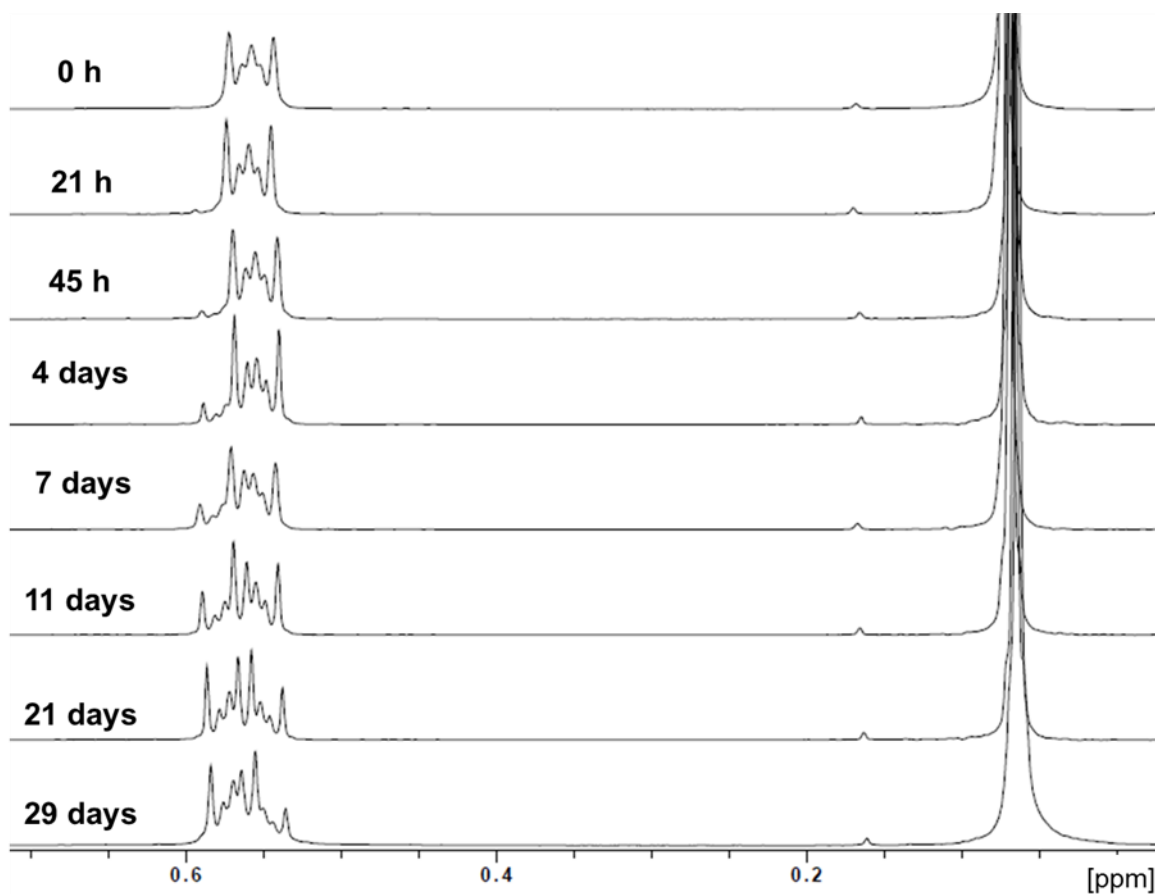


Figure S29. ^1H NMR spectra of **1a** at pH 7.4

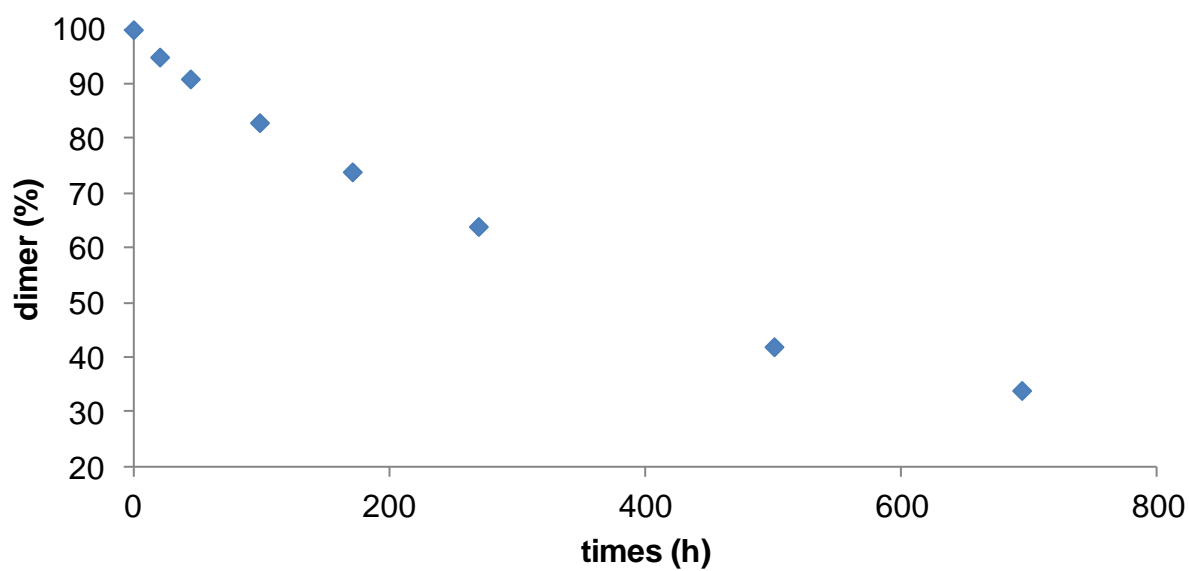


Figure S30. **1a** hydrolysis at pH 7.4 based on ^1H NMR kinetic studies

Homodimerization of unprotected peptides using hybrid hydroxydimethylsilane derivatives

We focused our attention on ^1H signals from $-\text{CH}_2\text{Si}$ and CH_3Si because they are the farthest signals from the peptide sequence in hybrid peptide displaying the dimethylpropylsiloxane dimerization arm. As a consequence, very few differences in chemical shifts and signal shapes are expected when changing the peptide sequence. Thus, NMR studies on the 1,3-bis(3-aminopropyl)tetramethyl disiloxane model can be generalized to hybrid peptides. In addition, these signals appear in a chemical shift area completely different from peptide signals which makes them easily identifiable and integrable. However, the methylene group in gamma position to the silicon is also a problem for the determination of monomer/dimer ratio (figure S31)

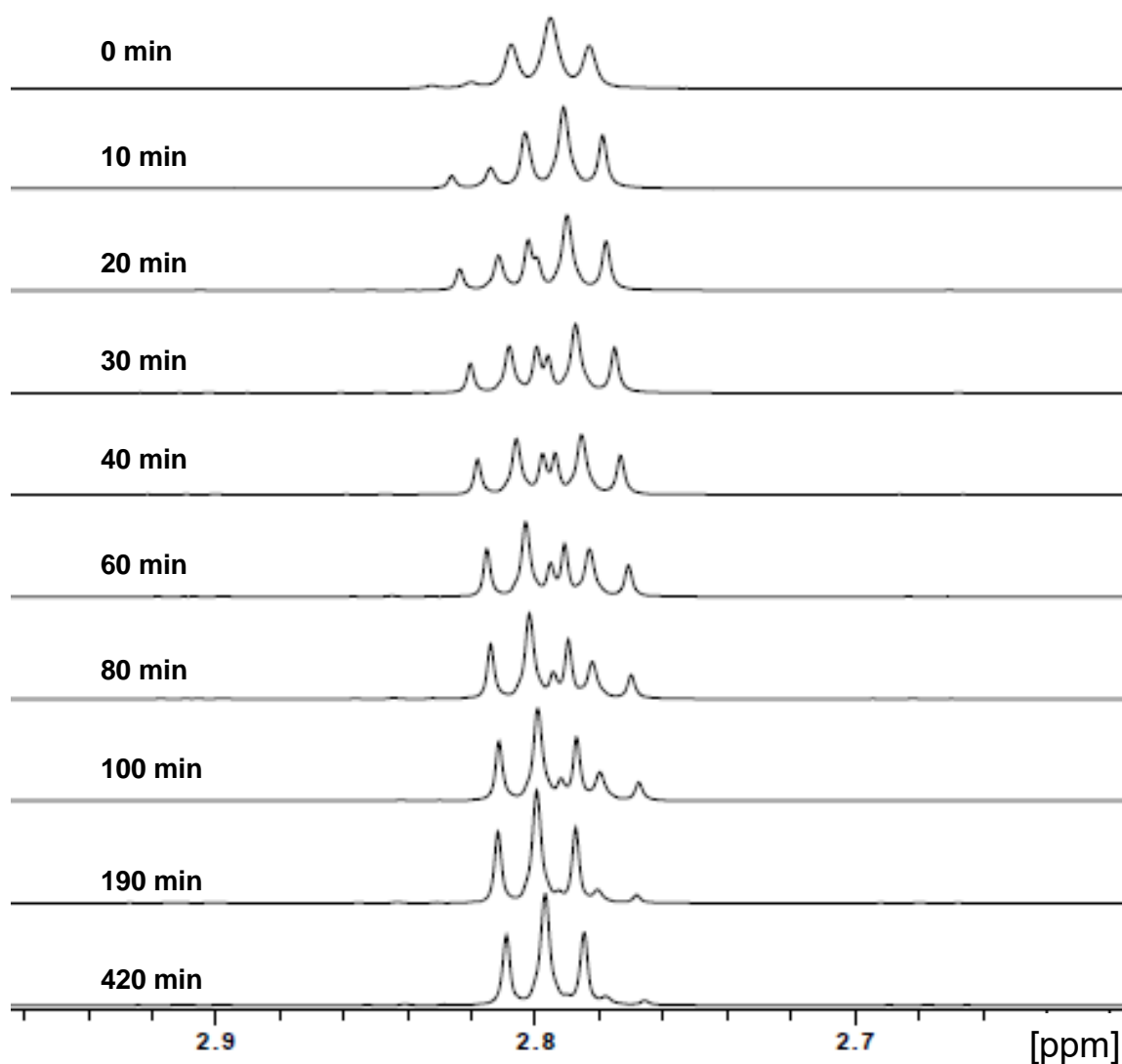


Figure S31. ^1H NMR spectra of **1a** at pH 10. Signals from the CH_2 group in gamma position to silicon

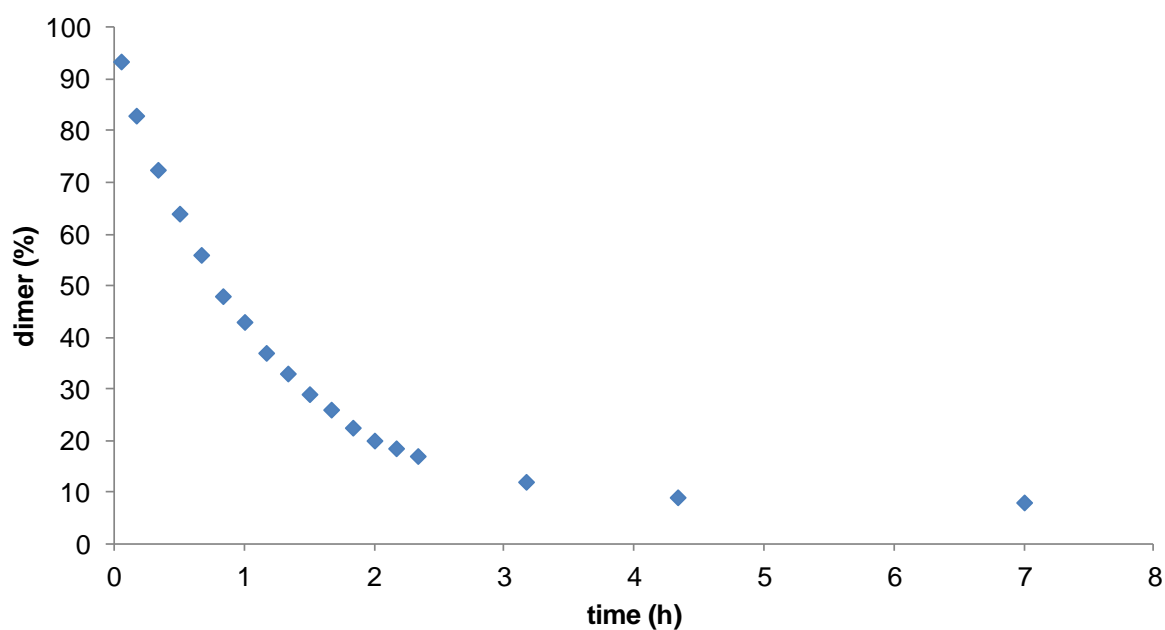


Figure S32. *1a* hydrolysis at pH 10 based on ^1H NMR kinetic studies

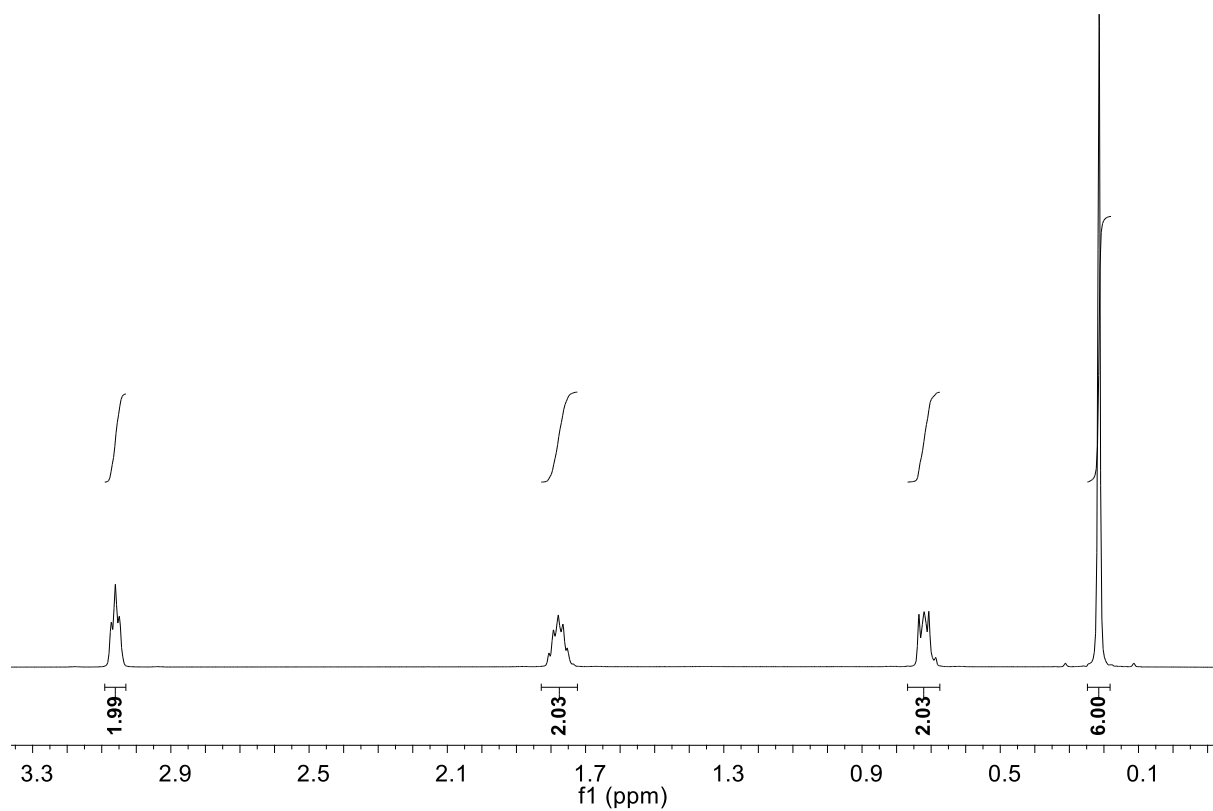


Figure S33. ^1H NMR spectrum of **1a** in D_2O 0.1% TFA at $t = 0$. Hydrolysis occurred immediately. Signals correspond to monomer **2a**.

Silanol condensation upon lyophilization

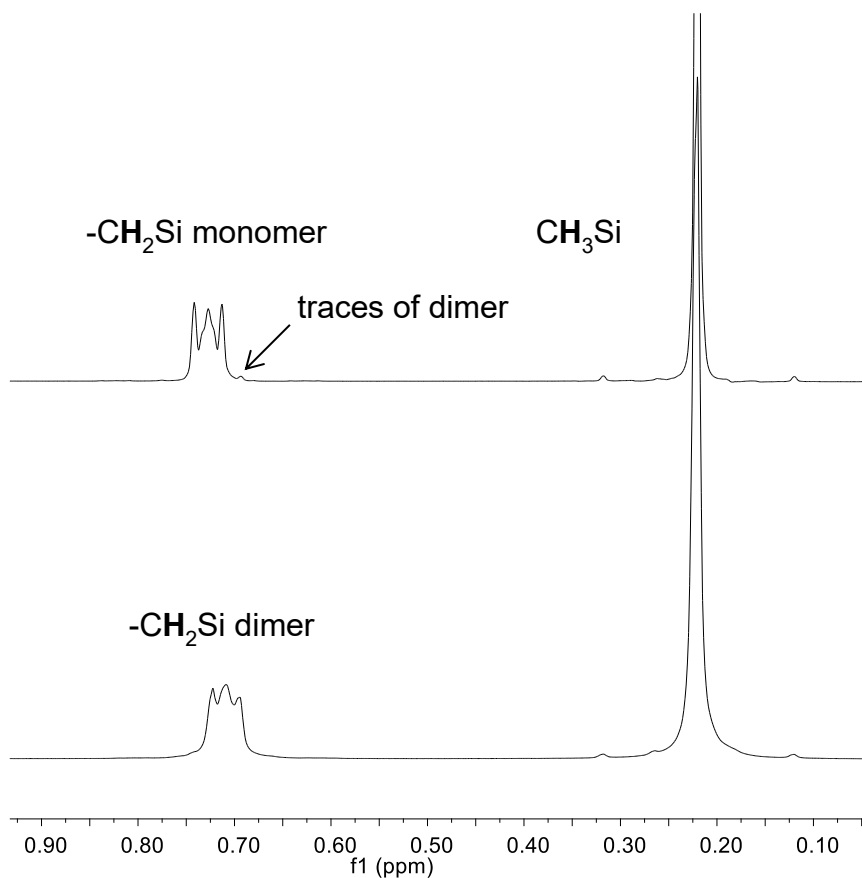


Figure S34. From monomer to dimer upon lyophilization. Top : ^1H NMR spectrum of **2a** in $\text{D}_2\text{O}/0.1\%$ TFA before lyophilization; bottom : ^1H NMR spectrum of the same sample after freeze-drying

N-ter hybrid monomer 4

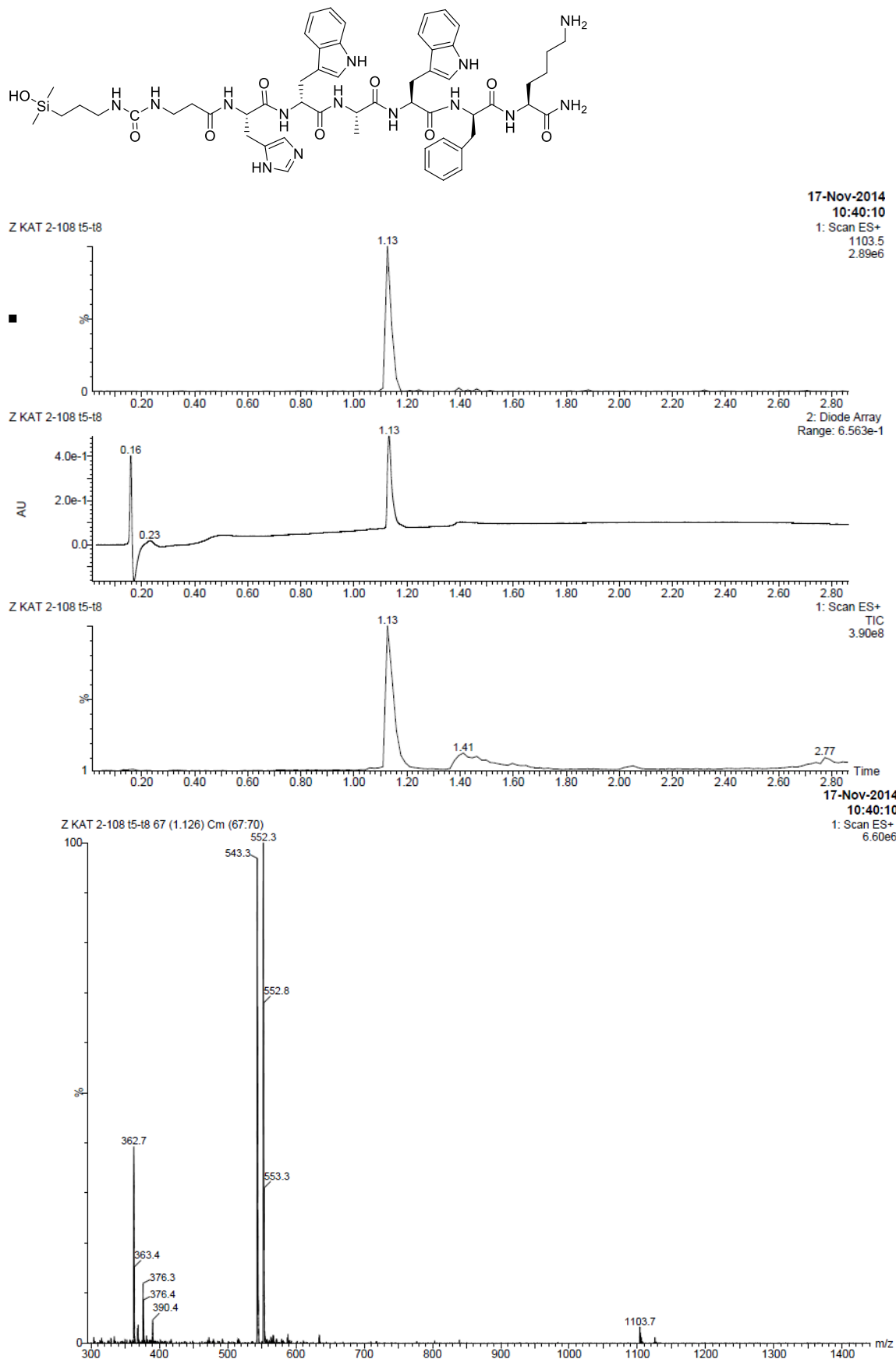


Figure S35. LC/MS spectrum of 4

N-ter hybrid dimer 5 (JMV 6187)

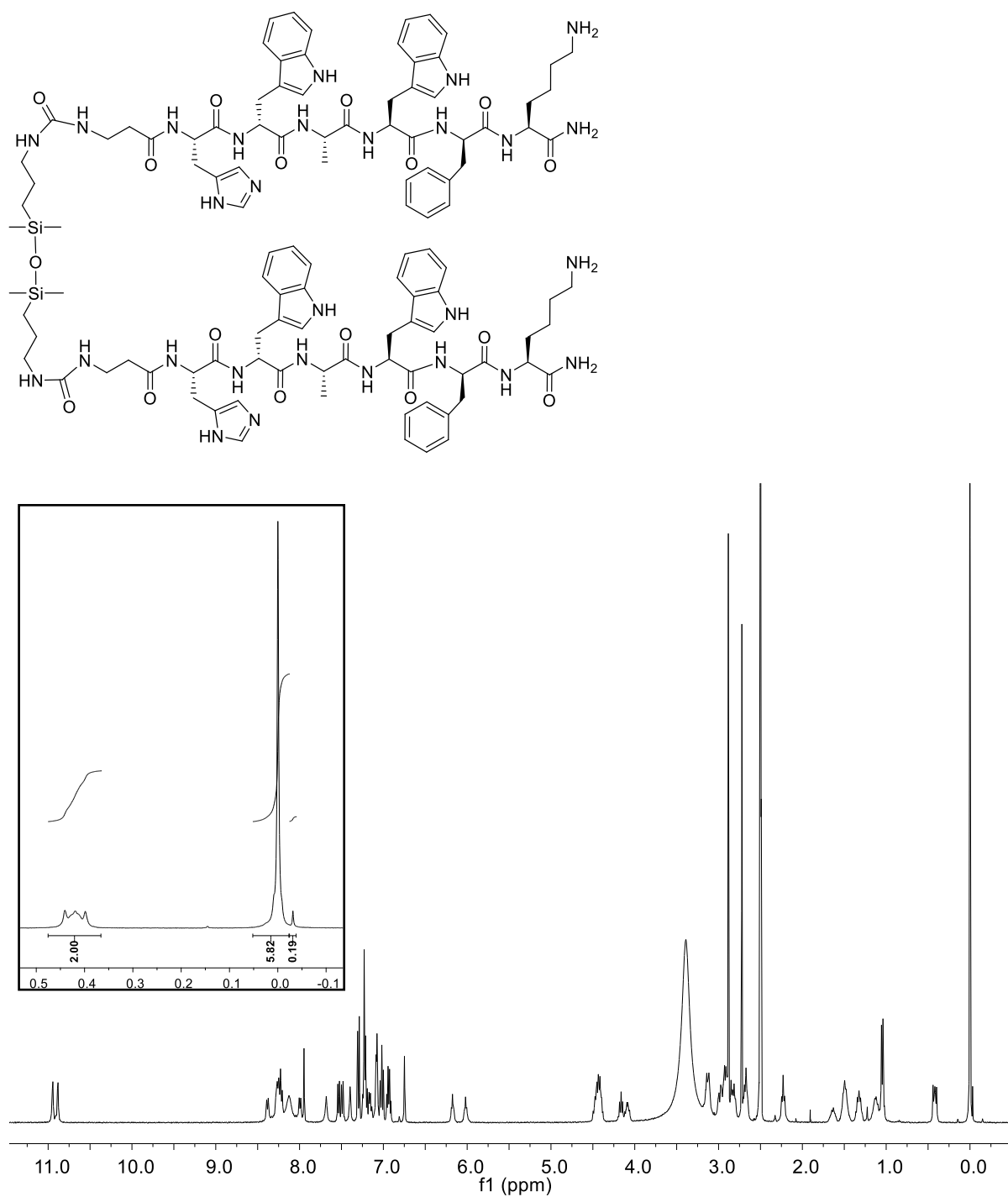


Figure S36. ¹H NMR spectrum of 5 in DMSO-d₆ (400 MHz)

Supporting information for publication n°1
Homodimerization of unprotected peptides using hybrid hydroxydimethylsilane derivatives

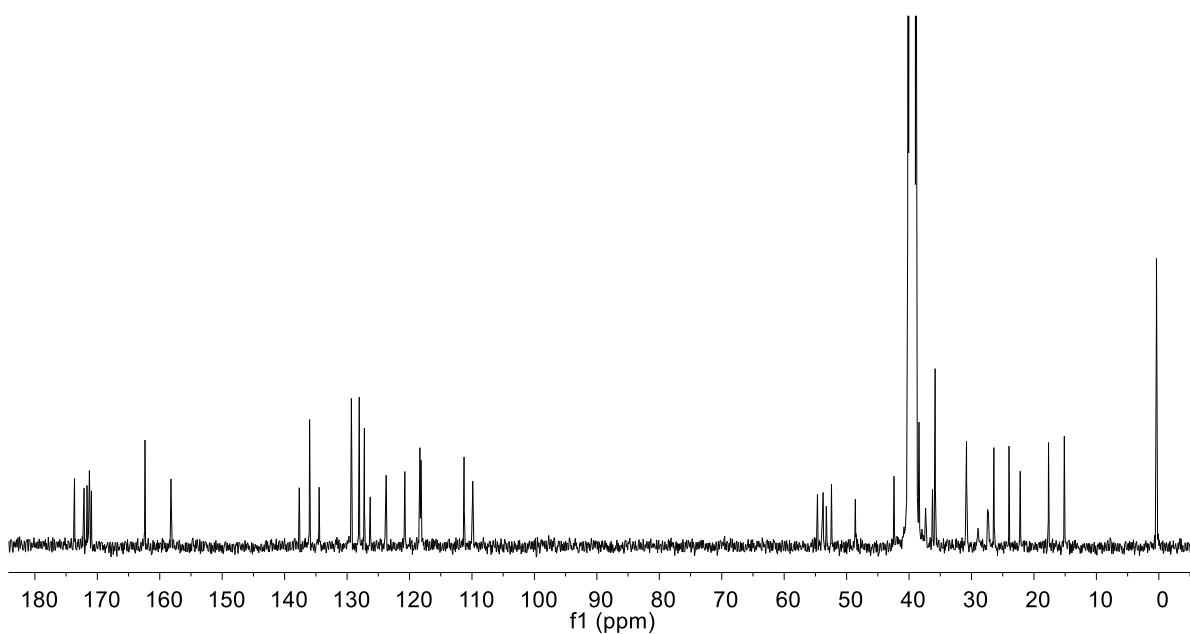
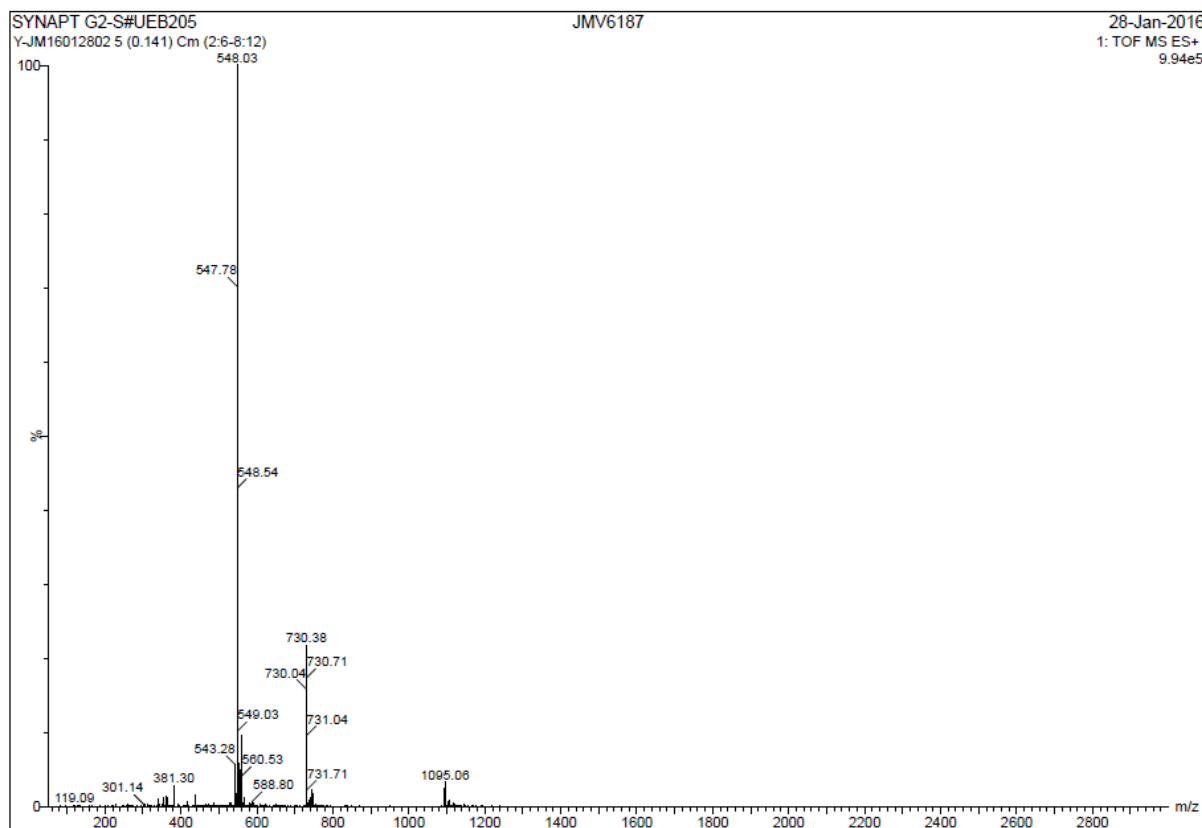


Figure S37. ^{13}C NMR spectrum of **5** in DMSO-d_6 (101 MHz)



Supporting information for publication n°1
Homodimerization of unprotected peptides using hybrid hydroxydimethylsilane derivatives

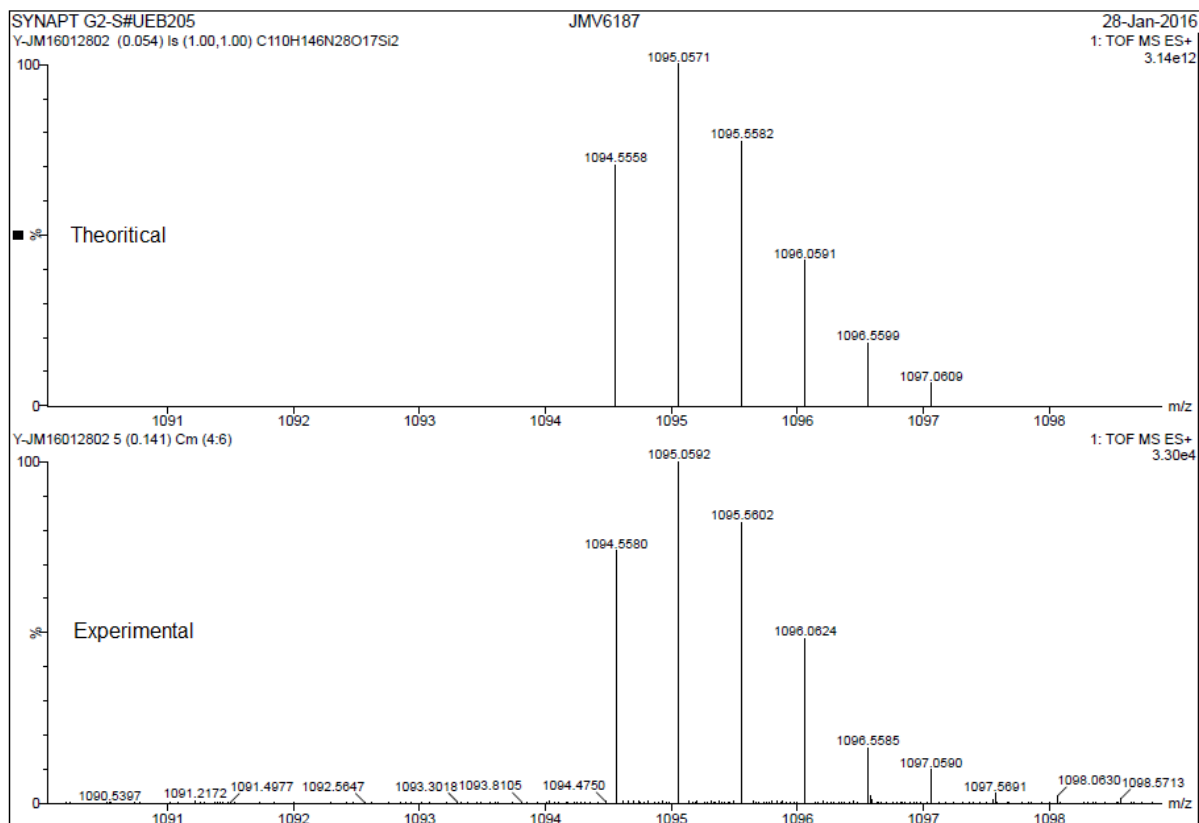
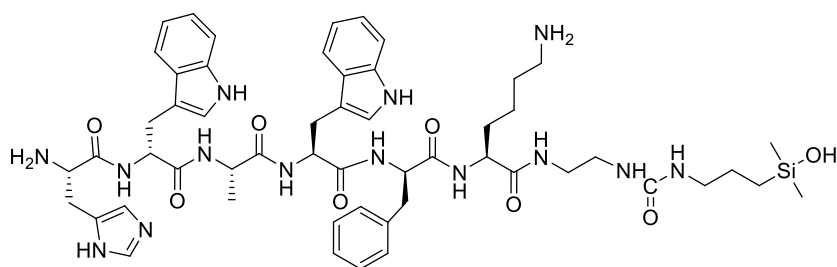


Figure S38. HR-MS analysis of **5**

C-ter hybrid monomer 6



Supporting information for publication n°1
Homodimerization of unprotected peptides using hybrid hydroxydimethylsilane derivatives

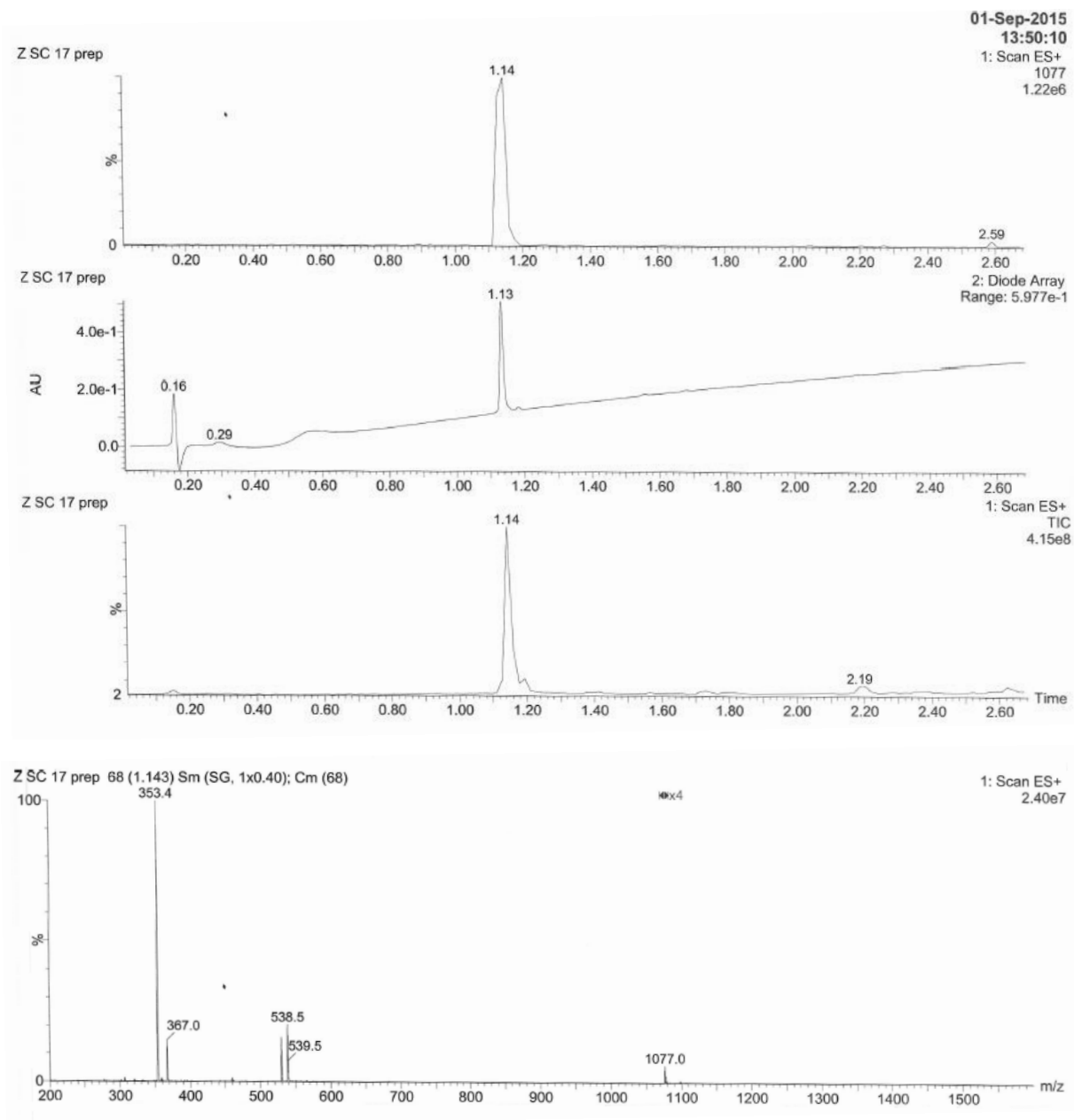


Figure S39. LC/MS spectrum of **6**

C-ter hybrid dimer 7 (JMV 6186)

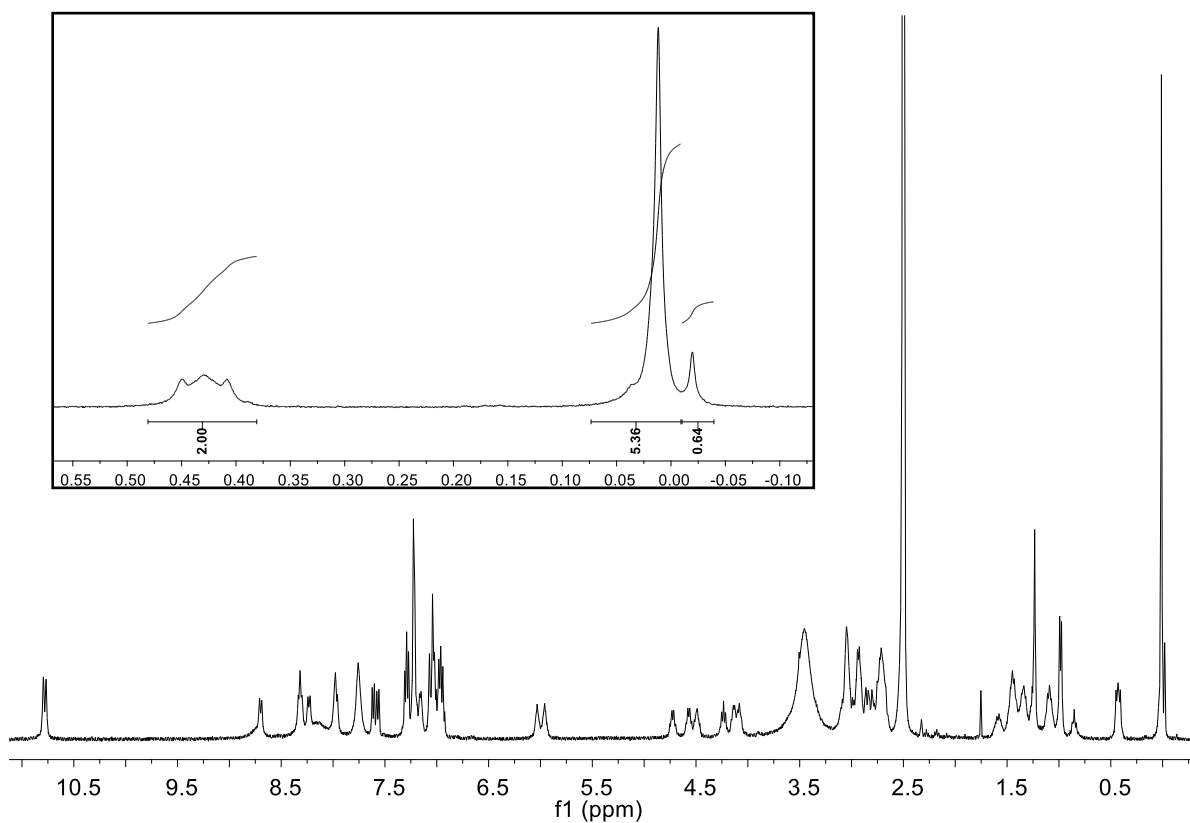
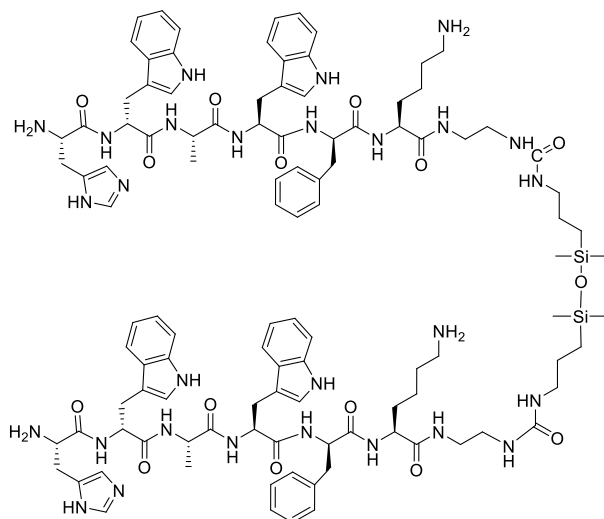


Figure S40. ^1H NMR spectrum of **7** in DMSO-d_6 (400 MHz)

Supporting information for publication n°1
Homodimerization of unprotected peptides using hybrid hydroxydimethylsilane derivatives

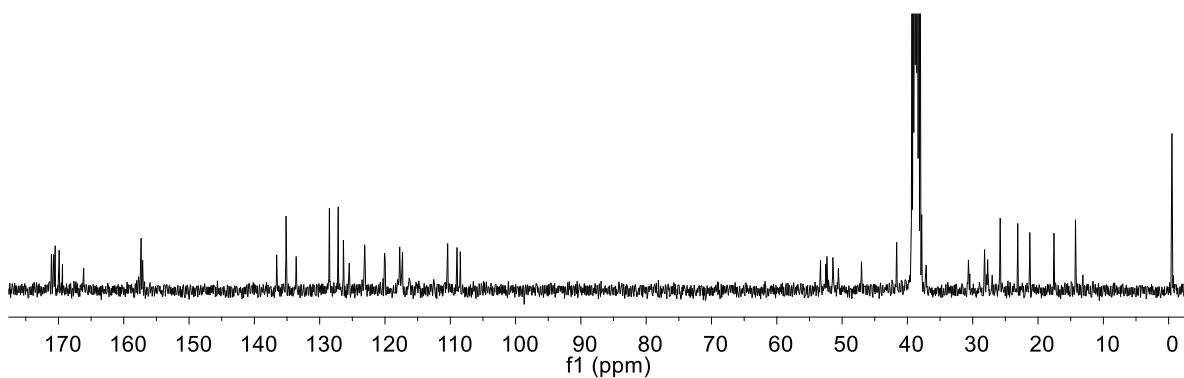
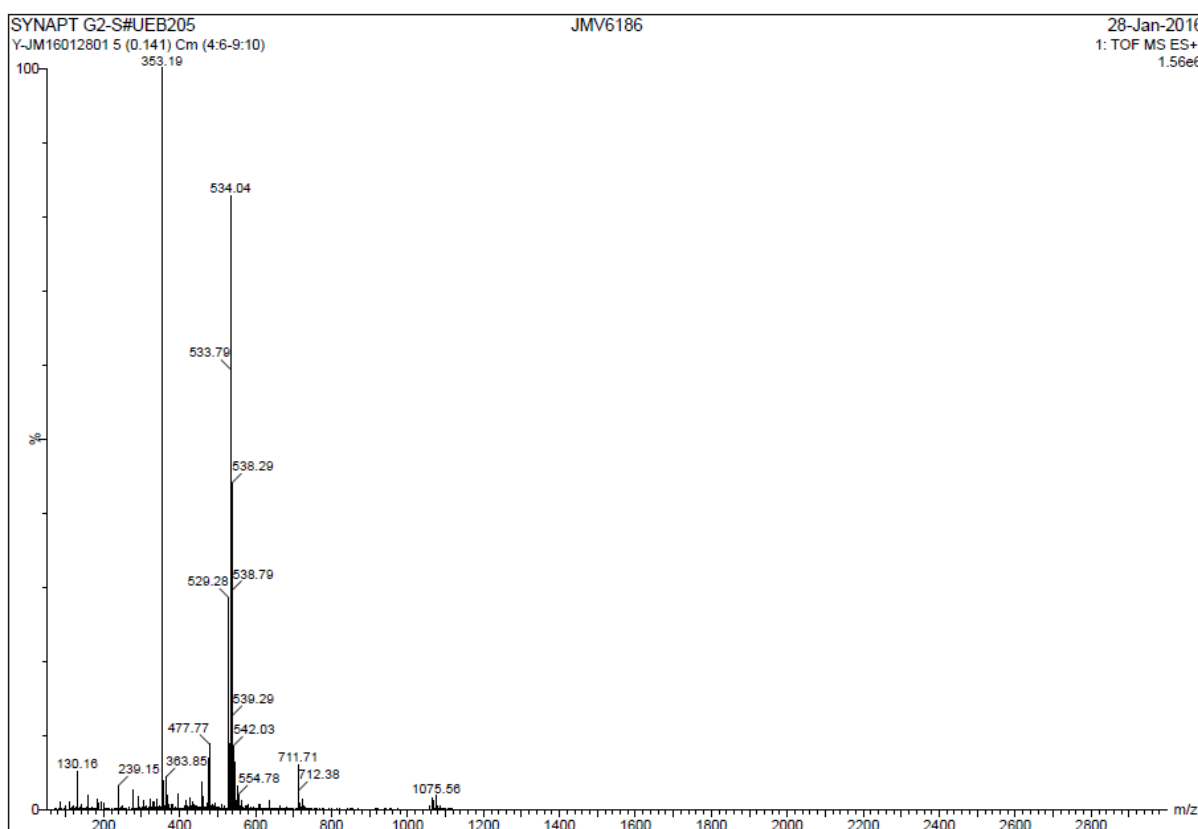


Figure S41. ^{13}C NMR spectrum of **7** in DMSO-d_6 (101 MHz)



Homodimerization of unprotected peptides using hybrid hydroxydimethylsilane derivatives

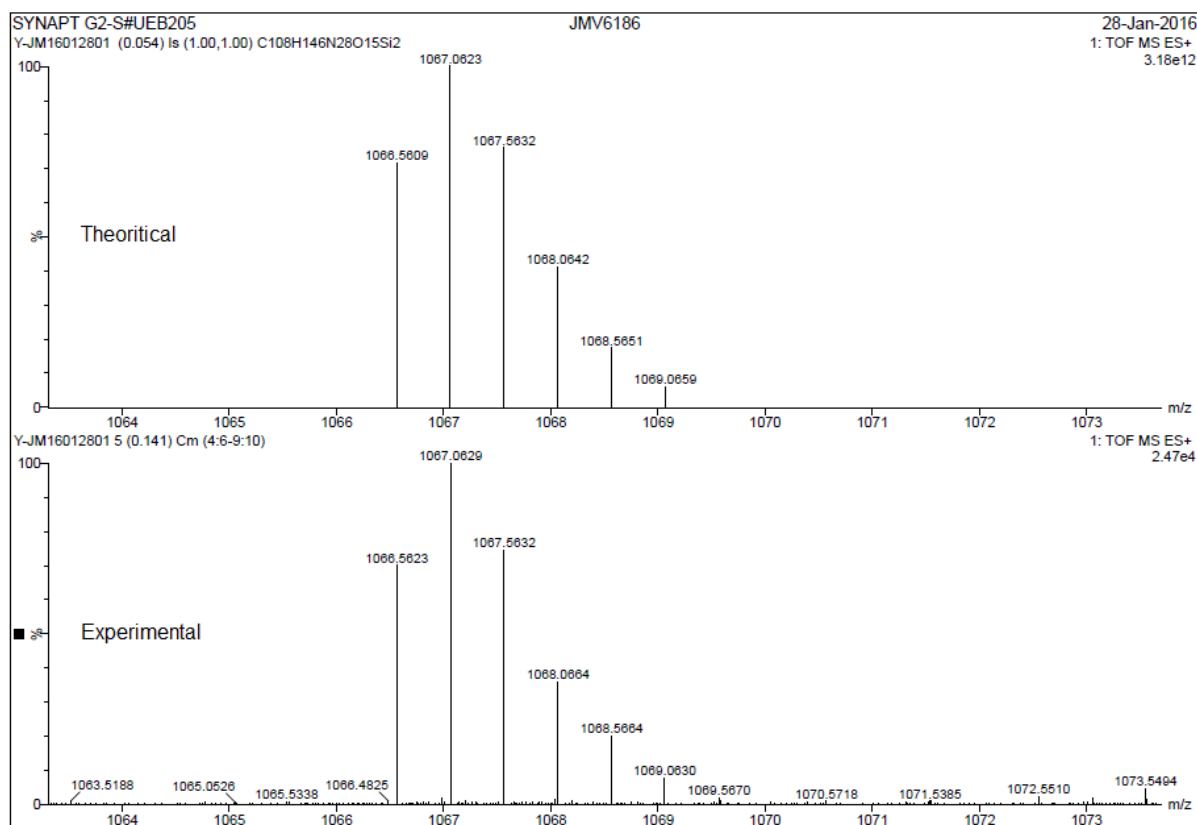
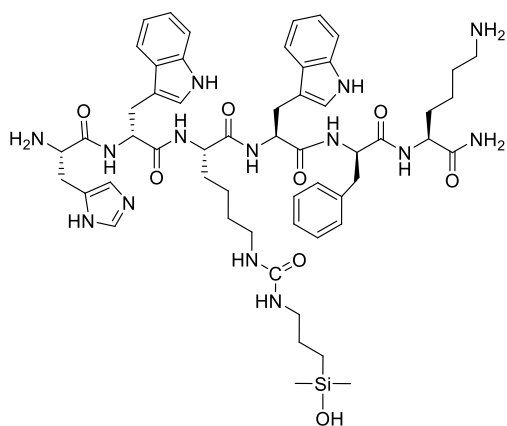


Figure S42. HR-MS analysis of 7

Lys³ hybrid monomer 8



Supporting information for publication n°1
Homodimerization of unprotected peptides using hybrid hydroxydimethylsilane derivatives

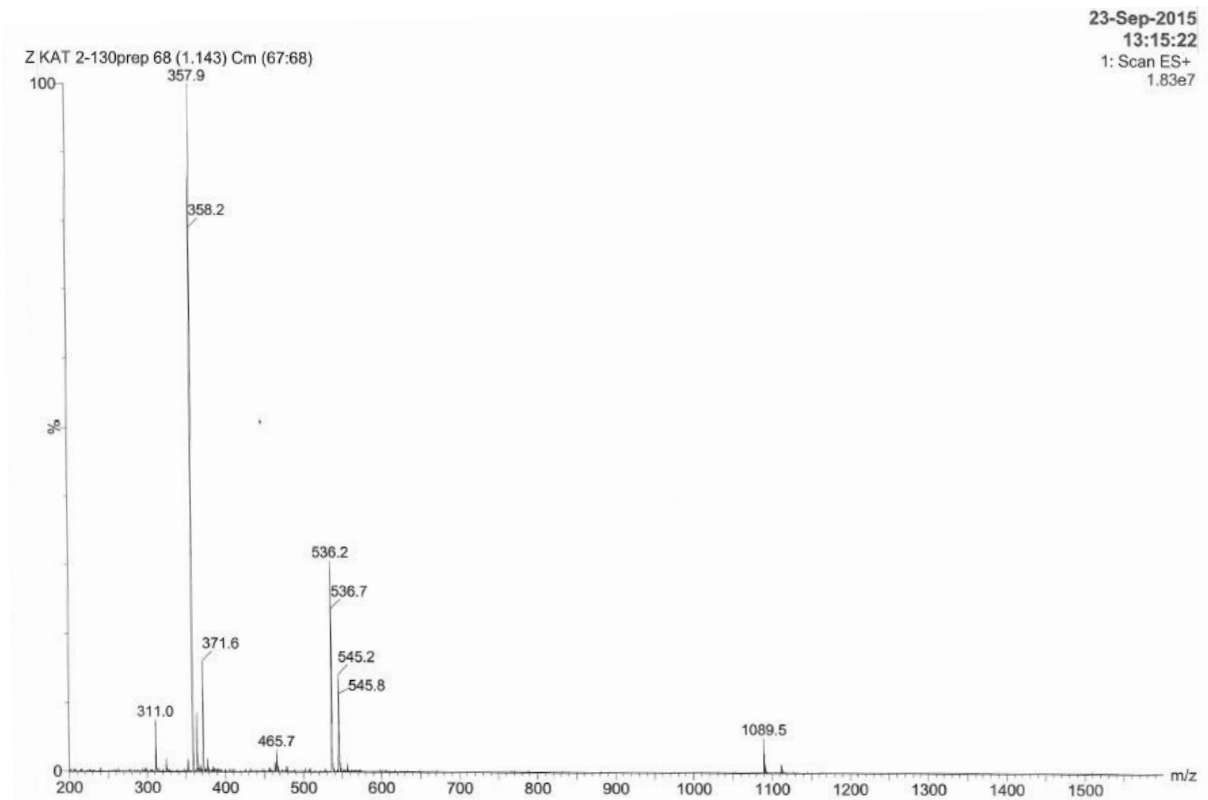
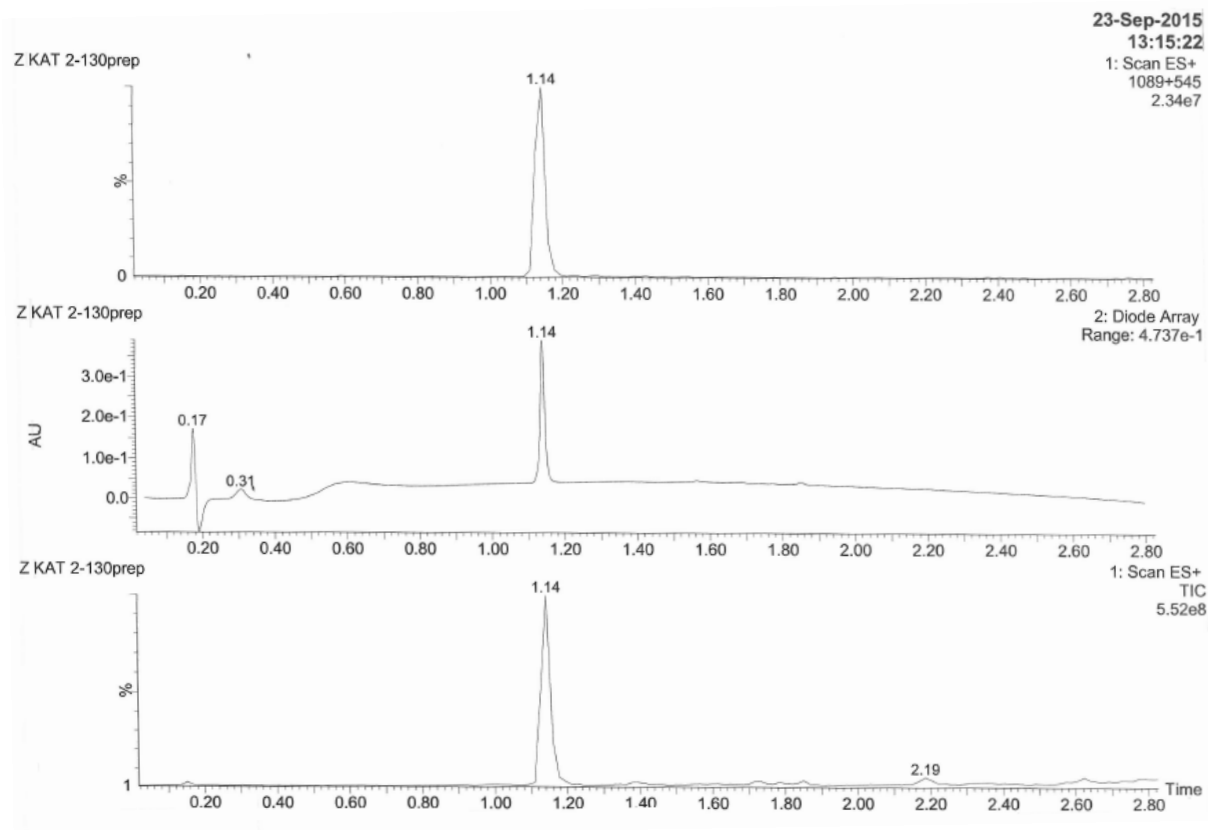
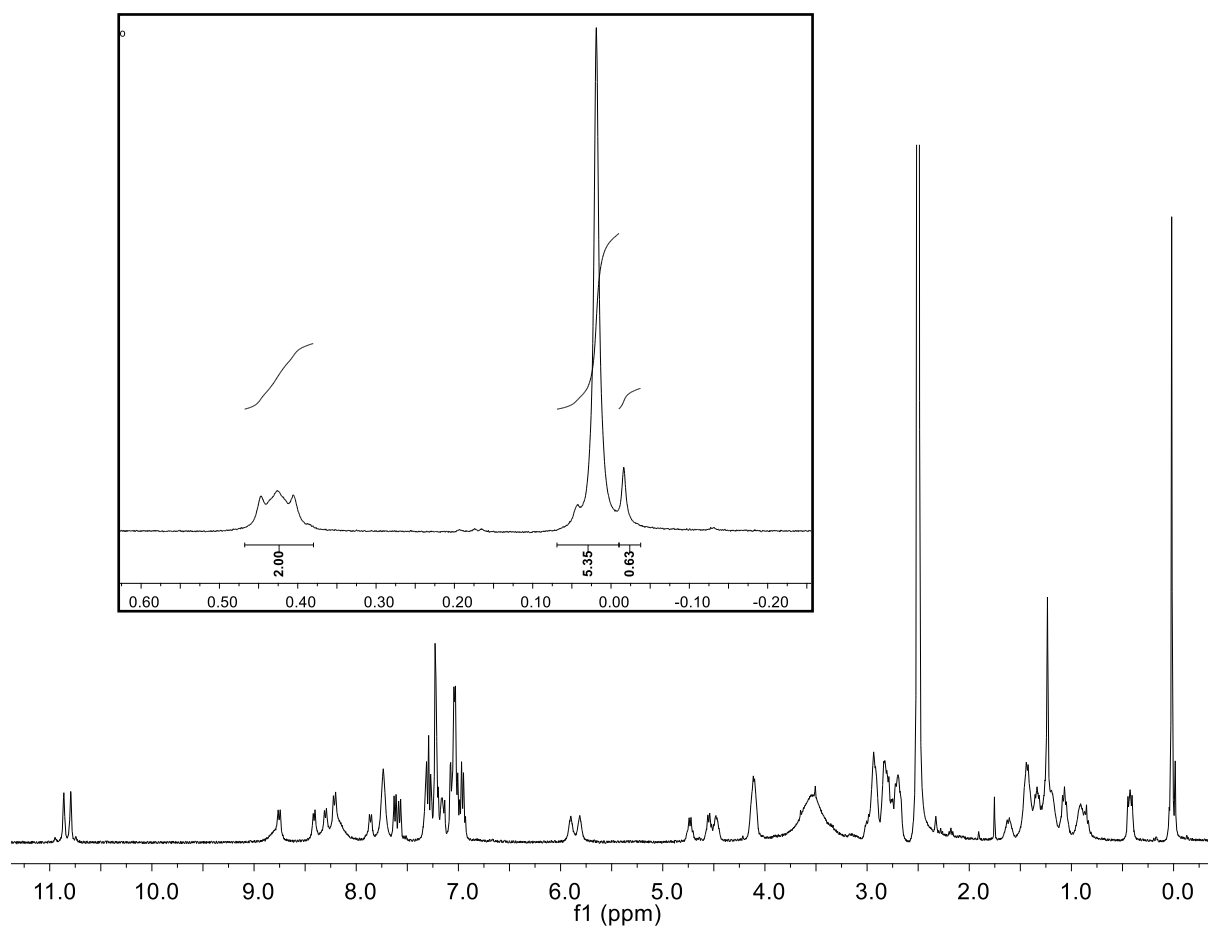
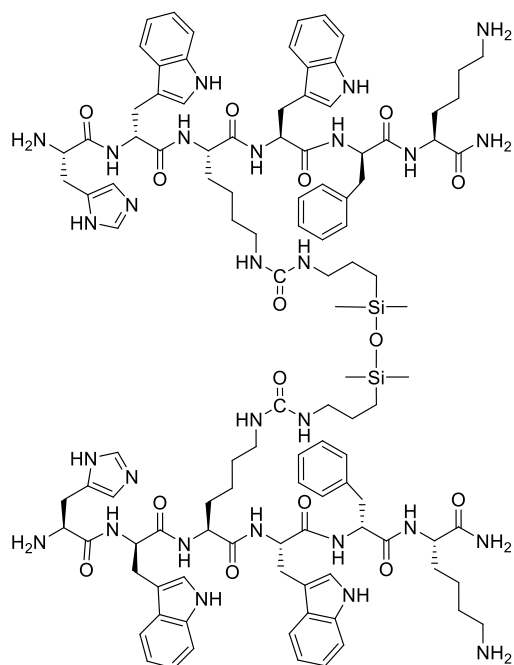


Figure S43. LC/MS spectrum of **8**

Lys³ hybrid dimer 9 (JMV 6185)**Figure S44.** ¹H NMR spectrum of **9** in DMSO-*d*₆ (400 MHz)

Supporting information for publication n°1
Homodimerization of unprotected peptides using hybrid hydroxydimethylsilane derivatives

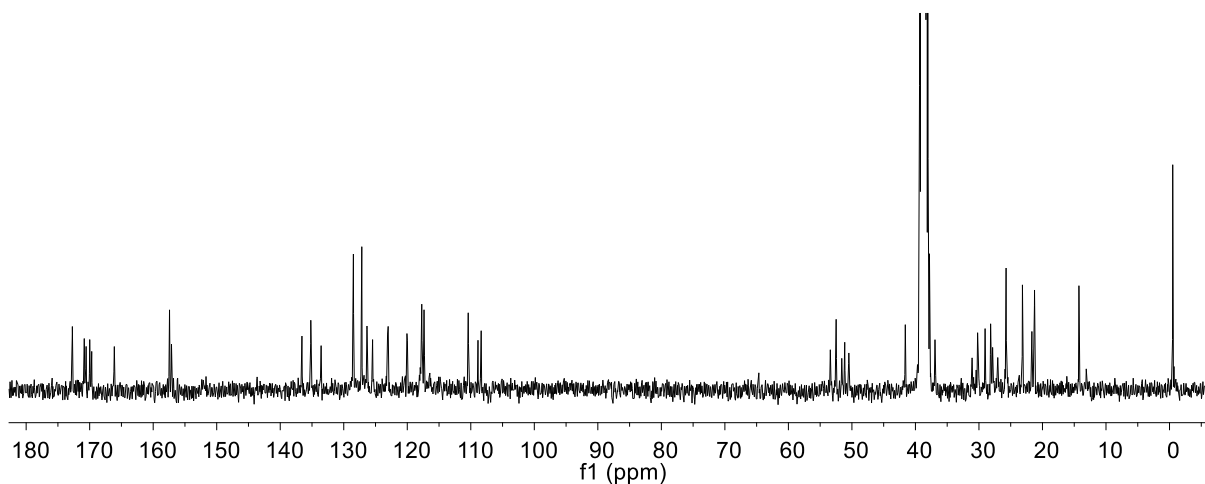
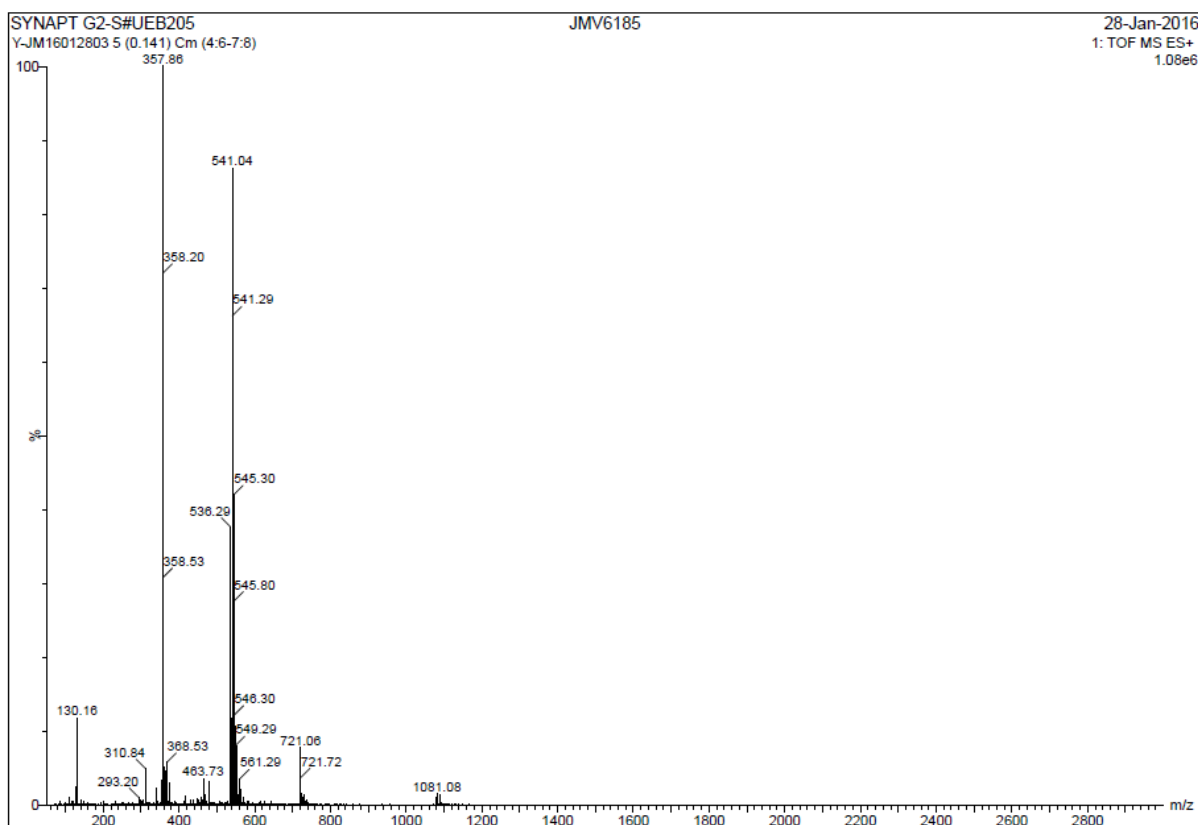


Figure S45. ^{13}C NMR spectrum of **9** in DMSO-d_6 (101 MHz)



Supporting information for publication n°1
 Homodimerization of unprotected peptides using hybrid hydroxydimethylsilane derivatives

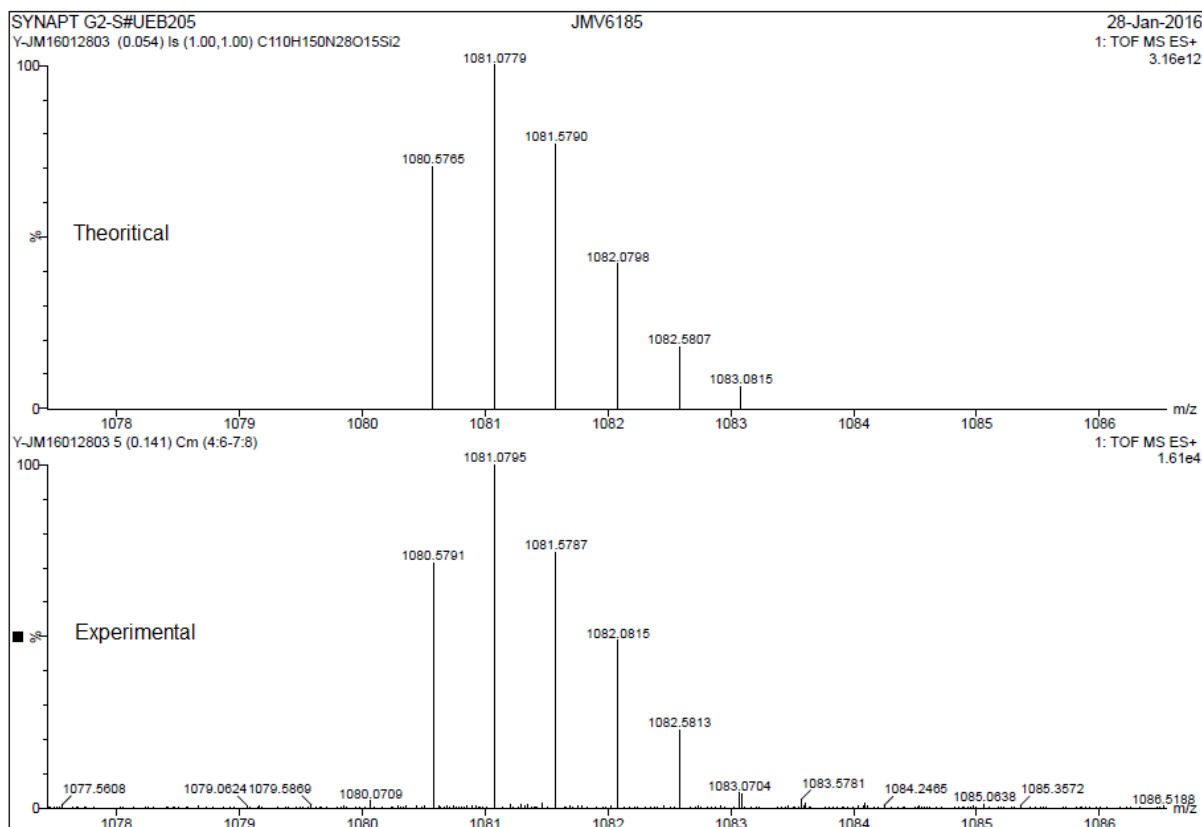
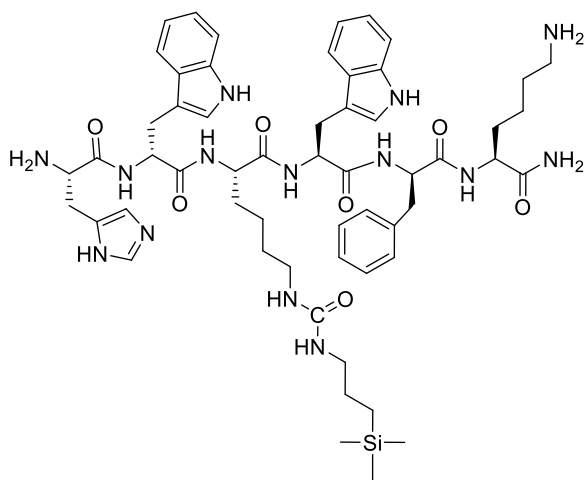


Figure S46. HR-MS analysis of **9**

Lys³(NH(CH₂)₃Si(CH₃)₃) monomer **10** (JMV 6246)



Supporting information for publication n°1
Homodimerization of unprotected peptides using hybrid hydroxydimethylsilane derivatives

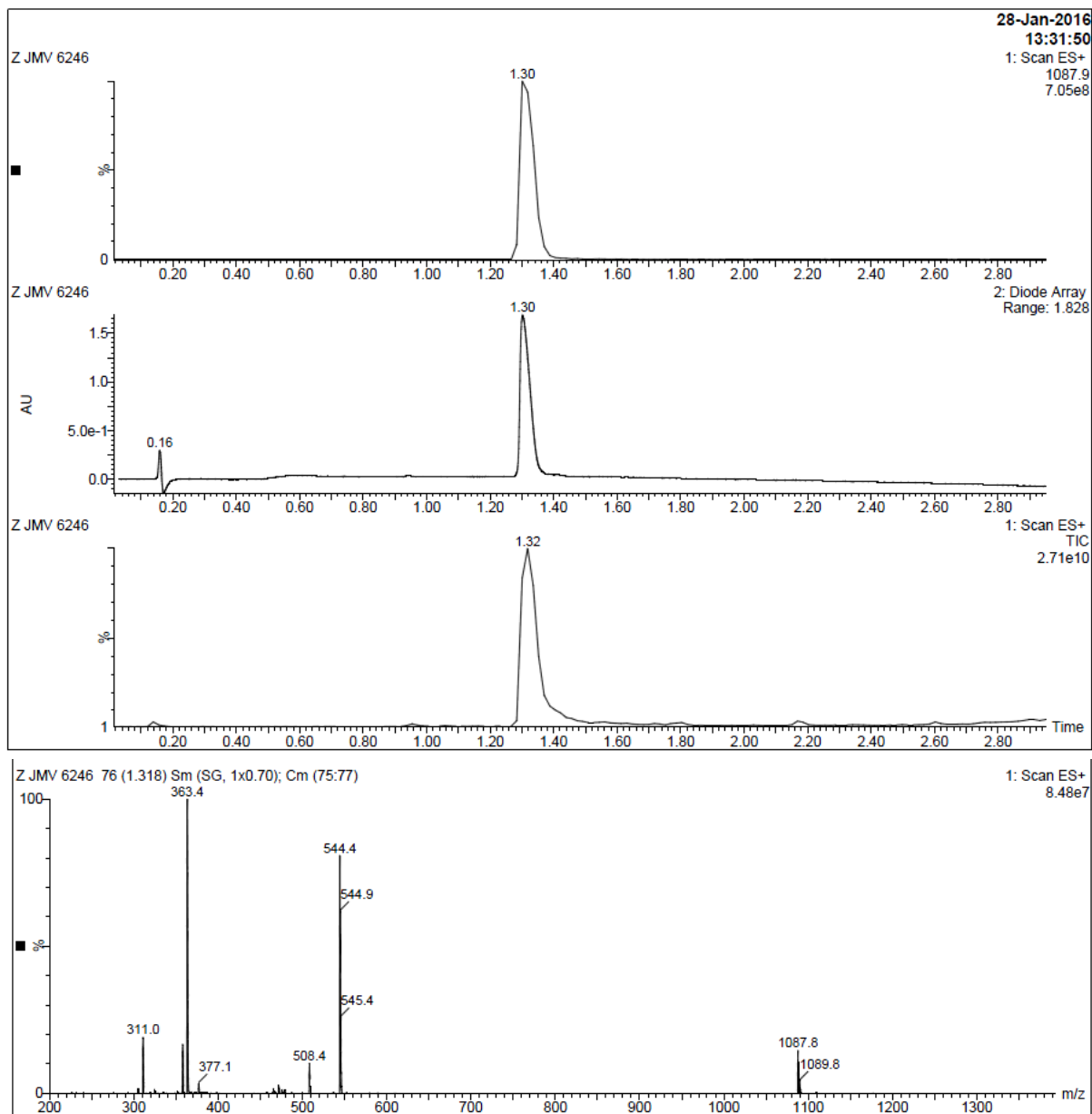


Figure S47. LC/MS spectrum of 10

Supporting information for publication n°1
Homodimerization of unprotected peptides using hybrid hydroxydimethylsilane derivatives

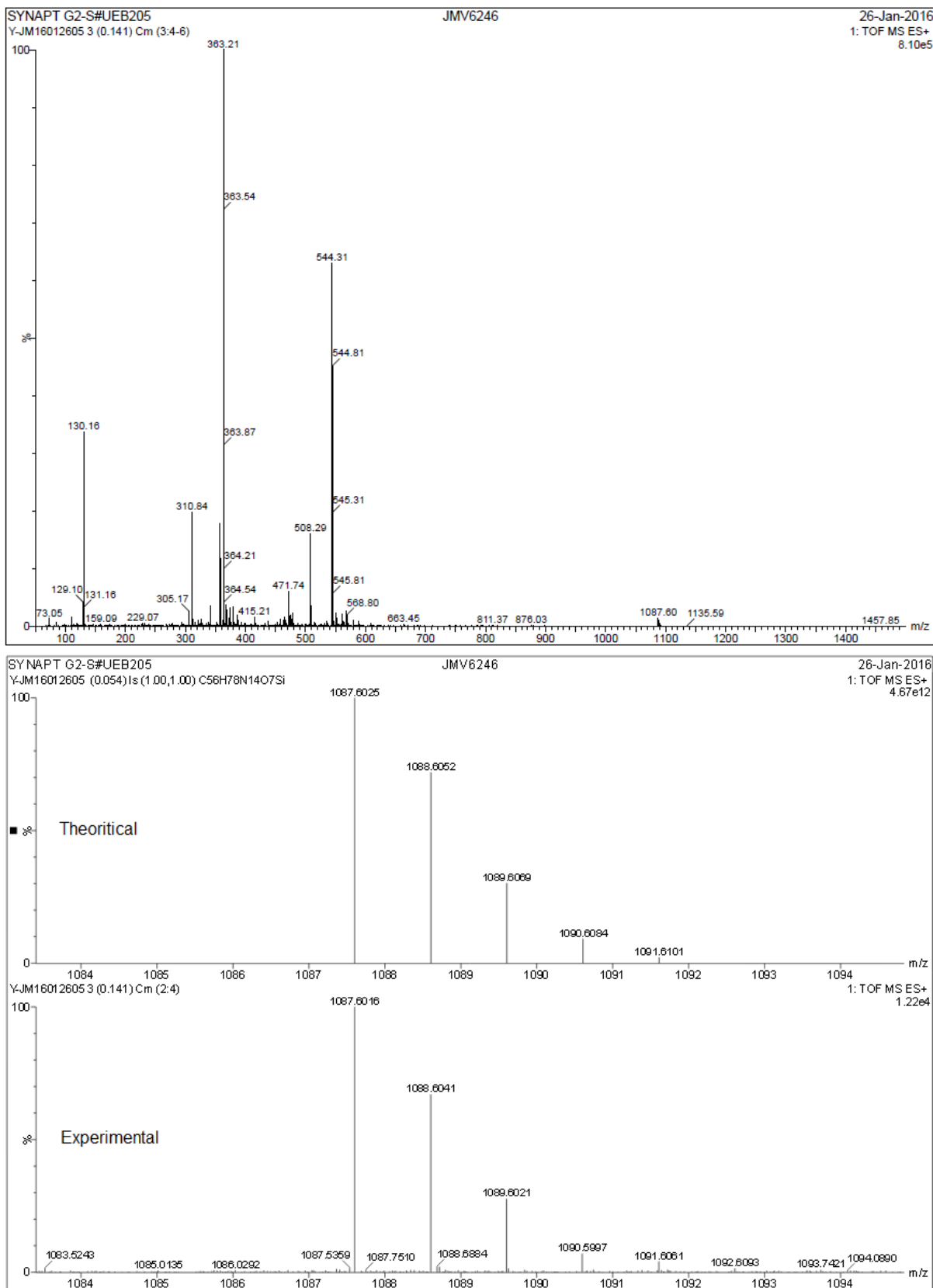
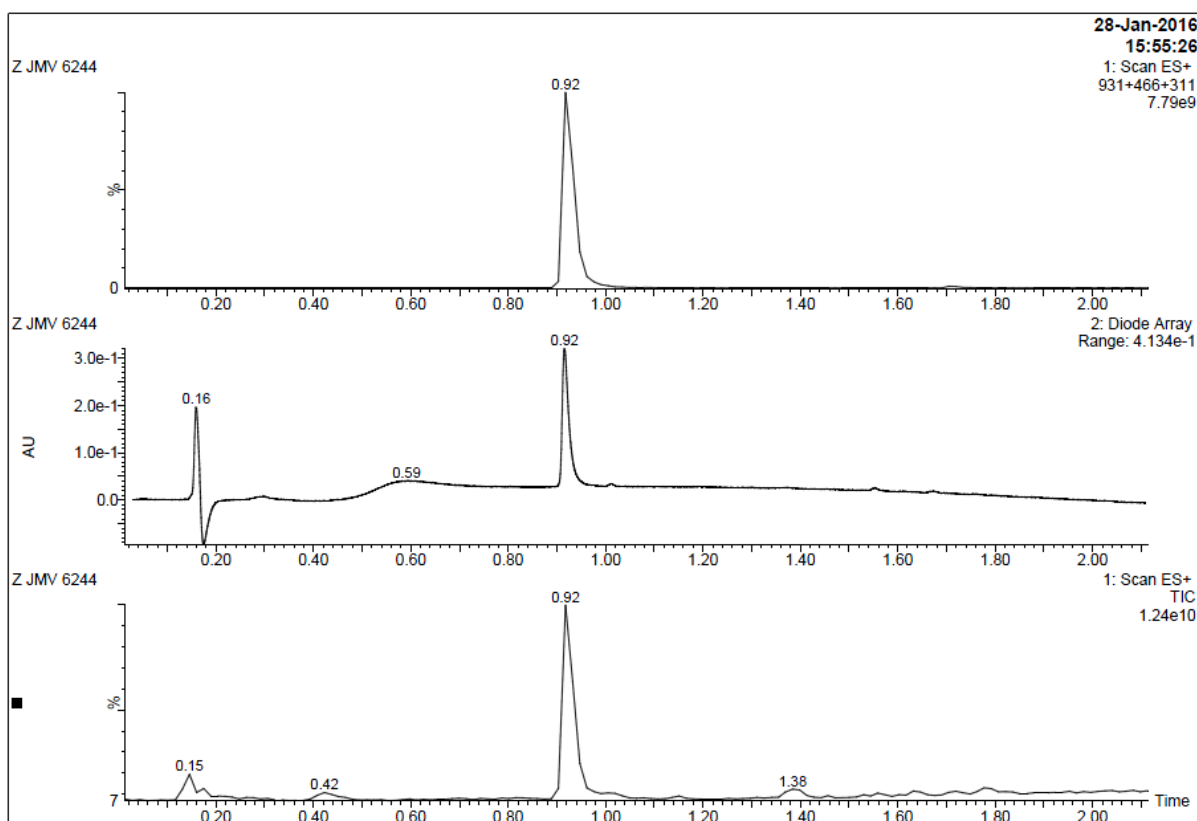
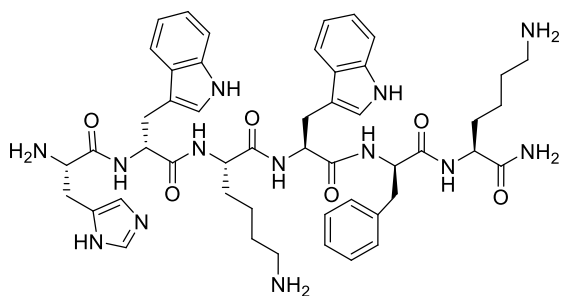


Figure S48. HR-MS analysis of 10

Lys³ monomer 11 (JMV 6244)



Supporting information for publication n°1
Homodimerization of unprotected peptides using hybrid hydroxydimethylsilane derivatives

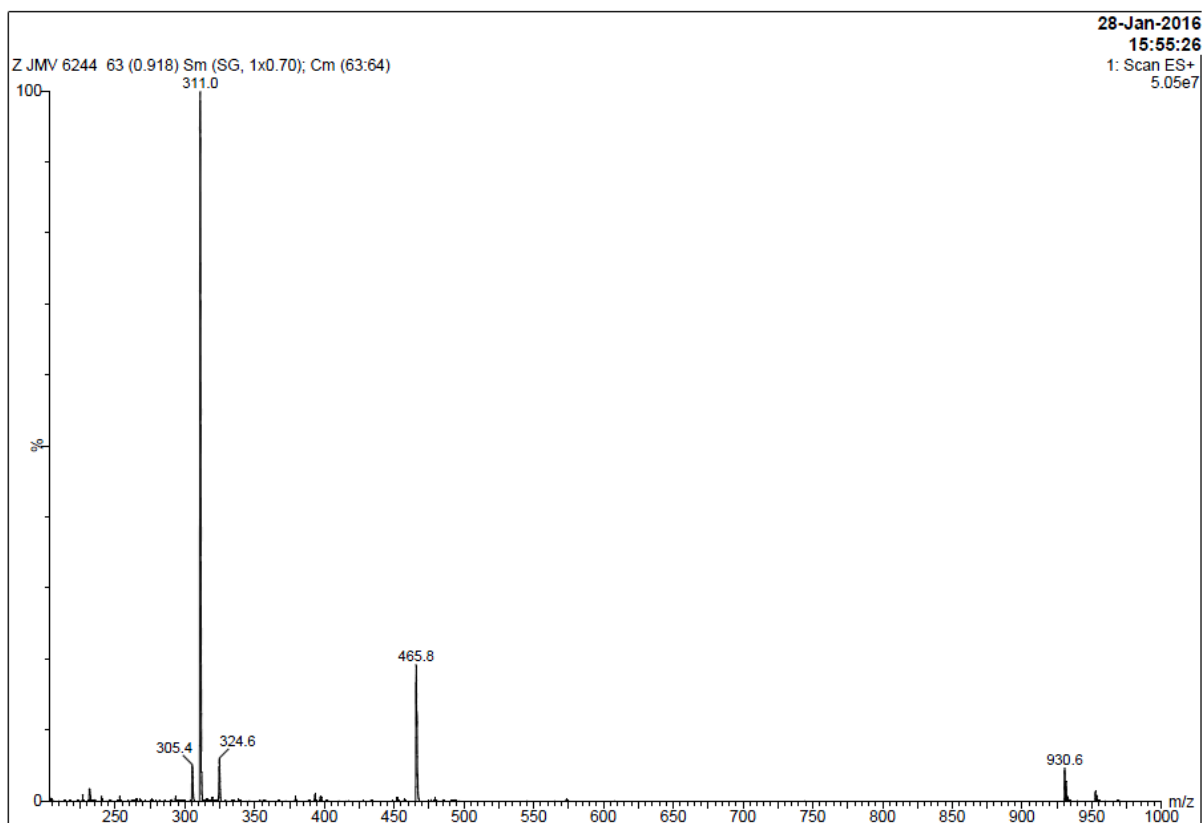


Figure S49. LC-MS spectrum of **11**

Supporting information for publication n°1
Homodimerization of unprotected peptides using hybrid hydroxydimethylsilane derivatives

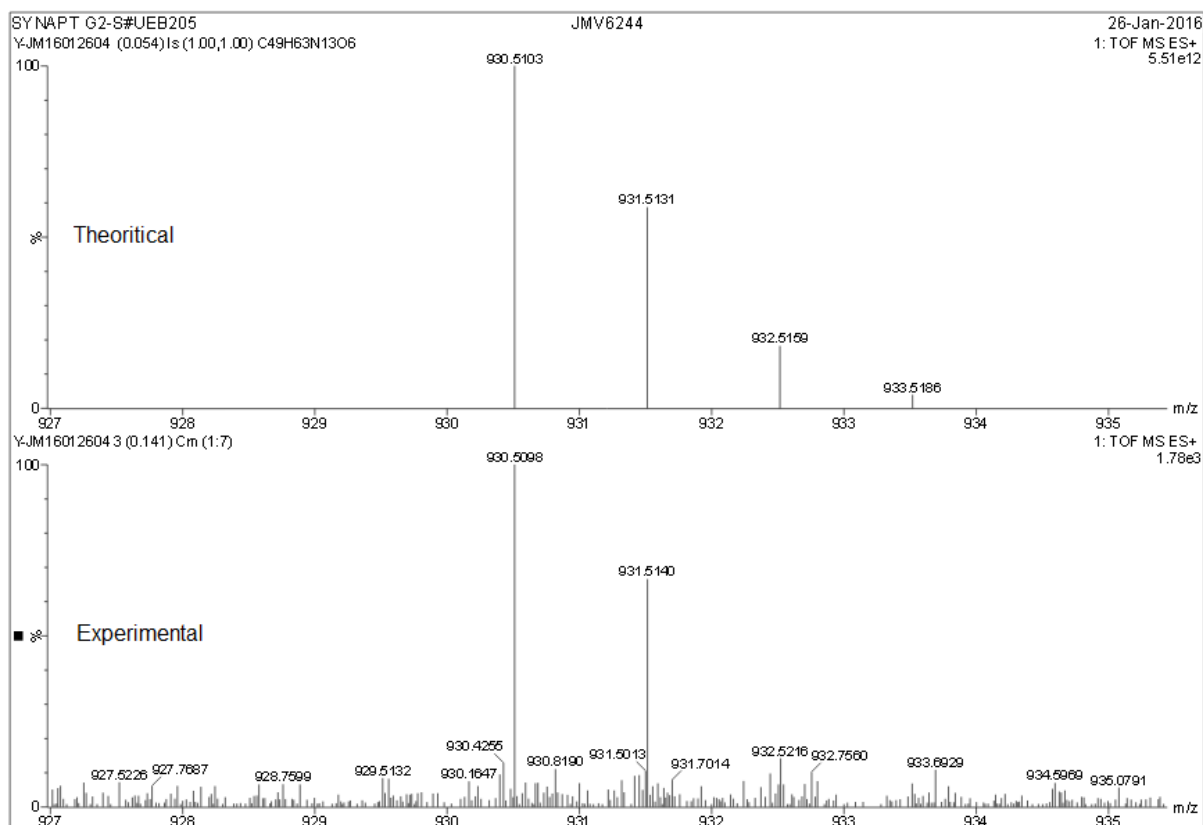
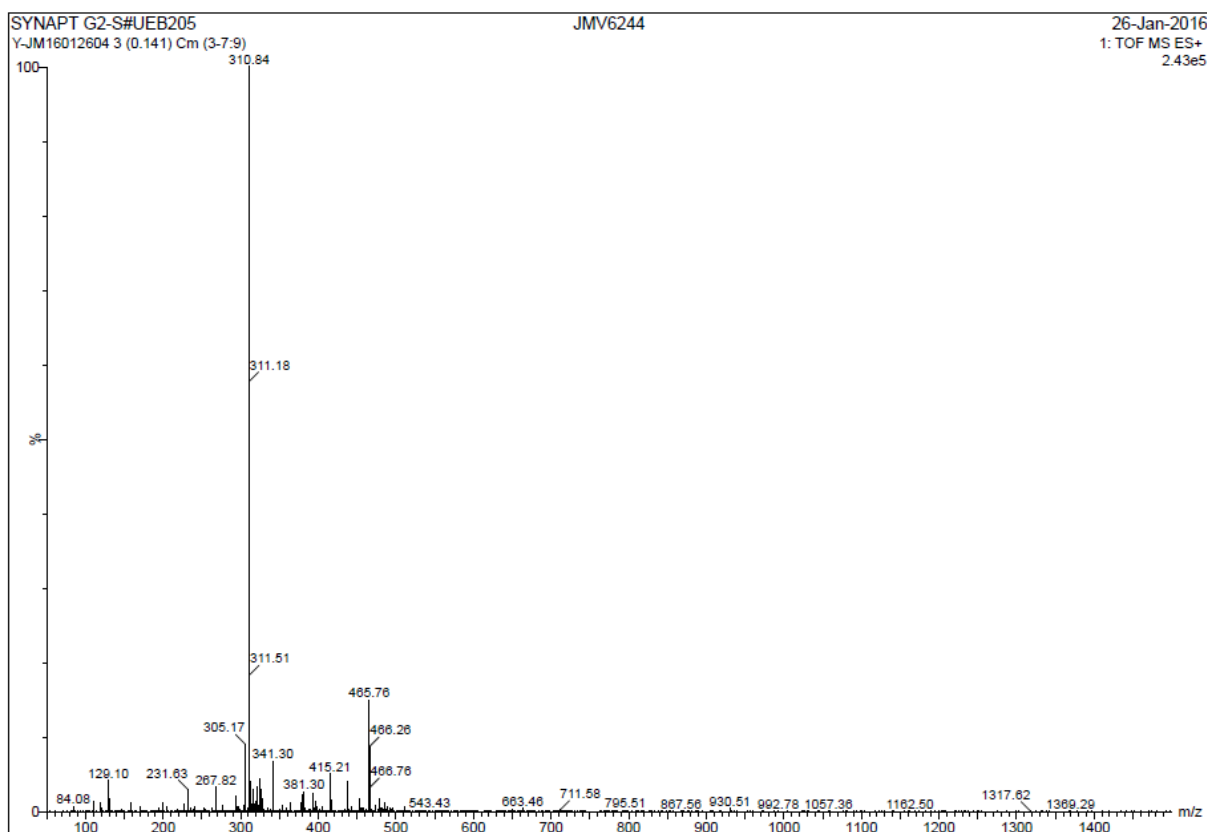
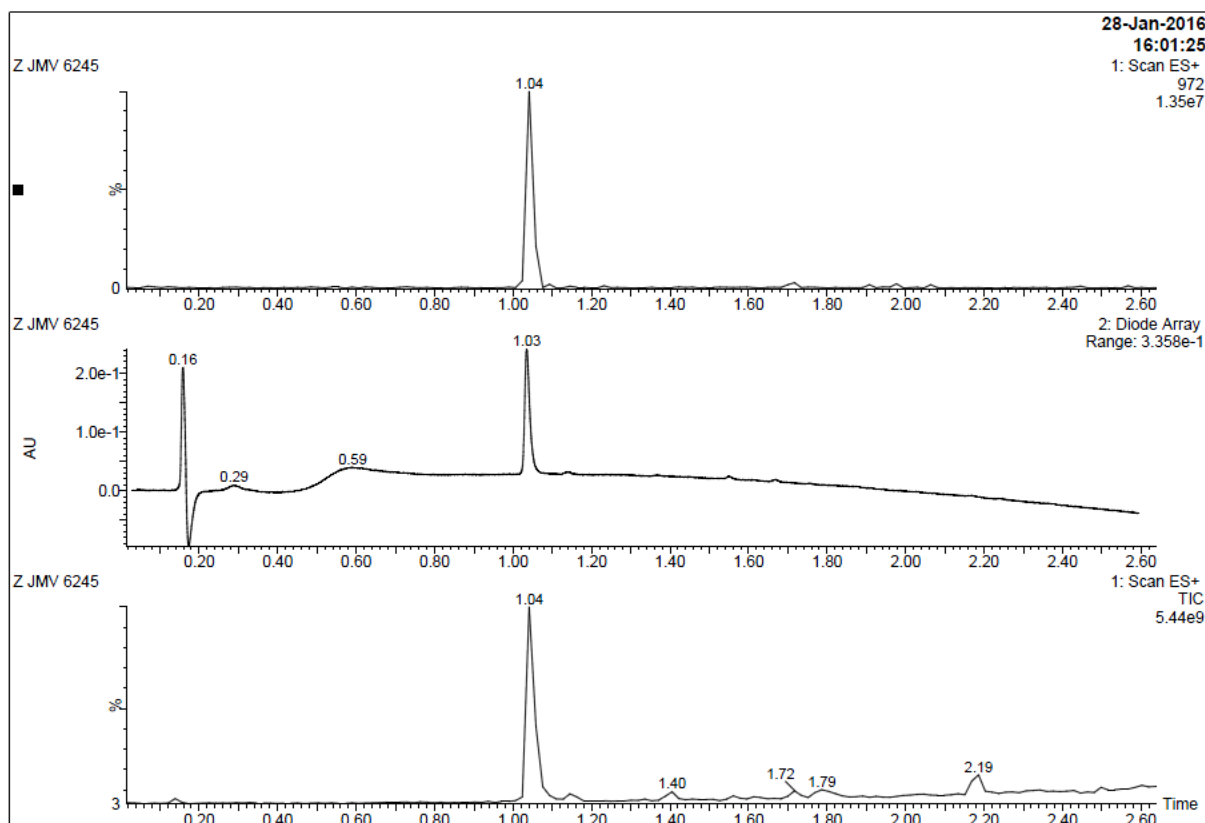
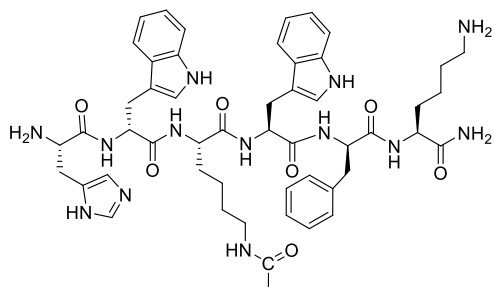


Figure S50. HR-MS analysis of 11

Lys³(Ac) monomer 12 (JMV 6245)



Supporting information for publication n°1
Homodimerization of unprotected peptides using hybrid hydroxydimethylsilane derivatives

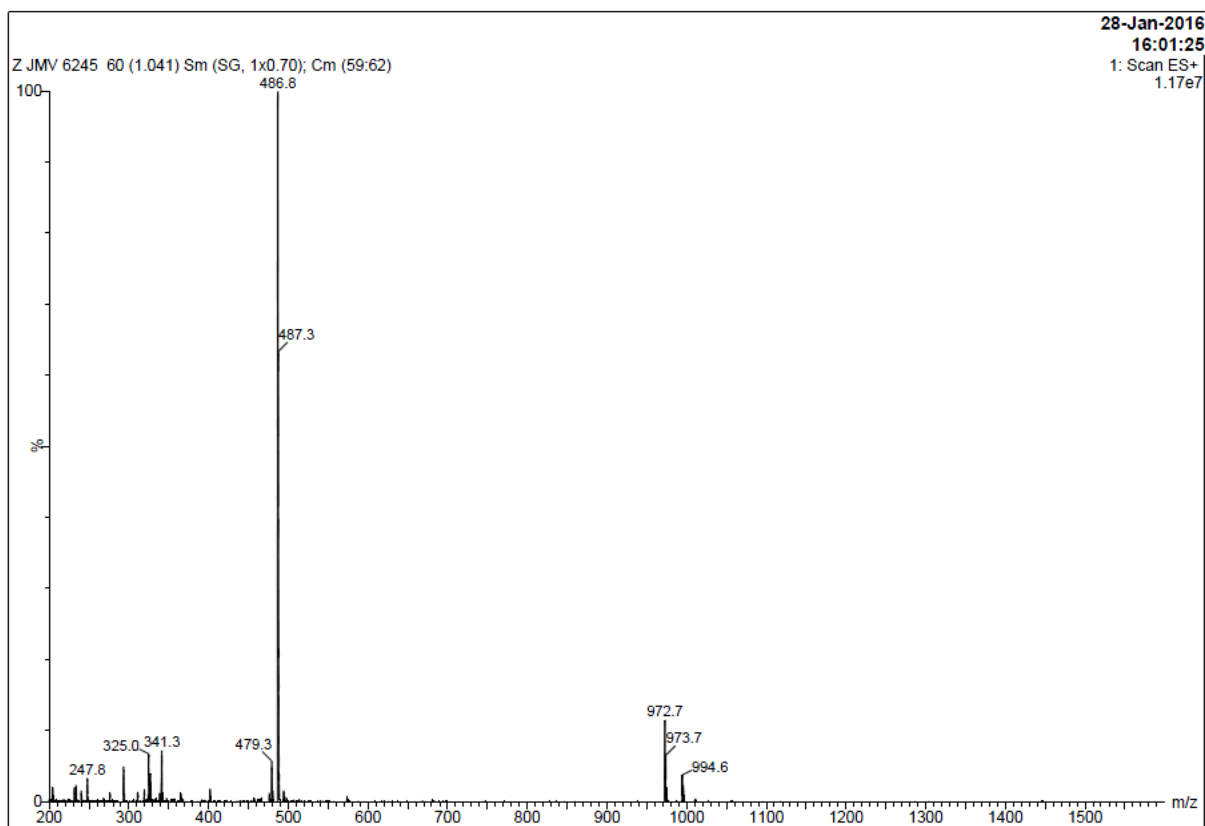


Figure S51. LC-MS spectrum of **12**

Supporting information for publication n°1
Homodimerization of unprotected peptides using hybrid hydroxydimethylsilane derivatives

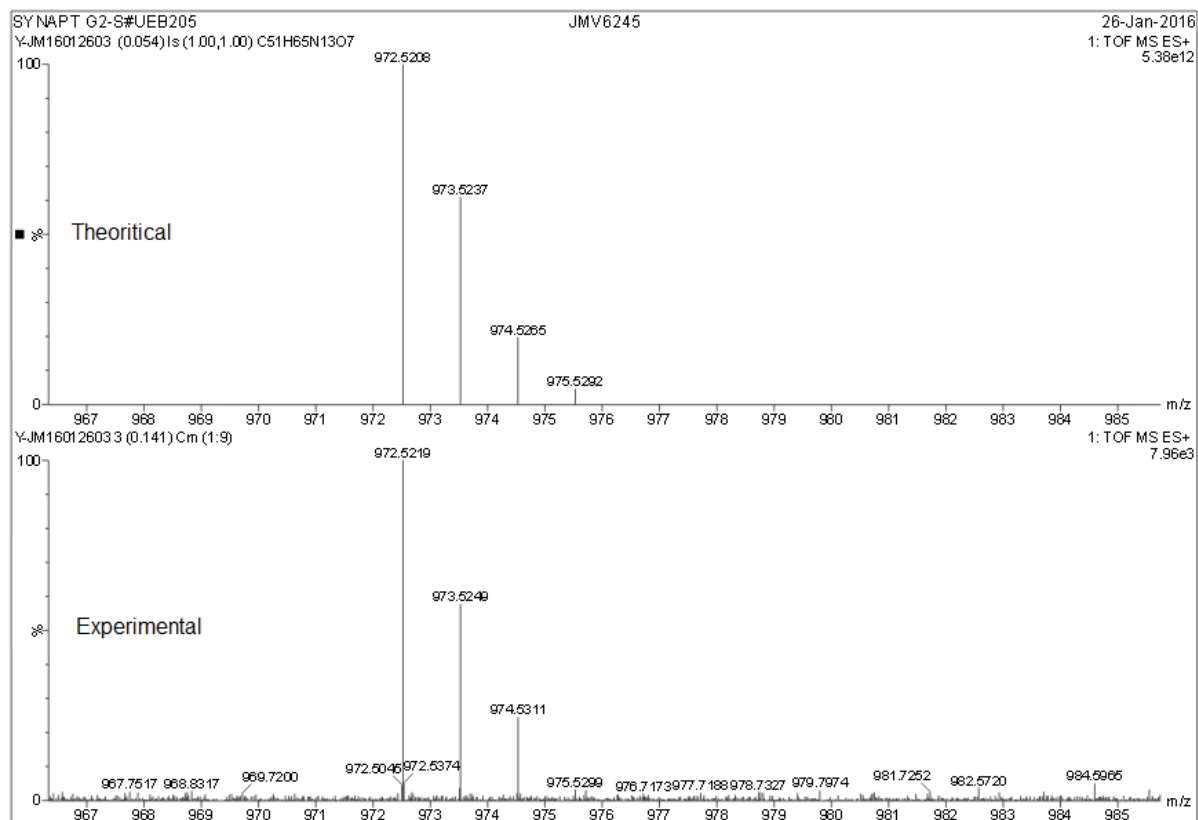
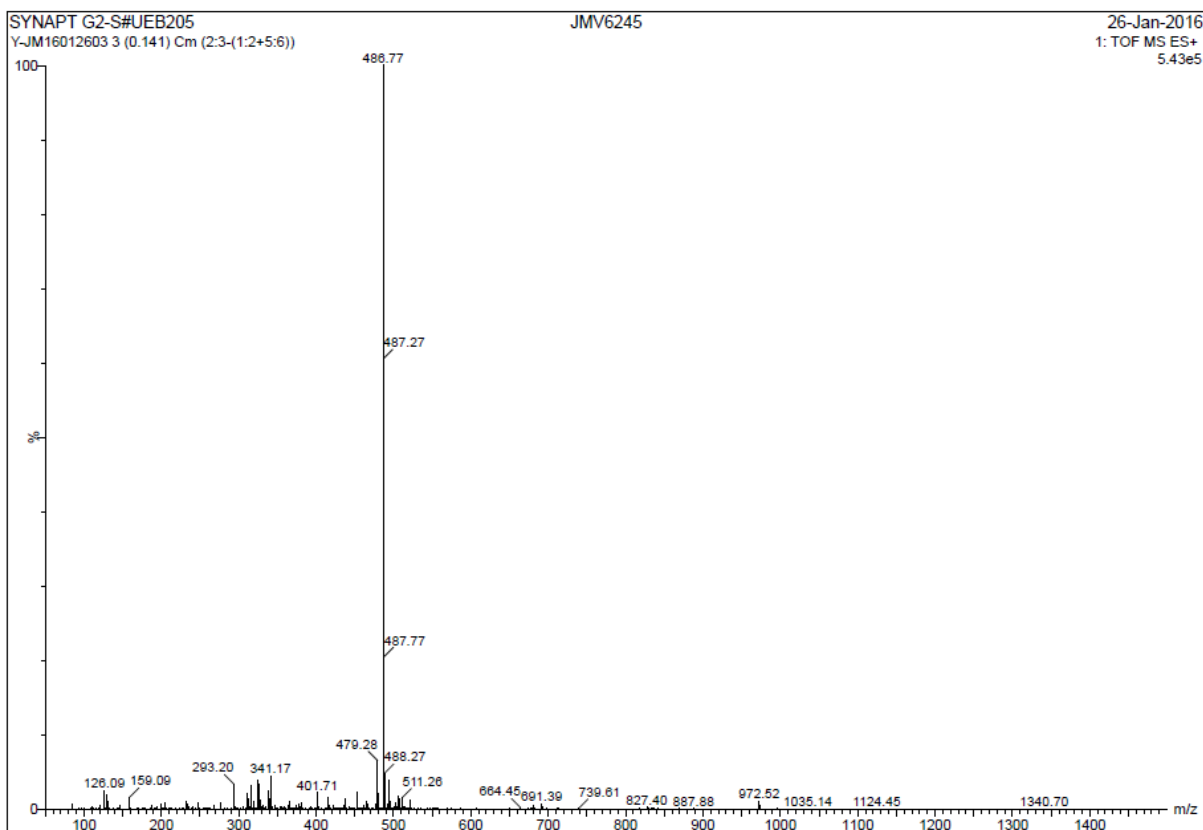


Figure S52. HR-MS spectrum of 12

Monomeric ligand binding assay

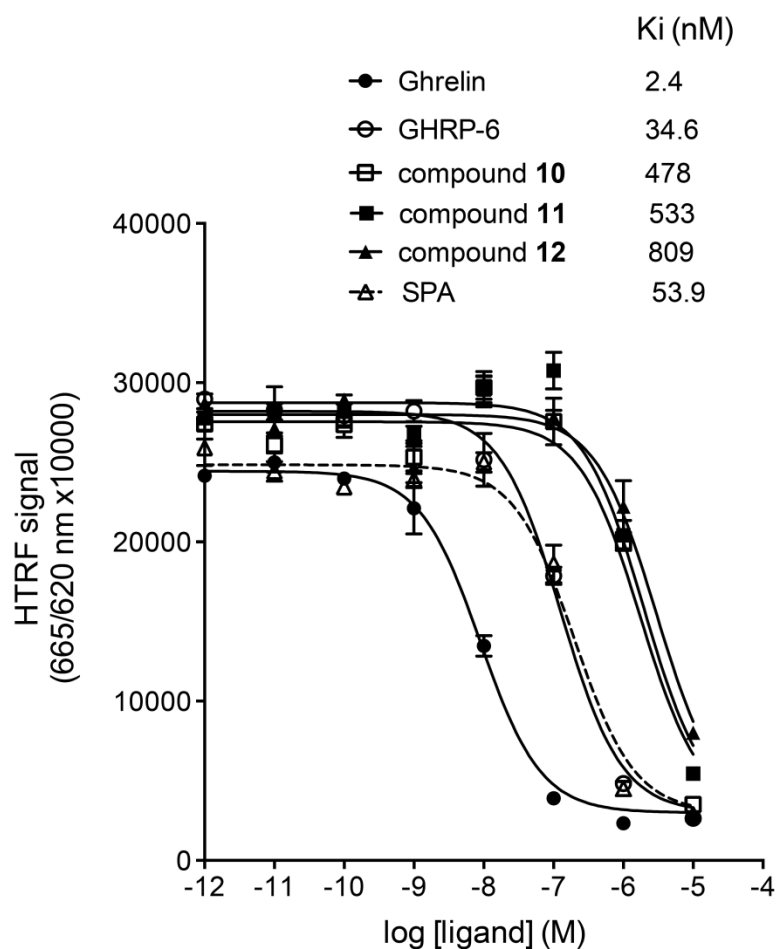


Figure S53. Binding of compounds 10, 11 and 12, monomeric analogues of dimer 9, to GHS-R1a. Ligands affinities were determined by HTRF-based competition binding assay performed on intact HEK293T cells as described in Materials and Methods. Results are from one representative experiment of two, each performed in triplicate.

Bioactivity of monomeric ligands

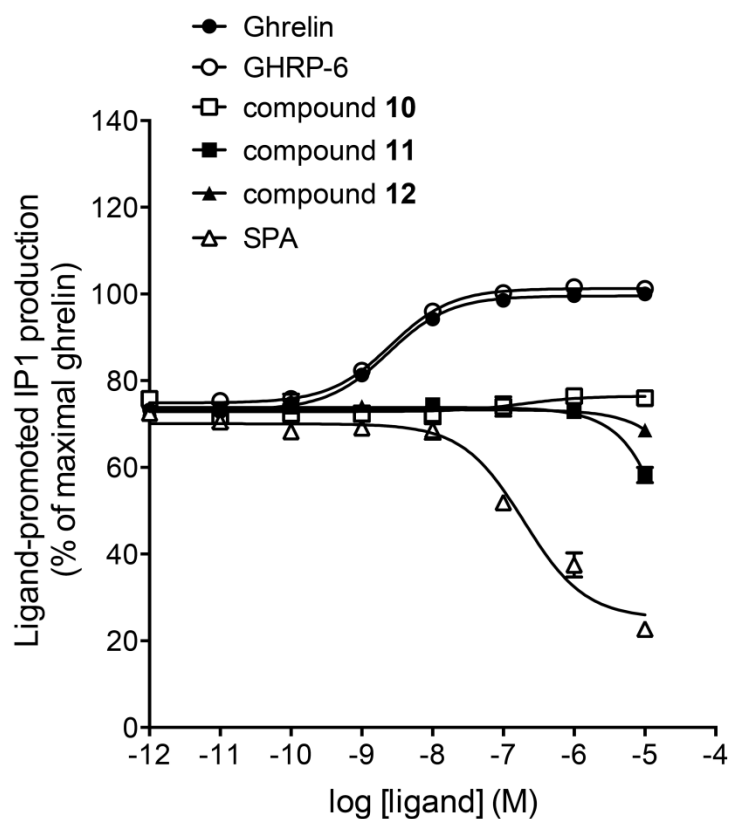


Figure S54. Signaling property of compounds 10, 11 and 12. Efficacy of ligands to stimulate IP1 production was measured on HEK293T cells expressing the GHS-R1a as described in Materials and Methods. Results are one representative experiment of two, each performed in triplicate.

Supporting information for publication n°2

An easy synthesis of tunable hybrid bioactive hydrogels

Cécile Echalier, Coline Pinese, Xavier Garric, Hélène Van Den Berghe, Estelle Jumas Bilak, Jean Martinez, Ahmad Mehdi,* Gilles Subra,*

Abbreviations.....	2
Material and Methods.....	2
Hybrid PEG 1	3
Hybrid PEG 1000	5
Hybrid PEG 6000	7
Peptide synthesis	9
Hybrid RGD peptide 2	9
Hybrid antibacterial peptide 3	12
Hybrid peptide 7	15
Non-silylated fluorescein 6	17
Triethoxysilyl fluorescein 4	20
Dimethylhydroxysilyl fluorescein 5	23
Hydrogel formation	27
Viscometry.....	27
Rheology	28
SEM images and BET	28
Cytotoxicity	29
Fluorescein release experience	29
Cell adhesion assays	30
Antibacterial assays	31

Supporting information for publication n°2
An easy synthesis of tunable hybrid bioactive hydrogels

Abbreviations

ACN, acetonitrile; Ahx, ϵ -aminohexanoic acid; Boc, t-utyloxycarbonyl; DCM, dichloromethane; CFU, colony-forming unit; DIEA, diisopropylethylamine; DMEM, Dulbecco's modified eagle medium; DMF, N,N'-dimethylformamide; DPBS, Dulbecco's phosphate buffered saline; ESI-MS, electrospray ionization mass spectrometry; Fmoc, fluorenylmethoxycarbonyl; HBTU, *N,N,N',N'*-tetramethyl-*O*-(1*H*-benzotriazol-1-yl)uronium hexafluorophosphate; HPLC, high performance liquid chromatography; HRMS, high resolution mass spectrometry; LC/MS, tandem liquid chromatography/ mass spectrometry; n. d., non determined; NMP, N-methyl-2-pyrrolidone; NMR, nuclear magnetic resonance; Pbf, 2,2,4,6,7-pentamethyldihydrobenzofuran-5-sulfonyl; PEG, polyethylene glycol; pip, piperidine; PLA, poly(L,D-lactic acid); PS, polystyrene; RT, room temperature; SPPS, solid phase peptide synthesis; TFA, trifluoroacetic acid; THF, tetrahydrofuran; TIS, triisopropylsilane; TSA, tryptic soy agar. Other abbreviations used were those recommended by the IUPAC-IUB Commission (Eur. J. Biochem. 1984, 138, 9-37).

Material and Methods

2-Chlorotriyl chloride resin (100-200 Mesh, 1.44 mmol Cl/g resin) and Fmoc-Rink Amide AM PS resin (100-200 Mesh, 0.94 mmol/g resin) were purchased from Iris Biotech and stored at 4°C. Protected amino acids and HBTU were purchased from Iris Biotech, Senn Chemicals and Bachem. PEG (MW = 2000 g/mol) was purchased from Alfa Aesar. All reagents and solvents were from Alfa Aesar, Acros, Sigma-Aldrich or Merck and were used without further purification.

Water sensitive reactions were carried out under an argon atmosphere with anhydrous solvents.

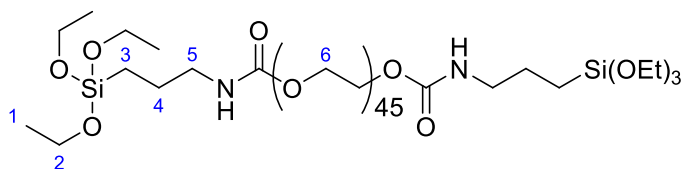
Preparative chromatographic purification was performed using Waters HPLC 4000 instrument, equipped with a UV detector 486 and Waters Delta-Pack 40×100 mm, 100Å, 15 µm, C₁₈ reversed-phase column using a flow rate of 50 mL/min. Solvents employed were water/0.1% TFA and ACN/0.1% TFA.

Samples for LC/MS analyses were prepared in acetonitrile/water (50:50, v/v) mixture, containing 0.1% TFA. The LC/MS system consisted of a Waters Alliance 2695 HPLC, coupled to a Water Micromass ZQ spectrometer (electrospray ionization mode, ESI+). All the analyses were carried out using a Phenomenex Onyx, 25 x 4.6 mm reversed-phase column. A flow rate of 3 mL/min and a gradient of (0-100)% B over 2.5 min were used. Eluent A: water/0.1% HCO₂H; eluent B: acetonitrile/0.1% HCO₂H. UV detection was performed at 214 nm. Electrospray mass spectra were acquired at a solvent flow rate of 200 µL/min. Nitrogen was used for both the nebulizing and drying gas. The data were obtained in a scan mode ranging from 100 to 1000 m/z or 250 to 1500 m/z to in 0.7 sec intervals. High Resolution Mass Spectrometric analyses were performed with a time of flight (TOF) mass spectrometer fitted with an Electrospray Ionisation source. All measurements were performed in the positive ion mode.

¹H, ¹³C and ²⁹Si NMR spectra were recorded at room temperature in deuterated solvents on a Bruker AMX/400 spectrometer operating at 400, 101 and 79 MHz respectively. Chemical shifts (δ) are reported in parts per million using residual non-deuterated solvents as internal references (CHCl₃ in CDCl₃, δ H = 7.26 ppm; DMSO-d₆, δ H = 2.50 ppm). Signals are indicated as s (singlet), d (doublet), t (triplet), q (quartet), dt (double triplet), m (multiplet), br (broad)... Coupling constants are measured in Hertz.

Supporting information for publication n°2
An easy synthesis of tunable hybrid bioactive hydrogels

Hybrid PEG 1 synthesis

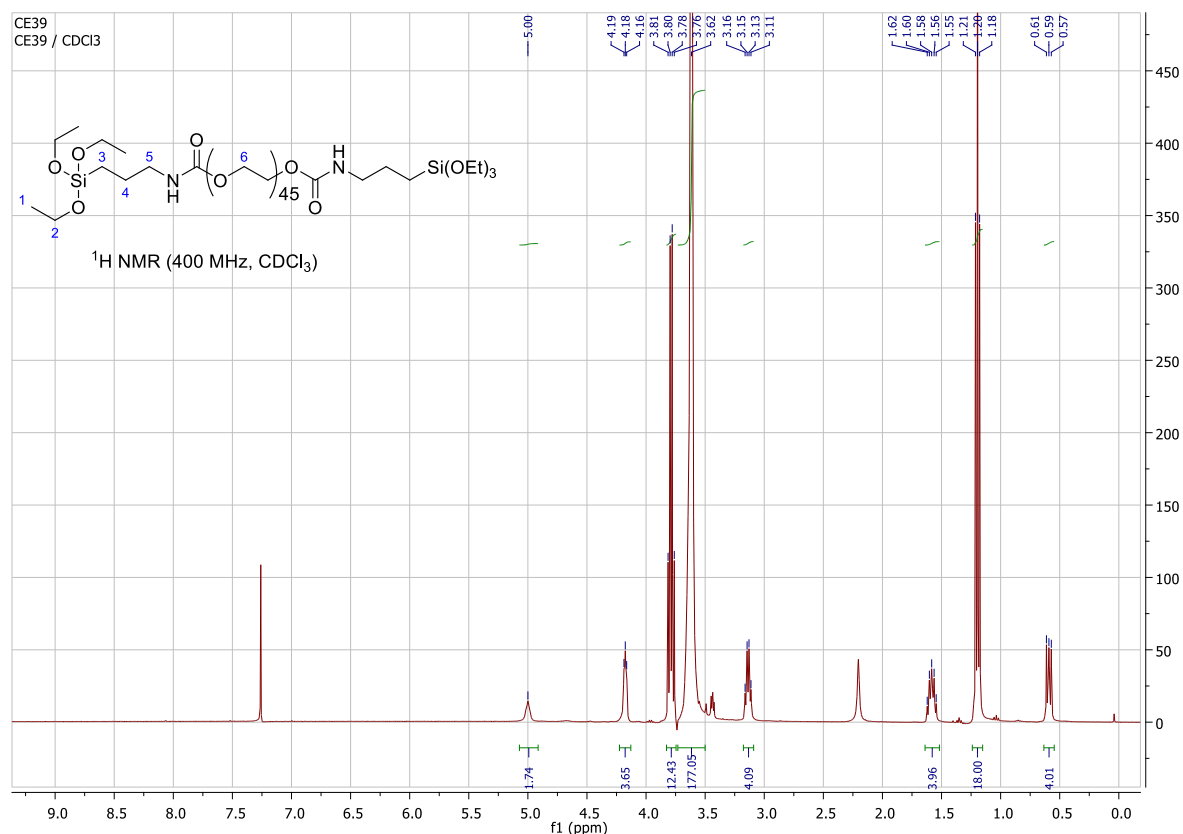


Polyethylene glycol 2000 (2.00 g, 1.00 mmol) was vacuum-dried overnight at 80°C and dissolved in anhydrous THF (12 mL) under argon. Triethylamine (1.66 mL, 12 mmol, 12 eq) and isocyanatopropyltriethoxysilane (744 μ L, 3 mmol, 3 eq) were added. The mixture was heated under reflux for 48 h. Then the solvents were removed under reduced pressure and the reaction mixture was precipitated in hexane. The white solid was washed 3 times with hexane and vacuum-dried. Hybrid PEG was then stored at 4°C under argon.

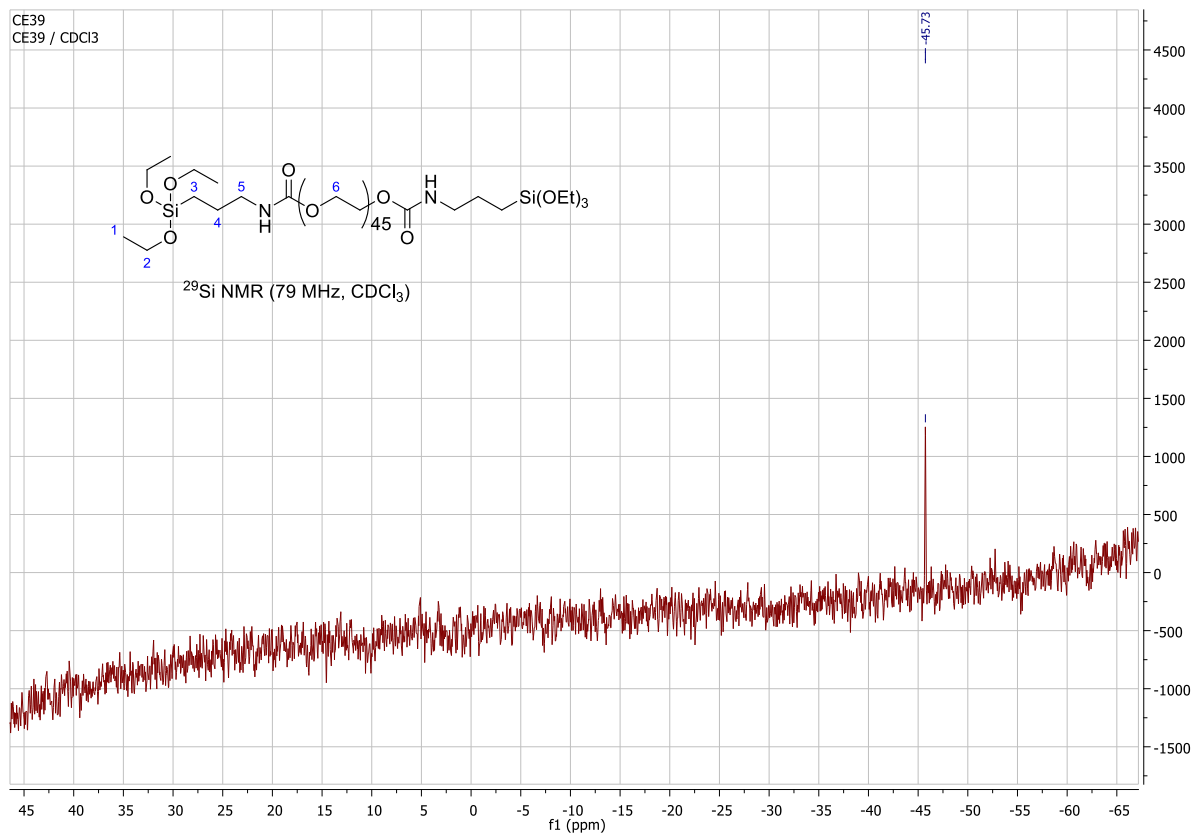
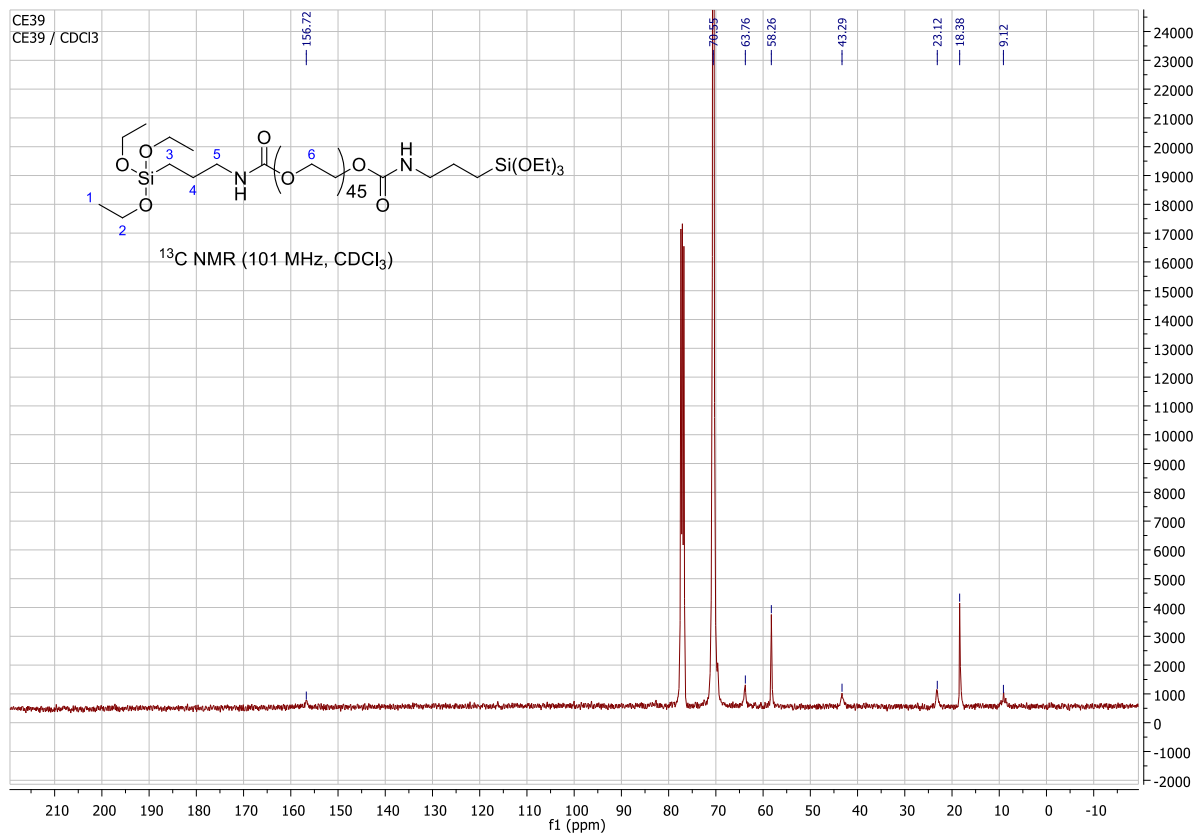
^1H NMR (400 MHz, CDCl_3) δ 5.00 (br s, 2H, NH), 4.18 (t, $J = 4.7$ Hz, 4H, H-6), 3.79 (q, $J = 7.0$ Hz, 12H, H-2), 3.62 (s, 177H, CH_2 PEG), 3.14 (dd, $J = 13.2, 6.7$ Hz, 4H, H-5), 1.58 (qu, $J = 7.7$ Hz, 4H, H-4), 1.20 (t, $J = 7.0$ Hz, 18H, H-1), 0.64 – 0.54 (m, 4H, H-3).

^{13}C NMR (101 MHz, CDCl_3) δ 156.72 (C), 70.55 (CH_2), 63.76 (CH_2), 58.26 (CH_2), 43.29 (CH_2), 23.12 (CH_2), 18.38 (CH_3), 9.12 (CH_2).

^{29}Si NMR (79 MHz, CDCl_3) δ -45.73 (s).

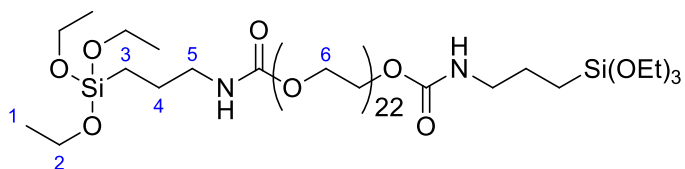


Supporting information for publication n°2
An easy synthesis of tunable hybrid bioactive hydrogels



Supporting information for publication n°2
An easy synthesis of tunable hybrid bioactive hydrogels

Hybrid PEG 1000

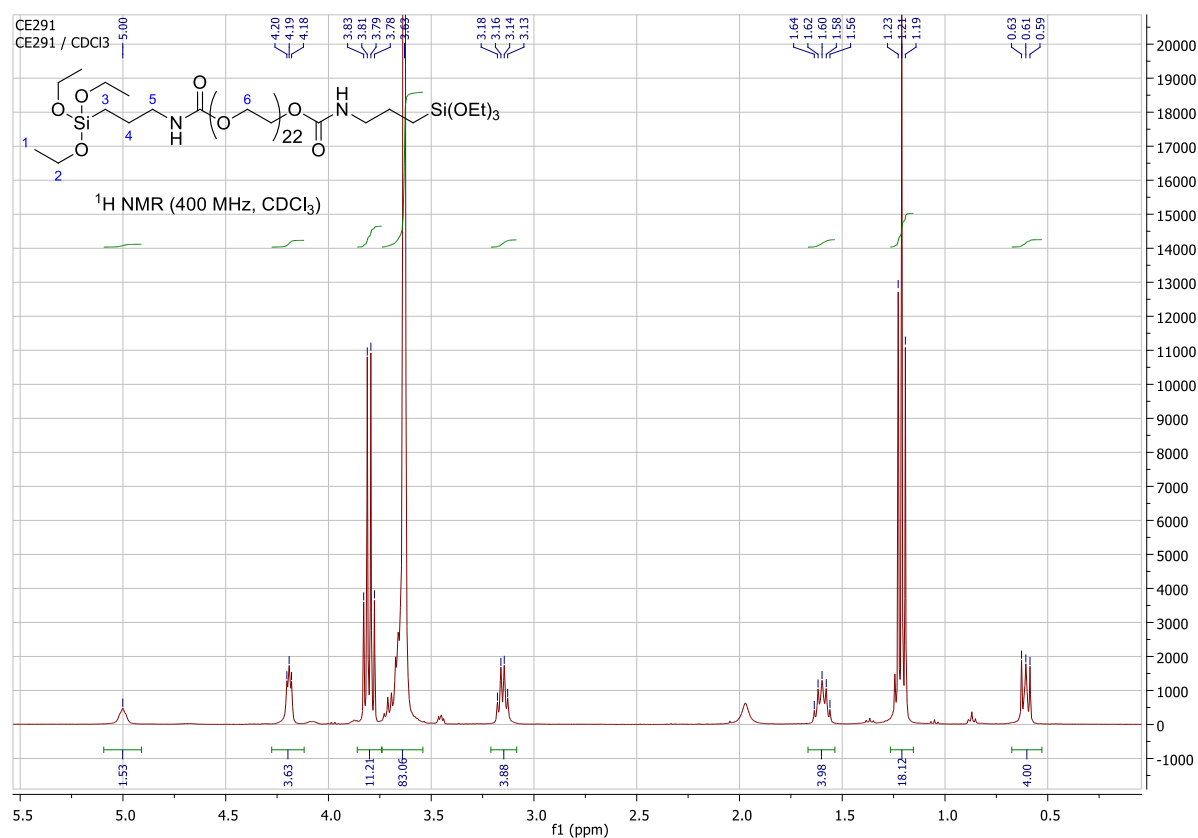


Hybrid PEG 1000 was prepared with the same experimental procedure as hybrid PEG 1 (2000).

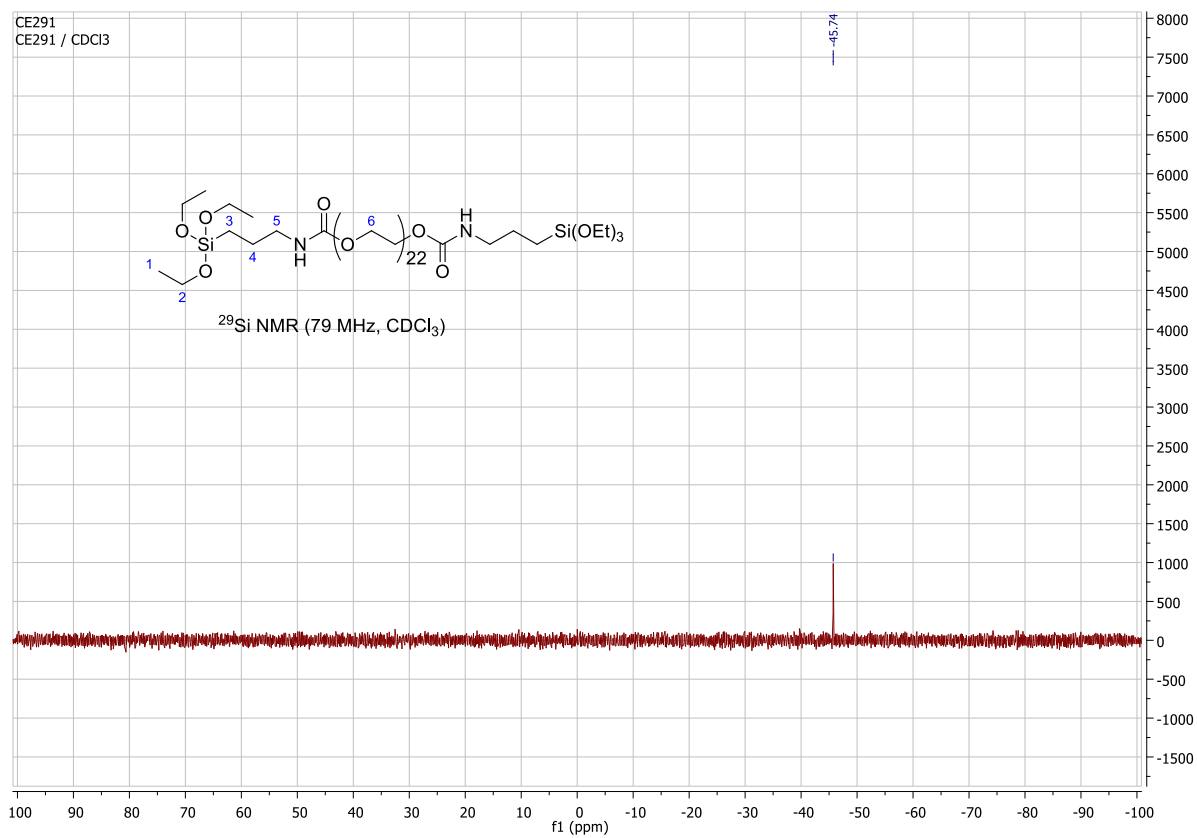
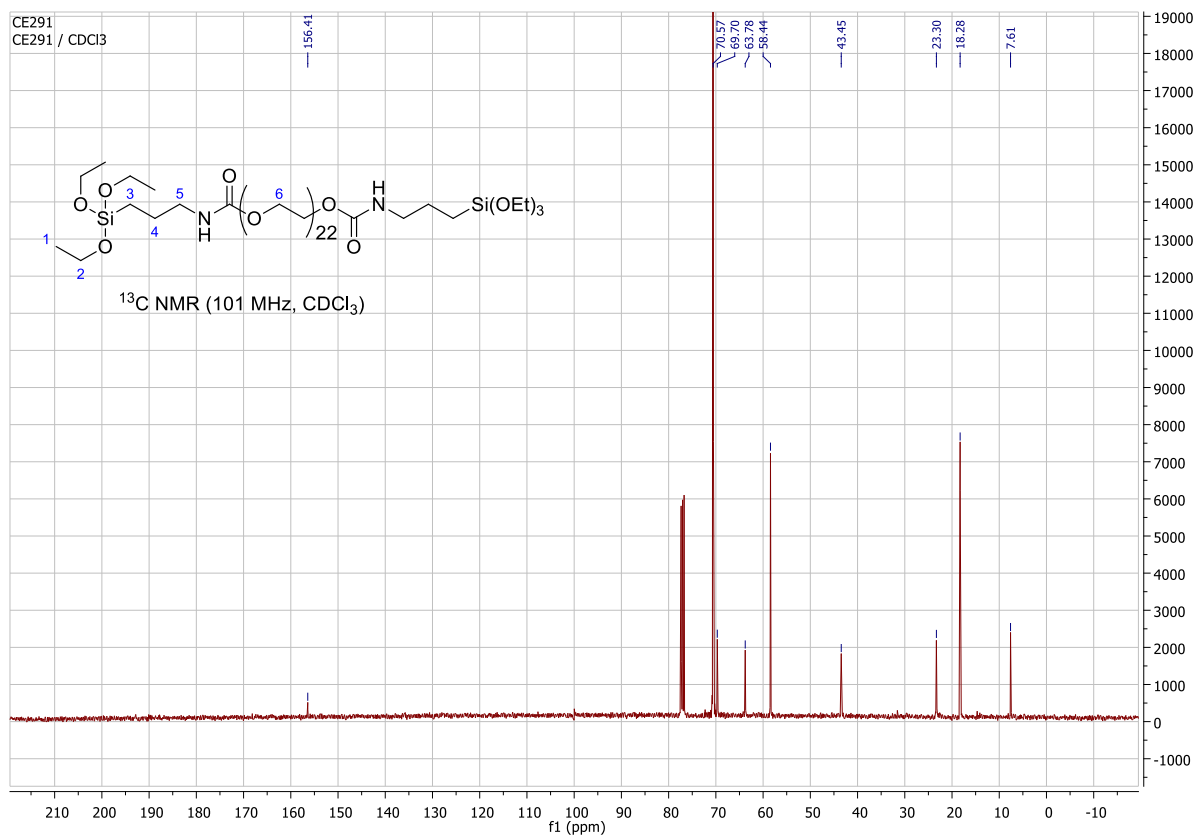
^1H NMR (400 MHz, CDCl_3) δ 5.00 (br s, 2H, NH), 4.19 (t, $J = 4.7$ Hz, 4H, H-6), 3.80 (q, $J = 7.0$ Hz, 12H, H-2), 3.63 (s, 83H, CH_2 PEG), 3.15 (dd, $J = 13.2, 6.7$ Hz, 4H, H-5), 1.60 (qu, $J = 7.7$ Hz, 4H, H-4), 1.21 (t, $J = 7.0$ Hz, 18H, H-1), 0.63 – 0.59 (m, 4H, H-3).

^{13}C NMR (101 MHz, CDCl_3) δ 156.41 (s), 70.57 (s), 69.70 (s), 63.78 (s), 58.44 (s), 43.45 (s), 23.30 (s), 18.28 (s), 7.61 (s).

^{29}Si NMR (79 MHz, CDCl_3) δ -45.74 (s).

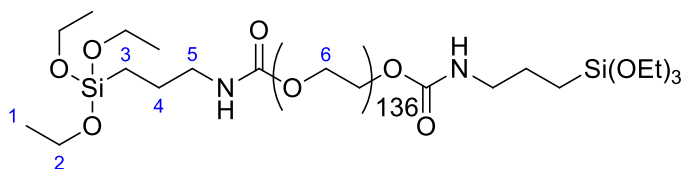


Supporting information for publication n°2
An easy synthesis of tunable hybrid bioactive hydrogels



Supporting information for publication n°2
An easy synthesis of tunable hybrid bioactive hydrogels

Hybrid PEG 6000

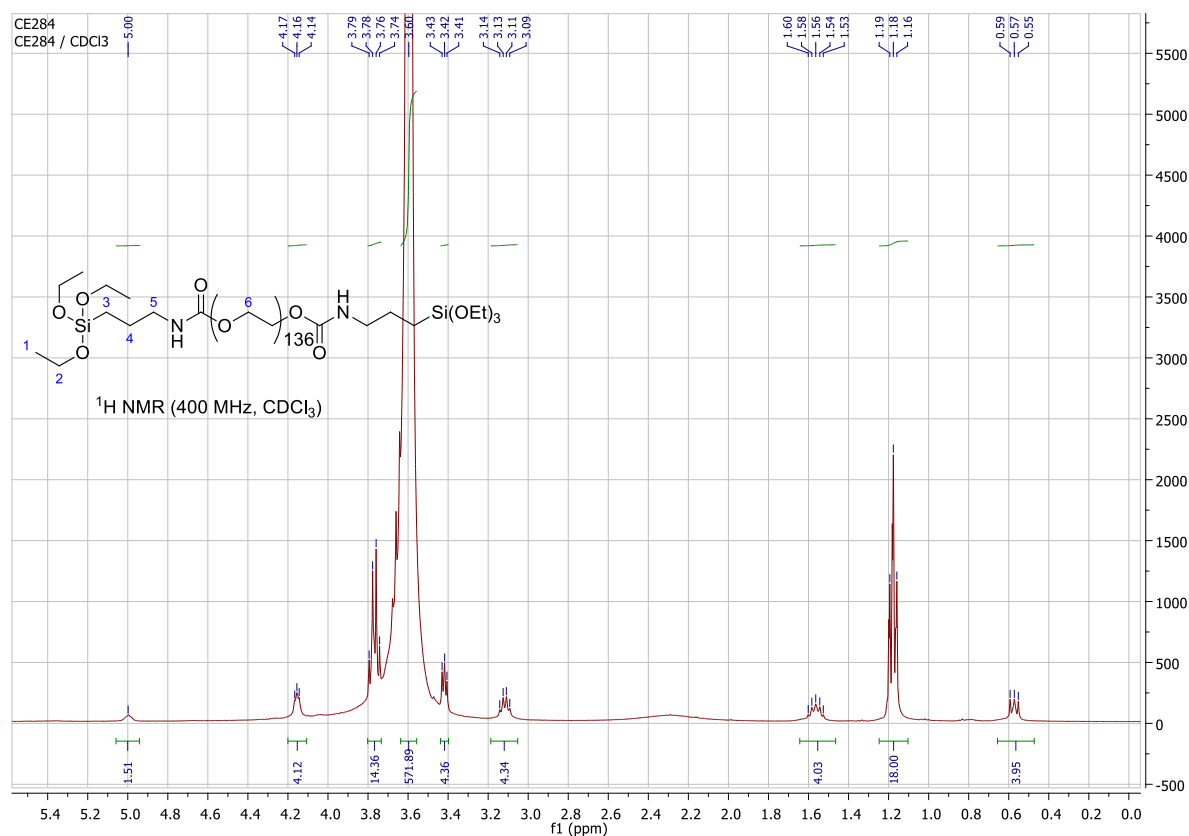


Hybrid PEG 6000 was prepared with the same experimental procedure as hybrid PEG 1 (2000).

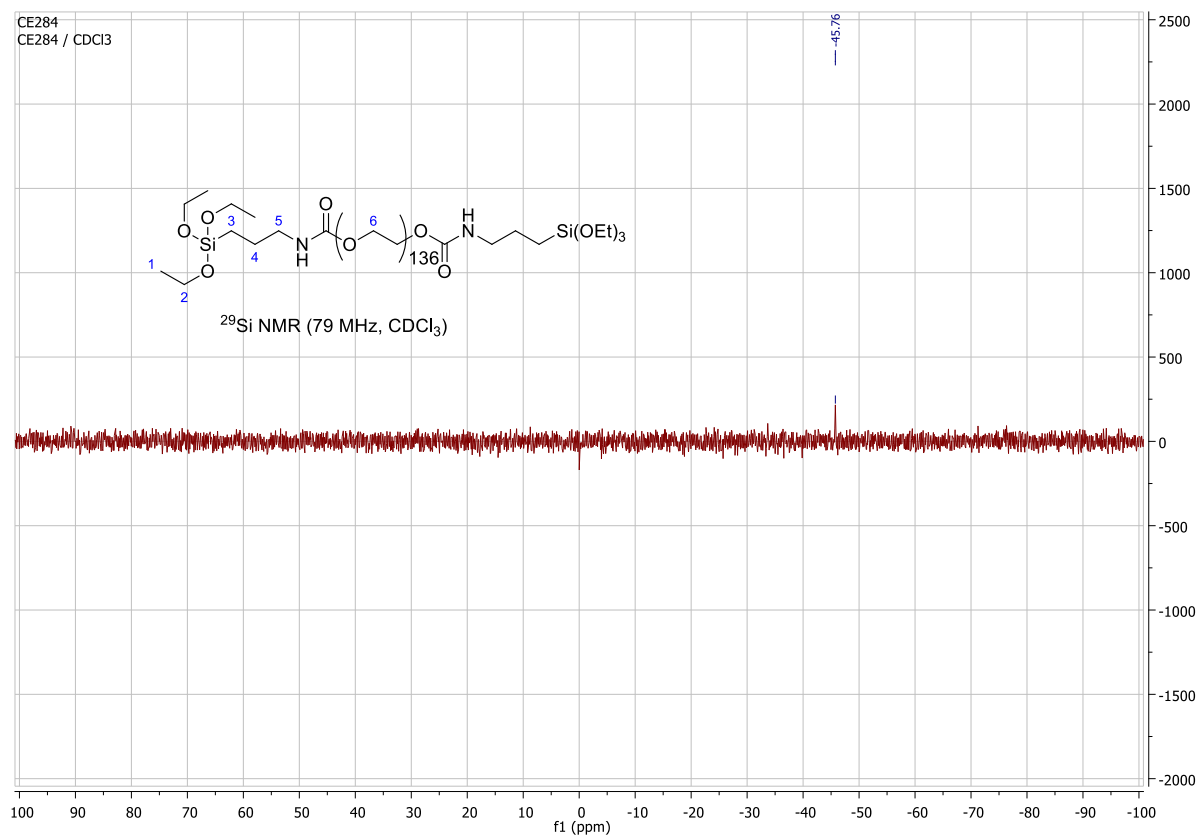
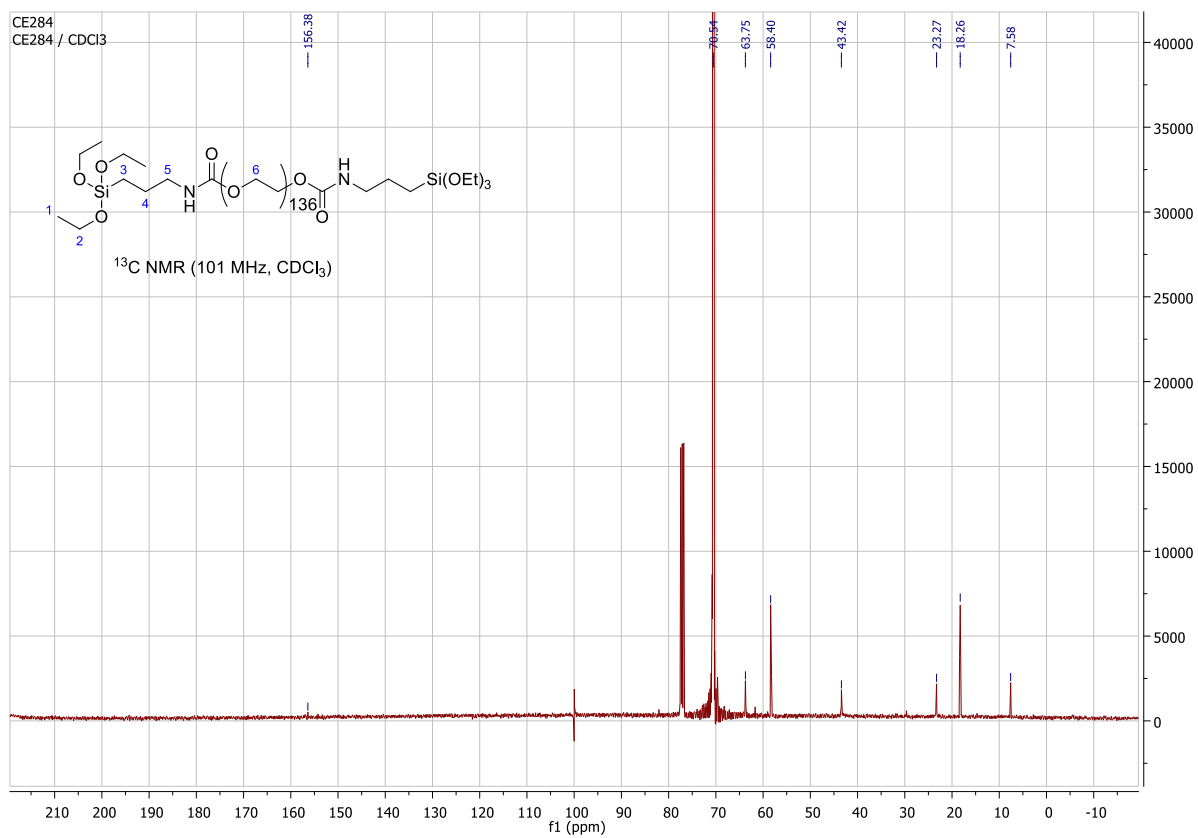
^1H NMR (400 MHz, CDCl_3) δ 5.00 (br s, 2H, NH), 4.16 (t, $J = 4.7$ Hz, 4H, H-6), 3.77 (q, $J = 7.0$ Hz, 12H, H-2), 3.60 (s, 544H, CH_2 PEG), 3.42 (t, $J = 4.9$ Hz, 4H, CH_2 PEG), 3.12 (dd, $J = 13.2, 6.7$ Hz, 4H, H-5), 1.56 (qu, $J = 7.7$ Hz, 4H, H-4), 1.18 (t, $J = 7.0$ Hz, 18H, H-1), 0.59 – 0.55 (m, 4H, H-3).

^{13}C NMR (101 MHz, CDCl_3) δ 156.38 (s), 70.54 (s), 63.75 (s), 58.40 (s), 43.42 (s), 23.27 (s), 18.26 (s), 7.58 (s).

^{29}Si NMR (79 MHz, CDCl_3) δ -45.76 (s).



Supporting information for publication n°2
An easy synthesis of tunable hybrid bioactive hydrogels



Supporting information for publication n°2
An easy synthesis of tunable hybrid bioactive hydrogels

Peptide synthesis

Fmoc-AA-OH anchoring on 2 chlorotriyl chloride resin

2-Chlorotriyl chloride resin (1.44 mmol Cl/g, 1eq) was placed in a solid-phase peptide synthesis flask fitted with a sintered glass. Fmoc-AA-OH (3 eq) was anchored to the resin in the presence of DIEA (5 eq) in DMF overnight. After standard washing steps using the following solvents (3×DMF, 1×MeOH and 1×DCM), Fmoc-AA-Cltrityl-resin was dried under vacuum for 12 h. Resin loading was determined by detection of piperidine-dibenzofulvene adduct from pip/DMF deprotection solution at 299 nm. A loading of 0.4 mmol/g was obtained for Fmoc-Pro-Cltrityl-resin.

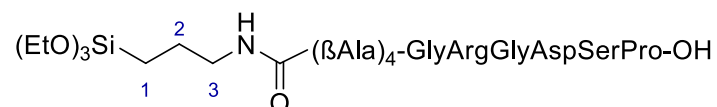
Fmoc deprotection

Fmoc-Rink Amide AM PS resin or Fmoc-peptidyl-resin was placed in a solid-phase peptide synthesis flask fitted with a glass sintered. Fmoc group was removed by two successive DMF-piperidine (80:20; v/v) treatments (2 x 20'). Between the two treatments, solution was filtered off and replaced by a new one. Standard washing steps were realized at the end of deprotection.

Standard protected aminoacid coupling step

The appropriate Fmoc-protected amino acid (3 eq.) was dissolved in DMF (75% of reactor volume) in presence of HBTU (3 eq.) and DIEA (3 eq.) for 10 min. This solution was then added to the free N-terminus peptidyl resin and placed under stirring at room temperature for 1 h 30' before washing steps.

Hybrid RGD peptide 2 synthesis: (EtO)₃Si-(CH₂)₃-NHCO-(βAla)₄GlyArgGlyAspSerPro-OH



H-(βAla)₄GlyArgGlyAspSerPro-OH was synthesized on 2-chlorochlorotriyl resin in Fmoc-SPPS strategy. Amino acid used were successively Fmoc-Pro-OH, Fmoc-Ser(tBu)-OH, Fmoc-Asp(tBu)-OH, Fmoc-Gly-OH, Fmoc-Arg(Pbf)-OH, Fmoc-Gly-OH and Fmoc-βAla-OH four times. Cleavage and side chain deprotection were realized in trifluoroacetic acid/triisopropylsilane/water 95/2.5/2.5 V/V/V for 4h. After precipitation, the peptide was purified on preparative HPLC (63%). Then, it was reacted with 3-isocyanatopropyltriethoxysilane (1,1 eq) in DMF at a concentration of 30 mM in presence of DIEA (3 eq). After concentration of the reaction mixture, the hybrid peptide was obtained by precipitation and washings with diethylether.

¹H NMR (400 MHz, DMSO-d₆) δ 8.61 – 8.40 (m, 2H, NH Asp and Gly), 8.21 – 8.04 (m, 2H, NH Gly N-ter and Arg), 7.99 – 7.78 (m, 3H, NH βAla), 7.58 – 7.42 (m, 1H, NH Ser), 7.34 – 6.98(m, 3H, OH Ser, COOH Asp and C-ter), 5.97 (t, J = 5.6 Hz, 1H, NH urea), 5.78 (t, J = 5.6 Hz, 1H, NH urea βAla), 4.56 (q, J = 6.9 Hz, 1H, H_α Ser), 4.49 – 4.38 (m, 1H, H_α Asp), 4.38 – 4.26 (m, 1H, H_α Arg), 4.22 (dd, J = 8.7, 4.1 Hz, 1H, H_α Pro), 4.02 – 3.75 (m, 4H, H_α Gly), 3.73 (q, J = 6.9 Hz, 6H, CH₂ ethoxy), 3.67 – 3.46 (m, 4H, H_δ Pro and H_β Ser), 3.46 – 3.28 (m, 2H, H_δ Arg), 3.28 – 3.11 (m, 8H, H_β βAla), 2.92 (q, J = 6.1 Hz, 2H, H-3), 2.60 – 2.48 (m, 2H, H_β Asp), 2.29 (t, J = 7.1 Hz, 2H, H_α βAla), 2.26 – 2.09 (m, 6H, H_α βAla), 1.87 (dd, J = 13.3, 6.5 Hz, 2H, H_γ Pro), 1.60 – 1.56 (m, 2H, H_β Arg), 1.55 – 1.42 (m, 2H, H_δ Arg), 1.38 (m, 2H, H-2), 1.19 – 1.09 (t, J = 7.2 Hz, 9H, CH₃ ethoxy), 0.55 – 0.42 (m, 2H, H-1).

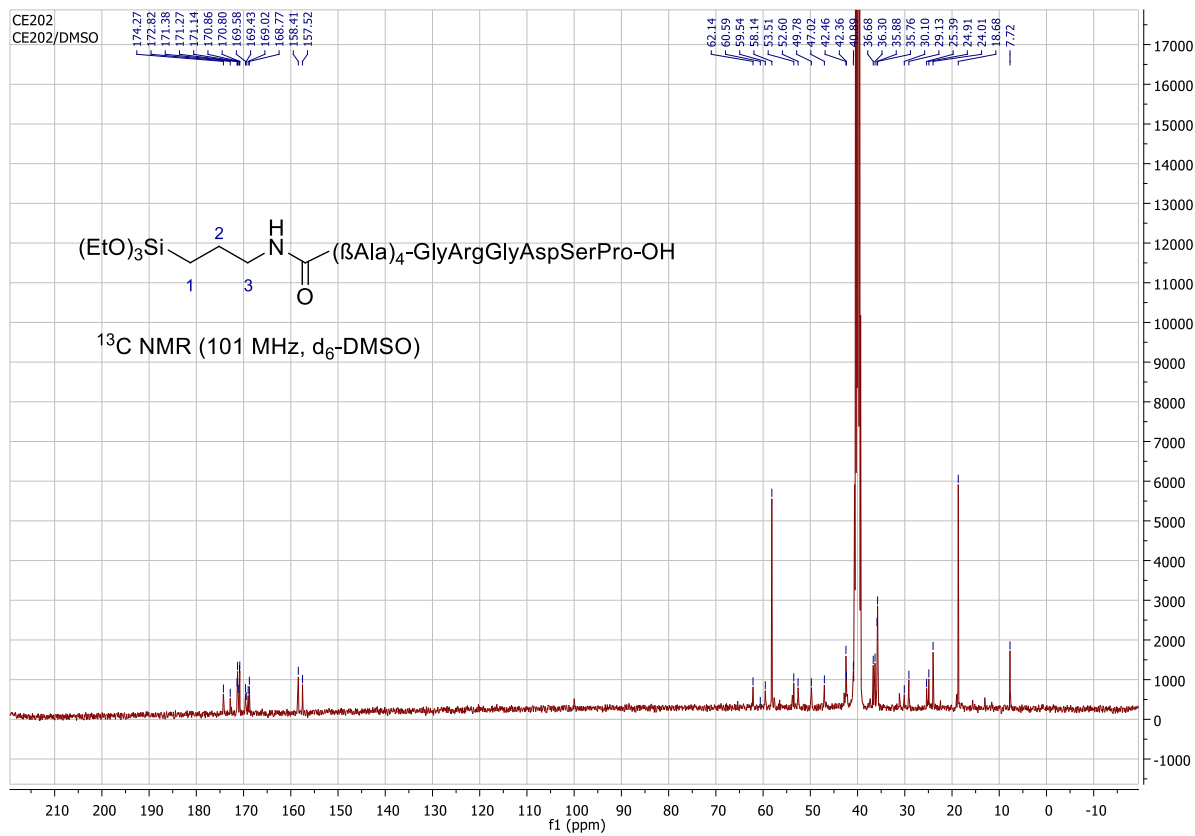
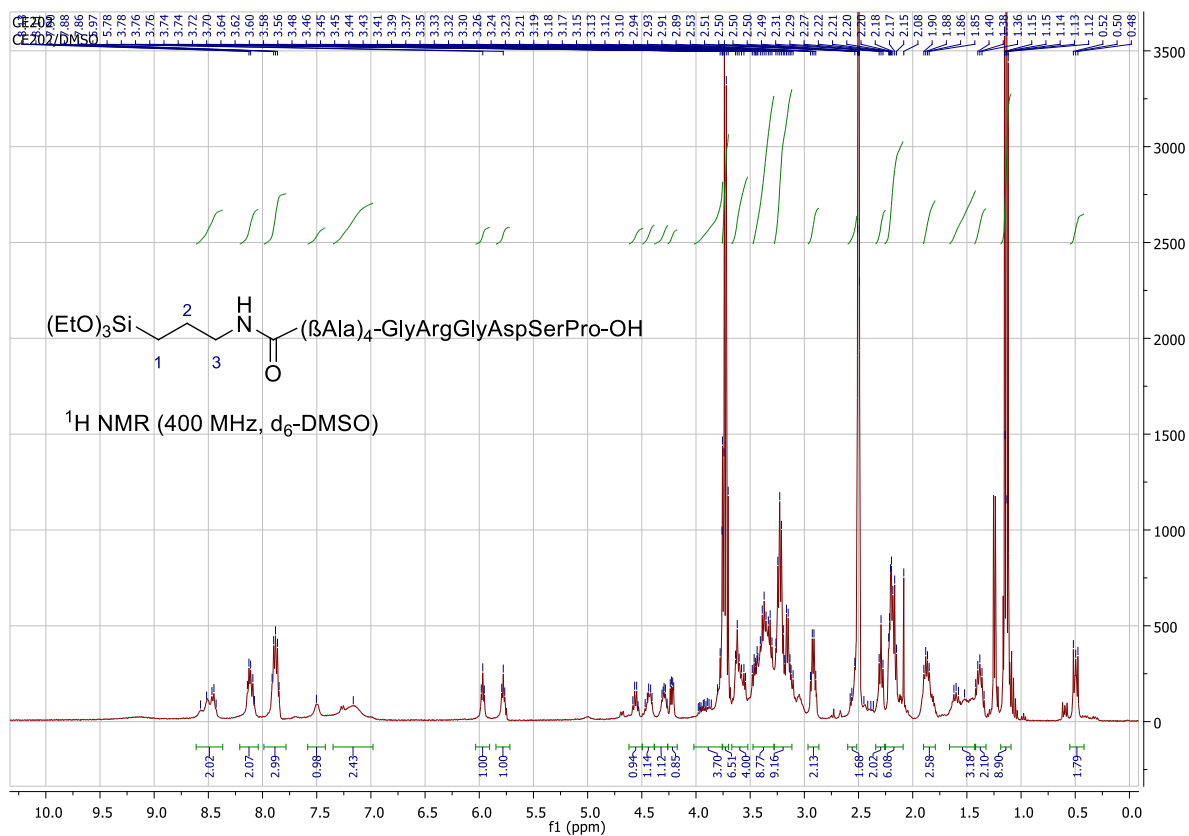
¹³C NMR (101 MHz, DMSO-d₆) δ 174.27 (C), 172.82 (C), 171.38 (C), 171.27 (C), 171.14 (C), 170.86 (C), 170.80 (C), 169.58 (C), 169.43 (C), 169.02 (C), 168.77 (C), 158.41 (C), 157.52 (C), 62.14 (CH₂), 59.54 (CH), 58.14 (CH₂), 53.51 (CH), 52.60 (CH), 49.78 (CH), 47.02 (CH₂), 42.46 (CH₂), 42.36 (CH₂), 40.89 (CH₂), 36.68 (CH₂), 36.30 (CH₂), 35.88 (CH₂), 35.76 (CH₂), 30.10 (CH₂), 29.13 (CH₂), 25.39 (CH₂), 24.91 (CH₂), 24.01 (CH₂), 18.68 (CH₃), 7.72 (CH₂).

²⁹Si NMR (79 MHz, DMSO-d₆) δ -45.10.

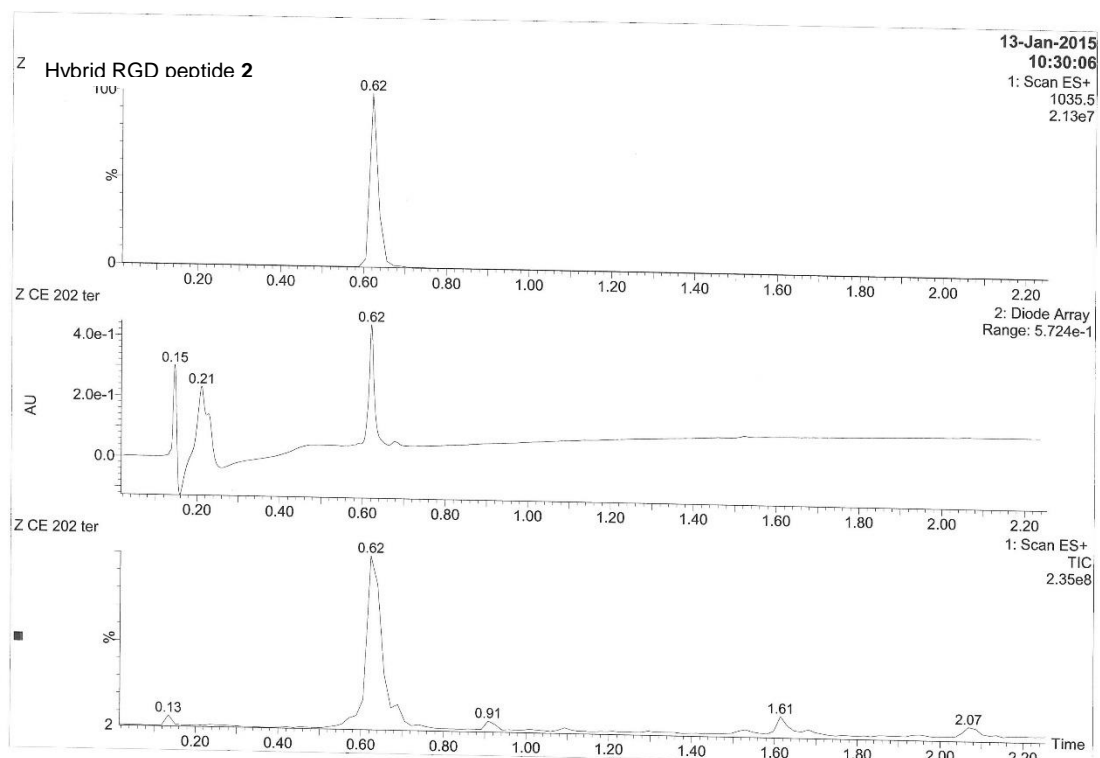
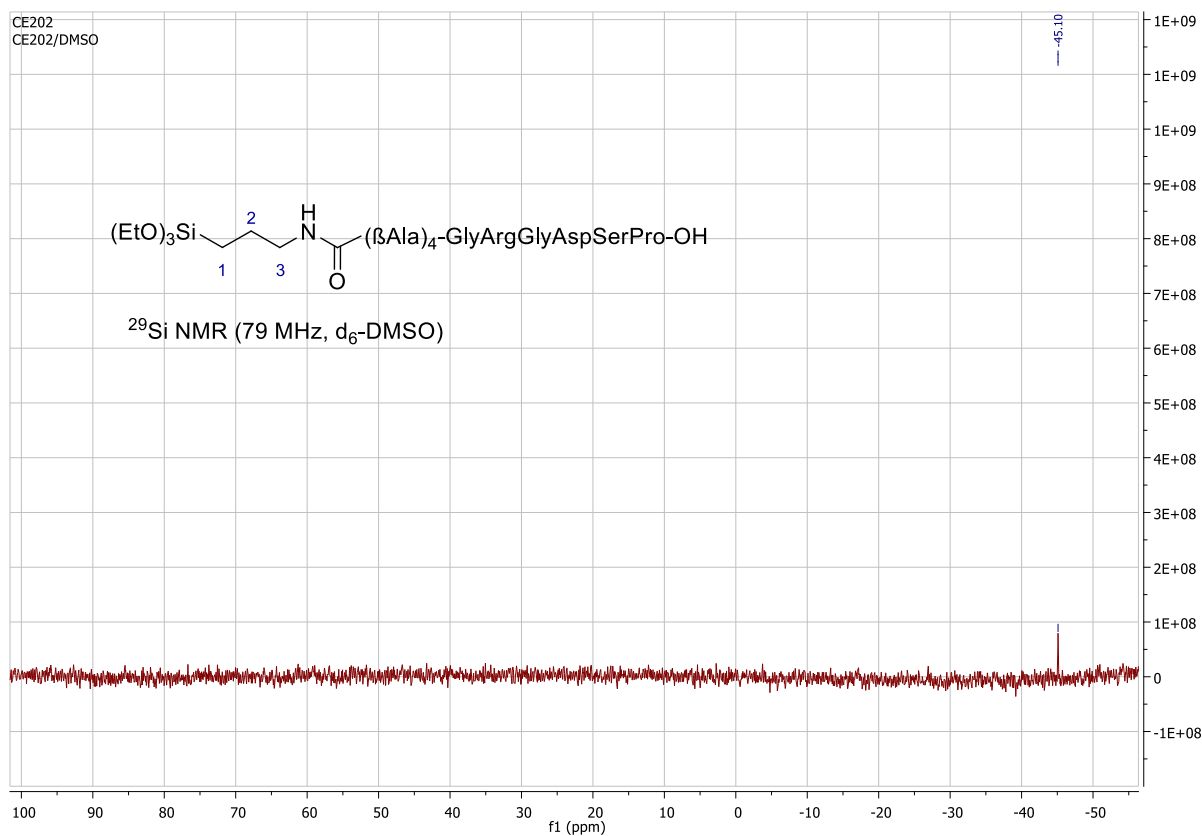
LC/MS (ESI⁺): Only the product of hydrolysis of ethoxysilyl groups into silanols is detected. t_R = 0.62 min, m/z 1035 ([M+H]⁺, 50%), 509 ([M+H-OH]²⁺, 60), 500 ([M-2OH]²⁺, 100).

HRMS: 1119.5481. C₄₅H₇₄N₁₈O₁₄Si requires [M+H]⁺, 1119.5479.

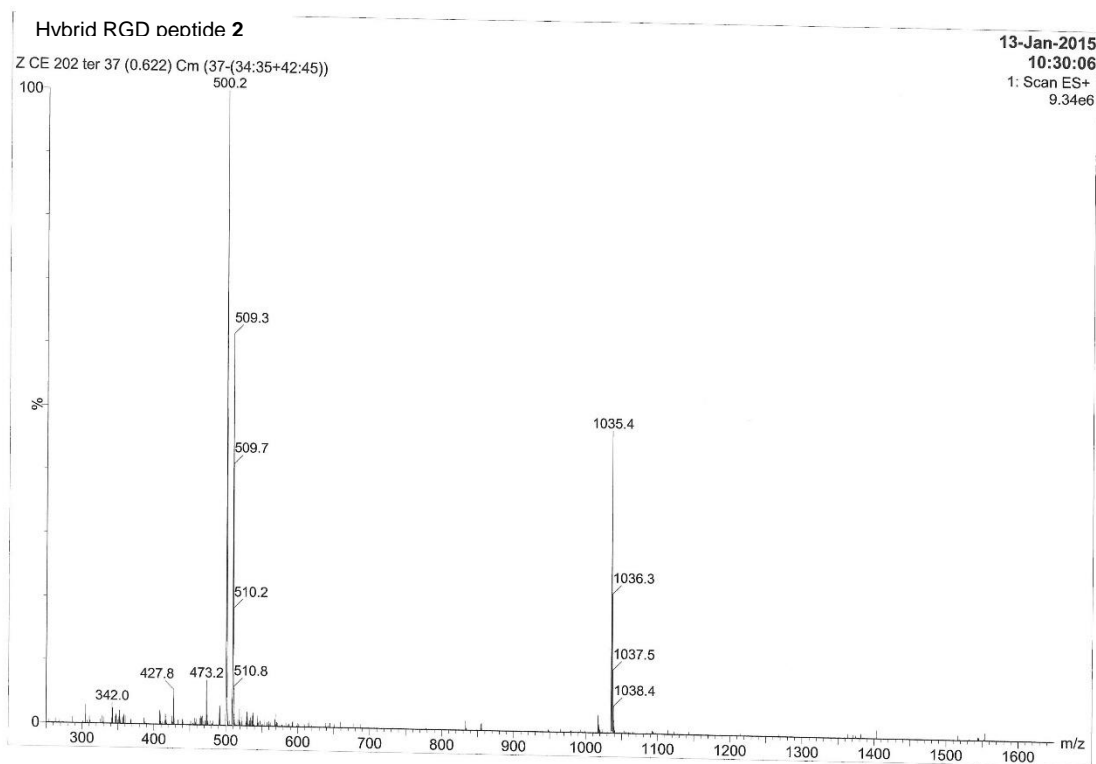
Supporting information for publication n°2
An easy synthesis of tunable hybrid bioactive hydrogels



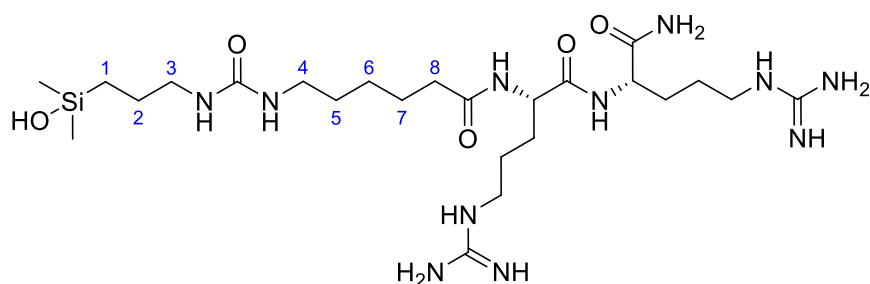
Supporting information for publication n°2
 An easy synthesis of tunable hybrid bioactive hydrogels



Supporting information for publication n°2
An easy synthesis of tunable hybrid bioactive hydrogels



Hybrid antibacterial peptide 3 synthesis: $(\text{CH}_3)_2(\text{HO})\text{Si}-(\text{CH}_2)_3-\text{NHCO}-\text{AhxArg}_2\text{NH}_2$



The hybrid antibacterial peptide was synthesized on Rink Amide resin using Fmoc-SPPS strategy. Amino acids used were Fmoc-Arg(Pbf)-OH twice and Fmoc- ϵ -amino hexanoic acid. After coupling and N-deprotection of Fmoc-Ahx-OH, the tripeptide was silylated in DMF (10 mL/g of resin) using 3-isocyanatopropyl dimethylchlorosilane (3 eq) in presence of diisopropylethylamine (3 eq) at room temperature overnight. After washings, the resin was cleaved in TFA for 5h. Cleavage solution was concentrated. The hybrid peptide was precipitated in diethyl ether and purified by preparative HPLC. Freeze drying gave the pure peptide as a white powder (68%).

^1H NMR (400 MHz, D_2O) δ 4.19 (ddd, $J = 14.4, 8.6, 5.7$ Hz, 2H, H_α Arg), 3.09 (t, $J = 6.9$ Hz, 4H, H_β Arg), 2.96 (td, $J = 6.8, 1.9$ Hz, 4H, H-3 and H-4), 2.17 (t, $J = 7.3$ Hz, 2H, H-8), 1.82 – 1.59 (m, 4H, H_β Arg), 1.59 – 1.44 (m, 6H, H-7 and H_γ Arg), 1.41 – 1.31 (m, 4H, H-2 and H-5), 1.24 – 1.12 (m, 2H, H-6), 0.53 – 0.41 (m, 2H, H-1), 0.00 (s, 6H, $\text{Si}(\text{CH}_3)_2$).

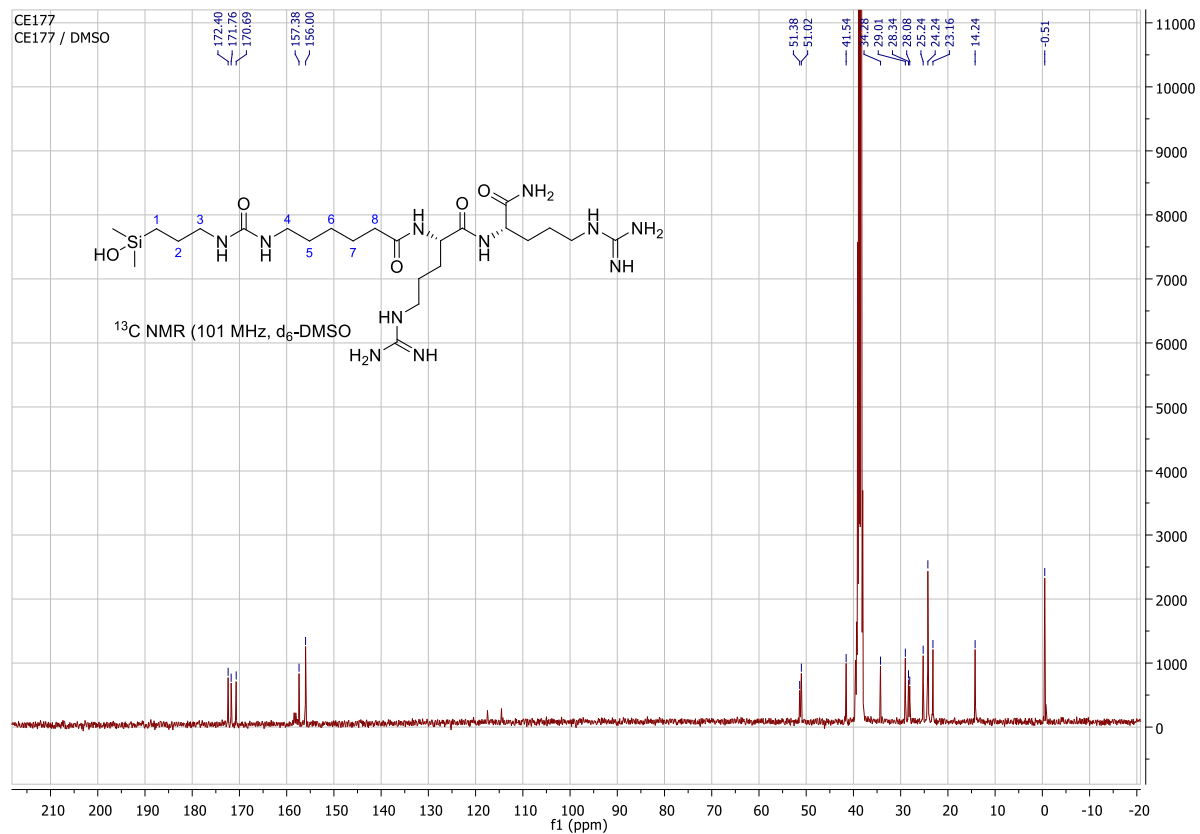
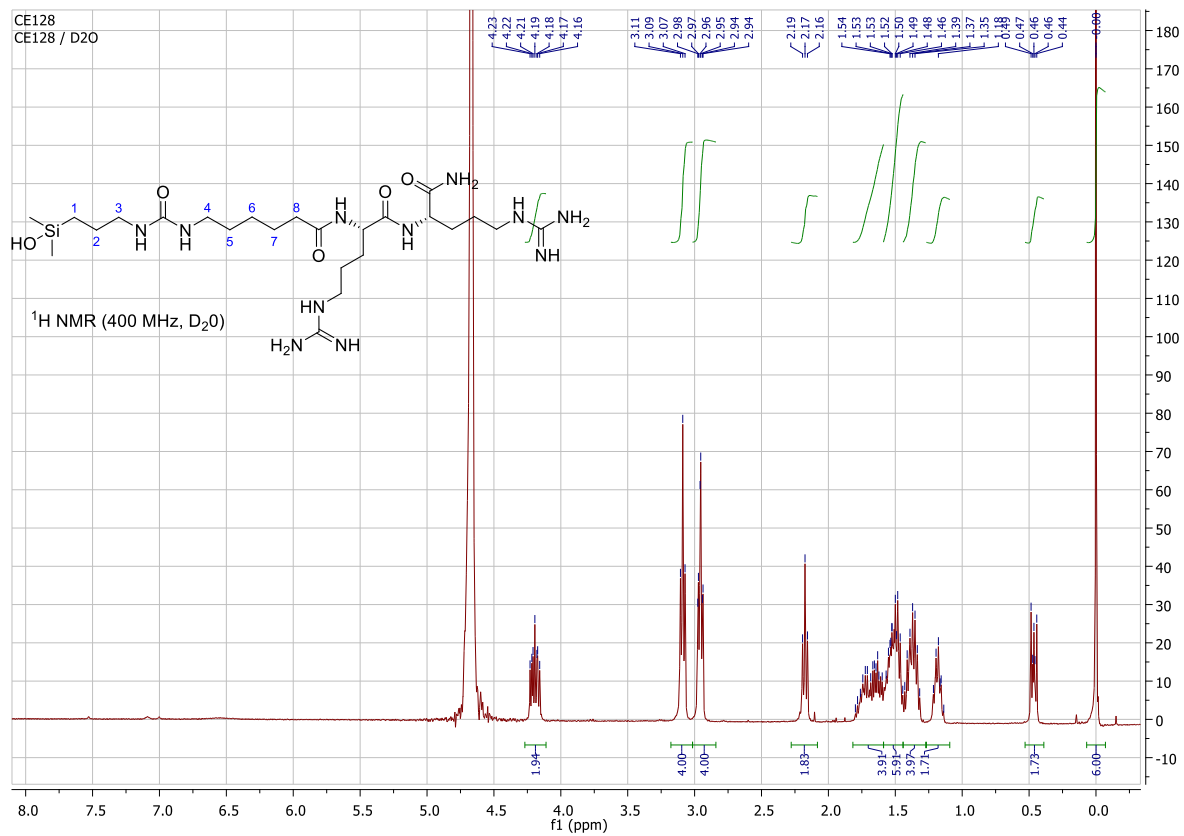
^{13}C NMR (101 MHz, DMSO- d_6) δ 172.40 (C), 171.76 (C), 170.69 (C), 157.38 (C), 156.00 (C), 51.38 (CH), 51.02 (CH), 41.54 (CH_2), 34.28 (CH_2), 29.01 (CH_2), 28.34 (CH_2), 28.08 (CH_2), 25.24 (CH_2), 24.24 (CH_2), 23.16 (CH_2), 14.24 (CH_2), -0.51 (CH_3).

^{29}Si NMR (79 MHz, DMSO- d_6) δ 7.97 (dimer).

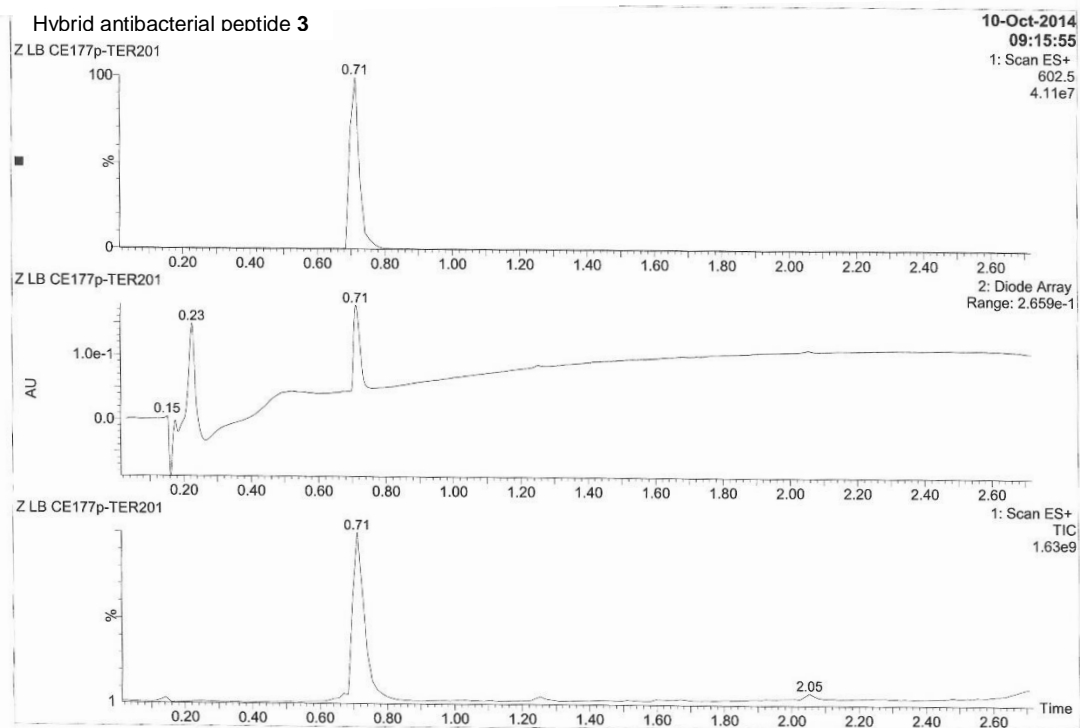
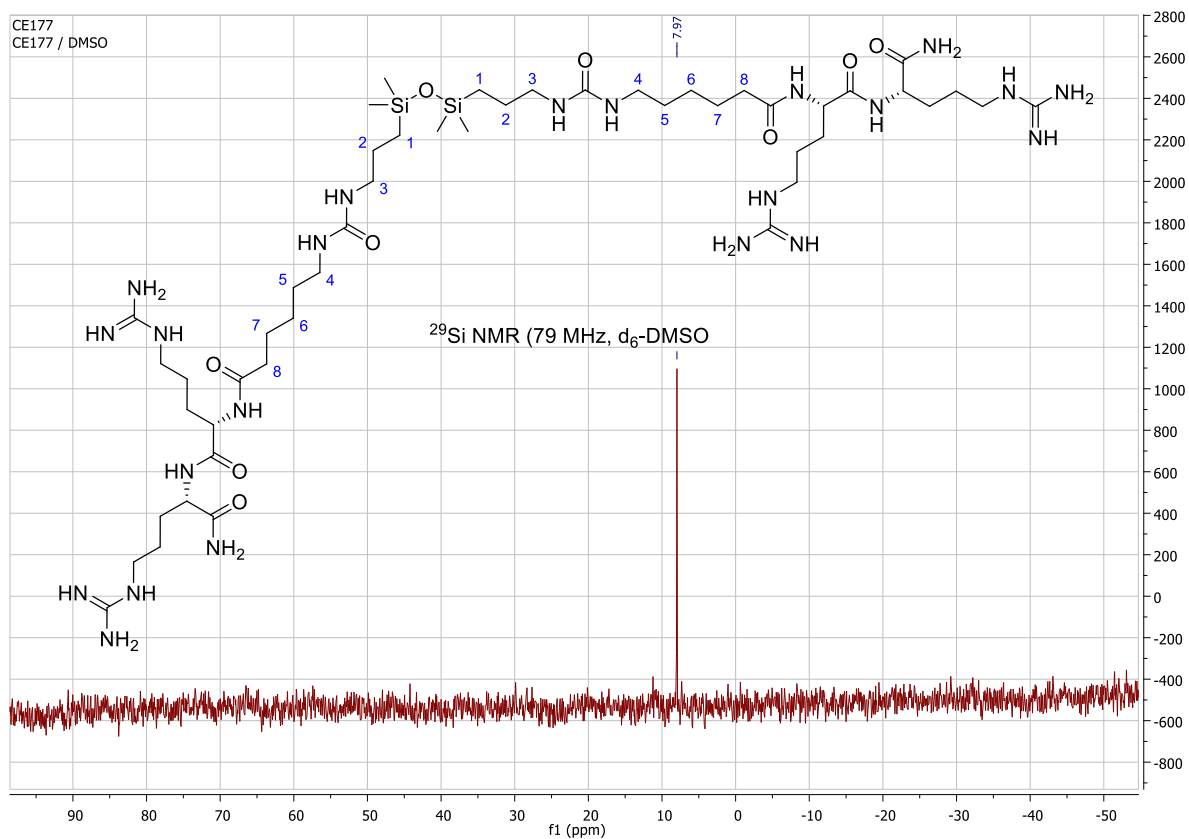
LC/MS (ESI $^+$): $t_R = 0.71$ min, m/z 602 ($[\text{M}+\text{H}]^+$, 10%), 302 ($[\text{M}+2\text{H}]^{2+}$, 100), 293 ($[\text{M}+2\text{H}-\text{NH}_3]^{2+}$, 30).

HRMS: 602.3926. $\text{C}_{24}\text{H}_{51}\text{N}_{11}\text{O}_5\text{Si}$ requires $[\text{M}+\text{H}]^+$, 602.3922.

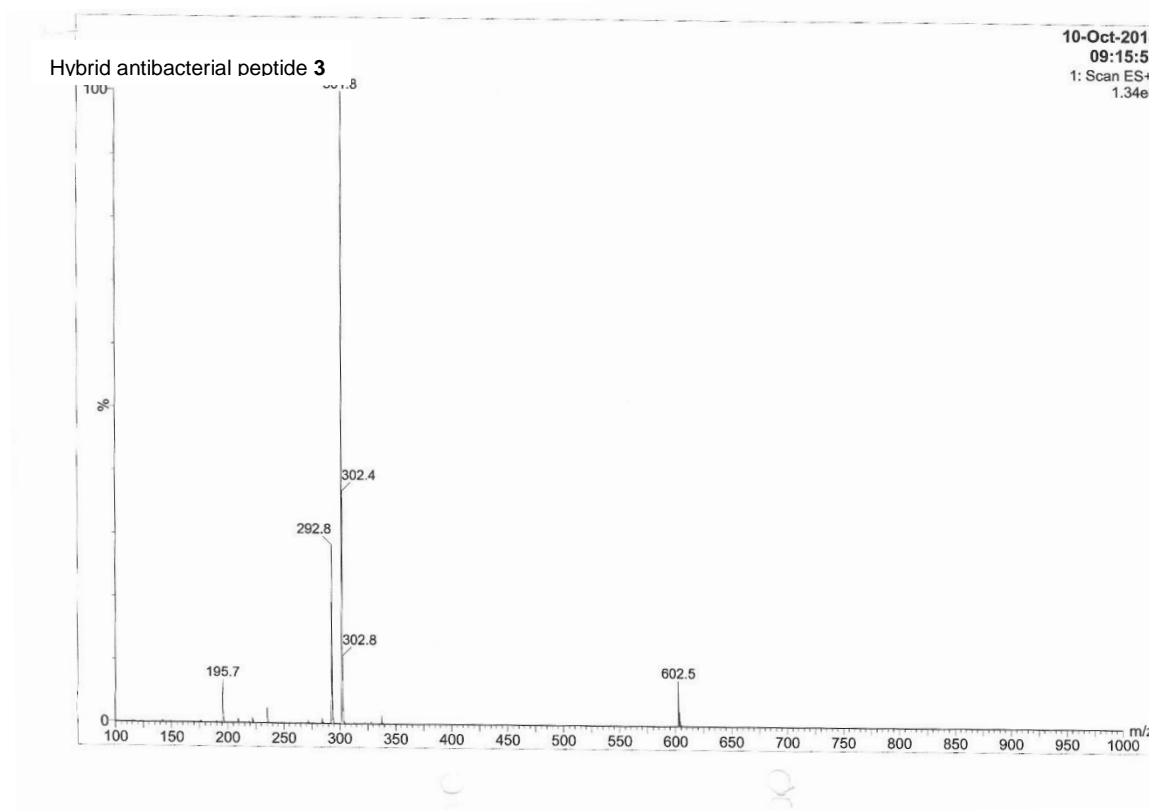
Supporting information for publication n°2
An easy synthesis of tunable hybrid bioactive hydrogels



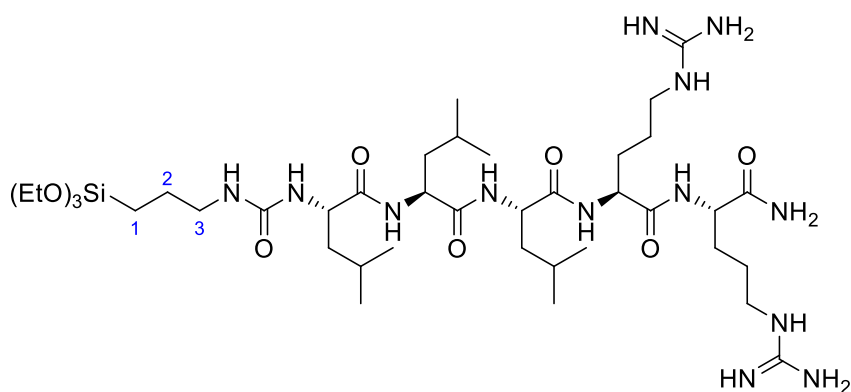
Supporting information for publication n°2
An easy synthesis of tunable hybrid bioactive hydrogels



Supporting information for publication n°2
An easy synthesis of tunable hybrid bioactive hydrogels



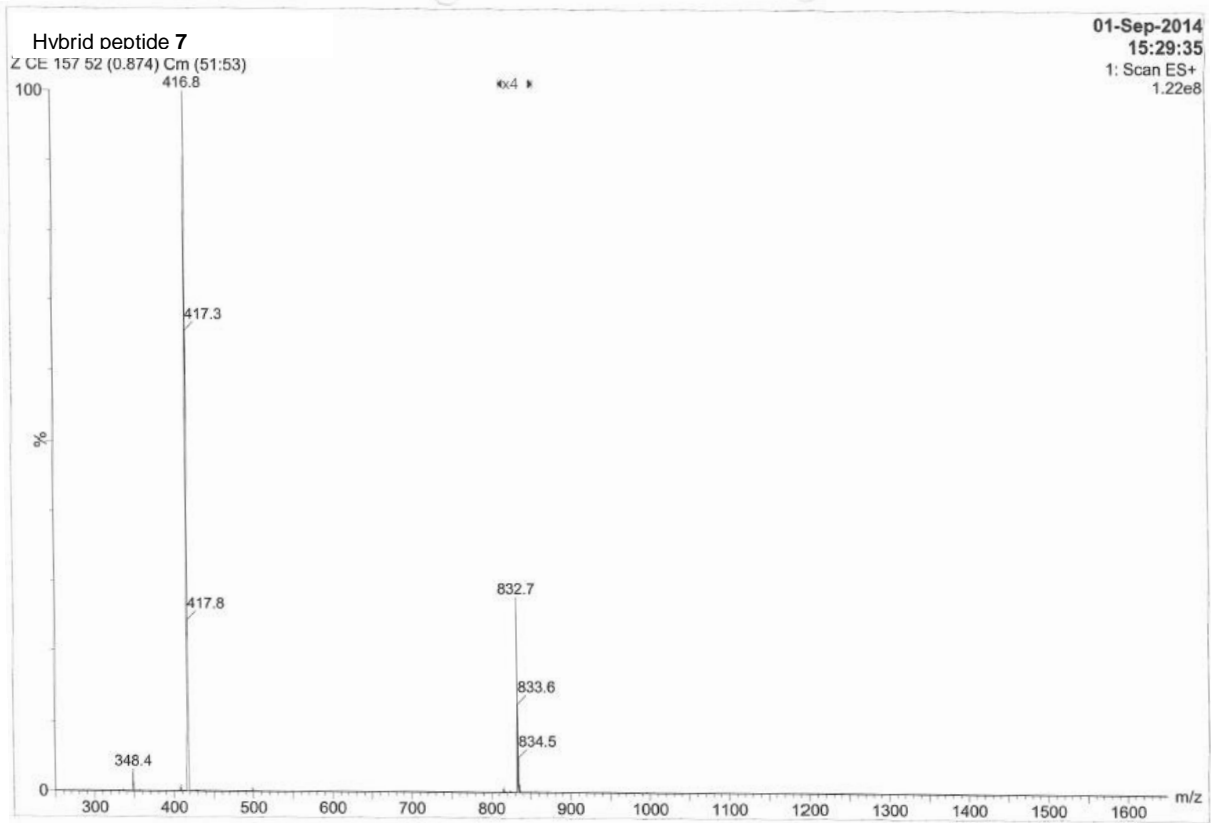
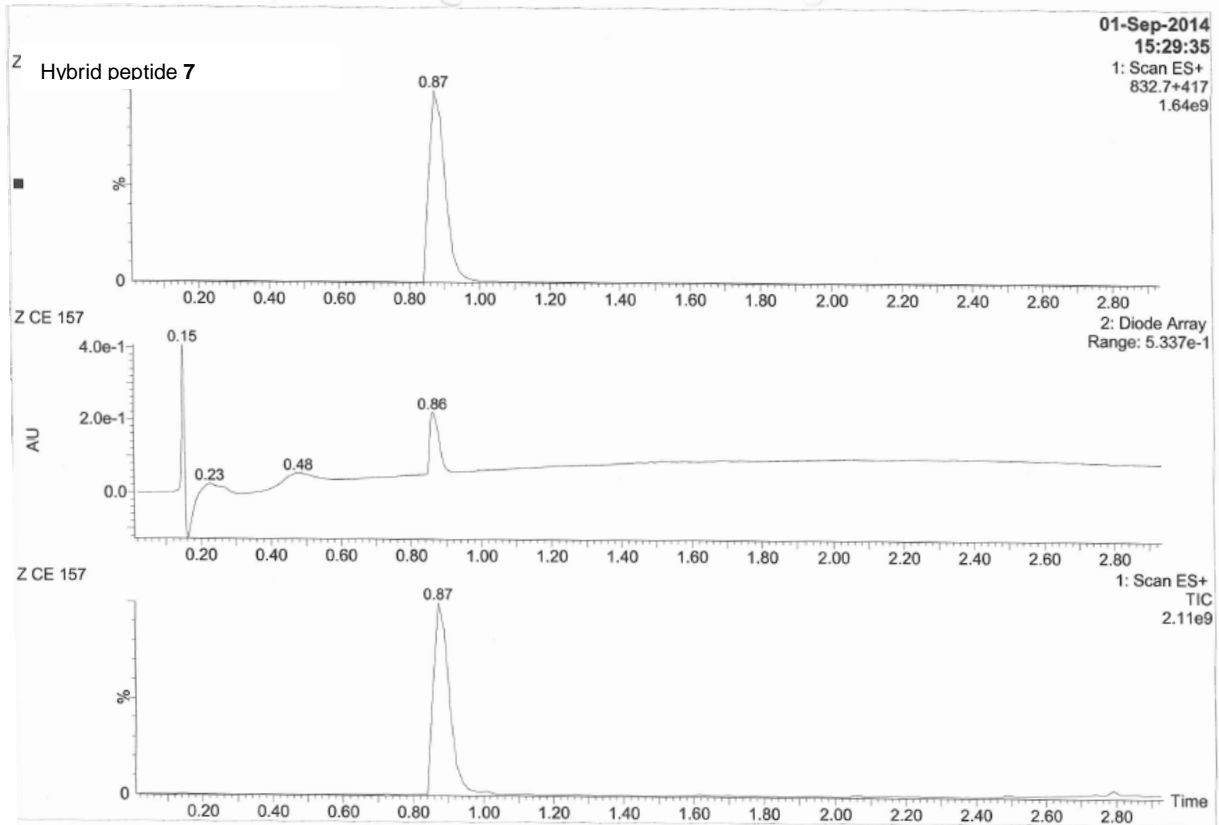
Hybrid peptide 7 synthesis: $(\text{EtO})_3\text{Si}-(\text{CH}_2)_3-\text{NHCO}-\text{Leu}_3\text{Arg}_2\text{NH}_2$



H-Leu₃Arg₂-NH₂ was synthesized on Rink Amide resin by a classical Fmoc-SPPS strategy. Amino acid used were successively Fmoc-Arg(Pbf)-OH twice and Fmoc-Leu-OH three times. Cleavage and side chain deprotection were realized in trifluoroacetic acid for 4h. After precipitation in diethylether, the peptide was purified on preparative HPLC (yield: 86%). Then, it was reacted with 3-isocyanatopropyltriethoxysilane (1,1 eq) in DMF at a concentration of 30 mM in presence of DIEA (3 eq). After concentration of the reaction mixture, the hybrid peptide was obtained by precipitation and washings with diethylether.

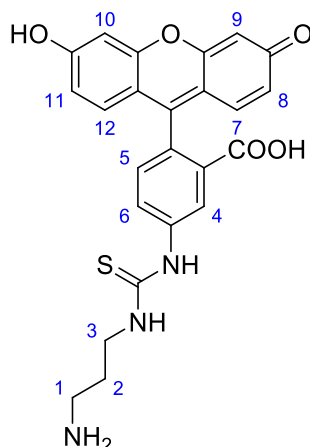
LC/MS (ESI⁺): Only the product of hydrolysis of ethoxysilyl groups into silanols was detected: t_R = 0.87 min, m/z 833 ([M+H]⁺, 30%), 417 ([M+2H]²⁺, 100).

Supporting information for publication n°2
An easy synthesis of tunable hybrid bioactive hydrogels



Supporting information for publication n°2
An easy synthesis of tunable hybrid bioactive hydrogels

Non-silylated fluorescein 6



N-Boc-1,3-propanediamine (56.4 mg, 0.324 mmol, 1.05 eq) was added to a solution of fluoresceine isothiocyanate (FITC, 120 mg, 0.308 mmol) in anhydrous DMF (3 mL) with DIEA (100 μ L). The reaction solution was stirred for 1 h under argon. Then the solvent was removed under reduced pressure. The protected amine was precipitated and washed with diethylether. The dried compound was solubilized in TFA (4 mL) and stirred for 1 h. The crude solution was concentrated and precipitated in diethylether. After centrifugation, fluoresceine amine was purified by preparative HPLC and obtained as a TFA salt (180 mg, 100%).

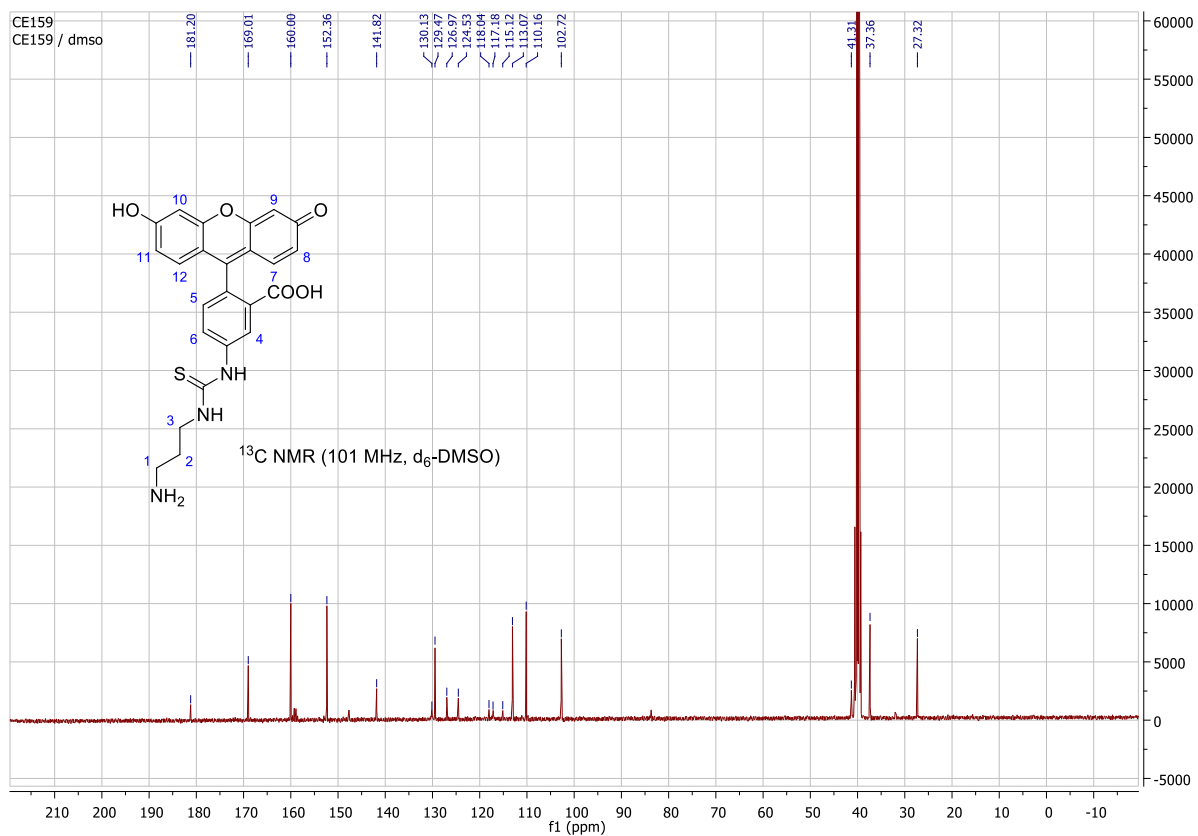
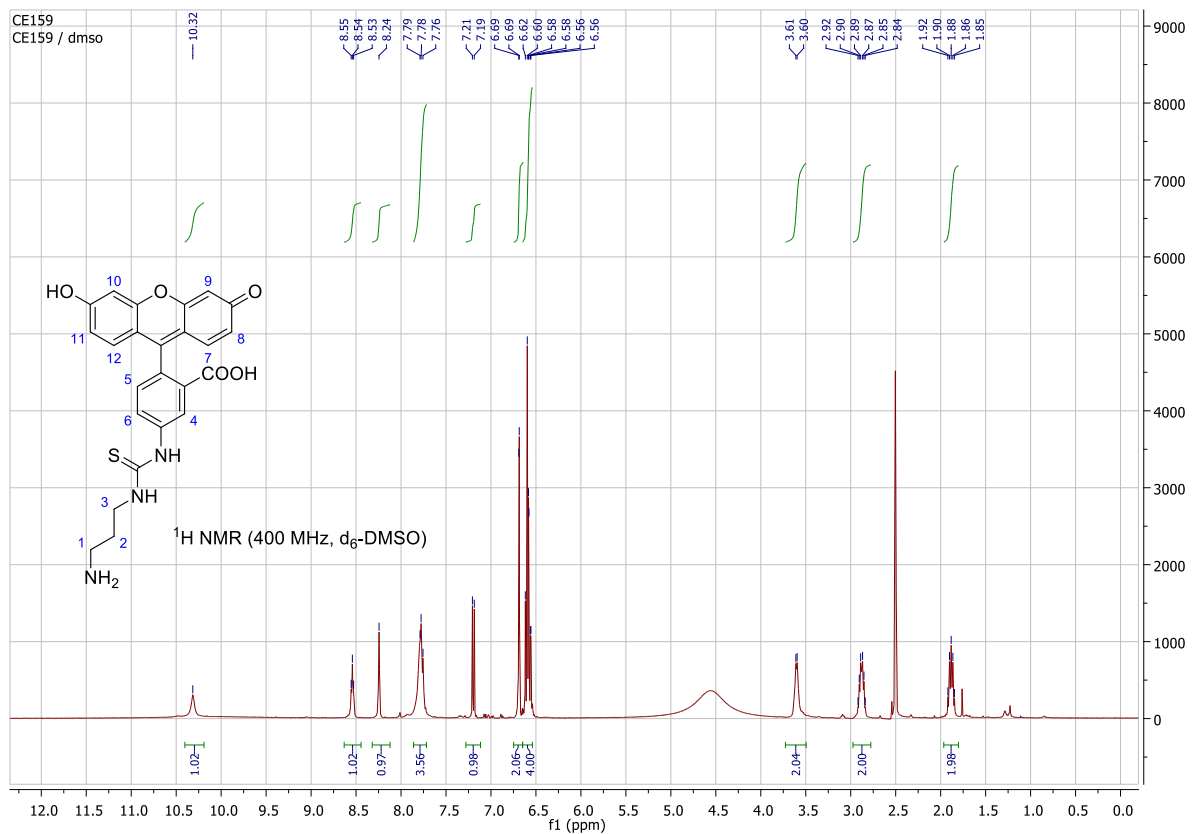
^1H NMR (400 MHz, DMSO- d_6) δ 10.32 (s, 1H, NH thiourea from FITC), 8.54 (t, J = 5.4 Hz, 1H, NH thiourea from diaminopropane), 8.24 (s, 1H, H-4), 7.86 – 7.72 (m, 3H, H-6 and NH_2), 7.20 (d, J = 8.3 Hz, 2H, H-5), 6.69 (d, J = 2.1 Hz, 2H, H-9 and H-10), 6.62 – 6.56 (m, 4H, H-7, H-8, H-11 and H-12), 3.60 (d, J = 5.5 Hz, 2H, H-3), 2.92 – 2.82 (m, 2H, H-1), 1.92 – 1.84 (m, 2H, H-2).

^{13}C NMR (101 MHz, DMSO- d_6) δ 181.20 (C), 169.01 (C), 160.00 (C), 152.36 (C), 141.82 (C), 130.13 (CH), 129.47 (CH), 126.97 (C), 124.53 (CH), 118.04 (C), 117.18 (CH), 115.12 (C), 113.07 (CH), 110.16 (C), 102.72 (CH), 41.31 (CH_2), 37.36 (CH_2), 27.32 (CH_2).

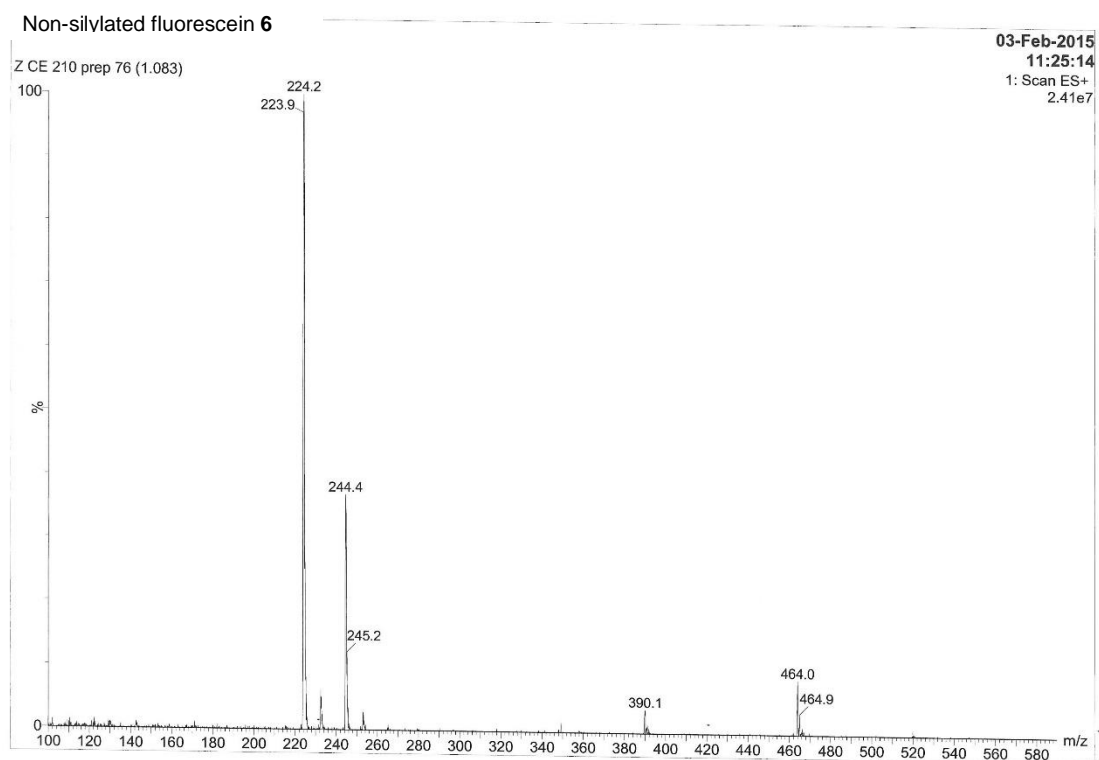
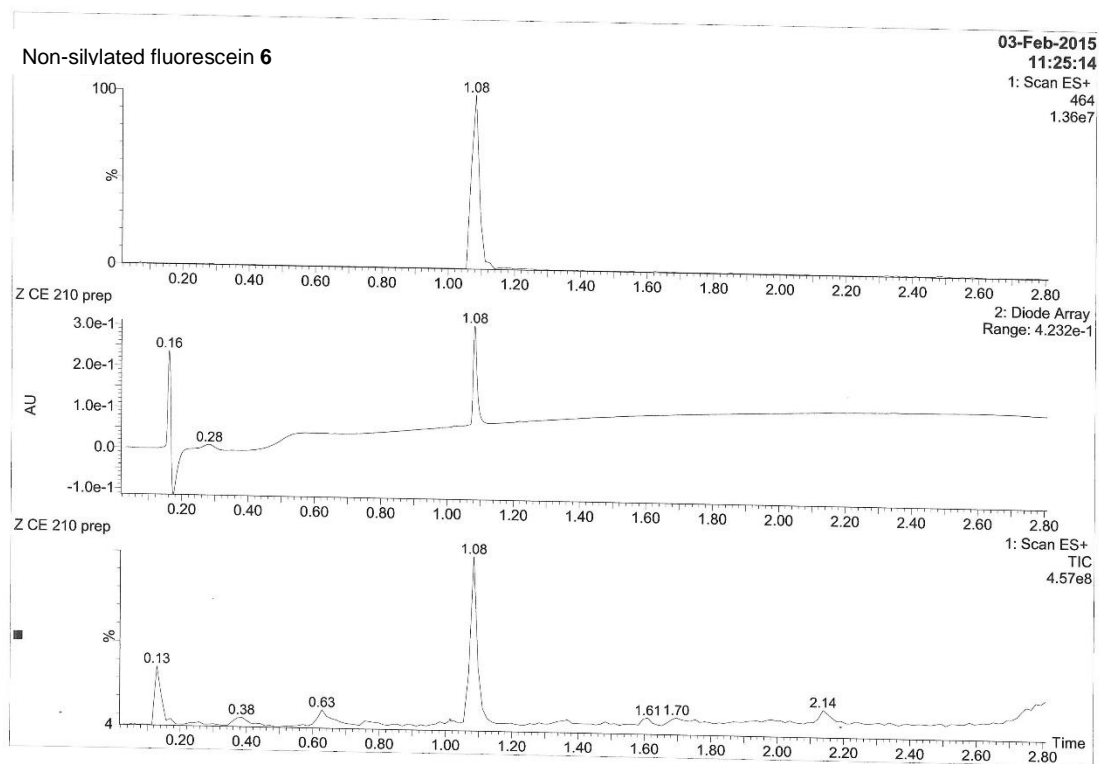
LC/MS (ESI $^+$): t_R = 1.08 min, m/z 464 ($[\text{M}+\text{H}]^+$, 9%), 390 ($[\text{M}+\text{H}-\text{NH}_2(\text{CH}_2)_3\text{NH}_2]^+$, 5%), 224 ($[\text{M}+2\text{H}-\text{NH}_3]^{2+}$, 100).

HRMS: 464.1278. $\text{C}_{24}\text{H}_{21}\text{N}_3\text{O}_5\text{S}$ requires $[\text{M}+\text{H}]^+$, 464,1280.

Supporting information for publication n°2
An easy synthesis of tunable hybrid bioactive hydrogels

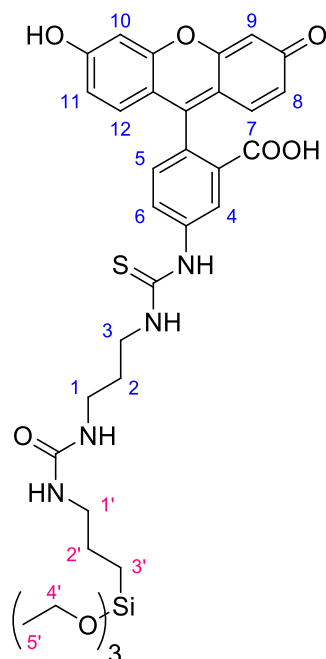


Supporting information for publication n°2
An easy synthesis of tunable hybrid bioactive hydrogels



Supporting information for publication n°2
An easy synthesis of tunable hybrid bioactive hydrogels

Triethoxysilyl fluorescein 4



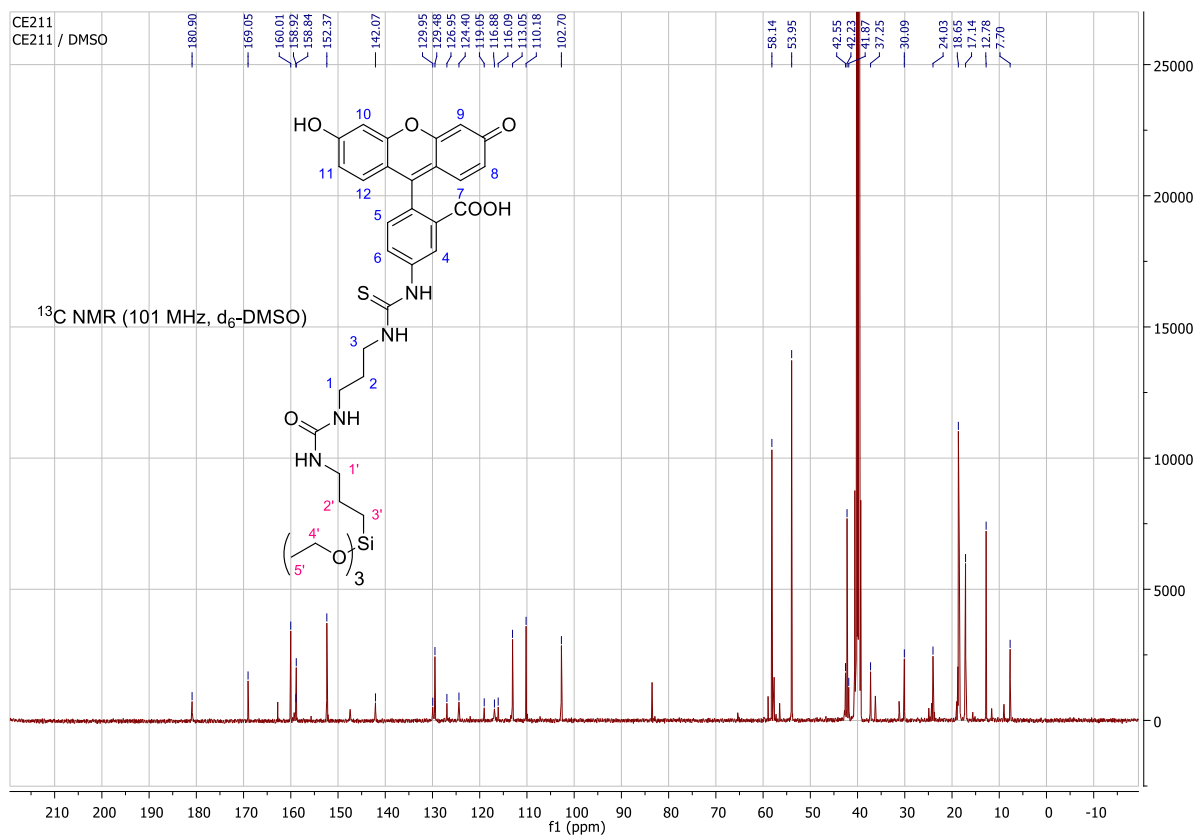
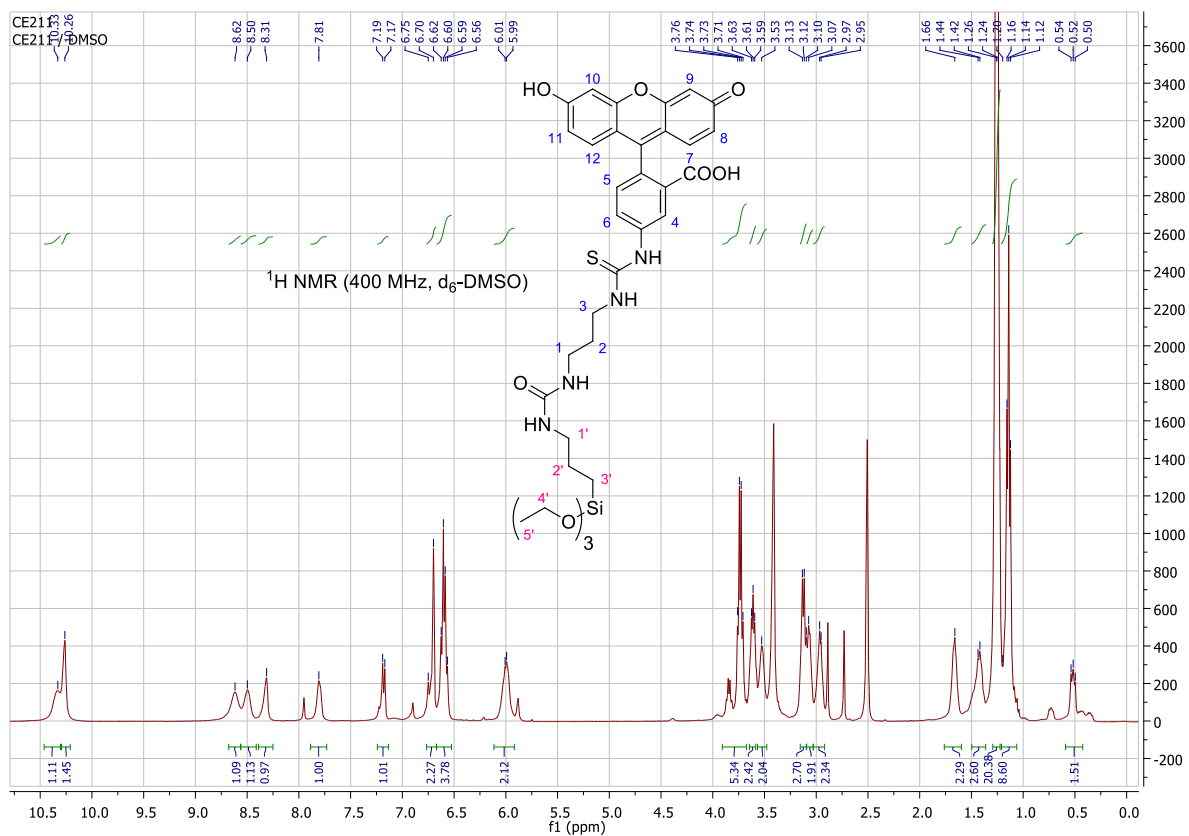
3-Isocyanatopropyltriethoxysilane (1.35 μL , $5.45 \cdot 10^{-3}$ mmol, 1.05 eq) was added to a solution of the non-silylated fluorescein **6** prepared precedently (3.00 mg, $5.19 \cdot 10^{-3}$ mmol) in anhydrous DMF (500 μL) with DIEA (1.35 μL , $7.79 \cdot 10^{-3}$ mmol, 1.5 eq). The solution was stirred under argon for 1 h. The solvent was removed under reduced pressure and triethoxysilyl fluoresceine **4** was obtained as a DIEA salt after precipitation and washings with diethylether (100%).

^1H NMR (400 MHz, DMSO- d_6) δ 10.33 (br s, 1H, COOH), 10.26 (s, 1H, NH thiourea from FITC), 8.62 (br s, 1H, NH DIEA), 8.50 (s, 1H, NH thiourea), 8.31 (s, 1H, H-4), 7.81 (s, 1H, H-6), 7.20 (d, $J = 11.2$ Hz, 1H, H-5), 6.70 (s, 2H, H-9 and H-10), 6.64 – 6.56 (m, 4H, H-7, H-8, H-11 and H-12), 6.00 (br s, 2H, NH urea), 3.73 (q, $J = 7.2$ Hz, 6H, H-4'), 3.64 – 3.58 (m, 2H, CH₂ DIEA), 3.53 (br s, 2H, H-3), 3.15 – 3.10 (m, 2H, CH DIEA), 3.09 – 3.03 (m, 2H, H-1), 3.01 – 2.93 (m, 2H, H-3'), 1.73 – 1.61 (m, 2H, H-2), 1.50 – 1.36 (m, 2H, H-2'), 1.30 – 1.21 (m, 15H, CH₃ DIEA), 1.14 (t, $J = 7.0$ Hz, 9H, H-5'), 0.59 – 0.42 (m, 2H, H-1').

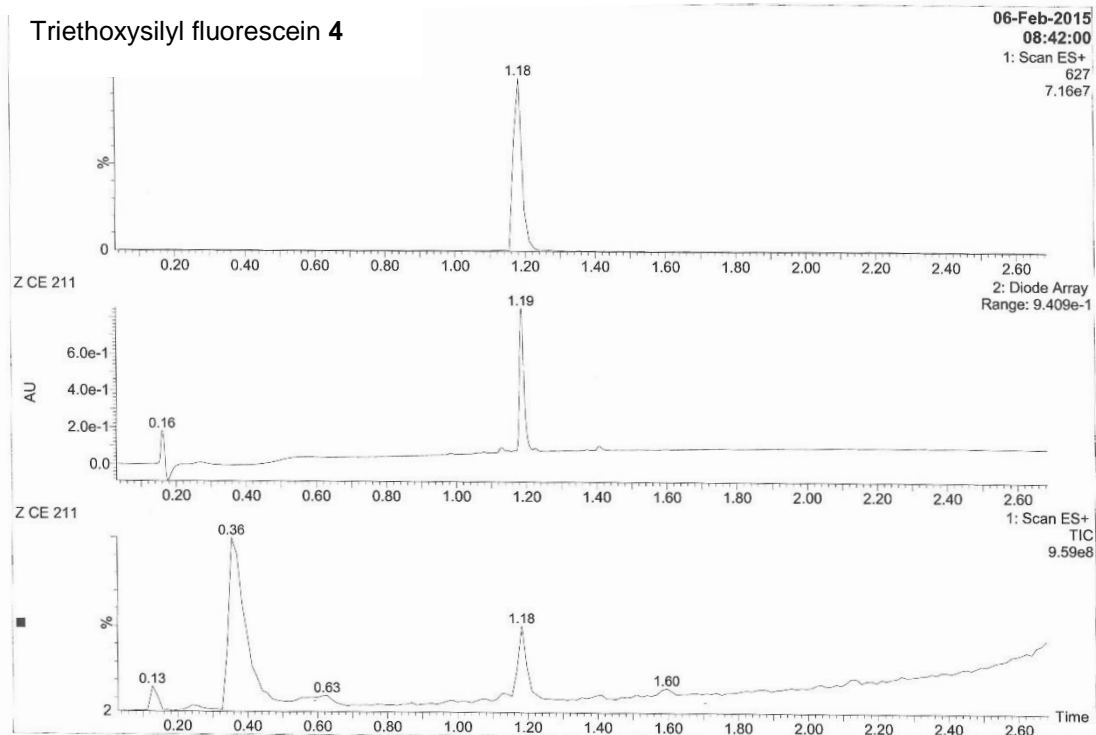
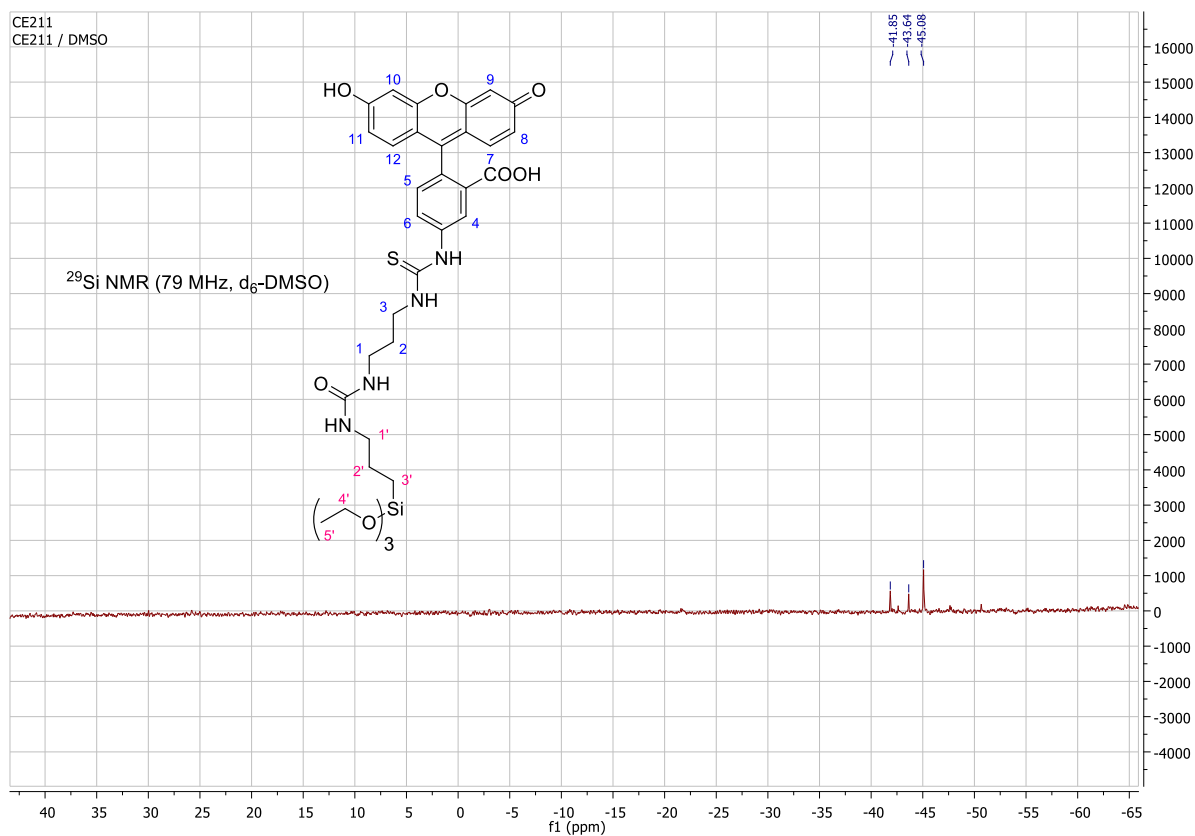
^{13}C NMR (101 MHz, DMSO- d_6) δ 180.90 (C), 169.05 (C), 160.01 (C), 158.92 (C), 158.84 (C), 152.37 (C), 142.07 (C), 129.95 (CH), 129.48 (CH), 126.95 (C), 124.40 (CH), 119.05 (C), 116.88 (CH), 116.09 (C), 113.05 (CH), 110.18 (C), 102.70 (CH), 58.14 (CH₂), 53.95 (CH₂), 42.55 (CH₂), 42.23 (CH), 41.87 (CH₂), 37.25 (CH₂), 30.09 (CH₂), 24.03 (CH₂), 18.65 (CH₃), 17.14 (CH₃), 12.78 (CH₃), 7.70 (CH₂).

^{29}Si NMR (79 MHz, DMSO- d_6) δ -41.85, -43.64, -45.08. Ethoxy group hydrolysis started during analysis. LC/MS (ESI⁺): $t_{\text{R}} = 1.18$ min, m/z 627 ([M+H]⁺, 70%), 609 ([M+H-H₂O]⁺, 20), 305 ([M+2H-H₂O]²⁺, 100). HRMS: 627.1587. C₂₈H₃₀N₄O₉SSi requires [M+H]⁺, 627,1581.

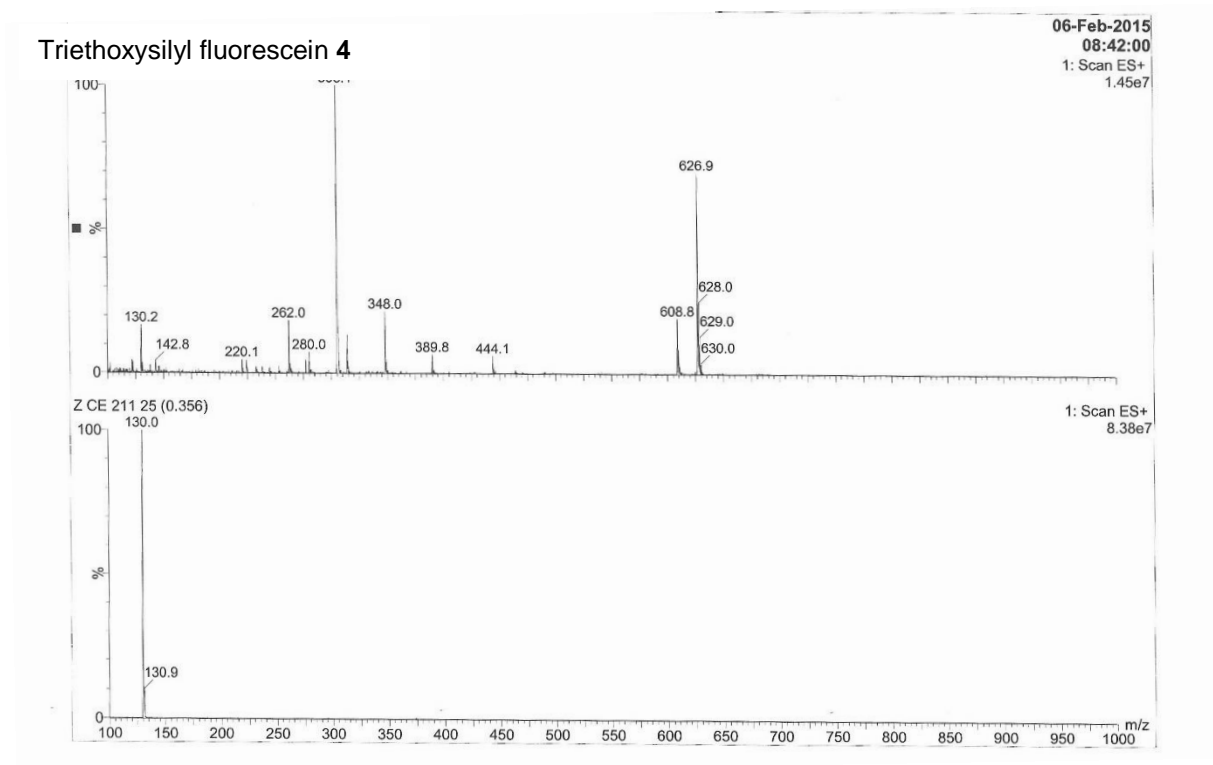
Supporting information for publication n°2
 An easy synthesis of tunable hybrid bioactive hydrogels



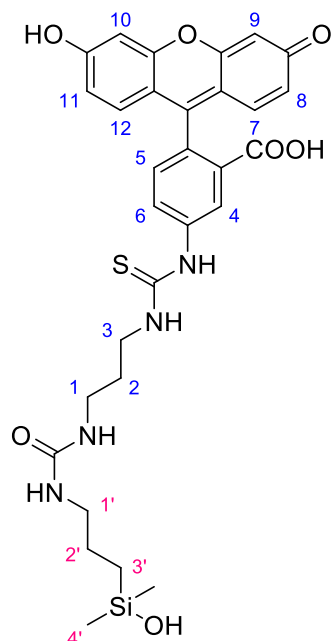
Supporting information for publication n°2
An easy synthesis of tunable hybrid bioactive hydrogels



Supporting information for publication n°2
An easy synthesis of tunable hybrid bioactive hydrogels



Dimethylhydroxysilyl fluorescein **5**



3-Isocyanatopropylchlorodimethylsilane (16.2 μL , 0.0910 mmol, 1.05 eq) was added to a solution of non-silylated fluorescein **6** prepared precedently (50.0 mg, 0.0867 mmol) in anhydrous DMF (2 mL) with DIEA (45.2 μL , 0.260 mmol, 3 eq). The solution was stirred under argon for 1 h. The solvent was removed under reduced pressure and the crude product was obtained by precipitation with diethylether. Purification by preparative HPLC gave dimethylhydroxysilyl fluoresceine **5** (42%).

Supporting information for publication n°2
An easy synthesis of tunable hybrid bioactive hydrogels

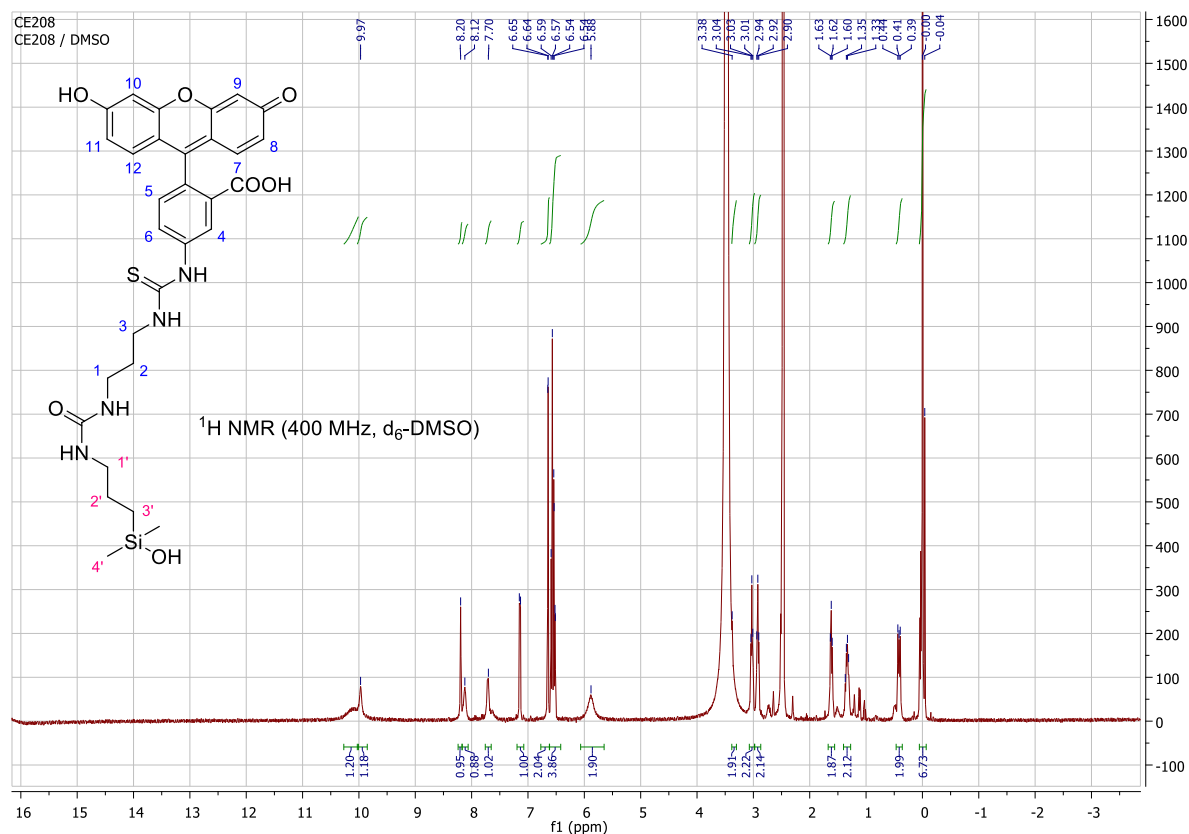
^1H NMR (400 MHz, DMSO- d_6) δ 10.01 (s br, 1H, COOH), 9.97 (s, 1H, NH thiourea from FITC), 8.20 (s, 1H, H-4), 8.12 (s, 1H, NH thiourea), 7.71 (d, $J = 7.6$ Hz, 1H, H-6), 7.14 (d, $J = 8.3$ Hz, 1H, H-5), 6.65 (d, $J = 2.2$ Hz, 2H, H-9 and H-10), 6.59 – 6.51 (m, 4H, H-7, H-8, H-11 and H-12), 5.88 (s br, 2H, NH urea), 3.43 – 3.38 (m, 2H, H-3), 3.03 (t, $J = 6.5$ Hz, 2H, H-1), 2.92 (t, $J = 6.9$ Hz, 2H, H-3'), 1.62 (qu, $J = 6.5$ Hz, 2H, H-2), 1.37 – 1.29 (m, 2H, H-2'), 0.47 – 0.36 (m, 2H, H-1'), 0.00 and -0.04 (2 s, 6H, H-4' from dimer and monomer respectively).

^{13}C NMR (101 MHz, DMSO- d_6) δ 179.51 (C), 167.65 (C), 158.62 (C), 157.51 (C), 151.02 (C), 140.47 (C), 128.75 (CH), 128.19 (CH), 125.68 (C), 123.18 (CH), 116.66 (C), 115.79 (CH), 114.24 (C), 111.71 (CH), 108.87 (C), 101.36 (CH), 41.55 (CH₂), 40.52 (CH₂), 35.85 (CH₂), 28.80 (CH₂), 23.13 (CH₂), 14.20 (CH₂), -0.51 (CH₃), -0.75 (CH₃).

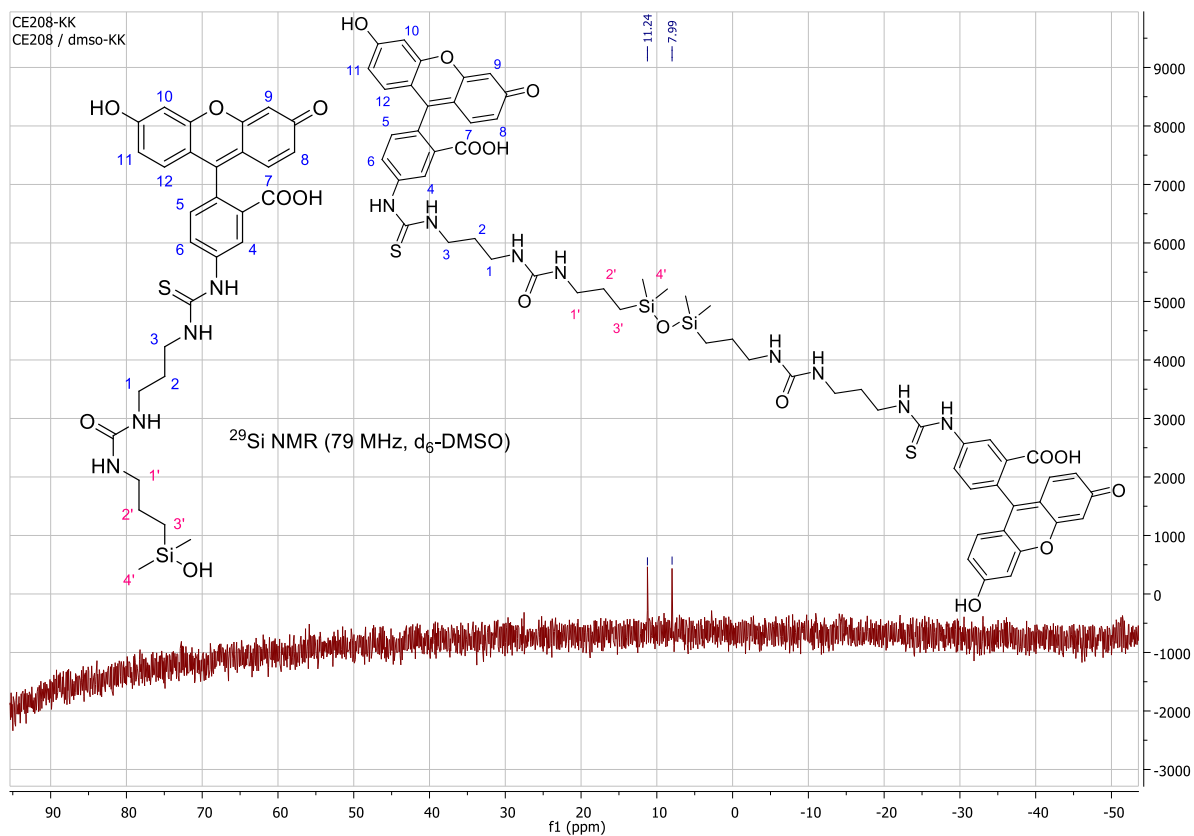
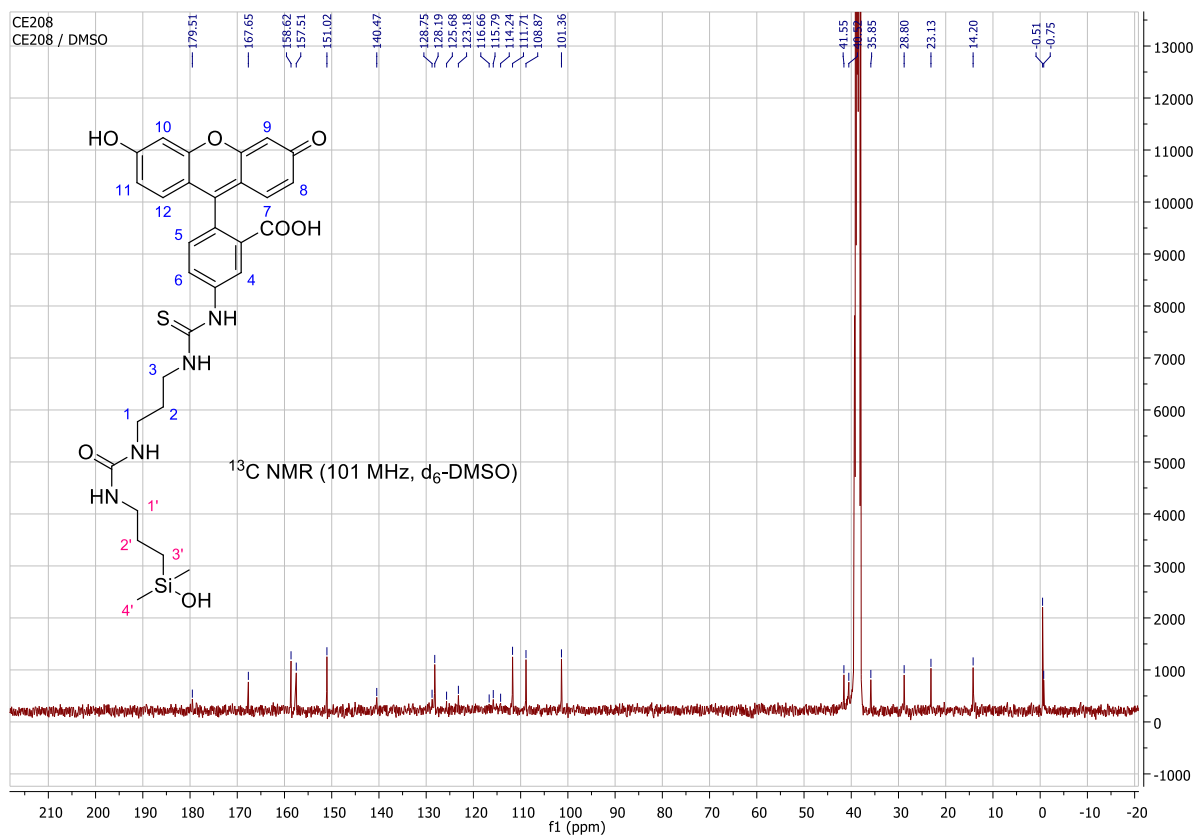
^{29}Si NMR (79 MHz, DMSO- d_6) δ 11.24 (monomer), 7.99 (dimer).

LC/MS (ESI⁺): $t_R = 1.33$ min, m/z 623 ([M+H]⁺, 60%), 390 ([M+H-NH₂(CH₂)₃NHCONH(CH₂)₃Si(CH₃)₂OH]⁺, 15), 312 ([M+2H]²⁺, 60), 303 ([M+2H-H₂O]²⁺, 100).

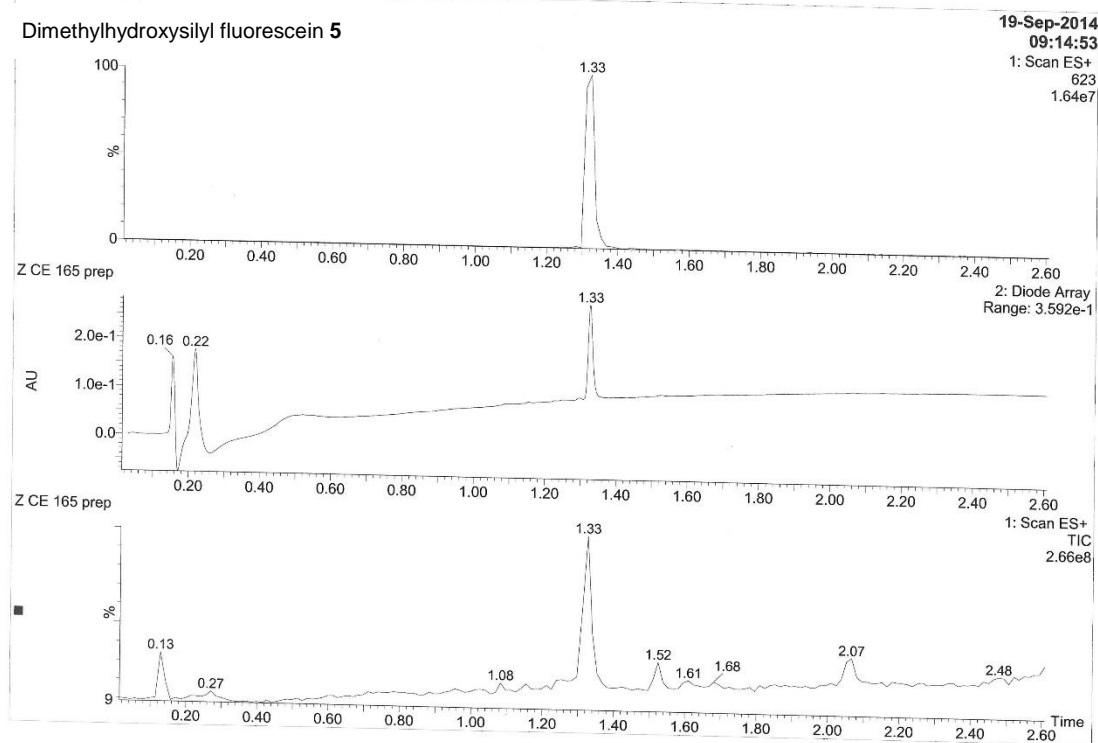
HRMS: 623.1996. C₃₀H₃₄N₄O₇SSi requires [M+H]⁺, 623,1996.



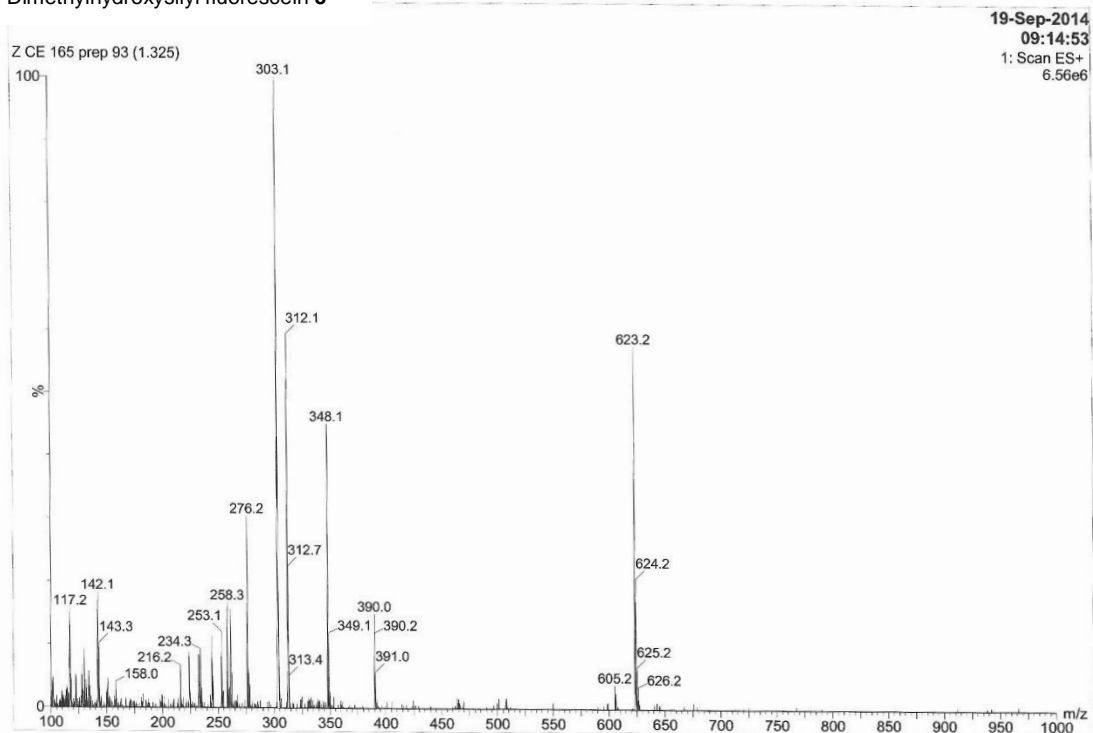
Supporting information for publication n°2
An easy synthesis of tunable hybrid bioactive hydrogels



Supporting information for publication n°2
An easy synthesis of tunable hybrid bioactive hydrogels



Dimethylhydroxysilyl fluorescein 5



Supporting information for publication n°2
An easy synthesis of tunable hybrid bioactive hydrogels

Hydrogel formation

Hybrid PEG is dissolved in Dulbecco's phosphate buffer (DPBS). For instance, 100 mg of hybrid PEG are dissolved in 1 mL of DPBS to obtain a 10 wt% hybrid PEG gel. The solution is filtered on a 0.22 μm pore size filter when sterile conditions are required. Sodium fluoride is added and the solution is incubated at 37°C to yield the hydrogel. Gelification time depends on NaF concentration (2 h at 37°C with 0.3 wt% NaF that is to say 3 mg/mL).



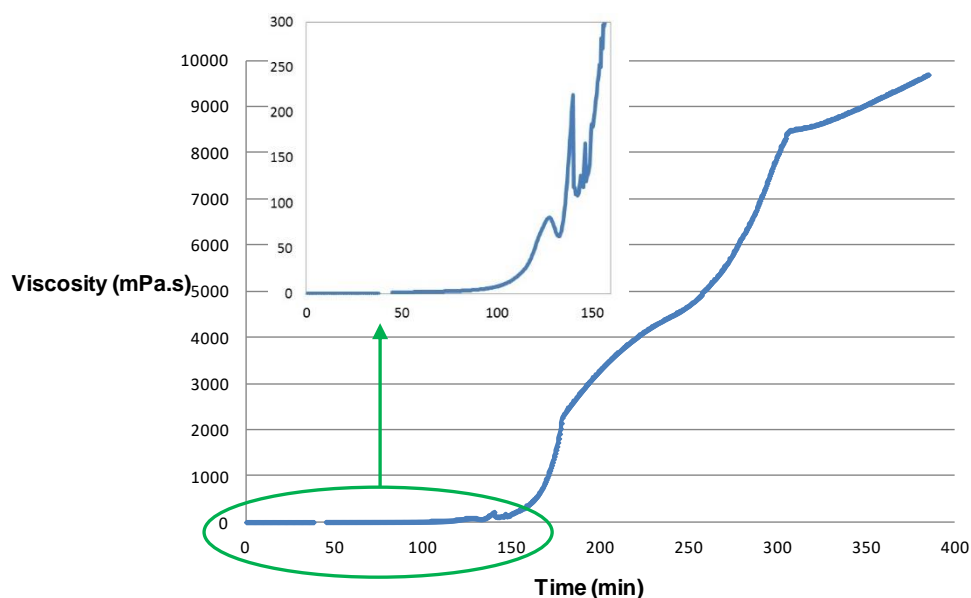
Left: 5 wt% hybrid PEG gel; middle: 10 wt% hybrid PEG gel; right: 20 wt% hybrid PEG gel.



Link to a hydrogel formation movie. Reactants in the order of addition: FITC, hybrid PEG 1, NaF in DPBS.

Viscometry

Viscometry measurements were carried out on a SV-10 sine-wave vibro viscometer. Viscosity was recorded as a function of time on 10 mL samples of hybrid PEG solutions.



Evolution of the viscosity of a 10 wt% hybrid PEG solution containing 0.3 wt% of NaF

Supporting information for publication n°2
An easy synthesis of tunable hybrid bioactive hydrogels

Rheology

Rheological measurements were carried out on an AR2000 rheometer from TA instruments, Inc. with a 20 mm diameter parallel geometry at 37°C in the oscillatory mode. Cylindrical gels with a diameter of 20 mm and a volume of 3 mL were prepared for these studies; they were unmoulded after 24 h at 37°C. Storage (G') and loss (G'') moduli were recorded as a function of frequency within the linear viscoelastic regime at 0,1% strain. The gap was controlled by maintaining a constant normal force at 1 ± 0.1 N. Viscoelastic moduli values were also recorded at 25°C and verified 4 and 7 days after by performing the same rheological experiments.

The effect of water/PEG ratio and NaF concentration on viscoelastic moduli was discussed in the article. The influence of hybrid PEG size on mechanical properties was also studied. Three hydrogels were prepared in DPBS with 10 wt% hybrid PEG (1000, 2000 or 6000 g/mol) and 2.5 wt% of NaF. Gelation time and storage moduli of these hydrogels at 1 Hz frequency are presented in the table below.

	Gelation time (min)	G' (Pa)
Hybrid PEG 1000	30	7973
Hybrid PEG 2000 (1)	35	10630
Hybrid PEG 6000	> 24 h	na

On the one hand, one can notice that G' value of hybrid PEG 1000 gel was lower than that of hybrid PEG 2000. Based on the evolution of the silica/organic ratio and the increase of the PEG chain length, which should induce a higher mesh size, we could suspect a reduction of G' for hybrid PEG 2000 gel. In our case, observed evolution can be explained by the higher cristallinity of PEG 2000 which could induce a self-assembly of PEG units in the gel. On the other hand, mechanical properties of hybrid PEG 6000 hydrogel could not be studied. Indeed, after 24 h at 37°C, hybrid PEG 6000 solution yielded a viscous liquid. This can be explained by a decrease in cross-links due to a higher silica/organic ratio.

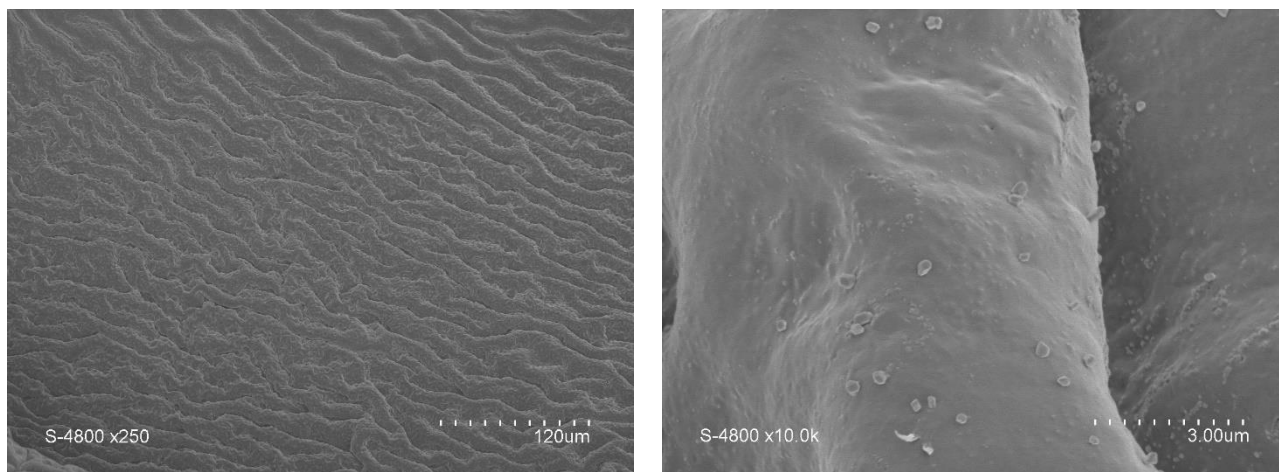


10 wt% hybrid PEG hydrogels after 24 h at 37°C. Top: hybrid PEG 2000; bottom: hybrid PEG 6000.

SEM images and BET

The morphology of the hydrogels was analyzed by Scanning Electron Microscopy (SEM) on a Hitachi S4800. Pieces of gels were affixed to SEM pucks using conductive carbon tape, they were freeze-dried and coated with a 2 nm gold layer. The images show a featureless homogeneous and dense matrix whether for broad and magnificated top views. It's worth noting that, observed crystals on the surface (right image) were generated from the DPBS.

Supporting information for publication n°2
An easy synthesis of tunable hybrid bioactive hydrogels



SEM images of 10 wt% hybrid PEG hydrogel containing 0,3 wt% of NaF

In addition, nitrogen sorption measurements show that these hybrid materials are also nonporous with a low surface area ($S_{\text{BET}} < 10 \text{ m}^2 \cdot \text{g}^{-1}$).

Cytotoxicity

Cell culture reagents were purchased from Gibco. Hydrogel cytotoxicity was measured with a LDH cytotoxicity kit II from PromoKine according to the ISO 10993-5 standard. L929 mouse fibroblasts were cultured in phenol red-containing Minimum Essential Media (MEM Alpha Medium) with 10% horse serum, 1% GlutaMAX and 1% penicillin-streptomycin at 37°C with a humidified 5% CO₂ atmosphere. Cells were detached using versene and trypsin. They were centrifugated, suspended in culture medium and counted with a hemacytometer. The suspension was diluted to a concentration of 50,000 cells per mL. Cells were seeded in a tissue culture treated 24 well cell culture plate (1 mL of cell suspension per well *i. e.* 50.000 cells, except background control wells which contain 1 mL of growth medium without cells). The plate was incubated at 37°C with 5% CO₂ for 24h to allow cell adhesion and proliferation. Cytotoxicity assays were run in tetraplicates following the supplier's protocol. After 24h, we added:

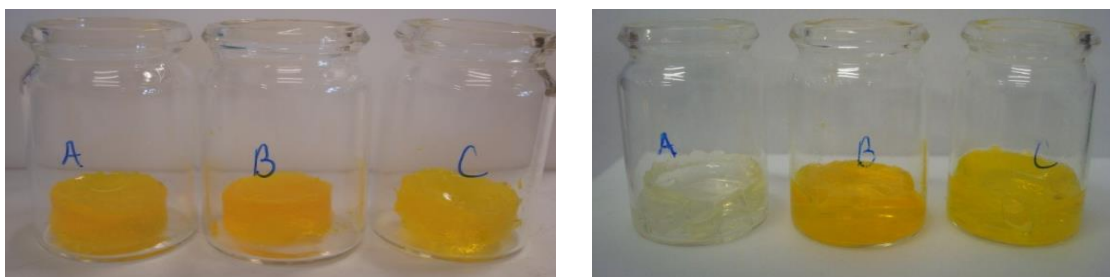
- 100 μL of DPBS in background control and low control wells,
- 100 μL of cell lysis solution in high control wells
- a 5 mm diameter cylindrical hydrogel whose volume is 100 μL in test sample wells
- a piece of PLA-50 whose surface is equivalent to hydrogel surfaces and 100 μL of DPBS in PLA controls.

The plate was placed again in an incubator for 24h. 10 μL of the homogenized media were transferred from the 24 well plate to an optically clear 96 well plate. LDH reaction mix (100 μL) was added to each well and allowed to react for 30 min at room temperature. The stop solution (10 μL per well) was then added and the absorbance of each well was read at 450 nm. Background values were subtracted from the other values.

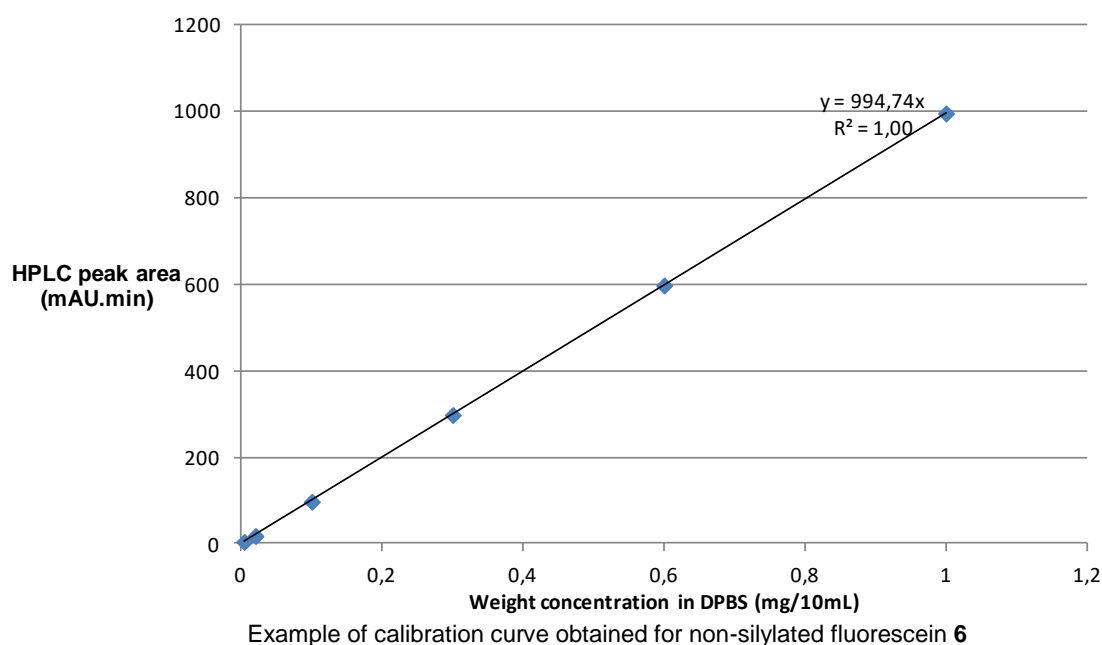
Fluorescein release experience

A 10 wt% solution of hybrid PEG in DPBS with 3 wt% of NaF (3 mL) was added to $5.2 \cdot 10^{-3}$ mmol of a fluorescein derivative (3.0 mg of non-silylated fluorescein **6** or 3.7 mg of triethoxysilyl fluorescein **4** or 3.2 mg of dimethylhydroxysilyl fluorescein **5**). N. B. dimethylhydroxysilyl fluorescein was first dissolved in DMF (100 μL) and water containing 1% TFA (v/v, 90 μL) was added to hydrolyse fluorescein dimers into monomers. Gelation occurred at 37°C overnight. Then, the gel tablets were placed in different flasks with 10 mL of DPBS and stored at RT. DPBS was regularly removed and replaced by fresh DPBS. The release of the different fluoresceins was measured out by HPLC from collected solutions of DPBS.

Supporting information for publication n°2
An easy synthesis of tunable hybrid bioactive hydrogels



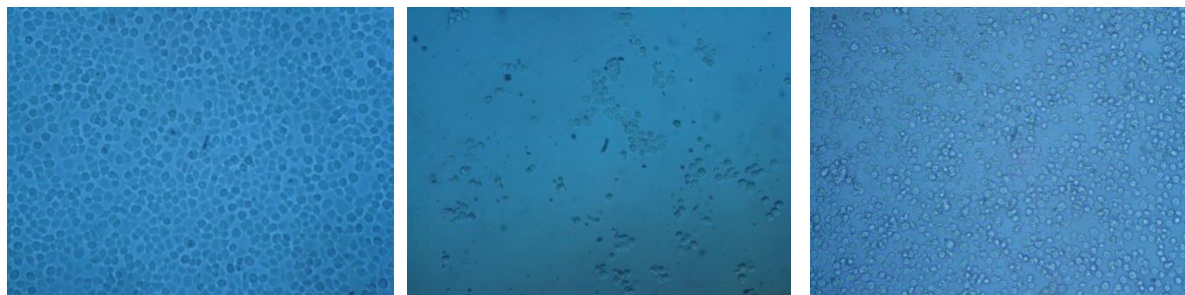
Fluorescein-containing gels at the beginning of the release experience (left) and after 8 days (right). A: non-silylated fluorescein **6** gel; B: triethoxysilyl fluorescein **4** gel; C: dimethylhydroxysilyl fluorescein **5** gel.



Cell adhesion assays

Adhesion properties of hybrid gels were measured on L929 mouse fibroblasts cultured in the same conditions as for cytotoxicity assays. 300 μ L of a 10 wt% solution of hybrid PEG containing 0.3 wt% of NaF and hybrid RGD peptide **2** (final concentration 0, 10 or 20 mol% compared to hybrid PEG **1**) were placed in a 24 well cell culture plate in triplicates. The plate was incubated at 37°C with a humidified 5% CO₂ atmosphere overnight. 200 000 cells in 40 μ L of culture medium were added on top of the gels. For high control wells, cells were seeded directly on tissue culture treated polystyrene. Cells were allowed to adhere for 30 min, 1h or 2h at 37°C. Then, all the wells were washed with DPBS and PrestoBlue (1 mL of a 10% (v/v) solution of PrestoBlue, Molecular probes by life technologies, in the culture medium) was added. 300 μ L of DPBS were added to high and low control (no cells) wells in order to reach the same dilution as the gel-containing wells. The plate was incubated for 1h. Then 200 μ L of each well were transferred to a 96 well black plate for fluorescence reading ($\lambda_{\text{excitation}} = 535 \text{ nm}$, $\lambda_{\text{emission}} = 615 \text{ nm}$).

Supporting information for publication n°2
An easy synthesis of tunable hybrid bioactive hydrogels

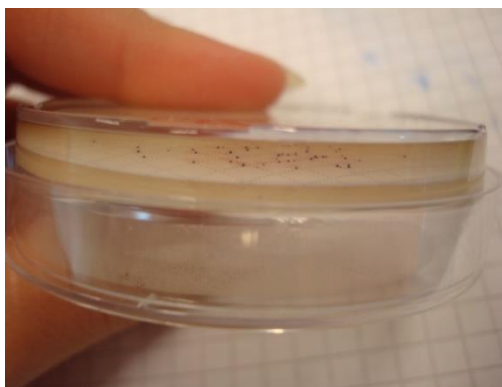


Cell observation after 30 min adhesion and 1h incubation with Prestoblue solution. Left : Tissue culture treated polystyrene; Middle: Hybrid PEG hydrogel without RGD; Right: 20 mol% hybrid RGD hydrogel.

Hybrid RGD promoted cell adhesion by providing attachment points to the cells. However, we observed that cells had difficulties spreading on the gel, indeed, PEG induced shrinkage. Nonetheless, the aim of this study was to prove that new biological properties could be given to hybrid PEG hydrogels by covalent incorporation of active peptides. Here, cell adhesion was enabled by hybrid RGD incorporation.

Antibacterial assays

Hybrid PEG was dissolved in DPBS at a 10 wt% concentration. The solution was filtered over a 0.22 μm pore size sterilizing nitrocellulose membrane. NaF was added at a 0.3 wt% concentration. Hybrid peptides **3** and **7** were dissolved in Milli-Q water (400 μL) containing 1‰ TFA (V/V) and added to the hybrid PEG solution. The same amount of acidic Milli-Q water without peptide was added to hybrid PEG solution to yield the reference hydrogel. This acidic addition resulted in a negligible variation in the buffer pH (variation of less than 0.1). Hybrid PEG solutions (5 mL) were poured in 55 mm diameter Petri dishes. Solutions were incubated at 37°C overnight to achieve gelification. Autoclaved granulated agar in DPBS (15 g/L) was used as a control sample. Bacteria strains (*Staphylococcus aureus* ATCC 6538, *Escherichia coli* ATCC 25922) were grown overnight at 37°C on tryptic soy agar. Bacteria were then suspended in DPBS and the turbidity of suspensions were adjusted to an equivalent 0.5 McFarland standard by measuring transmitted light at 620 nm (*E. Coli* 78%, *S. Aureus* 75%). Suspensions were diluted to 10^3 UFC/mL concentrations and added (500 μL *i. e.* approximately 500 UFC) onto hydrogels in Petri dishes. A 0.45 μm pore size nitrocellulose membrane was laid down on the inoculums before tryptic soy agar (TSA, 5 mL) was poured on top of the layers. Bacteria colonies were counted in each Petri dish after incubation at 37°C for 24h. To facilitate counting, bacteria were stained with MTT: 200 μL of a solution of 3-(4,5-dimethylthiazol-2-yl)-2,5-diphenyl tetrazolium bromide at a concentration of 0.5 mg/mL were sprayed onto TSA in each dish 1h before reading.



Picture of the experimental set-up for antibacterial assays. Upside-down Petri dish containing from top to bottom: hybrid PEG hydrogel, MTT stained bacteria, nitrocellulose membrane, tryptic soy agar culture medium.

Supporting information for publication n°3

Sol-gel synthesis of collagen-inspired peptide hydrogel

Cécile Echalié, Said Jebors, Guillaume Laconde, Luc Brunel, Pascal Verdié, Léa Causse, Audrey Bethry, Baptiste Legrand, Hélène Van Den Berghe, Xavier Garric, Danièle Noël, Jean Martinez, Ahmad Mehdi, Gilles Subra

Abbreviations	2
Material and Methods.....	2
Synthesis of undecapeptide 1	3
Silylation of undecapeptide 1	5
Preparation of a hydrogel	9
NMR study of 2 and monitoring of the gelation process.....	9
CD study	13
Rheology	14
Scanning Electron Microscopy	15
Cell adhesion	16
Cell proliferation	17
Encapsulation	17
Figure S1. Synthesis of undecapeptide 1 using Fmoc-ProHypGly-OH building block	3
Figure S2. LC/MS spectrum of 1	4
Figure S3. ¹ H NMR spectrum of 2 in DMSO- <i>d</i> ₆ (500 MHz).....	5
Figure S4. ¹³ C NMR spectrum of 2 in DMSO- <i>d</i> ₆ (125 MHz)	6
Figure S5. ²⁹ Si NMR spectrum of 2 in DMSO- <i>d</i> ₆ (99 MHz)	6
Figure S6. LC/MS spectrum of 2	7
Figure S7. HR-MS analysis of 2	8
Figure S8. Proposed mechanism for fluorine-catalyzed sol-gel process. A: hydrolysis step. B: condensation step.....	9
Figure S9. 1D ¹ H NMR spectra of the hybrid peptide 2 at 62 mM and 0.62 mM (10 and 0.1%) in DPBS buffer (10% D ₂ O) without NaF at 37°C, pH 7.2.	10
Figure S10. 1D ¹ H NMR spectra of the hybrid peptide 2 at 62 mM (10%) in DPBS buffer (10% D ₂ O) with and without NaF at 37°C, pH 7.2. Spectra were recorded after 5 and 60 min.....	11
Figure S11. Nomenclature and chemical shifts for the silylated arm (R = -H or -CH ₂ CH ₃)	12
Figure S12. 1D ¹ H NMR spectra at different intervals of the hybrid peptide 2 at 62 mM (10%) in DPBS buffer (10% D ₂ O) with NaF at 37°C, pH 7.2.	13
Figure S13. CD spectrum of the hybrid peptide 2 (0.062 mM) in DPBS buffer, pH 7.2 at 37°C.	14
Figure S14. Frequency sweep from 10 to 0.1 Hz at 25% strain. Black dots: G'; Grey dots: G''.	15
Figure S15. SEM image of a hydrogel (10 wt% of hybrid peptide 2 in DPBS with 0.3 wt% NaF) after freeze-drying.....	15
Figure S16. Cryo-SEM images of the hydrogel. A: before sublimation. B: after sublimation for 1 min at -96°C. C and D: after sublimation for 3 min at -87°C.....	16

Abbreviations

ACN, acetonitrile; Boc, t-butyloxycarbonyl; BBFO, broad band fluorine observation; CD, circular dichroism; DIEA, diisopropylethylamine; DMEM, Dulbecco's modified eagle medium; DMF, N,N'-dimethylformamide; DMSO, dimethylsulfoxide; DPBS, Dulbecco's phosphate buffered saline; ECM, extracellular matrix; ESI-MS, electrospray ionization mass spectrometry; FBS, fetal bovine serum; Fmoc, fluorenylmethoxycarbonyl; FPPS, fast parallel peptide synthesis; HATU, 1-/Bis(dimethylamino)methylene]-1H-1,2,3-triazolo[4,5-b]pyridinium 3-oxid hexafluorophosphate; HPMC, hydroxypropylmethylcellulose; ICPTES, 3-isocyanatopropyltriethoxysilane; LC/MS, tandem liquid chromatography/ mass spectrometry; mMSC, mouse mesenchymal stem cell; NIPAM, poly(*N*-isopropylacrylamide); NMR, nuclear magnetic resonance; pip, piperidine; PEG, polyethylene glycol; PHEMA, polyhydroxyethylmethacrylate; PLA, poly(lactic acid); PLGA, poly(lactic-co-glycolic acid); RP-HPLC, reversed phase high performance liquid chromatography; RT, room temperature; SEM, scanning electron microscopy; SPPS, solid phase peptide synthesis; TC-PS, tissue culture polystyrene; TFA, trifluoroacetic acid; TIS, triisopropylsilane; TMSP, trimethylsilyl-3-propionic acid 2,2,3,3-sodium salt; UV, ultra-violet, VEGF, vascular endothelial growth factor. Other abbreviations used were those recommended by the IUPAC-IUB Commission (Eur. J. Biochem. 1984, 138, 9-37).

Material and Methods

All solvents and reagents were used as supplied. Solvents used for LC/MS were of HPLC grade. DMF, DIEA, ACN, TIS, TFA and piperidine were obtained from Sigma-Aldrich. Fmoc amino acid derivatives and HATU were purchased from Iris Biotech (Marktredwitz, Germany). AmphiSpheres 40 RAM 0.37 mmol/g 75-150 μ m resin was purchased from Agilent Technologies. ICPTES and sodium fluoride were obtained from Alfa Aesar and Acros respectively.

Samples for LC/MS analyses were prepared in acetonitrile/water (50:50, v/v) mixture, containing 0.1% TFA. The LC/MS system consisted of a Waters Alliance 2695 HPLC, coupled to a Water Micromass ZQ spectrometer (electrospray ionization mode, ESI+). All the analyses were carried out using a Chromolith Flash 25 x 4.6 mm C18 reversed-phase column. A flow rate of 3 mL/min and a gradient of (0-100)% B over 2.5 min were used. Eluent A: water/0.1% HCO₂H; eluent B: acetonitrile/0.1% HCO₂H. UV detection was performed at 214 nm. Electrospray mass spectra were acquired at a solvent flow rate of 200 μ L/min. Nitrogen was used for both the nebulizing and drying gas. The data were obtained in a scan mode ranging from 100 to 1000 m/z or 250 to 1500 m/z to in 0.7 sec intervals.

High Resolution Mass Spectrometric analyses were performed with a Synapt G2-S (Waters) mass spectrometer fitted with an Electrospray Ionisation source. All measurements were performed in the positive ion mode. Capillary voltage: 1000 V; cone voltage: 30 V; source temperature: 120°C; desolvation temperature: 250°C. The data were obtained in a scan mode ranging from 0 to 2000 m/z.

NMR solvents and TMSP were obtained from Euriso-top. ²⁹Si, ¹³C and ¹H NMR spectra in DMSO-*d*₆ were collected on a Bruker AVANCE 500 MHz spectrometer equipped with a BBFO helium cryoprobe at 298 K. The deuterated solvent was used as an internal deuterium lock. Chemical shifts (δ) are reported in parts per million using residual non-deuterated solvents as internal references. Spectra were processed and visualized with Topspin 3.2 (Bruker Biospin).

Synthesis of undecapeptide 1

Convergent synthesis

A convergent synthesis strategy was first used to produce several grams of undecapeptide **1**. This strategy involved the solution phase synthesis of the Fmoc-ProHypGly-OH tripeptide. Boc-Hyp-OH was coupled on H-Gly-OBzl. Fmoc-Pro-OH was coupled on the resulting dipeptide after Boc removal in TFA. Removal of C-ter protecting group by catalyzed hydrogenation yielded the tripeptide ready to use as a building block for the synthesis of the undecapeptide **1**.

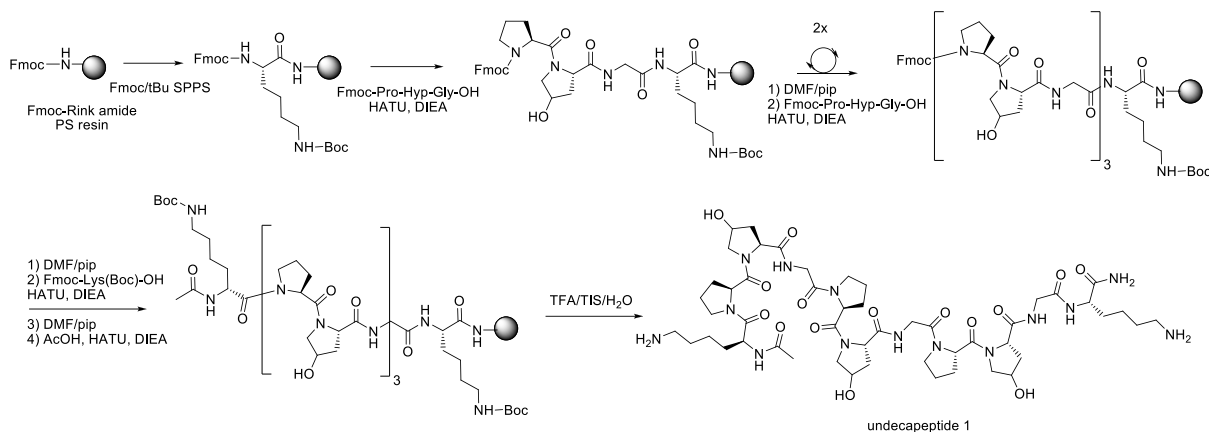


Figure S1. Synthesis of undecapeptide **1** using Fmoc-ProHypGly-OH building block

After purification, the undecapeptide **1** was obtained with 45% yield.

FPPS synthesis

The FPPS methodology developed in our group (Laconde, G. *et al.* Fast parallel peptide synthesis - FPPS: A methodology for the rapid and efficient preparation of peptide libraries. *Submitted*) was also applied to the synthesis of undecapeptide **1**. All the stages of the FPPS were realized under vortex stirring at 500 rpm, on a 0.5 mmol scale using the AmphiSpheres 40 RAM (0.37 mmol/g 75-150) μ m resin in DMF. Stock solutions of all Fmoc-protected amino acids (Fmoc-Lys(Boc)-OH, Fmoc-Gly-OH, Fmoc-Hyp(tBu)-OH, Fmoc-Pro-OH) and HATU were prepared in DMF at 0.5 M. The coupling reactions were performed using an amino acid (5 ml, 5 eq) / HATU (5 ml, 5 eq) / DIEA (0.87 ml, 10 eq) mixture for 5 minutes and repeated twice. Fast double couplings were replaced by a single 30 min coupling for Fmoc-Hyp(tBu)-OH. The Fmoc removal steps were realized using a piperidine/DMF 20/80 v/v solution (12 ml) for 1 minute and performed twice. All washings were done with DMF (12 ml). N-Terminal acetylation was performed with 20% Ac₂O in DMF and DIEA for 5 minutes twice. The peptide was cleaved from the resin with the cocktail TFA/TIS/H₂O (95/2.5/2.5 v/v/v), recovered by precipitation in diethyl ether, then taken up in ACN/H₂O 50/50 v/v mixture and freeze-dried. The crude peptide was solubilized in H₂O/ACN 98/2 v/v mixture with 1% TFA and purified by RP-preparative HPLC. The purification was performed on a NOVASEP HPLC system equipped with a C18 reversed-phase Luna column (Phenomenex 10 μ m, 250 \times 50 mm) with a flow rate of 120 mL/min. Eluents were H₂O 1% TFA (A) and ACN 1% TFA (B). The purification gradient started with 3 minutes at 0% of B and then increased from 0 to 20% of B in 20 min. UV detection was performed at 221 nm. Collected fractions were concentrated and freeze-dried to yield the pure undecapeptide **1** as a TFA salt with 50% yield. This yield was similar to the yield of the convergent strategy. However, the synthesis of the peptide was much faster with the FPPS methodology. As a consequence, this protocol was selected for large-scale synthesis of peptide **1**.

Supporting information for publication n°3
Sol-gel synthesis of collagen-inspired peptide hydrogel

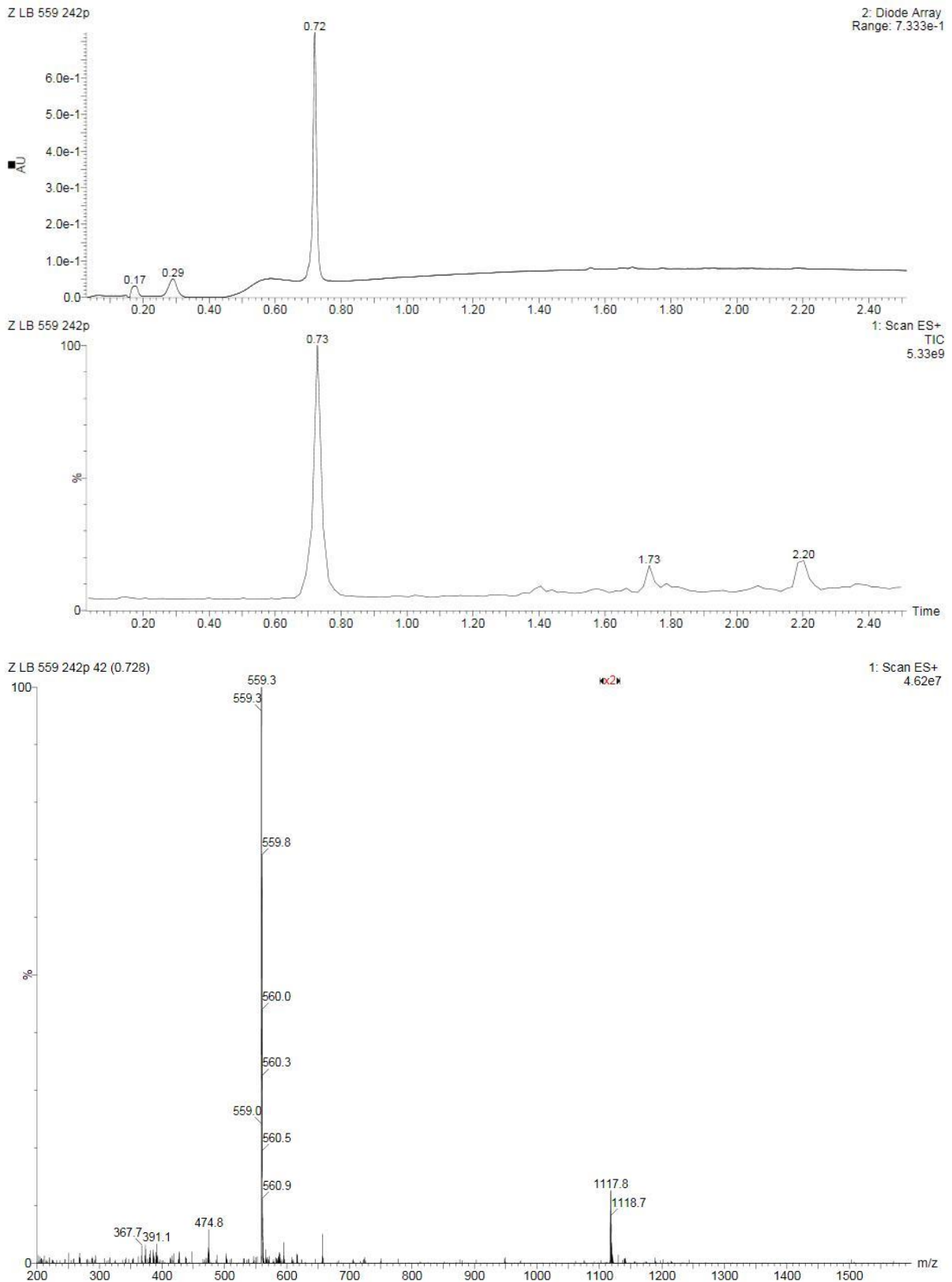


Figure S2. LC/MS spectrum of **1**

LC/MS (ESI⁺): t_R = 0.72 min, m/z 1118 ([M+H]⁺, 8%), 559 ([M+2H]²⁺, 100)

Silylation of undecapeptide **1**

Undecapeptide **1** was reacted with 3-isocyanatopropyltriethoxysilane (2.2 eq) in anhydrous DMF at a concentration of 100 mM in the presence of DIEA (4 eq) for 50 min under argon atmosphere. The completion of the reaction was checked by HPLC. The bis-silylated hybrid block **2** was obtained quantitatively after precipitation and washings with diethylether.

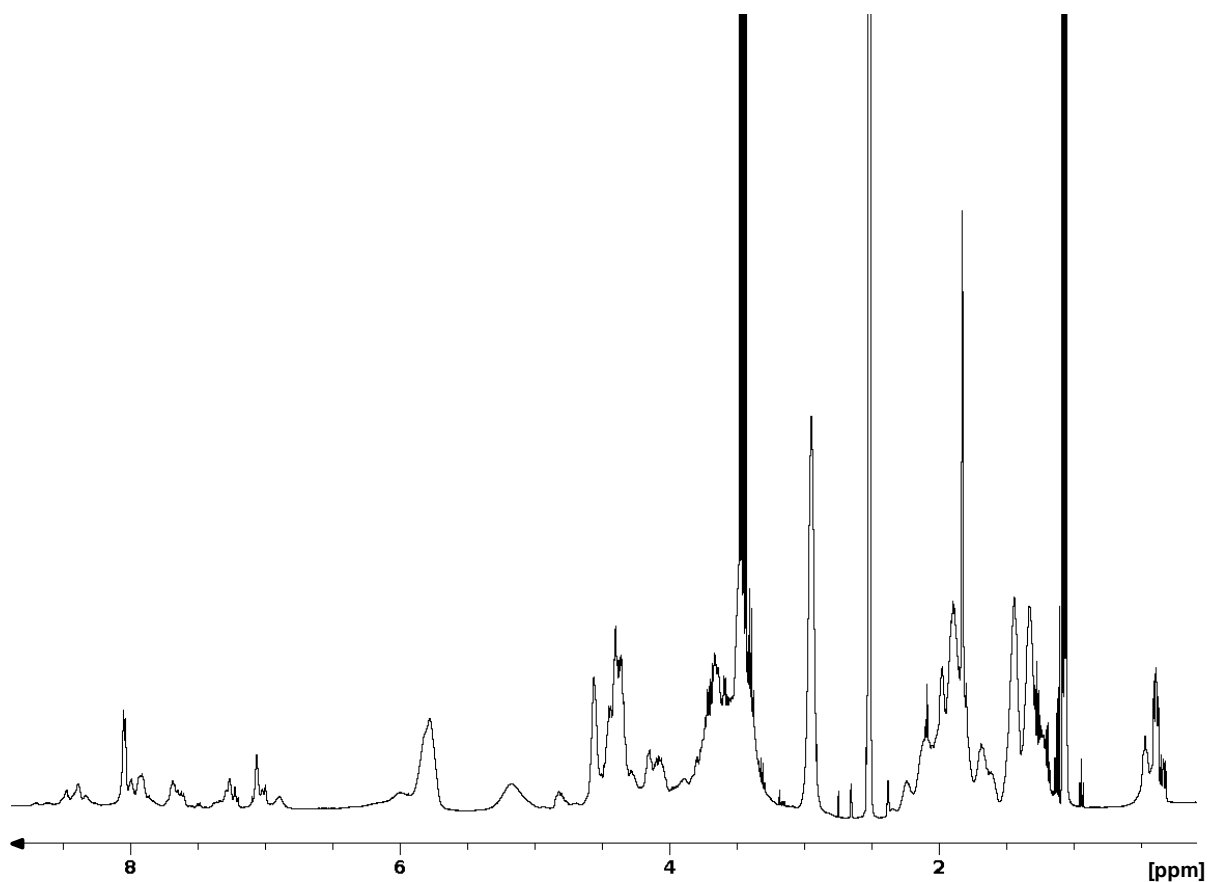


Figure S3. ¹H NMR spectrum of **2** in DMSO-*d*₆ (500 MHz)

Supporting information for publication n°3
Sol-gel synthesis of collagen-inspired peptide hydrogel

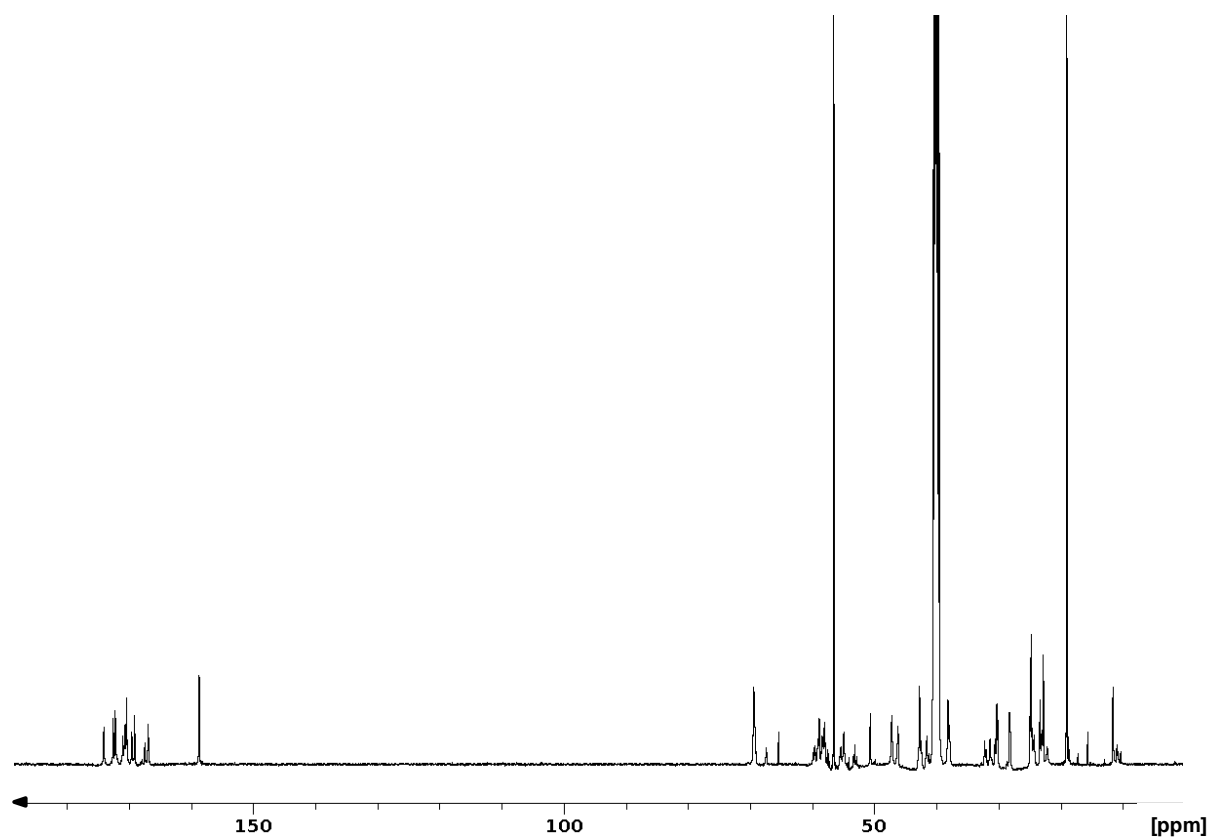


Figure S4. ^{13}C NMR spectrum of **2** in $\text{DMSO-}d_6$ (125 MHz)

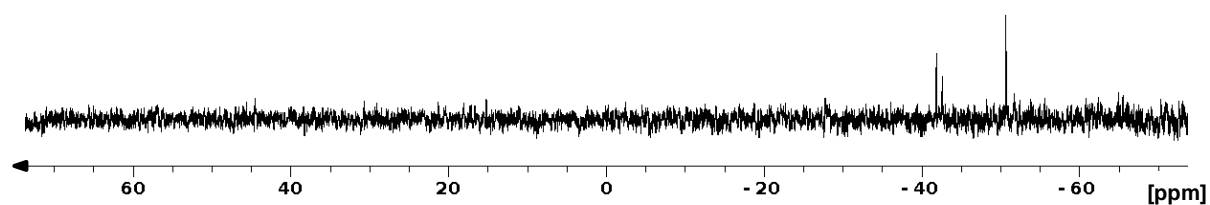


Figure S5. ^{29}Si NMR spectrum of **2** in $\text{DMSO-}d_6$ (99 MHz)

Noteworthy, 3 signals are observed on the ^{29}Si NMR spectrum corresponding to different states of hydrolysis and condensation of $-\text{Si}(\text{OEt})_3$ groups.

Supporting information for publication n°3
Sol-gel synthesis of collagen-inspired peptide hydrogel

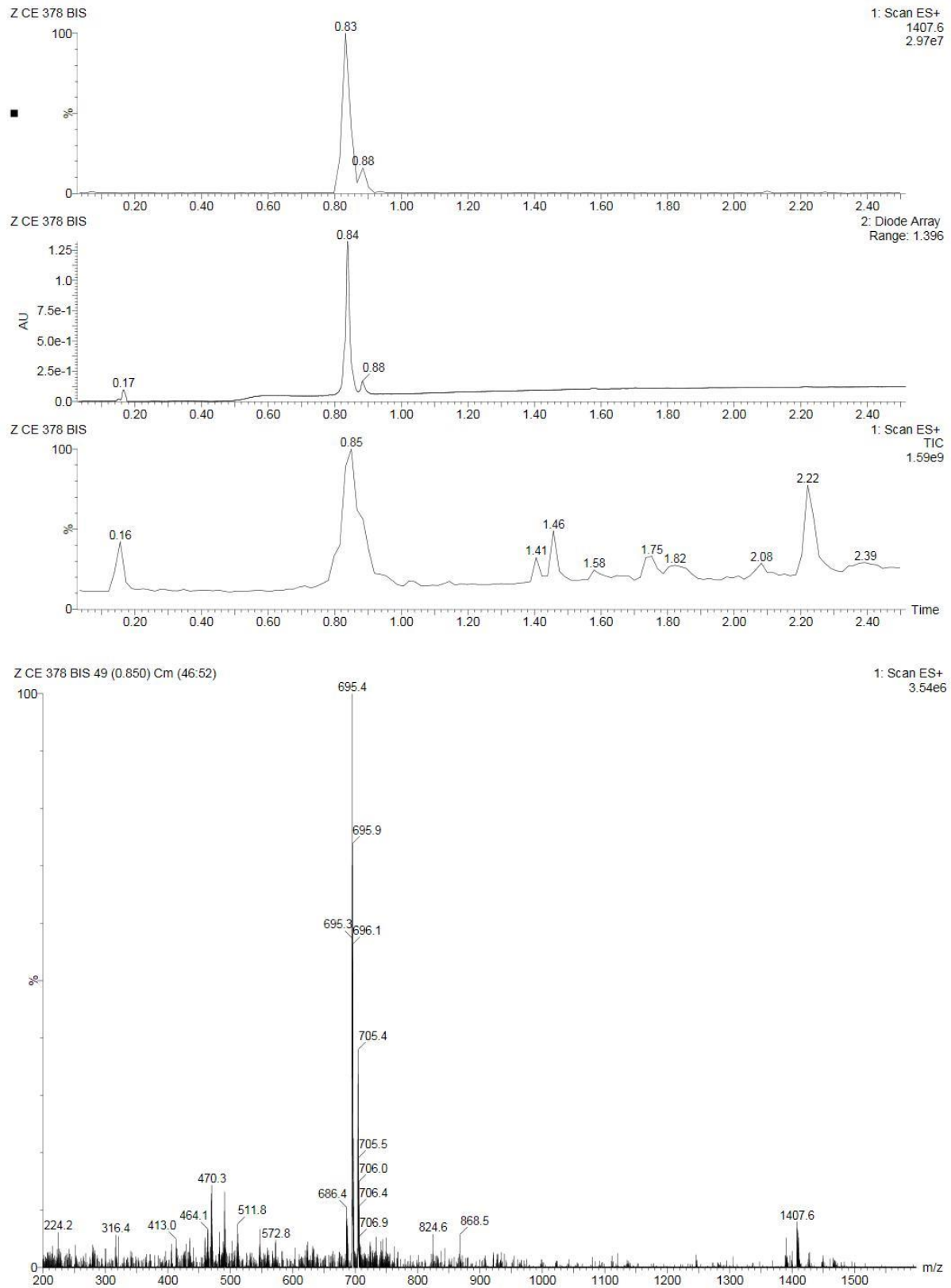


Figure S6. LC/MS spectrum of **2**

LC/MS (ESI⁺): Only the product of hydrolysis of ethoxysilyl groups into silanols is detected with several H₂O losses. t_R = 0.84 min, m/z 1408 ([M-2H₂O+H]⁺, 10%), 695 ([M-3H₂O+2H]²⁺, 100).

Supporting information for publication n°3
Sol-gel synthesis of collagen-inspired peptide hydrogel

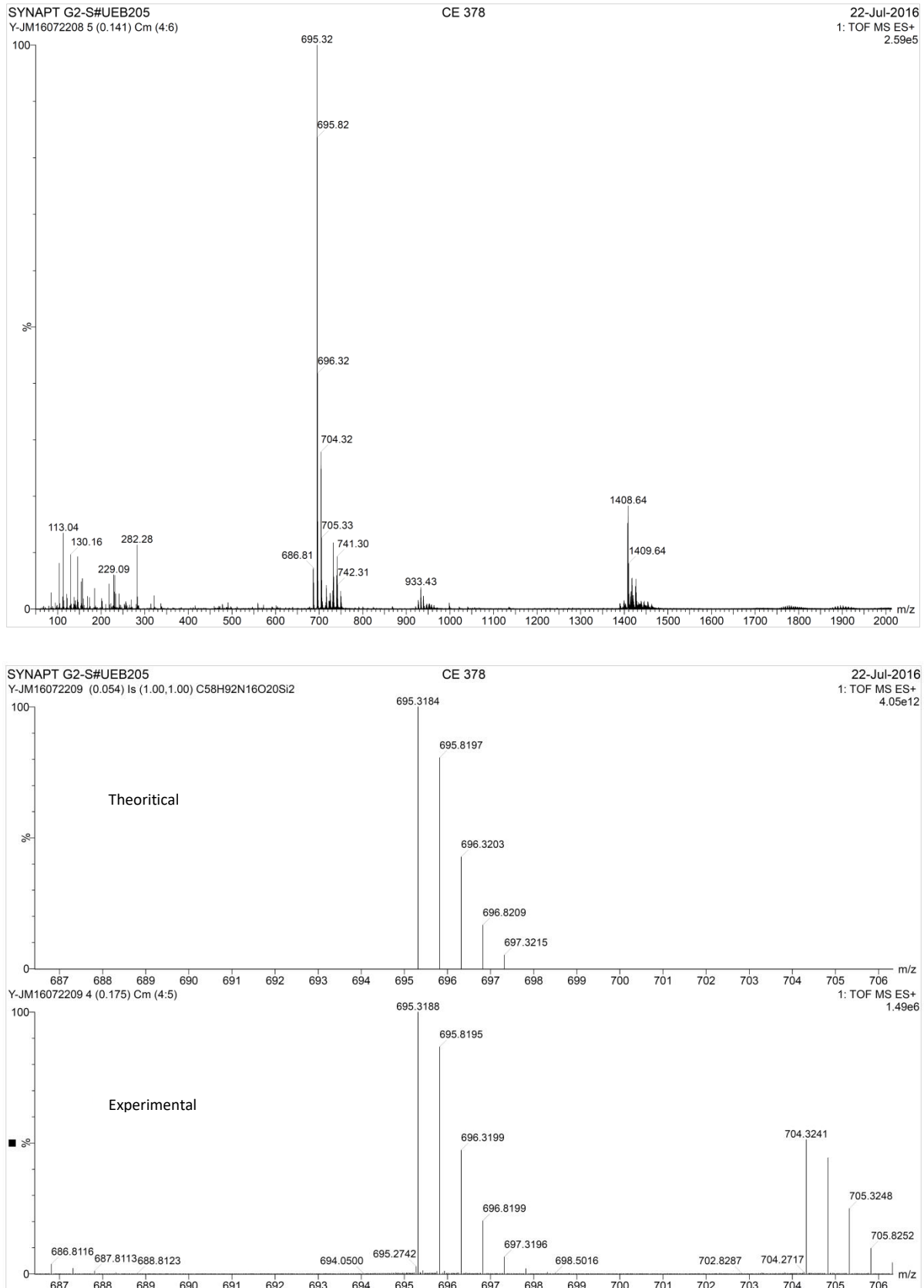


Figure S7. HR-MS analysis of **2**

HR/MS (ESI⁺): Only the product of hydrolysis of ethoxysilyl groups into silanols is detected with several H₂O losses. It is usual to observe $-\text{Si}^+(\text{OH})_2$ species when hybrid derivatives are analyzed by ESI⁺ MS.

Supporting information for publication n°3
Sol-gel synthesis of collagen-inspired peptide hydrogel

The most abundant ion at $m/z = 695.3188$ corresponds to $[M-3H_2O+2H]^{2+}$ with M the hydrolyzed hybrid peptide.

Preparation of a hydrogel

Hybrid bloc **2** (200 mg) was dissolved in 10% FBS supplemented DMEM (Gibco, ref. 31966, 2 mL) at a 10 wt% concentration. The solution was filtered on a 0.22 μm pore size filter to sterilize the solution when required. Sodium fluoride (0.3 wt%, 6 mg) was added. The hybrid solution was incubated at 37 $^\circ\text{C}$ overnight to yield the hybrid hydrogel.

The sol-gel process is catalyzed by fluoride ions. Here is a proposed mechanism for this process:

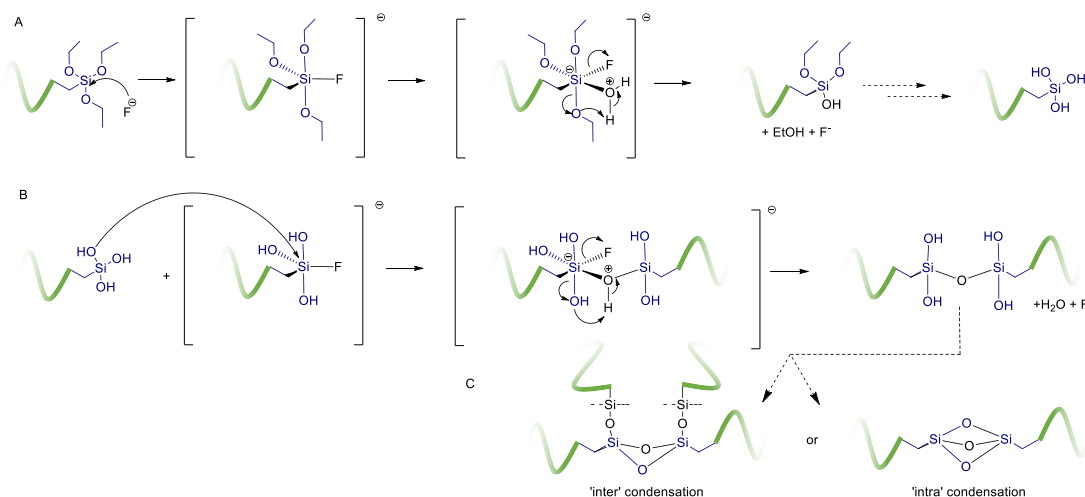


Figure S8. Proposed mechanism for fluoride-catalyzed sol-gel process. A: hydrolysis step. B: condensation step.

NMR study of **2** and monitoring of the gelation process

Preparation of samples

Two NMR samples containing the hybrid peptide **2** (0.062 M) were prepared in similar conditions, one with NaF catalyst and the other one without. The NaF-free sample was used to characterize the undecapeptide **2** in monomeric state since hydrolysis and condensation rates are very low in the absence of NaF. Gelation kinetics were then monitored using the NaF-containing solution.

Hybrid peptide **2** (20 mg, 0.0124 mmol) was dissolved in 200 μL of the following mixture: DPBS \times 10 (Gibco ref 14200, 100 μL), D_2O (100 μL), milliQ H_2O (800 μL), with or without NaF (3 mg). Microtubes were then used to record all spectra on a Bruker Avance 600 AVANCE III spectrometer equipped with a 5 mm quadruple-resonance probe (^1H , ^{13}C , ^{15}N , ^{31}P).

Characterization of the compound **2** at the monomeric state (NaF-free sample)

1D ^1H NMR spectra of compound **2** at 62 mM and 0.62 mM were first recorded to check the absence of self-assembly of this short sequence. Then, homonuclear 2D-spectra COSY, TOCSY (DIPS12) and ROESY were typically recorded in the phase-sensitive mode using the States-TPPI method as data matrices of 400 real (t_1) \times 2048 (t_2) complex data points; 4-32 scans per t_1 increment with 1.0 s recovery delay and spectral width of 6009 Hz in both dimensions were used. The mixing times were 80 ms for TOCSY and 300 ms for the ROESY experiments. Spectra were processed with Topspin (Bruker Biospin) and visualized with Topspin or NMRView (B. A. Johnson, R. A. Blevins, *J. Biomol. NMR*, 1994, **4**, 603-614) on a Linux station. The matrices were zero-filled to 1024 (t_1) \times 2048 (t_2) points after apodization by shifted sine-square multiplication and linear prediction in the F1 domain. Chemical shifts

Supporting information for publication n°3
Sol-gel synthesis of collagen-inspired peptide hydrogel

were referenced to the trimethylsilylpropanoic acid (TMSP). ^1H chemical shifts were assigned according to classical procedures (K. Wüthrich, NMR of Proteins and Nucleic acids; Wiley-Interscience: New York, 1986). The stereochemical assignment of proline and hydroxyproline geminal protons have been performed using the NOE correlations relative to the α protons on the ROESY spectrum. The absence of polymerization of **2** was confirmed performing 1D spectra at different times.

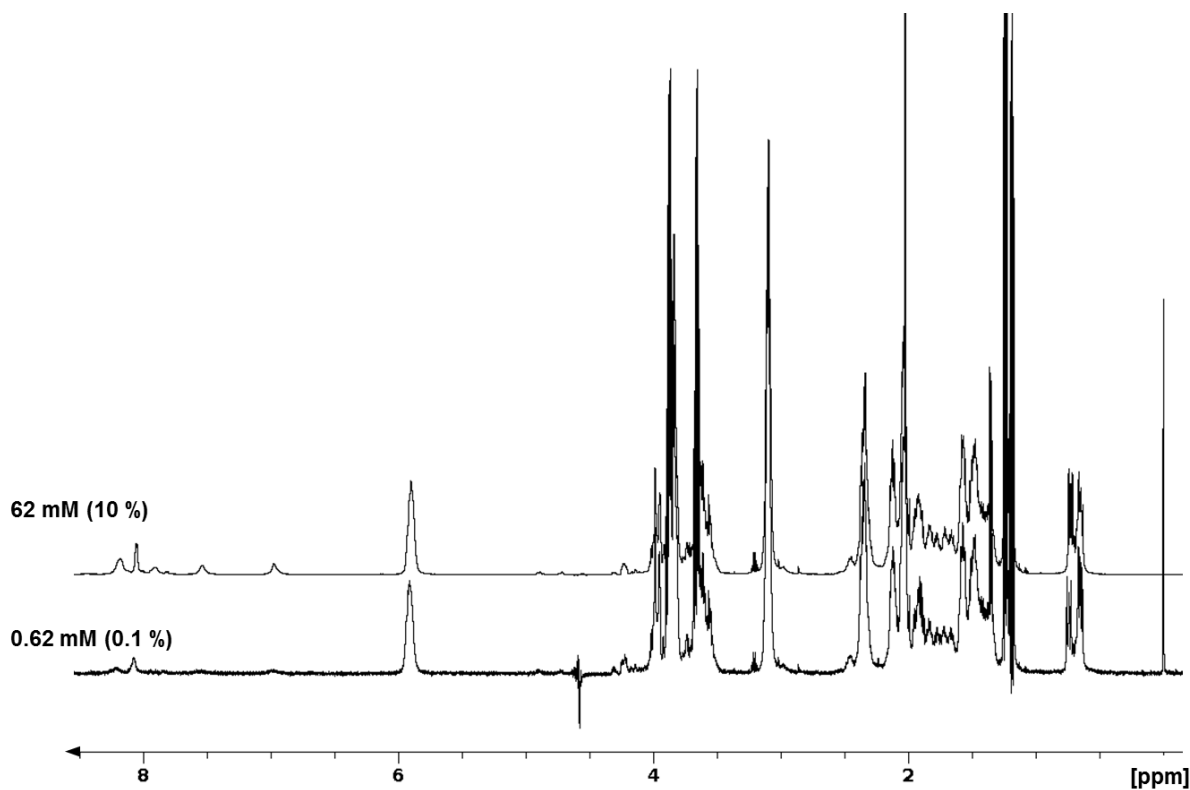


Figure S9. 1D ^1H NMR spectra of the hybrid peptide **2** at 62 mM and 0.62 mM (10 and 0.1%) in DPBS buffer (10% D_2O) without NaF at 37°C, pH 7.2.

Supporting information for publication n°3
Sol-gel synthesis of collagen-inspired peptide hydrogel

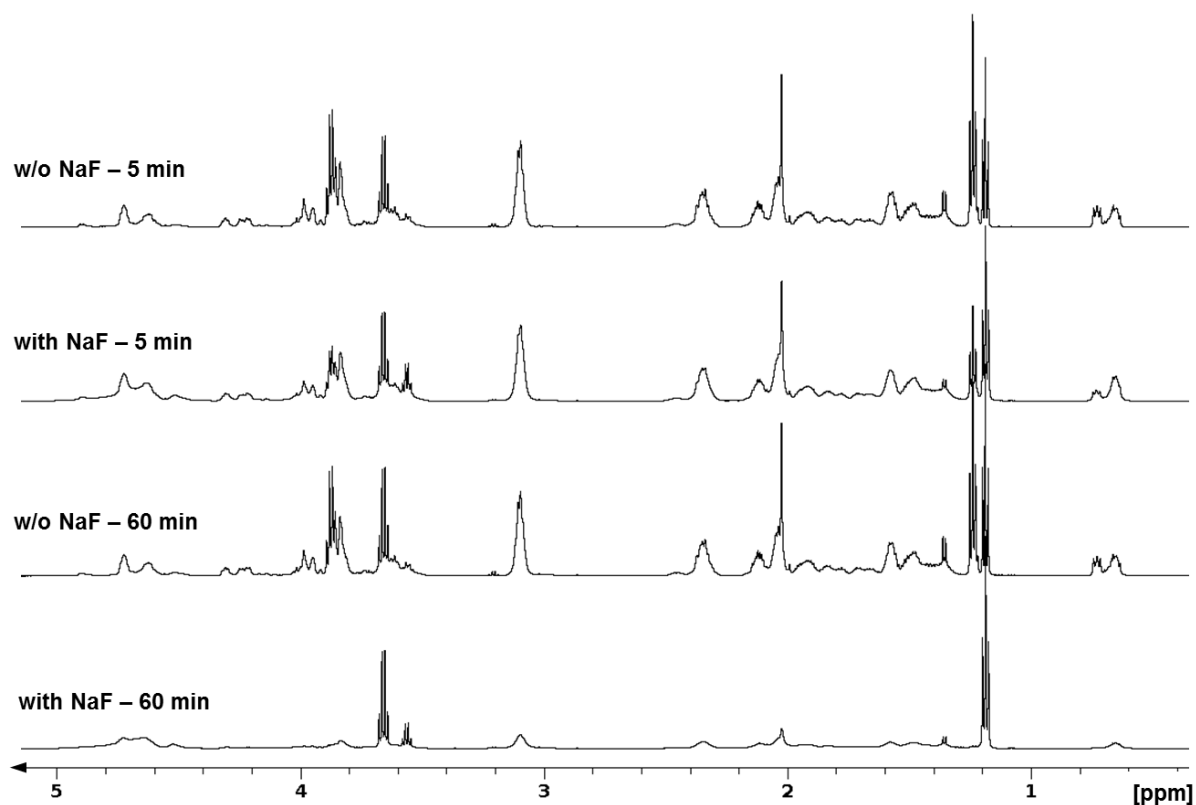


Figure S10. 1D ^1H NMR spectra of the hybrid peptide **2** at 62 mM (10%) in DPBS buffer (10% D_2O) with and without NaF at 37°C, pH 7.2. Spectra were recorded after 5 and 60 min.

Table S1. ^1H NMR chemical shifts of the peptide moieties of the compound **2** in DPBS buffer (10 % D_2O), pH 7.2 at 10°C.

Residue	H_N	H_α	H_β	H_γ	H_δ	Others
Lys 1	8.44	4.55	1.68, 1.80	1.46	1.51	H_ϵ 3.13; NH_ϵ 6.12; Ac 2.04
Pro 2	-	4.77	2.35, 1.92	2.06	3.91, 3.65	
Hyp 3	-	4.61	2.39, 2.11	4.66	3.90, 3.85	
Gly 4	8.59	3.98	-	-	-	
Pro 5	-	4.77	2.35, 1.92	2.06	3.61, 3.58	
Hyp 6	-	4.61	2.39, 2.11	4.66	3.90, 3.85	
Gly 7	8.59	3.99	-	-	-	
Pro 8	-	4.77	2.35, 1.92	2.06	3.69	
Hyp 9	-	4.61	2.39, 2.11	4.66	3.90, 3.85	
Gly 10	8.81	3.99	-	-	-	
Lys 11	8.22	4.31	1.74, 1.86	1.39	1.49	H_ϵ 3.11; NH_ϵ 6.12; NH_2 7.25, 7.82

Supporting information for publication n°3
Sol-gel synthesis of collagen-inspired peptide hydrogel

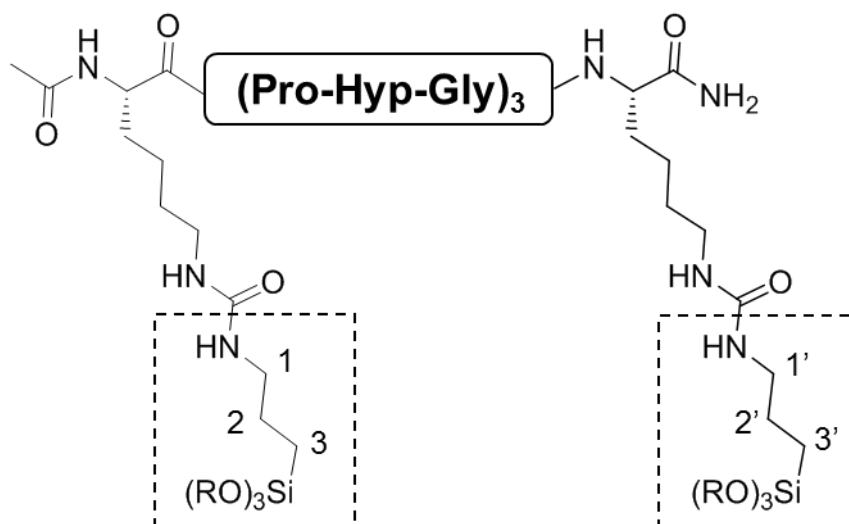


Figure S11. Nomenclature and chemical shifts for the silylated arm (R = -H or -CH₂CH₃)

SiOCH₂CH₃ silylated arm (R = CH₂CH₃): HN = 6.15 ppm; CH₂(1,1') = 3.12 ppm; CH₂(2,2') = 1.58 ppm; CH₂(3,3') = 0.77 ppm; OCH₂CH₃ = 3.90 and 1.24 ppm.

SiOH silylated arm (R = H): HN = 6.12 ppm; CH₂(1') = 3.11 ppm; CH₂(2') = 1.58 ppm; CH₂(3') = 0.66 ppm.

Ethanol NMR signals: CH₂ = 3.67 ppm; CH₃ = 1.18 ppm.

Note: The silylated arm was partially hydrolyzed even in absence of NaF.

Gelation kinetic measurement (NaF-containing sample)

1D ¹H NMR spectra of **2** in DPBS buffer (10 % D₂O) with NaF at pH 7.2 and 37°C were recorded at several intervals (5, 10, 15, 20, 30, 40, 50, 60, 70, 90 and 120 min) to monitor the kinetics of polymerization and gelation of **2**. Spectra were processed and integrals were measured using the Topspin software.

Supporting information for publication n°3
Sol-gel synthesis of collagen-inspired peptide hydrogel

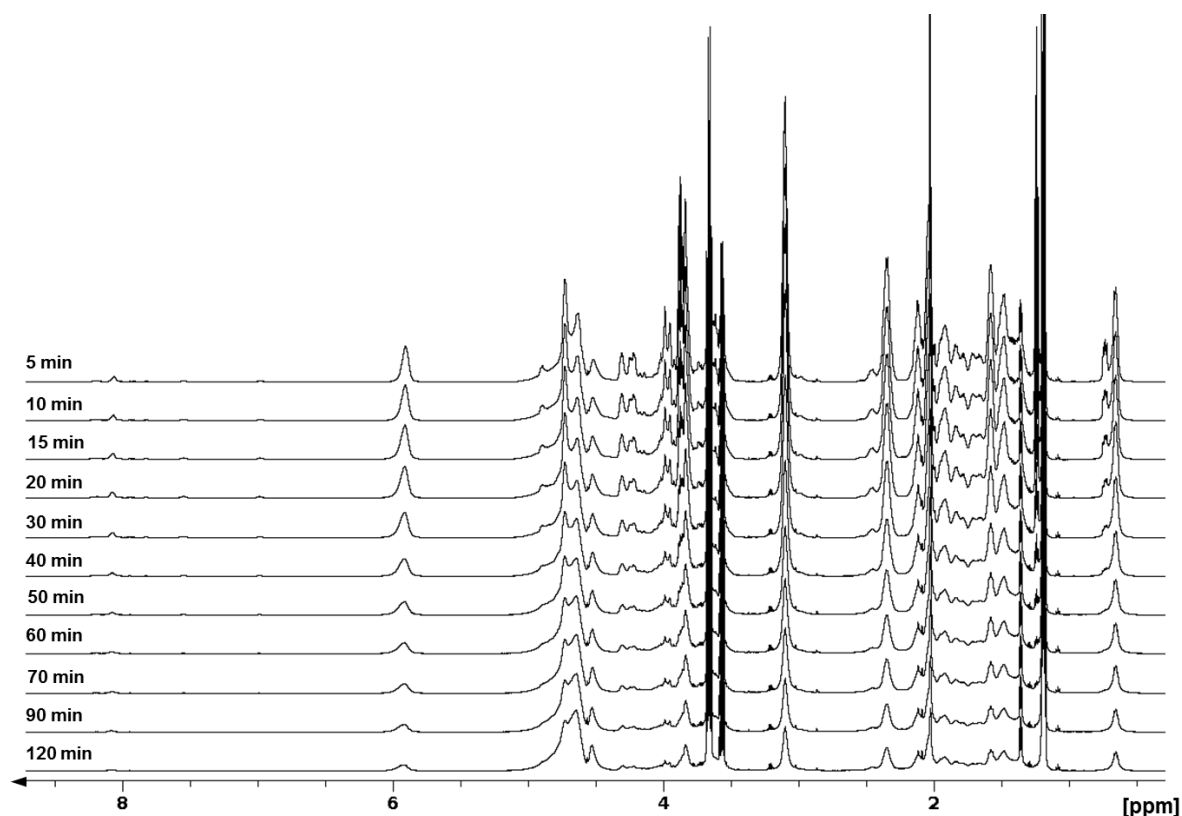


Figure S12. 1D ¹H NMR spectra at different intervals of the hybrid peptide **2** at 62 mM (10%) in DPBS buffer (10% D₂O) with NaF at 37°C, pH 7.2.

CD study

Circular dichroism experiments were carried out using a Jasco J815 spectropolarimeter. The spectra were obtained using a 1 mm path length CD cuvette, at 37°C, over a wavelength range of 190-260 nm. Continuous scanning mode was used, with a response of 1.0 s with 0.2 nm steps and a bandwidth of 2 nm. The signal to noise ratio was improved by acquiring each spectrum over an average of three scans. Baseline was corrected by subtracting the background from the sample spectrum.

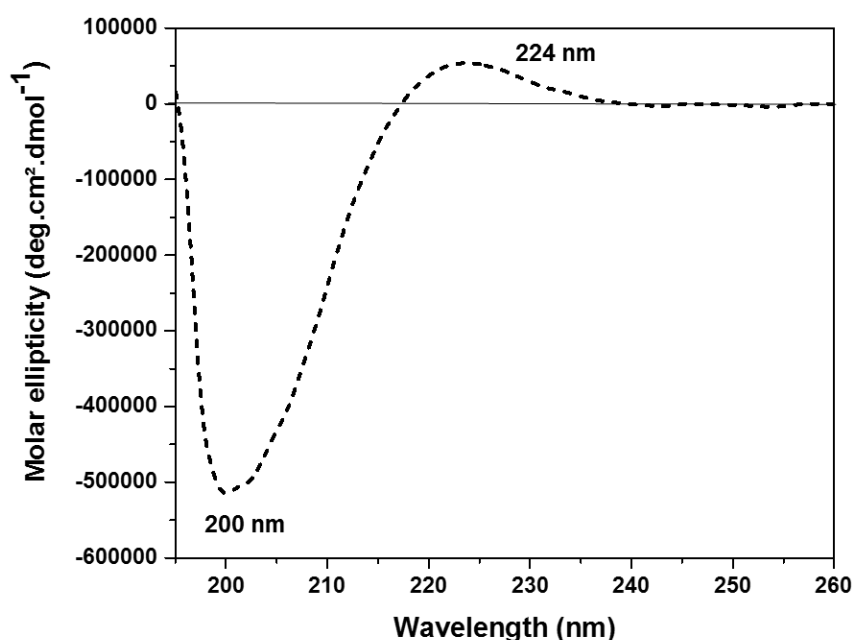


Figure S13. CD spectrum of the hybrid peptide 2 (0.062 mM) in DPBS buffer, pH 7.2 at 37°C.

Rheology

Rheological measurements were carried out on an AR 2000 rheometer from TA instruments, Inc. with a 20 mm diameter parallel geometry at 37°C in the oscillatory mode. The hybrid peptide 2 (50 mg) was dissolved in cell culture medium (10% FBS supplemented DMEM at 37°C, 500 µL) containing sodium fluoride (1.5 mg). The hybrid solution was immediately deposited on the Peltier plate and the gap was set at 500 µm. The excess solution was carefully removed with a pipette and a thin layer of silicone oil was applied to the air/sample interface to prevent dehydration of the sample. After 1 minute equilibration, storage (G') and loss (G'') moduli were recorded as a function of time for 5 hours within the linear viscoelastic regime at 25% strain and 1 Hz frequency. Frequency sweep experiment was also carried out at 25% strain.

Supporting information for publication n°3
Sol-gel synthesis of collagen-inspired peptide hydrogel

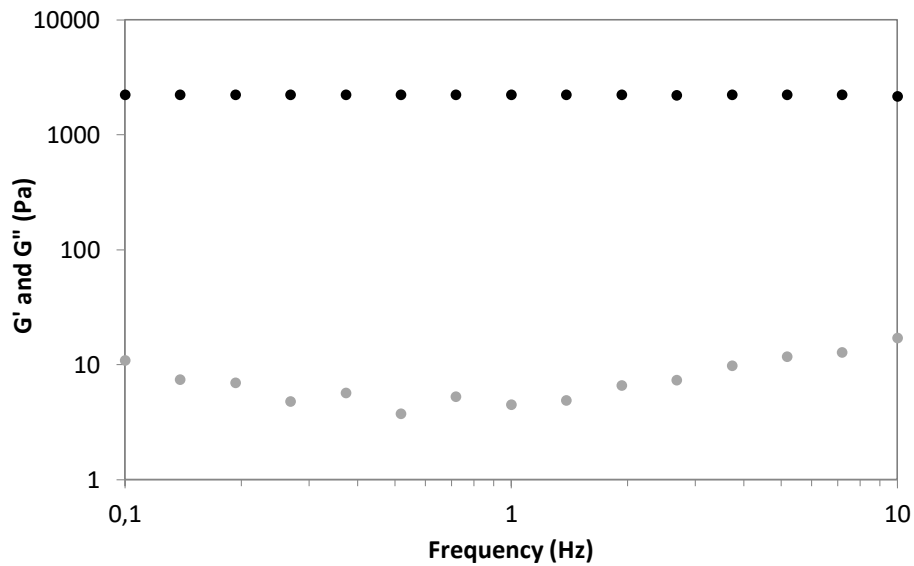


Figure S14. Frequency sweep from 10 to 0.1 Hz at 25% strain. Black dots: G' ; Grey dots: G'' .

Scanning Electron Microscopy

On the one hand, the morphology of the hydrogels was analyzed by Scanning Electron Microscopy (SEM) on a Hitachi S4800. Pieces of gels were affixed to SEM pucks using conductive carbon tape, they were freeze-dried and coated with a 2 nm gold layer.

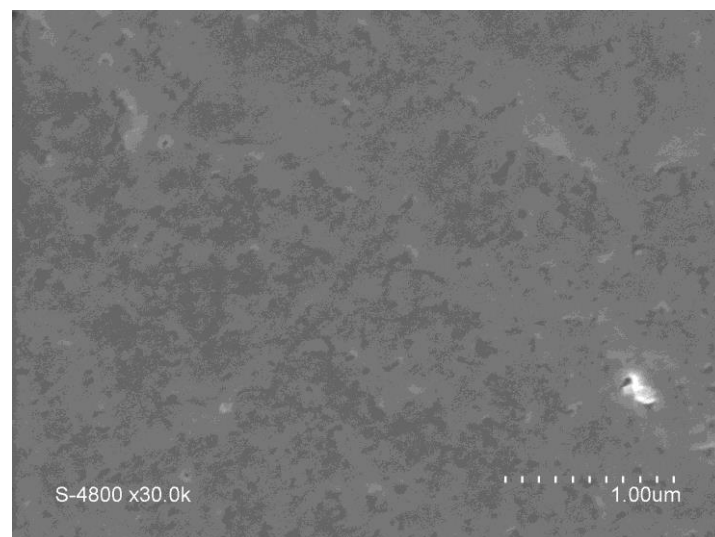


Figure S15. SEM image of a hydrogel (10 wt% of hybrid peptide 2 in DPBS with 0.3 wt% NaF) after freeze-drying

On the other hand, a 10 wt% hybrid peptide 2 hydrogel in cell culture medium was examined by cryo-SEM. The sample was frozen in slush nitrogen, fractured, sublimated for 1 minute at -96°C or 3 minutes at -87°C , coated with Palladium and analyzed at 5KV and -140°C on a FEI Quanta 250 SEM equipped with a Alto 2500 cryo-transfer system (GATAN).

Supporting information for publication n°3
Sol-gel synthesis of collagen-inspired peptide hydrogel

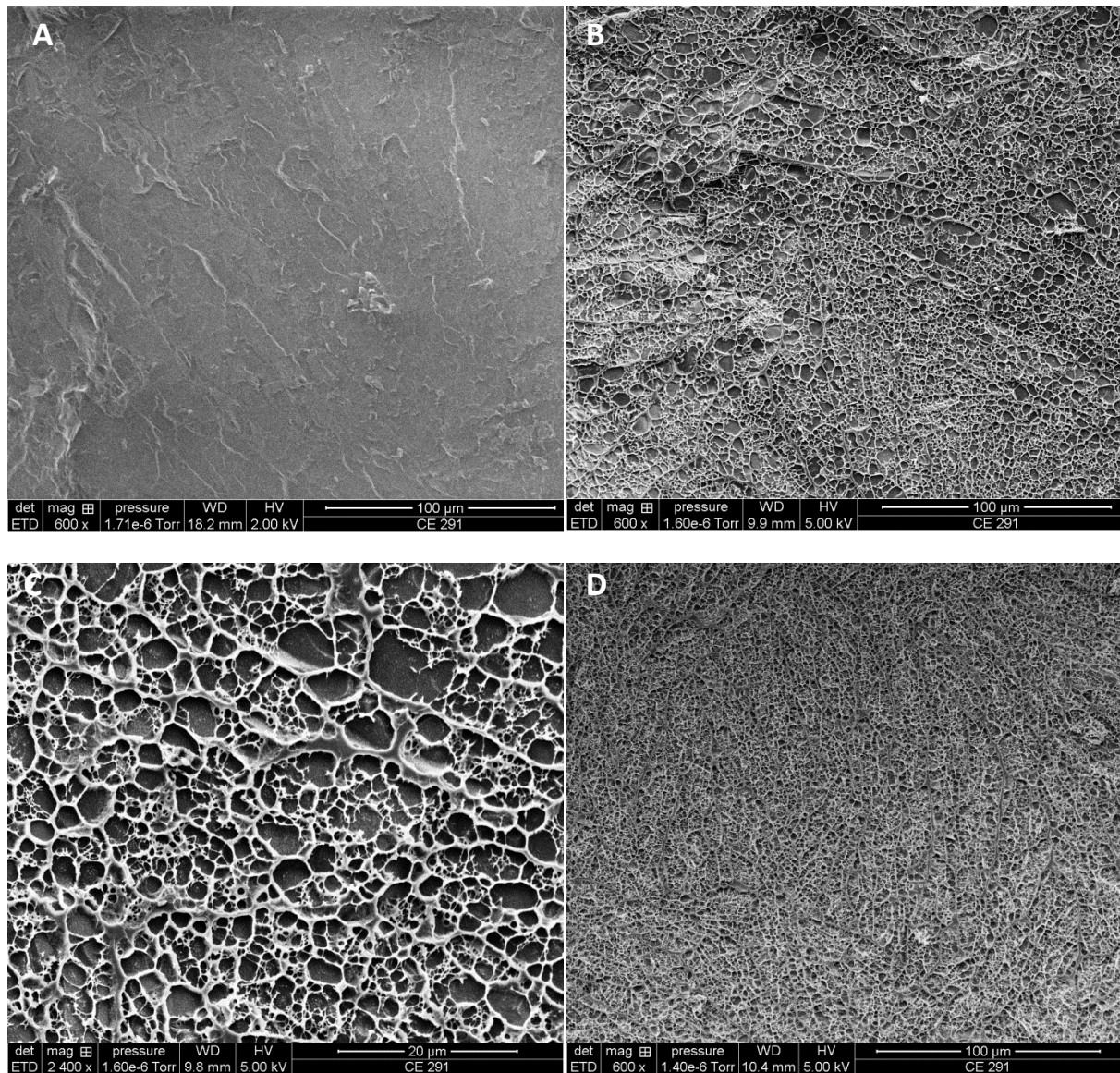


Figure S16. Cryo-SEM images of the hydrogel. A: before sublimation. B and C: after sublimation for 1 min at -96°C . D: after sublimation for 3 min at -87°C .

Cell adhesion

Cell culture reagents were purchased from Gibco and Sigma-Aldrich. Mouse mesenchymal stem cells (mMSC) from Black 6 mice were cultured in high glucose DMEM containing phenol red and GlutaMAX (Gibco ref. 31966) with 10% FBS and 1% penicillin-streptomycin at 37°C with a humidified 5% CO_2 atmosphere. All the assays were run in tetraplicates.

A 10 wt% hybrid peptide **2** solution in cell culture medium was prepared according to the protocol described above. After sterile-filtration, 30 μL of this solution were deposited in wells of a 96 well cell culture plate (flat bottom, TC-PS). A tetraplicate set was prepared for each adhesion time. The plate was incubated at 37°C overnight. The resulting hydrogels were washed with cell culture medium ($3 \times 200 \mu\text{L}$) before cell seeding. In parallel, collagen foams (ACE surgical supply co, ref DWFN14J1) were cut into discs of 6 mm in diameter, placed in the cell culture plate and washed with cell culture medium ($3 \times 200 \mu\text{L}$).

Supporting information for publication n°3 Sol-gel synthesis of collagen-inspired peptide hydrogel

Cells (passage n°23) were detached with trypsin (Trypsine-EDTA solution 0.25%) after washing with DPBS without calcium and magnesium. They were centrifugated, suspended in culture medium and counted with a hemacytometer. The suspension was diluted to a concentration of 60,000 cells per mL. Cells were seeded in the tissue culture treated 96 well cell culture plate, on the hydrogels and on the foams (3 000 cells per well, 50 μ L). The plate was incubated at 37°C. Cells were allowed to adhere for 30 min, 1h, 2h or 4h at 37°C. Then cell culture medium was removed, wells were washed with DPBS and 50 μ L of cell culture medium was added to each well. Only one set of samples was left intact after cell seeding to provide the value corresponding to 100% adhesion. Background wells contained only 50 μ L of cell culture medium (no cells). 50 μ L of CellTiter-Glo reagent (Promega) was added to each well. The plate was allowed to incubate at room temperature for 8 minutes. Then 50 μ L of each sample were transferred to a 96 well opaque white plate for luminescence reading (1 second per well). Background luminescence was subtracted from the obtained values and the results were presented as adherent cell percentage. All results were expressed as the mean \pm SD. Two way ANOVA test followed by Dukey's multiple comparison test was performed to analyze differences between groups and time points. P-values < 0.05 (*), P < 0.01 (**), P < 0.001 (***), or P < 0.0001 (****) were considered statistically significant. Analysis was performed using Graph-Pad Prism™ software (Graphpad, San Diego, CA, USA).

Cell proliferation

Cell proliferation on hybrid hydrogels were evaluated on mMSC cultured in the same conditions as for cell adhesion assays. Hydrogels and foam controls were also prepared according to the protocol described in the cell adhesion section. A cell suspension at a concentration of 20,000 cells per mL was prepared (passage n°20). 1 000 cells (50 μ L) were seeded in each well. On the first day, 50 μ L of CellTiter-Glo reagent were added to a set of samples (no prior washing). After incubation (8 minutes at RT), 50 μ L of each well was transferred to a 96 well opaque white plate and luminescence was recorded (1 second per well). 150 μ L of cell culture medium were added to the other sets of samples and the plates were allowed to incubate at 37°C. Each following day, culture medium was removed from a set of samples and replaced by 50 μ L of fresh medium. Cell proliferation was measured out with the CellTiter-Glo assay (50 μ L of the reagent) as previously detailed. Background luminescence was subtracted from the sample luminescence values. Besides, each day, a fresh suspension of cells was prepared, dispensed in a 96 well cell culture plate (50 μ L per well) and subjected to the CellTiter-Glo assay in order to measure the luminescence signal of known number of cells. This signal was used to normalize the sample signals and thus obtain the number of cells. All results were expressed as the mean \pm SD. Two way ANOVA test followed by Dukey's multiple comparison test was performed to analyze differences between groups and time points. P-values < 0.05 (*), P < 0.01 (**), P < 0.001 (***), or P < 0.0001 (****) were considered statistically significant. Analysis was performed using Graph-Pad Prism™ software (Graphpad, San Diego, CA, USA).

Cell encapsulation

The hybrid peptide **2** (30 mg) was dissolved in DMEM (150 μ L) at a 20 wt% concentration. NaF (0.3 mg/mL in DMEM, 100 μ L) was added. The resulting solution was incubated at 37°C for 17.3 hours until its viscosity got high enough to prevent cell sedimentation. 50 μ L of a suspension of mMSC in DMEM (passage n°27, 500 000 cells per mL) were added to the viscous hybrid solution. After homogenization, this solution was dispensed in a TC-PS 96 well plate (30 μ L per well). At the same time, 50 μ L of the same suspension of mMSC in DMEM were diluted with 250 μ L of DMEM to reach the same final cell concentration as in the hybrid solution. 30 μ L of this solution were also dispensed in the TC-PS 96 well plate, these wells were used as controls. The plate was incubated at 37°C for 25h. Then, 100 μ L of the live/dead cell staining solution (PromoKine live/dead cell staining kit II, 0.8 μ L of calcein-AM + 3.2 μ L of EthD-III in 1.6 mL of DPBS) were added on top of the gels and in the control

Supporting information for publication n°3
Sol-gel synthesis of collagen-inspired peptide hydrogel

wells. The plate was allowed to incubate at RT for 30 min and hydrogels were examined by laser confocal microscopy on a Leica Sp5-II microscope using the excitation and emission wavelengths recommended by the live/dead cell staining kit supplier. Images were recorded with a 15 μm pitch in z and were visualized with ImageJ.

Supporting information for publication n°4

Modular bioink for 3D printing of biocompatible hydrogels: sol-gel polymerization of hybrid peptides and polymers

Cécile Echalièr, Riccardo Levato, Miguel Angel Mateos Timoneda, Oscar Castaño, Stéphane Déjean, Xavier Garric, Coline Pinese, Danièle Noël, Elisabeth Engel, Jean Martinez, Ahmad Mehdi and Gilles Subra

Abbreviations.....	2
Preparation of the bioink	2
Viscometry.....	2
Hydrogel printing	3
PLA scaffold printing	3
Biological assessment.....	4
Microscopy	5
Figure S1. Viscosity of the hybrid solutions recorded as a function of time..	2
Figure S2. Aerotech rapid prototyping machine	3
Figure S3. Scaffold design.....	3
Figure S4. PLA scaffold	4
Figure S5. Hybrid hydrogel scaffold after autoclaving, swelling and cutting.....	4
Figure S6. Fluorescent microscopy images of mMSC after 4 days of culture on a PLA 3D- printed scaffold..	5

Supporting information for publication n°4
Modular bioink for 3D printing of biocompatible hydrogels: sol-gel polymerization of hybrid peptides and polymers

Abbreviations

3D, three-dimensional; CAD, computer-aided design; DMEM, Dulbecco's modified eagle medium; DPBS, Dulbecco's phosphate buffered saline; ECM, extracellular matrix; EthD-III, ethidium homodimer III; FBS, fetal bovine serum; ICPTES, 3-isocyanatopropyltriethoxysilane; mMSC, mouse mesenchymal stem cell; PA, polyacrylamide; PEG, polyethylene glycol; PHEMA, polyhydroxyethylmethacrylate; PLA, poly(lactic acid); RGD, ArgGlyAsp cell adhesion peptide sequence; RT, room temperature; TC-PS, tissue culture polystyrene; UV, ultra-violet. Other abbreviations used were those recommended by the IUPAC-IUB Commission (Eur. J. Biochem. 1984, 138, 9-37).

Preparation of the bioink

The syntheses of the hybrid blocks **1** and **2** were achieved following a previously described procedure (Echalier, C. et al. Easy Synthesis of Tunable Hybrid Bioactive Hydrogels. *Chem. Mater.* **2016**, *28*, 1261–1265). Hybrid PEG **1** (10 wt%, 300 mg) and hybrid GRGDSP peptide **2** (1 wt%, 30 mg) were dissolved in DPBS (3 mL, Gibco ref. 14190) containing sodium fluoride (0.3 wt%, 9 mg, Acros). The term bioink refers to this solution.

Viscometry

Viscosity measurements were performed using a SV-10 sine-wave vibro viscometer (A&D) equipped with a 10 mL sample cup (polycarbonate). The sample cup was filled with 10 mL of the bioink and fitted with a water jacket connected to a water tank. The temperature was set at 37°C. Viscosity was recorded automatically every 30 seconds. Full sets of data are presented in Figure S1.

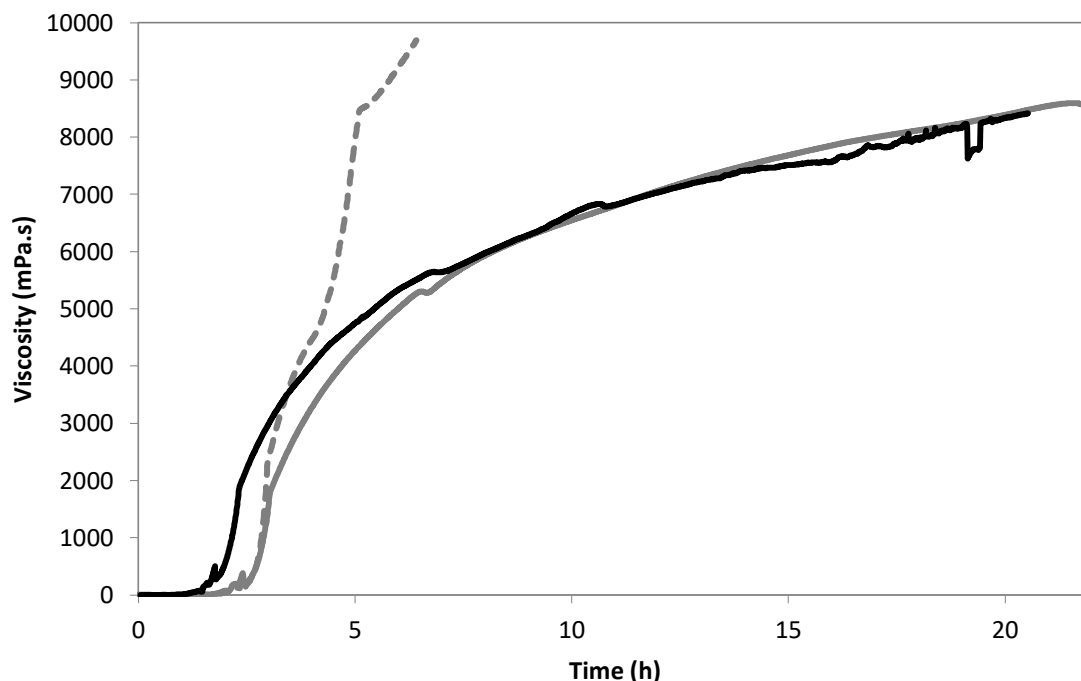


Figure S1. Viscosity of the hybrid solutions recorded as a function of time. Dashed grey line: hybrid PEG solution at 37°C; solid grey line: hybrid PEG solution at 37°C until gel point and then at 25°C; black line: hybrid PEG-RGD solution at 37°C until gel point and then at 25°C.

Supporting information for publication n°4
Modular bioink for 3D printing of biocompatible hydrogels: sol-gel polymerization of hybrid peptides and polymers

Hydrogel printing

All the printing assays were performed at RT on a nScrypt 3Dn-300 rapid prototyping machine (nScrypt, Orlando, FL). The bioink was placed in a clear 3 mL syringe barrel (optimum fluid dispensing system Nordson EFD 3 cc) equipped with a piston (Nordson EFD) and a 27G conical dispensing tip (Nordson EFD, ref. 7018417). Scaffolds were printed on microscope glass slides (Thermo Scientific, Superfrost). The script was written and visualized with Path2D software. The printer was controlled using the Machine tool software.

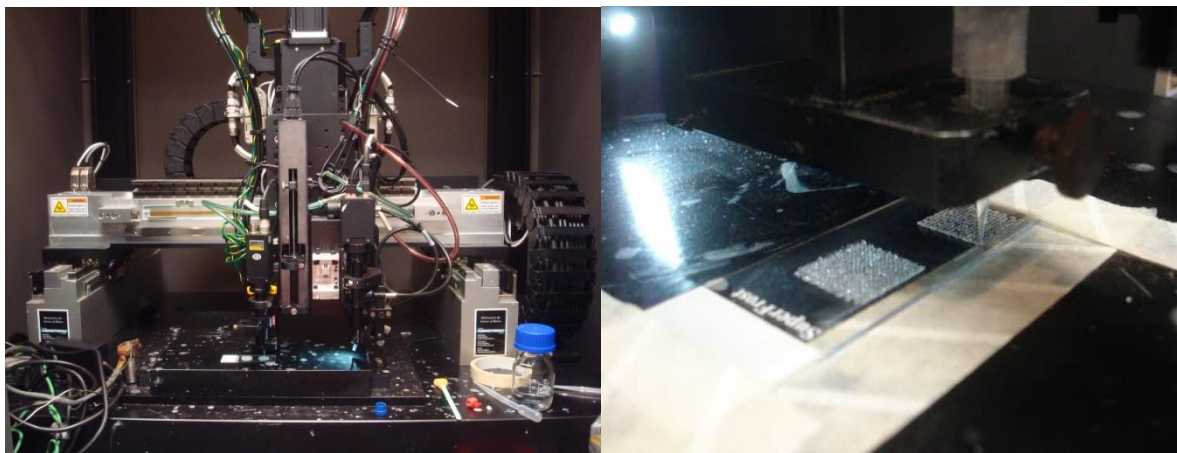


Figure S2. nScrypt 3Dn-300-TE rapid prototyping machine

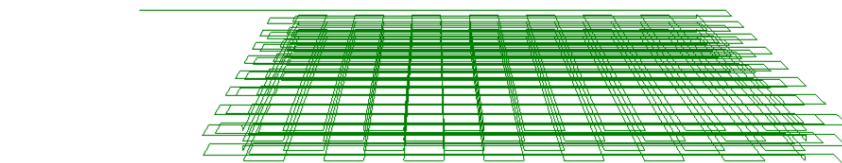


Figure S3. Scaffold design

PLA scaffold printing

PLA scaffolds were 3D-printed to be used as control for biological assessment of the hybrid hydrogel scaffolds. Printing was performed on a 3D Volumic Stream 20Pro printer. A black PLA filament (1.75 mm in diameter) was forced through the nozzle at 200°C. As the molten material was extruded, the nozzle followed a path designed to yield grid-patterned scaffolds similar to hydrogel scaffolds.

Supporting information for publication n°4
Modular bioink for 3D printing of biocompatible hydrogels: sol-gel polymerization of hybrid
peptides and polymers

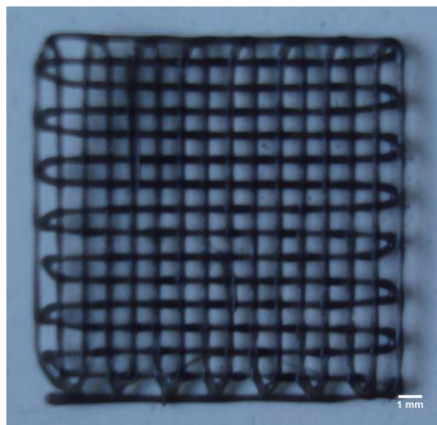


Figure S4. PLA scaffold

Biological assessment

Cell culture reagents were purchased from Gibco and Sigma-Aldrich. Mouse mesenchymal stem cells (mMSC) from Black 6 mice were cultured in high glucose DMEM containing phenol red and GlutaMAX (Gibco ref. 31966) with 10% FBS and 1% penicillin-streptomycin at 37°C with a humidified 5% CO₂ atmosphere.

Hydrogel scaffolds were sterilized by autoclaving on the glass slides used for printing. Then, they were detached with a blade, allowed to swell in cell culture medium and cut into discs of 7 mm in diameter with a punch. PLA scaffolds were sterilized in 70% ethanol baths, washed in cell culture medium and cut into discs of 7 mm in diameter with a punch.

Cells (passage n°18) were detached with trypsin (Trypsine-EDTA solution 0.25%) after washing with DPBS without calcium and magnesium. They were centrifugated, resuspended in culture medium and counted with a hemocytometer. The suspension was diluted to a concentration of 200,000 cells per mL. For each type of scaffolds, 4 samples were placed in a 1.5 mL Eppendorf tube with 1.5 mL of the cell suspension. The tubes were continuously rotated on a MACSmix tube rotator at 37°C for 4h. Then samples were put in 2 mL polypropylene tubes (Sarstedt) filled with cell culture medium. Non-adherent cells were removed by pipeting the media and the tubes were filled again with 400 μ L of cell culture media. Tubes were incubated at 37°C for 4 days with loose caps to allow gas exchange. After 4 days of proliferation, scaffolds were placed in a 24 well cell culture plate (non treated PS) and 400 μ L of the Live/Dead staining solution were added to each well (0.8 μ L of calcein-AM solution and 3.2 μ L of EthD-III solution in 1.6 mL of DPBS). Samples were observed 30 minutes later.

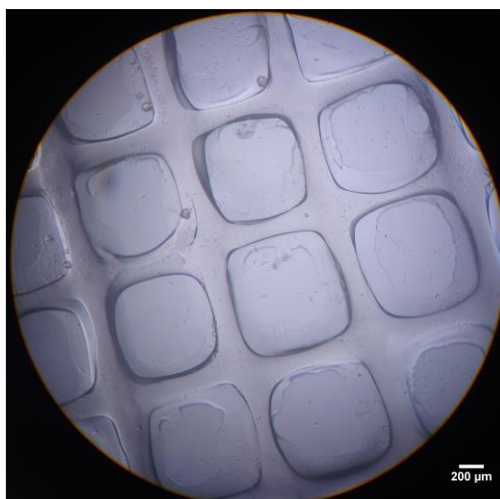


Figure S5. Hybrid hydrogel scaffold in cell culture medium after autoclaving, swelling and cutting

Supporting information for publication n°4
Modular bioink for 3D printing of biocompatible hydrogels: sol-gel polymerization of hybrid peptides and polymers

Microscopy

Stereomicroscopy images of the hydrogel scaffolds were taken on a Leica MZ16F stereomicroscope 24 hours after printing. Scaffolds were still on glass slides.

Fluorescence microscopy images were recorded on a Leica DM IRB inverted fluorescence microscope (objective lens $\times 4$, NA 0.1) equipped with a MicroMAX RS camera (Princeton instruments). Images were analyzed with ImageJ.

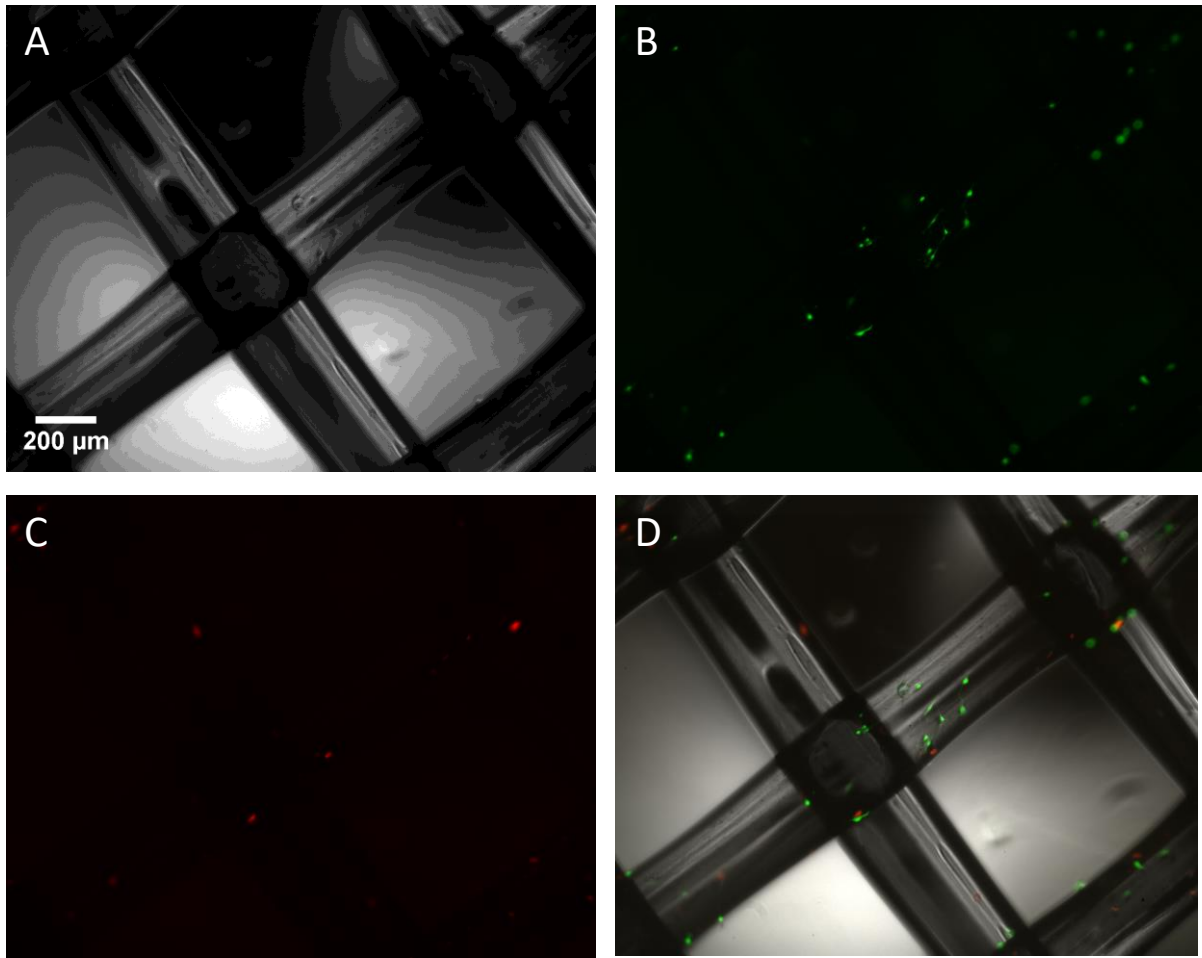


Figure S6. Fluorescent microscopy images of mMSC after 4 days of culture on a PLA 3D-printed scaffold. (A) transmitted light image; (B) calcein-AM stain showing live cells in green; (C) EthD-III stain showing dead cells in red; (D) merged images.

Annexes

Annexes

Publication: Simple and specific grafting of antibacterial peptides on silicone catheters

DOI: 10.1002/ (revision of adfm.201602240; em.advhealthmat.0.4c101d.79aa505a)

Article type: Full paper

Simple and specific grafting of antibacterial peptides on silicone catheters

Coline Pinese, Said Jebors, Cécile Echalié, Patricia Licznar-Fajardo, Xavier Garric, Vincent Humblot, Christophe Calers, Jean Martinez, Ahmad Mehdi, and Gilles Subra**

Dr. C. Pinese, Dr. S. Jebors, C. Echalié, Prof. X. Garric, Prof. J. Martinez, Prof. G. Subra, Institut des Biomolécules Max Mousseron (IBMM), UMR5247 CNRS, ENSCM, Université de Montpellier, France
E-mail: gilles.subra@umontpellier.fr

Prof. A. Mehdi,
Institut Charles Gerhardt (ICG), UMR5253 CNRS, ENSCM, Université de Montpellier France.
E-mail : ahmad.mehdi@umontpellier.fr

Prof. P. Licznar-Fajardo
HydroSciences Montpellier, UMR5569 CNRS, IRD, Université de Montpellier, France.

Dr. V. Humblot, Dr. C. Calers
Laboratoire de Réactivité de Surface(LRS), UMR 7197 Sorbonne Universités, UPMC Université de Paris 06, France.

Keywords: Silylated peptides, surface modification, antibacterial silicone, hybrid materials.

To fight against nosocomial infection initiated by colonization of medical devices, a strategy enabling the direct and fast functionalization of silicone surfaces is proposed. This strategy proceeds in a site-specific way using original hybrid silylated antibacterial peptides. This safe and up-scalable method guarantees a covalent and robust immobilization with the correct orientation of the bioactive moiety. Importantly it also avoids multi-step chemical modifications of the surface or multi-layer polymer coatings. As proof of concept, antibacterial

silicone catheter has been prepared whose immediate and long term efficiency is superior by comparison to similar silver-embedded materials.

1. Introduction

Bacterial colonization of implantable medical devices represents a serious public health care problem^[1] due to the associated risks of infection, high treatment costs and development of drug resistance. Nosocomial infections are estimated to 5-10% of hospital admission (2-4 millions admissions/year).^[2] Among them, 35% involve the urinary tract and 25% the surgical site. More than five millions of medical devices are implanted every year in the USA and 1 to 6% became infected.^[3] Antibiotics and silver particles have been already used as coatings to confer antifouling properties to the devices presenting a high risk of infection in particular silicone catheters, laryngeal masks or septum.^[4] However, the active substance has to be released from the surface in a time-dependent manner to exert its antibacterial activity by reaching an intracellular target. An interesting alternative is the use of antibacterial peptides^[5] acting as membrane-disruptors. Due to their 'mechanical' mode of action, they are less susceptible to promote the development of bacterial resistance^[6] and exhibit an activity spectrum against a wide range of microorganisms (Gram-positive and Gram-negative bacteria, protozoa, yeasts, fungi, viruses). Immobilization of antibacterial peptides has already been performed on several surfaces^[7], including silicone.^[8] On silicone, dendrimeric bioactive peptides have been also successfully grafted with peptide for cells adhesion.^[9] The covalent linking of peptides requires first functionalization of the surface with suitable functional groups (*i. e.* epoxide, primary amine) followed by reaction with a spacer, which finally enables the chemical grafting of the peptide. To obtain the desired orientation of the bioactive molecule on the surface, a single function within the peptide sequence has to react. It implies that unspecific chemistries such as N-hydroxysuccinimide-amine conjugation^[10] have to be avoided with compounds presenting several reactive functions. Alternatively, chemoselective ligation strategies, involving two

reactive functional groups (*i. e.* maleimide/thiol,^[11] thiol/ene,^[12] alkyne/azide^[13]), the first one belonging to the surface and the other to the peptide, may overcome this drawback. In both cases, the silicone is subjected to multistep chemical reactions, organic solvents, catalysts and even toxic reagents. This greatly impairs the transfer to such procedures to industrial scale treatment of medical devices.

2. Antibacterial hybrid peptide

In this context, we developed a straightforward strategy to immobilize antibacterial peptides on silicone surfaces, in a site-specific way. Our approach relies on the synthesis of hybrid peptide building blocks bearing a hydroxysilane group.^[14] We already demonstrated that trialkoxysilyl peptides may be immobilized either into pores of the mesoporous silica or on glass surfaces.^[15] The process is simple and requires neither any chemical reagent, nor toxic solvent, thus being compatible with the stability of biomolecules. Moreover, the peptide is immobilized *via* covalent SiOSi bonds, meaning that a long lasting effect can be expected. In this paper, we modified medical silicone catheter activated by plasma treatment, with a hybrid silylated analogue of the short cationic antibacterial peptide Palm-Arg-Arg-NH₂ **1**. Palm-Arg-Arg-NH₂ **1** was found to be active against Gram-negative bacilli *Escherichia coli*, *Pseudomonas aeruginosa* and the Gram-positive coccus *Staphylococcus aureus*, with a MIC in the micromolar range (**Supporting Information Table S2**). These three species are among the most representative bacterial species responsible for healthcare infections and are commonly found in contaminated medical devices.^[3,6] The palmitoylated dipeptide **1** possesses a comparable activity than “Sha”, a peptide of the temporin family with a well-known membrane-disrupting activity.^[16] Therefore, we designed a hybrid analogue of this amphipathic peptide bearing a dimethyl hydroxysilane moiety (compound **2**, **Figure 1**). Isocyanatopropyl dimethylchlorosilane (ICPDMCS) reacted with the amino group of the amino hexanoic acid

(Ahx) placed at the N terminus of the dipeptide. We hypothesized that, once attached to the surface, the N-terminal $-O-Si(Me)_2-(CH_2)_3-NHCO-Ahx$ spacer could mimic the palmitic acid in the antibacterial active sequence.

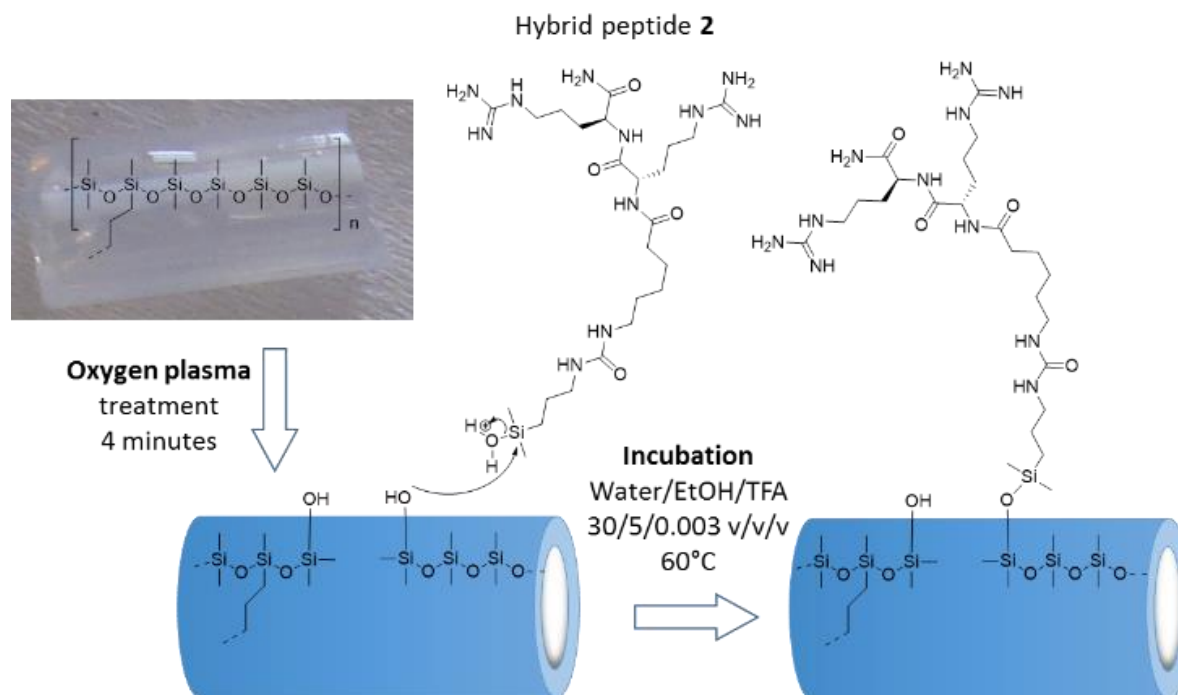


Figure 1. One-step specific grafting of antibacterial hybrid peptide **2** on activated silicone catheters.

2.1. Synthesis of hybrid peptide

Two syntheses of compound **2** were performed, the silylation step being performed either in solution (**Figure 2**) or on solid support (**Supporting Information Figure S1**). Due to the pKa (12.5) of guanidine moieties of the arginine side chains, it was theoretically possible to selectively react the N-terminus of the unprotected peptide H-Ahx-Arg-Arg-NH₂ with ICPDMCS. Our attempt in this strategy was unsuccessful due to the low solubility of the unprotected peptide in organic solvents. We thus decided to use the pentamethyldihydrobenzofuran-5-sulfonyl (Pbf) protected arginines for the reaction with ICPDMCS. The protected peptide H-Ahx-Arg(Pbf)-Arg(Pbf)-NH₂, prepared on a Sieber amide AM-PS resin was released by TFA/DMC 5/95, followed by treatment with ICPDMCS. Pbf

protecting groups were then removed by TFA treatment and the hybrid peptide **2** was precipitated in diethyl ether.

Interestingly, chlorodimethylsilyl group was converted into dimethylhydroxyl-silyl during TFA treatment. Several chlorodimethylsilylated peptides were already prepared by our group as precursors for GPCR ligand dimers. These peptide may undergo dimerization upon freeze drying or precipitation^[17] but are only observed in monomeric form when treated in acidic conditions, enabling their purification by classical RP HPLC in water/acetonitrile (with TFA, 1/1000 v/v) solvent system. The hybrid peptide **2** ‘ready to use’ was purified and characterized (See Supporting Information).

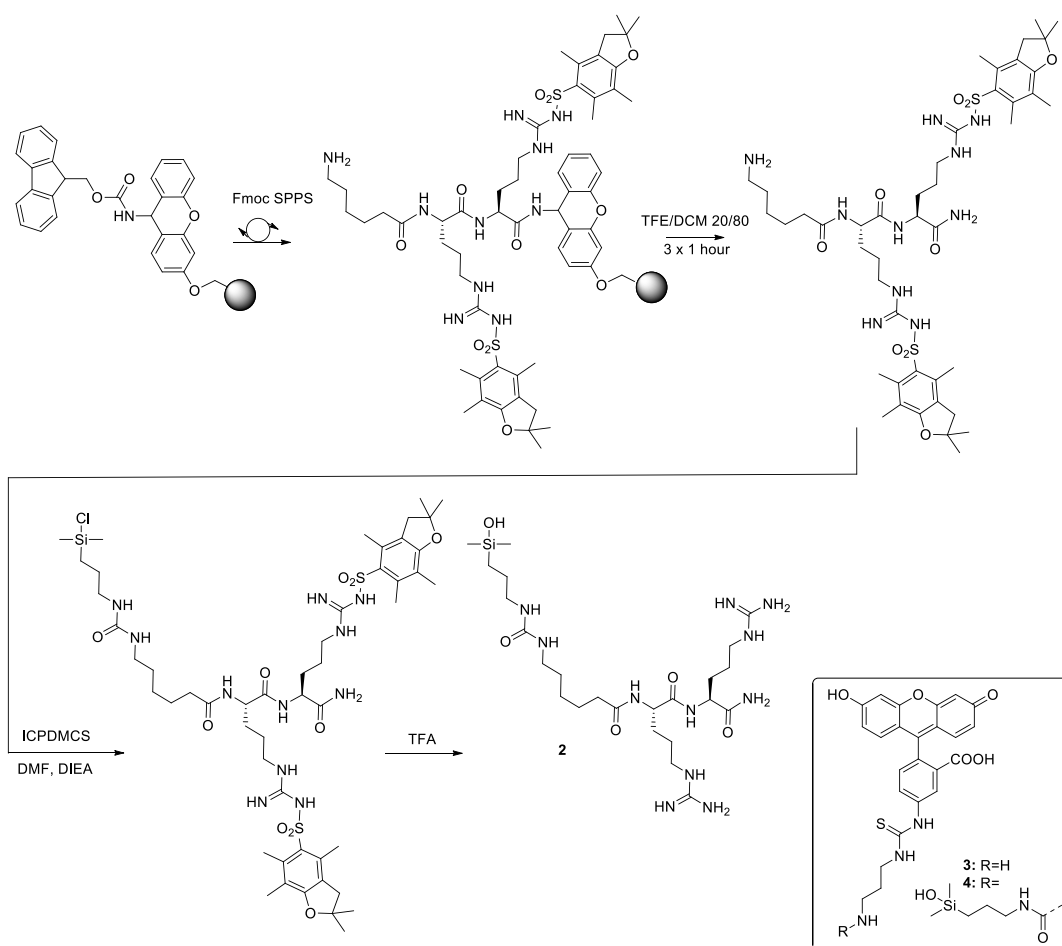


Figure 2. Syntheses of the hybrid dimethylhydroxylsilyl peptide **2**, hybrid fluorescent compound **3** and control compound **4**.

At this stage, we measured the MIC of hybrid peptide **2**. As it could have been expected, it was not antibacterial (MIC > 65 μ M, Table S2). Indeed, in solution compound **2** was a very different molecule from palmitoylated antimicrobial peptide **1**. Where the latter is an amphiphilic cationic molecule, the compound **2** displays a SiOH functional group at the end of the hydrophobic chain. This moiety, required for the grafting, completely changes the innermost nature of the peptide, turning it into a much more hydrophilic entity which should not be able to interact with bacteria membranes. Once attached to the surface, the amphipathic nature of compound **2** would be restored, the silanol group being converted to siloxane.

2.2. Grafting of hybrid peptide

In fact, the principle of grafting relies on the specific condensation of the hybrid peptide dimethylhydroxy-silyl with silanol functions on the surface (**Figure 1**). This type of chemistry had already been used to introduce simple organosilane compounds on the surface of silicones. Recently, modification of silicone surfaces by a zwitterionic silane has been reported and led to a super hydrophilic and antifouling material with high stability of siloxane bonds.^[18] Reactive groups on the surface of the silicone could be generated either by chemical treatments^[19] (strong acids or bases) or by plasma treatment.^[20] It is worth noting that in our case, any chemical treatment was excluded to avoid biomaterial damages and would have necessitated extensive washing steps to complete removal of the reagents from the catheter. We thus used oxygen plasma treatment, which preferentially generated silanol groups.

To optimize the grafting step, we first prepared the hybrid fluorescent derivative **4** as a convenient model to visualize the covalent surface modification (**Supporting information Figure S3**). Compound **4** was dissolved in water (1/1000 TFA)/ethanol, 30/5, v/v solution at a 30 mM concentration. Noteworthy we demonstrated that dimethylhydroxysilane peptides did not form dimers through intermolecular reaction in acidic solutions.^[17] Pieces of catheters were activated by oxygen plasma and immediately incubated in this solution at 60 °C for 12 hours.

As a control experiment, pieces of catheters were also incubated in a solution of the unsilylated fluorescein derivative **3**. As expected, silicone catheter pieces incubated in the solution containing compound **3** lost all their fluorescence during the washing steps. In contrast, catheter pieces that were incubated in the solution containing the hybrid fluorescent compound **4** retained the fluorescence after several washings in various solvent including DMF, H₂O and EtOH. It is important to note that the fluorescence remained stable even after 3 weeks incubation in PBS buffer (**Supporting Information Figure S3**). This qualitative experiment demonstrated the covalent nature of the grafting with the hybrid derivative **4**.

3. Antibacterial silicone catheter

3.1. Surface characterization

ATR-IR spectroscopy was first used to follow the surface modifications of the silicone and the apparition of SiOH groups which were indispensable for covalent anchoring of peptide. After plasma activation, a large peak at 3350 cm⁻¹, attributed to SiOH groups, appeared on the spectrum (**Figure S4**). After incubation for 12 hours, in a 30 mM solution containing hybrid peptide **2**, and washings, other peaks were observed at 3300, 1648 and 1553 cm⁻¹ corresponding to NH and CONH from immobilized peptide (**Figure S4**). Angle contacts were also measured before and after plasma activation. **Figure S5** shows clearly a dramatic decrease of the contact angle ($\theta = 26^\circ$), by comparison to starting silicone ($\theta = 112^\circ$), indicating a clear increase in hydrophilicity of the surface afforded by the SiOH groups generated by the plasma. In parallel, XPS analyses were also conducted. Spectra of non-grafted silicone catheters and of catheters incubated for 1 hour, in a 30 mM solution containing hybrid peptide **2**, are reported in **Figure S4**. Both analyses confirmed the presence of carbon and oxygen elements, together with the strong signature of silicone. A small contribution of nitrogen N1s around 400 eV was also observed on control catheters, suggesting some contamination of the commercial substrate. The

grafted catheters presented a clear and significant increase of the N1s peak, confirming the grafting of the hybrid peptide **2** after one hour incubation (see insert in **Figure S4**).

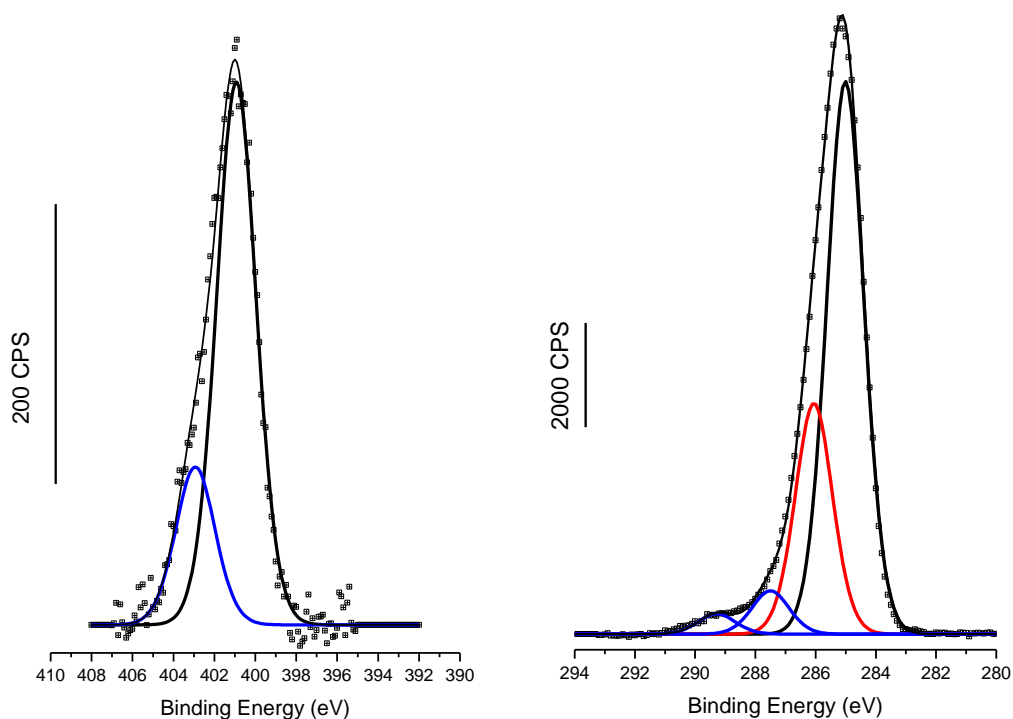


Figure 3. Deconvoluted N1s (left) and C1s (right) XPS spectra of catheters grafted with the hybrid peptide **2** after 24 hours incubation.

Then, to evaluate the impact of the incubation time on the density of peptides grafted on the silicone surface, several catheter samples were incubated in a 30 mM solution of the hybrid peptide **2** solution during different times (10 min, 1 h, 2 h 30 min, 12 h and 24 h) and washed thoroughly. High-resolution spectra were recorded in the four atomic regions to obtain quantitative atomic concentrations from C1s, O1s, Si2p and N1s (Supporting Information **Table S1**). As expected, the O/Si ratio remained constant (≈ 0.87). Interestingly, the N/Si ratio increased by two-fold (0.018 *vs.* 0.036) after 2 h 30 minutes of incubation and remained

constant afterwards. This confirmed a covalent grafting of a layer of hybrid peptides whose thickness reached a plateau during incubation. The XPS high-resolution spectra recorded on grafted catheters incubated for 24 h were used to assess precise attributions of atom environments. The C1s region was fitted with four components while the N1s region was decomposed into two contributions (**Figure 3**), in agreement with previous studies of arginine-containing peptide (details of components assignments are given in Supplementary Information).^[21] These observations prompted us to choose the N1s element as a marker to quantify the amount of molecules grafted on the silicone surface (see Supporting Information for detailed equations). The grafting was estimated to around 0.15 hybrid peptide per nm². In contrast, non-covalent adsorption of α -helical antimicrobial peptides on gold surface was found to be ~10 molecules/nm².^[22] In the same way, the density of Lasio-III antimicrobial peptide immobilized on a polymer layer grafted on silicone catheters was found to be ~21 molecules/nm².^[8] These important differences are related to the mode of association of the bioactive peptide with the silicone surface. Adsorption strategies lead to multi-layers of peptides randomly distributed on the material and post-grafting approaches on polymers requires first the establishment of a polymer layer of multi-nm thickness on which bioactive peptides are immobilized. In fact, hybrid peptide **2** imposed the formation of a bioactive monolayer on the surface of the silicone only *via* Si-O-Si covalent bonds.

Having demonstrated the efficiency of the grafting, catheter samples were prepared for the study of antibacterial properties. Hybrid peptide **2** was grafted in the same experimental conditions than the fluorescent derivative **4** (*i. e.* 12 hours incubation in water (1/1000 TFA)/ethanol, 30/5, v/v).

3.2. Anti-bacterial activity of hybrid peptide grafted catheters

More interestingly it had to be demonstrated that the relatively low density of active peptide was not detrimental to the bioactivity of the surface. Antibacterial properties of the catheters grafted with hybrid peptide **2** were evaluated against reference strains of *Escherichia coli*, *Pseudomonas aeruginosa* and *Staphylococcus aureus*. Catheter samples were incubated for 24 hours at 37 °C in a solution containing a known number of bacteria. Then, bacteria present on the silicone devices were recovered and counted (**Figure 4 A**). Whatever the bacterial species, the number of bacteria found on peptide-grafted surfaces was ~75% lower than the number found on non-grafted surfaces. This result demonstrated that the peptide kept its antibacterial properties when covalently grafted on silicone.

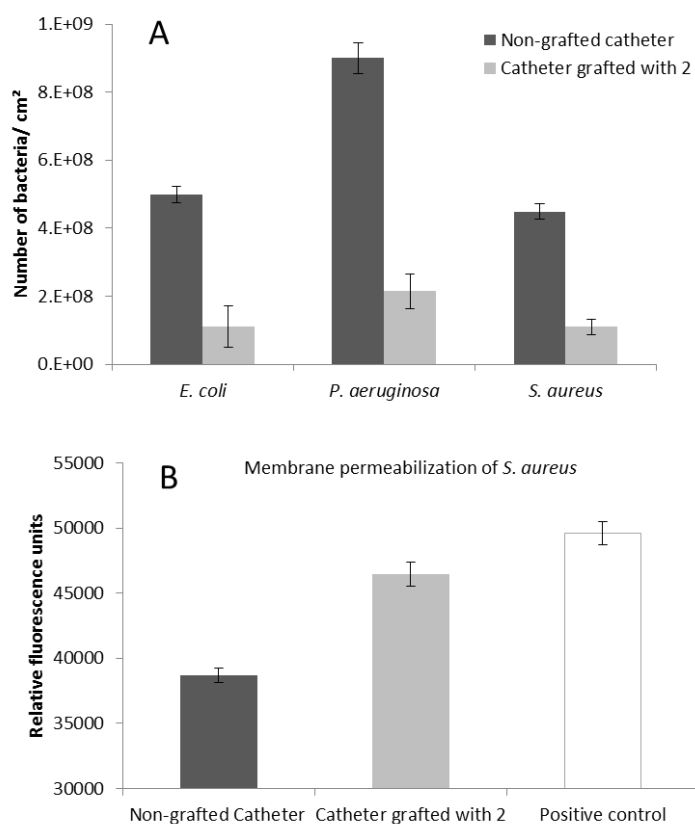


Figure 4. A: Antibacterial activity of catheters grafted with the hybrid peptide **2** after 24 h incubation with *E.coli*, *P. aeruginosa* and *S. aureus*. B: Membrane permeation assay against *S. aureus*. Propidium iodine (PI) fluorescence was measured after 1 h. Positive control was obtained by killing all bacteria with 70% ethanol/water solution.

To decipher if the reduction of the number of bacteria was due to either an anti-adhesive or a bactericidal property, a membrane permeation assay was performed to witness *S. aureus* death (**Figure 4 B**). Interestingly, it was observed that 92% of bacteria were killed on peptide-grafted catheters within one hour. In addition, bacteria death was significantly higher on grafted catheters than on the non-grafted surface. Taken together, these results are in favor of a dual anti adhesive/bactericidal effect of the hybrid peptide **2**. Taking these results into account, the potential of hybrid peptide-grafted silicones for the inhibition of biofilm growth was evaluated. The *Staphylococcus aureus* biofilm formation was studied for 30 days at 37 °C on three different catheters. Peptide **2**-grafted catheters were compared with non-grafted catheters but also with a commercially available antibacterial silicone catheter (Covidien) coated with a methyl vinyl ether maleic acid film, which enables the chelation of silver ions (noted ‘silver coated catheter’).^[23] It is worth noting that, despite being widely used as antibacterial agent, silver may lead to toxicity upon accumulation in tissues favoring the appearance of silver-resistant bacteria.^{[24][25]} As envisioned, peptide-grafted catheters conserved a significant anti-biofilm activity compared to untreated silicone catheters for at least one month (**Figure 5**).

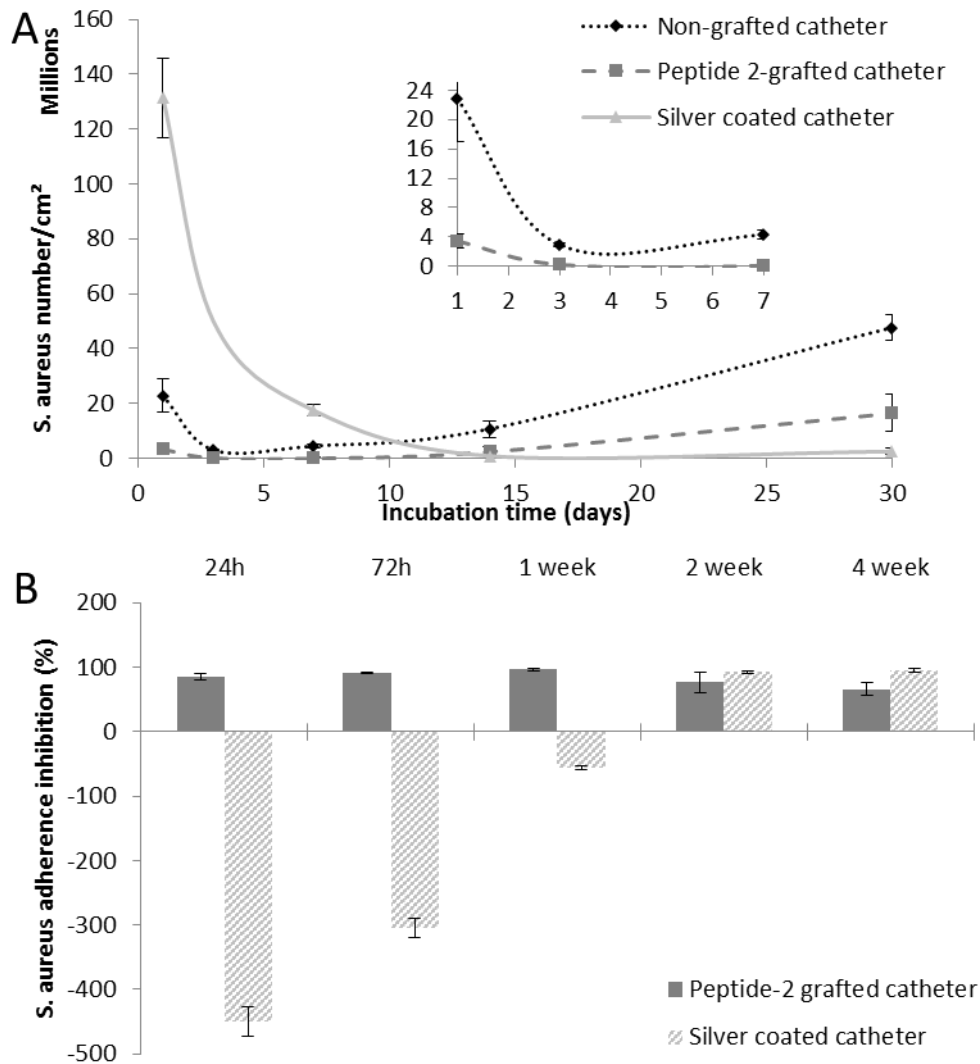


Figure 5. 30-days study of *S. aureus* biofilm formation and growth on catheters. A: Number of bacteria per cm² of catheter. B: Bacteria adherence of peptide 2-grafted catheter and silver coated catheter (striped bars) relative to non-grafted catheters expressed as: $100 - [(100 \times \text{number of bacteria on silver-coated or grafted-catheter}) / (\text{number of bacteria on non-grafted catheter})]$

In agreement with the previous results, the number of bacteria found after one day on peptide 2-treated catheters was significantly lower than on untreated catheters. After seven days, this ratio was 29-times lower (4.6 millions vs 140 000 bacteria, see insert in **Figure 5 A**). In contrast and very surprisingly, silver coated catheters did not present any anti-biofilm activity for the first days of incubation. During the first two weeks, the bacteria were more abundant on silver-embedded catheters (e.g. 17 millions at $t = 7$ days) than on untreated ones. One explanation could be that the methyl vinyl ether maleic acid coating was a better substrate for bacteria

adhesion than silicone which is inherently antiadhesive. This may explain the prominent drop in viable adherent bacteria after one day observed for the control catheters without any antimicrobial capabilities. A similar phenomenon has already been observed in the literature: *Staphylococcus epidermidis* adhered more to the surfaces of the silver-coated heart valves than to the uncoated surfaces.^[26] Subcutaneously implanted in rabbits, these silver-coated prosthetics did not protect against *S. aureus* colonization and device-related infections.^[27] However, the number of bacteria on silver-coated catheters decreased constantly to reach roughly the same number of bacteria that was found on peptide **2**-grafted catheters, after two weeks and maintained its antibacterial activity after that point. This late but constant effect of the commercial catheters could be related to the slow release of silver ions from the polymer in order to be effective. However, this delayed anti-bacterial effect will be beneficial only when the medical device stays implanted for more than 10 days, which is generally not the case. In addition, the major risk of contamination occurs during the short time of implantation of the device in the patient body. Thus, a rapid antibacterial effect is required to efficiently fight infections. The catheter grafted with hybrid peptide **2** immediately exhibited a significant antibacterial effect, which persisted over two weeks, allowing a constant biofilm growth inhibition, which corresponds to the common period of utilization of such devices in hospitals. Finally, to complete this study, we verified that catheters displaying covalently immobilized peptides were not cytotoxic (Supporting Information, **Figure S7**) and that their activity was not affected by gamma irradiation, an industrial sterilization process (**Figure S8**).

4. Conclusion.

This study confirmed once again the efficiency of antibacterial peptides when immobilized on a surface and highlighted their attractiveness over the use of silver ions. However, the covalent grafting of peptides as to be performed in a chemoselective way to avoid unspecific reactions of coupling reagents with reactive side chains and N or C extremities of peptides and to

guarantee the desired orientation. The use of a dimethylhydroxysilane function, introduced at a suitable position within the antibacterial peptide sequence, enabled to circumvent this difficulty and to obtain a Si-O-Si covalent bond between the peptide and the silicone surface. Avoiding chemical reagents, catalysts and toxic organic solvents, the grafting method is simple and safe. Further improvement involves the use of dip coating procedure instead of incubation to facilitate the large-scale treatment of other types of silicone medical devices.

Supporting Information

Supporting Information is available from the Wiley Online Library or from the author.

Acknowledgements

This work was supported by SATT AxLR maturation program. Peptide syntheses were performed using SynBio3 platform supported by IBSA and ITMO Cancer. The authors acknowledge IMPC (Institut des Matériaux de Paris Centre, FR2482) and the C' Nano projects of the Region Ile-de-France for Omicron XPS apparatus funding.

Received: ((will be filled in by the editorial staff))

Revised: ((will be filled in by the editorial staff))

Published online: ((will be filled in by the editorial staff))

- [1] R. O. Darouiche, *N. Engl. J. Med.* **2004**, *350*, 1422.
- [2] R. P. Wenzel, *Clin. Infect. Dis. Off. Publ. Infect. Dis. Soc. Am.* **2007**, *45 Suppl 1*, S85.
- [3] R. O. Darouiche, *Clin. Infect. Dis. Off. Publ. Infect. Dis. Soc. Am.* **2001**, *33*, 1567.
- [4] S. Saint, J. G. Elmore, S. D. Sullivan, S. S. Emerson, T. D. Koepsell, *Am. J. Med.* **1998**, *105*, 236.
- [5] K. V. R. Reddy, R. D. Yedery, C. Aranha, *Int. J. Antimicrob. Agents* **2004**, *24*, 536.
- [6] L. García-Aparicio, E. Blázquez-Gómez, O. Martin, L. Krauel, I. de Haro, J. Rodó, *Actas Urol. Esp.* **2015**, *39*, 53.
- [7] A. Lombana, Z. Raja, S. Casale, C.-M. Pradier, T. Foulon, A. Ladram, V. Humblot, *J. Pept. Sci.* **2014**, *20*, 563.
- [8] B. Mishra, A. Basu, R. R. Y. Chua, R. Saravanan, P. A. Tambyah, B. Ho, M. W. Chang, S. S. J. Leong, *J. Mater. Chem. B* **2014**, *2*, 1706.
- [9] H. Chen, M. A. Brook, H. D. Sheardown, Y. Chen, B. Klenkler, *Bioconjug. Chem.* **2006**, *17*, 21.
- [10] C. S. G. Daniel Hal Davis, *Biomaterials* **2002**, *23*, 4019.
- [11] S. D. Fontaine, R. Reid, L. Robinson, G. W. Ashley, D. V. Santi, *Bioconjug. Chem.* **2015**, *26*, 145.
- [12] L. Cheng, X. Zhang, Z. Zhang, H. Chen, S. Zhang, J. Kong, *Talanta* **2013**, *115*, 823.
- [13] H. Jiang, S. Qin, H. Dong, Q. Lei, X. Su, R. Zhuo, Z. Zhong, *Soft Matter* **2015**, *11*, 6029.

- [14] S. Jebors, S. Cecillon, C. Faye, C. Enjalbal, M. Amblard, A. Mehdi, G. Subra, J. Martinez, *J. Mater. Chem. B* **2013**, *1*, 6510.
- [15] S. Jebors, C. Enjalbal, M. Amblard, A. Mehdi, G. Subra, J. Martinez, *J. Mater. Chem. B* **2013**, *1*, 2921.
- [16] F. Abbassi, C. Galanth, M. Amiche, K. Saito, C. Piesse, L. Zargarian, K. Hani, P. Nicolas, O. Lequin, A. Ladram, *Biochemistry (Mosc.)* **2008**, *47*, 10513.
- [17] C. Echali er, A. Kalistratova, J. Ciccione, A. Lebrun, B. Legrand, E. Naydenova, D. Gagne, J.-A. Fehrentz, J. Marie, M. Amblard, A. Mehdi, J. Martinez, G. Subra, *RSC Adv.* **2016**, *6*, 32905.
- [18] S.-B. Yeh, C.-S. Chen, W.-Y. Chen, C.-J. Huang, *Langmuir* **2014**, *30*, 11386.
- [19] C. N. Hughes-Chinkhota, M. Banda, J. M. Smolinski, R. A. Thomas, D. M. Petibone, J. D. Tucker, G. W. Auner, *Sens. Actuators B Chem.* **2011**, *155*, 437.
- [20] C. Diaz Blanco, A. Ortner, R. Dimitrov, A. Navarro, E. Mendoza, T. Tzanov, *ACS Appl. Mater. Interfaces* **2014**, *6*, 11385.
- [21] A. Stypczyńska, T. Nixon, N. Mason, *Eur. Phys. J. D* **2014**, *68*, 1.
- [22] V. H. Margot Schlusshuber, *Appl. Microbiol. Biotechnol.* **2015**, *99*.
- [23] K. Amano, Y. Akaike, Antimicrobial medical implement containing silver ions **2008**.
- [24] S. L. Percival, P. G. Bowler, D. Russell, *J. Hosp. Infect.* **2005**, *60*, 1.
- [25] K. Mijndonckx, N. Leys, J. Mahillon, S. Silver, R. Van Houdt, *Biomaterials Int. J. Role Met. Ions Biol. Biochem. Med.* **2013**, *26*, 609.
- [26] G. Cook, J. W. Costerton, R. O. Darouiche, *Int. J. Antimicrob. Agents* **2000**, *13*, 169.
- [27] R. O. Darouiche, R. Meade, M. Mansouri, I. I. Raad, *J. Heart Valve Dis.* **1998**, *7*, 639.
- [28] M. Amblard, J. A. Fehrentz, J. Martinez, G. Subra, *Mol. Biotechnol.* **2006**, *33*, 239.
- [29] W. S. Hancock, J. E. Battersby, *Anal. Biochem.* **1976**, *71*, 260.
- [30] J. H. Scofield, *J. Electron Spectrosc. Relat. Phenom.* **1976**, *8*, 129.
- [31] S. Tanuma, C. J. Powell, D. R. Penn, *Surf. Interface Anal.* **1994**, *21*, 165.
- [32] H. H. Parker IV, R. B. Johnson, *J. Dent.* **1995**, *23*, 113.

Patent: Nouveaux hydrogels de structure silylée et procédé d'obtention

Inventors: MARTINEZ Jean; MEHDI Ahmad; SUBRA Gilles; JEBORS Said; ECHALIER Cécile

French patent application submitted on July 10th 2015 (FR 1556628).

International patent application submitted on July 7th 2016 (PCT/EP2016/066215).

L'objet de la présente invention concerne des hydrogels préparés au moyen de molécules organiques silylées (telles que des biomolécules silylées), leur procédé d'obtention et leurs utilisations.

Introduction

5 Il existe une recherche constante afin de trouver de nouveaux hydrogels, pouvant être fonctionnalisés, présentant des propriétés physico-chimiques ou biologiques précises, en particulier pour la médecine humaine.

Toutefois, il existe actuellement de nombreuses contraintes techniques avec ces matériaux. Par exemple, pour obtenir des matériaux possédant des propriétés biologiques, des biomolécules (peptides, protéines, saccharides, oligonucléotides, etc...) sont souvent
10 introduites dans ces matériaux de façon non covalente. Cette façon de faire est certes une technique d'introduction certaine des molécules actives dans les hydrogels présentant ainsi *ab initio* les propriétés biologiques et rhéologiques voulues. Elle présente néanmoins le désavantage que les hydrogels ainsi obtenus ne peuvent être envisagés pour être utilisés
15 *in vivo*, par exemple placés dans un patient, sans une libération de la/des molécules actives incorporées au sein de leur matrice. En outre, les hydrogels étant déjà formés et très visqueux (dans le meilleur des cas), leur administration par injection est très douloureuse pour le patient.

Ainsi, si l'on désire que l'hydrogel conserve une activité biologique sans relargage
20 intempestif, la liaison entre l'actif et la matrice de l'hydrogel doit être covalente. Toutefois, lier de manière covalente des biomolécules dans ces hydrogels sans en altérer fondamentalement les propriétés physico-chimiques reste difficile pour plusieurs raisons : les biomolécules étant généralement des molécules dont la chimie (de synthèse) est souvent particulière (e.g. des molécules possédant souvent de nombreuses fonctions
25 chimiques réactives), il est difficile de ne pas impliquer des réactions secondaires lors de la formation de l'hydrogel fonctionnalisé. En outre, il est difficile de lier de manière covalente ces biomolécules (souvent volumineuses) jusqu'au cœur de la matrice sans en altérer les propriétés physico-chimiques et/ou son intégrité quand on réalise une fonctionnalisation directe de l'hydrogel.

30 Le document brevet WO2011089267 traite, parmi d'autres sujets, de la fabrication d'hydrogels auxquels sont liées de manière covalente des biomolécules actives. Pour ce faire, c'est la chimie du silicium qui a été choisie complémentirement aux biomolécules choisies. Ainsi, deux types de biomolécules silylées sont synthétisées, l'une ayant pour rôle la matrice structurelle de l'hydrogel (en particulier HPMC silylé dans WO2011089267), et l'autre ayant le
35 rôle de fonctionnalisation biologique active de l'hydrogel. L'invention décrite dans

WO2011089267 apparaît donc séduisante. Toutefois, l'invention divulguée ne résout pas tous les problèmes techniques évoqués ci-dessus.

D'une part les propriétés rhéologiques des hydrogels sont difficilement contrôlables par la technique de WO2011089267. En effet, WO2011089267 divulgue des hydrogels formés à partir
5 d'une « biomolécule » possédant un seul groupement silylé, dont les propriétés vont essentiellement dépendre de la nature du fragment « biomolécule ». Ceci est un handicap car il est important de pouvoir finement contrôler la nature chimique de la matrice de l'hydrogel indépendamment de ses propriétés rhéologiques. Il est en outre fondamental que l'hydrogel assure par exemple une biocompatibilité selon le modèle étudié et/ou présente des fonctions
10 biologiques et/ou physico-chimiques particulières voulues selon le domaine concerné. L'un des aspects selon la présente invention a été donc de faciliter le contrôle de la rhéologie des hydrogels.

De plus, seul un procédé de fabrication des intermédiaires de synthèse (biomolécules silylées) est donné dans WO2011089267 (exemple 1 dudit document) et implique la suspension dans un
15 solvant comme de l'acétonitrile anhydre de la biomolécule d'intérêt à silyler. Ceci ne permet donc pas d'obtenir toutes les biomolécules silylées voulues. La purification apparaît donc être un réel problème quasiment non abordé dans WO2011089267. En effet, la purification décrite implique des lavages successifs du solide suspendu dans de l'acétonitrile afin d'en retirer toutes les impuretés. Or, une telle purification ne permet pas l'obtention d'un produit
20 (principe actif) d'une pureté nécessaire pour une utilisation médicale, et d'autre part nécessite que le produit obtenu soit également insoluble dans le solvant de lavage (acétonitrile anhydre dans WO2011089267). Les techniques de purification usuelles telle que la chromatographie en phase inverse (technique permettant une purification optimale pour la majorité des biomolécules) semblent être exclues de la technologie de WO2011089267 car les
25 molécules silylées décrites sont hautement réactives en milieu aqueux, résultant ainsi en une polymérisation une fois introduites dans une colonne HPLC en présence d'eau.

Ainsi, l'enseignement de WO2011089267, séduisant en première approche, ne permet pas de finement travailler avec les constituants des hydrogels afin de proposer des hydrogels fonctionnalisés de qualité médicale ou d'une qualité suffisante pour des domaines voisins
30 (recherche biomédicale en particulier).

Toutefois, même s'il existe d'autres exemples de molécules organiques silylées dans la littérature, tels que ceux trouvés dans WO2013190148 où est divulgué des conjugués peptidiques silylés, il n'est en revanche pas divulgué leur utilisation pour la fabrication d'hydrogels, ou une méthode de purification optimale impliquant par exemple l'HPLC en
35 phase inverse. En outre, seuls des « xérogels », formes non hydratées de gels, sont divulgués à

cette occasion. Or, le contrôle de la rhéologie d'hydrogels est également dépendant de leur taux d'hydratation.

En résumé, les hydrogels ont un potentiel d'utilisation considérable, en particulier dans le domaine médical. Néanmoins ce potentiel est actuellement limité par un mauvais contrôle
5 de la fabrication de ces hydrogels, une méconnaissance des moyens de contrôle des propriétés rhéologiques de ces hydrogels ou simplement l'impossibilité de réaliser des hydrogels biocompatibles actifs dont l'activité perdure dans le temps.

Ainsi, l'objet de la présente demande de brevet est de proposer au moins une solution technique pour pallier les méthodes incomplètes de l'art antérieur afin d'aboutir à l'obtention
10 d'hydrogels facilement modulables, pouvant en particulier être utilisés dans le domaine médical et les domaines voisins.

Afin de surmonter les problèmes rhéologiques des hydrogels, tout en permettant d'intégrer les (bio-)molécules voulues dans leur structure, il a été découvert de manière surprenante qu'en travaillant avec des (bio-)molécules au moins bi-silylées, il était possible de modifier les
15 propriétés rhéologiques des gels quasiment indépendamment de la nature des (bio-)molécules dites de structure. Ainsi, un modèle simple de polyéthylène glycol (PEG) intégré dans un hydrogel a permis, selon la longueur du PEG d'obtenir un hydrogel biocompatible avec les propriétés rhéologiques voulues. C'est en effet la taille de la maille formée par la matrice qui permet à celle-ci dans le cas particulier des hydrogels d'absorber plus ou moins d'eau et de lui
20 donner les propriétés rhéologiques voulues. En outre, en modifiant le nombre de groupements silylés introduits sur les (bio-)molécules de structure, il est possible de faire varier finement les propriétés rhéologiques de l'hydrogel quasiment indépendamment de la nature de ces (bio-)molécules de structure.

Un autre aspect de la présente invention concerne les techniques de purification des
25 précurseurs d'hydrogels éventuellement fonctionnalisés. La première de ces techniques implique une série de précipitations, en particulier dans un solvant inerte tel que l'éther diéthylique. Cette technique présente en effet l'intérêt que, la majorité des précurseurs synthétiques fonctionnalisés d'hydrogels sont insolubles dans l'éther et ne sont pas réactifs dans ce solvant. Par une succession de lavages par l'éther et éventuellement de dissolutions
30 dans un solvant adéquat, il est possible de proposer des précurseurs synthétiques fonctionnalisés d'hydrogels d'une pureté suffisante pour des molécules simples (peu coûteuses).

La présente invention propose en outre une méthode de purification par HPLC en phase
35 inverse impliquant un choix particulier de substituants de l'atome de Si. En effet, l'utilisation d'un seul groupement réactif, tel qu'un halogène ou un groupement hydroxyle ou un précurseur d'hydroxyle, sur l'atome de Si permet une purification sur colonne HPLC inverse de

la biomolécule silylée synthétisée, alors que les techniques selon l'art antérieur restent silencieuses quant à ce sujet. L'intérêt de pouvoir utiliser la HPLC en phase inverse, est de permettre l'obtention de molécules actives, telles que des biomolécules, avec un degré de pureté optimum, nécessaire dans le cadre d'une utilisation médicale.

5 Le choix des groupements portés sur l'atome de Si permet de pouvoir éviter dans la majorité des cas des réactions secondaires non voulues. Le potentiel de la présente invention réside donc également dans le fait qu'il semblerait que n'importe quelle biomolécule d'intérêt biologique (en particulier une séquence peptidique), puisse être introduite de façon contrôlée dans les hydrogels selon la présente invention pour leur
10 conférer des propriétés biologiques.

Il a été de plus trouvé de manière totalement opportune des caractéristiques physico-chimiques originales d'un hydrogel de polyéthylène glycol bi-silylé permettant de manière très facile le greffage de biomolécules silylées. L'hydrogel de polyéthylène glycol bi-silylé ainsi formé est biocompatible, biodégradable, totalement synthétique, et facilement modulable en
15 termes de taux d'hydratation (plus ou moins facilement imprégnable par des liquides par exemple aqueux). En outre il a été découvert que la matrice de l'hydrogel PEG(bi-silylé) peut être formée avec ou sans la présence d'eau, ce qui permet une flexibilité importante quant à l'utilisation de ce polymère (hydrogels déshydratés pouvant être hydratés par la suite). Néanmoins afin d'obtenir un hydrogel homogène en terme structurel (homogénéité de
20 structure et d'hydratation), il est préférable de former l'hydrogel dans un milieu majoritairement aqueux. De plus, la possibilité de modifier la réactivité du groupement silyle en diminuant ou augmentant le nombre de substituants réactifs sur celui-ci (1, 2 ou 3 substituants réactifs), permet de finement contrôler le degré de réticulation de l'hydrogel et ainsi de pouvoir en contrôler finement sa rhéologie.

25 Un autre aspect selon la présente invention concerne l'insertion d'hydrogels liquides dans l'organisme avec polymérisation de ces hydrogels *in situ*. En effet, un problème récurrent des hydrogels liquides préparés préalablement est que ceux-ci sont difficilement injectables à cause de leur viscosité, occasionnant lors de leur administration (locale) au patient des douleurs plus ou moins aiguës. La technique de WO2011089267, même si cela
30 est évoqué dans ce document, n'est pas utilisable en tant que telle car la pureté des biomolécules silylées n'est pas suffisante pour une application médicale avec une injection sous forme liquide et prise *in situ*. Les méthodes de purification évoquées ci-dessus permettent de surmonter ce problème technique.

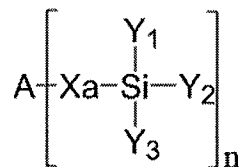
En effet, les hydrogels peuvent être préparés par simple dissolution des blocs hybrides
35 dans un tampon phosphate puis incubation de la solution à 37°C, ce qui permet d'envisager leur injection *in vivo* avec prise *in situ*.

Résumé de l'invention

L'objet de la présente invention concerne un procédé de fabrication d'un hydrogel comprenant les étapes de :

- a) polymérisation sol-gel d'au moins une molécule de formule (I) :

5



Formule (I)

dans laquelle :

10

- n est un nombre entier supérieur ou égal à 2 ; préférentiellement inférieur à 10, plus préférentiellement inférieur à 5 ou 4.
- A est un polymère organique de structure, préférentiellement d'origine synthétique (pouvant être par exemple choisi parmi les protéines, les peptides tels que des dérivés du collagène, en particulier les séquences comprenant des répétitions de tripeptides Pro-Hyp-Gly ou Pro-Pro-Gly ou Asp-Pro-Gly ou Pro-Lys-Gly, des séquences peptidiques d'autoassemblage comme Arg-Ala-Asp-Ala , des oligoprolines, des oligoalanines, les polysaccharides, tels que l'acide hyaluronique et ses dérivés, les oligonucléotides, des polymères de C₁-C₆-alkylènes-glycols, ou de polyvinylpyrrolidone);
- Xa est une liaison chimique ou un groupement espaceur préférentiellement représenté par un radical divalent dérivé d'une chaîne hydrocarbonée aliphatique saturée ou insaturée comportant de 1 à 10 atomes de carbone, dans laquelle sont éventuellement intercalés, un ou plusieurs chaînons structuraux choisis parmi le groupe arylène, ou les fragments -O-, -S-, -C(=O)-, -SO₂- ou -N(R₁)-, ladite chaîne étant non substituée ou substituée par un ou plusieurs radicaux choisis parmi les atomes d'halogène, les groupements hydroxyle, C₁-C₄ alkyle, benzyle et/ou phénéthyle ;
- R₁ représente un atome d'hydrogène, un groupement hydrocarboné aliphatique comportant de 1 à 6 atomes de carbones, un benzyle ou un phénéthyle ;
- Y₁, Y₂, Y₃, identiques ou différents, représentent chacun, indépendamment l'un de l'autre un atome d'hydrogène, d'halogène, un groupement -OR₂, un aryle ou une chaîne hydrocarbonée aliphatique saturée ou insaturée

15

20

25

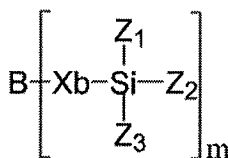
30

comportant de 1 à 6 atomes de carbone éventuellement substitués par un atome halogène, un groupement aryle ou hydroxyle ;

- R₂ représente un atome d'hydrogène, un groupement aryle ou une chaîne hydrocarbonée aliphatique saturée ou insaturée comportant de 1 à 6 atomes de carbone ;
 - au moins deux groupements Xa tels que définis ci-dessus étant reliés à des points d'accroches différents sur A;
- 5
- b) mise en présence d'eau, optionnellement conjointement à l'étape a) ; préférentiellement la qualité de l'eau étant de qualité médicale, et
 - 10 - c) récupération de l'hydrogel.

Le procédé de fabrication d'un hydrogel tel que défini ci-dessus peut en outre comprendre l'ajout conjointement ou successivement à l'étape a) au moins d'un type de molécule de formule (II) :

15



Formule (II)

dans laquelle :

- m est un nombre entier supérieur ou égal à 1; préférentiellement m est inférieur à 10, plus préférentiellement inférieur à 5 ou 4, encore plus préférentiellement égal à 1 ;
 - B est un principe actif, préférentiellement une biomolécule ou un fluorophore (pouvant être par exemple choisi parmi un peptide, un oligopeptide, une protéine, tel que le collagène, un acide désoxyribonucléique, un acide ribonucléique, un polysaccharide, tel qu'une pectine, un chitosane, un acide hyaluronique, un polysaccharide polyarabinose et polygalactose, et un glycolipide);
 - Xb est une liaison chimique ou un groupement espaceur préférentiellement représenté par un radical divalent dérivé d'une chaîne hydrocarbonée aliphatique saturée ou insaturée comportant de 1 à 10 atomes de carbone, dans laquelle sont éventuellement intercalés, un ou plusieurs chaînons
- 20
- 25
- 30

structuraux choisi parmi le groupe arylène, ou les fragments -O-, -S-, -C(=O)-, -SO₂- ou -N(R₃)-, ladite chaîne étant non substituée ou substituée par un ou plusieurs radicaux choisis parmi les atomes d'halogène, les groupements hydroxyle, C₁-C₄ alkyle, benzyle et/ou phénéthyle ;

- 5
- R₃ représente un atome d'hydrogène, un groupement hydrocarboné aliphatique comportant de 1 à 6 atomes de carbone, un benzyle ou un phénéthyle ;
 - Z₁, Z₂, Z₃, identiques ou différents, représentent chacun, indépendamment l'un de l'autre un atome d'hydrogène, d'halogène, un groupement -OR₄, un
- 10
- aryle ou une chaîne hydrocarbonée aliphatique saturée ou insaturée comportant de 1 à 6 atomes de carbone éventuellement substitués par un atome halogène, un groupement aryle ou hydroxyle ;
 - R₄ représente un atome d'hydrogène, un groupement aryle ou une chaîne hydrocarbonée aliphatique saturée ou insaturée comportant de 1 à 6 atomes
- 15
- de carbone ; et
 - avec préférentiellement un seul des groupements Z₁, Z₂, ou Z₃ comme atome d'halogène ou groupement OR₄.

L'objet de la présente invention, concerne donc un hydrogel susceptible d'être obtenu par le procédé tel que défini présentement.

- 20
- L'objet de la présente invention concerne en outre un hydrogel selon la présente invention pour son utilisation à des fins thérapeutiques et/ou chirurgicales, préférentiellement caractérisé en ce que ledit hydrogel permet la délivrance et/ou le transport de molécules actives, ou pour son utilisation *in vivo* en ingénierie tissulaire pouvant par exemple se faire
- 25
- par une polymérisation dudit hydrogel *in situ* dans un organisme vivant suite à la coulée ou l'injection des molécules de formule (I) et éventuellement (II) telles que définies ci-dessus.

- Ainsi, la présente invention concerne un hydrogel susceptible d'être obtenu par le procédé selon la présente invention pour son utilisation telle que définie ci-dessus, caractérisé en ce que la polymérisation dudit hydrogel est réalisée *in situ* dans un organisme vivant,
- 30
- c'est à dire un animal tel qu'un mammifère comme l'Homme, suite à la coulée ou l'injection, préférentiellement indolore ou peu douloureuse, des molécules de formule (I) et éventuellement (II) telles que définies ci-dessus.

Un autre objet de la présente invention concerne l'utilisation *in vitro* d'un hydrogel selon la présente invention en ingénierie tissulaire.

De plus, la présente invention concerne un procédé de purification d'un produit de formule (I) ou (II) tel que défini présentement, caractérisé en ce que ledit procédé comprend les étapes suivantes:

- 5 - a1) éventuelle solubilisation du produit de formule (I) ou (II) à purifier dans un solvant ;
- b1) précipitation du produit de formule (I) ou (II) à purifier, éventuellement en solution selon l'étape a1), dans un liquide de suspension, i.e. dans lequel les produits (I) ou (II) ne sont pas solubles ;
- c1) filtration du solide obtenu à l'étape (b1) ;
- 10 - d1) répétition au moins une fois des étapes a1) le cas échéant, b1) et c1) ; et
- e1) récupération du produit de formule (I) ou (II) purifié.

L'objet de la présente invention concerne de plus un procédé de purification d'un produit de formule (II) tel que défini présentement dans lesquels un seul des groupements Z_1 , Z_2 , Z_3 est un atome d'halogène ou un groupement $-OR_3$, caractérisé en ce que ledit procédé

15 comprend les étapes suivantes:

- a2) passage du produit de formule (II) à purifier sur une colonne de chromatographie en phase liquide, i.e. dans un solvant d'élution, préférentiellement en phase inverse ;
- b2) évaporation du solvant d'élution de l'étape a2), éventuellement par
- 20 lyophilisation ; et
- c2) récupération du produit de formule (II) purifié.

Ainsi, la présente invention concerne également un produit de formule (I) ou (II) tel que défini présentement, susceptible d'être obtenu par le procédé de purification de l'invention caractérisé en ce que ledit produit présente une pureté d'au moins 98% en

25 masse vis-à-vis du poids total de produit, préférentiellement supérieure à 99% en masse.

Définitions

« *Hydrogel* »

Un « hydrogel » est un type de matériau comportant une composante liquide aqueuse et

30 une composante solide. Structuellement, il est composé d'une matrice de chaînes polymères, gonflée par un fluide comprenant de l'eau, ce fluide, préférentiellement constitué essentiellement d'eau, étant préférentiellement en une proportion égale ou supérieure à 40% en poids dudit hydrogel, plus préférentiellement comprise entre 40 et

99% en poids, entre 50 et 98%, entre 60 et 97%, entre 70 et 96% ou encore entre 80% et 95%. De manière préférée ce fluide comprend au moins 95% d'eau en poids, voire 100% d'eau. Ce fluide peut en outre être un liquide d'origine biologique. La teneur en eau d'un hydrogel détermine également en grande partie ses caractéristiques physico-chimiques. Il est possible de retrouver ces hydrogels également pour diverses applications biomédicales notamment dans la libération de médicaments et dans le traitement de brûlures cutanées.

« *Polymère pouvant être réticulé* » ou « *polymère réticulable* »

Les hydrogels selon l'invention sont constitués de chaînes de polymères liées entre elles par des liaisons covalentes. Un polymère réticulé comprend des nœuds avec au moins 3 liaisons chimiques, préférentiellement covalentes. Cette réticulation permet aux hydrogels selon la présente invention de fournir un caractère dit "permanent" aux nœuds de réticulation car l'atome de silicium tétravalent génère 4 liaisons covalentes. Néanmoins, de par la double nature des hydrogels selon la présente invention (organique et inorganique), il est possible d'obtenir des propriétés remarquables : une rigidité partielle et une capacité à donner une réponse élastique à un stress mécanique. La nature organique permet une haute biocompatibilité et une non-toxicité des hydrogels produits. En outre, les hydrogels selon la présente invention ont un degré de flexibilité très similaire à celui des tissus naturels (induit par leur importante teneur en eau). Le terme « réticulable » fait donc préférentiellement référence ici à la capacité des atomes de silicium à générer au plus 3 liaisons covalentes avec au plus 3 groupements comprenant un atome de Si (tel que Si-OH).

« *Polymérisation sol-gel* »

Le procédé sol-gel permet de fabriquer un polymère inorganique par des réactions chimiques simples à une température proche de la température ambiante (en réalité applicable à des gammes de températures allant de 0°C à 150 °C, préférentiellement entre 20°C et 70°C, plus préférentiellement entre 35°C et 40°C). Typiquement, la synthèse est effectuée à partir d'alcoxysilanes ou de silanols de formule $\text{Si}(\text{OR})_n$ où R est un groupement organique alkyle $\text{C}_n\text{H}_{2n+1}$ ou un hydrogène.

Un des intérêts de ce procédé est que ces précurseurs sont soit liquides soit solides, dans ce cas ils sont, pour la plupart, solubles dans des solvants usuels. Il est donc possible de préparer des mélanges homogènes de monomères (précurseurs) ou oligomères.

Les réactions chimiques simples à la base du procédé sont déclenchées lorsque les précurseurs sont mis en présence d'eau : l'hydrolyse des groupements typiquement alcoxy (ou halogène le cas échéant) intervient tout d'abord, puis la condensation des produits hydrolysés conduit à la gélification du système, formant ainsi l'hydrogel.

5 « Polymère organique de structure »

Par « polymère organique de structure », il est compris selon la présente invention un polymère de nature organique, donc hydrocarboné, permettant de structurer l'hydrogel sous forme d'une matrice polymérique. Ceci est réalisé facilement à partir du moment où les monomères composant ledit polymère organique de structure sont contrôlés en terme
10 de structure chimique et de pureté ; i.e. par les techniques usuelles de chimie de synthèse ou de purification. En effet, en contrôlant la nature des monomères impliqués dans la polymérisation de l'hydrogel, il est possible de faire varier les caractéristiques physico-chimiques et rhéologiques du polymère obtenu *in fine*.

« Origine synthétique »

15 Les matières premières utilisées pour la production des matériaux synthétiques sont bien sûr issues de la Nature, comme le pétrole. Cependant, les matériaux synthétiques créés par l'Homme à partir de procédés chimiques, les différencient des autres matériaux. Selon la présente invention, l'expression « origine synthétique » implique que le produit considéré a été modifié au moins une fois par un procédé chimique mis au point par
20 l'Homme.

« Liaison chimique »

On appelle « liaison chimique » toute interaction attractive qui maintient au moins deux atomes à courte distance l'un de l'autre. Cette interaction peut être directionnelle comme la liaison entre deux atomes au sein d'une molécule, ou non directionnelle comme
25 l'interaction électrostatique qui maintient les ions d'un cristal ionique en contact. Elle peut être forte comme les deux précédents exemples, ou faible comme les interactions de van der Waals qui sont de nature dipolaire.

« Groupement espaceur »

On appelle « groupement espaceur » selon la présente invention, un fragment comprenant
30 au moins un atome. Préférentiellement, le groupement espaceur contient au moins un atome de carbone. Avantageusement le groupe espaceur permet d'éloigner au sein d'une même molécule, deux groupements chimiques, de diminuer la gêne stérique entre le

groupement A (ou B) et l'atome de Si. Plus avantageusement, le groupement espaceur permet au groupement silylé de réagir avec une gêne limitée du fragment A (ou B) ou au groupement A (ou B) d'interagir et de conserver ses propriétés biologiques, avec une gêne limitée du fragment contenant le Si. En outre le groupement espaceur permet une liaison stable entre le fragment A (ou B) et Si, tout en permettant au fragment silicate de réagir. Il est donc clair que le groupement espaceur ne peut pas être considéré comme un élément constitutif du fragment A (ou B), comme par exemple un résidu d'acide aminé si A (ou B) est un fragment peptidique).

Avantageusement, le groupement espaceur comprend, ou consiste en, une chaîne hydrocarbonée aliphatique saturée ou insaturée, préférentiellement comprise entre 1 et 10 atomes de carbone, plus préférentiellement entre 2 et 5 atomes de carbone. De manière préférée, le groupement espaceur est une chaîne hydrocarbonée aliphatique saturée.

Le groupement espaceur (en particulier lorsqu'il s'agit d'une chaîne hydrocarbonée aliphatique saturée ou insaturée telle que décrite ci-dessus) peut en outre inclure des hétéroatomes, en particulier choisis parmi N, O, S, ou encore P, et peut en plus être substitué, en particulier par des atomes d'halogènes, ou par des groupements hydroxyles, aryles, alkyles en C₁-C₄, sulfates, amines, ou encore phosphates. Toutefois, si des hétéroatomes sont présents dans le groupement espaceur, préférentiellement ces hétéroatomes ne sont pas directement reliés à Si.

Préférentiellement, le groupement espaceur est un fragment alkyle en C₁-C₄ linéaire ou ramifié. Plus préférentiellement, le groupement espaceur comprend un fragment -(CH₂)₂-, -(CH₂)₃-, -(CH₂)₄-. De manière plus préférée encore, le groupement espaceur comprend le fragment -(CH₂)₃-.

« *Radical divalent dérivé* »

Selon la présente invention, l'expression « radical divalent dérivé » concerne un élément ayant une valence de deux. La valence est le nombre de liaisons chimiques formées, qui peuvent être des liaisons covalentes, polaires, ou ioniques. Le terme « dérivé » fait simplement référence aux liaisons chimiques formées pour incorporer ledit radical dans la structure.

« *Chaîne hydrocarbonée aliphatique saturée ou insaturée* »

Par « chaîne hydrocarbonée aliphatique saturée ou insaturée », il est compris des fragments de type alkyle en C₁-C₁₀, alcène en C₂-C₁₀ ou alcyne en C₂-C₁₀, préférentiellement ces chaînes sont linéaires ou ramifiées.

« *Alkyle en C₁-C₁₀* »

- 5 Dans la présente invention, il est compris par « alkyle en C₁-C₁₀ », ou encore « alkyle de 1 à 10 atomes de carbone », un groupe aliphatique saturé, linéaire, ramifié, voire cyclique, comportant de 1 à 10 atomes de carbone, comme par exemple un groupement méthyle, éthyle, isopropyle, tertio-butyle, n-pentyle, cyclopropyle, cyclohexyle, etc.

« *Alcène en C₂-C₁₀* »

- 10 Par groupement « alcène en C₂-C₁₀ », ou encore « alcène de 2 à 10 atomes de carbone », on entend au sens de la présente invention, un groupe aliphatique mono- ou poly-insaturé, linéaire, ramifié ou cyclique comprenant de 2 à 10 atomes de carbone. Un groupe alcène selon l'invention comprend, de préférence, une ou plusieurs insaturations éthyléniques. A titre d'exemple, on peut citer les groupes éthylènes, propylène, propyl-2-ène ou propyl-3-ène, butylène, cyclobutène etc.

« *Alcyne en C₂-C₁₀* »

- Par groupement « alcyne en C₂-C₁₀ », ou encore « alcyne de 2 à 10 atomes de carbone », on entend au sens de la présente invention, un groupe aliphatique, linéaire, ramifié ou cyclique comprenant de 2 à 10 atomes de carbone et au moins une double insaturation, c'est-à-dire une triple liaison entre deux atomes de carbones. Un groupe alcyne selon 20 l'invention comprend, de préférence, une ou plusieurs doubles insaturations. A titre d'exemple, on peut citer les groupes acétylène, propyne, butyne, etc.

« *Aryle* »

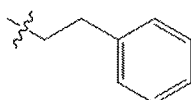
- Par groupement « aryle », on entend un groupement aromatique, comportant de 25 préférence de 5 à 10 atomes de carbone, comprenant un ou plusieurs cycles et comprenant éventuellement un ou plusieurs hétéroatome(s) en particulier un oxygène, un azote ou un soufre, comme par exemple un groupement phényle, furane, indole, pyridine, naphthalène, etc.

« *Arylène* »

Un groupement « arylène » représente un substituant d'un composé organique dérivé d'un fragment aryle dans lequel au moins un atome d'hydrogène a été retiré de deux carbones inclus dans l'aryle. Préférentiellement, il s'agit d'un groupement phénéthyle.

« *Phénéthyle* »

5 Le terme phénéthyle représente le fragment :



« *Halogène* »

10 Le terme halogène désigne les éléments chimiques de la 17^e colonne du tableau périodique, anciennement appelé groupe VII ou VIIA. Ces éléments chimiques sont préférentiellement : le fluor, le chlore, le brome et l'iode.

« *Hydroxyle* »

Le terme hydroxyle selon la présente invention concerne le fragment -OH, et éventuellement ses sels, par exemple de sodium ou potassium.

15 « *Xa reliés à des points d'accroches différents sur A* »;

Par l'expression « *Xa reliés à des points d'accroches différents sur A* », il est compris selon la présente invention que les groupements *Xa* ne sont pas reliés au même atome appartenant au polymère A. De manière préférée, les points d'accroches (i.e. les atomes d'accroche) sont positionnés de manière la plus éloignée possible sur le polymère A. Une manière pour évaluer cet éloignement peut être simplement de compter le nombre d'atomes entre les deux points d'accroche sur le polymère A. En effet, les propriétés physico-chimiques et rhéologiques sont plus facilement contrôlables lorsque l'entropie des polymères A est diminuée, ce qui se fait en principe en fixant les extrémités des chaînes de polymère.

25 « *Récupération* »

Par « *récupération* », il est compris selon la présente invention que les produits obtenus sont extraits selon les techniques communes de l'art, i.e. par l'intermédiaire d'un lavage biphasique comprenant par exemple un solvant organique et de l'eau ; alternativement, il est possible de récupérer les produits par suspension dans le liquide qui les contient, puis

de les filtrer. Une autre façon de récupérer les produits, peut être tout simplement d'évaporer ou lyophiliser le solvant qui les contient. Cette phase de récupération peut en outre contenir une purification par lavage ou passage sur colonne chromatographique, le cas échéant.

5 « *Eau de qualité médicale* »

Par « eau de qualité médicale », il est compris selon la présente invention que l'eau est de qualité ultra pure communément utilisée dans le milieu médical, éventuellement avec des adjuvants permettant de retrouver les conditions physiologiques de l'organisme humain, tel que des sels comme NaCl, KCl, CaCl₂, MgCl₂, etc. ; de tampon pH tel que des tampons phosphates pH 7,4, etc. ; ou encore des sucres tels que du glucose, du mannitol.

« *Principe actif* »

La définition générale d'un principe actif, est : le principe actif est la molécule qui dans un médicament possède un effet thérapeutique. Dans le contexte de la présente invention, qui concerne les hydrogels, le principe actif est la molécule présentant des caractéristiques physico-chimiques ou biologiques distinctives du polymère qui la porte. Par exemple, le principe actif peut être un médicament connu, une molécule biologique telle qu'une séquence peptidique permettant l'accroche de cellules biologiques, ou un colorant ou toute autre molécule présentant une ou des activités biologiques ou physico-chimiques. Le principe actif peut être d'origine naturelle ou synthétique.

20 De manière avantageuse, l'hydrogel selon la présente invention comprend un principe actif à activité antimicrobienne, antibiotique et/ou antifongique.

Préférentiellement, le principe actif est une biomolécule, par exemple choisie parmi un peptide, une protéine, un glycopeptide, une glycoprotéine, un acide déoxyribonucléique, un acide ribonucléique, une pectine, un chitosane, un acide hyaluronique, un saccharide, un oligosaccharide, un lipide, un glycolipide, ou leurs dérivés.

De manière avantageuse le principe actif est choisi parmi des molécules favorisant l'adhésion cellulaire, telles que des peptides contenant ou consistant en la séquence ArgGlyAsp, en particulier, le peptide H-GlyArgGlyAspSerPro-OH (Seq ID 1), des molécules favorisant la cicatrisation, telles que des peptides contenant ou consistant en la séquence H-GluGlyLeuGluProGly-OH (Seq ID 2), des molécules favorisant la production de matrice extracellulaire telles que des peptides contenant ou consistant en H-ValGlyValAlaProGly-OH (Seq ID 3) ou des molécules antibactériennes, telles que des peptides contenant ou consistant en H-AhxArgArg-NH₂, des molécules (e.g. peptides) antidouleurs, des molécules

(e.g. peptides) qui favorisent la coagulation du sang, des molécules (e.g. peptides) anticoagulantes, des molécules (e.g. peptides) antiprolifératives, ou un mélange de plusieurs de ces (bio-)molécules.

De manière avantageuse le principe actif peut être un colorant, un fluorophore ou un marqueur choisi parmi les composés suivants : fluorescéine, sel sodique de fluorescéine, 4',5'-Bis[*N,N*-bis(carboxyméthyl)-aminométhyl]fluorescéine, acide 6-[fluorescéine-5(6)-carboxamido]hexanoïque, acide 6-[fluorescéine-5(6)-carboxamido]hexanoïque, ester *N*-hydroxysuccinimide de fluorescéin-5(6)-isothiocyanate, fluorescéin- α -D-N-acétylneuraminide-polyacryl-amide, amidite de fluorescéine, fluorescéine-di(β -D-galactopyranoside), fluorescéin-di-(β -D-glucopyranoside), diacétate de fluorescéine, diacétate fluorescéin-5(6)-isothiocyanate, diacétate de fluorescéin-5-maleimide, diacétate de fluorescéin-6-isothiocyanate, dibutyrate de fluorescéine, fluorescéine dilaurate, sel de diphosphate de fluorescéine triammonium, acide fluorescéin-hyaluronique, isothiocyanate de fluorescéine- Dextran 500000-Conjugué, isomère I de l'isothiocyanate de fluorescéine, isothiocyanate de fluorescéine-dextran, acétate de mercure-fluorescéine, chlorhydrate de mono-*p*-guanidinobenzoate-fluorescéine, *O,O'*-diacrylate de fluorescéine, fluorescéine *O,O'*-diméthacrylate, fluorescéine *o*-acrylate, fluorescéine *O*-méthacrylate, ester *N*-hydroxysuccinimide de fluorescéine, fluorescéine-5-thiosemicarbazide, fluorescéin- α -D-galactosamine polyacrylamide, fluorescéin- α -D-mannopyranoside-polyacrylamide, 4(5)-(iodoacétamido)-fluorescéine, 5-(Bromométhyl)fluorescéine, 5-(iodoacétamido)fluorescéine, diacétate de l'ester *N*-succinimidyl-5-Carboxy-fluorescéine, diacétate de l'ester *N*-succinimidyl-6-Carboxy- fluorescéine, Aminophényl-fluorescéine, Biotin-4- fluorescéine, hydroxyphényl-fluorescéine, MTS-4- fluorescéine, chlorhydrate de poly(fluorescéine-isothiocyanate allylamine), poly(fluorescéine-*O*-acrylate), poly(fluorescéine-*O*-méthacrylate), acétate de PPHT-fluorescéine, chlorhydrate de 5-([4,6-dichlorotriazin-2-yl]amino) fluorescéine, chlorhydrate de 6-([4,6-dichlorotriazin-2-yl]amino) fluorescéine, poly[(méthylméthacrylate)-*co*-(fluorescéine-*O*-méthacrylate)], poly[méthylméthacrylate-*co*-(fluorescéine *O*-acrylate)], 5(6)-(Biotinamidohexanoylamido)pentylthioureidylfluorescéine, N-(5- fluorescéinyl)maléimide, sel disodique de Mercure-dibromo-fluorescéine, fluorescéin-di-[méthylène-*N*-méthylglycine], sel disodique de 2',4',5',7'-tétrakis-(acétoxymercuro)-fluorescéine, l'érythrosine B, l'éthyl éosine, 5-carboxy fluorescéine, ester *N*-succinimidyl de 5-carboxy fluorescéine, rhodamine B octadécyl, ester *N*-hydroxysuccinimide de 6-Carboxy-fluorescéine, dibenzyl fluorescéine, rhodol, 6-amino fluorescéine, rhodamine 6G, la rhodamine B ou encore la rhodamine 123. Ces colorants, fluorophores et/ou marqueurs

peuvent être incorporés dans l'hydrogel avec une biomolécule ou un mélange de plusieurs biomolécules.

Le terme « biomolécule » selon la présente invention concerne une molécule susceptible d'être trouvée dans le milieu biologique, i.e. synthétisée par un organisme vivant. Cette définition comprend également les analogues fonctionnels de ces molécules (qui deviennent donc des molécules de synthèse). En effet, il est par exemple commun dans l'art de modifier la structure des biomolécules afin d'uniquement en garder la région active ou le site actif, ou d'ajouter des groupements protecteurs des fonctions réactives, empêchant ainsi les réactions secondaires, par exemple.

10 Ces groupements protecteurs et leur utilisation sont décrits dans des ouvrages tels que par exemple Greene, "Protective Groups in Organic Synthesis", Wiley, New York, 2007 4e édition ; Harrison et al. "Compendium of Synthetic Organic Methods", Vol. 1 à 8 (J. Wiley & sons, 1971 to 1996).

« *Activité antimicrobienne* »

15 Une « activité antimicrobienne » selon la présente invention est la définition générique telle que comprise par l'homme du métier, c'est-à-dire un effet relatif à un agent antimicrobien. Un (agent) antimicrobien est une substance qui tue, ralentit la croissance ou bloque la croissance d'un ou de plusieurs microbes. Par « croissance » il est compris dans le cadre de la présente invention toute opération cellulaire permettant un
20 accroissement volumétrique de la cellule, une division cellulaire ou une reproduction cellulaire. Un microbe dans le cadre de la présente invention concerne tout organisme unicellulaire ou pluricellulaire pathogène ou parasitaire d'autres organismes vivants comme les humains.

Par exemple, les antimicrobiens peuvent être généralement choisis parmi les différentes
25 familles suivantes : les bêta-lactamines, les céphalosporines, la fosfomycine, les glycopeptides, les polymyxines, les gramicidines, la tyrocidine, les aminosides, les macrolides, les lincosamides, les synergistines, les phénicolés, les tétracyclines, l'acide fusidique, les oxazolidinones, les rifamycines, les quinolones, les fluoroquinolones, les produits nitrés, les sulfamides, la triméthoprime, et leurs mélanges.

30 De manière plus spécifique les antimicrobiens peuvent être choisis parmi la nystatine, le nitrate de miconazole, l'acide lauryl-oxypropyl-β-aminobutyrique, l'amphotéricine B, l'acide undécylénique, le chloroquinaldol, le nitrate d'éconazole, la natamycine, le cloprothiazole, le clotrimazole, le tolnaftate, la lucensomycine, la tétracycline, l'érythromycine, les pénicillines, l'oxacilline, la cloxaciline, l'ampicilline, l'amoxicilline, la
35 bacampicilline, la métampicilline, la pivampicilline, l'azlocilline, la mezlocilline, la

pipéracilline, la ticarcilline, le pivmécillinam, le sulbactam, le tazobactam, l'imipénème,
 la céfalexine, le céfadroxil, le céfador, la céfatrizine, la céfalotine, la céfapryrine, la
 céfazoline, la céfoxitine, le céfamandole, le céfotétan, le céfuroxime, le céfotaxime, le
 céfsulodine, le céfopérazone, le céfotiam, la céftazidime, le céftriaxone, le céfixime, le
 5 céfpodoxime, le céfépime, le latamoxef, l'aztréonam, la vancomycine, la vancocine, la
 téicoplanine, la polymyxine B, la colistine, la bacitracine, la tyrothricine, la
 streptomycine, la kanamycine, la tobramycine, l'amikacine, la sisomicine, la dibékacine, la
 nétilmicine, la spectinomycine, la spiramycine, l'érythromycine, la josamycine, la
 roxithromycine, la clarithromycine, l'azithromycine, la lincomycine, la clindamycine, la
 10 virginiamycine, la pristinamycine, la dalfopristine-quinupristine, le chloramphénicol, le
 thiamphénicol, la tétracycline, la doxycycline, la minocycline, l'acide fusidique, la
 linézolide, la rifamycine, la rifampicine, l'acide nalidixique, l'acide oxolinique, l'acide
 pipémidique, la fluméquine, la péfloxacine, la norfloxacin, l'ofloxacin, la ciprofloxacine,
 l'enoxacin, la sparfloxacin, la lévofloxacin, la moxifloxacin, la nitroxoline, le
 15 tilboquinol, la nitrofurantoïne, la nifuroxazide, la métronidazole, l'ornidazole, la
 sulfadiazine, le sulfaméthisol, le triméthoprime, l'isoniazide et leurs dérivés et mélanges.

Préférentiellement, les antimicrobiens greffés ont un mode d'action de contact.

En outre, toutes ces molécules antimicrobiennes présentent des fonctions chimiques plus
 ou moins réactives. Ainsi, l'homme du métier est tout à fait capable d'adapter l'objet de
 20 la présente invention afin d'utiliser l'une de ces fonctions comme point d'attache au
 fragment Xb.

« *Activité antibiotique* »

Une « activité antibiotique » (équivalent au terme « antibactérien ») selon la présente
 25 invention est la définition générique telle que comprise par l'homme du métier, c'est-à-
 dire un effet relatif à un agent antibiotique. Un (agent) antibiotique est une substance
 est une substance qui tue, ralentit la croissance ou bloque la croissance d'une ou de plusieurs
 bactéries. Par « croissance » il est compris dans le cadre de la présente invention toute
 opération cellulaire permettant un accroissement volumétrique de la cellule (bactérie),
 30 une division cellulaire (de la bactérie) ou une reproduction cellulaire (de la bactérie).

Par exemple les antibiotiques peuvent être généralement choisis parmi les différentes familles suivantes : les bêta-lactames, les monobactames, les pénicillines, les inhibiteurs

de beta lactamases, les aminoglycosides, les glycylycylcine, les tétracyclines, les quinolones, les glycopeptides, les lipopeptides, les macrolides, les ketolides, les lincosamides, les streptogramines, les oxazolidinones, les polymyxines.

De manière plus spécifique les antibiotiques peuvent être choisis parmi l'amikacine, la gentamycine, la tobramycine, l'imipénème, le méropénème, l'ertapénème, le composé
5 connu sous l'appellation PZ-601, la céfazoline, la céfépime, la céfotaxime, la céfoxitine, la ceftaroline, la ceftazidime, la ceftibiprole, la ceftriaxone, la céfuroxime, la céphalexine, l'aztréoname, l'amoxicilline, la clavulanate, l'ampicilline, le sulbactame, l'oxacilline, la pipéracilline, le tazobactame, la ticarcilline, la pénicilline, la doxycycline, la minocycline,
10 la tétracycline, la tigécycline, la ciprofloxacine, la gatifloxacine, la grépafloraxine, la lévofloxacine, la moxifloxacine, l'ofloxacine, l'azithromycine, la clarithromycine, la roxythromycine, la télithromycine, la colistine, la polymyxine B, la fosfomycine, le triméthoprim et le sulfaméthoxazole.

On peut encore citer comme exemples d'agents antibiotiques les alcools, les polyols en C2-
15 C8, les acétate, benzoate et diacétate d'aluminium, des conservateurs tels que le chlorure de benzalkonium, le chlorure de cétrimonium, la chlorhexidine, le climbazole, des citrates, l'oxyde et le sulfate d'argent, des acides tel que l'acide borique, l'acide usnique, l'acide pyroglutamique et dérivés, les acétate, borate, salicylate et sulfate de zinc, des peptides antimicrobiens tels que les béta-défensines, et leurs mélanges.

20 Préférentiellement, les antibiotiques greffés ont un mode d'action de contact.

Toutes ces molécules antibiotiques présentent des fonctions chimiques plus ou moins réactives. Ainsi, l'homme du métier est tout à fait capable d'adapter l'objet de la présente invention afin d'utiliser l'une de ces fonctions comme point d'attache au fragment Xb.

25

« *Activité antifongique* »

Une « activité antifongique » selon la présente invention est la définition générique telle que comprise par l'homme du métier, c'est-à-dire un effet relatif à un agent antifongique. Un (agent) antifongique est une substance qui tue, ralentit la croissance ou bloque la
30 croissance d'un ou de plusieurs champignons. Par « croissance » il est compris dans le cadre de la présente invention toute opération cellulaire permettant un accroissement

volumétrique de la cellule (champignon), une division cellulaire (du champignon) ou une reproduction cellulaire (du champignon).

Des exemples d'antifongiques peuvent en outre être choisis parmi les différentes familles suivantes : les polyènes, les imidazoles, les triazolés, les analogues nucléosidiques, les allylamines, les échinocandines, les sordarines, les morpholines, la griséofulvine, la ciclopiroxolamine, le sulfure de sélénium, et leurs mélanges.

Plus préférablement, l'agent antifongique est choisi parmi la nystatine, l'amphotéricine B, le kétoconazole, l'éconazole, le miconazole, le clotrimazole, le fluconazole, l'itraconazole, le voriconazole, le posaconazole, la 5-fluorocytosine, la naftafine, la terbinafine, la caspofongine, l'amorlfine, et leurs dérivés et mélanges.

Préférentiellement, les antifongiques greffés ont un mode d'action de contact.

Toutes ces molécules antifongiques présentent des fonctions chimiques plus ou moins réactives. Ainsi, l'homme du métier est tout à fait capable d'adapter l'objet de la présente invention afin d'utiliser l'une de ces fonctions comme point d'attache au fragment Xb.

« *Principe actif naturel* »

Un principe actif naturel, telle qu'une biomolécule naturelle, est un principe actif trouvé dans l'environnement sans intervention humaine directe (hormis son extraction/isolement)

« *Principe actif synthétique* »

Un principe actif synthétique est un principe actif qui n'est pas trouvé dans l'environnement sans intervention humaine directe (hormis son extraction/isolement). Par exemple, un principe actif tel qu'un peptide synthétique peut être une séquence d'un peptide naturel dans lequel au moins un acide aminé naturel a été remplacé par un autre, naturel ou synthétique.

« Peptide » et « protéine »

Les termes « peptide » (équivalent au terme « oligopeptide ») et « protéine » doivent être compris comme des polymères d'acides aminés, lesdits acides aminés étant reliés entre eux par une liaison peptidique et/ou pseudopeptidique. Un peptide contient généralement entre 2 et 80 à 100 acides aminés, la limite supérieure n'étant pas clairement définie. Au-delà de cette limite supérieure, on parlera plutôt de protéines. Préférentiellement le

principe actif peptidique selon la présente invention contient entre 2 et 80 acides aminés, plus préférablement entre 3 et 40, et encore plus préférablement entre 4 et 20.

Les peptides ou protéines peuvent être extraites d'un milieu biologique ou fabriquées de manière synthétique. Les techniques de synthèse peptidique sont décrites dans Paul Lloyd-Williams, Fernando Albericio, Ernest Giralt, "Chemical Approaches to the Synthesis of Peptides and Proteins", CRC Press, 1997 ou Houben-Weyl, "Methods of Organic Chemistry, Synthesis of Peptides and Peptidomimetics", Vol E 22a, Vol E 22b, Vol E 22c, Vol E 22d., M. Goodman Ed., Georg Thieme Verlag, 2002.

« *Acide aminé* »

10 L'expression « acide aminé » doit être comprise comme toute molécule présentant au moins un acide carboxylique, au moins une amine et au moins un carbone reliant cette amine et cet acide carboxylique. Préférentiellement, les acides aminés pouvant être utilisés dans le cadre de la présente invention sont les acides aminés dits « naturels » et/ou les acides aminés synthétiques tels que défini ci-dessous. Préférentiellement les
15 acides aminés de la présente invention sont de configuration L.

« *Acide aminé naturel* »

L'expression « acide aminé naturel » représente entre autres les acides aminés suivants : la glycine (Gly), l'alanine (Ala), la valine (Val), la leucine (Leu), l'isoleucine (Ile), la sérine (Ser), la thréonine (Thr), la phénylalanine (Phe), la tyrosine (Tyr), le tryptophane (Trp), la
20 cystéine (Cys), la méthionine (Met), la proline (Pro), l'acide aspartique (Asp), l'asparagine (Asn), la glutamine (Gln), l'acide glutamique (Glu), l'histidine (His), l'arginine (Arg) et la lysine (Lys). Les acides aminés naturels préférés selon la présente invention sont les acides aminés de la série L.

« *Acide aminé synthétique* »

25 Par acide aminé synthétique, il est compris tous les acides aminés non « codés » et non naturels tels que définis ci-dessus.

« *Glucide* »

Le terme "glucide" comprend les monosaccharides et polysaccharides.

Un monosaccharide, ou ose, est un polymère de carbones hydraté, lesquels carbones sont
30 reliés entre eux par une liaison C-C. Il existe deux types d'ose : les aldoses et les cétooses. Les monosaccharides sont en outre « cyclisables » par l'intermédiaire d'une fonction hémiacétal. Les monosaccharides préférés selon la présente invention sont les

monosaccharides de la série D. Les monosaccharides sont classés par nombre de carbones. Par exemples les monosaccharides à 6 carbones sont les hexoses de formule $C_6H_{12}O_6$ et peuvent être l'allose, l'altrose, le glucose, le mannose, le gulose, l'idose, le galactose ou le talose. Les monosaccharides à 5 carbones sont les pentoses de formule $C_5H_{10}O_5$ et peuvent être le ribose, l'arabinose, le xylose, ou le lyxose.

Un polysaccharide concerne un polymère fait de monosaccharides (préférentiellement de la série D) joints par des liaisons glycosidiques. Des exemples de polysaccharides sont la cellulose et ses dérivés, la pectine, le chitosane, ou encore l'acide hyaluronique. Les dérivés de cellulose comprennent l'hydroxypropylméthylcellulose (HPMC), l'hydroxyéthylcellulose (HEC), l'hydroxypropylcellulose (HPC), carboxyméthylcellulose (CMC).

Les glucides naturels ou synthétiques sont compris dans cette définition.

« *Glycopeptide* »

Un glycopeptide est un peptide relié à un glucide par l'intermédiaire d'au moins une liaison chimique.

« *Glycoprotéine* »

Une glycoprotéine est une protéine reliée à un glucide par l'intermédiaire d'au moins une liaison chimique.

« *Acide déoxyribonucléique* »

L'acide déoxyribonucléique, ou ADN, est une macromolécule biologique présente dans toutes les cellules ainsi que chez de nombreux virus. L'ADN contient toute l'information génétique, appelée génotype, permettant le développement et le fonctionnement des êtres vivants.

« *Acide ribonucléique* »

L'acide ribonucléique (ARN) est une molécule biologique présente chez pratiquement tous les êtres vivants, et aussi chez certains virus. L'ARN est une molécule très proche chimiquement de l'ADN et il est d'ailleurs en général synthétisé dans les cellules à partir d'une matrice d'ADN dont il est une copie. Les cellules vivantes utilisent en particulier l'ARN comme un support intermédiaire des gènes pour synthétiser les protéines dont elles ont besoin.

« *Pectine* »

Les pectines sont des polysaccharides caractérisés par un squelette d'acide α -D-galacturonique et de faibles quantités de α -L-rhamnose plus ou moins ramifiés.

« *Chitosane* »

Le chitosane ou chitosan est un polyoside composé de la distribution aléatoire de D-glucosamine liée en β -(1-4) (unité désacétylée) et de N-acétyl-D-glucosamine (unité acétylée).

« *Acide hyaluronique* »

Les acides hyaluroniques sont des polymères de disaccharides eux-mêmes composés d'acide D-glucuronique et de D-N-acétylglucosamine, liés entre eux par des liaisons glycosidiques alternées α 1,4 et α 1,3. Les polymères de cette unité récurrente peuvent avoir une taille moyenne entre 400 et 10^7 Da *in vivo*. Dans le cadre de la présente invention, les polymères de cette unité récurrente peuvent avoir une taille moyenne entre 1000 et $7 \cdot 10^6$ Da, préférentiellement entre 1500 et $5 \cdot 10^6$ Da, par exemple entre 2000 et 9000 Da ou entre 10^4 et $4 \cdot 10^6$, telle qu'entre 150000 et 500000 ou encore entre $2 \cdot 10^6$ et $3 \cdot 10^6$. Par exemple dans le cadre de la présente invention, les polymères de cette unité récurrente peuvent avoir une taille moyenne d'environ 6400 Da, $2 \cdot 10^5$ Da ou encore $2,6 \cdot 10^6$ Da.

« *Lipide* »

Les lipides comprennent plusieurs classes de molécules comprenant les acides gras, les glycérides, les phosphoglycérides, les sphingolipides, les stérols, les prénoles.

Les acides gras sont des acides carboxyliques à chaîne aliphatique. Les glycérides sont constitués d'un résidu de glycérol estérifié par un, deux ou trois acides gras, ce qu'on appelle respectivement monoglycérides, diglycérides et triglycérides. Les phosphoglycérides sont des phospholipides constitués de deux résidus d'acides gras estérifiant un résidu glycérol lui-même estérifié par un résidu phosphate. Les sphingolipides sont constitués d'un alcool aliphatique aminé, produit *de novo* à partir de la sérine et d'une acyl-coenzyme A à longue chaîne, et convertie entre autres en céramides, phosphosphingolipides, glycosphingolipides.

« *Glycolipide* »

Un glycolipide est un saccharide relié, préférentiellement par un groupement phosphate, à un lipide.

« *Polymérisation in situ* »

Par l'expression « polymérisation *in situ* », il est compris selon la présente invention que la polymérisation se fait après injection dans un organisme vivant, tel qu'un être humain.

Ceci est réalisable lorsque les conditions de la polymérisation sont celles du milieu physiologique de l'organisme vivant en question (pH, température, eau, tampon, etc). L'introduction du précurseur non polymérisé dans l'organisme vivant peut s'effectuer simplement en faisant couler ce précurseur sur ou dans l'organisme vivant, si celui-ci a été ouvert au préalable à l'aide d'instruments chirurgicaux. Alternativement, le précurseur de l'hydrogel peut être introduit dans l'organisme vivant en l'injectant à l'aide d'une seringue et d'une aiguille creuse adaptées. Le précurseur de l'hydrogel polymérise alors une fois en contact avec ledit organisme vivant. De manière avantageuse selon la présente invention, l'injection est peu douloureuse, car le précurseur peut être choisi pour être très fluide et donc, le moyen d'injection (seringue et surtout diamètre de l'aiguille) peut être de taille réduite favorisant son introduction dans l'organisme vivant de manière peu douloureuse. En outre, le liquide à injecter étant moins visqueux que si l'hydrogel a déjà été formé au préalable, le liquide une fois injecté prend beaucoup plus facilement sa place, sans distordre les tissus avoisinants, résultant en une injection moins douloureuse.

15 Description détaillée

Les caractéristiques physico-chimiques exceptionnelles des hydrogels selon la présente invention permettent des applications pharmaceutiques et biomédicales, notamment dans l'administration de médicaments (dans des nanosphères ou nanocapsules, par voie orale ou voie transdermique...). Les hydrogels selon la présente invention peuvent également être utilisés dans la lutte contre les brûlures cutanées. Ils peuvent aussi être utilisés pour une large gamme d'applications dans les essais cliniques de la médecine expérimentale comprenant : l'ingénierie tissulaire et la médecine de la régénération, le diagnostic, l'immobilisation cellulaire, la séparation de biomolécules ou de cellules, l'utilisation de matériaux "barrière" pour régler les adhérences biologiques.

25 Ainsi l'objet de la présente invention concerne un procédé de fabrication d'hydrogels tel que défini présentement caractérisé en ce que le groupement A de la formule (I) de l'hydrogel tel que défini est choisi parmi les protéines, les peptides tels que des séquences peptidiques issues des collagènes par exemple les séquences comprenant des répétitions de tripeptides Pro-Hyp-Gly ou Pro-Pro-Gly ou Asp-Pro-Gly ou Pro-Lys-Gly, des séquences peptidiques d'autoassemblage comme Arg-Ala-Asp-Ala (Seq ID 4), des oligoprolines, des oligoalanines, des polysaccharides, tels que l'acide hyaluronique* et ses dérivés, des oligonucléotides, des polymères de C₁-C₆-alkylènes-glycols, ou de polyvinylpyrrolidone.

* L'acide hyaluronique peut être utilisé pour ses propriétés structurantes et/ou pour ses activités biologiques.

L'objet de la présente invention concerne en outre un procédé de fabrication d'un hydrogel tel que défini ci-dessus, caractérisé en ce que le groupement B de la formule (II) de l'hydrogel tel que défini présentement est une biomolécule choisie parmi un peptide, un oligopeptide, une protéine, telle que le collagène, un acide désoxyribonucléique, un acide ribonucléique, un polysaccharide, tel qu'une pectine, un chitosane, un acide hyaluronique, un polysaccharide polyarabinose et polygalactose et un glycolipide.

De manière préférée, le fragment B de la formule (II), est un agent antimicrobien, antibiotique et/ou antifongique listés plus haut. De manière plus préférée le fragment B de la formule (II), est plus particulièrement un peptide antimicrobien choisi parmi les amphipathiques, les cationiques, la daptomycine, la polymyxine, la tachyplésine, la magainine, les défensines, les cathélicidines, les histatines, les cécropines, la mellitine, la temporines, les bombinines.

L'objet de la présente invention concerne de plus un procédé de fabrication d'un hydrogel tel que défini ci-dessus, caractérisé en ce que le procédé de polymérisation sol-gel est effectuée à pH physiologique, c'est-à-dire à un pH compris entre pH 6 et 9, préférentiellement entre pH 7 et 8, et encore plus préférentiellement à pH $7,4 \pm 0,1$, ou en ce que l'hydrogel est formé en présence d'une quantité suffisante d'eau pour que la teneur en eau de l'hydrogel soit d'au moins 50% en poids vis-à-vis du poids total de l'hydrogel formé.

L'objet de la présente invention concerne d'ailleurs un procédé de fabrication d'un hydrogel tel que défini ci-dessus, caractérisé en ce que l'hydrogel est formé en présence d'une quantité suffisante d'eau pour que la teneur en eau de l'hydrogel soit d'au moins 50% en poids vis-à-vis du poids total de l'hydrogel formé. De manière avantageuse, l'hydrogel selon la présente invention peut contenir entre 60 et 99% en poids d'eau vis-à-vis du poids total de l'hydrogel formé selon la présente invention, de manière plus avantageuse l'hydrogel selon la présente invention peut contenir entre 70 et 98% en poids d'eau et de manière encore plus avantageuse l'hydrogel selon la présente invention peut contenir entre 75 et 97%, voire entre 80 et 95% en poids d'eau vis-à-vis du poids total de l'hydrogel formé.

L'objet de la présente invention concerne également un procédé de fabrication d'un hydrogel tel que défini ci-dessus, caractérisé en ce que ledit hydrogel est polymérisé sur ou dans au moins un premier hydrogel en tant que support, résultant ainsi en un hydrogel multicouches. Toute technique connue de l'homme du métier afin d'obtenir un multicouche est applicable en l'espèce. De manière simple, un premier hydrogel peut être

coulé dans un fond de moule, puis un second hydrogel coulé sur ce premier hydrogel et ainsi de suite. En outre, les hydrogels selon la présente invention pouvant être découpés et façonnés à volonté, ce découpage peut avoir lieu avant la coulée d'un hydrogel supplémentaire sur un premier hydrogel ou multicouche découpé/façonné.

- 5 L'objet de la présente invention concerne en outre un hydrogel pour son utilisation à des fins thérapeutiques et/ou chirurgicales, telle que décrite ci-dessus, caractérisé en ce qu'il permet la délivrance et/ou le transport de molécules actives, ou pour son utilisation *in vivo* en ingénierie tissulaire.

Figures

- 10 Figure 1 : cette figure concerne des essais de cytotoxicité sur des fibroblastes L929. Le témoin « TC-PS » (colonne « témoins bas » dans la figure) représente la viabilité cellulaire sur TC-PS (i.e. sans hydrogel). Le témoin « cellules lysées » (colonne « témoins haut » dans la figure) correspond à la lyse complète des cellules et donc à un maximum de toxicité. Le témoin « PLA-50 » permet de vérifier la viabilité cellulaire en présence de poly (acide lactique). L'échantillon « hydrogel PEG silylé 2,5% NaF » concerne les cellules incubées 24 h en présence d'un hydrogel contenant 10% en masse de PEG silylé obtenu avec 2,5% en poids de NaF. L'échantillon « hydrogel PEG silylé 0,3% NaF » concerne les cellules incubées 24 h en présence d'un hydrogel contenant 10% en masse de PEG silylé obtenu avec 0,3% en poids de NaF.

- 20 Figure 2 : cette figure concerne des essais pour quantifier le relargage de fluorescéine à partir de différents hydrogels selon l'invention. Les hydrogels greffés par de la fluorescéine par liaison covalente affichent des taux de relargage bien moindres que l'hydrogel contenant de la fluorescéine simplement emprisonnée sans liaison covalente.

- Figure 3 : cette figure concerne des essais d'adhésion cellulaire sur les hydrogels selon la présente invention. Deux contrôles ont été choisis pour comparaison : l'un indique les valeurs mesurées de fluorescence du milieu de culture en l'absence de cellules et l'autre est la fluorescence mesurée pour les cellules déposées directement sur TC-PS. Sur cette base comparative, trois séries d'essais ont été réalisées avec des hydrogels de PEG silylé selon l'invention à 10% en masse de PEG silylé nus, puis avec 7,5% molaire ou 15 % molaire (par rapport au nombre de moles de PEG silylé) d'un peptide permettant l'adhésion cellulaire (« RGD ») lié par liaison covalente audit hydrogel.

Légende figure 3:

- Colonnes (de l'histogramme) en blanc (i.e. les 1^{ères} colonnes en partant de la gauche de l'histogramme): milieu de culture en absence de cellules ;
- Colonnes en gris clair (i.e. les 2^{èmes} colonnes en partant de la gauche de l'histogramme): cellules déposées sur hydrogel de PEG nu ;
- 5 • Colonnes en gris moyen (i.e. les 3^{èmes} colonnes en partant de la gauche de l'histogramme): cellules déposées sur hydrogel de PEG contenant 7.5% de peptide hybride RGD ;
- 10 • Colonnes en gris foncé (i.e. les 4^{èmes} colonnes en partant de la gauche de l'histogramme): cellules déposées sur hydrogel de PEG contenant 15% de peptide hybride RGD ;
- Colonnes en noir (i.e. les 5^{èmes} colonnes en partant de la gauche de l'histogramme): cellules déposées sur TCPS.

Figure 4 : cette figure concerne des essais antibactériens avec des hydrogels selon la présente invention. Les bactéries ayant fait l'objet du test sont *E. coli*, *S. aureus* et *P. aeruginosa*. Deux essais témoins ont été réalisés : l'un étant une évaluation du nombre de colonies bactériennes sur gel d'agar simple, l'autre sur l'hydrogel PEG silylé nu selon la présente invention (i.e. un hydrogel de PEG silylé à 10% en masse de PEG silylé). Un peptide antibactérien a été greffé sur ce même gel (i.e. hydrogel PEG nu) par liaisons covalentes à différents taux (7,5% en moles de peptide antibactérien et 15% en moles de peptide antibactérien par rapport au nombre de moles de PEG silylé). Les colonies bactériennes qui se sont formées au contact des gels sont comptées après 24 h d'incubation à 37°C.

Légende figure 4:

- Colonnes (de l'histogramme) en noir (i.e. les 1^{ères} colonnes en partant de la gauche de l'histogramme): coloniesensemencées sur Agar ;
- 25 • Colonnes en blanc (i.e. les 2^{èmes} colonnes en partant de la gauche de l'histogramme): coloniesensemencées sur hydrogel PEG nu ;
- Colonnes en gris clair (i.e. les 3^{èmes} colonnes en partant de la gauche de l'histogramme): coloniesensemencées sur hydrogel PEG avec 7.5% de peptide hybride antibactérien ;
- 30 • Colonnes en gris foncé (i.e. les 4^{èmes} colonnes en partant de la gauche de l'histogramme): coloniesensemencées sur hydrogel PEG avec 15% de peptide hybride antibactérien.

Exemples

Les exemples ci-dessous ne limitent en rien la portée de la protection convoitée et sont là à titre d'illustration selon la présente invention.

Abréviations

- 5 ACN, acétonitrile ; Ahx, acide ϵ -aminohexanoïque ; Boc, t-Butyloxycarbonyl ; DCM, dichlorométhane ; DIEA, diisopropyléthylamine ; DMF, N-N'-diméthylformamide ; DPBS, Dulbelcco's phosphate buffered saline ; ESI-MS, spectrométrie de masse avec ionisation électrospray ; Fmoc, fluorénylméthoxycarbonyl ; HBTU, N,N,N',N'-tétraméthyl-O-(1H-benzotriazol-1-yl)uronium hexafluorophosphate ; HPLC, chromatographie liquide haute
10 performance ; HRMS, spectrométrie de masse haute résolution ; LC/MS, spectrométrie de masse couplée à la chromatographie liquide ; Pbf, 2,2,4,6,7-pentaméthyl-dihydrobenzofuran-5-sulfonyl ; PEG, polyéthylène glycol ; pip, pipéridine ; PS, polystyrène ; RMN, résonance magnétique nucléaire ; TA, température ambiante , c'est-à-dire compris entre 20 et 25°C ; TFA, acide trifluoroacétique ; THF, tétrahydrofurane ; TIS,
15 triisopropylsilane.

Matériel et méthodes

Les HPLC analytiques ont été réalisées sur un appareil Agilent Infinity 1260 équipé d'une barette de diode et d'une colonne Kinetex C18 phase inverse, 2,6 μ m, 50 x 4.6 mm avec un gradient de 0% à 90% (% en volume) de B en 5 min avec éluant A : eau/0.1% TFA et éluant B
20 : ACN/0.1% TFA à un débit de 2,5 mL/min.

Les purifications par HPLC préparative ont été réalisées sur un appareil Waters HPLC 4000, équipé d'un détecteur UV 486 et d'une colonne en phase inverse C₁₈ Waters Delta-Pack 40x100 mm, 100 Å, 15 μ m, à un débit de 50 mL/min. Les solvants utilisés sont H₂O/0.1% TFA et ACN/0.1% TFA.

25 Les échantillons pour les analyses LC/MS ont été préparés dans un mélange eau/ACN (50:50, v/v) contenant 0.1% TFA. L'appareillage LC/MS est constitué d'une HPLC Waters Alliance 2695, couplée à un spectromètre Water Micromass ZQ (ionisation électrospray, mode positif). Les analyses ont été réalisées avec une colonne phase inverse Phenomenex Onyx, 25 x 4.6 mm à un débit de 3 mL/min avec un gradient de 0 à 100% (% en volume) de
30 B en 2,5 min avec éluant A : eau/0.1% HCO₂H ; éluant B : ACN/0.1% HCO₂H. La détection UV a été faite à 214 nm. Les spectres de masse ont été acquis avec un débit de solvant de 200 μ L/min. L'azote est utilisé comme gaz nébulisant et séchant. Les données sont obtenues en scannant les m/z de 100 à 1000 en 0,75 secondes ou de 200 à 1600 en 0,9

secondes. Les analyses de spectrométrie de masse haute résolution ont été réalisées en mode positif sur un spectromètre temps de vol (TOF) équipé d'une source d'ionisation électrospray.

Les spectres RMN ^1H , ^{13}C et ^{29}Si ont été enregistrés à température ambiante (TA) dans des solvants deutérés sur un spectromètre à 400, 101 et 79 MHz respectivement. Les déplacements chimiques (δ) sont donnés en parties par million en utilisant les solvants non deutérés résiduels comme références (CHCl_3 dans CDCl_3 , $\delta\text{H} = 7.26$ ppm; DMSO-d_6 , $\delta\text{H} = 2.50$ ppm). Les signaux sont notés s (singulet), d (doublet), t (triplet), q (quadruplet), dt (triplet dédoublé), m (multiplet)... Les constantes de couplage sont mesurées en Hertz.

10 **Accrochage d'un acide aminé sur la résine 2-chlorochlorotriyle :**

La résine 2-chlorochlorotriyle (1,44 mmol Cl/g, 1 éq) est placée dans un réacteur de synthèse peptidique en phase solide équipé d'un fritté. L'acide aminé protégé Fmoc-AA-OH (3 éq) est couplé sur la résine en présence de DIEA (5 éq) dans le DMF pendant une nuit. Après les lavages standards (3×DMF, 1×MeOH et 1×DCM), la résine Fmoc-AA-Cltrityle est séchée sous vide pendant 12 h. La charge de la résine est déterminée par détection à 299 nm de l'adduit pipéridine-dibenzofulvène qui se forme dans la solution de déprotection pip/DMF (20/80 v/v).

Déprotection du Fmoc :

La résine Fmoc-Rink Amide AM PS ou Fmoc-peptidyl-résine est placée dans un réacteur de phase solide muni d'un fritté. Le groupement Fmoc est retiré par deux traitements successifs avec une solution de DMF-pipéridine (80:20; v/v, 2 x 20 min). Entre les deux traitements, la solution est filtrée et remplacée par une solution fraîche. Les étapes classiques de lavage sont réalisées en fin de déprotection (3×DMF, 1×MeOH et 1×DCM).

Couplage d'un amino acide :

25 L'acide aminé protégé en N-ter par un groupement Fmoc (3 éq) est dissous dans le DMF (10 mL par g de résine) en présence d'HBTU (3 éq) et de DIEA (3 éq) pendant 10 min. Cette solution est ajoutée sur la peptidyl-résine dont le N-ter est libre. La résine est agitée à TA pendant 1h30 puis lavée (3×DMF, 1×MeOH et 1×DCM).

Exemple 1 : Silylation de PEG

30 Du polyéthylène glycol de masse moléculaire moyenne 2000 g/mol (2,00 g, 1,00 mmol) est séché sous vide à 80°C pendant une nuit puis il est dissous dans du THF anhydre (12 mL) sous argon. De la triéthylamine (1,66 mL, 12 mmol, 12 éq) et l'isocyanatopropyl-triéthoxysilane (744 μL , 3 mmol, 3 éq) sont ajoutés. Le mélange est chauffé à reflux pendant 48 h puis concentré sous pression réduite. Le PEG bi-silylé est alors précipité dans

l'hexane. Après centrifugation, il est lavé 3 fois à l'hexane et séché sous vide. Il est obtenu sous forme d'une poudre blanche stockée à 4°C sous argon. ¹H RMN (400 MHz, CDCl₃) δ 5.00 (sl, 2H, NH), 4.18 (t, J = 4.7 Hz, 4H, H-6), 3.79 (q, J = 7.0 Hz, 12H, H-2), 3.62 (s, 177H, CH₂ PEG), 3.14 (dd, J = 13.2, 6.7 Hz, 4H, H-5), 1.58 (qu, J = 7.7 Hz, 4H, H-4), 1.20 (t, J = 7.0 Hz, 18H, H-1), 0.64 - 0.54 (m, 4H, H-3). ¹³C RMN (101 MHz, CDCl₃) δ 156.72 (C), 70.55 (CH₂), 63.76 (CH₂), 58.26 (CH₂), 43.29 (CH₂), 23.12 (CH₂), 18.38 (CH₃), 9.12 (CH₂). ²⁹Si RMN (79 MHz, CDCl₃) δ -45.73 (s).

Exemple 2 : Synthèse d'un peptide dérivé du collagène et bi-silylé

Préparation du tripeptide : Fmoc-Pro-Hyp-Gly-OBzl

10 **Couplage de Boc-Hyp-OH :**

Dans un ballon monocol de 5000 mL sont introduits H-Gly-OBzl.HCl (11,42 g, 56,6 mmol, 1 éq) dissous dans AcN et de la DIEA (37,44 mL, 226,5 mmol, 4 éq). Dans un bécher, Boc-Hyp-OH (13,3 g, 56,6 mmol) est dissous dans AcN. La DIEA ainsi que le pyBOP (29,3 g, 56,63 mmol, 1 éq) sont ajoutés à cette solution. Les deux acides aminés sont mis en contact et agités à TA pendant 4h. Le suivi de la réaction est effectué par HPLC analytique.

Une fois la réaction terminée, AcN est évaporé et l'huile orangée obtenue est solubilisée dans de l'acétate d'éthyle. Cette solution est lavée par des solutions aqueuses de KHSO₄, NaHCO₃ et NaCl. La phase organique est ensuite séchée avec MgSO₄ et le solvant évaporé sous pression réduite.

20 **Déprotection N-ter du dipeptide :**

Le produit est mis ensuite en solution dans 150 ml de TFA pendant 40 min jusqu'à disparition complète de dégagement gazeux. Le TFA est alors évaporé sous pression réduite et le dipeptide est précipité dans l'éther diéthylique puis lyophilisé.

Couplage de Fmoc-Pro-OH :

25 Fmoc-Pro-OH est couplé sur H-Hyp-Gly-OBzl selon le même protocole que le couplage de Boc-Hyp-OH décrit ci-dessus. La réaction dure 2 h. A l'issue des lavages, le tripeptide est purifié sur gel de silice (appareil Biotage, colonne SNAP 340 g, gradient de 0% de MeOH dans le DCM à 10% de MeOH dans le DCM, sortie du produit à 50 % du gradient, rendement 71%).

30 **Déprotection C-ter :**

Dans un ballon monocol de 250 mL sont introduits Fmoc-Pro-Hyp-Gly-OBzl (20,4 g, 40,2 mmol) dissous dans EtOH et 200 mg de Pd/C. Le tout est mis sous bullage d'hydrogène pendant 6h à 60°C. Le suivi de la réaction est effectué par HPLC analytique. Une fois la réaction terminée, la solution est filtrée sur célite puis concentrée sous pression réduite.

35 Le solide est repris dans H₂O/AcN 50/50 V/V et lyophilisé (Rendement : 86%).

Synthèse du peptide Ac-Lys-(Pro-Hyp-Gly)₃-Lys-NH₂ (Seq ID 5) sur support à partir du bloc tripeptidique

La synthèse s'effectue dans une seringue munie d'un fritté sur une résine Rink Amide PS dont la charge est de 0,94 mmol/g avec une échelle de synthèse de 1 mmol. La résine est gonflée dans le DCM puis lavée au DMF. Elle est déprotégée grâce à deux traitements avec la solution de déprotection pip/DMF (15 mL pendant 5 min, 3 lavages au DMF, 15 mL pendant 20 min puis lavages (3×DMF, 3×DCM, 1×DMF)). Les conditions de couplage habituelles sont légèrement modifiées. Les couplages sont allongés à 2 h et se font avec 1,5 éq de Fmoc-Lys(Boc)-OH ou Fmoc-(Pro-Hyp-Gly)₃-OH, 5 éq de DIEA et 1,5 éq d'HATU qui remplace l'HBTU. En fin de couplage, la résine est lavée avec les solvants suivants : (3×DMF, 3×DCM, 1×DMF). Le dernier couplage est lui aussi suivi d'une déprotection du groupement Fmoc. Puis la peptidyl-résine est acétylée avec de l'acide acétique (2 éq) dans le DCM (10 mL) en présence de BOP (2 éq) et de DIEA (4 éq) pendant 1h30. La résine est lavée puis clivée dans un mélange TFA/TIS/H₂O (95/2,5/2,5 v/v/v, 50 ml). La solution de "clivage" est concentrée sous pression réduite et le peptide est précipité à l'éther. Après centrifugation et élimination du surnageant, le peptide brut est repris dans un mélange eau/ACN et lyophilisé. Il est enfin purifié par HPLC préparative sur une colonne Luna C₁₈ phase inverse (15 µm, 250 x 50 mm) à un débit de 120 mL/min avec un gradient de 0 à 6% de B en 6 min, de 6% à 10% de B en 8 min et de 10% à 18% en 24 min avec éluant A : H₂O/0,1% TFA et éluant B : ACN/0,1% TFA. Rendement : 49% ; pureté > 99%. LC/MS (ESI⁺): t_R = 0.73 min, 1118 ([M+H]⁺, 5%), 559 ([M+2H]²⁺, 100).

Silylation

Ac-Lys-(Pro-Hyp-Gly)₃-Lys-NH₂ (20 mg, 14,9 µmol) est dissous dans le diméthylformamide anhydre (300 µL) sous argon. La diisopropyléthylamine (12,4 µL, 71,3 µmol, 4,8 éq) puis le 3-isocyanatopropyltriéthoxysilane (9,7 µL, 39,3 µmol, 2,6 éq) sont ajoutés à la solution de nonapeptide. Le mélange réactionnel est laissé 50 min sous agitation. La fin de la réaction est contrôlée par LC/MS. Le solvant est évaporé sous pression réduite. Puis le nonapeptide silylé est précipité à l'éther diéthylique. Après centrifugation, le peptide hybride est lavé à 3 reprises à l'éther diéthylique puis la poudre obtenue est séchée sous vide. LC/MS (ESI⁺): t_R = 0.82 min, 704 ([M+2H-2H₂O]²⁺, 100%), 695 ([M+2H-3H₂O]²⁺, 80) et t_R = 0.87 min (conformère), 704 ([M+2H-2H₂O]²⁺, 70%), 695 ([M+2H-3H₂O]²⁺, 100).

Exemple 3 : Préparation d'un hydrogel constitué d'une molécule de formule (I)

Une molécule de formule (I), par exemple le PEG bi-silylé préparé dans l'exemple 1 ou le peptide bi-silylé dérivé du collagène synthétisé dans l'exemple 2, est dissous dans du tampon phosphate à pH 7,4 (DPBS Dulbecco's phosphate buffered saline), de préférence à une concentration de 10 % en masse, en présence de fluorure de sodium (3 mg de NaF par

mL de DPBS). La solution non visqueuse est incubée à 37°C, il se forme alors un gel. Le temps de gélification dépend de la nature de la molécule de formule (I) et de sa concentration.

Exemple 4 : Synthèse du peptide silylé (EtO)₃Si-(CH₂)₃-NHCO-(BAla)₄-Gly-Arg-Gly-Asp-Ser-Pro-OH (Seq ID 6)

H-(BAla)₄-Gly-Arg-Gly-Asp-Ser-Pro-OH (Seq ID 6) est synthétisé sur une résine 2-chlorochlorotriyle (charge : 1,44 mmol/g, échelle de synthèse : 0,5 mmol) en stratégie Fmoc/tBu. Les acides aminés utilisés sont successivement Fmoc-Pro-OH, Fmoc-Ser(tBu)-OH, Fmoc-Asp-(tBu)-OH, Fmoc-Gly-OH, Fmoc-Arg(Pbf)-OH, Fmoc-Gly-OH et Fmoc-BAla-OH quatre fois. Chaque couplage d'acide aminé est suivi d'une déprotection du groupement Fmoc en N-ter. Le "clivage" du peptide et la déprotection des chaînes latérales sont effectués dans un mélange TFA/TIS/H₂O 95/2.5/2.5 V/V/V pendant 4 h. Après précipitation, le peptide est purifié par HPLC préparative sur une colonne C₁₈. Il est obtenu après lyophilisation avec un rendement de 63%. Il est ensuite silylé par réaction avec le 3-isocyanatopropyltriéthoxysilane (1,1 éq) dans le DMF à une concentration de 30 mM en présence de DIEA (3 éq). La réaction est suivie par HPLC analytique. Le DMF est ensuite évaporé sous pression réduite et le peptide silylé est précipité dans l'éther diéthylique. Il est récupéré par centrifugation à l'issue de 3 lavages dans l'éther diéthylique.

¹H RMN (400 MHz, DMSO-d₆) δ 8.61 - 8.40 (m, 2H, NH Asp et Gly), 8.21 - 8.04 (m, 2H, NH Gly N-ter et Arg), 7.99 - 7.78 (m, 3H, NH BAla), 7.58 - 7.42 (m, 1H, NH Ser), 7.34 - 6.98(m, 3H, OH Ser, COOH Asp et C-ter), 5.97 (t, J = 5.6 Hz, 1H, NH urée), 5.78 (t, J = 5.6 Hz, 1H, NH urée BAla), 4.56 (q, J = 6.9 Hz, 1H, H_α Ser), 4.49 - 4.38 (m, 1H, H_α Asp), 4.38 - 4.26 (m, 1H, H_α Arg), 4.22 (dd, J = 8.7, 4.1 Hz, 1H, H_α Pro), 4.02 - 3.75 (m, 4H, H_α Gly), 3.73 (q, J = 6.9 Hz, 6H, CH₂ éthoxy), 3.67 - 3.46 (m, 4H, H_δ Pro et HB Ser), 3.46 - 3.28 (m, 2H, H_δ Arg), 3.28 - 3.11 (m, 8H, HB BAla), 2.92 (q, J = 6.1 Hz, 2H, H-3), 2.60 - 2.48 (m, 2H, HB Asp), 2.29 (t, J = 7.1 Hz, 2H, H_α BAla), 2.26 - 2.09 (m, 6H, H_α BAla), 1.87 (dd, J = 13.3, 6.5 Hz, 2H, H_γ Pro), 1.60 - 1.56 (m, 2H, HB Arg), 1.55 - 1.42 (m, 2H, H_δ Arg), 1.38 (m, 2H, H-2), 1.19 - 1.09 (t, J = 7.2 Hz, 9H, CH₃ éthoxy), 0.55 - 0.42 (m, 2H, H-1). ¹³C RMN (101 MHz, DMSO-d₆) δ 174.27 (C), 172.82 (C), 171.38 (C), 171.27 (C), 171.14 (C), 170.86 (C), 170.80 (C), 169.58 (C), 169.43 (C), 169.02 (C), 168.77 (C), 158.41 (C), 157.52 (C), 62.14 (CH₂), 59.54 (CH), 58.14 (CH₂), 53.51 (CH), 52.60 (CH), 49.78 (CH), 47.02 (CH₂), 42.46 (CH₂), 42.36 (CH₂), 40.89 (CH₂), 36.68 (CH₂), 36.30 (CH₂), 35.88 (CH₂), 35.76 (CH₂), 30.10 (CH₂), 29.13 (CH₂), 25.39 (CH₂), 24.91 (CH₂), 24.01 (CH₂), 18.68 (CH₃), 7.72 (CH₂). ²⁹Si RMN (79 MHz, DMSO-d₆) δ -45.10. LC/MS (ESI⁺): Seuls les produits d'hydrolyse des groupements éthoxysilanes en silanols sont détectés. t_R = 0.62 min, 1035 ([M+H]⁺, 50%), 509 ([M+H-OH]²⁺, 60), 500 ([M-2OH]²⁺, 100). HRMS: 1119.5481. C₄₅H₇₄N₁₈O₁₄Si implique [M+H]⁺, 1119.5479.

Exemple 5 : Synthèse du peptide silylé HO(CH₃)₂Si-(CH₂)₃-NHCO-Ahx-Arg-Arg-NH₂

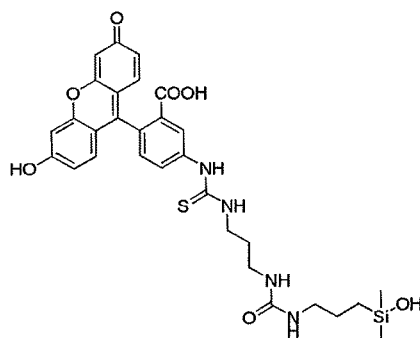
Le peptide antibactérien H-Ahx-Arg-Arg-NH₂ est synthétisé sur une résine Rink Amide (charge 0,94 mmol/g, échelle de synthèse : 3 mmol) en stratégie Fmoc/tBu. Les acides aminés utilisés sont successivement Fmoc-Arg(Pbf)-OH deux fois et l'acide Fmoc-ε-aminohexanoïque. Chaque couplage est suivi d'une déprotection du groupement Fmoc en N-ter. Le tripeptide est ensuite silylé sur support dans le DMF (10 mL/g de résine) en utilisant le 3-isocyanatopropyldiméthylchlorosilane (3 éq) en présence de DIEA (3 éq). La réaction de silylation est laissée sous agitation pendant une nuit puis la résine est lavée (3×DMF, 1×MeOH et 1×DCM) et clivée dans le TFA pendant 5 h. La solution de « clivage » est concentrée sous pression réduite puis le peptide antibactérien silylé est précipité dans l'éther diéthylique et enfin purifié par HPLC préparative sur une colonne C₁₈ (Eluant A : H₂O/0,1% TFA, éluant B : ACN/0,1% TFA, gradient : de 0 à 7% de B en 2 min puis de 7% à 30% de B en 23 min, sortie du produit à 16% de B). Après lyophilisation, le peptide antibactérien silylé est obtenu sous forme d'une poudre blanche (Rendement : 68%, pureté > 98%).

¹H RMN (400 MHz, D₂O) δ 4.19 (ddd, J = 14.4, 8.6, 5.7 Hz, 2H, H_α Arg), 3.09 (t, J = 6.9 Hz, 4H, H_δ Arg), 2.96 (td, J = 6.8, 1.9 Hz, 4H, H-3 et H-4), 2.17 (t, J = 7.3 Hz, 2H, H-8), 1.82 - 1.59 (m, 4H, H_B Arg), 1.59 - 1.44 (m, 6H, H-7 et H_γ Arg), 1.41 - 1.31 (m, 4H, H-2 et H-5), 1.24 - 1.12 (m, 2H, H-6), 0.53 - 0.41 (m, 2H, H-1), 0.00 (s, 6H, Si(CH₃)₂).

¹³C RMN (101 MHz, DMSO-d₆) δ 172.40 (C), 171.76 (C), 170.69 (C), 157.38 (C), 156.00 (C), 51.38 (CH), 51.02 (CH), 41.54 (CH₂), 34.28 (CH₂), 29.01 (CH₂), 28.34 (CH₂), 28.08 (CH₂), 25.24 (CH₂), 24.24 (CH₂), 23.16 (CH₂), 14.24 (CH₂), -0.51 (CH₃).

²⁹Si RMN (79 MHz, DMSO-d₆) δ 7.97 (dimère). LC/MS (ESI⁺): t_R = 0.71 min, 602 ([M+H]⁺, 10%), 302 ([M+2H]²⁺, 100), 293 ([M+2H-NH₃]²⁺, 30). HRMS: 602.3926. C₂₄H₅₁N₁₁O₅Si implique [M+H]⁺, 602.3922.

Exemple 6 : Synthèse d'une hydroxydiméthylsilyl fluorescéine



25

La N-Boc-1,3-propanediamine (56,4 mg, 0,324 mmol, 1,05 éq) est ajoutée à une solution de fluorescéine isothiocyanate (FITC, 120 mg, 0,308 mmol) dans le DMF anhydre (3 mL) en présence de DIEA (100 µL). Le mélange réactionnel est agité pendant 1 h à TA sous argon.

Puis le DMF est évaporé sous pression réduite. La Boc-amino fluorescéine est précipitée et lavée dans l'éther diéthylique puis séchée. Elle est ensuite solubilisée dans le TFA (4 mL) et cette solution est agitée pendant 1 h. Le mélange réactionnel est concentré et précipité dans l'éther diéthylique. Après centrifugation, le surnageant est retiré. La fluorescéine amine est purifiée par HPLC préparative sur une colonne C₁₈ (Eluant A : H₂O/0,1% TFA, éluant B : ACN/0,1% TFA, gradient : de 0 à 15% de l'éluant B en 3 min puis de 15% à 40% de l'éluant B en 25 min, sortie du produit à 22% de l'éluant B) et obtenue sous forme de sel de TFA (180 mg, 100%, pureté = 95%).

Le 3-isocyanatopropylchlorodiméthylsilane (16,2 µL, 0,0910 mmol, 1,05 éq) est ajouté à une solution de fluorescéine amine purifiée précédemment (50,0 mg, 0,0867 mmol) dans le DMF anhydre (2 mL) en présence de DIEA (45,2 µL, 0,260 mmol, 3 éq). Le mélange réactionnel est agité sous argon pendant 1 h. Le solvant est évaporé sous pression réduite et le produit brut est obtenu par précipitation dans l'éther diéthylique. La hydroxydiméthylsilyl fluorescéine est purifiée par HPLC préparative sur une colonne C₁₈ (Eluant A : H₂O/0,1% TFA, éluant B : ACN/0,1% TFA, gradient : de 0 à 20% de l'éluant B en 4 min, de 20 à 26% de l'éluant B en 6 min puis de 26% à 46% de l'éluant B en 30 min, sortie du produit à 32% de l'éluant B, rendement : 42%, pureté : 97%) ¹H RMN (400 MHz, DMSO-d₆) δ 10.01 (sl, 1H, COOH), 9.97 (s, 1H, NH thiourée provenant de la FITC), 8.20 (s, 1H, H-4), 8.12 (s, 1H, NH thiourée), 7.71 (d, J = 7.6 Hz, 1H, H-6), 7.14 (d, J = 8.3 Hz, 1H, H-5), 6.65 (d, J = 2.2 Hz, 2H, H-9 et H-10), 6.59 - 6.51 (m, 4H, H-7, H-8, H-11 et H-12), 5.88 (s br, 2H, NH urée), 3.43 - 3.38 (m, 2H, H-3), 3.03 (t, J = 6.5 Hz, 2H, H-1), 2.92 (t, J = 6.9 Hz, 2H, H-3'), 1.62 (qu, J = 6.5 Hz, 2H, H-2), 1.37 - 1.29 (m, 2H, H-2'), 0.47 - 0.36 (m, 2H, H-1'), 0.00 et -0.04 (2 s, 6H, H-4' du dimère et du monomère respectivement). ¹³C RMN (101 MHz, DMSO-d₆) δ 179.51 (C), 167.65 (C), 158.62 (C), 157.51 (C), 151.02 (C), 140.47 (C), 128.75 (CH), 128.19 (CH), 125.68 (C), 123.18 (CH), 116.66 (C), 115.79 (CH), 114.24 (C), 111.71 (CH), 108.87 (C), 101.36 (CH), 41.55 (CH₂), 40.52 (CH₂), 35.85 (CH₂), 28.80 (CH₂), 23.13 (CH₂), 14.20 (CH₂), -0.51 (CH₃), -0.75 (CH₃). ²⁹Si RMN (79 MHz, DMSO-d₆) δ 11.24 (monomère), 7.99 (dimère). LC/MS (ESI⁺): t_R = 1.33 min, 623 ([M+H]⁺, 60%), 390 ([M+H-NH₂(CH₂)₃NH-CONH(CH₂)₃Si(CH₃)₂OH]⁺, 15), 312 ([M+2H]²⁺, 60), 303 ([M+2H-H₂O]²⁺, 100). HRMS: 623.1996. C₃₀H₃₄N₄O₇SSi implique [M+H]⁺, 623,1996.

Exemple 7 : Préparation d'hydrogels comportant une molécule de formule (I) et une molécule de formule (II)

Une molécule de formule (I), par exemple le PEG bi-silylé préparé dans l'exemple 1 ou le peptide bi-silylé dérivé du collagène synthétisé dans l'exemple 2, est dissous dans du tampon phosphate à pH 7,4 (DPBS Dulbecco's phosphate buffered saline), de préférence à

une concentration de 10 % en masse, en présence de fluorure de sodium (3 mg de NaF par mL de DPBS). Une molécule de formule (II), par exemple le peptide silylé contenant la séquence Arg-Gly-Asp synthétisé dans l'exemple 4 ou le peptide silylé antibactérien préparé dans l'exemple 5 ou la fluorescéine silylée décrite dans l'exemple 6, est ajouté à la solution de molécule de formule (I) à une concentration comprise entre 1% et 15 mol% par rapport à la molécule de formule (I). La solution non visqueuse est incubée à 37°C, il se forme alors un gel. Le temps de gélification dépend de la nature des molécules choisies et de leur concentration.

10 **Exemple 8 : exemples d'applications d'un hydrogel selon l'invention**

- Optimisation de la synthèse

L'unité bi-fonctionnelle $(\text{EtO})_3\text{-Si}-(\text{CH}_2)_3\text{-NHCO}-(\text{PEG}2000)\text{-OCONH}-(\text{CH}_2)_3\text{-Si}-(\text{OEt})_3$ (i.e. « bloc PEG hybride bi-silylé ») a été synthétisée en faisant réagir le polyéthylène glycol (PM = 2000 Da) avec du 3-isocyanatopropyltriéthoxysilane. Ensuite, le bloc PEG hybride bi-silylé a été engagé dans le procédé sol-gel, consistant en l'hydrolyse des éthoxysilyles en silanols et leur condensation pour former des liaisons siloxanes. Ce processus a été réalisé à 37 ° C, à pH 7,2-7,4 dans un tampon phosphate (DPBS). Le fluorure de sodium (NaF) a été utilisé en tant que catalyseur nucléophile pour accélérer les réactions de condensation. Différentes concentrations de PEG hybride bi-silylé et de fluorure de sodium ont été testées démontrant ainsi leur influence sur le temps de gélification (tableau 1) :

Tableau 1 : Temps de gélification de solutions de PEG hybride bi-silylé dans le DPBS à 37°C et modules visco-élastiques des hydrogels obtenus

Composition du gel		Temps de gélification (min)	G' (Pa)	G'' (Pa)
Bloc PEG hybride bi-silylé (% massique)	NaF (% massique)			
20	5.0	10	n. d.	n. d.
20	2.5	15	77 750	204
10	5.0	20	n. d.	n. d.
10	2.5	35	18 960	49
10	0.3	120	9 947	61
5	5.0	50	n. d.	n. d.
5	2.5	220	5413	39

L'effet du rapport PEG/eau et de la concentration en NaF sur les propriétés mécaniques des hydrogels a également été étudié. La réponse viscoélastique des hydrogels a été mesurée en oscillation sur un rhéomètre AR 2000 (TA Instruments, Inc.) avec une géométrie parallèle de 20 mm de diamètre (force normale = 2 N). L'évolution des modules de conservation (G') et de perte (G'') a été suivie en fonction de la fréquence d'oscillation dans le domaine linéaire visco-élastique (0,1 % de déformation, de 0,01 Hz à 10 Hz) pour des gels de compositions différentes. Les valeurs des modules pour une fréquence de 10 Hz sont présentées dans le tableau 1. Tous les échantillons présentent les propriétés d'un solide avec G' supérieur à G'' . Les modules de conservation ont été utilisés comme mesure de l'élasticité des hydrogels. Ils sont restés stables pendant une semaine. S'étendant de 5 000 à 80 000 Pa selon la composition du gel, ils couvrent une large gamme de rigidité. Très peu de variations ont été observées sur les modules de perte pour l'ensemble des échantillons. Ainsi selon l'application visée, la rigidité des gels peut être ajustée en faisant varier les concentrations en PEG hybride bi-silylé et/ou en NaF.

- Tests de cytotoxicité de l'hydrogel nu

Des essais de cytotoxicité ont été effectués sur deux des hydrogels présentés ci-dessus contenant chacun 10% massique de PEG hybride bi-silylé par rapport à la masse de solvant et 0,3% ou 2,5% massique de NaF respectivement.

Des fibroblastes murins de la lignée L929 ont étéensemencés dans des puits en polystyrène traités pour la culture de tissus. Après 24 h de prolifération, ces cellules ont été incubées avec les hydrogels pendant 24 h supplémentaires. La cytotoxicité a ensuite été mesurée à l'aide d'un test mettant en évidence la libération de lactate déshydrogénase par les cellules. Comme prévu, les hydrogels contenant la plus forte concentration de NaF se sont révélés toxiques. Cependant, plus de 80% de la viabilité cellulaire a été observée pour une concentration en NaF de 3 mg / ml, ce qui signifie que ce dernier hydrogel n'est pas toxique pour les cellules (Figure 1).

Ces résultats ont été confirmés par des observations microscopiques qui ont montré des cellules saines fusiformes.

- Vérification de la fonctionnalisation de l'hydrogel

Afin de montrer l'incorporation covalente d'une (bio-)molécule dans le gel et l'absence de relargage dans le temps des molécules greffées, des dérivés de fluorescéine ont été choisis pour être liés chimiquement aux hydrogels conformément à la présente invention (cf. figure 2 pour les formules exactes). Ainsi, s'il devait y avoir un relargage des molécules greffées, l'utilisation de la fluorescéine permettrait de le détecter aisément.

L'isothiocyanate de fluorescéine (FITC) a été utilisé pour préparer deux types de dérivés de fluorescéine donnant des liaisons covalentes (triéthoxysilane et diméthylhydroxysilane),

ainsi qu'une molécule non-silylée servant de témoin/contrôle. Chaque dérivé de la fluorescéine a été dissous à une concentration de 5,2 mM dans une solution de PEG hybride bi-silylé lui-même à une concentration de 10% massique par rapport à la masse de DPBS servant de solvant. Le fluorure de sodium a été ajouté et les solutions ont été
5 homogénéisées. Des hydrogels hybrides fluorescents ont été obtenus à 37 °C en 30 minutes. Les différents hydrogels ont été placés dans du tampon phosphate (10 ml) et la libération de fluorescéine a été contrôlée par HPLC. Dans le cas de l'emprisonnement non-covalent, un relargage complet de fluorescéine a été observé dans les 72h. Comme on s'y attendait, le relargage de fluorescéine est limité (au regard du contrôle) dans le cas des
10 dérivés covalents et atteint un plateau après 72 heures. Ceci indique la stabilité des liaisons covalentes hybrides. Un maximum de 9% et 20% (par rapport à la quantité totale de fluorescéine introduite) de libération a été observé pour les hydrogels obtenus avec la « triéthoxysilylfluorescéine » et la « diméthylhydroxyfluorescéine », respectivement (figure 2). Ce relargage pourrait être attribué à des molécules hybrides piégées de façon
15 non-covalente qui n'auraient pu réagir pendant le processus de gélification. Ceci est cohérent avec le fait que le dérivé triéthoxysilyle devrait être plus réactif que le diméthylhydroxysilyle lors de la réaction de condensation.

- Test d'adhésion cellulaire

Un peptide contenant la séquence RGD a été choisi pour favoriser l'adhérence cellulaire. Il
20 s'agit de la séquence GRGDSP (SEQ ID 7).

Le peptide déprotégé H-GRGDSP-OH (Seq ID 7) a tout d'abord été préparé par synthèse peptidique sur support solide en stratégie Fmoc / tBu et fonctionnalisé par un groupement triéthoxysilyle en utilisant l'ICPTES (3-isocyanatopropyltriéthoxysilane). Une solution de PEG hybride bi-silylé à 10% massique par rapport à la masse de DPBS) contenant 0,3%
25 massique en NaF a été préparée et le peptide hybride GRGDSP silylé a été ajouté à cette solution. La concentration relative en GRGDSP silylé dans le mélange avant réaction a été fixée à 7,5% (1^{ère} solution) et à 15% (2^{ème} solution) en moles par rapport au nombre de moles de PEG hybride bi-silylé. Ces deux solutions ont été placées à 37 ° C pendant une nuit, pour fournir deux hydrogels de « PEG / RGD-silylés ».

30 Des fibroblastes L929 ont étéensemencés à la surface des hydrogels de PEG/RGD-silylés et sur un hydrogel hybride de PEG non fonctionnalisé (« hydrogel nu »). Les cellules adhérentes après 30 min, 1 h et 2 h d'incubation ont été mises en évidence et dosées à l'aide d'un réactif de viabilité « PrestoBlue Cell Viability Reagent ® » (figure 3). Aucune adhésion cellulaire n'a été constatée sur l'hydrogel nu. En revanche, l'adhésion cellulaire a
35 été très efficace dans le cas de l'hydrogel contenant 15% molaire en RGD silylé (solution

2). En effet, l'adhésion sur ce dernier après 30 min d'incubation est meilleure que sur le polystyrène traité pour la culture de tissus (TC-PS), et ce pour des surfaces d'adhésion de taille identique.

5 • Tests antibactériens

De même, des hydrogels avec des propriétés antibactériennes ont été préparés en utilisant la séquence peptidique H-Ahx-Arg-Arg-NH₂ convenablement silylé du côté N-terminal. Pour ce faire, le peptide H-Ahx-Arg(Pbf)-Arg(Pbf)-NH- sur résine rinkamide a été fonctionnalisé à l'extrémité N-terminale par un groupement diméthylhydroxysilyle avant clivage de la
10 résine et déprotection des chaînes latérales. Le peptide hybride résultant a été ajouté à des solutions de PEG hybride bi-silylé selon le protocole décrit précédemment pour l'hydrogel «PEG-RGD silylés». L'activité antibactérienne des hydrogels a été évaluée contre *Escherichia coli*, *Staphylococcus aureus* et *Pseudomonas aeruginosa*. Les hydrogels ont été inoculés en surface avec des bactéries et recouverts de gélose trypticase soja.
15 Après 24 h d'incubation à 37 ° C, les colonies bactériennes ont été comptées (Figure 4). Les hydrogels de PEG « nus » semblent inhiber la croissance de *P. aeruginosa* même en l'absence de peptide. Pour *E. coli* et *S. aureus*, l'effet antibactérien a été apporté par le peptide greffé. En effet, 15 mol% en peptide antibactérien ont induit une inhibition complète de la croissance de *S. aureus* et ont réduit la croissance d'*E. Coli* de 80%.

20 • Conclusion

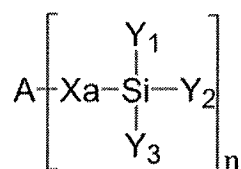
Il a été démontré la facilité de synthèse et d'utilisation des hydrogels selon la présente invention. Ces hydrogels ont été valablement utilisés avec des molécules de structures chimiques diverses prouvant la flexibilité du procédé selon la présente invention. Il a ainsi pu être préparé des hydrogels présentant des propriétés rhéologiques, biologiques et/ou
25 physico-chimiques satisfaisantes avec très peu de variation (voire aucune variation) des conditions opératoires, hormis la nature des molécules greffées.

REVENDEICATIONS

1. Procédé de fabrication d'un hydrogel comprenant les étapes de :

- a) polymérisation sol-gel d'au moins une molécule de formule (I) :

5



Formule (I)

dans laquelle :

- n est un nombre entier supérieur ou égal à 2 ;
- A est un polymère organique de structure, préférentiellement d'origine synthétique pouvant être par exemple choisi parmi les protéines, les peptides tels que des dérivés du collagène, en particulier les séquences comprenant des répétitions de tripeptides Pro-Hyp-Gly ou Pro-Pro-Gly ou Asp-Pro-Gly ou Pro-Lys-Gly, des séquences peptidiques d'autoassemblage comme Arg-Ala-Asp-Ala (SEQ ID 4), des oligoprolines, des oligoalanines, les polysaccharides, tels que l'acide hyaluronique et ses dérivés, les oligonucléotides, des polymères de C₁-C₆-alkylènes-glycols, ou de polyvinylpyrrolidone;
- Xa est une liaison chimique ou un groupement espaceur préférentiellement représenté par un radical divalent dérivé d'une chaîne hydrocarbonée aliphatique saturée ou insaturée comportant de 1 à 10 atomes de carbone, dans laquelle sont éventuellement intercalés, un ou plusieurs chaînons structuraux choisis parmi le groupe arylène, ou les fragments -O-, -S-, -C(=O)-, SO₂ ou -N(R₁)-, ladite chaîne étant non substituée ou substituée par un ou plusieurs radicaux choisis parmi les atomes d'halogène, les groupements hydroxyle, C₁-C₄ alkyle, benzyle et/ou phénéthyle ;
- R₁ représente un atome d'hydrogène, un groupement hydrocarboné aliphatique comportant de 1 à 6 atomes de carbones, un benzyle ou un phénéthyle ;
- Y₁, Y₂, Y₃, identiques ou différents, représentent chacun, indépendamment l'un de l'autre un atome d'hydrogène, d'halogène, un groupement -OR₂, un aryle ou une chaîne hydrocarbonée aliphatique saturée ou insaturée

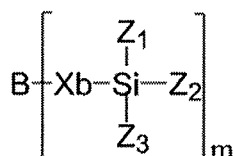
30

comportant de 1 à 6 atomes de carbone éventuellement substitués par un atome halogène, un groupement aryle ou hydroxyle ;

- R_2 représente un atome d'hydrogène, un groupement aryle ou une chaîne hydrocarbonée aliphatique saturée ou insaturée comportant de 1 à 6 atomes de carbone ;
 - au moins deux groupement X_a tels que définis ci-dessus étant reliés à des points d'accroches différents sur A;
- b) mise en présence d'eau, optionnellement conjointement à l'étape a) ; et
- c) récupération de l'hydrogel.

10

2. Procédé de fabrication d'un hydrogel selon la revendication 1, caractérisé en ce que ledit procédé comprend l'ajout conjointement ou successivement à l'étape a) d'au moins un type de molécule de formule (II) :



15

Formule (II)

dans laquelle :

- m est un nombre entier supérieur ou égal à 1, préférentiellement égal à 1 ;
- B est un principe actif, préférentiellement une biomolécule ou un fluorophore, pouvant être par exemple choisi parmi un peptide, un oligopeptide, une protéine, telle que le collagène, un acide désoxyribonucléique, un acide ribonucléique, un polysaccharide, tel qu'une pectine, un chitosane, un acide hyaluronique, un polysaccharide polyarabinose et polygalactose, et un glycolipide;
- X_b est une liaison chimique ou un groupement espaceur préférentiellement représenté par un radical divalent dérivé d'une chaîne hydrocarbonée aliphatique saturée ou insaturée comportant de 1 à 10 atomes de carbone, dans laquelle sont éventuellement intercalés, un ou plusieurs chaînons structuraux choisis parmi le groupe arylène, ou les fragments $-O-$, $-S-$, $-C(=O)-$, SO_2 ou $-N(R_3)-$, ladite chaîne étant non substituée ou substituée par

30

un ou plusieurs radicaux choisis parmi les atomes d'halogène, les groupements hydroxyle, C₁-C₄ alkyle, benzyle et/ou phénéthyle ;

- 5 • R₃ représente un atome d'hydrogène, un groupement hydrocarboné aliphatique comportant de 1 à 6 atomes de carbones, un benzyle ou un phénéthyle ;
- 10 • Z₁, Z₂, Z₃, identiques ou différents, représentent chacun, indépendamment l'un de l'autre un atome d'hydrogène, d'halogène, un groupement -OR₄, un aryle ou une chaîne hydrocarbonée aliphatique saturée ou insaturée comportant de 1 à 6 atomes de carbone éventuellement substitués par un atome halogène, un groupement aryle ou hydroxyle ;
- 15 • R₄ représente un atome d'hydrogène, un groupement aryle ou une chaîne hydrocarbonée aliphatique saturée ou insaturée comportant de 1 à 6 atomes de carbone ; et
- avec préférentiellement un seul des groupements Z₁, Z₂, ou Z₃ comme atome d'halogène ou groupement OR₄.

3. Procédé de fabrication d'un hydrogel selon la revendication 1 ou 2, caractérisé en ce que le procédé de polymérisation sol-gel est effectuée à pH physiologique ou en ce que l'hydrogel est formé en présence d'une quantité suffisante d'eau pour que la teneur en eau de l'hydrogel soit d'au moins 50% en poids vis-à-vis du poids total de l'hydrogel formé.

4. Procédé de fabrication d'un hydrogel selon l'une quelconque des revendications 1 à 3 caractérisé en ce que ledit hydrogel est polymérisé sur ou dans au moins un premier hydrogel en tant que support, résultant ainsi en un hydrogel multicouches.

5. Hydrogel susceptible d'être obtenu par le procédé selon l'une quelconque des revendications 1 à 4.

6. Hydrogel selon la revendication 5 pour son utilisation à des fins thérapeutiques et/ou chirurgicales, préférentiellement caractérisé en ce que ledit hydrogel permet la délivrance et/ou le transport de molécules actives, ou pour son utilisation *in vivo*

en ingénierie tissulaire pouvant par exemple se faire par une polymérisation dudit hydrogel *in situ* dans un organisme vivant suite à la coulée ou l'injection des molécules de formule (I) et éventuellement (II) telles que définies dans la revendication 1 ou 2.

5

7. Utilisation *in vitro* d'un hydrogel selon la revendication 5, en ingénierie tissulaire.

8. Procédé de purification d'un produit de formule (I) ou (II) tels que définis selon l'une quelconque des revendications 1 ou 2 caractérisé en ce que ledit procédé comprend les étapes suivantes:

10

- a1) éventuelle solubilisation du produit de formule (I) ou (II) à purifier dans un solvant ;
- b1) précipitation du produit de formule (I) ou (II) à purifier, éventuellement en solution selon l'étape a1), dans un liquide de suspension ;
- c1) filtration du solide obtenu à l'étape (b1) ;
- d1) répétition au moins une fois des étapes a1) le cas échéant, b1) et c1) ; et
- e1) récupération du produit de formule (I) ou (II) purifié.

15

9. Procédé de purification d'un produit de formule (II) tel que défini selon la revendication 2 dans laquelle un seul des groupements Z_1 , Z_2 , Z_3 est un atome d'halogène ou un groupement $-OR_3$, caractérisé en ce que ledit procédé comprend les étapes suivantes:

20

- a2) passage du produit de formule (II) à purifier sur une colonne de chromatographie en phase liquide, préférentiellement en phase inverse ;
- b2) évaporation du solvant d'élution de l'étape a2), éventuellement par lyophilisation ;
- c2) récupération du produit de formule (II) purifié.

25

10. Produit de formule (I) ou (II) tel que défini selon la revendication 1 ou 2, susceptible d'être obtenu par le procédé selon la revendication 8 ou 9 caractérisé en ce que ledit produit présente une pureté d'au moins 98% en masse vis-à-vis du poids total de produit obtenu, préférentiellement supérieure à 99% en masse.

30

TITRE

Nouveaux hydrogels de structure silylée et procédé d'obtention

5

ABREGE DESCRIPTIF

L'objet de la présente invention concerne des hydrogels préparés au moyen de molécules organiques silylées (telles que des biomolécules silylées), leur procédé d'obtention et leurs utilisations

1/2

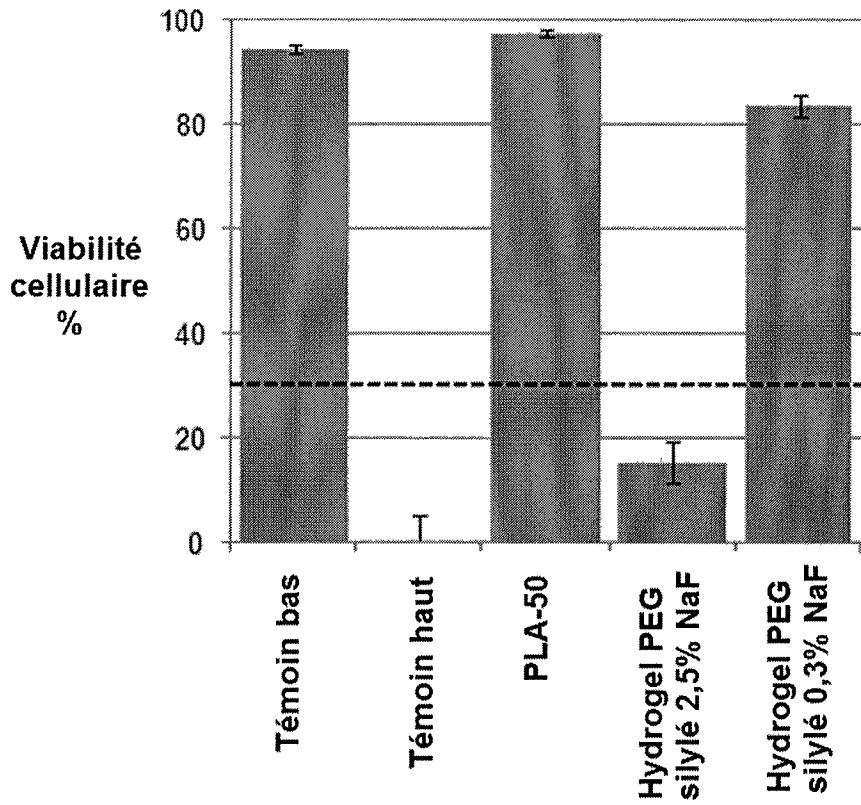


Figure 1

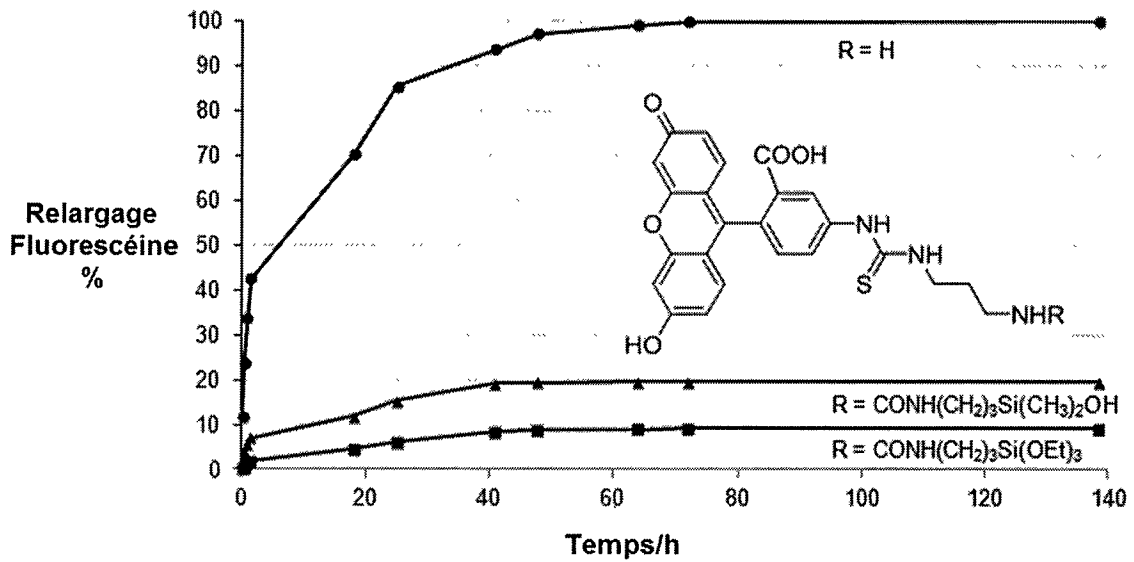


Figure 2

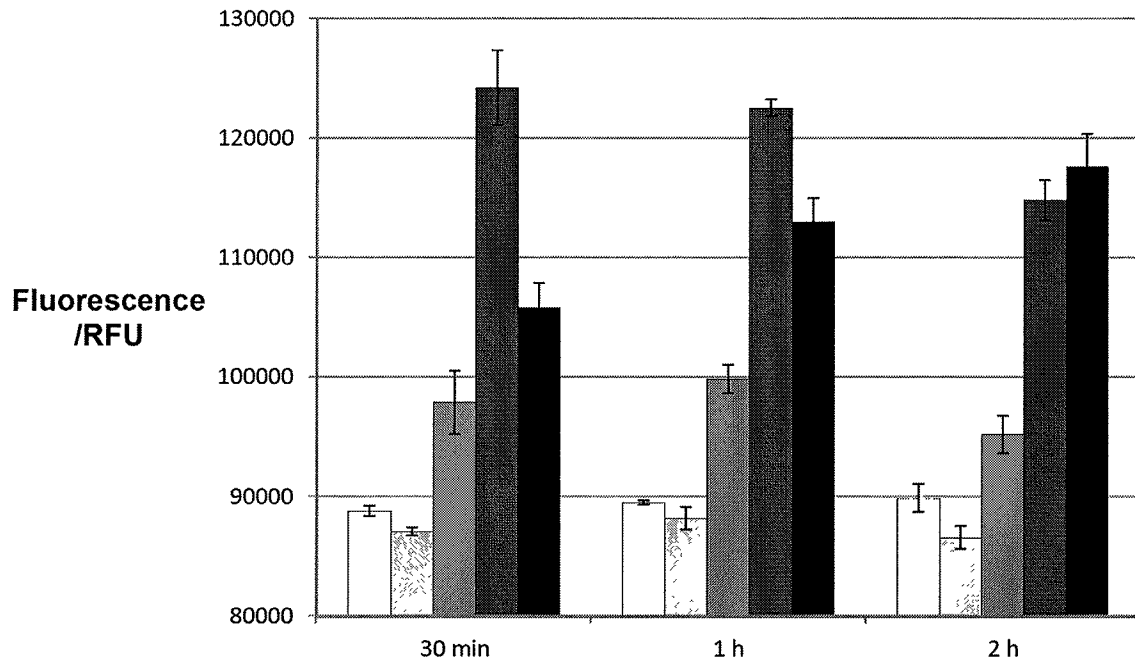


Figure 3

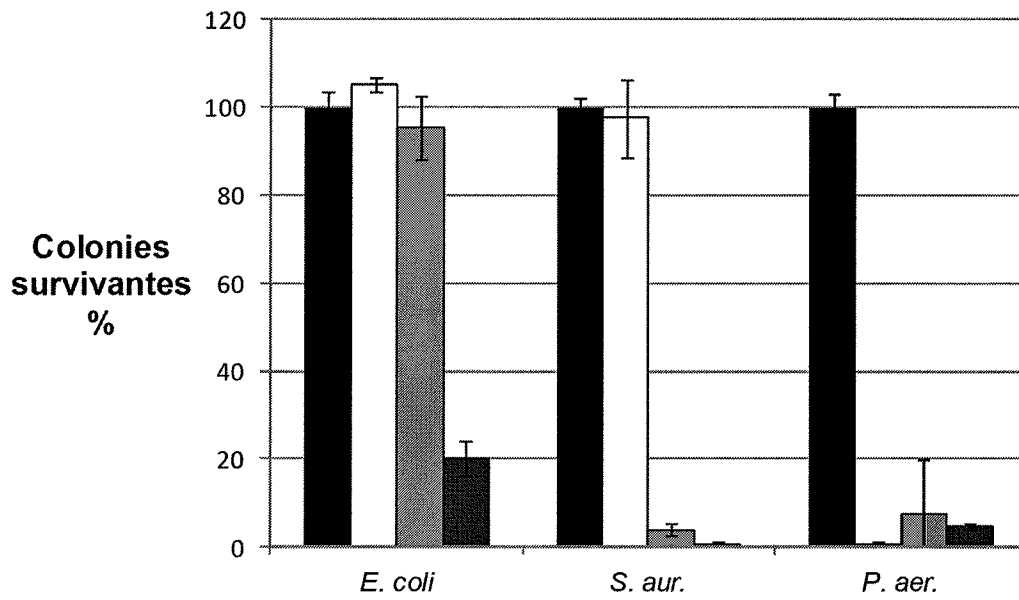


Figure 4

Résumé : Nous avons imaginé et développé une méthode pour la préparation d'hydrogels par procédé sol-gel à partir de blocs hybrides (bio)organiques-inorganiques. Les blocs hybrides sont obtenus par introduction de groupements silylés, triéthoxysilanes ou hydroxydiméthylsilanes, sur des polymères synthétiques ou des molécules d'intérêt biologique telles que des peptides. Ces blocs hybrides peuvent être combinés dans des proportions choisies pour former des hydrogels multifonctionnels. Le procédé de gélification se déroule à 37°C à pH 7.4 dans un tampon physiologique. L'hydrolyse et la condensation des précurseurs silylés conduit à la formation d'un réseau tridimensionnel covalent dans lequel les entités organiques sont reliées par des liaisons siloxanes. Dans un premier temps, cette méthode a été appliquée à la synthèse d'hydrogels à base de PEG. Nous avons ensuite montré que ces hydrogels pouvaient être fonctionnalisés de façon covalente par des entités bioactives au cours de leur préparation. Des hydrogels possédant des propriétés antibactériennes ou favorisant l'adhésion cellulaire ont ainsi été préparés. Dans un deuxième temps, un peptide hybride inspiré du collagène naturel a été synthétisé et a permis l'obtention d'hydrogels qui présentent des propriétés de prolifération cellulaire similaires à celles observées sur des substrats de collagène naturel. La biocompatibilité du procédé sol-gel a été démontrée par l'encapsulation de cellules souches dans l'hydrogel au cours de sa formation. Enfin, l'impression 3D d'hydrogels hybrides a été réalisée. Ce travail de thèse met donc en lumière le potentiel de la chimie sol-gel pour la conception à façon de matériaux biomimétiques particulièrement prometteurs pour des applications en ingénierie tissulaire.

Mots-clés : peptide, silane, hybride, sol-gel, hydrogel et biomatériau

Biomimetic Peptide Hybrid Materials

Abstract: We designed and developed a method for the preparation of hydrogels through the sol-gel process. It is based on (bio)organic-inorganic hybrid blocks obtained by functionalization of synthetic polymers or bioactive molecules, such as peptides, with silyl groups (triethoxysilanes or hydroxydimethylsilanes). These hybrid blocks can be combined in desired ratio and engaged in the sol-gel process to yield multifunctional hydrogels. Gelation proceeds at 37°C at pH 7.4 in a physiological buffer. Hydrolysis and condensation of silylated precursors result in a three-dimensional covalent network in which molecules are linked through siloxane bonds. First, this method was applied to the synthesis of PEG-based hydrogels. Then, we demonstrated that hydrogels could be covalently functionalized during their formation. Thus, hydrogels exhibiting antibacterial properties or promoting cell adhesion were obtained. Secondly, a hybrid peptide whose sequence was inspired from natural collagen was synthesized and used to prepare hydrogels that provided a cell-friendly environment comparable to natural collagen substrates. Stem cells could be encapsulated in these hydrogels with high viability. Finally, hybrid hydrogels were used as bio-inks to print 3D scaffolds. This PhD work highlights the potential of the sol-gel chemistry for the design of tailor-made biomimetic scaffolds that could be particularly promising for tissue engineering applications.

Keywords: peptide, silane, hybrid, sol-gel, hydrogel and biomaterial

Noms et adresses des laboratoires

Institut des Biomolécules Max Mousseron (IBMM)
UMR 5247 – Université de Montpellier, CNRS, ENSCM
Faculté de Pharmacie,
15 Avenue Charles Flahault
34093 MONTPELLIER, FRANCE

Institut Charles Gerhardt Montpellier (ICGM)
UMR 5253 - Université de Montpellier, CNRS, ENSCM
Campus Triolet
Place Eugène Bataillon
34095 MONTPELLIER, FRANCE